Functional analysis of candidate terpenoid biosynthetic genes isolated from grapevine

by

Ilse-marie Bezuidenhout

Dissertation presented for the degree of

Doctor of Philosophy

(Agricultural Sciences)

at

Stellenbosch University

Department of Viticulture and Oenology, Institute for Wine Biotechnology, Faculty of AgriSciences

Supervisor: Dr. Philip Richard Young

Co-supervisor: Prof. Melané Alethea Vivier

March 2021

Declaration

By submitting this dissertation electronically, I declare that the entirety of the work contained therein is my own, original work, that I am the sole author thereof (save to the extent explicitly otherwise stated) that reproduction and publication thereof by Stellenbosch University will not infringe any third party rights and that I have not previously in its entirety or in part submitted it for obtaining any qualification.

Date: 01/03/2021

Summary

Terpenoids are a group of compounds found in various organisms, with diverse functions, and can be broadly grouped into primary or specialised (secondary) metabolites. This compound diversity is achieved from the universal precursors for terpenoids, isopentenyl diphosphate (IPP) and dimethylallyl diphosphate (DMAPP), through the activity of various enzymes. Isoprenyl diphosphate synthases (IDSs) incorporate the IPP and DMAPP precursors into compounds of varying lengths that can then serve as the substrate for terpene synthases (TPSs) to produce terpenes. Each of these steps incorporates the opportunity to further increase terpene diversity. In addition, terpenes can be modified into other products through the activity of various enzymes to increase the product range even further.

Terpenoids play an important role in *Vitis vinifera* (grapevine), not only in the normal functioning of the plant, but also in more specialised roles involving plant–environment interactions. In terms of their economic value, terpenes, such as mono- and sesquiterpenes, contribute to wine aroma – which has supported the study of these compounds and how these metabolites are biosynthesised. Grapevine genome annotation has shown a moderately sized IDS gene family and a TPS gene family that has undergone extensive expansion. However, many of these genes have not been functionally characterised. Putative annotation based on sequences is not always accurate or does not provide a realistic indication of gene function.

Functional characterisation of IDS and TPS genes involves heterologous expression followed by analysis of the produced compounds. In this study, various heterologous systems were used and evaluated with the aim of characterising grapevine genes that putatively encode IDS and TPS enzymes. In this study, the novel annotation of a eucalyptol synthase and the re-annotation of a previously characterised gene to α-thujene synthase was achieved. Various expression systems were assessed, with *Saccharomyces cerevisiae* deemed a viable alternative to the typical use of *Escherichia coli.* Different plant systems were also investigated, with *Nicotiana benthamiana* found to be a good option in terms of ease of use and results obtained.

An in-depth study of geranylgeranyl diphosphate synthase (*VviGGPS*) was also conducted using an established transgenic tobacco population. The population was characterised in terms of morphology, physiology, and metabolites. The possible role of gibberellin was also determined based on the results of these analyses.

Opsomming

Terpene is 'n groep metaboliete wat in verskillende organismes voorkom, met 'n wye verskeidenheid van funksies, en wat breedvoerig in primêre of gespesialiseerde (sekondêre) metaboliete opgedeel kan word. Terpeen diversiteit word bewerkstellig vanaf die universele voorlopers, isopentenieldifosfaat (IPP) en dimetielallieldifosfaat (DMAPP), deur die aktiwiteit van verskeie ensieme. Isoprenieldifosfaat-sintases (IDSs) inkorporeer die IPP en DMAPP voorlopers binne-in verbindings van wisselende lengtes in wat dan as die substrate vir terpeen-sintases (TPSs) kan dien vir die biosintese van terpene. Elkeen van hierdie stappe bied 'n geleentheid om terpeen diversiteit te vermeerder. Terpene kan ook gemodifiseer word na ander produkte toe deur die aktiwiteit van verskeie ensieme om sodoende die terpeen produkreeks selfs meer te vermeerder.

Terpene speel 'n belangrike rol in *Vitis vinifera* (wingerd); nie net in die normale funksionering van die plant nie, maar ook in 'n meer gespesialiseerde rol in plant–omgewing interaksies. In terme van ekonomiese waarde dra terpene soos mono- en seskwiterpene by tot die aroma van wyn – wat gedien het as ondersteuning vir die bestudering van hierdie verbindigs asook die biosintese daarvan. Annotering van die wingerd genoom het aangedui dat dit beskik oor 'n gemiddelde-grootte IDS geenfamilie en 'n TPS geenfamilie wat ekstensiewe vergroting ondergaan het. Baie van hierdie gene is egter nog nie gekarakteriseer in terme van funksie nie. Die vermeende benaming van gene gebaseer op nukleotied- of aminosuurvolgorde is ook nie altyd akkuraat nie of verskaf nie 'n realistiese indikasie van geenfunksie nie.

Funksionele karakterisering van IDS en TPS gene behels heteroloë uitdrukking gevolg deur die analise van die geproduseerde metaboliete. Verskeie heteroloë sisteme is in hierdie studie gebruik en geëvalueer met die doel om wingerd gene wat kodeer vir vermeende IDS en TPS ensieme te karakteriseer. In hierdie studie is die nuwe annotering van 'n eukaliptol-sintase asook die annotasie van 'n voorheen gekaraktiseerde geen na α-thujene-sintase. Verskeie sisteme was ondersoek en *Saccharomyces cerevisiae* is gevind as 'n goeie alternatief tot die tipiese gebruik van *Escherichia coli*. Verskeie plantsisteme is ook oorweeg en *Nicotiana benthamiana* is gevind as 'n goeie opsie in terme van gebruikersvriendelikheid en resultate wat verkry is.

'n In-diepte studie van 'n geranielgeranieldifosfaat-sintase (*VviGGPS*) is ook uitgevoer deur die bestudering van 'n gevestigde transgeniese tabak populasie. Die populasie is gekaraktiriseer in terme van morfologie, fisiologie en metaboliete. Die moontlike rol van gibberelien gebasseer op hierdie analises, is ook bepaal.

This dissertation is dedicated to

My parents, for their unerring support
and belief that I can climb any
mountain on my path.

Biographical sketch

Ilse-marie Bezuidenhout was born in Pretoria, South Africa on 21 November 1984 and was raised on a farm close to Tzaneen. She matriculated from Merensky High School in 2002 and commenced her studies at the University of Stellenbosch in 2008 where she enrolled for a BSc degree in Molecular Biology and Biotechnology. After graduating in 2010, she pursued postgraduate studies, obtaining an HonsBSc degree in Wine Biotechnology Cum Laude in 2011 before enrolling for an MSc degree in 2012 Wine biotechnology that was upgraded to a PhD degree in 2013.

Acknowledgements

I wish to express my sincere gratitude and appreciation to the following persons and institutions:

- **Dr Philip Young**, who acted as my supervisor since my Honours studies, for his encouragement, for being a never-ending fountain of ideas and knowledge and for giving me that last push to let go and hand in my thesis.

- **Prof Melané Vivier,** who acted as my co-supervisor and encouraging me to upgrade my MSc to a PhD, for her insight and guidance during my studies.

- **The National Research Foundation (NRF), Institute for Wine Biotechnology (IWBT) and WineTech** for financial assistance.

- Past and present staff of IWBT, CAF and SUN as mentioned in the different chapters but also special thanks to **Anke Berry, Thalitha Mostert, Karin Vergeer** and **Lucky Mokwena** for always be willing to assist.

- **Prof. Alisdair Fernie, Dr Takayuki Tohge, Dr Saleh Alseekh, and Dr Igor Florez** and the rest of the group for making my research visit to MPIMP so enjoyable while still learning a lot!

- My lab maatjies, **Dr Kari du Plessis and Dr Helmien Barkhuizen:** we started this PhD journey together and I am also lucky enough to call you friends, thank you for all the support, encouragement, and of course all the coffee/wine drinking sessions.

- All my friends and colleagues at IWBT. Special thanks to **Dr Florent Weiller,** we started and finished our PhDs together, it was a long journey, but it was easier with a friend along the way! **Dr Jay Belli-Kullan** for your encouragement.

- My past and present colleagues at Scistaff, thank you **Thea van der Merwe** for being so supportive during the writing-up phase and **Janca Ferreira** for being a great cheerleader and generous spirit!

- **Dr Anneke Brand and Ed Burger:** Anneke for assistance with the editing and moral support during the last stretch, Ed for not complaining when we continued to work into the late hours to get the thesis in on time!

- All my friends outside of the lab who patiently listened to all my complaints and celebrated my achievements with me, special thanks to **Michelle Jelbert** for just being an awesome friend and along with her mother, **Nerine Davies** and the rest of her family for always making me feel welcome**, Derick Schmidt** who I can always call if I need help and for being such a supportive friend and great listener**, Emma Livesey** for checking-in and listening to all my troubles and being such fun during the celebrations.

- The Wentzel family, **Ben** for your continuous encouragement even through the difficult times, tannie **Winnie** and the late oom **Manus** for making Langdraai a haven from the demands of a PhD, I will always remember the wonderful holidays on the farm and at the sea with the Wentzel family.

- My family especially my parents, **Dr Jurg Bezuidenhout** and **Carlo Bezuidenhout** for all the support before and during my PhD, I am very lucky to have parents who never doubt my ability to succeed. My sisters**, Lydia Bester** for knowing when to be understanding and when give me a push, **Hilda van der Schyff** for your loving support. **Julané** and **John Wagenaar,** for always being willing to help. Lastly to Mr. **McGyver**, we managed to help each other through a tough year!

Preface

This dissertation is presented as a compilation of six chapters. Each chapter is introduced separately and is written according to the style of the *South African Journal of Enology and Viticulture.*

Chapter 1   **General Introduction, literature overview, and specific project aims and objectives**

Chapter 2   **Research results**
Development and validation of yeast and plant expression systems for functional characterisation of genes involved in grapevine terpenoid biosynthesis

Chapter 3   **Research results**
Characterisation of a eucalyptol and α-thujene synthase from *Vitis vinifera*

Chapter 4   **Research results**
Annotation and evaluation of a tobacco population overexpressing the *VviGGPS1*

Chapter 5   **Research results**
Overexpression of the grapevine geranylgeranyl diphosphate synthase (*VviGGPS1*) gene in tobacco alters plant morphology and chemotypes indicative of changes in gibberellin metabolism

Chapter 6   **General discussion and conclusions**

Table of Contents

Chapter 3 Characterisation of a eucalyptol and α-thujene synthase from *Vitis vinifera* 94

Chapter 4 Annotation and evaluation of a tobacco population overexpressing the *VviGGPS1*

List of Abbreviations and Acronyms

ABA	abscisic acid
alt-ORFs	alternative open reading frames
CAF	Central Analytical Facility
CAS	Chemical Abstracts Service
CCC	chair-chair-chair
CCD	carotenoid cleavage dioxygenase
CL	carlactone
CLD	chain-length determination
CPS	*ent*-Copalyl diphosphate synthase
CR_LL	climaroom under low light
CT	computed tomography
cTP	chloroplastic transit peptide
CWSI	Crop Water Stress Index
DLI	daily light integral
DMAPP	dimethyl diphosphate
DMNT	4,8-dimethylnona-1,3,7-triene
EIM	electron impact mode
FARM	first aspartate-rich motif
FPP	farnesyl diphosphate
FPS	Farnesyl diphosphate synthase
GA	gibberellin
GC	gas chromatography
GC-MS	gas chromatography mass spectroscopy
GGPP	geranylgeranyl diphosphate
GH	greenhouse
GH_HL	greenhouse under high light
GPP	geranyl diphosphate
GPS	geranyl diphosphate synthase
GS	genomic selection
GWA	genome-wide association
HGL-DTG	17-hydroxygeranyllinalool diterpenoid glycoside
HMG	3-hydroxy-3-methylglutaryl coenzyme A reductase
HS	headspace
HS-SPME	headspace solid phase microextraction
IDS	isoprenyl diphosphate synthase

IPP	isopentenyl diphosphate
IPTG	isopropyl-β-D-thiogalactopyranoside
IRGA	infrared gas analyser
IS	internal standard
IWBT	Institute for Wine Biotechnology
KI	Kovats Index
KS	*ent*-kaurene synthase
LD	linkage disequilibrium
LD	long day
LMA	leaf mass (fresh weight) per area
LSU	large subunit
MBO	methylbutenol
MeJA	methyl jasmonate
MEP	methylerythritol phosphate
MOG	materials other than grapes
MS	mass spectrum
MS	mass spectrometry
MS	Murashige and Skoog
MSA	multiple sequence alignments
mTP	mitochondrial transit peptide
MVA	mevalonate
NCED	9'-*cis*-epoxycarotenoid dioxygenases
NIST	United States National Institute of Standards & Technology (NIST)
NPP	neryl diphosphate
NPS	neryl diphosphate synthase
OD	optical density
OPLS-DA	orthogonal projections to latent structures discriminant analysis
OSC	oxidosqualene cyclase
PAR	photosynthetically active radiation
PPPS	polyprenyl diphosphate synthase
PTFE	polytetrafluorothylene
RI	Retention Index
RP-UPLC	reverse-phase ultra-performance liquid chromatography
RT	retention time
SAGWRI	South African Grape and Wine Research Institute
SARM	second aspartate-rich motif
SB	Sauvignon blanc

SDs	segmental duplications
SIC	selected ion count
SIM	selected ion monitoring
SMRT	single-molecule real-time
SNP	single nucleotide polymorphism
SPME	solid phase microextraction
SSU	small subunit
SSUII	small subunit of the heterodimeric GPS
TMTT	4,8,12-trim- ethyltrideca-1,3,7,11-tetraene
VOC	volatile organic compound
WGD	whole genome duplication
YPD	yeast extract peptone dextrose

Chapter 1 General introduction, literature overview, and specific project aims and objectives

1.1 Introduction

Terpenoids are the most chemically and structurally diverse natural products, with a current estimation of more than 80 000 compounds grouped in this family (Christianson, 2017). The C5 building blocks for terpenoid biosynthesis, isopentenyl diphosphate (IPP) and its isomer dimethylallyl diphosphate (DMAPP), are produced via two pathways in plants and pluricellular green algae (**Figure 1.1),** these two pathways being the mevalonate (MVA) pathway, localised to the cytosol and endoplasmic reticulum (ER), and the methylerythritol phosphate (MEP) pathway compartmentalised to the plastids (Wright, 1961; Rohmer *et al.*, 1996; Lichtenthaler *et al.*, 1997). Other organisms are limited to only one pathway, non-plant eukaryotes as well as archaea have the MVA pathway while the MEP pathway is found in prokaryotes and unicellular green algae. However, there are exceptions to this rule as the MVA pathway has been found in some bacteria. Possible reasons for this being recent horizontal gene transfer (HGT) events or the MVA pathway is an ancestral metabolic route common to three domains of life (Boucher & Doolittle, 2000; Wilding *et al.*, 2000; Lombard & Moreira, 2011). In plants, the MEP pathway is utilised for the biosynthesis of hemiterpenes (C5), monoterpenes (C10), diterpenes (C20) and tetraterpenes/carotenoids (C40) as well various phytohormones and photosynthetic compounds while the MVA pathway is required for sesquiterpene (C15), triterpene (C30), sterol and brassinosteroid production (**Figure 1.1**). However, the two pathways do not operate in isolation and crosstalk between these two pathways can take place (Bick & Lange, 2003; Hemmerlin *et al.*, 2003, 2012; Schuhr *et al.*, 2003).

IPP and DMAPP are the substrates for the condensation reactions catalysed by isoprenyl diphosphate synthases (IDSs) to produce isoprenyl diphosphates of various lengths. The isoprenyl diphosphates can then be converted to the basic terpene structure by terpene synthases (TPSs), terpenes can be further modified through various reactions such as hydroxylation, dehydrogenation, acylation and glycosylation to produce the wide array of terpenoids found in nature (Dudareva, 2004). Alternatively, the isoprenyl diphosphates can be shunted to the biosynthesis of the various other compounds derived from the terpenoid pathway (**Figure 1.1**).
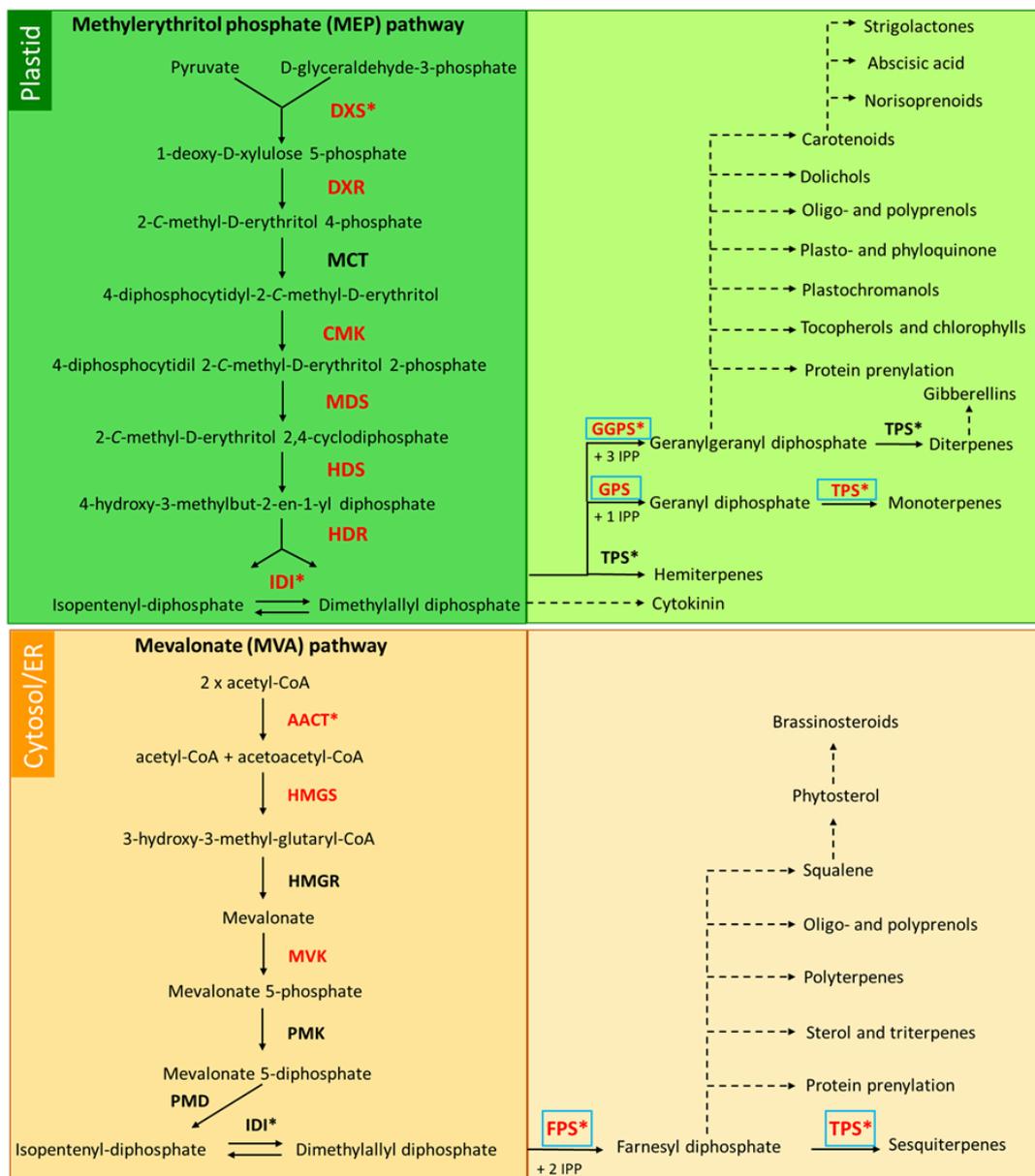
Figure 1.1 Description of the two terpenoid pathways found in plants, based on pathways constructed for *Arabidopsis thaliana* by (Vranová *et al.*, 2011). Dashed lines indicate multiple reactions. Enzymes responsible for catalysing reactions are shown in bold. The MEP pathway enzymes: **DXS**, 1-deoxy-D-xylulose-5-phosphate synthase; **DXR**, 1-deoxy-D-xylulose-5-phosphate reductoisomerase; **MCT**, 2-C-methyl-D-erythritol-4-phosphate cytidyltransferase; **CMK**, 4-diphosphocytidyl-2-C-methyl-D-erythritol kinase; **MDS,** 2-C-methyl-D-erythritol 2,4-cyclodiphosphate synthase; **HDS**, 4-hydroxy-3-methylbut-2-en-1-yl diphosphate synthase; **HDR**, 4-hydroxy-3-methylbut-2-enyl diphosphate reductase; **IDI**, isopentenyl-diphosphate δ-isomerase; **GPS**, geranyl-diphosphate synthase; **GGPS**, geranylgeranyl diphosphate synthase. MVA pathway enzymes: **AACT**, acetyl-CoA acetyltransferase; **HMGS**, 3-hydroxy-3-methylglutaryl-CoA synthase; **HMGR**, 3-hydroxy-3-methylglutaryl-CoA reductase; **MVK**, mevalonate kinase; **PMK**, phosphomevalonate kinase; **PMD**, diphospho-mevalonate decarboxylase; **IDI**, isopentenyl-diphosphate δ-isomerase.; **FPS**, farnesyl diphosphate synthase; **TPS**, terpene synthase. * indicates multiple genes and/or protein variants found in *A. thaliana* with predicted or confirmed differences in subcellular localisation (Aubourg *et al.*, 2002; Vranová *et al.*, 2013). Isolation of various grapevine terpenoid genes has been done with the enzymes which these genes putatively encode for highlighted in red. Enzymes enclosed in blue blocks are those targeted in this study for characterisation.

2

Terpenoids have a variety of functions in the plants and can be broadly grouped into primary and secondary metabolites (Karunanithi & Zerbe, 2019). A useful definition for distinguishing between primary and secondary metabolism is given by Hartmann (2007), wherein primary metabolism relates to all processes necessary for growth and development while secondary metabolism is required for an individual to survive its environment. Although all terpene synthases share an evolutionary origin, the split between those enzymes responsible for primary and secondary metabolism in plants seems to have occurred before the branching of angiosperms and gymnosperms (Singh & Sharma, 2015). Secondary metabolism genes are characterised by their high plasticity, which enables relatively rapid adaptations based on selective pressure from the environment (Hartmann, 2007; Moore *et al.*, 2019). Terpenoids such as gibberellin (hormone), ubiquinone (electron carrier), carotenoids and chlorophyll (photosynthetic pigments) play a vital role in normal plant functioning and can be found across all plant species. These compounds are therefore categorized as primary metabolites and form a relatively small fraction of the total terpenoids found in nature (McGarvey & Croteau, 1995; Pichersky & Gang, 2000). The majority of the terpenoids in plants are classified as secondary, also called specialised, metabolites, which enable the plant to interact with its environment (Chen *et al.*, 2011; Pichersky & Lewinsohn, 2011). Secondary metabolite terpenoids include hemiterpenes (C_5), monoterpenes (C_{10}), sesquiterpenes (C_{15}), homoterpenes (C_{11} and C_{16}) and diterpenes (C_{20}) (Dudareva *et al.*, 2006). However, the classification can sometimes be blurred with some terpenoids having roles that can be classified as essential for plant function (primary metabolite) but also play a more specialised role. An example being the carotenoids that have a photoprotective role which can be seen as an essential function but carotenoids are also responsible for the colour of some fruits which function in attracting seed dispersers and therefore plays a more specialised role(Pott *et al.*, 2019).

Based on their varied functions in plants it is therefore not surprising that terpenoids and the genes responsible for the biosynthesis thereof have received a lot of attention across plant species. Following the release of the grapevine genome in 2007 and the subsequent annotation of the terpene synthase gene family there has been a significant gain in momentum regarding research into the grapevine terpenoid pathway genes (Jaillon *et al.*, 2007; Velasco *et al.*, 2007; Martin *et al.*, 2010). This thesis will focus on the functional characterisation of selected genes involved in terpenoid biosynthesis. To give context to the scope of this study, the current knowledge regarding terpenoids and terpenoid pathway genes will be briefly discussed.

3

1.2 Literature overview – The plant gene families encoding isoprenyl diphosphate synthases and terpene synthases and functional characterisation of these genes

1.2.1 Introduction

The development of a sophisticated metabolic network in plants enabled these sessile organisms to flourish in an ever-changing environment. Most plant metabolites can be categorised as secondary (or specialised) compounds, with terpenoids representing a significant fraction thereof. Selective pressure, whether natural or through crop domestication, has exploited this intricate metabolic network, with the result being a large repertoire of terpenoids found in nature. In this literature overview the aim was to look at the current knowledge regarding the evolution of the genes encoding for IDSs and TPSs. The IDSs synthesise the substrates used by TPSs to produce terpenes and both groups can be viewed as branchpoint enzymes since these enzymes shuttle the universal terpenoid precursors, IPP and DMAPP, in a specific avenue of terpenoid production. The biological roles terpenoids play in normal plant functioning as well as in plant–environment interactions are discussed with a specific focus on specialised terpenes in grapevine. Lastly, the difficulties associated with the characterisation of these genes are described and linked to the evolutionary beginning of these genes.

1.2.2 Evolution of *IDSs* and *TPSs* – the basis for terpenoid diversity

The IDSs can be broadly subdivided into *trans*-IDSs and *cis*-IDSs based on the product stereochemistry (Ogura & Koyama, 1998; Liang *et al.*, 2002). Even though these two enzyme classes produce similar products they do not seem to share a common ancestor and have no structural or sequence homology (Wang & Ohnuma, 2000). Studies regarding *cis*-IDSs are limited, but generally these enzymes are responsible for the biosynthesis of long-chain IPPs (>C50) although *cis*-IDSs capable of producing short-chain (<C25) IPPs have been characterised (Sallaud *et al.*, 2009; Schilmiller *et al.*, 2009; Akhtar *et al.*, 2013; Surmacz *et al.*, 2014). However, the focus of this review will be on the *trans*-IDSs since these enzymes produce most of the substrates for terpene biosynthesis. The *trans*-IDSs synthesise the C10-C50 isoprenyl diphosphates, with the short-chain IDSs (C10-C25) forming a subgroup thereof. The short-chain IDSs produce the substrates used by TPSs to form monoterpenes (C10), sesquiterpenes (C15), diterpenes (C20) and sesterterpenes (C25) (Vandermoten *et al.*, 2009; Jia & Chen, 2016; Wang *et al.*, 2016). It is thought that all *trans*-IDSs share a common ancestor, with archaeal GGPSs proposed to be the closest relative to this common ancestor (Chen *et al.*, 1994; Wang & Ohnuma, 1999). However, as more sequences become available for analysis this hypothesis has been brought under dispute (Tachibana *et al.*,

2000). Phylogenetic analysis by Vandermoten et al. (2009) did show two groupings of *trans*-IDSs with animal (insect) GPSs and eukaryotic FPSs in one subfamily while all other *trans*-IDSs grouped in another subfamily. This is indicative of a common prokaryotic ancestor, although the frequency of horizontal gene transfer in prokaryotes will make it difficult to pinpoint the specific ancestor to *trans*-IDSs (Dagan *et al.*, 2008). Phylogenetic analysis by Jia & Chen (2016) assigned plant *trans*-IDSs into five subfamilies. The subfamilies also represent functional groups with *trans*-IDS-a representing farnesyl diphosphate synthase (FPS), *trans*-IDS-b the solanesyl diphosphate synthases (SPS), *trans*-IDS-c the polyprenyl diphosphate synthase (PPS) and *trans*-IDS-e the small subunit (SSU) of the heterodimeric geranyl diphosphate synthase (GPS). The *trans*-IDS-d subfamily includes geranylgeranyl diphosphate synthase (GGPS), geranylfarnesyl diphosphate synthase (GFPS) and PPS. The divergence of these subfamilies seems to have taken place early in plant evolution based on the subfamilies of *trans*-IDS already being observed in green algae (Jia & Chen, 2016). Adal *et al.* (2017) expanded on this phylogenetic tree with the inclusion of the large subunit (LSU) GPSs into the *trans*-IDS-d subfamily. The *trans*-IDS-e clade was also subdivided into GPS-SSUI and GPS-SSUII.

A hypothesis formulated by Reardon and Farber (1995) states that enzymes involved in sequential reactions are likely to share an ancestor with divergent evolution allowing for functional differentiation. Based on the structural similarity between IDSs and TPSs, it is believed that these enzymes are evolutionarily related. Major sequence differences have occurred since the split from the ancestral enzyme, but since the three-dimensional structure evolves much more slowly, the strong relation between these enzymes can still be seen (Reardon & Farber, 1995; Liang *et al.*, 2002). In terms of the direction of evolution, it has been hypothesised by Beran *et al.* (2016) that *TPSs* might have evolved from *IDSs.* Support for this theory is given by the bifunctional nature of a GPS from bark beetle which produces both GPP and myrcene (Gilg *et al.*, 2009), isolated sequences from insects with high similarity to IDSs producing sesquiterpenes in heterologous studies (Beran *et al.*, 2016; Lancaster *et al.*, 2018) as well as an α-farnesene synthase from apple which also possesses FPS activity (Green *et al.*, 2007).

Within the gene family, the *TPSs* in higher plants are thought to have evolved from an ancestral gene encoding bifunctional copalyl synthase (CPS) / kaurene synthase (KS) (Keeling *et al.*, 2010; Chen *et al.*, 2011). Duplication and subsequent subfunctionalisation of this ancestral *CPS/KS* has resulted in loss of function in one of the two domains with either the N-terminal domain (active site of CPS) or the C-terminal domain (active site of KS) remaining functional. This split in the functional domains gave rise to the class I (KS domain) and class II (CPS domain) terpene synthases identified in higher plants. The subdivision of TPSs into class I and II also describes the way in which the isoprenyl diphosphate substrate is converted to the carbocation intermediate. Class I TPSs ionises

5

the diphosphate substrate while class II creates the intermediate through protonation and scaffold rearrangement without breaking the diphosphate ester bond. The majority of plant TPSs involved in secondary metabolism fall under the class I grouping but there are exceptions to this rule with some diterpene synthases in gymnosperms still having both functional domains (Peters *et al.*, 2000; Jiang *et al.*, 2019).

Based on phylogenetic analysis of full-length TPS protein sequences from gymnosperms and angiosperms, the gene family was divided into seven subfamilies (Bohlmann *et al.*, 1998; Dudareva *et al.*, 2003; Martin *et al.*, 2004; Chen *et al.*, 2011). The initial analysis grouped the TPSs into subfamilies TPS-a, -b, -c, -d, -e and -f (Bohlmann *et al.*, 1998) but Chen *et al.*, (2011) expanded on this analysis with the following two alterations. Inclusion of additional sequences found that TPS-f is derived from TPS-e which resulted in the merging of these two subfamilies. The TPS-e/f subfamily is found in vascular plants and contains KS but also other unique TPSs (Dudareva *et al.*, 1996; Herde *et al.*, 2008; Martin *et al.*, 2010; Chen *et al.*, 2011). Additionally, a new subfamily TPS-h was created containing the TPSs from *Selaginella moellendorffii* which could not be defined as TPS-c or TPS-e/f. Two additional members to subfamily-h were also found in *Marchantia polymorpha* in a more recent analysis of plant genomes (Jiang *et al.*, 2019)*.* TPS-a consists of sesquiterpene synthases and can be further subdivided into TPS-a-1 found in eudicots and TPS-a-2 which is found in monocots. Generally the TPS-a clade is over-represented in monocots and eudicots but in some species, such as *Carica papaya* and *Citrus clementina,* there are no representatives of this subfamily (Jiang *et al.*, 2019). The TPS-b subfamily consists of monoterpene and isoprene synthases from angiosperms, mostly eudicots but TPSs from *Sorghum bicolor* is also represented in this clade. TPS-g is another angiosperm-specific clade which includes mono-, sesqui- and diterpene synthases. Together, the TPS-a, -b and -g subfamilies form the basis of terpene secondary metabolism in angiosperms. Based on the analysis by Chen *et al.*, (2011) the TPS-d subfamily is gymnosperm-specific but an expanded analysis by Jiang *et al.*, (2019) also found this subfamily in *Ananas comosus* (pineapple) and *M. polymorpha* (liverwort). TPSs involved in gymnosperm secondary metabolism are grouped in the TPS-d subfamily with three further subdivisions made within this group (Chen *et al.*, 2011). The bifunctional CPS/KS as well as the monofunctional CPS from land plants are subdivided into TPS-c, based on the hypothesis that TPSs evolved from CPS/KS this subfamily would constitute the root of the phylogenetic tree (Chen *et al.*, 2011).

1.2.3   Creating terpenoid diversity

Metabolite diversity can be achieved through various mechanisms at the DNA, mRNA and protein levels (Schwab, 2003). Although the review by Schwab, (2003) was addressing the discrepancy between the small number of genes compared to the multitude of metabolites produced, the

6

mechanisms discussed serve as a good basis for examining the systems that could be used to achieve terpenoid diversity in plants.

The two events listed in the Schwab (2003) study for increasing metabolite diversity on a DNA level are via gene fusion and alternative open reading frames. Gene fusions are known to occur mostly in prokaryotes but evidence of these mechanisms functioning in plants have been surfacing (Hagel & Facchini, 2017). Gene fusion can enable a single gene to encode a protein with dual enzyme activity (Velayos *et al.*, 2000). A less extreme form of gene fusion, and possibly the evolutionary basis thereof is functional gene clusters, akin to the operons found in bacteria, and has been described for genes involved in plant terpene production (Qi *et al.*, 2004; Wilderman *et al.*, 2004; Shimura *et al.*, 2007; Matsuba *et al.*, 2013; Boycheva *et al.*, 2014). Another method to increase metabolite diversity on the DNA level is alternative open reading frames (alt-ORFs), allowing the overlapping of protein-coding genes. It is a common occurrence in viruses (Mir & Schober, 2014) but has recently been found in bacterial and eukaryotic systems. The alt-ORFs function in a regulatory role, with some encoding proteins with cellular functions (Orr *et al.*, 2020).

An additional event not mentioned in the study by Schwab (2003) is gene duplication, either through whole-genome duplication (WGD), segmental or tandem duplication. Gene duplication has played a significant role in evolution since duplicated genes are freed from their previous function and allowed to have another function, with plants having a much higher rate of gene duplications than other organisms (Zhang, 2003; Taylor & Raes, 2004; Giannuzzi *et al.*, 2011; Panchy *et al.*, 2016; Leebens-Mack *et al.*, 2019). Gene duplication is an important contributor to the expansion of gene families in specialised metabolism (Ober, 2005; Chen *et al.*, 2011; Chae *et al.*, 2014; Tohge & Fernie, 2020). Analysis of the duplicated genes in *Arabidopsis thaliana, Physcomitrella patens* (moss), *Oryza sativa japonica* (rice) and *Populus trichocarpa* (poplar) by Hanada *et al.* (2008) indicated that genes in orthologous groups that underwent tandem duplications tended to be associated with plant response to biotic stress and environmental cues. The stress-responsive genes also displayed a higher retention rate. A higher incidence of tandem duplicates was also observed in genes involved in biotic stress, the possible reason for this being that tandem duplicated genes provide a larger selection of genes which can be used to respond to the constant arms race between host and pathogen than can be provided by non-tandem gene duplications (Hanada *et al.*, 2008). The gene families involved in terpenoid biosynthesis are no exception to the expansive capabilities of gene duplication (Coman *et al.*, 2014; Liu *et al.*, 2016; Ilc *et al.*, 2018; Jiang *et al.*, 2019).

On the level of mRNA, alternative splicing of the pre-mRNA can result in multiple proteins. Alternative splicing in *TPSs* has been identified (Du *et al.*, 2019; Jin *et al.*, 2019) as well as in other secondary

metabolite genes (Qiao *et al.*, 2019) and has also been shown as a method by which *TPS* expression can be affected (Song *et al.*, 2017).

Another important contributor to terpenoid diversity occurs at the protein level. Terpenoid biosynthesis occurs via multiple steps, with each reaction presenting an opportunity for increasing the diversity in compounds being produced. The first step towards terpenoid diversity is the condensation reaction of IPP with DMAPP, catalysed by IDSs. These reactions can occur in a regular (head-to-tail) manner or the C5 isoprene units can be coupled in an irregular fashion, with a total of nine different joining patterns possible (Christianson, 2007; Thulasiram *et al.*, 2007). However, the 1'-4 linkage (head-to-tail) is the most prevalent coupling reaction with the variable lengths of isoprenyl diphosphates catalysed by IDSs in a very product-specific manner (Wang & Ohnuma, 2000; Thulasiram *et al.*, 2007).

These backbone compounds are then utilised by TPSs to produce terpenes. TPSs have been labelled as the "gatekeepers" of terpenoid pathways by Karunanithi and Zerbe (2019), enabling the species-specific biosynthesis of specialised terpenoids. The natural diversity of terpenes can be largely attributed to the many different *TPSs* found. TPSs are responsible for channelling terpenoid biosynthesis to produce the terpene backbone structures, which can then be further modified to produce the multitude of terpenoids found in nature (Dudareva, 2004; Fridman & Pichersky, 2005; Pichersky, 2006; Tholl, 2006; Degenhardt *et al.*, 2009; Martin *et al.*, 2010). According to Sacchettini and Poulter (1997), terpenoid diversity is due to three factors, namely the manner in which the substrate folds within the active site, the method of stabilising the carbocation intermediate, and how the positive charge is quenched at the end of the reaction. An important feature of class I TPSs is the multitude of bond rearrangements that are possible with the carbocation intermediate, this aspect allows for the biosynthesis of multiple terpene products by a single TPS (Chen *et al.*, 2011; Vattekkatte & Boland, 2020).

The terpene scaffold generated by TPSs can then be further modified through various reactions such as oxidation, hydroxylation, peroxidation, methylation, acylation, or glycosylation. These modifications affect the physical properties and may alter their biological activities (Chen *et al.*, 2011; Yonekura-Sakakibara & Hanada, 2011). An important group of enzymes involved in the modifications of plant terpenes is the cytochromes P450 (CYP). The presence of TPS/CYP gene pairs in various plant genomes studied is an indication of the strong relationship between these enzymes (Boutanaev *et al.*, 2015). The CYPs can catalyse various reactions including hydroxylation, oxidations, ring rearrangements and closures. In addition to increasing terpenoid diversity, these modifications also provide starting points for various transferases (Boachon *et al.*, 2015; Bathe & Tissier, 2019). Secondary modification of terpenes produced can also occur, with non-specific

glycosyltransferases being able to metabolise various terpenes to their glycoside form (Schwab, 2003; Yonekura-Sakakibara, 2009). The ability to act on multiple substrates is most likely an important basis for rapid functional divergence of enzymes, a characteristic of specialised metabolism enzymes (Pichersky, 2006).

1.2.4   Role of terpenes in normal plant functioning and plant–environment interaction

Terpenoids can be broadly subdivided into primary and secondary (specialised) metabolites based on the biological role these metabolites play in the plant.

1.2.4.1   Primary terpenoid metabolites

The primary metabolites derived from the terpenoid pathway will be briefly discussed in terms of the biosynthesis thereof as well as the general roles of these metabolites to give context to the importance the two pathways play in plant physiology.

Covalent addition of FPP or GGPP to conserved cysteine residues close to or at the C-terminus of proteins is often used as a method of controlling localisation and activity of the proteins. This type of modification is termed protein prenylation (Casey, 1992; Cox & Der, 1992; Schafer & Rine, 1992; Zhang & Casey, 1996; Wang & Casey, 2016).

Sterols and triterpenes mostly consist of a cyclic structure containing a 1-5 ring system. In plants, the basic structure is synthesised through the conversion of squalene into oxidosqualene by the enzyme squalene epoxidase, followed by the cyclisation reaction catalysed by oxidosqualene cyclase (OSC) to produce (*3S*)-2,3-oxidosqualene. For sterol biosynthesis, the (*3S*)-2,3-oxidosqualene is cyclised to cycloartenol via the chair-boat-chair (CBC) conformation. Sterols are important components of membranes and also play a role in signalling within plants (Kushiro & Ebizuka, 2010; Thimmappa *et al.*, 2014).

Various compounds involved in photosynthesis are produced via the MEP pathway with GGPP as the starting substrate (Schwender *et al.*, 1996; Lichtenthaler *et al.*, 1997; Lichtenthaler, 1999). One of the most well-known compounds in nature is chlorophyll playing the essential role of photosynthetic carbon fixation and which is composed of a chlorin ring, produced via the tetrapyrrole pathway, and an isoprenoid tail which is derived from GGPP (Von Wettstein *et al.*, 1995; Eckhardt *et al.*, 2004; Bollivar, 2006; Kim *et al.*, 2013). Phylloquinones (Vitamin K) consist of a phytyl-diphosphate side-chain, produced through the reduction of GGPP or through chlorophyll hydrolysis, and a naphthoquinone ring produced from chorismite, a product of the shikimate pathway (Basset *et al.*, 2017). Phylloquinones are crucial for photosystem I functioning as these compounds serve as electron carriers (Reumann, 2013).

Carotenoid biosynthesis starts with the formation of phytoene from two GGPP molecules through the enzymatic activity of phytoene synthase (von Lintig *et al.*, 1997). Two major classes of carotenoids are produced from phytoene, namely the carotenes and the xanthophylls (Tanaka *et al.*, 2008). Carotenoids are responsible for the autumn colours of leaves when chlorophyll levels are reduced and give the distinctive colours to fruits such as pumpkin, tomato and oranges. In terms of photosynthesis, carotenoids are required for light collection and photoprotection (Toledo-Ortiz *et al.*, 2010; Ruiz-Sola & Rodríguez-Concepción, 2012).

Various phytohormones are produced via the terpenoid pathway or require a terpenoid sidechain to function. Although the biological roles of these phytohormones are discussed in isolation, these compounds do not function in isolation (Llanes *et al.*; Cox *et al.*, 2004; Loreti *et al.*, 2008; Golldack *et al.*, 2013; Du *et al.*, 2015; Ito *et al.*, 2017; Ahmad *et al.*, 2018).

The polyhydroxylated steroidal brassinosteroids (BRs) are involved in promoting growth in the plant with cell elongation and division, tolerance to stress, differentiation of the vascular system and morphogenesis (both in light and darkness) controlled by these phytohormones (Choe, 2006; Chung & Choe, 2013). Biosynthesis of the different BRs found in nature starts with campesterol (CR), which is produced via various enzymatic steps from squalene (Sakurai, 1999; Chung & Choe, 2013).

Cytokinins are either produced with an aromatic side chain or through the transfer of the isopentenyl moiety from the C_5 terpenoid starting substrate, DMAPP, to adenine (ATP/ADP) at the N^6 position, with the isoprene side chain cytokinins being more widespread in nature. The isoprene side chain can then undergo further modification through hydroxylation in the *cis-* or *trans*-terminal position to form zeatin, with the double-bond of zeatin reduced to form dihydrozeatin [N6-(4-hydroxy-3-methylbutyl)adenine] (Argueso *et al.*, 2009; Frébort *et al.*, 2011). In plants, cytokinins function in various aspects of growth and development, while bacteria such as *Agrobacterium tumefaciens* utilise this phytohormone as a tool to induce uncontrolled cell proliferation (tumour induction) in plants for its own benefit (Sakakibara, 2005; Frébort *et al.*, 2011; Albrecht & Argueso, 2016).

The biosynthesis of gibberellin (GA) starts with the formation of *ent*-Kaurene from the precursor GGPP via the enzymatic activity of *ent*-Copalyl diphosphate synthase (CPS) and *ent*-Kaurene synthase (KS) (van Schie *et al.*, 2012). The *ent*-Kaurene is then oxidised to GA[12]-aldehyde, the general GA precursor for plants, fungi, and bacteria. In higher plants, GA[12]-aldehyde is either further oxidised or first hydroxylated and then oxidised to produce the various forms of GAs found in nature (Salazar-Cerezo *et al.*, 2018). This phytohormone plays an important role throughout the life of a plant, affecting seed germination, stem elongation, mediation of environmental stimuli, flower development as well as seed development (Hedden & Kamiya, 1997).

Abscisic acid (ABA) is a role player in many processes of the plant, including stomatal closure, seed germination, cuticular wax accumulation, bud dormancy and leaf senescence. Generally, ABA is linked to the plant responding to environmental stresses such as a drought (Chen *et al.*, 2020). Biosynthesis of ABA in plants occurs through the cleavage of *cis*-xanthophylls, 9'-*cis*-Neoxanthin and 9'-*cis*-Violaxanthin, by 9'-*cis*-epoxycarotenoid dioxygenases (NCED) (Nambara & Marion-Poll, 2005).

The most recently discovered phytohormone, strigolactones (SLs) are best known for affecting shoot branching but the phytohormone also plays a role in leaf senescence, root architecture and stress response (biotic and abiotic) (Lopez-Obando *et al.*, 2015). Like ABA, SLs are also synthesised via the carotenoid pathway. β-carotene is converted to carlactone (CL) through the enzymatic activity of an isomerase (D27) and the sequential cleavage of 9'-*cis*-β-carotene by two carotenoid cleavage dioxygenases (CCD7 and CCD8) (Lopez-Obando *et al.*, 2015; Saeed *et al.*, 2017).

1.2.4.2 Biological relevance of specialised terpenoids

Specialised terpenoid metabolites have been extensively studied in both model and crop plants, particularly from the perspective of their involvement in plant stress and signalling behaviour. Terpenes with a low molecular weight, such as isoprenes, monoterpenes and sesquiterpenes, form a large part of the volatile organic compounds (VOCs) produced by plants with biological roles which include attracting pollinators, seed disseminators and other beneficial organisms, defence against herbivores and pathogens, as well as in plant-plant communication (Pare & Tumlinson, 1999; Wink, 2003; Arimura *et al.*, 2008; Attaran *et al.*, 2008; Dudareva & Pichersky, 2008; Abbas *et al.*, 2017; Tamiru *et al.*, 2017). These compounds are also involved in mediating plant responses to abiotic stress (Vickers, Gershenzon, *et al.*, 2009; Lee *et al.*, 2015; Korankye *et al.*, 2017).

Hemiterpenes, such as isoprene (2-methyl-1,3-butadiene) and methylbutenol (MBO), are produced in abundance by certain plants through enzymatic activity with the reactions being light- and temperature-dependent (Silver & Fall, 1991; Fisher *et al.*, 2000). Hemiterpenes are not thought to play an important role in plant-herbivore interactions, but caterpillar feeding has been deterred on transgenic tobacco plants emitting isoprene (Laothawornkitkul *et al.*, 2008). Various studies have shown that isoprene plays an important role in biosphere-atmosphere interaction by allowing the plant to recover from a rapid increase in light and temperature, and that it can also protect plants against oxidative damage (Silver & Fall, 1991; Sharkey & Yeh, 2001; Sharkey *et al.*, 2001; Rosenstiel *et al.*, 2002; Behnke *et al.*, 2007; Vickers, Possell, *et al.*, 2009). Although the exact mechanisms with which isoprene protects the plant are not fully understood, it has been shown that isoprene improves thylakoid membrane integrity at high temperatures (Lantz *et al.*, in press; Velikova *et al.*, 2011).

11

Various essential oils, high in monoterpene and sesquiterpene content, have been shown to have antimicrobial activity (Cox *et al.*, 2000; Zeng *et al.*, 2012; Mabrouk *et al.*, 2013; Martins *et al.*, 2013; Sadgrove *et al.*, 2014). Monoterpenes have also been shown to have antifungal against plant pathogenic fungi (Marei *et al.*, 2012). Although these studies did not directly measure antimicrobial or antifungal activity *in planta,* they do indicate the potential role these compounds might have in plants. However, studies have shown direct evidence of the antimicrobial and/or antifungal role of mono or sesquiterpenes in plants (Taniguchi *et al.*, 2014; Yoshitomi *et al.*, 2016; Souleyre *et al.*, 2019). Ectopic expression of a (*S*)-limonene synthase in rice confers increased resistance to the fungus *Magnaporthe oryzae* which is responsible for rice blast disease, while silencing of the *TPS* gene resulted in higher susceptibility to the pathogen (Chen *et al.*, 2018). The expression of various *TPS* genes encoding for mono- and sesquiterpenes is induced with methyl jasmonate (MeJA) treatment, a phytohormone known to be involved in the plant defensive response, which further supports the role many of these compounds play in the plant (Taniguchi *et al.*, 2014; Adal *et al.*, 2017; Muchlinski *et al.*, 2019).

Mono- and sesquiterpenes can also convey plant resistance to insects with the defensive mechanism being either indirect, through recruitment of parasitoids (predators) of the herbivores or through direct deterrence (Turlings *et al.*, 1995; Degenhardt, 2009; Aljbory & Chen, 2018). For example, geraniol has an indirect defence function through the attraction of the natural enemy of an herbivore attacking the plant (Hamachi *et al.*, 2018) and (+)-3-carene, a monoterpene produced in Sitka spruce, is associated with resistance against white pine weevil (Roach *et al.*, 2014), while the sesquiterpenes farnesene and (*E*)-β-caryophyllene have been associated with defence against insect feeding on the plant. (Schnee *et al.*, 2006; Zhuang *et al.*, 2012; Muchlinski *et al.*, 2019). Release of (*E*)-β-caryophyllene from certain lines of maize in response to larvae feeding of the roots attracts an entomopathogenic nematode which preys on these herbivores (Rasmann *et al.*, 2005; Köllner *et al.*, 2008). Silencing of a rice terpene synthase gene resulted in the transgenic plants being vulnerable to aphid attacks (Sun *et al.*, 2017), while caterpillar feeding on *Arabidopsis* increases expression of a terpene synthase gene involved in myrcene biosynthesis, with the herbivore-induced plant volatile profile attracting parasitoids (Van Poecke *et al.*, 2001). Some terpenoid volatiles, like β-ocimene, produced in a plant because of herbivore feeding, have also been shown to elicit a defensive response in neighbouring plants (Arimura *et al.*, 2000). The volatiles produced by plants is a method of communication, sometimes unintended, with other organisms, as can be seen by the attraction of the parasitoid wasp to rice infected by the rice brown planthopper. When the infestation density was either too low or too high, the wasp was not attracted to the infected plant. The proposed reason for this was that the eggs of the parasitoid wasp need a certain amount of food, but the plant also needs to still be alive when the wasps emerge. The volatile profile produced by the plants

differed based on infestation density (Lou *et al.*, 2005). Non-volatile zealexins are acidic sesquiterpenoids which are found across maize species with phytoalexin/antifungal activity and are produced *in planta* at levels which would make these compounds effective phytoalexins (Huffaker *et al.*, 2011). Pesticide application could also have the unwanted effect of reducing the plants' endogenous response to pathogen infestation as described by Yang *et al.* (2012) where (+)-δ-cadinene synthase expression was negatively affected by omethoate (a pesticide) treatment in cotton.

Monoterpene and sesquiterpenes are important components of many flower bouquets, functioning as attractants to pollinators, but also act in defending the flower against florivores (Pichersky & Gershenzon, 2002; Kessler *et al.*, 2013; Muhlemann *et al.*, 2014; Burkle & Runyon, 2017). Pollinators are also able to distinguish between male and female flowers based on the volatile produced by the dimorphic flowers (Ashman *et al.*, 2005). Feeding experiments showed that linalool and β-caryophyllene, mono- and sesquiterpenes frequently found as part of the floral volatile profile, were deterrents to a facultative florivore (Junker *et al.*, 2010). Inhibition of terpenoid production in *Phlox paniculate* resulted in lowering of linalool levels in the flowers and a loss in the plant's ability to repel *Lasius niger* ants, but not in its ability to attract pollinators (Junker *et al.*, 2011). The irregular acyclic homoterpenes, 4,8-dimethylnona-1,3,7-triene (DMNT) and 4,8,12-trim- ethyltrideca-1,3,7,11-tetraene (TMTT), are also associated with indirect defence against herbivores. The compounds are produced through the oxidative degradation of (*E*)-nerolidol and (*E,E*)-geranyl linalool, two sesquiterpenes, through the enzymatic activity of cytochrome P450 monooxygenase (Tholl *et al.*, 2011; Richter *et al.*, 2016).

Diterpenes, being less volatile than mono- and sesquiterpenes, do not generally form part of the VOCs but these compounds have been shown to play a defensive role in conifers where they are a major component of the oleoresin (Keeling & Bohlmann, 2006; Hall *et al.*, 2013), as well as in monocots such as rice and maize, where they are produced in response to pathogen infection (Schmelz *et al.*, 2014) with labdane-related diterpenoids displaying anti-fungal activity in rice (*Oryza sativa*) (Prisic *et al.*, 2004; Peters, 2006). An increase in diterpene synthase gene expression, with the concomitant increase in the terpene produced by the enzyme, was observed in switchgrass (*Panicum virgatum*) following oxidative stress and ultraviolet irradiation treatment (Pelot *et al.*, 2018).

Triterpenoid saponins are synthesised through the cyclisation of 2,3-oxidosqualene by the enzymatic activity of oxidosqualene cyclase (OSC). The 2,3-oxidosqualene is then cyclised to the chair-chair-chair (CCC) conformation, with secondary modifications of the diverse skeletal structure catalysed by cytochrome P450 monooxygenases and uridine diphosphate-dependent glycosyltransferases producing the different saponins found in nature (Haralampidis *et al.*, 2002; Kushiro & Ebizuka, 2010;

13

Sawai & Saito, 2011; Thimmappa *et al.*, 2014). Saponins are mainly associated with plant defence against insects and plant pathogens, stored in the glycosidic form and often located close to the surface for quick release when the plant is attacked (Francis *et al.*, 2002; Sparg *et al.*, 2004; Kuzina *et al.*, 2009; Szakiel *et al.*, 2011).

Modification of terpenes can increase product diversity and is a common method used by plants to switch from non-active to biologically active compounds. For example the volatile sesquiterpene β-selinene is converted to the non-volatile β-costic acid, most likely through the activity of a cytochrome P450 monooxygenase, which has antibiotic activity protecting the maize roots against fungal infection (Ding *et al.*, 2017).

1.2.5   Specialised terpenoids in grapevine

As in other plant species, grapevine produce terpenoid metabolites involved in basic plant physiology and various terpenoid compounds that have specialised functions within the grapevine. A growing body of evidence has confirmed that secondary terpenoids are produced in pathogen defence responses, in response to environmental stresses such as drought as well as due to trophic interactions between the grapevine and insect pests (Hampel *et al.*, 2005; Gil *et al.*, 2012a; Chalal *et al.*, 2015; Schwab & Wüst, 2015; Salvagnin *et al.*, 2016; Savoi *et al.*, 2016). For example, treatment of grapevine leaves with MeJA and sulfated laminarine activated the biosynthesis and/or release of mono- and sesquiterpenes, indicating that these volatile compounds are produced as part of the defence response (Hampel *et al.*, 2005; Chalal *et al.*, 2015; Schwab & Wüst, 2015). Similarly, treatment with UV-B radiation resulted in the accumulation of various terpenoids in grapevine leaves (Gil *et al.*, 2012b), whereas environmental stress, such as drought has been shown to affect the terpenoid pathway in grapevine. Long-term drought conditions lead to increased zeaxanthin levels and various monoterpenes in a white grape cultivar, indicating a possible role for these compounds in drought tolerance (Savoi *et al.*, 2016). Contrary to the above-mentioned defensive role of terpenes, these compounds can also be utilised by pests to find their plant hosts. This knowledge can be exploited as shown in the study by Salvagnin *et al.* (2018), where altering the sesquiterpene ratio in grapevine interfered with the ability of *Lobesia botrana* (European grapevine moth) to find its host.

Although the biological functions of terpenoids in grapevines are being studied, the focus on these compounds has traditionally been on their accumulation in grape berries and their contribution to perceived grape and wine quality impact factors. Mono- and sesquiterpenes are the more odoriferous of the terpene compounds and therefore contribute significantly to the grape aroma and the resulting products made thereof (Wendt & Schulz, 1998; Lukić *et al.*, 2010; May & Wüst, 2012; Slaghenaufi & Ugliano, 2018). Most monoterpenes present in the grape berry are found in the exocarp and occur as odourless glycosides (Lund & Bohlmann, 2006; Bönisch *et al.*, 2014; Liu, Zhu,

et al., 2017). Only monoterpenes in the aglycon-free form (unbound) possess an odorous quality. Winemaking conditions can release the sugar moiety to produce the (unbound) aromatic terpene compounds (Ribéreau-Gayon, Dubourdieu, *et al.*, 2006; Matarese *et al.*, 2013a). Grapevine cultivars can be broadly classified according to the concentration of free monoterpenes found in the grape berry. The floral and sweet aromas characteristic of the aromatic cultivars like Muscat, Riesling and Gewürztraminer are due to higher levels of monoterpenes compared to what is found in more neutral cultivars (Gunata *et al.*, 1985; Ribéreau-Gayon, Glories, *et al.*, 2006; Darriet *et al.*, 2012; Schwab & Wüst, 2015). The aromatic cultivars generally also have a higher ratio of unbound terpene compounds (Ribéreau-Gayon, Dubourdieu, *et al.*, 2006).

Monoterpenes have also been detected in the leaves and roots of grapevine, although much less studied than in the grape berry and wines made from it (Lawo *et al.*, 2011; Chalal *et al.*, 2015). In a study by Wirth *et al.* (2001), the glycoconjugates in the leaves and berries of Shiraz and Muscat of Alexandria were analysed, in both cultivars higher levels of monoterpenes were found in the leaves when compared to the berry, with overall higher levels of monoterpenes found in the leaves and berries of Muscat of Alexandria compared to Shiraz.

Due to their importance in winemaking, the focus has previously always been more on the monoterpenes present the grape berry. However, the relatively recent discovery of rotundone, a sesquiterpene ketone responsible for the characteristic peppery aroma of cool-climate Australian Shiraz wine and the balsamic odour in wines made from Corvina and Corvinone grapes, has initiated significant interest in the grapevine sesquiterpenes (Slaghenaufi & Ugliano, 2018). As with monoterpenes, there has not been an abundance of studies focusing on sesquiterpenes in grapevine organs other than berries. However, there are some studies detailing the localisation of sesquiterpene biosynthesis to the pollen grain of flower from Cabernet Sauvignon (Martin *et al.*, 2009) as well as sesquiterpene profiling in flowers of various cultivars (Smit *et al.*, 2019) and characterisation of sesquiterpene synthases isolated from flower tissue cDNA (Lücker, Bowen, *et al.*, 2004; Smit *et al.*, 2019). The biological roles and importance of these compounds for plant functioning and stress protection provide motivation to study the biosynthesis of the terpenoids (Gil *et al.*, 2012b; Chalal *et al.*, 2015; Salomon *et al.*, 2016).

Another group of compounds derived from the terpenoid pathway that influences grape and wine aroma are the norisoprenoids. These are biosynthesised from carotenoids in the ripening stages of berry development through the enzyme activity of carotenoid cleavage dioxygenases (CCDs) and include volatile compounds such as β-ionone, β-damascenone, TDN (1,1,6-trimethyl-1,2-dihydronaphthalene), TPB (1-(2,3,6-trimethylphenyl)buta-1,3-diene), (Z)-vitispirane and actinidol (Mendes-Pinto, 2009; Keller, 2010; Darriet *et al.*, 2012; Young *et al.*, 2012; Günata, 2013). Many of

15

the these compounds contribute to wine aroma, with odour descriptors associated with some of these compounds being the "cooked apple/floral/quince" aroma of β-damascenone and the "violet/woody/raspberry" aroma of β-ionone, with the specific type of descriptor dependent on the concentration as well as the matrix (Sefton *et al.*, 1993, 1994, 1996; Sefton, 1998; Mendes-Pinto, 2009; Robinson, 2011). These compounds can also sometimes provide cultivar-specific aromas, such as TDN which imparts the characteristic "petroleum" aroma to aged Riesling wine (Darriet *et al.*, 2012).

1.2.6   Difficulties associated with functional characterisation of *IDSs* and *TPSs*

Thousands of organisms have been sequenced but accurate annotation of genes is still a major bottleneck (Bradbury *et al.*, 2013). With the advent of next-generation sequencing technologies, it has become possible to perform genome annotation, gene expression profiling as well as discovery and profiling of small non-coding RNAs of various organisms. Comparative genomics is an important method to analyse the data and involves analysing the genomic context, gene fusions, distribution and co-expression to determine gene function (Bradbury *et al.*, 2013; Grassi *et al.*, 2013; Butler *et al.*, 2017; Khan *et al.*, 2017; Tabidze *et al.*, 2017).

The various other methods used to assign gene function in plants has been reviewed in detail by Abdeeva et al. (2012) with some mentioned in context with the functional characterisation of *IDS* and *TPS* genes. Using homology with annotated genes from other species as an indication of gene function can be used to group genes into families and subfamilies but requires supportive analyses, especially in the case of *GGPSs* and *TPSs* genes which have been shown to belong to extended gene families (Coman *et al.*, 2014) with sequence similarity not necessarily indicating a similar product profile. Generally this method is used as a first step towards terpenoid pathway gene annotation, where predicted genes are aligned (BLAST) against the protein sequences of previously characterised terpenoid pathway genes (Martin *et al.*, 2010). Characteristic motifs are also identified to further support classification of the gene of interest (Aubourg *et al.*, 2002; Martin *et al.*, 2010; Coman *et al.*, 2014).

Gene-targeted mutagenesis, which generally involves loss-of-function mutagenesis or gene silencing, is not always suitable for genes that belong to gene families where redundancy can prevent an observable phenotype. The suitability of this method for *IDSs* and *TPSs* is therefore limited since a large portion of plant genes are part of gene families (Panchy *et al.*, 2016) with *TPS* genes having undergone multiple gene duplication events which have resulted in an expanded gene family (Martin *et al.*, 2010). This method is also not suitable for genes involved in crucial pathways required in early development. Since terpene synthase expression can be organ and/or developmental stage specific the use of gene silencing to determine gene function is not a feasible

16

option. However, gene silencing was successfully utilised in the study by Jassbi *et al.* (2008) to determine the role of 17-hydroxygeranyllinalool diterpenoid glycosides (HGL-DTGs) in *Nicotiana attenuata.* RNA interference has also been used to study the defensive roles of two *TPS* genes in *Solanum lycopersicon* (tomato) (Coppola *et al.*, 2018).

The gain-of-function approach involves either increasing expression of endogenous genes or expressing the genes in a heterologous system. Within this approach, various methods can be utilised. Generally, this method is suitable for genes belonging to an extended gene family since a single gene can be over-expressed with the resulting phenotype attributed to this gene without interference from other family members. This method is often used for terpenoid pathway genes, especially *TPS* genes (Martin *et al.*, 2010). This technique (both homologous and heterologous expression) was used by Salvagnin *et al.* (2018) to alter the scent ratio produced by grapevine, with the resulting effect this had on European grapevine moth behaviour then being studied.

Characterisation of *TPSs* through molecular cloning and heterologous expression methods is made difficult since the specialised function of these enzymes mean that gene expression is often restricted to certain specialised cells, developmental stages or in response to external/environmental cues. Isolation of mRNA therefore needs to be done using tissue known to have high terpene content, at a time where terpene production is increased, or terpene synthase expression should be induced. However, the problem with all these methods is that prior knowledge is required and there is a likelihood that some TPSs will be overlooked (Bohlmann *et al.*, 1998).

Connecting the terpenoid compounds produced in a plant to specific genes can be a challenging task since determining terpene synthase gene function based solely on sequence homology is not possible as only a few nucleotide differences can alter the product profile. An example of this type of variation can be seen with the functional characterisation of the gene encoding for the VviGuaS enzyme which catalyses the reaction that produces α-guaiene, the precursor to rotundone biosynthesis. It was shown that this gene is an allele of the *VviTPS24* gene with two nucleotide substitutions resulting in the gene encoding for a VvGuaS in the Shiraz cultivar instead of the Selinene synthase encoded for in the Pinot noir cultivar (Drew *et al.*, 2016). Functional characterisation of terpene synthase genes in specific cultivars and not only on a species level is therefore necessary to elucidate gene function. This sequence variation is also an example of the genetic diversity within the *Vitis* species which can form the basis for the phenotypic variation seen between cultivars (Martinez-Zapater *et al.*, 2010). It is likely that the TPS gene family could be over-represented in cultivars known for their high terpene content, such as the Muscat cultivars, as shown for the polyphenol biosynthesis gene family in the Tannat cultivar (Da Silva *et al.*, 2013). Other obstacles in functional characterisation of TPS-encoding genes is that they are not constitutively

expressed, making the isolation of transcripts from cDNA problematic; many terpene synthases are also able to catalyse the biosynthesis of multiple terpene compound and can sometimes accept more than one type of prenyl diphosphate as substrate (Martin *et al.*, 2010). Terpenes are also inherently unstable, the method used to analyse the terpene products can have a significant impact on the results, as was shown in a study to try and characterise the gene responsible for the characteristic terpin-4-ol found in *Melaleuca alternifolia* (Shelton *et al.*, 2004). Even the choice of the heterologous expression system can affect the product profile and hinder the functional characterisation of a gene (Fischer *et al.*, 2013).

Functional characterisation of a gene also needs to consider the localisation of the enzyme and the gene expression profile. In *Arabidopsis thaliana*, twelve paralogous geranylgeranyl diphosphate synthase (*GGPS*) genes were identified (Lange & Ghassemian, 2003). Some of these genes are likely to be pseudogenes, but 10 of the GGPS isozymes have been shown to produce GGPP. Even though all of these enzymes produce the same terpenoid branchpoint substrate the function of the enzymes differs based on their localisation within the cell and their expression pattern (Ruiz-Sola, Coman, *et al.*, 2016). The significance of compartmentalisation in functional characterisation could bring into question the accuracy of using microbial systems for functional annotation of genes (Schwab, 2003). However, transgenic plants could also be negatively affected by the ectopic expression of terpenoid pathway genes, especially if expressed under the control of a strong constitutive promoter. An example of this was the susceptibility of a transgenic *Nicotiana tabacum* population overexpressing a geraniol synthase-encoding gene to cold and heat stress (Hamachi *et al.*, 2018).

The main disadvantage with using a bacterial system is the additional steps required for enzyme purification or extensive pathway manipulation necessary for adequate production of GPP and FPP *in vivo*. These steps are mostly unnecessary when using a yeast system, although some pathway manipulation might still be required. The advantage of using a plant system is the endogenous availability of GPP and FPP, although it does not always offer a null background, making functional characterisation of terpene synthases more complicated. The study by Fischer *et al.*, (2013) compared monoterpene production in various systems using a geraniol synthase (GES) isolated from *Ocimum basilicum* as the indicator TPS. Based on the results, *Vitis vinifera* and *Nicotiana benthamiana* were deemed as the better systems in terms of monoterpene accumulation compared to *Arabidopsis thaliana.* However, it was observed that the monoterpene profile can differ among the microbial and various plant systems, which begs the question of which system is better to most accurately determine the terpene profile that a specific TPS catalyses.

In order to obtain the most accurate results during functional characterisation the use of a homologous system is preferential (Jelly *et al.*, 2014). In grapevine, stable transformation is possible but it is a time consuming process with random gene insertion events requiring a large population for functional genomic studies (Vidal *et al.*, 2010). An alternative is the use of transient expression, with various methods developed including cell suspension cultures, somatic embryos, leaves or whole plantlets (Jelly *et al.*, 2014).

Benefits of using biolistics instead of *Agrobacterium* for transformation are the relative ease of using the system and the simplified plasmid construction with the possibility to eliminate plasmid DNA insertion sequence. Compared to *Agrobacterium*-mediated transformation, it is also easier to co-transform with multiple transgenes when using a biolistic system (Vidal *et al.*, 2006). However gene transfer efficiency is lower, the cost associated with this technology is higher, and gene silencing due to multiple gene insertions is more prevalent than is found with *Agrobacterium*-mediated transformation (Vidal *et al.*, 2010).

1.2.7 Knowledge gained and what is still unknown

Following the two Pinot noir genome projects, various transcriptome and genome studies were undertaken in grapevine (Jaillon *et al.*, 2007; Velasco *et al.*, 2007). The availability of a reference genome has enabled more comprehensive transcriptome studies such as the NimbleGen-based gene atlas, numerous RNAseq studies with particular focus on the grape berry, and an analysis of alternative splicing (Zenoni *et al.*, 2010; Fasoli *et al.*, 2012; Dal Santo *et al.*, 2013; Degu *et al.*, 2014; Vitulo *et al.*, 2014; Kelloniemi *et al.*, 2015; du Plessis *et al.*, 2017). Genome studies included an exploration of the diversity within the species, a reference-based genome sequence assembly of the grape cultivar Tannat and a *de novo* approach to assemble the genome sequence of the Thompson seedless table grape cultivar (Giannuzzi *et al.*, 2011; Da Silva *et al.*, 2013; Di Genova *et al.*, 2014; Cardone *et al.*, 2016). Recently, advances in the assembly of heterozygous genomes assisted in the sequencing and assembly of *V. vinifera* cv. Cabernet sauvignon (Chin *et al.*, 2016; Minio *et al.*, 2017). In addition, Myles *et al.* (2010) recommended a stronger focus on whole genome sequencing in order to link genome wide association (GWA) mapping and genomic selection (GS) since usage of single nucleotide polymorphism (SNP) array for GWA in grapevine is an unsuitable method as the species as undergone rapid linkage disequilibrium (LD) decay.

However there is still a large gap between the functional characterisation of the genes and those annotated in the genome (Martinez-Zapater *et al.*, 2010). The *TPS* gene annotation study by (Martin *et al.*, 2010) included a large-scale functional characterisation of some of the *TPS* genes, utilising *in vitro* and *in vivo* methods with *Escherichia coli* as the heterologous expression system. Thirty-nine of the putative *VvTPSs* sequences isolated from Gewürztraminer, Pinot noir, and Cabernet

19

sauvignon grapevine cultivars were functionally characterised in terms of enzyme activity. Various other studies have also endeavoured to functionally characterise grapevine TPSs and connecting traits observed to specific genes (Lücker, Bowen, *et al.*, 2004; Martin & Bohlmann, 2004; Matarese *et al.*, 2013b, 2014; Drew *et al.*, 2016). Nevertheless, there are still many uncharacterised TPS-encoding genes playing a role in plant defence, diversity between cultivars and potentially contributing to grape and wine character. Linking characterised VviTPSs to specific traits found in grapes and wine can be exploited during grapevine crop improvement (Velasco *et al.*, 2007; Degenhardt *et al.*, 2009; Martinez-Zapater *et al.*, 2010; Gray *et al.*, 2014).

1.2.7.1 Grapevine terpenoid gene family

The economic importance of grapevine as well as its potential to be utilised as a model organism for woody perennial fruit species, supported the genome sequencing studies undertaken of this crop (Velasco *et al.*, 2007). In 2007, two genome sequencing projects of *V. vinifera* Pinot noir were published. While Velasco et al. (2007) undertook to sequence the ENTAV 115 Pinot noir clone, the heterozygous nature of the grapevine genome made contig assembly difficult. The selection of the highly homozygous PN40024 Pinot noir clone by Jaillon et al. (2007) for sequencing overcame some of the difficulties associated with the high genome heterozygosity. Even though these two grapevine genome sequences contain gaps, possibly missing large sections of repetitive sequences, they provide the basis on which to analyse specific gene sequences and the biological functions thereof as well as giving an understanding of the genetic potential of grapevine (Martinez-Zapater *et al.*, 2010; Minio *et al.*, 2017).

A similar situation is seen in grapevine where segmental duplications (SD) were predominantly observed in genes involved biosynthesis of compounds required for plant–environment interactions (Giannuzzi *et al.*, 2011). Due to the high plasticity associated with secondary metabolite genes, *TPS* genes are continuously evolving, whereby minimal genetic changes can alter the amino acid sequence of TPSs thereby changing the product profile of a terpene synthase (Lesburg *et al.*, 1998; Hyatt & Croteau, 2005; Tholl, 2006; Hartmann, 2007). Many terpene synthases are also able to catalyse the production of multiple terpenes, which further increases terpene diversity (Shimada *et al.*, 2004; Xie *et al.*, 2012).

With the exception of two *Eucalyptus* species, grapevine has the largest *TPS* gene family when compared to other annotated plant genomes indicating the importance of terpenoids in the grapevine (Külheim *et al.*, 2015; Butler *et al.*, 2018). Annotation of the Pinot noir PN40042 genome revealed that the terpene synthase (*TPS*) gene family is highly represented, with a predicted 89 functional *TPSs* and 27 pseudogenes, with gene duplication and diversification as the most likely cause of the expanded gene family (Jaillon *et al.*, 2007). Re-annotation by Martin *et al.* (2010) adapted the

number to 69 putatively functional *TPS* genes, 20 partial genes and 63 pseudogenes. Phylogenetic analysis indicated the existence of species-specific gene clusters but also of a few orthologous genes which have likely maintained gene function throughout speciation events. Sequence analysis showed an expanded *TPS-a* subfamily with genes grouped under this subfamily generally encoding for sesquiterpene and sometimes diterpene synthases involved in secondary metabolism. The *TPS-g* subfamily, known to encode for acyclic monoterpene synthases, was also shown to be extensive compared to *Arabidopsis* (Martin *et al.*, 2010).

1.2.8   Conclusion

Terpenoids have various roles within plants, ranging from primary to specialised metabolites. Within grapevine these compounds have been shown to have various defensive roles as well as contributing to wine aroma. The basis of terpenoid diversity is the extended gene families associated with the biosynthesis of these compounds. The *IDS* and *TPS* gene families have undergone extensive expansion throughout plant evolution with gene duplication and subsequent sub- and neo-functionalisation attributed as an important factor in this expansion. Understanding function of the genes involved in creating the terpenoid diversity seen in nature requires an integrated approach that needs to be tailored to specific genes.

1.3   Rationale, scope, and aims of the study

Linking terpenoid compounds to specific genes is difficult in general and particularly complicated with the terpene synthase genes. The expanded TPS gene family in grapevine combined with the significant cultivar diversity observed within the species supports the need to functionally characterise these genes. Functional characterisation of terpenoid pathway genes requires a holistic approach of combining the results obtained from various methods, with an understanding of the limitations of each, in order to build a sound hypothesis of the functions of the various genes in the plant.

1.3.1   Specific research aims

The aim of this study was the functional characterisation of a selection of grapevine terpenoid genes. This study benefited from previous work in the Institute for Wine Biotechnology (IWBT) that lead to the isolation of multiple grapevine terpenoid genes. The isolated genes were analysed in terms of their sequence and the predicted enzymes and subcellular localisation are shown in **Figure 1.1**. Functional complementation in *Escherichia coli* was done for genes putatively encoding for DXS, IDI, GGPS, FPS and HMGS. However, only IDI and GGPS could be shown to be functional (Young, 2004). Stable transgenic plant populations were established for some of the isolated genes, these being *VviGGPS, VviIDI* and two *VviTPSs.* Initial phenotypic characterisation of the parental *Nicotiana*

21

tabacum VviGGPS transgene population showed a severe aberrant leaf and flower phenotype. These early observations lead to a full genotypic characterisation of the *VviGGPS* transgene plant population.

Prior work formed the basis of the aim to target important branchpoint genes in the pathway, as well as the terpene synthases that would convert the various branchpoint substrates into terpenes. The predicted enzymes encoded by the genes targeted are indicated by the blue blocks in **Figure 1.1**. The genes targeted included *VviGPS*, *VviFPS* and *VviGGPS*, encoding three branchpoint enzymes which catalyses the biosynthesis of the three prenyl diphosphates GPP, FPP and GGPP. In addition, *VviTPS27, VviTPS39, VviTPS41* and *VviTPS44* encoding for putative terpene synthases were included.

The approach for this study was to utilise the current knowledge, as briefly discussed in the introduction, to expand on the available information for the selected genes. This included *in silico* analysis of the available grapevine genome annotations, the gene atlas, and other gene expression platforms to contextualise the functional analysis that were pursued. For the functional analysis, heterologous gene expression was used to generate terpenoid products which could be analysed. A yeast expression system has the advantages of having a null background for terpene synthases but still being able to produce geranyl diphosphate (GPP) as an intermediate to farnesyl diphosphate (FPP) via the MVA pathway. The precursors for mono- and sesquiterpene synthesis are therefore available and this system does not require excessive pathway manipulation (Asadollahi *et al.*, 2008; Herrero *et al.*, 2008). Previous studies have successfully utilised *Saccharomyces cerevisiae* for plant terpene synthase expression, which supports the use of this system in this study *(Herrero et al. 2008; Rico et al. 2010; Siddiqui et al.* 2012; Xie *et al.* 2012).

The yeast system was used to determine gene functionality while transient expression in a plant system was included for some of the genes to support the functional characterisation done in a yeast. A comparison of the terpenes produced by a yeast and plant system as well as the benefits and shortcoming of each system were evaluated. Although heterologous expression in a yeast system and transient expression in a plant system is useful to establish whether the targeted gene functions in terpenoid production and allows the profiling and quantification of the terpenoids in a direct strategy, these systems do not provide information on the functional impact of the gene and the terpenoids produced on the plant. A study of plants stably expressing terpenoid genes would add valuable information regarding the regulation of terpenoid production as well as possible functions of these enzymes within the plant (Aharoni *et al.*, 2003, Kappers *et al.*, 2005, Lücker *et al.*, 2012). For this purpose, the analysis of the available transgenic tobacco population overexpressing the

VviGGPS gene was included in the study. To attain the aims of this study the following research objectives are summarised in Figure 1.2:
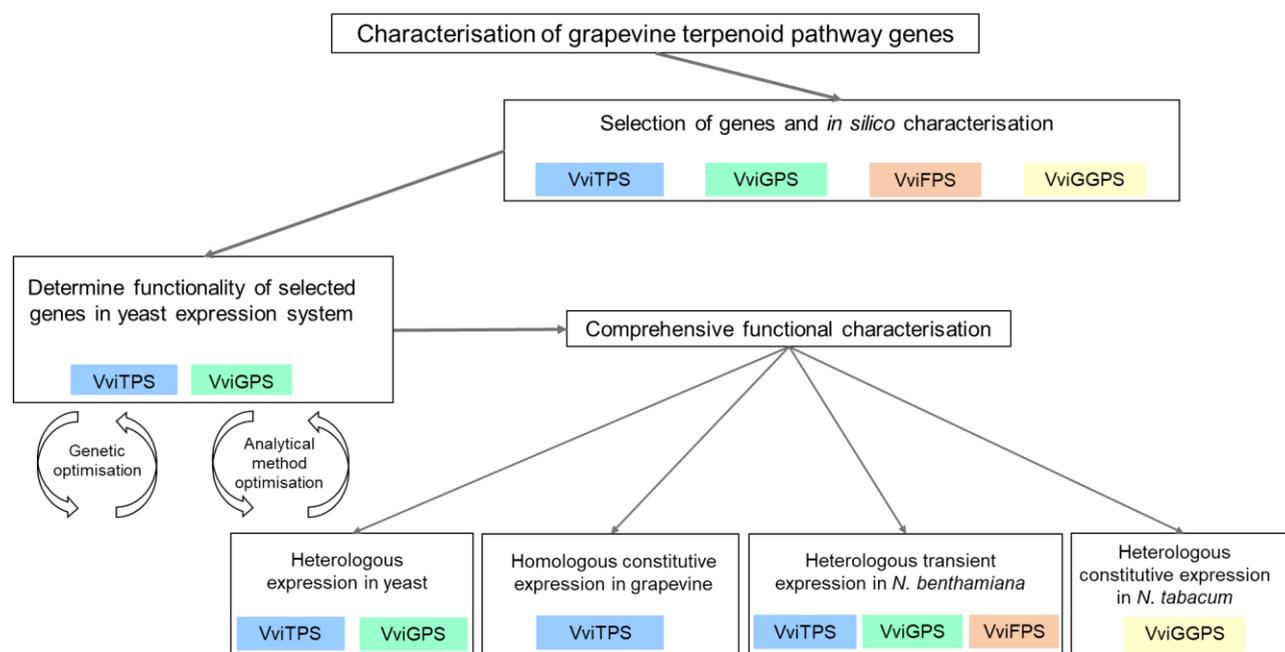
Figure 1.2 Diagrammatic representation of the genes studied, and the methodology used to functionally characterise the genes.

1.3.1.1   Objective 1: In silico analysis of the cDNA sequences of the selected genes, as well as the predicted amino acid sequence

The analysis included characteristic motif identification, prediction of cell localisation, protein modelling as well as comparison to previously characterised terpenoid pathway genes to putatively assign gene function. In addition, the cDNA sequences were used to construct an expression profile using available transcriptomic datasets to further contextualise possible gene function.

1.3.1.2   Objective 2: Heterologous expression of selected genes in a yeast expression system and analysis of the product profile

Since the yeast expression system needed to be established for the functional characterisation of terpenoid genes, this objective also included some optimisation steps with a focus on increasing the substrate available for heterologous terpenoid biosynthesis as well as the methods used to analyse the terpenoids. The optimised yeast expression system was used to determine whether the genes being studied are functional and to assign gene function.

1.3.1.3 Objective 3: Heterologous expression of selected genes in a plant expression system

This objective tied in with the previous Objective 2 whereby selected terpenoid genes were expressed in a plant system with the resulting terpenoid profile compared to the results obtained from the yeast system.

1.3.1.4 Objective 4: In-depth analysis of a model plant (Nicotiana tabacum) population over-expressing a grapevine terpenoid branchpoint gene (VviGGPS)

This objective dealt with the question of how altering the expression of the selected branchpoint terpenoid pathway gene in a model plant affected the population phenotype? The transgene plant population was phenotypically characterised under various growth conditions in comparison to the control plants. The phenotypic evaluation included general observation of vegetative and reproductive organ development and morphology as well as physiological analysis targeting photosynthetic parameters, given that various compounds involved in photosynthesis are terpenoids (**Figure 1.1**). The lines were also be subjected to chemotypic characterisation to complement the phenotypic description and physiological analysis.

The results obtained from the completing the above objectives enabled a better understanding of the biological role the various terpenoid pathway genes play in grapevine. Assigning a specific function to an isolated gene will also assist in future efforts to improve grapevine as an economically important crop.

1.4 References

Abbas, F., Ke, Y., Yu, R., Yue, Y., Amanullah, S., Jahangir, M.M. & Fan, Y., (2017). Volatile terpenoids: multiple functions, biosynthesis, modulation and manipulation by genetic engineering *Planta* **246**, 5, 803–816.

Abdeeva, I., Abdeev, R., Bruskin, S. & Piruzi, E., (2012). Transgenic Plants as a Tool for Plant Functional Genomics In: Transgenic Plants - Adv. Limitations. InTech.

Adal, A.M., Sarker, L.S., Lemke, A.D. & Mahmoud, S.S., (2017). Isolation and functional characterization of a methyl jasmonate-responsive 3-carene synthase from Lavandula x intermedia *Plant Mol. Biol.* **93**, 6, 641–657.

Aharoni, A., Giri, A.P., Deuerlein, S., Griepink, F., De Kogel, W.-J.J., Verstappen, F.W.A.A., Verhoeven, H.A., Jongsma, M.A., Schwab, W. & Bouwmeester, H.J., (2003). Terpenoid Metabolism in Wild-Type and Transgenic Arabidopsis Plants *Plant Cell* **15**, December, 2866–2884.

Ahmad, F., Singh, A. & Kamal, A., (2018). Crosstalk of brassinosteroids with other phytohormones under various abiotic stresses *J. Appl. Biol. Biotechnol.* **6**, 1, 56–62.

Akhtar, T.A., Matsuba, Y., Schauvinhold, I., Yu, G., Lees, H.A., Klein, S.E. & Pichersky, E., (2013). The tomato cis-prenyltransferase gene family *Plant J.* **73**, 4, 640–652.

Albrecht, T. & Argueso, C.T., (2016). Should I fight or should I grow now? The role of cytokinins in plant growth and immunity and in the growth–defence trade-off *Ann. Bot.* (November, 17), mcw211.

Aljbory, Z. & Chen, M., (2018). Indirect plant defense against insect herbivores: a review *Insect Sci.* **25**, 1, 2–23.

Argueso, C.T., Ferreira, F.J. & Kieber, J.J., (2009). Environmental perception avenues: The interaction of cytokinin and environmental response pathways *Plant, Cell Environ.* **32**, 9, 1147–1160.

Arimura, G., Ozawa, R., Shimoda, T., Nishioka, T., Boland, W. & Takabayashi, J., (2000). Herbivory-induced volatiles elicit defence genes in lima bean leaves *Nature* **406**, 6795, 512–515.

Arimura, G.I., Garms, S., Maffei, M., Bossi, S., Schulze, B., Leitner, M., Mithöfer, A. & Boland, W., (2008).

Herbivore-induced terpenoid emission in Medicago truncatula: Concerted action of jasmonate, ethylene and calcium signaling *Planta* **227**, 2, 453–464.

Asadollahi, M.A., Maury, J., Møller, K., Nielsen, K.F., Schalk, M., Clark, A. & Nielsen, J., (2008). Production of Plant Sesquiterpenes in Saccharomyces cerevisiae: Effect of ERG9 Repression on Sesquiterpene Biosynthesis *Biotechnol. Bioeng.* **99**, 3, 666–677.

Ashman, T.-L., Bradburn, M., Cole, D.H., Blaney, B.H. & Raguso, R.A., (2005). The Scent of a Male: The Role of Floral Volatiles in Pollination of a Gender Dimorphic Plant *Ecology* **86**, 8, 2099–2105.

Attaran, E., Rostás, M. & Zeier, J., (2008). *Pseudomonas syringae* Elicits Emission of the Terpenoid (E,E)-4,8,12-Trimethyl-1,3,7,11-Tridecatetraene in *Arabidopsis* Leaves Via Jasmonate Signaling and Expression of the Terpene Synthase TPS4 *Mol. Plant-Microbe Interact.* **21**, 11, 1482–1497.

Aubourg, S., Lecharny, a & Bohlmann, J., (2002). Genomic analysis of the terpenoid synthase (AtTPS) gene family of Arabidopsis thaliana. *Mol. Genet. Genomics* **267**, 6, 730–45.

Basset, G.J., Latimer, S., Fatihi, A., Soubeyrand, E. & Block, A., (2017). Phylloquinone (Vitamin K1): Occurrence, Biosynthesis and Functions *Mini-Reviews Med. Chem.* **17**, 12.

Bathe, U. & Tissier, A., (2019). Cytochrome P450 enzymes: A driving force of plant diterpene diversity *Phytochemistry* October.

Behnke, K., Ehlting, B., Teuber, M., Bauerfeind, M., Louis, S., Hänsch, R., Polle, A., Bohlmann, J. & Schnitzler, J.P., (2007). Transgenic, non-isoprene emitting poplars don't like it hot *Plant J.* **51**, 3, 485–499.

Beran, F., Rahfeld, P., Luck, K., Nagel, R., Vogel, H., Wielsch, N., Irmisch, S., Ramasamy, S., Gershenzon, J., Heckel, D.G. & Köllner, T.G., (2016). Novel family of terpene synthases evolved from trans-isoprenyl diphosphate synthases in a flea beetle *Proc. Natl. Acad. Sci. U. S. A.* **113**, 11, 2922–2927.

Bick, J.A. & Lange, B.M., (2003). Metabolic cross talk between cytosolic and plastidial pathways of isoprenoid biosynthesis: unidirectional transport of intermediates across the chloroplast envelope membrane *Arch. Biochem. Biophys.* **415**, 2, 146–154.

Boachon, B., Junker, R.R., Miesch, L., Bassard, J.E., Hofer, R., Caillieaudeaux, R., Seidel, D.E., Lesot, A., Heinrich, C., Ginglinger, J.F., Allouche, L., Vincent, B., Wahyuni, D.S., Paetz, C., Beran, F., Miesch, M., Schneider, B., Leiss, K. & Werck-Reichhart, D., (2015). CYP76C1 (Cytochrome P450)-Mediated Linalool Metabolism and the Formation of Volatile and Soluble Linalool Oxides in Arabidopsis Flowers: A Strategy for Defense against Floral Antagonists. Vol. 27.

Bohlmann, J., Meyer-Gauen, G. & Croteau, R., (1998). Plant terpenoid synthases: molecular biology and phylogenetic analysis. *Proc. Natl. Acad. Sci. U. S. A.* **95**, 8, 4126–33.

Bollivar, D.W., (2006). Recent advances in chlorophyll biosynthesis *Photosynth. Res.* **89**, 3.

Bönisch, F., Frotscher, J., Stanitzek, S., Rühl, E., Wüst, M., Bitz, O., Schwab, W., Products, N., München, T.U. & Germany, F.B., (2014). Activity-Based Profiling of a Physiologic Aglycone Library Reveals Sugar Acceptor Promiscuity of Family 1 UDP-Glucosyltransferases from Grape *Plant Physiol.* **166**, 1, 23–39.

Boucher, Y. & Doolittle, W.F., (2000). The role of lateral gene transfer in the evolution of isoprenoid biosynthesis pathways. *Mol. Microbiol.* **37**, 4, 703–16.

Boutanaev, A.M., Moses, T., Zi, J., Nelson, D.R., Mugford, S.T., Peters, R.J., Osbourn, A., Reuben, J., Osbourn, A., Peters, R.J. & Osbourn, A., (2015). Investigation of terpene diversification across multiple sequenced plant genomes *Proc. Natl. Acad. Sci.* **112**, 1, 1–8.

Boycheva, S., Daviet, L., Wolfender, J.-L. & Fitzpatrick, T.B., (2014). The rise of operon-like gene clusters in plants *Trends Plant Sci.* (February), 1–13.

Bradbury, L.M.T., Niehaus, T.D. & Hanson, A.D., (2013). Comparative genomics approaches to understanding and manipulating plant metabolism *Curr. Opin. Biotechnol.* **24**, 2, 278–284.

Burkle, L.A. & Runyon, J.B., (2017). The Smell of Environmental Change: Using Floral Scent to Explain Shifts in Pollinator Attraction *Appl. Plant Sci.* **5**, 6, 1600123.

Butler, J.B., Vaillancourt, R.E., Potts, B.M., Lee, D.J., King, G.J., Baten, A., Shepherd, M. & Freeman, J.S., (2017). Comparative genomics of Eucalyptus and Corymbia reveals low rates of genome structural rearrangement *BMC Genomics* **18**, 1, 397.

Butler, J.B., Freeman, J.S., Potts, B.M., Vaillancourt, R.E., Grattapaglia, D., Silva-Junior, O.B., Simmons, B.A., Healey, A.L., Schmutz, J., Barry, K.W., Lee, D.J., Henry, R.J., King, G.J., Baten, A. & Shepherd, M., (2018). Annotation of the Corymbia terpene synthase gene family shows broad conservation but dynamic evolution of physical clusters relative to Eucalyptus *Heredity (Edinb).* **121**, 1, 87–104.

Cardone, M.F., D'Addabbo, P., Alkan, C., Bergamini, C., Catacchio, C.R., Anaclerio, F., Chiatante, G., Marra, A., Giannuzzi, G., Perniola, R., Ventura, M. & Antonacci, D., (2016). Inter-varietal structural variation in grapevine genomes *Plant J.* **88**, 4, 648–661.

Casey, P.J., (1992). Biochemistry of protein prenylation *J. Lipid Res.* **33**, 12, 1731–1740.

Chae, L., Kim, T., Nilo-Poyanco, R. & Rhee, S.Y., (2014). Genomic Signatures of Specialized Metabolism in

25

Plants *Science (80-.).* **344**, 6183, 510–513.

Chalal, M., Winkler, J.B., Gourrat, K., Trouvelot, S., Adrian, M., Schnitzler, J.-P., Jamois, F. & Daire, X., (2015). Sesquiterpene volatile organic compounds (VOCs) are markers of elicitation by sulfated laminarine in grapevine *Front. Plant Sci.* **6**, May, 1–9.

Chen, A., Dale Poulter, C. & Kroon, P. a, (1994). Isoprenyl diphosphate synthases: Protein sequence comparisons, a phylogenetic tree, and predictions of secondary structure *Protein Sci.* **3**, 4, 600–607.

Chen, F., Tholl, D., Bohlmann, J. & Pichersky, E., (2011). The family of terpene synthases in plants: a mid-size family of genes for specialized metabolism that is highly diversified throughout the kingdom. *Plant J.* **66**, 1, 212–29.

Chen, K., Li, G., Bressan, R.A., Song, C., Zhu, J. & Zhao, Y., (2020). Abscisic acid dynamics, signaling, and functions in plants *J. Integr. Plant Biol.* **62**, 1, 25–54.

Chen, X., Chen, H., Yuan, J.S., Köllner, T.G., Chen, Y., Guo, Y., Zhuang, X., Chen, X., Zhang, Y. jun, Fu, J., Nebenführ, A., Guo, Z. & Chen, F., (2018). The rice terpene synthase gene OsTPS19 functions as an (S)-limonene synthase in planta, and its overexpression leads to enhanced resistance to the blast fungus Magnaporthe oryzae *Plant Biotechnol. J.* **16**, 10, 1778–1787.

Chin, C.S., Peluso, P., Sedlazeck, F.J., Nattestad, M., Concepcion, G.T., Clum, A., Dunn, C., O'Malley, R., Figueroa-Balderas, R., Morales-Cruz, A., Cramer, G.R., Delledonne, M., Luo, C., Ecker, J.R., Cantu, D., Rank, D.R. & Schatz, M.C., (2016). Phased diploid genome assembly with single-molecule real-time sequencing *Nat. Methods* **13**, 12, 1050–1054.

Choe, S., (2006). Brassinosteroid biosynthesis and inactivation *Physiol. Plant.* **126**, 4, 539–548.

Christianson, D.W., (2007). CHEMISTRY: Roots of Biosynthetic Diversity *Science (80-.).* **316**, 5821, 60–61.

Christianson, D.W., (2017). Structural and Chemical Biology of Terpenoid Cyclases *Chem. Rev.* **117**, 17, 11570–11648.

Chung, Y. & Choe, S., (2013). The Regulation of Brassinosteroid Biosynthesis in Arabidopsis *CRC. Crit. Rev. Plant Sci.* **32**, 6, 396–410.

Coman, D., Altenhoff, A., Zoller, S., Gruissem, W. & Vranová, E., (2014). Distinct evolutionary strategies in the GGPPS family from plants. *Front. Plant Sci.* **5**, May, 230.

Coppola, M., Cascone, P., Bossi, S., Corrado, G., Garonna, A., Maffei, M., Rao, R. & Guerrieri, E., (2018). TPS Genes Silencing Alters Constitutive Indirect and Direct Defense in Tomato *Int. J. Mol. Sci.* **19**, 9.

Cox, A.D. & Der, C.J., (1992). Protein prenylation: more than just glue? *Curr. Opin. Cell Biol.* **4**, 6, 1008–1016.

Cox, M.C.H., Benschop, J.J., Vreeburg, R.A.M., Wagemaker, C.A.M., Moritz, T., Peeters, A.J.M. & Voesenek, L.A.C.J., (2004). The roles of ethylene, auxin, abscisic acid, and gibberellin in the hyponastic growth of submerged Rumex palustris petioles. *Plant Physiol.* **136**, 2, 2948–60; discussion 3001.

Cox, S.D., Mann, C.M., Markham, J.L., Bell, H.C., Gustafson, J.E., Warmington, J.R. & Wyllie, S.G., (2000). The mode of antimicrobial action of the essential oil of Melaleuca alternifolia (tea tree oil). *J. Appl. Microbiol.* **88**, 1, 170–5.

Dagan, T., Artzy-Randrup, Y. & Martin, W., (2008). Modular networks and cumulative impact of lateral transfer in prokaryote genome evolution *Proc. Natl. Acad. Sci. U. S. A.* **105**, 29, 10039–10044.

Dal Santo, S., Tornielli, G.B., Zenoni, S., Fasoli, M., Farina, L., Anesi, A., Guzzo, F., Delledonne, M., Pezzotti, M., Santo, S.D., Tornielli, G.B., Zenoni, S., Fasoli, M., Farina, L., Anesi, A., Guzzo, F., Delledonne, M. & Pezzotti, M., (2013). The plasticity of the grapevine berry transcriptome. *Genome Biol.* **14**, 6, r54.

Darriet, P., Thibon, C. & Dubourdieu, D., (2012). Aroma and Aroma Precursors in Grape Berry In: Biochem. Grape Berry. 111–136.

Degenhardt, J., (2009). Indirect defense responses to herbivory in grasses *Plant Physiol.* **149**, 1, 96–102.

Degenhardt, J., Köllner, T.G. & Gershenzon, J., (2009). Monoterpene and sesquiterpene synthases and the origin of terpene skeletal diversity in plants. *Phytochemistry* **70**, 15–16, 1621–37.

Degu, A., Hochberg, U., Sikron, N., Venturini, L., Buson, G., Ghan, R., Plaschkes, I., Batushansky, A., Chalifa-Caspi, V., Mattivi, F., Delledonne, M., Pezzotti, M., Rachmilevitch, S., Cramer, G.R. & Fait, A., (2014). Metabolite and transcript profiling of berry skin during fruit development elucidates differential regulation between Cabernet Sauvignon and Shiraz cultivars at branching points in the polyphenol pathway. *BMC Plant Biol.* **14**, 1, 188.

Ding, Y., Huffaker, A., Köllner, T.G., Weckwerth, P., Robert, C.A.M., Spencer, J.L., Lipka, A.E. & Schmelz, E.A., (2017). Selinene Volatiles Are Essential Precursors for Maize Defense Promoting Fungal Pathogen Resistance *Plant Physiol.* **175**, 3, 1455–1468.

Drew, D.P., Andersen, T.B., Sweetman, C., Møller, B.L., Ford, C. & Simonsen, H.T., (2016). Two key polymorphisms in a newly discovered allele of the Vitis vinifera TPS24 gene are responsible for the production of the rotundone precursor α-guaiene *J. Exp. Bot.* **67**, 3, 799–808.

Du, F., Wang, T., Fan, J., Liu, Z., Zong, J., Fan, W., Han, Y. & Grierson, D., (2019). Volatile composition and

classification of Lilium flower aroma types and identification, polymorphisms, and alternative splicing of their monoterpene synthase genes *Hortic. Res.* **6**, 1, 110.

Du, H., Chang, Y., Huang, F. & Xiong, L., (2015). GID1 modulates stomatal response and submergence tolerance involving abscisic acid and gibberellic acid signaling in rice *J. Integr. Plant Biol.* **57**, 11, 954–968.

Dudareva, N., (2004). Biochemistry of Plant Volatiles *PLANT Physiol.* **135**, 4, 1893–1902.

Dudareva, N. & Pichersky, E., (2008). Metabolic engineering of plant volatiles *Curr. Opin. Biotechnol.* **19**, 2, 181–189.

Dudareva, N., Cseke, L., Blanc, V.M. & Pichersky, E., (1996). Evolution of floral scent in Clarkia: novel patterns of S-linalool synthase gene expression in the C. breweri flower. *Plant Cell* **8**, 7, 1137–1148.

Dudareva, N., Martin, D., Kish, C.M., Kolosova, N., Gorenstein, N., Fäldt, J., Miller, B. & Bohlmann, J., (2003). (E)-B-Ocimene and Myrcene Synthase Genes of Floral Scent Biosynthesis in Snapdragon : Function and Expression of Three Terpene Synthase Genes of a New Terpene Synthase Subfamily *Plant Cell* **15**, May, 1227–1241.

Dudareva, N., Negre, F., Nagegowda, D. a. & Orlova, I., (2006). Plant Volatiles: Recent Advances and Future Perspectives *CRC. Crit. Rev. Plant Sci.* **25**, 5, 417–440.

Eckhardt, U., Grimm, B. & Hörtensteiner, S., (2004). Recent advances in chlorophyll biosynthesis and breakdown in higher plants *Plant Mol. Biol.* **56**, 1, 1–14.

Fasoli, M., Dal Santo, S., Zenoni, S., Tornielli, G.B., Farina, L., Zamboni, A., Porceddu, A., Venturini, L., Bicego, M., Murino, V., Ferrarini, A., Delledonne, M. & Pezzotti, M., (2012). The Grapevine Expression Atlas Reveals a Deep Transcriptome Shift Driving the Entire Plant into a Maturation Program *Plant Cell* **24**, 9, 3489–3505.

Fischer, M.J.C., Meyer, S., Claudel, P., Perrin, M., Ginglinger, J.F., Gertz, C., Masson, J.E., Werck-Reinhardt, D., Hugueney, P. & Karst, F., (2013). Specificity of Ocimum basilicum geraniol synthase modified by its expression in different heterologous systems. *J. Biotechnol.* **163**, 1, 24–9.

Fisher, A.J., Baker, B.M., Greenberg, J.P. & Fall, R., (2000). Enzymatic Synthesis of Methylbutenol from Dimethylallyl Diphosphate in Needles of Pinus sabiniana *Arch. Biochem. Biophys.* **383**, 1, 128–134.

Francis, G., Kerem, Z., Makkar, H.P.S. & Becker, K., (2002). The biological action of saponins in animal systems: a review *Br. J. Nutr.* **88**, 6, 587–605.

Frébort, I., Kowalska, M., Hluska, T., Frébortová, J. & Galuszka, P., (2011). Evolution of cytokinin biosynthesis and degradation *J. Exp. Bot.* **62**, 8, 2431–2452.

Fridman, E. & Pichersky, E., (2005). Metabolomics, genomics, proteomics, and the identification of enzymes and their substrates and products. *Curr. Opin. Plant Biol.* **8**, 3, 242–8.

Di Genova, A., Almeida, A., Muñoz-Espinoza, C., Vizoso, P., Travisany, D., Moraga, C., Pinto, M., Hinrichsen, P., Orellana, A. & Maass, A., (2014). Whole genome comparison between table and wine grapes reveals a comprehensive catalog of structural variants *BMC Plant Biol.* **14**, 1, 7.

Giannuzzi, G., D'Addabbo, P., Gasparro, M., Martinelli, M., Carelli, F.N., Antonacci, D. & Ventura, M., (2011). Analysis of high-identity segmental duplications in the grapevine genome *BMC Genomics* **12**.

Gil, M., Pontin, M., Berli, F., Bottini, R. & Piccoli, P., (2012a). Metabolism of terpenes in the response of grape (Vitis vinifera L.) leaf tissues to UV-B radiation *Phytochemistry* **77**, 89–98.

Gil, M., Pontin, M., Berli, F., Bottini, R. & Piccoli, P., (2012b). Metabolism of terpenes in the response of grape (Vitis vinifera L.) leaf tissues to UV-B radiation *Phytochemistry* **77**, 89–98.

Gilg, A.B., Tittiger, C. & Blomquist, G.J., (2009). Unique animal prenyltransferase with monoterpene synthase activity *Naturwissenschaften* **96**, 6, 731–735.

Golldack, D., Li, C., Mohan, H. & Probst, N., (2013). Gibberellins and abscisic acid signal crosstalk: Living and developing under unfavorable conditions *Plant Cell Rep.* **32**, 7, 1007–1016.

Grassi, S., Piro, G., Lee, J.M., Zheng, Y., Fei, Z., Dalessandro, G., Giovannoni, J.J. & Lenucci, M.S., (2013). Comparative genomics reveals candidate carotenoid pathway regulators of ripening watermelon fruit. *BMC Genomics* **14**, November 2013, 781.

Gray, D.J., Li, Z.T. & Dhekney, S.A., (2014). Precision breeding of grapevine (Vitis vinifera L.) for improved traits *Plant Sci.* **228**, 3–10.

Green, S., Friel, E.N., Matich, A., Beuning, L.L., Cooney, J.M., Rowan, D.D. & MacRae, E., (2007). Unusual features of a recombinant apple α-farnesene synthase *Phytochemistry* **68**, 2, 176–188.

Gunata, Y.Z.Z., Bayonove, C.L.L., Baumes, R.L.L. & Cordonnier, R.E.E., (1985). The aroma of grapes. Extraction and determination of free and glycosidically bound fractions of some grape aroma components *J. Chromatogr.* **331**, 83–90.

Günata, Z., (2013). Biosynthesis of C13-norisoprenoids in vitis vinifera: Evidence of carotenoid cleavage dioxygenase (ccd) and secondary transformation of norisoprenoid compounds *ACS Symp. Ser.* **1134**, i,

97–107.

Hagel, J.M. & Facchini, P.J., (2017). Tying the knot: Occurrence and possible significance of gene fusions in plant metabolism and beyond *J. Exp. Bot.* **68**, 15, 4029–4043.

Hall, D.E., Zerbe, P., Jancsik, S., Quesada, A.L., Dullat, H., Madilao, L.L., Yuen, M. & Bohlmann, J., (2013). Evolution of Conifer Diterpene Synthases: Diterpene Resin Acid Biosynthesis in Lodgepole Pine and Jack Pine Involves Monofunctional and Bifunctional Diterpene Synthases *Plant Physiol.* **161**, 2, 600–616.

Hamachi, A., Nisihara, M., Saito, S., Rim, H., Takahashi, H., Islam, M., Uemura, T., Ohnishi, T., Ozawa, R., Maffei, M.E. & Arimura, G., (2018). Overexpression of geraniol synthase induces heat stress susceptibility in Nicotiana tabacum *Planta* 0123456789.

Hampel, D., Mosandl, A. & Wüst, M., (2005). Induction of de Novo Volatile Terpene Biosynthesis via Cytosolic and Plastidial Pathways by Methyl Jasmonate in Foliage of Vitis vinifera L. *J. Agric. Food Chem.* **53**, 7, 2652–2657.

Hanada, K., Zou, C., Lehti-Shiu, M.D., Shinozaki, K. & Shiu, S.-H.H., (2008). Importance of lineage-specific expansion of plant tandem duplicates in the adaptive response to environmental stimuli *Plant Physiol.* **148**, 2, 993–1003.

Haralampidis, K., Trojanowska, M. & Osbourn, A.E., (2002). Biosynthesis of Triterpenoid Saponins in Plants In: Adv. Biochem. Eng. Biotechnol. Vol. 75 31–49.

Hartmann, T., (2007). From waste products to ecochemicals: Fifty years research of plant secondary metabolism *Phytochemistry* **68**, 22–24, 2831–2846.

Hedden, P. & Kamiya, Y., (1997). GIBBERELLIN BIOSYNTHESIS: Enzymes, Genes and Their Regulation *Annu. Rev. Plant Physiol. Plant Mol. Biol.* **48**, 1, 431–460.

Hemmerlin, A., Hoeffler, J.-F., Meyer, O., Tritsch, D., Kagan, I. a, Grosdemange-Billiard, C., Rohmer, M. & Bach, T.J., (2003). Cross-talk between the cytosolic mevalonate and the plastidial methylerythritol phosphate pathways in tobacco bright yellow-2 cells. *J. Biol. Chem.* **278**, 29, 26666–76.

Hemmerlin, A., Harwood, J.L. & Bach, T.J., (2012). A raison d'être for two distinct pathways in the early steps of plant isoprenoid biosynthesis? *Prog. Lipid Res.* **51**, 2, 95–148.

Herde, M., Gärtner, K., Köllner, T.G., Fode, B., Boland, W., Gershenzon, J., Gatz, C. & Tholl, D., (2008). Identification and regulation of TPS04/GES, an Arabidopsis geranyllinalool synthase catalyzing the first step in the formation of the insect-induced volatile C16-homoterpene TMTT *Plant Cell* **20**, 4, 1152–1168.

Herrero, O., Ramón, D., Orejas, M., Ramo, D. & Ã, M.O., (2008). Engineering the Saccharomyces cerevisiae isoprenoid pathway for de novo production of aromatic monoterpenes in wine. *Metab. Eng.* **10**, 2, 78–86.

Huffaker, A., Kaplan, F., Vaughan, M.M., Dafoe, N.J., Ni, X., Rocca, J.R., Alborn, H.T., Teal, P.E.A. & Schmelz, E.A., (2011). Novel acidic sesquiterpenoids constitute a dominant class of pathogen-induced phytoalexins in maize *Plant Physiol.* **156**, 4, 2082–2097.

Hyatt, D.C. & Croteau, R., (2005). Mutational analysis of a monoterpene synthase reaction: altered catalysis through directed mutagenesis of (-)-pinene synthase from Abies grandis. *Arch. Biochem. Biophys.* **439**, 2, 222–33.

Ilc, T., Arista, G., Tavares, R., Navrot, N., Duchêne, E., Velt, A., Choulet, F., Paux, E., Fischer, M., Nelson, D.R., Hugueney, P., Werck-Reichhart, D. & Rustenholz, C., (2018). Annotation, classification, genomic organization and expression of the Vitis vinifera CYPome *PLoS One* **13**, 6, 1–22.

Ito, S., Yamagami, D., Umehara, M., Hanada, A., Yoshida, S., Sasaki, Y., Yajima, S., Kyozuka, J., Ueguchi-Tanaka, M., Matsuoka, M., Shirasu, K., Yamaguchi, S. & Asami, T., (2017). Regulation of strigolactone biosynthesis by gibberellin signaling *Plant Physiol.* **174**, 2, 1250–1259.

Jaillon, O., Aury, J.-M., Noel, B., Policriti, A., Clepet, C., Casagrande, A., Choisne, N., Aubourg, S., Vitulo, N., Jubin, C., Vezzi, A., Legeai, F., Hugueney, P., Dasilva, C., Horner, D., Mica, E., Jublot, D., Poulain, J., Bruyère, C., Billault, A., Segurens, B., Gouyvenoux, M., Ugarte, E., Cattonaro, F., Anthouard, V., Vico, V., Del Fabbro, C., Alaux, M., Di Gaspero, G., Dumas, V., Felice, N., Paillard, S., Juman, I., Moroldo, M., Scalabrin, S., Canaguier, A., Le Clainche, I., Malacrida, G., Durand, E., Pesole, G., Laucou, V., Chatelet, P., Merdinoglu, D., Delledonne, M., Pezzotti, M., Lecharny, A., Scarpelli, C., Artiguenave, F., Pè, M.E., Valle, G., Morgante, M., Caboche, M., Adam-Blondon, A.-F., Weissenbach, J., Quétier, F. & Wincker, P., (2007). The grapevine genome sequence suggests ancestral hexaploidization in major angiosperm phyla. *Nature* **449**, 7161, 463–7.

Jassbi, A.R., Gase, K., Hettenhausen, C., Schmidt, A. & Baldwin, I.T., (2008). Silencing geranylgeranyl diphosphate synthase in Nicotiana attenuata dramatically impairs resistance to tobacco hornworm *Plant Physiol.* **146**, 3, 974–986.

Jelly, N.S., Valat, L., Walter, B. & Maillot, P., (2014). Transient expression assays in grapevine: A step towards genetic improvement *Plant Biotechnol. J.* **12**, 9, 1231–1245.

Jia, Q. & Chen, F., (2016). Catalytic Functions of the Isoprenyl Diphosphate Synthase Superfamily in Plants:

28

A Growing Repertoire *Mol. Plant* **9**, 2, 189–191.

Jiang, S.Y., Jin, J., Sarojam, R. & Ramachandran, S., (2019). A Comprehensive Survey on the Terpene Synthase Gene Family Provides New Insight into Its Evolutionary Patterns *Genome Biol. Evol.* **11**, 8, 2078–2098.

Jin, B., Guo, J., Tang, J., Tong, Y., Ma, Y., Chen, T., Wang, Y., Shen, Y., Zhao, Y., Lai, C., Cui, G. & Huang, L., (2019). An alternative splicing alters the product outcome of a class I terpene synthase in Isodon rubescens *Biochem. Biophys. Res. Commun.* **512**, 2, 310–313.

Junker, R.R., Heidinger, I.M.M. & Blüthgen, N., (2010). Floral Scent Terpenoids Deter the Facultative Florivore Metrioptera bicolor (Ensifera, Tettigoniidae, Decticinae) *J. Orthoptera Res.* **19**, 1, 69–74.

Junker, R.R., Gershenzon, J. & Unsicker, S.B., (2011). Floral Odor Bouquet Loses its Ant Repellent Properties After Inhibition of Terpene Biosynthesis *J. Chem. Ecol.* **37**, 12, 1323–1331.

Kappers, I.F., Aharoni, A., van Herpen, T.W.J.M., Luckerhoff, L.L.P., Dicke, M. & Bouwmeester, H.J., (2005). Genetic engineering of terpenoid metabolism attracts bodyguards to Arabidopsis. *Science* **309**, 5743, 2070–2.

Karunanithi, P.S. & Zerbe, P., (2019). Terpene Synthases as Metabolic Gatekeepers in the Evolution of Plant Terpenoid Chemical Diversity *Front. Plant Sci.* **10**, October, 1–23.

Keeling, C.I. & Bohlmann, J., (2006). Diterpene resin acids in conifers. *Phytochemistry* **67**, 22, 2415–23.

Keeling, C.I., Dullat, H.K., Yuen, M., Ralph, S.G., Jancsik, S. & Bohlmann, J., (2010). Identification and functional characterization of monofunctional ent-copalyl diphosphate and ent-kaurene synthases in white spruce reveal different patterns for diterpene synthase evolution for primary and secondary metabolism in gymnosperms *Plant Physiol.* **152**, 3, 1197–1208.

Keller, M., (2010). Developmental Physiology In: M. Keller (ed). Sci. Grapevines Anat. Physiol. (1st ed.). Elsevier Inc. 169–225.

Kelloniemi, J., Trouvelot, S., Héloir, M.-C., Simon, A., Dalmais, B., Frettinger, P., Cimerman, A., Fermaud, M., Roudet, J., Baulande, S., Bruel, C., Choquer, M., Couvelard, L., Duthieuw, M., Ferrarini, A., Flors, V., Le Pêcheur, P., Loisel, E., Morgant, G., Poussereau, N., Pradier, J.-M., Rascle, C., Trdá, L., Poinssot, B. & Viaud, M., (2015). Analysis of the Molecular Dialogue Between Gray Mold (Botrytis cinerea) and Grapevine (Vitis vinifera) Reveals a Clear Shift in Defense Mechanisms During Berry Ripening *Mol. Plant-Microbe Interact.* **28**, 11, 1167–1180.

Kessler, D., Diezel, C., Clark, D.G., Colquhoun, T.A. & Baldwin, I.T., (2013). Petunia flowers solve the defence/apparency dilemma of pollinator attraction by deploying complex floral blends *Ecol. Lett.* **16**, 3, 299–306.

Khan, S., Upadhyay, S., Khan, F., Tandon, S., Shukla, R.K., Ghosh, S., Gupta, V., Banerjee, S. & ur Rahman, L., (2017). Comparative transcriptome analysis reveals candidate genes for the biosynthesis of natural insecticide in Tanacetum cinerariifolium *BMC Genomics* **18**, 1, 54.

Kim, S., Schlicke, H., Van Ree, K., Karvonen, K., Subramaniam, A., Richter, A., Grimm, B. & Braam, J., (2013). Arabidopsis chlorophyll biosynthesis: An essential balance between the methylerythritol phosphate and tetrapyrrole pathways *Plant Cell* **25**, 12, 4984–4993.

Köllner, T.G., Held, M., Lenk, C., Hiltpold, I., Turlings, T.C.J., Gershenzon, J. & Degenhardta, J., (2008). A maize (E)-β-caryophyllene synthase implicated in indirect defense responses against herbivores is not expressed in most American maize varieties *Plant Cell* **20**, 2, 482–494.

Korankye, E.A., Lada, R., Asiedu, S. & Caldwell, C., (2017). Plant Senescence: The Role of Volatile Terpene Compounds (VTCs) *Am. J. Plant Sci.* **08**, 12, 3120–3139.

Külheim, C., Padovan, A., Hefer, C., Krause, S.T., Köllner, T.G., Myburg, A.A., Degenhardt, J. & Foley, W.J., (2015). The Eucalyptus terpene synthase gene family. *BMC Genomics* **16**, 1, 450.

Kushiro, T. & Ebizuka, Y., (2010). Triterpenes In: Compr. Nat. Prod. II. Elsevier 673–708.

Kuzina, V., Ekstrøm, C.T., Andersen, S.B., Nielsen, J.K., Olsen, C.E. & Bak, S., (2009). Identification of defense compounds in barbarea vulgaris against the herbivore phyllotreta nemorum by an ecometabolomic approach *Plant Physiol.* **151**, 4, 1977–1990.

Lancaster, J., Lehner, B., Khrimian, A., Muchlinski, A., Luck, K., Köllner, T.G., Weber, D.C., Gundersen-Rindal, D.E. & Tholl, D., (2018). An IDS-Type Sesquiterpene Synthase Produces the Pheromone Precursor (Z)-α-Bisabolene in Nezara viridula *J. Chem. Ecol.* Tholl 2015.

Lange, B.M. & Ghassemian, M., (2003). Genome organization in Arabidopsis thaliana: a survey for genes involved in isoprenoid and chlorophyll metabolism. *Plant Mol. Biol.* **51**, 6, 925–48.

Lantz, A.T., Allman, J., Weraduwage, S.M. & Sharkey, T.D., (in press). Control of rate and physiological role of isoprene emission from plants *Plant. Cell Environ.* July, pce.13629.

Laothawornkitkul, J., Paul, N.D., Vickers, C.E., Possell, M., Taylor, J.E., Mullineaux, P.M. & Hewitt, C.N., (2008). Isoprene emissions influence herbivore feeding decisions *Plant, Cell Environ.* **31**, 10, 1410–1415.

Lawo, N.C., Weingart, G.J.F., Schuhmacher, R. & Forneck, A., (2011). The volatile metabolome of grapevine roots: First insights into the metabolic response upon phylloxera attack *Plant Physiol. Biochem.* **49**, 9, 1059–1063.

Lee, G.W., Lee, S., Chung, M.-S., Jeong, Y.S. & Chung, B.Y., (2015). Rice terpene synthase 20 (OsTPS20) plays an important role in producing terpene volatiles in response to abiotic stresses *Protoplasma* **252**, 4, 997–1007.

Leebens-Mack, J.H., Barker, M.S., Carpenter, E.J., Deyholos, M.K., Gitzendanner, M.A., Graham, S.W., Grosse, I., Li, Z., Melkonian, M., Mirarab, S., Porsch, M., Quint, M., Rensing, S.A., Soltis, D.E., Soltis, P.S., Stevenson, D.W., Ullrich, K.K., Wickett, N.J., DeGironimo, L., Edger, P.P., Jordon-Thaden, I.E., Joya, S., Liu, T., Melkonian, B., Miles, N.W., Pokorny, L., Quigley, C., Thomas, P., Villarreal, J.C., Augustin, M.M., Barrett, M.D., Baucom, R.S., Beerling, D.J., Benstein, R.M., Biffin, E., Brockington, S.F., Burge, D.O., Burris, J.N., Burris, K.P., Burtet-Sarramegna, V., Caicedo, A.L., Cannon, S.B., Çebi, Z., Chang, Y., Chater, C., Cheeseman, J.M., Chen, T., Clarke, N.D., Clayton, H., Covshoff, S., Crandall-Stotler, B.J., Cross, H., dePamphilis, C.W., Der, J.P., Determann, R., Dickson, R.C., Di Stilio, V.S., Ellis, S., Fast, E., Feja, N., Field, K.J., Filatov, D.A., Finnegan, P.M., Floyd, S.K., Fogliani, B., García, N., Gâteblé, G., Godden, G.T., Goh, F. (Qi Y., Greiner, S., Harkess, A., Heaney, J.M., Helliwell, K.E., Heyduk, K., Hibberd, J.M., Hodel, R.G.J., Hollingsworth, P.M., Johnson, M.T.J., Jost, R., Joyce, B., Kapralov, M. V., Kazamia, E., Kellogg, E.A., Koch, M.A., Von Konrat, M., Könyves, K., Kutchan, T.M., Lam, V., Larsson, A., Leitch, A.R., Lentz, R., Li, F.W., Lowe, A.J., Ludwig, M., Manos, P.S., Mavrodiev, E., McCormick, M.K., McKain, M., McLellan, T., McNeal, J.R., Miller, R.E., Nelson, M.N., Peng, Y., Ralph, P., Real, D., Riggins, C.W., Ruhsam, M., Sage, R.F., Sakai, A.K., Scascitella, M., Schilling, E.E., Schlösser, E.M., Sederoff, H., Servick, S., Sessa, E.B., Shaw, A.J., Shaw, S.W., Sigel, E.M., Skema, C., Smith, A.G., Smithson, A., Stewart, C.N., Stinchcombe, J.R., Szövényi, P., Tate, J.A., Tiebel, H., Trapnell, D., Villegente, M., Wang, C.N., Weller, S.G., Wenzel, M., Weststrand, S., Westwood, J.H., Whigham, D.F., Wu, S., Wulff, A.S., Yang, Y., Zhu, D., Zhuang, C., Zuidof, J., Chase, M.W., Pires, J.C., Rothfels, C.J., Yu, J., Chen, C., Chen, L., Cheng, S., Li, J., Li, R., Li, X., Lu, H., Ou, Y., Sun, X., Tan, X., Tang, J., Tian, Z., Wang, F., Wang, J., Wei, X., Xu, X., Yan, Z., Yang, F., Zhong, X., Zhou, F., Zhu, Y., Zhang, Y., Ayyampalayam, S., Barkman, T.J., Nguyen, N. phuong, Matasci, N., Nelson, D.R., Sayyari, E., Wafula, E.K., Walls, R.L., Warnow, T., An, H., Arrigo, N., Baniaga, A.E., Galuska, S., Jorgensen, S.A., Kidder, T.I., Kong, H., Lu-Irving, P., Marx, H.E., Qi, X., Reardon, C.R., Sutherland, B.L., Tiley, G.P., Welles, S.R., Yu, R., Zhan, S., Gramzow, L., Theißen, G. & Wong, G.K.S., (2019). One thousand plant transcriptomes and the phylogenomics of green plants *Nature* **574**, 7780, 679–685.

Lesburg, C. a., Caruthers, J.M., Paschall, C.M. & Christianson, D.W., (1998). Managing and manipulating carbocations in biology: Terpenoid cyclase structure and mechanism *Curr. Opin. Struct. Biol.* **8**, 6, 695–703.

Liang, P.H., Ko, T.P. & Wang, A.H.J., (2002). Structure, mechanism and function of prenyltransferases *Eur. J. Biochem.* **269**, 14, 3339–3354.

Lichtenthaler, H.K., (1999). The 1-Deoxy-D-Xylulose-5-Phosphate Pathway of Isoprenoid Biosynthesis in Plants *Annu. Rev. Plant Physiol. Plant Mol. Biol.* **50**, 1, 47–65.

Lichtenthaler, H.K., Schwender, J., Disch, a & Rohmer, M., (1997). Biosynthesis of isoprenoids in higher plant chloroplasts proceeds via a mevalonate-independent pathway. *FEBS Lett.* **400**, 3, 271–4.

von Lintig, J., Welsch, R., Bonk, M., Giuliano, G., Batschauer, A. & Kleinig, H., (1997). Light-dependent regulation of carotenoid biosynthesis occurs at the level of phytoene synthase expression and is mediated by phytochrome in Sinapis alba and Arabidopsis thaliana seedlings. *Plant J.* **12**, 3, 625–34.

Liu, J., Zhu, X.-L., Ullah, N. & Tao, Y.-S., (2017). Aroma Glycosides in Grapes and Wine *J. Food Sci.* **82**, 2, 248–259.

Liu, Y., Luo, S., Schmidt, A., Wang, G., Sun, G.-L., Grant, M., Kuang, C., Yang, M.-J., Jing, S.-X., Li, C.-H., Schneider, B., Gershenzon, J. & Li, S.-H., (2016). A Geranylfarnesyl Diphosphate Synthase Provides the Precursor for Sesterterpenoid (C 25) Formation in the Glandular Trichomes of the Mint Species Leucosceptrum canum *Plant Cell* **28**, 3, 804–822.

Llanes, A., Varela, C. & Luna, V., Crosstalk between gibberellins and abscisic acid under drought and salinity.

Lombard, J. & Moreira, D., (2011). Origins and early evolution of the mevalonate pathway of isoprenoid biosynthesis in the three domains of life *Mol. Biol. Evol.* **28**, 1, 87–99.

Lopez-Obando, M., Ligerot, Y., Bonhomme, S., Boyer, F.D. & Rameau, C., (2015). Strigolactone biosynthesis and signaling in plant development *Dev.* **142**, 21, 3615–3619.

Loreti, E., Povero, G., Novi, G., Solfanelli, C., Alpi, A. & Perata, P., (2008). Gibberellins, jasmonate and abscisic acid modulate the sucrose-induced expression of anthocyanin biosynthetic genes in Arabidopsis *New Phytol.* **179**, 4, 1004–1016.

Lou, Y.G., Ma, B. & Cheng, J.A., (2005). Attraction of the parasitoid Anagrus nilaparvatae to rice volatiles induced by the rice brown planthopper Nilaparvata lugens *J. Chem. Ecol.* **31**, 10, 2357–2372.

Lücker, J., Bowen, P. & Bohlmann, J., (2004). Vitis vinifera terpenoid cyclases: functional identification of two sesquiterpene synthase cDNAs encoding (+)-valencene synthase and (−)-germacrene D synthase and expression of mono- and sesquiterpene synthases in grapevine flowers and berries *Phytochemistry* **65**, 19, 2649–2659.

Lücker, J., Schwab, W., Hautum, B. Van, Blaas, J., Der, L.H.W. Van, Bouwmeester, H.J., Verhoeven, H.A., Liickerl, J., Schwab, W., Hautum, B. Van, Blaas, J. & Plas, L.H.W. Van Der, (2004). Increased and Altered Fragrance of Tobacco Plants after Metabolic Engineering Using Three Monoterpene Synthases from Lemon *Plant Physiol.* **134**, 1, 510–519.

Lukić, I., Miličević, B., Banović, M., Tomas, S., Radeka, S. & Peršurić, Đ., (2010). Characterization and Differentiation of Monovarietal Grape Marc Distillates on the Basis of Varietal Aroma Compound Composition *J. Agric. Food Chem.* **58**, 12, 7351–7360.

Lund, S.T. & Bohlmann, J., (2006). The Molecular Basis for Wine Grape Quality-A Volatile Subject *Science (80-.).* **311**, 5762, 804–805.

Mabrouk, S., Salah, K.B.H., Elaissi, A., Jlaiel, L., Jannet, H. Ben, Aouni, M. & Harzallah-Skhiri, F., (2013). Chemical Composition and Antimicrobial and Allelopathic Activity of Tunisian *Conyza sumatrensis* (Retz .) E. Walker Essential Oils *Chem. Biodivers.* **10**, 2, 209–223.

Marei, G.I.K., Abdel Rasoul, M. a. & Abdelgaleil, S. a. M., (2012). Comparative antifungal activities and biochemical effects of monoterpenes on plant pathogenic fungi *Pestic. Biochem. Physiol.* **103**, 1, 56–61.

Martin, D.M. & Bohlmann, J., (2004). Identification of Vitis vinifera (-)-alpha-terpineol synthase by in silico screening of full-length cDNA ESTs and functional characterization of recombinant terpene synthase. *Phytochemistry* **65**, 9, 1223–9.

Martin, D.M., Fäldt, J. & Bohlmann, J., (2004). Functional characterization of nine Norway spruce TPS genes and evolution of gymnosperm terpene synthases of the TPS-d subfamily *Plant Physiol.* **135**, 4, 1908–1927.

Martin, D.M., Toub, O., Chiang, A., Lo, B.C., Ohse, S., Lund, S.T. & Bohlmann, J., (2009). The bouquet of grapevine (Vitis vinifera L. cv. Cabernet Sauvignon) flowers arises from the biosynthesis of sesquiterpene volatiles in pollen grains. *Proc. Natl. Acad. Sci. U. S. A.* **106**, 17, 7245–50.

Martin, D.M., Aubourg, S., Schouwey, M.B., Daviet, L., Schalk, M., Toub, O., Lund, S.T. & Bohlmann, J., (2010). Functional annotation, genome organization and phylogeny of the grapevine (Vitis vinifera) terpene synthase gene family based on genome assembly, FLcDNA cloning, and enzyme assays. *BMC Plant Biol.* **10**, 1, 226.

Martinez-Zapater, J., Carmona, M., Diaz-Riquelme, J., Fernandez, L. & Lijavetzky, D., (2010). Grapevine genetics after the genome sequence: Challenges and limitations *Aust. J. Grape Wine Res.* **16**, 33–46.

Martins, M.D.R., Arantes, S., Candeias, F., Teresa Tinoco, M. & Cruz-Morais, J., (2013). Antioxidant, antimicrobial and toxicological properties of Schinus molle L. essential oils. *J. Ethnopharmacol.* (November, 11), 1–8.

Matarese, F., Scalabrelli, G. & D'Onofrio, C., (2013a). Analysis of the expression of terpene synthase genes in relation to aroma content in two aromatic Vitis vinifera varieties *Funct. Plant Biol.* **40**, 6, 552.

Matarese, F., Scalabrelli, G. & D'Onofrio, C., (2013b). Analysis of the expression of terpene synthase genes in relation to aroma content in two aromatic Vitis vinifera varieties *Funct. Plant Biol.* **40**, 6, 552–565.

Matarese, F., Cuzzola, A., Scalabrelli, G. & D'Onofrio, C., (2014). Expression of terpene synthase genes associated with the formation of volatiles in different organs of Vitis vinifera *Phytochemistry* **105**, 12–24.

Matsuba, Y., Nguyen, T.T.H., Wiegert, K., Falara, V., Gonzales-Vigil, E., Leong, B., Schäfer, P., Kudrna, D., Wing, R. a, Bolger, A.M., Usadel, B., Tissier, A., Fernie, A.R., Barry, C.S. & Pichersky, E., (2013). Evolution of a complex locus for terpene biosynthesis in solanum. *Plant Cell* **25**, 6, 2022–36.

May, B. & Wüst, M., (2012). Temporal development of sesquiterpene hydrocarbon profiles of different grape varieties during ripening *Flavour Fragr. J.* **27**, 4, 280–285.

McGarvey, D.J. & Croteau, R., (1995). Terpenoid metabolism. *Plant Cell* **7**, 7, 1015–26.

Mendes-Pinto, M.M., (2009). Carotenoid breakdown products the-norisoprenoids-in wine aroma *Arch. Biochem. Biophys.* **483**, 2, 236–245.

Minio, A., Lin, J., Gaut, B.S. & Cantu, D., (2017). How Single Molecule Real-Time Sequencing and Haplotype Phasing Have Enabled Reference-Grade Diploid Genome Assembly of Wine Grapes *Front. Plant Sci.* **8**, May, 1–6.

Mir, K. & Schober, S., (2014). Selection pressure in alternative reading frames *PLoS One* **9**, 10, 1–7.

Moore, B.M., Wang, P., Fan, P., Leong, B., Schenck, C.A., Lloyd, J.P., Lehti-Shiu, M.D., Last, R.L., Pichersky, E. & Shiu, S.-H., (2019). Robust predictions of specialized metabolism genes through machine learning

Proc. Natl. Acad. Sci. **116**, 6, 2344–2353.

Muchlinski, A., Chen, X., Lovell, J.T., Köllner, T.G., Pelot, K.A., Zerbe, P., Ruggiero, M., Callaway, L., Laliberte, S., Chen, F. & Tholl, D., (2019). Biosynthesis and Emission of Stress-Induced Volatile Terpenes in Roots and Leaves of Switchgrass (*Panicum virgatum* L.) *Front. Plant Sci.* **10**, September, 1–16.

Muhlemann, J.K., Klempien, A. & Dudareva, N., (2014). Floral volatiles: From biosynthesis to function *Plant. Cell Environ.* **37**, 8, 1936–1949.

Myles, S., Chia, J.-M., Hurwitz, B., Simon, C., Zhong, G.Y., Buckler, E. & Ware, D., (2010). Rapid genomic characterization of the genus vitis. *PLoS One* **5**, 1, e8219.

Nambara, E. & Marion-Poll, A., (2005). Abscisic Acid Biosynthesis and Catabolism *Annu. Rev. Plant Biol.* **56**, 1, 165–185.

Ober, D., (2005). Seeing double: gene duplication and diversification in plant secondary metabolism. *Trends Plant Sci.* **10**, 9, 444–9.

Ogura, K. & Koyama, T., (1998). Enzymatic Aspects of Isoprenoid Chain Elongation. *Chem. Rev.* **98**, 4, 1263–1276.

Orr, M.W., Mao, Y., Storz, G. & Qian, S.B., (2020). Alternative ORFs and small ORFs: shedding light on the dark proteome *Nucleic Acids Res.* **48**, 3, 1029–1042.

Panchy, N., Lehti-Shiu, M. & Shiu, S.-H., (2016). Evolution of Gene Duplication in Plants *Plant Physiol.* **171**, 4, 2294–2316.

Pare, P.W. & Tumlinson, J.H., (1999). Plant Volatiles as a Defense against Insect Herbivores *Plant Physiol.* **121**, 2, 325–331.

Pelot, K.A., Chen, R., Hagelthorn, D.M., Young, C.A., Addison, J.B., Muchlinski, A., Tholl, D. & Zerbe, P., (2018). Functional diversity of diterpene synthases in the biofuel crop switchgrass *Plant Physiol.* **178**, 1, 54–71.

Peters, R.J., (2006). Uncovering the complex metabolic network underlying diterpenoid phytoalexin biosynthesis in rice and other cereal crop plants *Phytochemistry* **67**, 21, 2307–2317.

Peters, R.J., Flory, J.E., Jetter, R., Ravn, M.M., Lee, H.J., Coates, R.M. & Croteau, R.B., (2000). Abietadiene synthase from grand fir (Abies grandis): characterization and mechanism of action of the "pseudomature" recombinant enzyme. *Biochemistry* **39**, 50, 15592–602.

Pichersky, E., (2006). Biosynthesis of Plant Volatiles: Nature's Diversity and Ingenuity *Science (80-.).* **311**, 5762, 808–811.

Pichersky, E. & Gang, D.R., (2000). Genetics and biochemistry of secondary metabolites in plants: an evolutionary perspective. *Trends Plant Sci.* **5**, 10, 439–45.

Pichersky, E. & Gershenzon, J., (2002). The formation and function of plant volatiles: perfumes for pollinator attraction and defense. *Curr. Opin. Plant Biol.* **5**, 3, 237–43.

Pichersky, E. & Lewinsohn, E., (2011). Convergent Evolution in Plant Specialized Metabolism *Annu. Rev. Plant Biol.* **62**, 1, 549–566.

du Plessis, K., Young, P.R., Eyéghé-Bickong, H.A. & Vivier, M.A., (2017). The Transcriptional Responses and Metabolic Consequences of Acclimation to Elevated Light Exposure in Grapevine Berries *Front. Plant Sci.* **8**, July.

Van Poecke, R.M., Posthumus, M.A. & Dicke, M., (2001). Herbivore-induced volatile production by Arabidopsis thaliana leads to attraction of the parasitoid Cotesia rubecula: chemical, behavioral, and gene-expression analysis. *J. Chem. Ecol.* **27**, 10, 1911–28.

Pott, D.M., Osorio, S. & Vallarino, J.G., (2019). From Central to Specialized Metabolism: An Overview of Some Secondary Compounds Derived From the Primary Metabolism for Their Role in Conferring Nutritional and Organoleptic Characteristics to Fruit *Front. Plant Sci.* **10**, June.

Prisic, S., Xu, M., Wilderman, P.R. & Peters, R.J., (2004). Rice Contains Two Disparate ent -Copalyl Diphosphate Synthases with Distinct Metabolic Functions *Plant Physiol.* **136**, 4, 4228–4236.

Qi, X., Bakht, S., Leggett, M., Maxwell, C., Melton, R. & Osbourn, A., (2004). A gene cluster for secondary metabolism in oat: Implications for the evolution of metabolic diversity in plants *Proc. Natl. Acad. Sci. U. S. A.* **101**, 21, 8233–8238.

Qiao, D., Yang, C., Chen, J., Guo, Y., Li, Y., Niu, S., Cao, K. & Chen, Z., (2019). Comprehensive identification of the full-length transcripts and alternative splicing related to the secondary metabolism pathways in the tea plant (Camellia sinensis) *Sci. Rep.* **9**, 1, 2709.

Rasmann, S., Köllner, T.G., Degenhardt, J., Hiltpold, I., Toepfer, S., Kuhlmann, U., Gershenzon, J. & Turlings, T.C.J., (2005). Recruitment of entomopathogenic nematodes by insect-damaged maize roots *Nature* **434**, 7034, 732–737.

Reardon, D. & Farber, G.K., (1995). The structure of alpha/beta barrel proteins *FASEB J.* **9**, 7, 497–503.

Reumann, S., (2013). Biosynthesis of Vitamin K1 (Phylloquinone) by Plant Peroxisomes and Its Integration

into Signaling Molecule Synthesis Pathways In: Subcell. Biochem. Vol. 69 213–229.

Ribéreau-Gayon, P., Glories, Y., Maujean, A. & Dubourdieu, D. Eds., (2006). Handbook of Enology. Volume 2: The Chemistry of Wine Stabilization and Treatments. (2nd editio ed.). John Wiley & Sons, Ltd.

Ribéreau-Gayon, P., Dubourdieu, D., Doneche, B. & Lonvaud, A., (2006). Handbook of Enology, The Microbiology of Wine and Vinifications. Vol. 1.

Richter, A., Schaff, C., Zhang, Z., Lipka, A.E., Tian, F., Köllner, T.G., Schnee, C., Preiß, S., Irmisch, S., Jander, G., Boland, W., Gershenzon, J., Buckler, E.S. & Degenhardt, J., (2016). Characterization of Biosynthetic Pathways for the Production of the Volatile Homoterpenes DMNT and TMTT in Zea mays *Plant Cell* **28**, 10, 2651–2665.

Rico, J., Pardo, E. & Orejas, M., (2010). Enhanced production of a plant monoterpene by overexpression of the 3-hydroxy-3-methylglutaryl coenzyme A reductase catalytic domain in Saccharomyces cerevisiae. *Appl. Environ. Microbiol.* **76**, 19, 6449–54.

Roach, C.R., Hall, D.E., Zerbe, P. & Bohlmann, J.J., (2014). Plasticity and Evolution of (+)-3-Carene Synthase and (-)-Sabinene Synthase Functions of a Sitka Spruce Monoterpene Synthase Gene Family associated with Weevil Resistance. *J. Biol. Chem.* **289**, 34, 23859–23869.

Robinson, A.L., (2011). Environmental Influences on Grape Aroma Potential.

Rohmer, M., Seemann, M., Horbach, S., Bringer-Meyer, S. & Sahm, H., (1996). Glyceraldehyde 3-phosphate and pyruvate as precursors of isoprenic units in an alternative non-mevalonate pathway for terpenoid biosynthesis *J. Am. Chem. Soc.* **118**, 11, 2564–2566.

Rosenstiel, T.N., Fisher, A.J., Fall, R. & Monson, R.K., (2002). Differential accumulation of dimethylallyl diphosphate in leaves and needles of isoprene- and methylbutenol-emitting and nonemitting species. *Plant Physiol.* **129**, 3, 1276–1284.

Ruiz-Sola, M.Á. & Rodríguez-Concepción, M., (2012). Carotenoid Biosynthesis in Arabidopsis: A Colorful Pathway *Arab. B.* **10**, e0158.

Ruiz-Sola, M.Á., Coman, D., Beck, G., Barja, M.V., Colinas, M., Graf, A., Welsch, R., Rütimann, P., Bühlmann, P., Bigler, L., Gruissem, W., Rodríguez-Concepción, M. & Vranová, E., (2016). Arabidopsis GERANYLGERANYL DIPHOSPHATE SYNTHASE 11 is a hub isozyme required for the production of most photosynthesis-related isoprenoids *New Phytol.* **209**, 1, 252–264.

Sacchettini, J.C. & Poulter, C.D., (1997). Creating isoprenoid diversity. *Science* **277**, 5333, 1788–9.

Sadgrove, N.J., Telford, I.R.H., Greatrex, B.W. & Jones, G.L., (2014). Composition and antimicrobial activity of the essential oils from the *Phebalium squamulosum* species complex (Rutaceae) in New South Wales, Australia *Phytochemistry* **97**, 38–45.

Saeed, W., Naseem, S. & Ali, Z., (2017). Strigolactones biosynthesis and their role in abiotic stress resilience in plants: A critical review *Front. Plant Sci.* **8**, August, 1–13.

Sakakibara, H., (2005). Cytokinin Biosynthesis and Regulation In: Vitam. Horm. Vol. 72 271–287.

Sakurai, A., (1999). Brassinosteroid biosynthesis *Plant Physiol. Biochem.* **37**, 5, 351–361.

Salazar-Cerezo, S., Martínez-Montiel, N., García-Sánchez, J., Pérez-y-Terrón, R. & Martínez-Contreras, R.D., (2018). Gibberellin biosynthesis and metabolism: A convergent route for plants, fungi and bacteria *Microbiol. Res.* **208**, January, 85–98.

Sallaud, C., Rontein, D., Onillon, S., Jabès, F., Duffé, P., Giacalone, C., Thoraval, S., Escoffier, C., Herbette, G., Leonhardt, N., Causse, M. & Tissier, A., (2009). A novel pathway for sesquiterpene biosynthesis from Z,Z-farnesyl pyrophosphate in the wild tomato Solanum habrochaites. *Plant Cell* **21**, 1, 301–317.

Salomon, M.V., Purpora, R., Bottini, R. & Piccoli, P., (2016). Rhizosphere associated bacteria trigger accumulation of terpenes in leaves of Vitis vinifera L. cv. Malbec that protect cells against reactive oxygen species *Plant Physiol. Biochem.* **106**, 295–304.

Salvagnin, U., Carlin, S., Angeli, S., Vrhovsek, U., Anfora, G., Malnoy, M. & Martens, S., (2016). Homologous and heterologous expression of grapevine E-(β)-caryophyllene synthase (VvGwECar2) *Phytochemistry* **131**, 76–83.

Salvagnin, U., Malnoy, M., Thöming, G., Tasin, M., Carlin, S., Martens, S., Vrhovsek, U., Angeli, S. & Anfora, G., (2018). Adjusting the scent ratio: using genetically modified Vitis vinifera plants to manipulate European grapevine moth behaviour *Plant Biotechnol. J.* **16**, 1, 264–271.

Savoi, S., Wong, D.C.J., Arapitsas, P., Miculan, M., Bucchetti, B., Peterlunger, E., Fait, A., Mattivi, F. & Castellarin, S.D., (2016). Transcriptome and metabolite profiling reveals that prolonged drought modulates the phenylpropanoid and terpenoid pathway in white grapes (Vitis vinifera L.) *BMC Plant Biol.* **16**, 1, 67.

Sawai, S. & Saito, K., (2011). Triterpenoid biosynthesis and engineering in plants *Front. Plant Sci.* **2**, JUN, 1–8.

Schafer, W.R. & Rine, J., (1992). Protein Prenylation: Genes, Enzymes, Targets, and Functions *Annu. Rev.*

33

Genet. **26**, 1, 209–237.

van Schie, C.C.N., Haring, M.A. & Schuurink, R.C., (2012). Prenyldiphosphate Synthases and Gibberellin Biosynthesis In: Isoprenoid Synth. Plants Microorg. Springer New York, New York, NY 213–232.

Schilmiller, A.L., Schauvinhold, I., Larson, M., Xu, R., Charbonneau, A.L., Schmidt, A., Wilkerson, C., Last, R.L. & Pichersky, E., (2009). Monoterpenes in the glandular trichomes of tomato are synthesized from a neryl diphosphate precursor rather than geranyl diphosphate. *Proc. Natl. Acad. Sci. U. S. A.* **106**, 26, 10865–70.

Schmelz, E.A., Huffaker, A., Sims, J.W., Christensen, S.A., Lu, X., Okada, K. & Peters, R.J., (2014). Biosynthesis, elicitation and roles of monocot terpenoid phytoalexins *Plant J.* **79**, 4, 659–678.

Schnee, C., Köllner, T.G., Held, M., Turlings, T.C.J., Gershenzon, J., Degenhardt, J., Kollner, T.G., Held, M., Turlings, T.C.J., Gershenzon, J. & Degenhardt, J., (2006). The products of a single maize sesquiterpene synthase form a volatile defense signal that attracts natural enemies of maize herbivores *Proc. Natl. Acad. Sci. U. S. A.* **103**, 4, 1129–1134.

Schuhr, C. a., Radykewicz, T., Sagner, S., Latzel, C., Zenk, M.H., Arigoni, D., Bacher, A., Rohdich, F. & Eisenreich, W., (2003). Quantitative assessment of crosstalk between the two isoprenoid biosynthesis pathways in plants by NMR spectroscopy *Phytochem. Rev.* **2**, 1/2, 3–16.

Schwab, W., (2003). Metabolome diversity: Too few genes, too many metabolites? *Phytochemistry* **62**, 6, 837–849.

Schwab, W. & Wüst, M., (2015). Understanding the Constitutive and Induced Biosynthesis of Mono- and Sesquiterpenes in Grapes (Vitis vinifera): A Key to Unlocking the Biochemical Secrets of Unique Grape Aroma Profiles *J. Agric. Food Chem.* **63**, 49, 10591–10603.

Schwender, J., Seemann, M., Lichtenthaler, H.K. & Rohmer, M., (1996). Biosynthesis of isoprenoids (carotenoids, sterols, prenyl side-chains of chlorophylls and plastoquinone) via a novel pyruvate/glyceraldehyde 3-phosphate non-mevalonate pathway in the green alga Scenedesmus obliquus *Biochem. J.* **316**, 1, 73–80.

Sefton, M. a., Francis, I.L. & Williams, P.J., (1994). Free and Bound Volatile Secondary Metabolites of Vitis Vhifera Grape cv. Sauvignon Blanc *J. Food Sci.* **59**, 1, 142–147.

Sefton, M.A., (1998). Hydrolytically-released volatile secondary metabolites from a juice sample of Vitis vinifera grape cvs Merlot and Cabernet Sauvignon *Aust. J. Grape Wine Res.* **4**, 1, 30–38.

Sefton, M.A., Francis, I.L. & Williams, P.J., (1993). The Volatile Composition of Chardonnay Juices: A Study by Flavor Precursor Analysis *Am. J. Enol. Vitic.* **44**, 4, 359–370.

Sefton, M.A., Frances, I.L. & Williams, P.J., (1996). The free and bound volatile secondary metabolites of Vitis vinifera grape cv. Semillon *Aust. J. Grape Wine Res.* **2**, 3, 179–183.

Sharkey, T.D. & Yeh, S., (2001). Isoprene Emission from Plants *Annu. Rev. Plant Physiol. Plant Mol. Biol.* **52**, 1, 407–436.

Sharkey, T.D., Chen, X. & Yeh, S., (2001). Isoprene increases thermotolerance of fosmidomycin-fed leaves *Plant Physiol.* **125**, 4, 2001–2006.

Shelton, D., Zabaras, D., Chohan, S., Wyllie, S.G., Baverstock, P., Leach, D. & Henry, R., (2004). Isolation and partial characterisation of a putative monoterpene synthase from Melaleuca alternifolia *Plant Physiol. Biochem.* **42**, 11, 875–882.

Shimada, T., Endo, T., Fujii, H., Hara, M., Ueda, T., Kita, M. & Omura, M., (2004). Molecular cloning and functional characterization of four monoterpene synthase genes from Citrus unshiu Marc. *Plant Sci.* **166**, 1, 49–58.

Shimura, K., Okada, A., Okada, K., Jikumaru, Y., Ko, K.W., Toyomasu, T., Sassa, T., Hasegawa, M., Kodama, O., Shibuya, N., Koga, J., Nojiri, H. & Yamane, H., (2007). Identification of a biosynthetic gene cluster in rice for momilactones *J. Biol. Chem.* **282**, 47, 34013–34018.

Siddiqui, M.S., Thodey, K., Trenchard, I. & Smolke, C.D., (2012). Advancing secondary metabolite biosynthesis in yeast with synthetic biology tools *FEMS Yeast Res.* **12**, 2, 144–170.

Da Silva, C., Zamperin, G., Ferrarini, A., Minio, A., Dal Molin, A., Venturini, L., Buson, G., Tononi, P., Avanzato, C., Zago, E., Boido, E., Dellacassa, E., Gaggero, C., Pezzotti, M., Carrau, F. & Delledonne, M., (2013). The High Polyphenol Content of Grapevine Cultivar Tannat Berries Is Conferred Primarily by Genes That Are Not Shared with the Reference Genome *Plant Cell* **25**, 12, 4777–4788.

Silver, G.M. & Fall, R., (1991). Enzymatic synthesis of isoprene from dimethylallyl diphosphate in aspen leaf extracts. *Plant Physiol.* **97**, 4, 1588–1591.

Singh, B. & Sharma, R. a., (2015). Plant terpenes: defense responses, phylogenetic analysis, regulation and clinical applications *3 Biotech* **5**, 2, 129–151.

Slaghenaufi, D. & Ugliano, M., (2018). Norisoprenoids, Sesquiterpenes and Terpenoids Content of Valpolicella Wines During Aging: Investigating Aroma Potential in Relationship to Evolution of Tobacco and Balsamic

Aroma in Aged Wine *Front. Chem.* **6**, March, 1–13.

Smit, S.J., Vivier, M.A. & Young, P.R., (2019). Linking Terpene Synthases to Sesquiterpene Metabolism in Grapevine Flowers *Front. Plant Sci.* **10**, February, 1–18.

Song, J., Liu, H., Zhuang, H., Zhao, C., Xu, Y., Wu, S., Qi, J., Li, J., Hettenhausen, C. & Wu, J., (2017). Transcriptomics and alternative splicing analyses reveal large differences between maize lines B73 and Mo17 in response to aphid Rhopalosiphum padi infestation *Front. Plant Sci.* **8**, October, 1–17.

Souleyre, E.J.F., Bowen, J.K., Matich, A.J., Tomes, S., Chen, X., Hunt, M.B., Wang, M.Y., Ileperuma, N.R., Richards, K., Rowan, D.D., Chagné, D. & Atkinson, R.G., (2019). Genetic control of α-farnesene production in apple fruit and its role in fungal pathogenesis *Plant J.* **100**, 6, 1148–1162.

Sparg, S.G., Light, M.E. & Van Staden, J., (2004). Biological activities and distribution of plant saponins *J. Ethnopharmacol.* **94**, 2–3, 219–243.

Sun, Y., Huang, X., Ning, Y., Jing, W., Bruce, T.J.A., Qi, F., Xu, Q., Wu, K., Zhang, Y. & Guo, Y., (2017). TPS46, a Rice Terpene Synthase Conferring Natural Resistance to Bird Cherry-Oat Aphid, Rhopalosiphum padi (Linnaeus) *Front. Plant Sci.* **08**, February, 1–11.

Surmacz, L., Plochocka, D., Kania, M., Danikiewicz, W. & Swiezewska, E., (2014). cis-Prenyltransferase AtCPT6 produces a family of very short-chain polyisoprenoids in planta. *Biochim. Biophys. Acta* **1841**, 2, 240–250.

Szakiel, A., Pączkowski, C. & Henry, M., (2011). Influence of environmental biotic factors on the content of saponins in plants *Phytochem. Rev.* **10**, 4, 493–502.

Tabidze, V., Pipia, I., Gogniashvili, M., Kunelauri, N., Ujmajuridze, L., Pirtskhalava, M., Vishnepolsky, B., Hernandez, A.G., Fields, C.J. & Beridze, T., (2017). Whole genome comparative analysis of four Georgian grape cultivars *Mol. Genet. Genomics* **292**, 6, 1377–1389.

Tachibana, A., Yano, Y., Otani, S., Nomura, N., Sako, Y. & Taniguchi, M., (2000). Novel prenyltransferase gene encoding farnesylgeranyl diphosphate synthase from a hyperthermophilic archaeon, Aeropyrum pernix. Molecular evolution with alteration in product specificity *Eur. J. Biochem.* **267**, 2, 321–328.

Tamiru, A., Bruce, T.J.A., Richter, A., Woodcock, C.M., Midega, C.A.O., Degenhardt, J., Kelemu, S., Pickett, J.A. & Khan, Z.R., (2017). A maize landrace that emits defense volatiles in response to herbivore eggs possesses a strongly inducible terpene synthase gene *Ecol. Evol.* **7**, 8, 2835–2845.

Tanaka, Y., Sasaki, N. & Ohmiya, A., (2008). Biosynthesis of plant pigments: Anthocyanins, betalains and carotenoids *Plant J.* **54**, 4, 733–749.

Taniguchi, S., Hosokawa-Shinonaga, Y., Tamaoki, D., Yamada, S., Akimitsu, K. & Gomi, K., (2014). Jasmonate induction of the monoterpene linalool confers resistance to rice bacterial blight and its biosynthesis is regulated by JAZ protein in rice *Plant, Cell Environ.* **37**, 2, 451–461.

Taylor, J.S. & Raes, J., (2004). Duplication and Divergence: The Evolution of New Genes and Old Ideas *Annu. Rev. Genet.* **38**, 1, 615–643.

Thimmappa, R., Geisler, K., Louveau, T., O'Maille, P. & Osbourn, A., (2014). Triterpene biosynthesis in plants *Annu. Rev. Plant Biol.* **65**, September, 225–257.

Tholl, D., (2006). Terpene synthases and the regulation, diversity and biological roles of terpene metabolism. *Curr. Opin. Plant Biol.* **9**, 3, 297–304.

Tholl, D., Sohrabi, R., Huh, J.-H. & Lee, S., (2011). The biochemistry of homoterpenes--common constituents of floral and herbivore-induced plant volatile bouquets. *Phytochemistry* **72**, 13, 1635–46.

Thulasiram, H. V., Erickson, H.K. & Poulter, C.D., (2007). Chimeras of two isoprenoid synthases catalyze all four coupling reactions in isoprenoid biosynthesis *Science (80-.).* **316**, 5821, 73–76.

Tohge, T. & Fernie, A.R., (2020). Co-regulation of Clustered and Neo-functionalized Genes in Plant-Specialized Metabolism *Plants* **9**, 5, 622.

Toledo-Ortiz, G., Huq, E. & Rodríguez-Concepción, M., (2010). Direct regulation of phytoene synthase gene expression and carotenoid biosynthesis by phytochrome-interacting factors. *Proc. Natl. Acad. Sci. U. S. A.* **107**, 25, 11626–31.

Turlings, T.C.J., Loughrin, J.H., Mccall, P.J., Röse, U.S.R., Lewis, W.J. & Tumlinson, J.H., (1995). How caterpillar-damaged plants protect themselves by attracting parasitic wasps *Proc. Natl. Acad. Sci. U. S. A.* **92**, 10, 4169–4174.

Vandermoten, S., Haubruge, É. & Cusson, M., (2009). New insights into short-chain prenyltransferases: structural features, evolutionary history and potential for selective inhibition *Cell. Mol. Life Sci.* **66**, 23, 3685–3695.

Vattekkatte, A. & Boland, W., (2020). Biosynthetic Origin of Complex Terpenoid Mixtures by Multiproduct Enzymes , Metal Cofactors , and Substrate Isomers *Nat. Prod. Chem. Res.* **8**, 1, 372.

Velasco, R., Zharkikh, A., Troggio, M., Cartwright, D. a, Cestaro, A., Pruss, D., Pindo, M., Fitzgerald, L.M., Vezzulli, S., Reid, J., Malacarne, G., Iliev, D., Coppola, G., Wardell, B., Micheletti, D., Macalma, T., Facci,

M., Mitchell, J.T., Perazzolli, M., Eldredge, G., Gatto, P., Oyzerski, R., Moretto, M., Gutin, N., Stefanini, M., Chen, Y., Segala, C., Davenport, C., Demattè, L., Mraz, A., Battilana, J., Stormo, K., Costa, F., Tao, Q., Si-Ammour, A., Harkins, T., Lackey, A., Perbost, C., Taillon, B., Stella, A., Solovyev, V., Fawcett, J. a, Sterck, L., Vandepoele, K., Grando, S.M., Toppo, S., Moser, C., Lanchbury, J., Bogden, R., Skolnick, M., Sgaramella, V., Bhatnagar, S.K., Fontana, P., Gutin, A., Van de Peer, Y., Salamini, F. & Viola, R., (2007). A high quality draft consensus sequence of the genome of a heterozygous grapevine variety. *PLoS One* **2**, 12, e1326.

Velayos, A., Eslava, A.P. & Iturriaga, E.A., (2000). A bifunctional enzyme with lycopene cydase and phytoene synthase activities is encoded by the carRP gene of Mucor circinelloides *Eur. J. Biochem.* **267**, 17, 5509–5519.

Velikova, V., Várkonyi, Z., Szabó, M., Maslenkova, L., Nogues, I., Kovács, L., Peeva, V., Busheva, M., Garab, G., Sharkey, T.D. & Loreto, F., (2011). Increased thermostability of thylakoid membranes in isoprene-emitting leaves probed with three biophysical techniques *Plant Physiol.* **157**, 2, 905–916.

Vickers, C.E., Gershenzon, J., Lerdau, M.T. & Loreto, F., (2009). A unified mechanism of action for volatile isoprenoids in plant abiotic stress. *Nat. Chem. Biol.* **5**, 5, 283–91.

Vickers, C.E., Possell, M., Cojocariu, C.I., Velikova, V.B., Laothawornkitkul, J., Ryan, A., Mullineaux, P.M. & Nicholas Hewitt, C., (2009). Isoprene synthesis protects transgenic tobacco plants from oxidative stress *Plant, Cell Environ.* **32**, 5, 520–531.

Vidal, J.R., Kikkert, J.R., Donzelli, B.D., Wallace, P.G. & Reisch, B.I., (2006). Biolistic transformation of grapevine using minimal gene cassette technology *Plant Cell Rep.* **25**, 8, 807–814.

Vidal, J.R., Gomez, C., Cutanda, M.C., Shrestha, B.R., Bouquet, A., Thomas, M.R. & Torregrosa, L., (2010). Use of gene transfer technology for functional studies in grapevine *Aust. J. Grape Wine Res.* **16**, SUPPL. 1, 138–151.

Vitulo, N., Forcato, C., Carpinelli, E.C., Telatin, A., Campagna, D., D'Angelo, M., Zimbello, R., Corso, M., Vannozzi, A., Bonghi, C., Lucchin, M. & Valle, G., (2014). A deep survey of alternative splicing in grape reveals changes in the splicing machinery related to tissue, stress condition and genotype. *BMC Plant Biol.* **14**, 1, 99.

Vranová, E., Hirsch-Hoffmann, M. & Gruissem, W., (2011). AtIPD: A Curated Database of Arabidopsis Isoprenoid Pathway Models and Genes for Isoprenoid Network Analysis *Plant Physiol.* **156**, 4, 1655–1660.

Vranová, E., Coman, D., Gruissem, W., Vranov, E., Coman, D., Gruissem, W., Vranová, E., Coman, D. & Gruissem, W., (2013). Network Analysis of the MVA and MEP Pathways for Isoprenoid Synthesis *Annu. Rev. Plant Biol.* **64**, 1, 665–700.

Wang, C., Chen, Q., Fan, D., Li, J., Wang, G. & Zhang, P., (2016). Structural Analyses of Short-Chain Prenyltransferases Identify an Evolutionarily Conserved GFPPS Clade in Brassicaceae Plants *Mol. Plant* **9**, 2, 195–204.

Wang, K. & Ohnuma, S., (1999). Chain-length determination mechanism of isoprenyl diphosphate synthases and implications for molecular evolution. *Trends Biochem. Sci.* **24**, 11, 445–51.

Wang, K.C. & Ohnuma, S., (2000). Isoprenyl diphosphate synthases. *Biochim. Biophys. Acta* **1529**, 1–3, 33–48.

Wang, M. & Casey, P.J., (2016). Protein prenylation: unique fats make their mark on biology *Nat. Rev. Mol. Cell Biol.* **17**, 2, 110–122.

Wendt, K.U. & Schulz, G.E., (1998). Isoprenoid biosynthesis: manifold chemistry catalyzed by similar enzymes. *Structure* **6**, 2, 127–33.

Von Wettstein, D., Gough, S. & Kannangara, C.G., (1995). Chlorophyll biosynthesis *Plant Cell* **7**, 7, 1039–1057.

Wilderman, P.R., Xu, M., Jin, Y., Coates, R.M. & Peters, R.J., (2004). Identification of syn-pimara-7,15-diene synthase reveals functional clustering of terpene synthases involved in rice phytoalexin/allelochemical biosynthesis *Plant Physiol.* **135**, 4, 2098–2105.

Wilding, E.I., Brown, J.R., Bryant, A.P., Chalker, A.F., Holmes, D.J., Ingraham, K.A., Iordanescu, S., So, C.Y., Rosenberg, M. & Gwynn, M.N., (2000). Identification, evolution, and essentiality of the mevalonate pathway for isopentenyl diphosphate biosynthesis in gram-positive cocci. *J. Bacteriol.* **182**, 15, 4319–27.

Wink, M., (2003). Evolution of secondary metabolites from an ecological and molecular phylogenetic perspective *Phytochemistry* **64**, 1, 3–19.

Wirth, J., Guo, W., Baumes, R. & Günata, Z., (2001). Volatile compounds released by enzymatic hydrolysis of glycoconjugates of leaves and grape berries from Vitis vinifera Muscat of Alexandria and Shiraz cultivars. *J. Agric. Food Chem.* **49**, 6, 2917–2923.

Wright, L.D., (1961). Biosynthesis of Isoprenoid Compounds *Annu. Rev. Biochem.* **30**, 1, 525–548.

36

Xie, X., Kirby, J. & Keasling, J.D., (2012). Functional characterization of four sesquiterpene synthases from Ricinus communis (Castor bean) *Phytochemistry* **78**, 20–28.

Yang, W.L., Shi, X.Y., Zhong, L., Liang, P., Song, D.L., Gao, X.W., Wen-ling, Y., Xue-yan, S.H.I., Li, Z., Pei, L., Dun-lun, S. & Xi-wu, G.A.O., (2012). Omethoate-Induced Changes of (+)-δ-Cadinene Synthase Activity and Gossypol Content in Cotton Seedlings *J. Integr. Agric.* **11**, 10, 1682–1690.

Yonekura-Sakakibara, K., (2009). Functional genomics of family 1 glycosyltransferases in Arabidopsis *Plant Biotechnol.* **26**, 3, 267–274.

Yonekura-Sakakibara, K. & Hanada, K., (2011). An evolutionary view of functional diversity in family 1 glycosyltransferases. *Plant J.* **66**, 1, 182–93.

Yoshitomi, K., Taniguchi, S., Tanaka, K., Uji, Y., Akimitsu, K. & Gomi, K., (2016). Rice terpene synthase 24 (OsTPS24) encodes a jasmonate-responsive monoterpene synthase that produces an antibacterial γ-terpinene against rice pathogen *J. Plant Physiol.* **191**, 120–126.

Young, P.R., (2004). Molecular analyses of candidate carotenoid biosynthetic genes in *Vitis vinifera* L. Stellenbosch University.

Young, P.R., Lashbrooke, J.G., Alexandersson, E., Jacobson, D., Moser, C., Velasco, R. & Vivier, M. a, (2012). The genes and enzymes of the carotenoid metabolic pathway in Vitis vinifera L. *BMC Genomics* **13**, 1, 243.

Zeng, W.-C., Zhang, Z., Gao, H., Jia, L.-R. & He, Q., (2012). Chemical composition, antioxidant, and antimicrobial activities of essential oil from pine needle (*Cedrus deodara*). *J. Food Sci.* **77**, 7, C824-9.

Zenoni, S., Ferrarini, A., Giacomelli, E., Xumerle, L., Fasoli, M., Malerba, G., Bellin, D., Pezzotti, M. & Delledonne, M., (2010). Characterization of transcriptional complexity during berry development in Vitis vinifera using RNA-Seq. *Plant Physiol.* **152**, 4, 1787–95.

Zhang, F.L. & Casey, P.J., (1996). Protein Prenylation: Molecular Mechanisms and Functional Consequences *Annu. Rev. Biochem.* **65**, 1, 241–269.

Zhang, J., (2003). Evolution by gene duplication: an update *Trends Ecol. Evol.* **18**, 6, 292–298.

Zhuang, X., Köllner, T.G., Zhao, N., Li, G., Jiang, Y., Zhu, L., Ma, J., Degenhardt, J. & Chen, F., (2012). Dynamic evolution of herbivore-induced sesquiterpene biosynthesis in sorghum and related grass crops *Plant J.* **69**, 1, 70–80.

Chapter 2   Development and validation of yeast and plant expression systems for functional characterisation of genes involved in grapevine terpenoid biosynthesis

2.1   Introduction

Terpenoid biosynthesis can occur via two routes, namely the mevalonate (MVA) pathway and the methylerythritol phosphate (MEP) pathway. However, both these pathways produce the same end-products, isopentenyl diphosphate (IPP) and dimethyl diphosphate (DMAPP). These universal terpenoid precursors are directed to their respective terpene substrates through the activity of isoprenyl diphosphate synthases (IDSs). The reactions catalysed by a subgroup of IDSs, the short-chain IDSs, are summarised in **Figure 2.1** (Wang & Ohnuma, 1999). The head-to-tail condensation of IPP to DMAPP, catalysed by geranyl diphosphate synthase (GPS), produces geranyl diphosphate (GPP) – the main substrate for the synthesis of monoterpenes (Dubey *et al.*, 2003; Schilmiller *et al.*, 2009; Gao *et al.*, 2012). An alternative substrate for monoterpene synthesis is the *cis*-isomer of GPP, neryl diphosphate (NPP), and is synthesised by neryl diphosphate synthase (NPS) (Schilmiller *et al.*, 2009). Farnesyl diphosphate synthase (FPS) catalyses the sequential addition of two IPP molecules to DMAPP to produce farnesyl diphosphate (FPP) – the substrate for sesquiterpenes and several other terpenoids (Szkopińska & Płochocka, 2005). Geranylgeranyl diphosphate (GGPP) synthesis in plants results from the successive addition of IPP to DMAPP, GPP or FPP to produce the C_{20} substrate. GGPP is utilised in the biosynthesis of diterpenes but also various other compounds (Vandermoten *et al.*, 2009).

Short-chain isoprenyl diphosphates can be converted to a multitude of terpenes through terpene synthases (TPSs). Identification and quantification of the terpene compounds produced through the activity of a specific TPS, typically via heterologous expression studies, are necessary to functionally characterise *TPS* genes (Martin & Bohlmann, 2004). Various approaches, each with its own inherent advantages and disadvantages, can be utilised to determine product profile of isolated TPSs (Fischer *et al.*, 2013; Li & Pfeifer, 2014).

Characterisation of IDSs and TPSs generally occurs through *in vitro* studies whereby the putative genes are expressed in *Escherichia coli.* The heterologously-produced proteins are then purified and incubated with potential substrates, after which the products are analysed (Pan *et al.*, 1996; Burke *et al.*, 1999, 2004; Burke & Croteau, 2002a; Shelton *et al.*, 2004; Iijima *et al.*, 2004; Schmidt & Gershenzon, 2008; Jones *et al.*, 2008; Wang & Dixon, 2009; Schmidt *et al.*, 2010; Martin *et al.*, 2010; Keim *et al.*, 2012; Del Terra *et al.*, 2013; Kulkarni *et al.*, 2013; Alquézar *et al.*, 2017; Rusdi *et al.*, 2018; Zhang *et al.*, 2019). In addition, *in vivo* bacterial functional complementation can be utilised

for genes that are predicted to encode proteins involved in carotenoid biosynthesis. During these studies the production and accumulation of carotenoids in *E. coli* is used to determine gene functionality (Cunningham *et al.*, 1994; Zhu, Suzuki, Okada, Tanaka, Nakagawa, Kawamukai & Matsuda, 1997; Young, 2004; Thabet *et al.*, 2012; Kulkarni *et al.*, 2013).
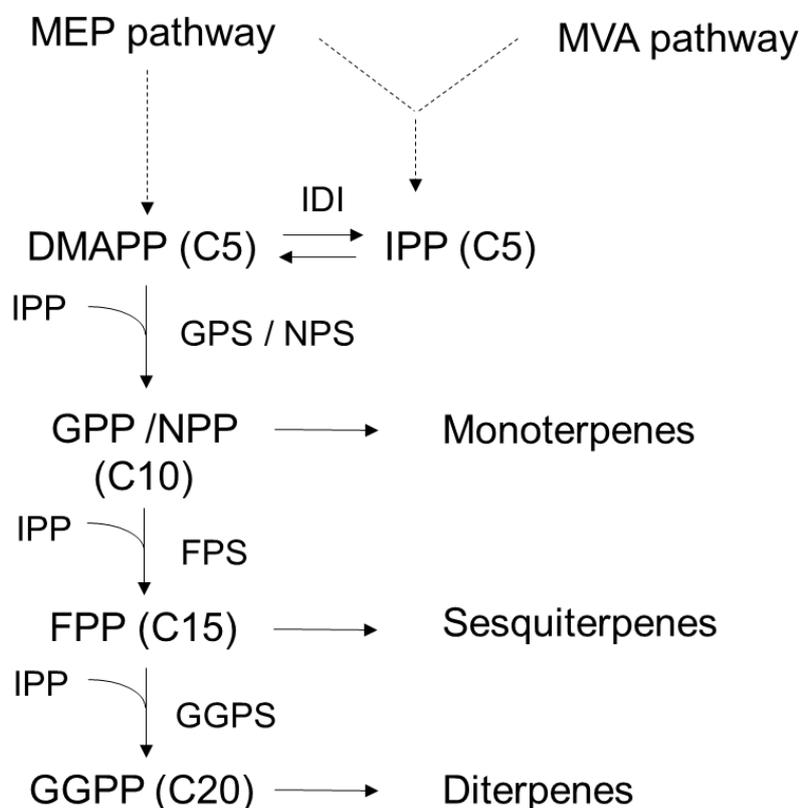
Figure 2.1 Simplified diagram to illustrate the production of substrates used by terpene synthases (adapted from Schilmiller *et al.*, 2009; Chen *et al.*, 2011). Dotted lines indicate multiple reactions. The methylerythritol phosphate (MEP) and mevalonate (MVA) pathways produce isopentenyl diphosphate (IPP) and dimethylallyl diphosphate (DMAPP). DMAPP can be produced directly by the MEP pathway with isopentenyl diphosphate isomerase (IDI) catalysing the isomerisation reaction to form either IPP or DMAPP. These C5 compounds are the building blocks for all terpenoids. The short-chain prenyl diphosphate synthases [geranyl diphosphate synthase (GPS), neryl diphosphate synthase (NPS), farnesyl diphosphate synthase (FPS), geranylgeranyl diphosphate synthase (GGPS)] utilise these compounds in condensation reactions to produce the short-chain diphosphates [geranyl diphosphate (GPP) and its isomer neryl diphosphate (NPP), farnesyl diphosphate (FPP), geranylgeranyl diphosphate GGPP)] which is used by terpene synthases (TPSs) to produce terpenes.

As an alternative to the conventional *in vitro* assays involving *E. coli* (bacterial system) for characterisation, an *in vivo* production system in yeast was implemented and evaluated in this study. *TPS* expression in *Saccharomyces cerevisiae* has been used in previous studies (Scalcinati *et al.*, 2012; Chen *et al.*, 2019). The substantial genetic information and molecular tools available for *S. cerevisiae* allow its application as a microbial production host with relative ease (Göpfert *et al.*, 2009;

39

Fischer *et al.*, 2011; Xie *et al.*, 2012). The benefit of using this system, compared to that of *E. coli*, is that it is a eukaryotic system. Therefore, it does not require codon optimisation, although it has the usability associated with microbial hosts. Although *S. cerevisiae* does not have a dedicated GPS that can produce GPP for monoterpene production, it does have an FPS that catalyses the condensation reaction of IPP with DMAPP – producing GPP as a transient intermediate (Eberhardt & Rilling, 1975; Anderson *et al.*, 1989). Oswald *et al.* (2007) found that the wild-type yeast strains contained adequate amounts of free GPP, which could be used by the heterologously-expressed geraniol synthase. Due to the economic importance of terpenoids, the production of these compounds – either through heterologous methods or increased flux through the terpenoid pathway *in situ* – has received significant attention over the last two decades (Besumbes *et al.*, 2004; van Herpen *et al.*, 2010; Jiang *et al.*, 2012; Xiao & Zhong, 2016; Shi *et al.*, 2017). Increased heterologous terpene production in yeast has also been reported (Takahashi *et al.*, 2007; Farhi *et al.*, 2011; Ignea *et al.*, 2011, 2014; Kampranis & Makris, 2012; Liu, Redden, *et al.*, 2013; Rodriguez *et al.*, 2014; Zhuang & Chappell, 2015). The increase is created either through altered growth conditions or through manipulation of the MVA pathway or other genes indirectly involved in the production of terpene substrates. This further supports the use of yeasts in the expression of *TPSs*. Furthermore, two *S. cerevisiae* MVA pathway genes, encoding isopentenyl diphosphate isomerase (*ScIDI1*) and 3-hydroxy-3-methyl-glutaryl-coenzyme A reductase (*ScHMG1*), were targeted for overexpression to increase the flux towards terpene production in the yeast strain that was used in this study (Jackson *et al.*, 2003; Asadollahi, 2008; Ajikumar *et al.*, 2010; Rico *et al.*, 2010; Ignea *et al.*, 2011; Liu *et al.*, 2013a; Wriessnegger & Pichler, 2013).

Although *in vitro* and *in vivo* studies in microbial hosts have the potential to provide valuable information about gene functionality, they cannot provide the invaluable insights that are generated with *in planta* studies (Van Schie *et al.*, 2012; Yin *et al.*, 2017). In comparison to microbial systems, plant-based expression systems for characterisation of grapevine terpenoid pathway genes have a major advantage in that the genes are expressed in higher organisms (plants). Therefore, they share common plant cellular compartmentalisation, cofactors, and coenzymes.

The aim of this study was to evaluate various heterologous and analytical systems for their respective suitability to functionally characterise grapevine putative *IDS* and *TPS* genes. Heterologous and homologous expression systems were implemented, optimised, and compared. The homologous ectopic expression of *VviTPS* in grapevine and its heterologous transient expression in *Nicotiana benthamiana* were evaluated as alternative methods for TPS functional characterisation. Ectopic expression of *Vitis vinifera* genes for functional characterisation has the benefit of imitating the native endogenous conditions and will also be evaluated in this study. However, grapevine transformation and recovery and maintenance of transgenic plants are

40

comparatively slow processes (Vidal *et al.*, 2010; Jelly *et al.*, 2014; Salvagnin *et al.*, 2018). Utilising an *Agrobacterium tumefaciens*-mediated transformation of *N. benthamiana* for the transient expression of various plant proteins has been widely used and it is also relatively easily utilised, enabling faster screening of gene function within a plant system (Green *et al.*, 2012; Reed & Osbourn, 2018). To test these systems, a *VviTPS* that was previously shown to encode an (-)-α-terpineol synthase (Martin & Bohlmann, 2004) and an uncharacterised *VviIDS,* putatively encoding a GPS*,* was utilised. *VviTPS* was used in all three expression systems (yeast, grapevine, and tobacco), whereas *VviIDS* was used for co-expression studies with *VviTPS* in the yeast and tobacco systems.

2.2   Materials and methods

2.2.1   Microbial strains, transformation, and culture conditions

Unless otherwise stated, all methods for DNA isolation, manipulations, and cloning were performed as described by Sambrook *et al*. (1989). For cloning experiments and plasmid propagation, *E. coli* DH5α [*endA1 hsdR17 gyrA96 thi-1 relA1 supE44 recA1 ΔlacU169* (φ80 *lacZ*ΔM15), Life Technologies] was used – except for the propagation of constructs containing the *ccd*b gene. In these cases, *E. coli* DB3.1 [F⁻ *gyrA462 endA1 glnV44 Δ(sr1-recA) mcrB mrr hsdS20 (r_B⁻, m_B⁻) ara14 galK2 lacY1 proA2 rpsL20 (Smʳ) xyl5 Δleu mtl1),* Invitrogen®] was used instead. The *E. coli* cultures were maintained in Luria–Bertani (LB) medium (1% w/v tryptone, 0.5% w/v yeast extract, 1% w/v NaCl) with or without 100 μg/mL ampicillin, 40 μg/mL isopropyl-β-D-thiogalactopyranoside (IPTG), and 40 μg/mL 5-bromo-4-chloro-indolyl-galactopyranoside (X-gal). For the Gateway® cloning, the *E. coli* cultures were maintained on low-salt LB medium (1% w/v tryptone, 0.5% w/v yeast extract, 0.5% w/v NaCl, adjusted to pH 7) and Zeocin™ (50 μg/mL) for selection. The *E. coli* cultures were incubated at 37°C.

Saccharomyces cerevisiae W303-1A (MAT *a ade2-1 can1-100 ura3-1 leu2-3,112 his3-11,15 trp1*-1) (Thomas & Rothstein, 1989) was used for yeast expression studies and the lithium acetate method for yeast transformation (Agatep *et al.*, 1998; Gietz & Woods, 2002). Yeast strains were maintained in yeast extract peptone dextrose (YPD) medium (1% w/v yeast extract, 2% w/v bacteriological peptone, and 2% w/v glucose) or synthetic complete (SC) medium without the amino acids necessary for auxotrophic marker selection (Gietz *et al.*, 1997). Yeast cultures were incubated at 30°C.

For terpene analysis, either SC medium (complete with all the amino acids) was used, or SC drop-out medium without uracil (SC-URA) when continued selection was needed for the extra-chromosomal expression vectors. Where the induction of gene expression was required, glucose

41

was substituted with galactose (2% w/v) and raffinose (1% w/v). The yeast cells were cultured up to the exponential phase after which the cells were harvested and resuspended in galactose media with sampling 12 h after galactose induction. For terpene analysis, media was prepared in the same way as the SC media (described above), except that for these analyses, it was also buffered with citric acid (11 mM) and Na_2HPO_4 (44 mM) to pH 6 and with the addition of $MgSO_4$ (5 mM of Mg^{2+}) unless stated otherwise. For creation of the growth curve, the yeast cultures were grown in triplicate in 50 mL SC media in a 250 mL flask at 30°C with continuous agitation. Samples were taken from the cultures every 2 h for optical density (OD) measurements at 600 nm on a LAMDA25 UV/Vis Spectrophotometer (PerkinElmer, Waltham, MSA, USA).

Agrobacterium tumefaciens strain EHA105 (Hood *et al.*, 1993) was used for grapevine transformation and strain LBA4404 (Ooms *et al.*, 1981) for the transient expression of genes in *N. benthamiana*. *A. tumefaciens* culture conditions were maintained according to Wang (2006). To maintain the selection of both strains, rifampicin (10 µg/L) was added to the growth media. Electrocompetent *A. tumefaciens* preparation and transformation was based on a protocol outlined by Bach *et al.* (2014), with the only adaptation being the resuspension of the *A. tumefaciens* cells with ice-cold 1 mM HEPES buffer (Merck KGaA, Darmstadt, Germany) instead of water. MicroPulser™ electroporation apparatus (Bio-Rad Laboratories Ltd., Johannesburg, South Africa) was used for transformation according to the supplier's instructions. Transformation-positive colonies were selected through the addition of either 100 µg/L spectinomycin for the pART27 expression vectors or 50 µg/L kanamycin for the p19 and pCB355-GFP expression vectors.

2.2.2   Grapevine gene isolation

A previously characterised gene isolated from *V. vinifera* cv. Gewürztraminer, previously shown to encode a multi-product (-)-α-terpineol synthase, was targeted for isolation from *V. vinifera* cv. Sauvignon blanc (SB) in this study (Martin & Bohlmann, 2004). The predicted sequence for *GPS* (AY351862.1) publicly available on the NCBI database (https://www.ncbi.nlm.nih.gov/) was used as the template for primer design for *VviGPS* isolation from *V. vinifera* cv. Pinotage. Leaf tissue harvested from *V. vinifera* (cv. SB and cv. Pinotage) was used for total RNA extraction and cDNA synthesis according to the method described by Lashbrooke *et al.* (2013). The coding sequences of *VviTPS* and *VviGPS* were isolated from the synthesised cDNA by using gene-specific primer pairs (**Table A-i**).

All PCR products were amplified with the Expand High-fidelity PCR System (Merck). PCR-generated fragments were gel-purified and cloned into the pGEM-T Easy vector system according to the specifications of the supplier (Promega, Madison, Wisconsin, USA). Sequencing was performed with

42

an ABI Prism 3100 Genetic Analyser (Thermo Fisher Scientific, Wilmington, DE, USA) at the Central Analytical Facility, Stellenbosch University, South Africa.

2.2.3 Construction of expression vectors

The primers that were used for gene isolation and subsequent cloning into the expression vectors are listed in **Table A-i**. In addition, the vectors that were used are listed in **Table A-ii** with construction of the vectors described below.

Construction of the yeast expression cassette, containing a constitutive promoter for the integration of isolated *VviTPSs*, into the yeast genome was performed as follows. The *PGK1* promoter was amplified through PCR from a 2μ multi-copy expression vector (pCEL15) using PGK1p-5'/PGK1p-3' primers and cloned into pGEM-T Easy. Similarly, the URA3 fragment was amplified from YIplac211 (Gietz & Akio, 1988), using the primer pair ScURA3-5'/ScURA3-3', and cloned into pGEM-T-Easy to yield pGEM-URA3. An expression cassette containing the *MET25* promoter and the *CYC1* terminator was excised from p424MET25 (Mumberg *et al.*, 1994) and cloned into pBluescript SK II+ yielding pBS-METp. Following that, a *SspI*/*KpnI* fragment containing the URA3 gene was excised from pGEM-URA3 and cloned into the corresponding *SspI*/*Kpn*l sites of pBS-METp – yielding pBS-METp-URA3. The *PGK1p* promoter was also excised from pGEM-PGK1p as a *SspI*/*Xba*l fragment and cloned into the *Pvu*II/*Xba*l sites of pBS-METp-URA3 – yielding pBS-PGK1p-URA3 with the *PGK1* promoter replacing the *MET25* promoter. The *VviTPS* gene was excised from pGEM-TPSx with the restriction enzymes that are listed in **Table A-i** and cloned into the corresponding sites of pBS-PGK1p-URA3 to yield pBS-PGK1p-VvTPSx.

In order to increase the flux in the MVA pathway towards the terpene substrates, two *S. cerevisiae* genes were targeted for overexpression. The isopentenyl diphosphate isomerase gene (*IDI1*) (SGD accession: YPL117C) was isolated from *S. cerevisiae* genomic(g)DNA using the primer pairs IDI1-5'/IDI1-3' and cloned into the pGEM-T-Easy vector to yield pGEM-ScIDI1. The *IDI1* gene was excised from pGEM-ScIDI1 with *SalI* and cloned into the corresponding sites of pBS-PGK1p-URA3 to yield pBS-PGK1p-IDI1. The PGK1p-IDI1-CYCt expression cassette was amplified through PCR from pBS-PGK1-IDI1-URA3 and cloned into pGEM-T-Easy to yield pGEM-PGK1p-IDI1. The *ADE2* gene was PCR-amplified from gDNA extracted from a prototrophic yeast strain using the ADE2-5'/ADE2-3' primers and cloned into pGEM-T-Easy. The PGK1p-IDI1-CYCt expression cassette was excised from pGEM-PGK1p-IDI1-CYCt with *PvuII/SalI* and cloned into pGEM-ADE2 which had been digested with *Ec113611/SalI* to yield pGEM-PGK1p-IDI1-ADE2. The catalytic domain of 3-hydroxy-3-methylglutaryl coenzyme A reductase (tHMG1), encoded by *HMG1* gene (SGD accession: YML075C), was also amplified with PCR from *S. cerevisiae* gDNA using the primer pairs tHMG1-5'/tHMG1-3' and cloned into the pGEM-T-Easy vector to yield pGEM-tHMG1. The truncated *HMG1*

43

gene was excised from pGEM-tHMG1with *SalI* and cloned into the corresponding sites of pBS-PGK1p-URA3 to yield pBS-PGK1p-tHMG1. Finally, the PGK1p-tHMG1-CYCt expression cassette was excised from pBS-PGK1-IDI1-URA3 using *SspI/PstI* and cloned into YIplac128 (Gietz & Akio, 1988) to yield YIplac128-PGK1p-tHMG1.

In addition to the two yeast MVA pathway genes evaluated, a grapevine gene putatively encoding for geranyl diphosphate synthase (VviGPS) (NCBI accession: AY351862.1) was expressed in *S. cerevisiae*. A truncated version of the *VviGPS* was isolated which did not include the plastid targeting sequence. The TRP1 fragment was PCR-amplified from YIplac204 (Gietz & Akio, 1988) using the primer pair ScTRP1-5'/ScTRP1-3' and cloned into pGEM-T-Easy to yield pGEM-TRP1. An expression cassette containing the *MET25* promoter and *CYC1* terminator was excised from p424MET25 (Mumberg *et al.*, 1994) and cloned into pBluescript SK II+ yielding pBS-METp. In addition, an *SspI*/*KpnI* fragment containing the TRP1 gene was excised from pGEM-TRP1 and cloned into the corresponding sites of pBS-METp yielding pBS-METp-TRP1. The *MET25* promoter was replaced by the *PGK1p* promoter, as described above for the pBS-PGK1p-URA1 expression vector. The *VviGPS* truncated coding sequence was excised from pGEM-VviGPS with *SalI* and *SpeI* and cloned into the corresponding sites of pBS-PGK1p-TRP1 to yield pBS-PGK1p-VvGPS.

The coding sequence for the *VviTPS* used in this study was isolated from *Vitis vinifera* cv. SB and mapped to the *VviTPS39* gene model (Martin *et al.*, 2010) with the sequence analysis and annotation described in the following chapter. The predicted targeting sequence was removed from *VviSBTPS39* with the truncated version referred to as *VviSBTPS39*trunc, cloned into the Gateway® compatible yeast expression vector pAG426GAL (Alberti *et al.*, 2007). The Gateway® compatible plasmid, pDONR™/Zeo, was used as the entry vector (pEntry). The pDONR™/Zeo plasmid and the BP and LR clonases were acquired from Thermo Fisher Scientific. The yeast Gateway® vector kit was obtained from the Addgene plasmid repository (http://www.addgene.org/yeast_gateway) (Alberti *et al.*, 2007). The genes were amplified from pGEM-VviTPS via the two-step PCR protocol using the gene-specific primers and the universal adapter primers containing the Gateway® cloning adaptable *att*B sites (**Table A-i**). Phusion High-fidelity DNA Polymerase (Thermo Fisher Scientific) was used for amplification according to the manufacturer's instructions. PCR products were subjected to agarose gel electrophoresis and fragments were excised and purified with the Zymoclean™ Gel DNA Recovery Kit (Zymo Research Corporation, Irvine, CA, USA). DNA concentration was determined with a Nanodrop 2000 Spectrophotometer (Thermo Fisher Scientific).

Fragments with attached *att*B sites were cloned into pDONR™/Zeo with an overnight BP reaction according to the supplier's instructions and transformed into electrocompetent *E. coli* DH5α cells and streaked out onto the appropriate media. The pEntry clones were isolated with the GenElute plasmid

44

miniprep kit (Merck) and cloning was confirmed through restriction enzyme (RE) digestion and sequencing. Following confirmation of gene integration, the pEntry constructs were used to introduce the genes into the high-copy 2μ extra-chromosomal pAG426GAL yeast expression vector with an overnight LR reaction (**Table A-ii** in the Appendix to this chapter).

The construction of the *VviTPS39* plant expression vector was performed by excising the sequence from pGEM with *Sal*I and *EcoR*I and cloning it into the *Xho*I and *EcoR*I sites of pART7 (Gleave, 1992). In turn, the expression cassette with the inserted gene was sub-cloned from pART7-VviTPS into the corresponding *Not*I sites of pART27 to produce pART27-VviTPS with *VviTPS* under the control of the constitutive CaMV 35S promoter and nopaline synthase (NOS) terminator with the *npt*II gene for kanamycin selection (Gleave, 1992). A similar method was used to construct the vector containing *VviGPS* (**Table A-ii**). The sequences were excised from respective pGEM with *Xho*I and *EcoR*I and cloned into the corresponding RE sites of pART7. Finally, the expression cassette with the inserted gene was subcloned from pART7-VviGPS into the *Not*I sites of pART27 to give pART27-VviGPS. The plant expression constructs were transformed into *A. tumefaciens* as described in section 2.2.1.

2.2.4   Yeast transformation and genetic characterisation

The yeast expression vectors were transformed into *E. coli* and positive colonies were inoculated into LB broth with the addition of the appropriate selection antibiotic. Plasmids were isolated from the culture after incubation for 16 h and gene integration was verified with PCR screening, RE digestion, and sequencing. The integrating expression vectors were linearised in the selectable yeast marker with the appropriate RE, as listed in **Table A-ii**, before being transformed into the yeast. The various constructs were transformed into *S. cerevisiae* according to the method described in section 2.2.1. The genetic modifications that were made are summarised in **Table A-iii**.

PCR screening and northern hybridisation were used to confirm gene integration into the yeast genome. Total RNA and gDNA were isolated from *S. cerevisiae* as described by Hoffman and Winston (1987). RNA was removed from the gDNA isolations with RNase A treatment (0.1 mg/mL RNase A) and incubation at 37°C for 10 min. *S. cerevisiae* gDNA was subjected to PCR screening using GoTaq® DNA polymerase (Promega, Madison, Wisconsin, USA) with gene-specific primers (**Table A-i**) to verify transformation. Gel electrophoresis, RNA transfer, hybridisation, and detection were performed as described in the DIG application manual (Merck). Probes for northern hybridisations were randomly labelled with digoxigenin (DIG) high-prime (Merck) according to the supplier's instructions. The gene sequences of the various isolated genes were used as templates for the random labelling.

2.2.5 Grapevine transformation and genetic characterisation

The genetically transformed and established stable grapevine population ectopically expressing the *VviSBTPS39* gene was obtained from the transformation platform at the Institute for Wine Biotechnology (IWBT), Stellenbosch University. Briefly, the immature anthers were used to initiate somatic embryogenic cultures and transformed via *A. tumefaciens* strain EHA105 to yield putatively transformed lines of *V. vinifera* cv. Merlot according to the method described by Lashbrooke *et al.* (2013). After transformation, the transgenic callus culture was regenerated under kanamycin selection (100 µg/mL) on Murashige and Skoog (MS) medium (Murashige & Skoog, 1962) at 25°C under F36W/GRO fluorescent tubes (Feilo Sylvania Europe Ltd., Newhaven, UK) set at a long day (LD) cycle (16 h light, 8 h dark). The established population consisted of six putative transgenic lines with the *in vitro* plantlets and a population of untransformed controls maintained in tissue culture with clonal propagation on selection-free media after regeneration under selection.

For genetic characterisation of putative transgenic grapevine plantlets, gDNA extraction was performed according to the method described by Reid *et al.* (2006) followed by treatment with RNase A. Subsequently, PCR screening was performed with primers designed for the kanamycin-resistant gene and primers specific to the CaMV 35S promoter and the inserted gene (**Table A-i**). GoTaq® DNA polymerase (Promega) was used to confirm the integration of the expression cassette into the genome. Young healthy tissue, which included young leaves, stems, and tendrils, were harvested from putative transgenic plants (and controls) growing under greenhouse conditions for RNA extraction. Approximately 50 mg of plant tissue was homogenised in a mortar and pestle with liquid nitrogen and subjected for RNA extraction using the Spectrum™ Plant Total RNA Kit (Sigma-Aldrich, Saint-Louis, MO, USA) according to supplier's instructions. The RNA was eluted from the column with the elution buffer containing RiboLock™ RNase Inhibitor (Thermo Fischer Scientific) at the supplier's recommended concentration. Samples were stored at -80°C until later use for northern hybridisations and cDNA synthesis. For cDNA synthesis, the samples were treated with DNase I (Merck) and purified with the RNeasy Mini Protocol for RNA cleanup (Qiagen SA (Pty) Ltd., Johannesburg, South Africa) before cDNA synthesis was performed using the SensiFAST™ cDNA Synthesis Kit (Celtic Molecular Diagnostics (Pty) Ltd., Cape Town, South Africa).

For northern hybridisation, the conditions used were the same as those used for the genetic characterisation of the yeast strains (Section 2.2.4). The probes were generated via random labelling of the two *VviTPS* sequences as well as a fragment of *VviActin* (VIT_204s0044g00580) used as a positive control. In addition to northern hybridisation, transgene expression in grapevine was also verified through PCR screening of prepared cDNA samples using gene-specific primers in combination with the *VviActin* primers as a positive control (**Table A-i**).

The confirmed transgenic grapevine plantlets were hardened off by cutting the growth point just below the first two leaves and transferring it into Grodan rockwool plugs (Grodan A/S, Denmark) hydrated with a solution of dH$_2$O and 0.1% (v/v) Sporekill (Hygrotech, Pretoria, South Africa) in clear plastic tubs with lids. The lids were kept closed until plantlets had started to form roots, after which the lids were gradually opened. The plants were fertilised with 0.5% (w/v) Nutrifeed (Starke Ayres, South Africa) suspended in dH$_2$O every two weeks. During the hardening-off process, the plants were grown at 26°C with a LD photoperiod under F36W/GRO fluorescent tubes (Feilo Sylvania Europe Ltd.). The plants were subsequently transferred into a peat:potting soil:perlite:vermiculite (1:1:1:1) mixture treated overnight with a 1% (v/v) Sporekill (Hygrotech) solution and fertilised every two weeks with 0.5% (v/v) Nitrosol natural organic plant food (Efekto, Isando, South Africa). After being acclimatised to the soil mixture, the plants were moved to greenhouse conditions under natural light with the temperature maintained below 30°C and watering according to need.

2.2.6   *Agrobacterium tumefaciens* infiltration of tobacco for transient expression studies

Nicotiana benthamiana seeds were sown directly onto Hygromix:Vermiculite (1:1) pretreated with 1% (v/v) Sporekill® (Hygrotech) and grown at 26°C with LD photoperiod under F36W/GRO fluorescent tubes (Sylvania, Erlangen, Germany) and humidity maintained at ≥50% with a humidifier during the light hours. The seedlings were kept well-watered and fertilised with 0.5 g/L Hygrofert (Hygrotech) every two weeks. Plants were ready for infiltration when five to six mature leaves had formed.

For agroinfiltration, *A. tumefaciens* freeze cultures were streaked out onto LB medium containing the appropriate antibiotics (10 μg/mL rifampicin and 100 μg/mL spectinomycin or 50 μg/mL kanamycin) and incubated at 25°C for 3 to 4 days. After this, 10 to 15 single colonies were used to inoculate 50 mL LB (with the appropriate antibiotics) in 250 mL flasks and incubated with continuous agitation at 25°C for 18 to 20 h at which time the culture had reached an OD$_{600}$ ≥1. The cells were harvested through centrifugation (2500 RCF for 15 min) and washed three times with 0.9% (w/v) NaCl to remove all the antibiotics. The cells were then resuspended in MMA (10 mM MES hydrate [2-[N-morpholino] ethanesulfonic acid hydrate] pH 5.6 with NaOH, 10 mM MgCl2, 200 μM acetosyringone [freshly prepared 200 mM stock solution in DMSO]).

Based on the results (not shown) of the agroinfiltration with the pCB355-GFP construct (M Campa, unpublished), a protocol was developed for transient expression. The OD$_{600}$ was measured, and the cultures were incubated for at least 1 h with continuous agitation at room temperature before infiltration. *A. tumefaciens* cultures were diluted to OD$_{600}$=0.5 for infiltration. For co-expression studies where *VviSBTPS39* and *VviGPS* were co-infiltrated, the two cultures were mixed at equal densities to a final combined OD$_{600}$=0.5. An *A. tumefaciens* culture containing the p19 construct was

included in each infiltration mixture to enhance transgene protein expression levels (Silhavy *et al.*, 2002). As a control, some of the leaves were infiltrated with *A. tumefaciens* containing the pCB355-GFP construct and fluorescence was detected using the longwave UV-A (365 nm) setting of the SPECTROLINE® ENF-260C lamp (SPECTROLINE®, Westbury, NY, USA). Infiltration with an *A. tumefaciens* culture containing an empty expression cassette in pART27 was used as the negative control. Young, fully expanded *N. benthamiana* leaves were pressure-infiltrated using a 1 mL syringe without a needle and harvested at day 4 after infiltration. To reduce any variability between the various plant populations, the growth conditions were kept consistent, and plants of similar size and leaf ages were selected for infiltration with sampling on day 4 after infiltration.

2.2.7 Terpene analysis

Volatile terpene analysis was conducted using headspace (HS) solid phase microextraction (SPME) coupled with gas chromatography (GC) – mass spectrometry (MS) with the analytical method adapted for various purposes during the study. Unless otherwise mentioned, the control used during the yeast expression studies was a yeast strain with the same modifications of the MVA pathway genes as the yeast expressing the *VviTPS*.

2.2.7.1 Total potential volatile terpene analysis

For the analysis of the yeast cultures, pre-warmed media flasks were inoculated to an $OD_{600}=0.1$ from an overnight culture and grown for ~ 24 h at 30°C with continuous agitation. For sampling, 5 mL of the yeast culture was added to 20 mL SPME vials with 3-octanol (Merck) as an internal standard (IS) at a final concentration of 50 µg/L. The vials were incubated at 100°C for 1 h and allowed to cool to room temperature before being placed in the autosampler. The sample vial was pre-incubated for 5 min at 60°C in the autosampler heating chamber and agitated at 250 rpm. After the equilibration, the 50/30 µm grey DVB/CAR/PDMS SPME fibre (Merck), pre-conditioned according to the manufacturer's specifications, was inserted into the vial through the septa. The fibre was exposed to the sample headspace (HS) for 30 min at 60°C with constant agitation of the vial at 250 rpm.

The sample preparation method described by Moyo (2017) was used for grapevine tissue culture plants that were homogenised with liquid nitrogen. In addition to the 2 mL tartaric acid buffer containing 50 µg/L 3-octanol (Merck) as an IS, 500 mg of NaCl was also added to the 20 mL SPME vial before being sealed with a polytetrafluorothylene (PTFE) septa cap (Merck) and heat treatment at 100°C.

Separation and detection of compounds were performed on an Agilent 6890N GC system using the Agilent DB-FFAP capillary column (60 m × 0.25 mm × 0.5 µm) coupled to a CTC CombiPal Analytics

48

autosampler and an Agilent 5975B inert XL EI/CI MSD mass spectrometer detector through a transfer line (Chemetrix Export (Pty) Ltd., Johannesburg, South Africa). Desorption of the DVB/CAR/PDMS SPME fibre was performed in the injection port at 250°C in pulsed splitless mode for 20 min. The purge flow was set at 50 mL/min for 1 min and the column operating head pressure was raised from 111 KPa to obtain a pulse pressure of 300 KPa for 1 min. Helium was used as carrier gas with a constant flow rate of 1 mL/min. The oven parameters were as follows: the initial temperature was set at 40°C and maintained for 2 min, followed by a linear increase to a final temperature of 240°C at a rate of 5°C/min, after which the temperature was held at 240°C for 2 min with a total run time of 44 min.

Detection was performed in electron impact mode (EIM) (70 eV) and operated in selected ion monitoring (SIM), utilising the mass spectra of the authentic standards analysed, and scan mode. The scan parameters were set at *m/z* ranging from 35 to 350. The SIM parameters for monoterpenes and the IS were set based on the ion fragmentation of the selected terpene standards with the dwell time for each selected ion set between 30 and 100 ms. MSD ChemStation E.02.01.1177 software (Agilent, Santa Clara, USA) was used for data processing.

2.2.7.2   *Volatile terpene analysis of the accumulated headspace*

The effects of the genetic modifications of the MVA pathway in yeast as well as the impact of high temperature before and during terpene analysis were studied using the following sample preparation method. The terpene analysis media was inoculated to an OD_{600} of 0.1 and 10 mL aliquots representing biological repeats of inoculated media were added to 20 mL SPME vials and sealed with PTFE septa caps (Merck) with 50 µg/L 3-octanol (Merck) used as an IS. The vials were placed on a rotating wheel and incubated at 30°C for ~12 h. The cultures were sampled for OD_{600} readings using a sterile needle and syringe. To inhibit further yeast growth, natamycin was used as an antifungal agent. Delvo®Cid (DSM Food Specialties, Heerlen, Netherlands) was dissolved in 0.1 M NaOH at 40 mg/mL and injected into the vials to a final concentration of 1 mg/mL (equivalent to 0.5 mg/mL natamycin). The vials were kept at room temperature until analysis. To study the effect that high temperatures before extraction might have had on the monoterpene composition, the vials were incubated at 100°C for 1 h and allowed to cool down to room temperature before analysis.

When the effect of extraction temperature on monoterpene levels was studied, the temperature was increased to 60°C from 30°C. Extraction, separation, and detection of compounds were performed as described in the previous section, except for a decrease in extraction temperature from 60°C to 30°C (unless otherwise stated) and an increase in the holding time of final temperature during GC runs from 2 to 5 min at 240°C with a resulting increase of the total GC runtime to 47 min.

49

2.2.7.3   Volatile terpene analysis for profile determination

The yeast strain expressing the episomal Gateway® expression vector was used for these analyses. Galactose induction was based on a method described by Ignea *et al.* (2011). An overnight pre-culture grown in 2% (w/v) glucose SC-URA medium (with buffering but without added $MgSO_4$) was used to inoculate 100 mL of the same media in a 250 mL flask to an OD_{600} of 0.1The culture was grown for approximately 7 h at 30°C with continuous agitation until an OD_{600} reading of 0.5 to 0.7 (exponential phase) was reached. At that point, the 100 mL culture was divided in half, 50 mL for galactose induction and the other half was kept in glucose medium as control. The yeast cells were harvested through centrifugation at 2500 RCF for 5 min and washed twice with a 0.9% (w/v) NaCl solution. The yeast cells were resuspended in either 50 mL 2% (w/v) galactose with 1% w/v raffinose SC-URA medium for induction, or 50 mL 2% (w/v) glucose SC-URA medium for a negative control in 250 mL flasks. The cultures were then incubated at 30°C with continuous agitation for 12 h until sampling. First, an OD_{600} reading was taken for normalisation before 10 mL of the culture, 3 g NaCl, and Anisole-d_8 (Merck) at a final concentration of 7.5 µg/L as an IS were added into 20 mL SPME vials and sealed with screwcaps with Macherey-Nagel™ silicone/PTFE septa (Thermo Fisher Scientific). Samples were agitated at 30°C for 60 min before being placed in the autosampler.

For the sample preparation of agroinfiltrated *N. benthamiana* leaves, the method that was described above for the terpene analysis of grapevine tissue was used for homogenised tissue with the following adjustments. The leaves were harvested and homogenised with liquid nitrogen: approximately 300 mg of the frozen tissue was weighed into a 20 mL SPME vial and 2 mL of the tartaric acid buffer with 100 µg/L 3-octanol and anisole-d_8 (Merck) with 500 mg NaCl were added to each vial. The contents were mixed well before being placed on the autosampler for analysis. The fibre was exposed to the sample HS for 60 min at 35°C with agitation at 250 rpm. In addition, volatiles from whole leaves were analysed based on the whole-leaf SPME methods described by Aharoni *et al.* (2003) and Bach *et al.* (2014). Two to three leaves were cut at the petiole and placed into 20 mL a clear SPME vial containing 2 mL dH_2O, taking care not to damage the leaves and ensuring that the upper part of the vial was not obstructed. The vials were sealed with Macherey-Nagel™ silicone blue tr./PTFE septa screwcaps (Thermo Fisher Scientific) and kept in the growth room for at least 24 h before the HS volatiles were analysed. Conditions for volatile extraction and analysis for *N. benthamiana* tissue were the same as described for the yeast cultures, except for increasing the extraction time from 30 to 60 min and omitting the addition of IS.

The sample vial was pre-incubated for 2 min at 30°C without agitation. After equilibration, the 50/30 µm grey DVB/CAR/PDMS SPME fibre (Merck), pre-conditioned at 250°C for 1 min, was inserted into

the vial through the septa. The fibre was exposed to the sample HS for 40 min at room temperature without agitation.

The separation and detection of compounds were carried out on an Agilent 7890N GC system coupled to a CTC CombiPal Analytics auto-sampler and an Agilent 5977B inert XL EI/CI MSD mass spectrometer detector through a transfer line. Separation was performed using the HP-5MS (Agilent) capillary column (30 m × 250 μm × 0.25 μm). Desorption of the DVB/CAR/PDMS SPME fibre was performed in the injection port at 250°C in pulsed splitless mode for 5 min. The fibre was maintained in the injection port for 5 min for cleaning. The purge flow was set at 15 mL/min for 0.75 min. Helium was used as carrier gas with a constant flow rate of 1 mL/min. The oven parameters were as follows: the initial temperature was set at 40°C and maintained for 2 min, followed by a linear increase to a final temperature of 240°C at a rate of 8°C/min, held for 2 min with a total run time of 29 min. A solvent delay of 2.6 min was programmed to avoid the detection of acetonitrile. Detection was performed in EIM (70 eV) with the scan parameters set at m/z ranging from 35 to 350.

The following authentic standards were used for compound identification and absolute quantification: myrcene, α-terpinene, (-)-terpinen-4-ol, α-terpineol, γ-terpinene, R-(+)-β-citronellol, eucalyptol (1,8-cineole), R-(+)-limonene, and ± linalool (Merck).

2.2.8   Data analysis

MassHunter MS Qualitative and Quantitative software (Version B.07.00, Agilent) was used for the identification and relative quantification of GC-MS peaks. For unknown compounds, the initial identification was done by comparing the mass spectra to the United States National Institute of Standards & Technology (NIST) and Wiley275.L mass spectral libraries. Relative quantification of peaks was carried out through selected ion count (SIC) of characteristic ions. Absolute quantification of compounds was performed through external standard calibration based on standard curves that were plotted using the peak areas of each standard relative to the peak area of the IS versus the concentration (μg/L) of a standard dilution series in the control culture using the same method. The resulting concentrations in μg/L were normalised to the cell count (OD_{600}). The Kovats index (KI) for temperature-programmed chromatography was determined for all identified compounds using the retention times of 0.1 μg/mL C7 – C40 saturated alkane mixture (Sigma-Aldrich). As a further compound identification method, the calculated KIs were compared to KIs from previous studies that were determined by using the same column.

The data were analysed with the following software: SIMCA® (version 16, Sartorius Stedim Biotech, Göttingen, Germany), Microsoft Office Excel 2016 (Microsoft Corporation, Redmond, WA, USA) and Statistica™ (version 13.2, Dell, Round Rock, USA).

2.3   Results

2.3.1   Yeast expression system

2.3.1.1   Volatile analysis of VviTPS in Saccharomyces cerevisiae

The full-length *VviSBTPS39* cDNA was cloned into a yeast expression vector containing the constitutive *PGK1* promoter and the *CYC1* terminator (**Table A-ii**), and the expression cassette was integrated into the genome of an *S. cerevisiae* W303-1A strain (**Table A-iii**). PCR screening of yeast gDNA verified successful transformation and gene expression was confirmed by northern hybridisation (results not shown).

To determine TPS functionality in the expression system, an HS-SPME GC-MS method was used in combination with a sample preparation method that included heat treatment of samples coupled with high extraction temperatures during analysis to determine the terpene-producing potential. High temperature before and during extraction increases signal intensity and has the advantage of thermally lysing the yeast cells and releasing cell contents (Čajka *et al.*, 2007; Robinson *et al.*, 2011; Islam *et al.*, 2017). The volatile data are presented in **Table B-i** and peak identification was confirmed with authentic standards where possible.

Comparative analysis of the terpenes detected in the yeast cultures showed a clear difference in the *VviTPS*-expressing strain relative to the control strain that was transformed with an empty vector (**Figure 2.2**). Various monoterpenes were produced by the *VviSBTPS39*-expressing strain that were not detected in the control yeast strain culture. Two peaks, identified as (-)-terpinen-4-ol and putatively as γ-terpinene, showed the highest peak areas. A peak identified as α-terpineol was also present in the *VviSBTPS39*-expressing yeast strain culture. However, the peak area was very small in comparison to the other monoterpene peak areas and was also detected in the control yeast culture.
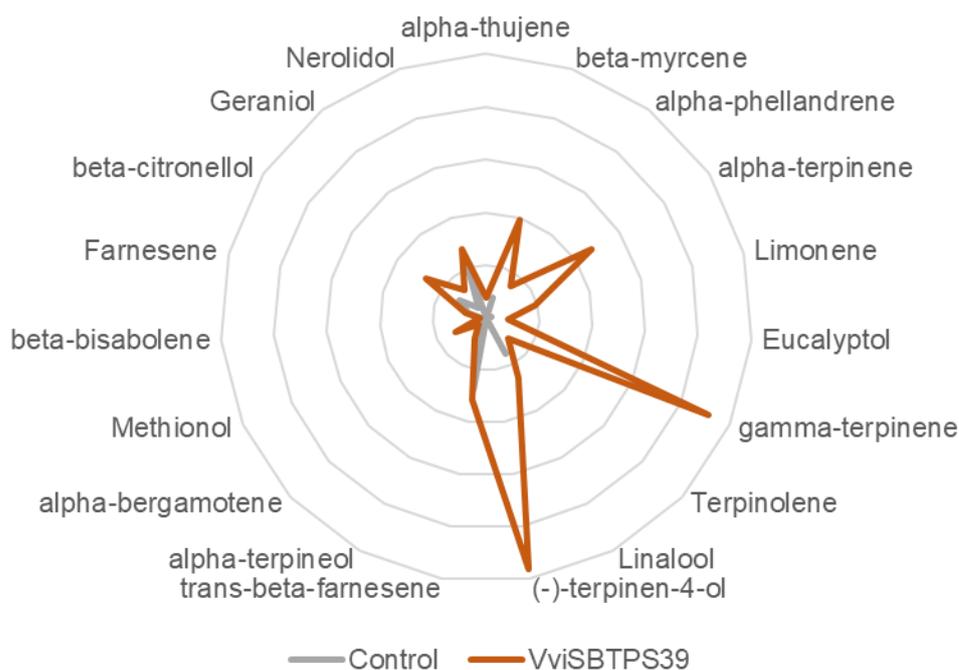
Figure 2.2 Terpene analysis results of the yeast culture heterologously expressing *VviSBTPS39* (dark orange line) in comparison to the control yeast culture (grey line). The average peak area (selected ion count) normalised to the IS (3-octanol) and the cell count (OD_{600} reading) is shown.

2.3.1.2 *Improvement of the yeast expression system for functional characterisation of heterologous terpene synthases*

The VviSBTPS39 yeast system produced several unique monoterpenes that were not detected in the control strain culture (as illustrated in **Figure 2.2**). The system was therefore used to evaluate certain aspects of the sample preparation system, discussed below, to minimise artefacts in monoterpene profiles. These steps were important to ensure that the terpene profile produced via the heterologous expression system is an accurate representation of the TPS enzyme activity in its native environment. The optimisation of monoterpene production in yeast was also assessed.

2.3.1.2.1 Effects of temperature on the monoterpene profile

Aiming to determine the effects of high temperature on the monoterpene profile before and during extraction, samples were either left untreated or subjected to a temperature of 100°C for 1 h before extraction, with SPME performed at 30°C or 60°C (**Table C-i**). The monoterpene compounds were broadly divided into four clusters (A to D) based on the effect that temperature had on the relative peak percentage before and during extraction.

The relative peak area percentage of α-thujene, β-pinene, sabinene, and α-phellandrene (Cluster A) decreased with heat treatment as well as 60°C extraction temperature. A reciprocal increase in the

peak area percentages of linalool, (-)-terpinen-4-ol, α-terpineol, β-citronellol and geraniol (Cluster C) was observed.

Cluster B consisted of monoterpene compounds that showed an intermediate response to the 60°C extraction temperature and the heat treatment before extraction. Heat treatment increased the relative peak area if the extraction was performed at 30°C for all the monoterpenes in cluster B except for β-phellandrene, which did not show a significant change. However, the compounds reacted inconsistently with the other combinations of heat treatment and extraction temperatures. Increased extraction temperature resulted in lower peak area percentages for β-myrcene, α-terpinene, and limonene where the samples underwent heat treatment beforehand. Without the pre-treatment, either no significant differences were observed, or the relative peak area was slightly increased (e.g., limonene). The relative peak area for β-phellandrene was only altered with an increase in extraction temperature where the samples had been subjected to heat pre-treatment. The peak area percentage of ρ-cymene remained stable except for an increase observed in untreated samples extracted at 60°C compared to 30°C.

The two compounds subdivided into Cluster D showed an increase in peak area with heat treatment when extracted at either 30°C or 60°C in comparison to the untreated samples. Increased extraction temperature had a positive effect on the relative peak area only when no heat treatment was done.

The sesquiterpene compounds, nerolidol and farnesol, were detected with the 60°C extraction temperature only. Heat treatment beforehand resulted in a decrease in the farnesol peak area together with an increase in the peak area of nerolidol.

The rearrangement pathway for sabinene, as proposed by Wrolstad & Jennings (1963), was used to provide context to the volatile analysis results from this study at different temperatures. The relative peak areas (expressed as a percentage of the total monoterpene peak areas) of the shared compounds in the context of the degradation pathway is shown in **Figure 2.3**. The low extraction temperatures that were applied without heat pre-treatment of samples resulted in the highest ratio to total monoterpenes of sabinene and α-thujene. In contrast, heat treatment in combination with high extraction temperatures lowered the relative ratio of these two compounds the most, leading to a higher ratio of other compounds further down in the proposed degradation pathway **Figure 2.3**. These results show that heat pre-treatment results in the degradation of sabinene and α-thujene into other monoterpenes.
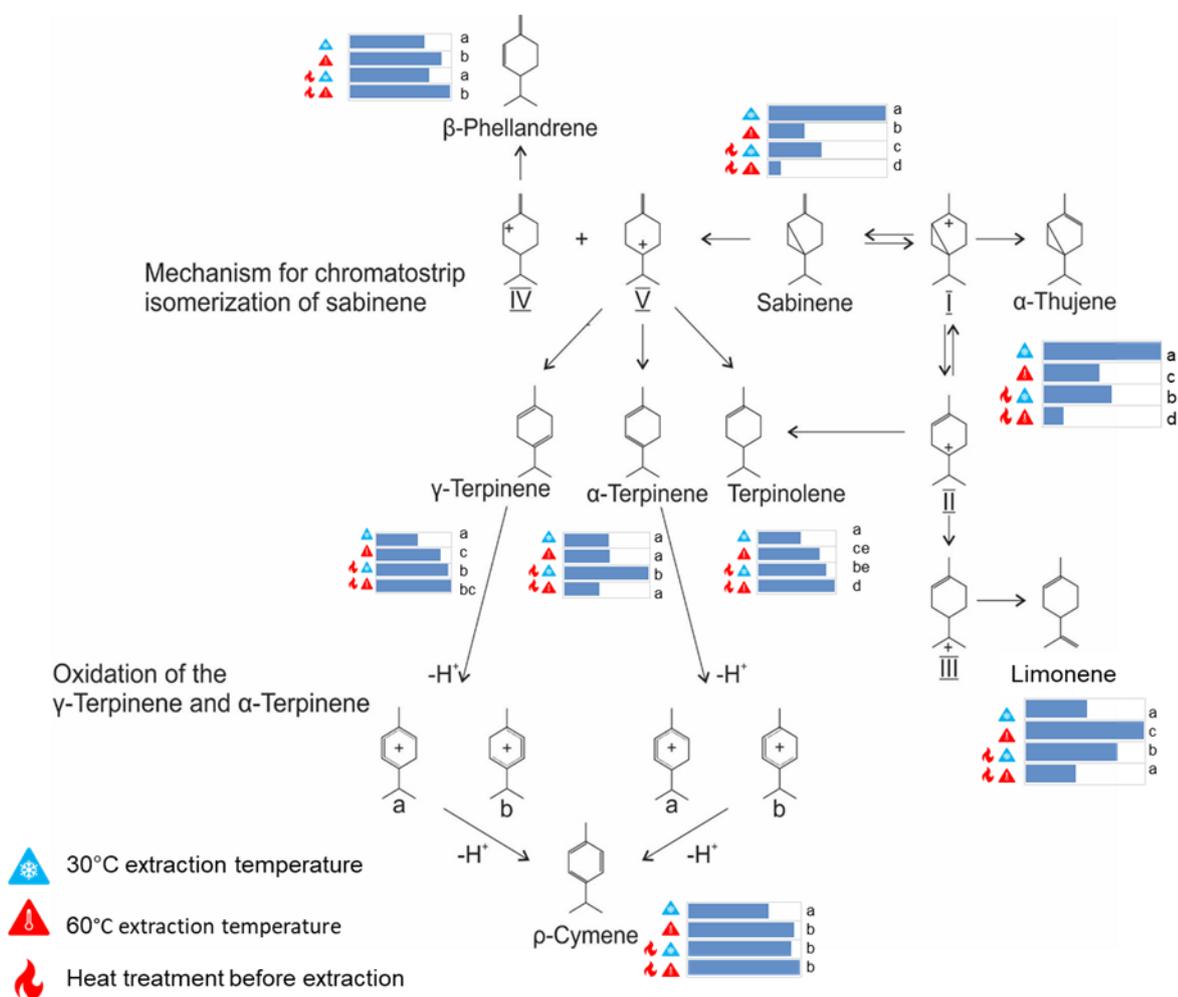
Figure 2.3 Proposed rearrangement pathway adapted from Wrolstad and Jennings (1963) with the peak area percentage of the various compounds relative to the total monoterpene peak area shown when samples are analysed at two different SPME extraction temperatures (30° and 60°C) as well as when samples are treated at 100°C for 1 h before SPME (heat treatment). Formation of a cyclopropylcarbonyl (I) through attack of a hydrogen ion on the exocyclic double bond. α-thujene is formed by the loss of a hydrogen ion while the breakage of the 3-membered ring results in a tertiary carbonium ion (II) being formed with dehydrogenation leading to the formation of terpinolene, γ-terpinene, and α-terpinene. The transfer of a hydrogen ion from carbon number 8 to 4 of II forms a carbonium ion (III) from which limonene and terpinolene can be formed. β-phellandrene can be formed through the breakage of the 3-membered ring of sabinene that results in the formation of two carbonium ions (IV and V). Hydrogen loss from IV results in β-phellandrene while dehydrogenation of V with isomerisation of the double bond can lead to the formation of terpinolene, γ-terpinene, and α-terpinene. Oxidation of γ-terpinene and α-terpinene is attributed to the formation of ρ-cymene. Significant differences ($p<0.05$) determined with student t-test are shown next to bar graph with letters.

The most pronounced effect that the high temperatures before and during extraction had on the monoterpene profile was that the compounds with lower volatility (higher retention time), had increased peak area ratios. Based on these results, all subsequent analyses for terpene profiling and quantification were carried out at low extraction temperatures (30 to 35°C) without heat pre-treatment. However, omitting the heat treatment of samples before analysis does mean that only the non-glycosylated terpenes were analysed.

55

2.3.1.2.2 Engineering of the MVA pathway in yeast and removal of the plastid-targeting sequence

Volatile terpene analysis was used to evaluate the MVA pathway optimisation steps, using the *VviSBTPS39* gene as an indicator monoterpene synthase (**Table D-i**). The impact of the removal of the targeting signals from *VviSBTPS39* is presented in **Table D-ii**.

To determine whether the production of monoterpenes affected normal cell functioning, growth curves were created for the yeast strain overexpressing *ScIDI1* – either with the empty vector (negative control) or in conjunction with *VviSBTPS39* under the control of the constitutive *PGK1* promoter. There were no significant differences between the growth dynamics of the monoterpene-producing strain and the control strain (**Figure 2.9**).

Individual overexpression of *SctHMG1, ScIDI1*, and *VviGPS* in conjunction with *VviSBTPS39* did not result in significantly different levels of the total monoterpene peak areas when normalised to cell count. However, the normalised peak areas of some of the monoterpenes were significantly higher in the yeast strain overexpressing *IDI1* in combination with *VviSBTPS39.* The same trend was observed in the combinatorial overexpression of *tHMG1, IDI1*, and *VviSBTPS39*, which resulted in higher normalised peak areas of some monoterpenes but not the total monoterpene peak area. The only combination that resulted in significantly ($p < 0.05$) higher levels of the total normalised monoterpene peak area was seen in the strain that was overexpressing *IDI1, VviGPS*, and *VviSBTPS39,* which had a threefold increase in the total monoterpene area compared to the strain that was overexpressing *VviSBTPS39* only (**Table D-i**). Removal of the targeting sequence from *VviSBTPS39* significantly ($p < 0.05$) increased the normalised total monoterpene peak area (**Table D-ii**).

The results of the various MVA pathway manipulations in combination with *VviSBTPS39* expression as well as the removal of the predicted targeting sequence from *VviSBTPS39* are summarised in **Figure 2.4**. The various points in the MVA pathway that were targeted, are highlighted in the figure. The total monoterpene peak area (normalised to the IS and cell count) expressed as a percentage of the control are also presented. As indicated in **Figure 2.4**, the co-expression of *IDI1* and *VviGPS* with *VviSBTPS39* significantly increased the total monoterpene peak area. Removal of the targeting sequence also had a significant impact on this increase.
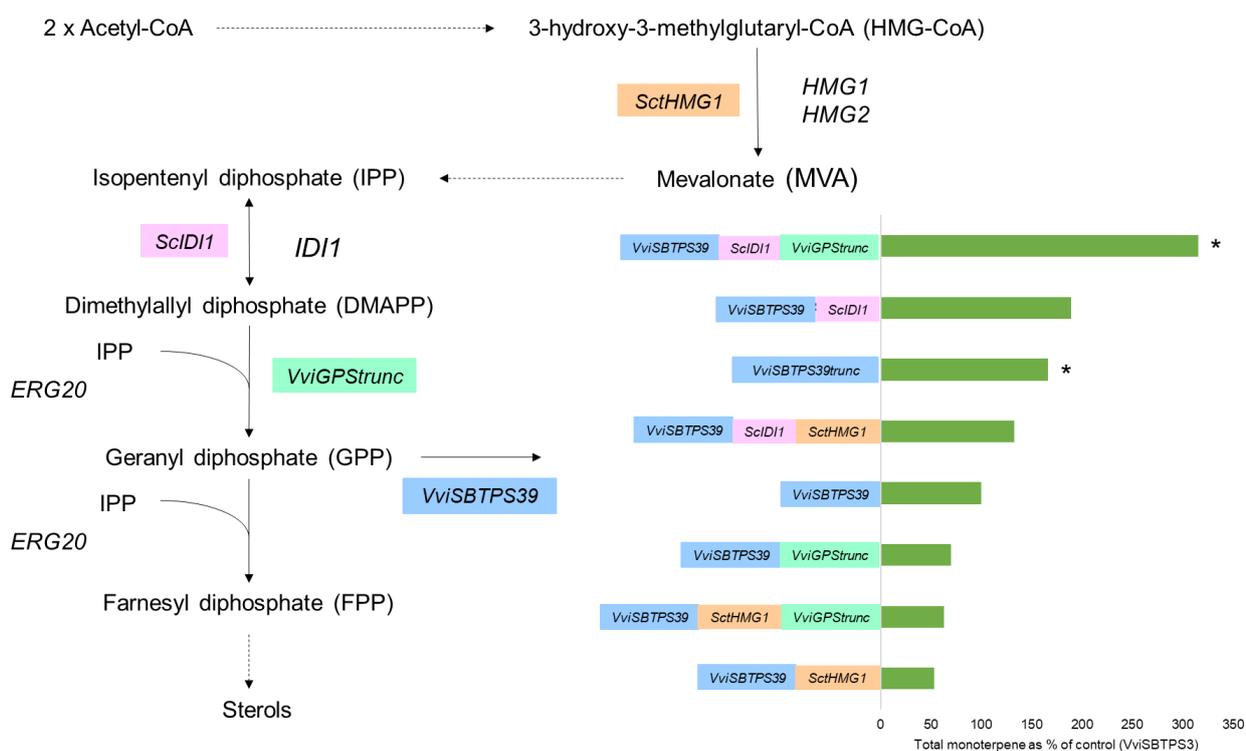
Figure 2.4 Simplified diagram of the mevalonate (MVA) pathway in *Saccharomyces cerevisiae* summarising the results from the MVA pathway manipulation investigated in this study. The genes encoding the enzymes responsible for catalysing the reactions in yeast are shown in italics. Dotted lines indicate multiple reactions. The points in the pathway that were targeted with genetic modification are shown in different coloured boxes. Two endogenous yeast genes and one grapevine gene were overexpressed in combination with the grapevine terpene synthase (*VviSBTPS39*) with the aim of increasing the heterologous monoterpene production. These genes included a truncated version of 3-hydroxy-3-methylglutaryl coenzyme A reductase (*SctHMG1),* isopentenyl diphosphate isomerase (*ScIDI1*) and a truncated geranyl diphosphate synthase (*VviGPS*). In addition, the full-length *VviSBTPS39* and a truncated version of the grapevine gene (*VviSBTPS39trunc*) were also compared. The effect of the various genetic optimisations on the total monoterpene peak area (normalised to the IS and cell count) as a percentage of the control (yeast strain expressing full-length *VviTPS39*) is shown in the green bar graph with significant differences (student's *t*-test with p < 0.05) between triplicates indicated with asterisks.

2.3.2   Plant expression systems

2.3.2.1   *Ectopic expression of VviTPSs in grapevine*

2.3.2.1.1 Genetic characterisation of grapevine population

The results of the genetic characterisation of the grapevine population transformed via *A. tumefaciens* with *VviSBTPS39* under the control of a constitutive promoter are summarised in **Table 2.1**. Transgene integration was determined with PCR screening using gDNA as template and primers specific to the pART27 construct (**Table A-i**). The results for the transformed grapevine population indicate that all the lines were successfully transformed with the expression vector containing *TPS*. Gene expression was determined with northern hybridisation with gene-specific probes and PCR

screening of cDNA using gene-specific primers. Probes and primers specific to the actin gene (VIT_204s0044g00580) in *V. vinifera* were used as the positive control (**Table A-i**). Based on these results the grapevine population transformed with *VviSBTPS39* showed no detectable transgene expression.

Table 2.1 Summary of the genetic characterisation of the *V. vinifera* cv. Merlot population transformed with *VviSBTPS39.*

Transgenic lines	Gene integration		Gene expression			
	nptII PCR with gDNA	CaMVp & VviTPS27 PCR with gDNA	Northern blot with actin probe (control)	Actin PCR with cDNA (control)	Northern blot with VviTPS27 probe	VviTPS27 PCR with cDNA
Merlot_#WT	-	-	+	+	-	-
Merlot_#3	+	+	+	+	-	-
Merlot_#5	+	+	+	+	-	-
Merlot_#6	+	+	+	+	-	-
Merlot_#12	+	+	+	+	-	-
Merlot_#19	+	+	+	+	-	-
Merlot_#25	+	+	+	+	-	-

2.3.2.1.2 Volatile analysis of the grapevine population

Metabolic characterisation of the plant population was performed through volatile analysis of tissue culture plants. Various compounds were detected in the control as well as the transformed plants, most of which were monoterpenoids in addition to a few norisoprenoids. Interestingly, no sesquiterpenes could be detected with the analysis method that was used (**Table F-i**). Orthogonal projections to latent structures discriminant analysis (OPLS-DA) was subsequently performed using the normalised peak areas as variables to determine which variables, if any, drove the separation between the control and transgene plant populations. Interestingly, separation was seen between the control plants and the lines transformed with *VviSBTPS39* (**Figure 2.5**) even though ectopic overexpression could not be detected during genetic characterisation (**Table 2.1**).
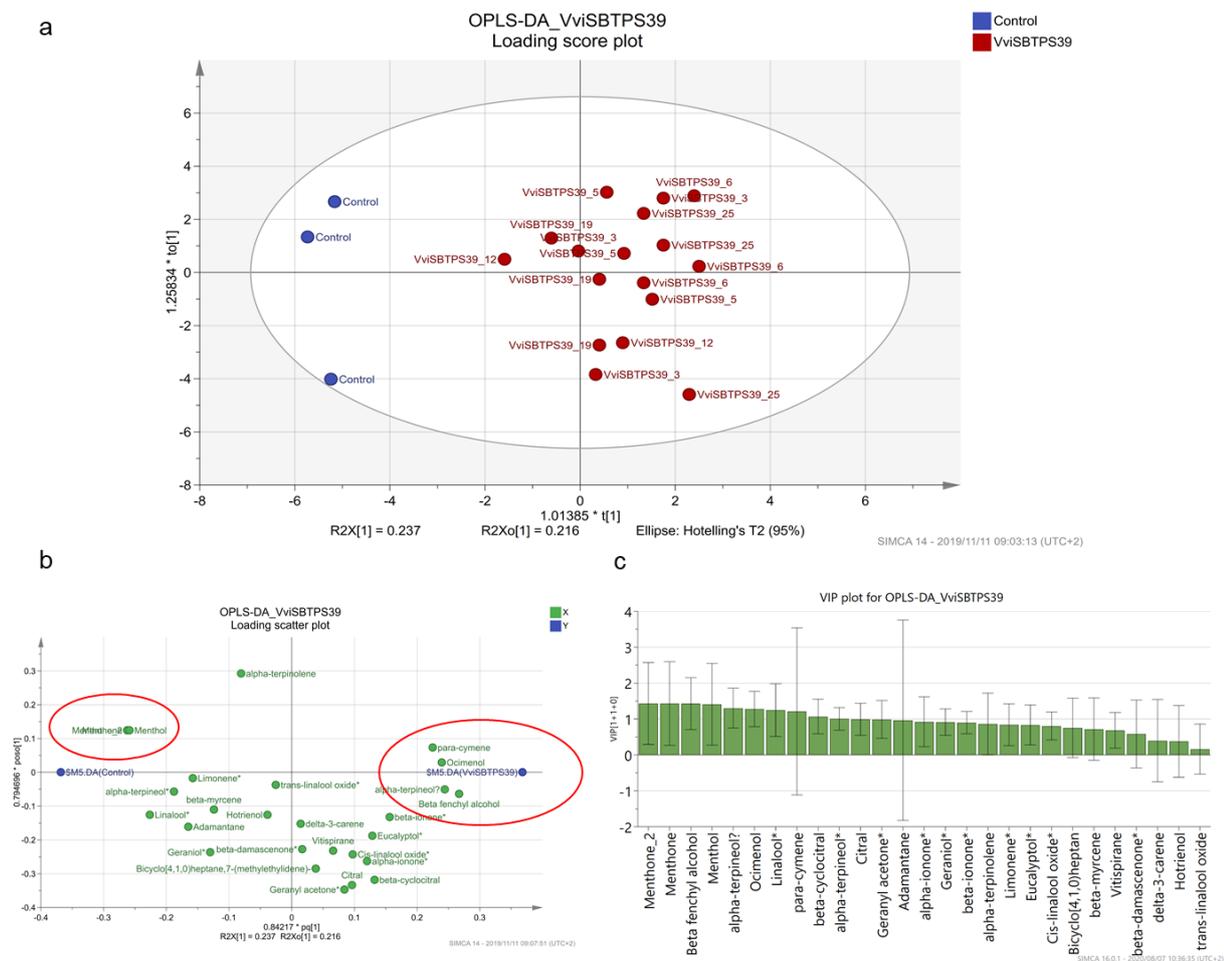
Figure 2.5 Orthogonal projections to latent structures discriminant analysis (OPLS-DA) of volatiles detected in tissue culture plants of *Vitis vinifera* L. cv. Merlot transformed with *VviSBTPS39*, in comparison to untransformed plants. The loading score plot (a) indicates the grouping of the samples while the loading score plot (b) indicates the variables that drove the separation between the samples (a).

The variables shown to drive the separation between the control plants and plants transformed with *VviSBTPS39*, are circled in red (Figure 2.5b). The population transformed with *VviSBTPS39* showed increased levels of the peaks putatively identified as ρ-cymene, α-terpineol-like (peak identity unconfirmed with authentic standard), β fenchyl alcohol, and ocimenol (Figure 2.6a to 6d). Significantly higher levels of the peaks putatively identified as menthone (two peaks), linalool (peak identity confirmed with authentic standard), menthol, and α-terpineol (peak identity confirmed with authentic standard) (Table F-i) were detected in the control plants compared to both transformed populations.

59
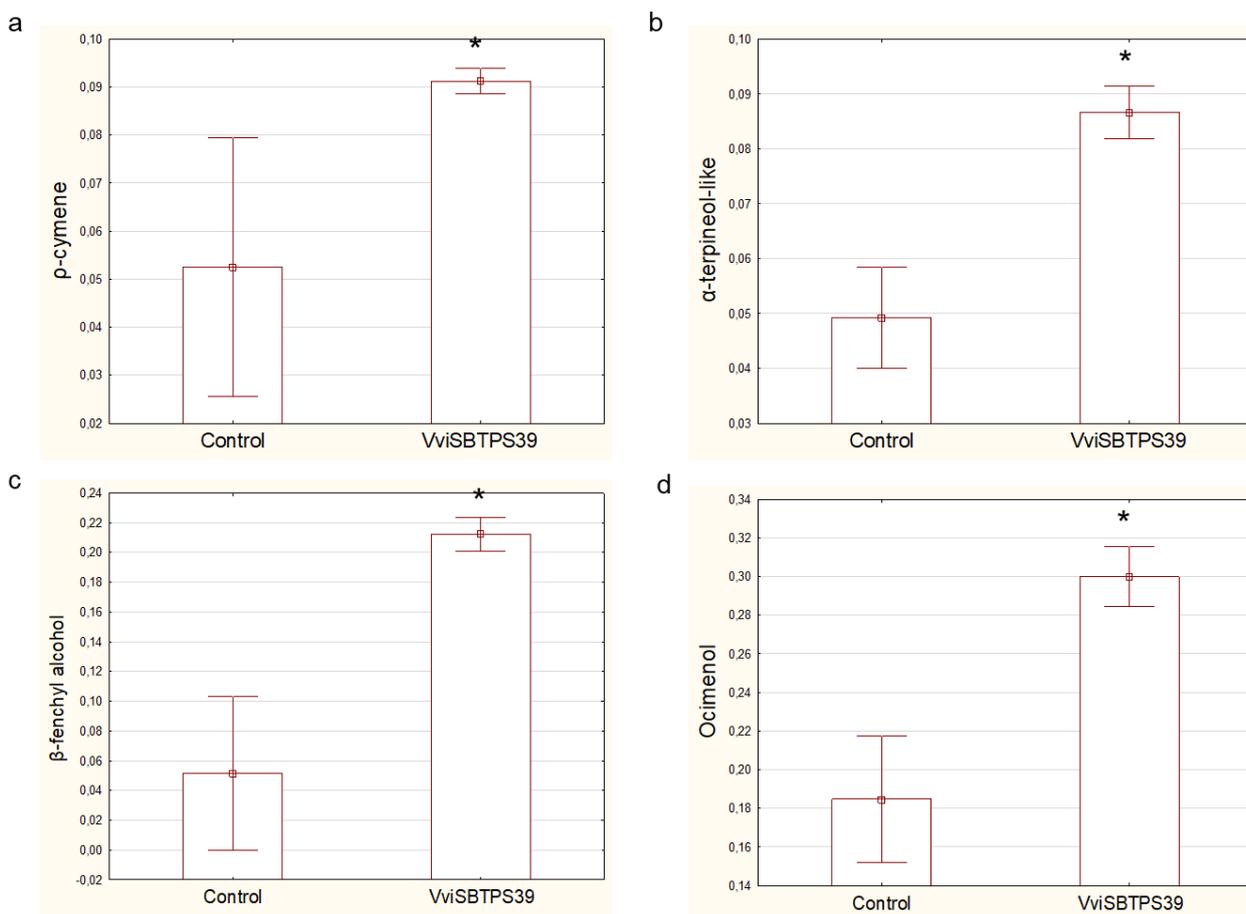
Figure 2.6 Bar graphs of compounds (variables) identified as drivers of the separation between the control plants and plants transformed with *VviSBTPS39* under the control of a constitutive promoter. Bar graph values are presented as average normalised peak area (IS and fresh weight) with whiskers indicating standard deviation. Asterisks (*) indicate significantly higher levels in the plants transformed with *VviSBTPS39* while hashes (#) indicates significantly lower levels in the plants transformed with *VviSBTPS39* compared to the control plants.

2.3.2.2 Terpene production utilising a heterologous plant expression platform: transient expression in <u>Nicotiana benthamiana</u>

The same plant expression construct that was used for the transformation of the grapevine population, was also used for agroinfiltration into *N. benthamiana* for the transient expression of *VviSBTPS39.* Optimisation of the agroinfiltration protocol included various factors such as the use of p19 (gene silencing repressor) in co-infiltration, the infiltration buffer, *A. tumefaciens* cell density used for infiltration, as well as the sampling date. The fluorescence signal produced by GFP was used as a visual indicator during optimisation and to serve as a positive control during agroinfiltration experiments. The infiltrated leaves were sampled and either the whole leaf (without normalisation) or ground tissue (normalised to net weight and IS) was analysed.

The non-normalised peak areas of volatiles detected with the whole-leaf analysis method were used as the variables for OPLS-DA to determine whether the control population could be separated from the *VviTPS*-infiltrated plants (**Figure 2.7**). Based on the results, the plants separated according to the construct with which they had been infiltrated. Multiple monoterpenes were detected in the *VviSBTPS39*-infiltrated plants, which drove the separation of these plants from the control plants. The results are summarised in **Table G-i** with the peaks which were significantly different from the control plants, highlighted in red.
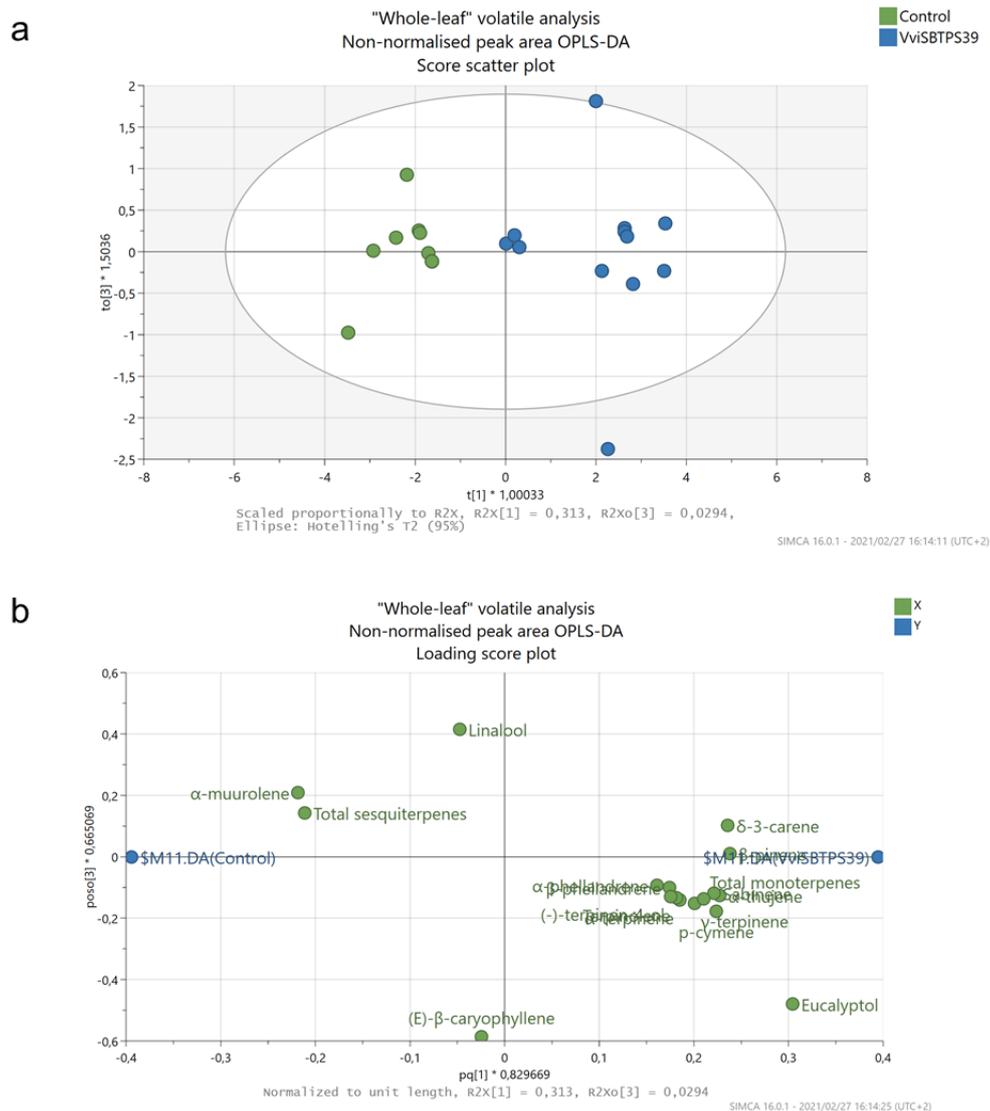
Figure 2.7 Orthogonal projections to latent structures discriminant analysis (OPLS-DA) of headspace volatiles produced by *Nicotiana benthamiana* plants agroinfiltrated with either an empty expression vector (control) or *VviSBTPS39* with the score scatter plot (a) showing separation between samples of control and *VviSBTPS39*. The loading scatter plot (b) illustrates the variables driving the separation of the control plants samples from those infiltrated with *VviSBTPS39*.

In addition to the whole-leaf analysis, volatile analysis of ground tissue was performed to normalise the peak area for a relative quantitative comparison between plants. The *N. benthamiana* plants were agroinfiltrated with pART27-VviTPS39 in combination with either pART27-empty (control) or pART27-VviGPS. The peak areas of the identified compounds were normalised to the IS peak area (Anisole-d_8) and the fresh weight (g) of each sample. In the *VviSBTPS39*-infiltrated plants, there was only one compound, putatively identified as β-cyclocitral, of which the levels were significantly higher ($p < 0.05$) in plants co-infiltrated with *VviGPS* (**Table G-ii**).

2.3.3   Terpene profiling determination of monoterpene synthases

The monoterpene profiles of the *VviSBTPS39*-expressing yeast and *N. benthamiana* were compared in terms of compounds identified as well as the relative ratio of the peaks. The results of this comparison are illustrated in **Figure 2.8** and show 15 monoterpenes that were detected in both expression systems. The monoterpene profile of these shared compounds was consistent across the two systems (**Figure 2.8**b). However, there are monoterpenes which were unique to each specific expression system, as listed in the table (**Figure 2.8**a).

Yeast	Plant
β-citronellol	α-fenchene
Isoterpinolene	α-citral
4-Terpinenyl acetate	β-cyclocitral
Camphene	Nerol
Limonene	β-phellandrene
Isogeraniol	
Menthol	
Fenchone	
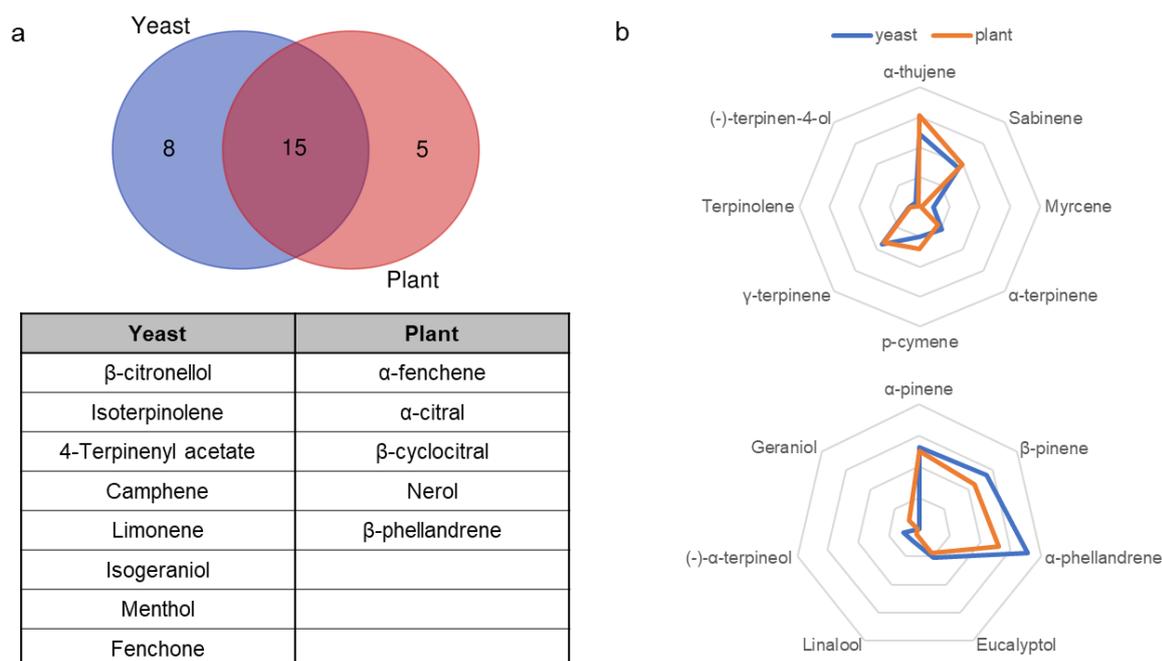
Figure 2.8 Comparison of the monoterpene profile of *VviSBTPS39* when expressed in a yeast (*Saccharomyces cerevisiae*) or plant (*Nicotiana benthamiana*) system. Many compounds were detected in both expression systems but some of the compounds were unique to a specific system, as listed in the tables (a). The relative ratio profile of the communal compounds is shown in (b) with the monoterpenes with the highest peak areas shown in the top spider plot and the minor monoterpenes in terms of peak area shown in the bottom plot.

62

The monoterpenes produced by VviSBTPS39 in the yeast expression system using the Gateway® expression vector, as well as the monoterpenes produced by VviSBTPS39 in the *N. benthamiana* plant expression system, are listed in **Table 2.2**. The monoterpene synthases form multiple products, but the profile remained consistent between repeats. The main compound produced by VviSBTPS39 in both the yeast and the plant systems was α-thujene in terms of the relative peak area under the conditions used for analysis.

Table 2.2 Monoterpene profile for the two monoterpene synthases. [a]Components listed in the order of elution on HP 5MS capillary column and named according to identification methods listed in the ID column. [b] Chemical Abstracts Service (CAS) number of compounds listed. [c]Retention time (RT) in minutes of the compounds detected. [d]Compound identification method: MS – comparison of mass spectra (MS) with MS libraries (Wiley and NIST), RI – comparison of calculated retention index (RI) with those reported in literature, Std – identification based on comparison with authentic standard. [e]Compounds detected in the yeast expression system overexpressing *VviSBTPS39*. [f]Compounds detected in the plant (*N. benthamiana*) expression system transiently expressing *VviSBTPS39*. [e-f]Terpenes were analysed in the headspace at ambient temperature, expressed as percentage ratio of the total monoterpene peak area with ± standard deviation. The main compounds in terms of relative peak area for each expression system are presented in red. Asterisks (*) indicate compounds for which an authentic standard was available for comparison. ND = not detected.

Compound[a]	CAS[b]	RT[c]	ID[d]	VviSBTPS39[e] (%)	VviSBTPS39[f] (%)
α-thujene	2867-05-2	7.278	MS, RI	24.3 ± 1.4	30.4 ± 2.4
α-pinene	80-56-8	7.402	MS, RI	1.3 ± 0.4	1.2 ± 0.2
Camphene	79-98-5	7.722	MS, RI	0.03 ± 0.005	ND
Sabinene	3387-41-5	8.262	MS, RI	18.1 ± 1.1	20.2 ± 4.7
β-pinene	127-91-3	8.328	MS, RI	1.4 ± 0.3	1.1 ± 0.2
Myrcene*	123-35-3	8.602	MS, RI, Std	4.4 ± 0.9	0.6 ± 0.9
α-phellandrene	99-83-2	8.885	MS, RI	1.8 ± 0.5	1.3 ± 0.4
α-terpinene*	99-86-5	9.149	MS, RI, Std	10.5 ± 1.1	8.7 ± 1.7
p-cymene	99-87-6	9.313	MS, RI	10.2 ± 3.2	13.9 ± 3.4
β-phellandrene	555-10-2	9.389	MS, RI	ND	2 ± 0.4
Limonene*	138-86-3	9.404	MS, RI, Std	2.8 ± 0.2	ND
Eucalyptol*	470-82-6	9.458	MS, RI, Std	0.5 ± 0.1	0.4 ± 0.2
γ-terpinene*	99-85-4	10.025	MS, RI, Std	17.8 ± 0.5	16.7 ± 2.3
Terpinolene	586-62-9	10.604	MS, RI	3.6 ± 0.6	3.1 ± 0.6
Linalool*	78-70-6	10.79	MS, RI, Std	0.2 ± 0.02	0.1 ± 0.2
Menthol	89-78-1	12.224	MS, RI	0.1 ± 0.1	ND
(-)-terpinen-4-ol*	562-74-3	12.335	MS, RI, Std	2.1 ± 0.6	0.4 ± 0.4
α-terpineol*	10482-56-1	12.57	MS, RI, Std	0.3 ± 0.1	0.03 ± 0.05
α-fenchene	471-84-1	12.808	MS	ND	0.3 ± 0
Fenchone	2774-84-7	12.873	MS	0.1 ± 0.1	ND
β-cyclocitral	432-25-7	13.122	MS	ND	0.03 ± 0.03
β-Citronellol*	106-22-9	13.193	MS, Std	0.7 ± 0.5	ND
Geraniol*	106-24-1	13.668	MS, RI, Std	ND	0.2 ± 0.2

2.4   Discussion

The advancement in next-generation sequencing technologies has made it feasible to gather extensive knowledge on the genome and transcriptome of various organisms including non-model plant species. Based on the data generated it has become clear that plants possess expanded gene families involved in specialised metabolism (Xiao *et al.*, 2013; Mutwil, 2020). However, identifying these genes is just the first step in annotation with further functional characterisation required which can often be very time-consuming. One of the reasons being the wide variation in chemical structures and properties seen in specialised metabolites which requires tailored analysis thereof. Different methods can be used but the most important factor to consider is whether the results generated can lead to an accurate characterisation of the gene and its function within the plant.

2.4.1   Yeast as a heterologous host for functional characterisation of terpene synthases

Functional characterisation of TPSs typically involves heterologous overexpression of the relevant gene with many studies utilising a bacterial (*E. coli*) expression system. In general, the latter requires protein extraction followed by the addition of substrates for terpene biosynthesis. The benefits of using such a system are the ability to control the various aspects of the enzymatic reaction as well as the option to determine the enzyme kinetics and substrate specificity (Shelton *et al.*, 2004; 2008; Martin *et al.*, 2010; Del Terra *et al.*, 2013; Alquézar *et al.*, 2017; Rusdi *et al.*, 2018; Zhang *et al.*, 2019). Some studies have described the construction of pathways for GPP biosynthesis (Carter *et al.*, 2003) or optimisation of the native MEP pathway to increase flux to FPP (Martin *et al.*, 2010), rendering the protein extraction and addition of substrates steps unnecessary. However, there are several difficulties associated with using this expression system. For instance, codon optimisation for expression in *E. coli* is often required for the expression of a eukaryotic gene in a prokaryotic host. In addition, if present, the plastid-targeting sequence needs to be removed because the bacteria will not be able to process the full-length protein. Sequence analysis can be used to predict which substrate would be best to use. For example, the presence of a plastid-targeting sequence is a good indication that the TPS will be either a monoterpene (with GPP as substrate) or a diterpene (with GGPP as substrate) synthase. On the contrary, the absence of this sequence suggests that it will be a sesquiterpene synthase (with FPP as substrate). Nevertheless, prediction of the targeting sequence is not infallible, and common practice is to incubate the protein extract with all the possible substrates, with characterisation based on the ability of an enzyme to utilise a certain substrate. To add to these difficulties, some TPSs can utilise more than one type of substrate, thereby producing monoterpenes with GPP, sesquiterpenes with FPP and/or diterpenes with GGPP (Martin *et al.*, 2010). In addition, while most isoprenyl diphosphates utilised in terpenoid production is in the *trans*

(*E*) configuration, the *cis*-isomer can also sometimes form the substrate for terpene synthase (Akhtar *et al.*, 2013).

Instead of using the bacterial system for the functional characterisation of *VviTPSs,* a yeast system was assessed in this study with previous successes supporting the use thereof (Oswald *et al.*, 2007; Takahashi *et al.*, 2007; Nguyen *et al.*, 2012; Scalcinati *et al.*, 2012; Chen *et al.*, 2019). Results in this study showed that a measurable accumulation of monoterpenes was formed without any MVA pathway manipulation except for the heterologous expression of *VviSBTPS39* when using the *yeast* strain *S. cerevisiae* W303-1A.

Terpene analysis revealed that terpenes were also detected in the cultures of the *S. cerevisiae* strains not expressing the *VviTPS.* The implementation of high temperatures before and during extraction was especially conducive to terpene detection in the control strains. These compounds included monoterpenes such as linalool, α-terpineol, β-citronellol and geraniol, and the sesquiterpene, nerolidol. Generally, *S. cerevisiae* is considered a null background for terpene synthase characterisation, but it has been found to produce trace amounts of farnesol (Hock *et al.*, 1984). Some wine yeast strains are also able to produce other monoterpenes and sesquiterpenes with a higher concentration of assimilable nitrogen and microaerobic conditions found to be more favourable to terpene production (Carrau *et al.*, 2005). The yeast background could alter the product profile, with specific terpenes considered as characteristic yeast by-products. The stereospecific conversion of geraniol to citronellol has previously been described and is attributed to the activity of an endogenous yeast reductase (Gramatica *et al.*, 1982; Fischer *et al.*, 2011). All the aforementioned terpenes detected in the control yeast culture of this study were also detected in the *S. cerevisiae* strains studied by Carrau *et al.* (2005), who proposed an alternative pathway for monoterpenes in some yeast strains. In this study, the strains were overexpressing MVA pathway genes with a potential excess of substrates being produced that were not converted by the heterologously expressed *VviTPS* into specific terpenes. Instead, the additional substrates could have been transformed to terpenes by endogenous yeast enzymes or through non-enzymatic activity. Nevertheless, only trace amounts of terpenes were detected in the control strain and levels were much lower than what was produced in the strains overexpressing *VviSBTPS39.* Switching to ambient temperatures during extraction with no heat pre-treatment, as well as expressing the *VviTPS* on a high-copy episomal expression plasmid under the control of an inducible promoter, further reduced terpene levels in the control strain.

The results from this study support those from previous studies where yeast was used as a heterologous expression system for terpene production (Jackson *et al.*, 2003; Fischer *et al.*, 2011; 2013; Pardo *et al.*, 2015). Terpene production in yeast can be achieved without protein extraction,

substrate addition or extensive pathway manipulation since both GPP and FPP are produced by the yeast (Asadollahi *et al.*, 2008; Herrero *et al.*, 2008). Yeast could thereby function as a viable alternative for the functional characterisation of TPSs, although care should be taken when using this system since the yeast background could alter the terpene profile (Fischer *et al.*, 2013).

2.4.2   Optimisation of the yeast expression and analytical systems

2.4.2.1   Heat treatment

Initially, the preferred method that was used for volatile analysis included a heat treatment step and high extraction temperatures as a means of increasing volatiles in the headspace. However, studies have shown that terpenes are generally unstable, with various factors determining their stability (Varming *et al.*, 2006; Turek & Stintzing, 2013). In a study by Cornwell *et al.* (1999), the effect of temperature on monoterpenes was monitored through (-)-terpenin-4-ol detection in the steam distillate from the leaves of three *Melaleuca* species, which were correlated to the presence of (+)-sabinene and *cis*- and *trans*-sabinene hydrate in the fresh plant material. Another study showed that wine that was spiked with different monoterpenes and stored at 60°C resulted in the formation of various monoterpenes which were dependent on the identity of the added monoterpene and the treatment time (Slaghenaufi & Ugliano, 2018).

The effects that acidity levels have on terpene stability was investigated through the isomerisation of sabinene during thin-layer chromatography with the formation of α-thujene, α-terpinene, limonene, β-phellandrene, γ-terpinene, and terpinolene as the rearrangement products (Wrolstad & Jennings, 1963). Treatment with NaOH to "neutralise" the chromatostrips before compound separation significantly reduced the formation of these compounds. Many of the degradation monoterpenes listed in these studies were also detected in this study. This indicates that the inherent instability of the main monoterpenes produced could contribute to the formation of various other rearrangement products after its synthesis by VviSBTPS39, with acidity and/or high temperature contributing to their formation.

Extraction temperature is another important factor to consider when analysing volatile compounds such as monoterpenes with low boiling points. Increased temperatures do not always lead to increased vaporisation into the headspace. Instead, it can cause desorption from the fibre (Hamm *et al.*, 2003). Previous studies where HS-SPME was used for volatile analysis have reported the formation of artefacts in response to increased extraction temperatures (Čajka *et al.*, 2007; Robinson *et al.*, 2011). In this study, the relatively high extraction temperature of 60°C resulted in the detection of various terpenes with higher boiling points and a decrease in the peak area of the low-boiling-point (LBP) terpenes. The two sesquiterpene compounds, nerolidol and farnesol, detected at the higher extraction temperature could be due to activity of the modified yeast strains producing excess

66

substrates (discussed in Section 0). The increased extraction temperature forces these less-volatile compounds into the headspace where it can be detected (Carrau *et al.*, 2005).

Our results have highlighted the effect that temperature has on terpene analysis. Although the profile undergoes some change as the temperature is increased (or decreased), the volatile profile that is interesting and relevant in terms of the biological role in plants, would be at the temperature range wherein a plant grows. Therefore, the samples were not heated and HS-SPME for terpene analysis was performed at 35°C, which was the lowest temperature that could accurately be maintained in the equilibration chamber. In addition to the temperature, steps were also taken to avoid highly acidic conditions during terpene analyses. In nature, plant cells maintain a pH ranging from slightly acidic (pH 5) in the vacuole to relatively more alkaline (pH 8) in the peroxisome, plastidial stroma, and the mitochondrial matrix (Shen *et al.*, 2013). The maintenance of more neutral conditions during terpene analysis is therefore a closer approximation of the native conditions found within the plant cell.

2.4.2.2 *Increasing precursor availability*

Because the availability of precursors could influence terpene production in yeast, several studies have focused on this aspect, as reviewed by Marienhagen and Bott (2013) and Bian *et al.* (2017). Various enzymes have been shown to catalyse rate-limiting reactions within the MVA pathway or indirectly affect flux through this pathway (Jackson *et al.*, 2003; Muntendam *et al.*, 2009; Ignea *et al.*, 2011; Kampranis & Makris, 2012). The two *S. cerevisiae* MVA pathway genes that were targeted for overexpression in this study, encoded isopentenyl diphosphate isomerase (*ScIDI1*) and a truncated version of 3-hydroxy-3-methylglutaryl coenzyme A reductase (*SctHMG1*), as illustrated in **Figure 2.4**. Previous studies have shown that increased expression of these genes can lead to higher levels of terpenes formation via a heterologous expression system (Donald *et al.*, 1997; Carter *et al.*, 2003; Martin *et al.*, 2003; Rico *et al.*, 2010b; Ignea *et al.*, 2011). The GPP used for monoterpene production is formed as an intermediate to FPP synthesis (Dhar *et al.*, 2013) in yeast. As a result, the expression of *VviSBTPS39* diverts substrates needed for sterol biosynthesis. To produce an alternative pool of GPP, *VviGPS* with its targeting sequence removed was heterologously expressed in yeast.

The results from the MVA pathway manipulation in yeast show that the greatest impact on monoterpene levels was achieved with the overexpression of *IDI1* in combination with *VviGPS.* IDI catalyses an important isomerisation reaction at the end of the MVA pathway whereby IPP is converted to DMAPP (Berthelot *et al.*, 2012). Increasing the conversion of IPP to DMAPP could therefore increase the flux towards FPP (and GPP) production that can subsequently be utilised for terpene biosynthesis (Ignea *et al.*, 2011). The overexpression of GPS-encoding genes has also been shown to increase flux towards monoterpene production in yeast and other expression platforms (Mahmoud & Croteau, 2002; Alonso-Gutierrez *et al.*, 2013; Zhao *et al.*, 2016). It, therefore, seems

as if the combination of these two enzymes effectively increases the availability of GPP, which is then utilised by VviSBTPS39.

It has been shown that the reaction catalysed by 3-hydroxy-3-methylglutaryl coenzyme A reductase (HMG) is a major regulatory point in the MVA pathway (Hampton *et al.*, 1996). It is possible to increase MVA pathway end-product levels in *S. cerevisiae* through the removal of the regulatory DNA sequences of the *HMG1* gene, yielding *tHMG1,* and overexpression of the DNA sequence encoding the catalytic domain of Hmg1p (Donald *et al.*, 1997; Polakowski *et al.*, 1998; Verwaal *et al.*, 2007). The overexpression of *tHMG1* and *VviGPS* on their own or in combination did not result in an increase of monoterpene levels – instead, it reduced the monoterpene peak area when normalised to cell count (Table D-i). The combinatorial overexpression of *tHMG1* and *IDI1* also did not affect monoterpene levels more than the overexpression of *IDI1* alone*.* This is in contrast to a study conducted by Rico *et al.* (2010) in which *tHMG1* overexpression resulted in a 1.5 to twofold increase of linalool levels. From these results, it can thus be postulated that HMG1 is not a rate-limiting enzyme in the W303-1A strain under the growth conditions and with the specific TPS used in this study and that instead, the availability of DMAPP is more limiting to heterologous monoterpene production. Although this is speculative and will need to be verified, it does highlight the effect the yeast genotype, growth conditions and transgene has on metabolic engineering studies. Combinatorial expression of *IDI1* and *VviGPS* allows for higher levels of DMAPP, that can be utilised for dedicated GPP biosynthesis. However, the impact of the overexpression of *IDI1* and *VviGPS* could also be dependent on the enzyme activity of the specific TPS. It could be that a TPS with higher enzyme activity is needed to compete more aggressively with the endogenous yeast FPS to release the GPP intermediate. Because this is an *in vivo* system it is not possible to determine the enzyme activity – as can be done when using an *in vitro* system. Therefore, no direct comparison can be made of enzyme activity between VviSBTPS39 used in this study and the linalool synthase used by Rico *et al.* (2010) where *tHMG1* expression in yeast did result in a significant increase in monoterpene production.

Additional enzymes functioning in the terpene metabolic pathway as well as outside this pathway can be targeted in future studies to further increase the flux towards terpene biosynthesis (Asadollahi *et al.*, 2008; Farhi *et al.*, 2011; Chung *et al.*, 2013; Liu *et al.*, 2013b; Wriessnegger & Pichler, 2013; Ignea *et al.*, 2014). For functional characterisation of most of the *VviTPSs* used in this study, additional manipulation of the MVA pathway was not necessary because the resulting enzymes exhibited enough activity to produce quantifiable levels of most terpene products. However, not all the terpene synthases have similar enzyme activities and it might be necessary to increase substrate availability to facilitate functional characterisation (Lücker *et al.*, 2002).

In yeast, the MVA pathway is used to produce sterols. Because sterols are essential components of the membrane, manipulation of the biosynthetic pathway for the heterologous production of terpenes might affect yeast cell viability (Daum *et al.*, 1998). Terpenes have also been shown, in many studies, to possess a broad range of anti-microbial activity (Friedman *et al.*, 2002; Hammer *et al.*, 2003; Baydar *et al.*, 2004; Carson *et al.*, 2006; Bourgou *et al.*, 2010). The possible antifungal activity of the terpenes formed by the yeast strains overexpressing *VviSBTPS39* could therefore also affect the viability of the yeast culture. However, results from growth curves (Figure) did not indicate that the yeast was affected negatively by heterologous monoterpene production in this study. Despite this, the use of a high-copy episomal expression vector instead of the genome-integrating expression vector could have resulted in terpenes being produced at quantities that could have affected yeast growth. The *GAL1* promoter has been used in previous studies (Ignea *et al.*, 2011, 2014; Kirby *et al.*, 2014) and has the benefit of regulating the expression of *VviTPS* with the carbon source (Johnston & Davis 1984, Mumberg *et al.* 1994). Consequently, in this study, the *GAL1* promoter was used instead of the constitutive *PGK1* promoter, which would have allowed for biomass accumulation before *TPS* gene expression was induced.

2.4.2.3 *Plastid-targeting sequence removal*

Monoterpene synthases have an N-terminal plastid-targeting sequence that is required for the enzymes' subcellular localisation to the plant chloroplast where monoterpene synthesis occurs (Gavel & von Heijne, 1990; Bohlmann *et al.*, 1998; Bruce, 2001). Because yeast and bacteria do not have chloroplasts, they are unable to process the transit peptide to form the mature peptide. In most heterologous expression studies, the targeting sequence is removed prior to cloning into the expression vector to improve the functionality of the monoterpene synthase (Shelton *et al.*, 2004; Simkin *et al.*, 2013). Decreased enzyme activity with the transit peptide can therefore be expected when expressed in yeast, or any other organism used for protein expression, which does not have the post-translational mechanisms required for removal of the targeting sequence (Williams *et al.* 1998; Jarvis & Robinson 2004). The results from this study support those from previous studies in that higher levels were achieved with VviSBTPS39 when the gene was truncated (Table). However, the enzymes with the targeting sequences attached were still functional and able to produce terpenes. It is therefore recommended that the predicted plastid-targeting sequences be removed before heterologous expression in yeast. However, this step is not always needed for accurate functional characterisation to proceed and the necessity thereof can be assessed based on circumstances.

2.4.3   Comparison of bacterial, yeast, and plant expression systems

In this study, the functionally characterised α-terpineol synthase sequence from Martin and Bohlmann (2004) was used to design primers to isolate *VviTPS39* from *V. vinifera* cv. SB. The α-terpineol synthase gene, characterised with an *in vitro* system, mapped to the same gene model as *VviSBTPS39* and was also shown to encode multi-product monoterpene synthase. However, (-)-α-terpineol was the main product, at around 50% of the total monoterpene peak area (Martin & Bohlmann, 2004). Sequence alignment between the cDNA isolates from the two studies showed very high similarity (96% identity). Although there are coinciding monoterpenes being produced by the respective monoterpene synthases, the relative quantities differed and sabinene hydrate was not detected in this study. The most notable difference is that in this study, α-thujene and sabinene were the major monoterpenes produced in the headspace at ambient extraction temperature. There are multiple possible explanations for why the two enzymes produce different major products. It is possible, for instance, that the amino acid differences, although very little, could have allowed for a change in the enzymes' product profiles (Roach *et al.*, 2014). These sequence differences can most likely be attributed to cultivar differences (Kollner *et al.*, 2004). Another factor that needs to be considered is the heterologous system that was used here to functionally characterise monoterpene synthases. Fischer *et al.* (2013) found that the expression of the geraniol synthase gene from *Ocimum basilicum* in various heterologous systems could result in some product variation. This study utilised an *in vivo* system with *S. cerevisiae* as the heterologous host for functional characterisation of the *VviTPSs* and not an *in vitro* system with *E. coli*, as in the Martin and Bohlmann (2004) study. Therefore, the possible role that each system might have on the monoterpene product profile needs to be considered. Lastly, the methods that were used for the extraction of monoterpenes also differed between the two studies. HS-SPME was chosen for this study to determine the volatile product profile of VviSBTPS39, in contrast to the pentane overlay used by Martin and Bohlmann (2004). The inherent instability of sabinene, as discussed in the previous Section (2.4.2.1), could be a possible explanation for the differences in product profiles detected.

The monoterpene profile produced by *VviSBTPS39* when expressed in a yeast system compared to a plant system was equivalent. However, a few of the minor monoterpenes produced were only detected in one of the expression systems but not both. A comprehensive study by Fischer *et al.* (2013), wherein geraniol synthase was heterologously expressed in various microbiological and plant systems showed that the expression system can impact the terpene profile. The ability of bacteria, yeast, fungi and plants to transform terpenes (biotransformation) possibly through the activity of endogenous enzymes has been shown (Duetz *et al.*, 2003; Gamero *et al.*, 2011; Çorbacı, 2020). Notable among the species-specific monoterpenes were limonene (yeast expression system) and β-phellandrene (plant expression system). Wrolstad & Jennings, (1963) proposed a

70

rearrangement pathway for sabinene wherein it is chemically rearranged to various compounds, all of which have been detected in the yeast and plant systems expressing *VviSBTPS39,* with limonene and β-phellandrene at the opposite ends of this pathway (**Figure 2.3**). It can therefore be hypothesised that each expression system promotes the conversion of sabinene to a different endpoint. In both these systems, the main compound detected in terms of peak area at low extraction temperatures (≤35°C) was α-thujene, followed by sabinene and λ-terpinene produced in relatively equal amounts (**Table 2.2**). The other two main monoterpenes that were produced were ρ-cymene and α-terpinene with the rest of the monoterpenes detected at much lower levels. Although the two expression systems analysed were quite consistent in terms of the monoterpene profile, the greatest variation occurred among the minor monoterpenes produced (**Table 2.2**).

Grapevine was also evaluated as a plant expression system for this study but ectopic expression of *VviSBTPS39* could not be shown (

Table 2.1) and could be a result of gene silencing at a transcriptional or post-transcriptional level (Jin & Guo, 2015). Although ectopic expression of *VviSBTPS39* was not detected in the transformation-positive lines, the volatile profile of the transformed population differed from the control plants (**Table F-i**). The three peaks putatively identified as β-fenchyl alcohol, α-terpineol (comparison to an authentic standard confirmed that this peak was not α-terpineol), and ocimenol were significantly higher in the *VviSBTPS39*-transformed population. Sabinene, α-thujene, γ-terpinene, and α-terpinene, which are the main compounds in the *S. cerevisiae* and *N. benthamiana* systems, were not detected during volatile analysis. This could be partly ascribed to the volatile analysis method that was analogous to the initial high-heat method used for yeast cultures. However, this cannot be the only reason, since α-thujene, γ-terpinene and α-terpinene were still detected in the yeast culture even when analysed under those initial conditions. Because several terpenes were also detected in the control plants, this system cannot be considered as a null background. In addition, the processes of transformation, regeneration, and genetic characterisation do not allow high throughput in this system.

A comparison of the terpene synthase expression systems that were used in this study to the commonly used *in vitro* system in *E. coli*, are summarised in **Table 2.3**. Yeast proved to be a good alternative to *E. coli* for the microbial expression of *TPSs* because extensive pathway manipulation was not required (although it is possible if higher terpene levels are required). In terms of a plant system, transient expression in *N. benthamiana* provided a means for the relatively quick introduction of the transgene and volatile analysis thereafter, although it remained slower than a microbial system. The monoterpene profile for *VviSBTPS39* in both the yeast and tobacco systems remained

consistent although there were some discrepancies, especially among the minor products, which can be attributed to the genetic background.

Table 2.3 Comparison of the frequently used *E. coli* expression system to the expression systems investigated in this study.

E. coli (*in vitro*)	*S. cerevisiae* (*in vivo*)	*N. benthamiana* (transient expression)	*V. vinifera* (constitutive expression)
Codon optimisation Removal of targeting sequence	Removal of targeting sequence	No sequence optimisation necessary	No sequence optimisation necessary
In vitro system requires protein purification and incubation with substrates	*In vivo* system, but pathway manipulation might be necessary to produce enough substrate	*In vivo* system with the plant producing all the required substrates	*In vivo* system with the plant producing all the required substrates
In vitro system enables regulation of pH, temperature etc. with the option of determining enzyme activity	*In vivo* system, but able to regulate growth conditions more easily than with plants	*In vivo* system with limited capability for regulation of growth conditions	*In vivo* system with limited capability for regulation or growth conditions
Considered a null background	Considered a null background, but certain yeast strains and/or culture conditions can result in *de novo* terpene production	Able to produce terpenes, but very low levels observed in control under conditions used	Able to produce terpenes, various terpenes detected with volatile analysis method used
The impact of endogenous enzymes is reduced since it is an *in vitro* system	Endogenous enzymes can alter the terpenes produced by TPSs to produce wider array of terpenes	Endogenous enzymes able to modify terpenes produced, but tobacco does not glycosylate terpenes	Endogenous enzymes able to modify terpenes produced (i.e., glucosyltransferases, cytochromes P450) – benefit of giving the most authentic terpene profile but encumbers the characterisation process
Transformation of *E. coli* and production of TPSs are relatively quick (can be done within a week) with easy storage of cultures (freeze cultures)	Transformation of *S. cerevisiae* and production of terpenes are relatively quick (can be done within a week) with easy storage of cultures (freeze cultures)	Growing plants is relatively quick compared to other plants (5 to 6 weeks) with an additional week needed for agroinfiltration and volatile analysis	Transformation, regeneration, and genetic characterisation is time-consuming Transgene plants can be maintained in tissue culture but require regular maintenance and specialised growth rooms

The truncated version of the putative *VviGPS* gene was used during MVA pathway manipulation in *S. cerevisiae* with *VviSBTPS39* as the indicator TPS. Heterologous expression of *VviGPS* in *S. cerevisiae* only increased monoterpene levels when expressed in combination with *ScIDI1.* During

72

transient expression in *N. benthamiana*, co-infiltration of *VviGPS* (full-length) with *VviSBTPS39* did not result in a significant difference in the levels of measured monoterpenes. These results indicate that *VviGPS* is likely to be functional, but other enzymes can affect the activity of the heterologously expressed *VviGPS*. Usually, the method used for the functional characterisation of IDSs is similar to what is used for TPSs. In a typical situation, the predicted isoprenyl diphosphate synthase genes are heterologously-expressed in *E. coli*, followed by *in vitro* assays with possible substrates and analysis of the resulting products (Burke & Croteau, 2002a; Schmidt & Gershenzon, 2008; Alcaíno *et al.*, 2014; Zhao *et al.*, 2015). The indirect method of IDS functional characterisation evaluated in this study is dependent on various factors that could adversely affect results and is therefore not the optimal method for determining *IDS* gene functionality.

2.5   Conclusion

With the advent of next-generation sequencing and the exponential increase in generated sequencing data, the greatest bottleneck for understanding gene function remains the functional characterisation of identified genes. This is especially true for genes involved in specialised (secondary) metabolism, which displays a high level of plasticity. Based on the results from this study and previous studies, the inherent instability of terpenes hampers the production and analysis thereof. The most important aspect when choosing a specific expression system for TPS functional characterisation is that the measured terpene profile provides the most accurate depiction of the true nature of the characterised terpene synthase characterised. Consequently, the method for subsequent analysis was the closest imitation of the conditions within the plant cell where the enzyme is active. The use of a microbial expression system (*in vitro* and *in vivo*) for functional characterisation of terpenoid pathway genes has its benefits. However, transient expression in *N. benthamiana* is a viable alternative since it is a relatively quick plant-based system with comparatively low background noise.

2.6   Acknowledgements

2.7   References

Agatep, R., Kirkpatrick, R.D., Parchaliuk, D.L., Woods, R.A. & Gietz, R.D., (1998). Transformation of *Saccharomyces cerevisiae* by the lithium acetate/single-stranded carrier DNA/polyethylene glycol protocol *Tech. Tips Online* **3**, 1, 133–137.

Aharoni, A., Giri, A.P., Deuerlein, S., Griepink, F., De Kogel, W.-J.J., Verstappen, F.W.A.A., Verhoeven, H.A., Jongsma, M.A., Schwab, W. & Bouwmeester, H.J., (2003). Terpenoid Metabolism in Wild-Type and Transgenic Arabidopsis Plants *Plant Cell* **15**, December, 2866–2884.

Ajikumar, P.K., Xiao, W.-H., Tyo, K.E.J., Wang, Y., Simeon, F., Leonard, E., Mucha, O., Phon, T.H., Pfeifer, B. & Stephanopoulos, G., (2010). Isoprenoid pathway optimization for Taxol precursor overproduction in *Escherichia coli*. *Science* **330**, 6000, 70–4.

Akhtar, T.A., Matsuba, Y., Schauvinhold, I., Yu, G., Lees, H.A., Klein, S.E. & Pichersky, E., (2013). The tomato cis-prenyltransferase gene family *Plant J.* **73**, 4, 640–652.

Alberti, S., Gitler, A.D. & Lindquist, S., (2007). A suite of Gateway cloning vectors for high-throughput genetic analysis in *Saccharomyces cerevisiae Yeast* **24**, 10, 913–919.

Alcaíno, J., Romero, I., Niklitschek, M., Sepúlveda, D., Rojas, M.C., Baeza, M. & Cifuentes, V., (2014). Functional characterization of the *Xanthophyllomyces dendrorhous* farnesyl pyrophosphate synthase and geranylgeranyl pyrophosphate synthase encoding genes that are involved in the synthesis of isoprenoid precursors *PLoS One* **9**, 5, 1–12.

Alonso-Gutierrez, J., Chan, R., Batth, T.S., Adams, P.D., Keasling, J.D., Petzold, C.J. & Lee, T.S., (2013). Metabolic engineering of *Escherichia coli* for limonene and perillyl alcohol production *Metab. Eng.* **19**, 33–41.

Alquézar, B., Rodríguez, A., de la Peña, M. & Peña, L., (2017). Genomic Analysis of Terpene Synthase Family and Functional Characterization of Seven Sesquiterpene Synthases from *Citrus sinensis Front. Plant Sci.* **8**, August, 1481.

Anderson, M.S., Yarger, S.J.G., Burck, C.L. & Poultersii, C.D., (1989). Farnesyl Diphosphate Synthetase *J. Biol. Chem.* **264**, 32, 19176–19184.

Asadollahi, M.A., (2008). Establishment of Yeast Platform for Isoprenoid Production.

Asadollahi, M.A., Maury, J., Møller, K., Nielsen, K.F., Schalk, M., Clark, A. & Nielsen, J., (2008). Production of Plant Sesquiterpenes in *Saccharomyces cerevisiae*: Effect of ERG9 Repression on Sesquiterpene Biosynthesis *Biotechnol. Bioeng.* **99**, 3, 666–677.

Bach, S.S., Bassard, J.-É., Andersen-Ranberg, J., Møldrup, M.E., Simonsen, H.T. & Hamberger, B., (2014). High-Throughput Testing of Terpenoid Biosynthesis Candidate Genes Using Transient Expression in Nicotiana benthamiana In: M. Rodríguez-concepción (ed). Plant Isoprenoids. 245–255.

Baydar, H., Sağdiç, O., Özkan, G. & Karadoğan, T., (2004). Antibacterial activity and composition of essential oils from Origanum, Thymbra and Satureja species with commercial importance in Turkey *Food Control* **15**, 3, 169–172.

Berthelot, K., Estevez, Y., Deffieux, A. & Peruch, F., (2012). Isopentenyl diphosphate isomerase: A checkpoint to isoprenoid biosynthesis. *Biochimie* **94**, 8, 1621–34.

Besumbes, O., Sauret-gueto, S., Phillips, M.A., Imperial, S., Rodriguez-Concepcion, M., Boronat, A., Sauret-gu, S., Phillips, M.A. & Imperial, S., (2004). Metabolic engineering of isoprenoid biosynthesis in Arabidopsis for the production of Taxadiene, the first committed precursor of Taxol *Biotechnol. Bioeng.* **88**, 2, 168–175.

Bian, G., Deng, Z. & Liu, T., (2017). Strategies for terpenoid overproduction and new terpenoid discovery *Curr. Opin. Biotechnol.* **48**, 234–241.

Bohlmann, J., Meyer-Gauen, G. & Croteau, R., (1998). Plant terpenoid synthases: molecular biology and phylogenetic analysis. *Proc. Natl. Acad. Sci. U. S. A.* **95**, 8, 4126–33.

Bourgou, S., Pichette, a., Marzouk, B. & Legault, J., (2010). Bioactivities of black cumin essential oil and its main terpenes from Tunisia *South African J. Bot.* **76**, 2, 210–216.

Bruce, B.D., (2001). The paradox of plastid transit peptides: conservation of function despite divergence in primary structure. *Biochim. Biophys. Acta* **1541**, 1–2, 2–21.

Burke, C. & Croteau, R., (2002). Geranyl diphosphate synthase from Abies grandis: cDNA isolation, functional expression, and characterization *Arch. Biochem. Biophys.* **405**, 1, 130–136.

Burke, C., Klettke, K. & Croteau, R., (2004). Heteromeric geranyl diphosphate synthase from mint: Construction of a functional fusion protein and inhibition by bisphosphonate substrate analogs *Arch.*

Biochem. Biophys. **422**, 1, 52–60.

Burke, C.C., Wildung, M.R. & Croteau, R., (1999). Geranyl diphosphate synthase: cloning, expression, and characterization of this prenyltransferase as a heterodimer. *Proc. Natl. Acad. Sci. U. S. A.* **96**, 23, 13062–7.

Čajka, T., Hajšlová, J., Cochran, J., Holadová, K. & Klimánková, E., (2007). Solid phase microextraction–comprehensive two-dimensional gas chromatography–time-of-flight mass spectrometry for the analysis of honey volatiles *J. Sep. Sci.* **30**, 4, 534–546.

Carrau, F.M., Medina, K., Boido, E., Farina, L., Gaggero, C., Dellacassa, E., Versini, G. & Henschke, P. a, (2005). De novo synthesis of monoterpenes by Saccharomyces cerevisiae wine yeasts. *FEMS Microbiol. Lett.* **243**, 1, 107–15.

Carrau, F.M., Medina, K., Farina, L., Boido, E., Henschke, P. a. & Dellacassa, E., (2008). Production of fermentation aroma compounds by Saccharomyces cerevisiae wine yeasts: effects of yeast assimilable nitrogen on two model strains. *FEMS Yeast Res.* **8**, 7, 1196–1207.

Carson, C., Hammer, K. & Riley, T., (2006). Melaleuca alternifolia (Tea Tree) oil : a review of antimicrobial and other medicinal properties *Clin. Microbiol. Rev.* **19**, 1, 50–62.

Carter, O. a., Peters, R.J. & Croteau, R., (2003). Monoterpene biosynthesis pathway construction in Escherichia coli *Phytochemistry* **64**, 2, 425–433.

Chen, F., Tholl, D., Bohlmann, J. & Pichersky, E., (2011). The family of terpene synthases in plants: a mid-size family of genes for specialized metabolism that is highly diversified throughout the kingdom. *Plant J.* **66**, 1, 212–29.

Chen, H., Zhu, C., Zhu, M., Xiong, J., Ma, H., Zhuo, M. & Li, S., (2019). High production of valencene in Saccharomyces cerevisiae through metabolic engineering *Microb. Cell Fact.* **18**, 1, 195.

Chung, B.K.-S., Lakshmanan, M., Klement, M., Mohanty, B. & Lee, D.-Y., (2013). Genome-scale in silico modeling and analysis for designing synthetic terpenoid-producing microbial cell factories *Chem. Eng. Sci.* **103**, 100–108.

Çorbacı, C., (2020). Biotransformation of terpene and terpenoid derivatives by Aspergillus niger NRRL 326 *Biologia (Bratisl).* **75**, 9, 1473–1481.

Cornwell, C.P., Leach, D.N. & Wyllie, S.G., (1999). The Origin of Terpinen-4-ol in the Steam Distillates of Melaleuca argentea, M. dissitiflora and M. linariifolia *J. Essent. Oil Res.* **11**, 1, 49–53.

Cunningham, F.X., Sun, Z., Chamovitz, D., Hirschberg, J. & Gantt, E., (1994). Molecular structure and enzymatic function of lycopene cyclase from the cyanobacterium Synechococcus sp strain PCC7942. *Plant Cell* **6**, 8, 1107–1121.

Daum, G., Lees, N.D., Bard, M. & Dickson, R., (1998). Biochemistry, cell biology and molecular biology of lipids of Saccharomyces cerevisiae. *Yeast* **14**, 16, 1471–510.

Dhar, M.K., Koul, A. & Kaul, S., (2013). Farnesyl pyrophosphate synthase: a key enzyme in isoprenoid biosynthetic pathway and potential molecular target for drug development. *N. Biotechnol.* **30**, 2, 114–23.

Donald, K. a, Hampton, R.Y. & Fritz, I.B., (1997). Effects of overproduction of the catalytic domain of 3-hydroxy-3-methylglutaryl coenzyme A reductase on squalene synthesis in Saccharomyces cerevisiae. *Appl. Environ. Microbiol.* **63**, 9, 3341–4.

Dubey, V.S., Bhalla, R., Luthra, R., Microbes, P., Dubey, V.S., Bhalla, R. & Luthra, R., (2003). An overview of the non-mevalonate pathway for terpenoid biosynthesis in plants *J. Biosci.* **28**, 5, 637–646.

Duetz, W. a, Bouwmeester, H., van Beilen, J.B. & Witholt, B., (2003). Biotransformation of limonene by bacteria, fungi, yeasts, and plants. *Appl. Microbiol. Biotechnol.* **61**, 4, 269–77.

Eberhardt, N.L. & Rilling, H.C., (1975). Prenyltransferase from Saccharomyces cerevisiae. Purification to homogeneity and molecular properties. *J. Biol. Chem.* **250**, 3, 863–866.

Farhi, M., Marhevka, E., Masci, T., Marcos, E., Eyal, Y., Ovadis, M., Abeliovich, H. & Vainstein, A., (2011). Harnessing yeast subcellular compartments for the production of plant terpenoids. *Metab. Eng.* **13**, 5, 474–481.

Fischer, M.J.C., Meyer, S., Claudel, P., Bergdoll, M. & Karst, F., (2011). Metabolic engineering of monoterpene synthesis in yeast. *Biotechnol. Bioeng.* **108**, 8, 1883–92.

Fischer, M.J.C., Meyer, S., Claudel, P., Perrin, M., Ginglinger, J.F., Gertz, C., Masson, J.E., Werck-Reinhardt, D., Hugueney, P. & Karst, F., (2013). Specificity of Ocimum basilicum geraniol synthase modified by its expression in different heterologous systems. *J. Biotechnol.* **163**, 1, 24–9.

Friedman, M., Henika, P.R. & Mandrell, R.E., (2002). Bactericidal activities of plant essential oils and some of their isolated constituents against Campylobacter jejuni, Escherichia coli, Listeria monocytogenes, and Salmonella enterica. *J. Food Prot.* **65**, 10, 1545–60.

Gamero, a., Manzanares, P., Querol, a. & Belloch, C., (2011). Monoterpene alcohols release and bioconversion by Saccharomyces species and hybrids *Int. J. Food Microbiol.* **145**, 1, 92–97.

Gao, Y., Honzatko, R.B. & Peters, R.J., (2012). Terpenoid synthase structures: a so far incomplete view of complex catalysis. *Nat. Prod. Rep.* **29**, 10, 1153–75.

Gavel, Y. & von Heijne, G., (1990). A conserved cleavage-site motif in chloroplast transit peptides. *FEBS Lett.* **261**, 2, 455–8.

Gietz, R.D. & Akio, S., (1988). New yeast-Escherichia coli shuttle vectors constructed with in vitro mutagenized yeast genes lacking six-base pair restriction sites *Gene* **74**, 2, 527–534.

Gietz, R.D. & Woods, R. a, (2002). Transformation of yeast by lithium acetate/single-stranded carrier DNA/polyethylene glycol method. *Methods Enzymol.* **350**, 2001, 87–96.

Gietz, R.D., Triggs-Raine, B., Robbins, A., Graham, K.C. & Woods, R.A., (1997). Identification of proteins that interact with a protein of interest: applications of the yeast two-hybrid system. *Mol. Cell. Biochem.* **172**, 1–2, 67–79.

Gleave, A.P., (1992). A versatile binary vector system with a T-DNA organisational structure conducive to efficient integration of cloned DNA into the plant genome *Plant Mol. Biol.* **20**, 6, 1203–1207.

Göpfert, J.C., Macnevin, G., Ro, D.-K. & Spring, O., (2009). Identification, functional characterization and developmental regulation of sesquiterpene synthases from sunflower capitate glandular trichomes. *BMC Plant Biol.* **9**, 86.

Gramatica, P., Manitto, P., Ranzi, B.M., Delbianco, A. & Francavilla, M., (1982). Stereospecific reduction of geraniol to (R)-(+)-citronellol by *Saccharomyces cerevisiae Experientia* **38**, 7, 775–776.

Green, S. a, Chen, X. & Matich, A.J., (2012). In planta transient expression analysis of monoterpene synthases. (1st ed.). Vol. 515. Elsevier Inc.

Hamm, S., Lesellier, E., Bleton, J. & Tchapla, A., (2003). Optimization of headspace solid phase microextraction for gas chromatography/mass spectrometry analysis of widely different volatility and polarity terpenoids in olibanum *J. Chromatogr. A* **1018**, 1, 73–83.

Hammer, K. a., Carson, C.F. & Riley, T.V., (2003). Antifungal activity of the components of Melaleuca alternifolia (tea tree) oil *J. Appl. Microbiol.* **95**, 4, 853–860.

Hampton, R., Dimster-denk, D. & Rine, J., (1996). The biology of HMG-CoA reductase: the pros of contra-regulation *Trends Biochem. Sci.* **21**, 140–145.

van Herpen, T.W.J.M., Cankar, K., Nogueira, M., Bosch, D., Bouwmeester, H.J. & Beekwilder, J., (2010). Nicotiana benthamiana as a Production Platform for Artemisinin Precursors *PLoS One* **5**, 12, e14222.

Herrero, O., Ramón, D., Orejas, M., Ramo, D. & Ã, M.O., (2008). Engineering the Saccharomyces cerevisiae isoprenoid pathway for de novo production of aromatic monoterpenes in wine. *Metab. Eng.* **10**, 2, 78–86.

Hock, R., Benda, I. & Schreier, P., (1984). Formation of terpenes by yeasts during alcoholic fermentation *Z. Lebensm. Unters. Forsch.* **179**, 6, 450–452.

Hoffman, C.S. & Winston, F., (1987). A ten-minute DNA preparation from yeast efficiently releases autonomous plasmids for transformations of Escherichia coli. *Gene* **57**, 2–3, 267–272.

Hood, E.E., Gelvin, S.B., Melchers, L.S. & Hoekema, A., (1993). New Agrobacterium helper plasmids for gene transfer to plants *Transgenic Res.* **2**, 4, 208–218.

Ignea, C., Cvetkovic, I., Loupassaki, S., Kefalas, P., Johnson, C.B., Kampranis, S.C. & Makris, A.M., (2011). Improving yeast strains using recyclable integration cassettes, for the production of plant terpenoids. *Microb. Cell Fact.* **10**, 1, 4.

Ignea, C., Pontini, M., Maffei, M.E., Makris, A.M. & Kampranis, S.C., (2014). Engineering Monoterpene Production in Yeast Using a Synthetic Dominant Negative Geranyl Diphosphate Synthase. *ACS Synth. Biol.* **3**, 5, 298–306.

Iijima, Y., Gang, D.R., Fridman, E., Lewinsohn, E. & Pichersky, E., (2004). Characterization of geraniol synthase from the peltate glands of sweet basil. *Plant Physiol.* **134**, 1, 370–379.

Islam, M.S., Aryasomayajula, A. & Selvaganapathy, P.R., (2017). A review on macroscale and microscale cell lysis methods *Micromachines* **8**, 3.

Jackson, B.E., Hart-Wells, E. a & Matsuda, S.P.T., (2003). Metabolic engineering to produce sesquiterpenes in yeast. *Org. Lett.* **5**, 10, 1629–32.

Jarvis, P. & Robinson, C., (2004). Mechanisms of protein import and routing in chloroplasts. *Curr. Biol.* **14**, 24, R1064-77.

Jelly, N.S., Valat, L., Walter, B. & Maillot, P., (2014). Transient expression assays in grapevine: A step towards genetic improvement *Plant Biotechnol. J.* **12**, 9, 1231–1245.

Jiang, M., Stephanopoulos, G. & Pfeifer, B. a, (2012). Downstream reactions and engineering in the microbially reconstituted pathway for Taxol. *Appl. Microbiol. Biotechnol.* **94**, 4, 841–9.

Jin, Y. & Guo, H.S., (2015). Transgene-induced gene silencing in plants *Plant Gene Silenc. Methods Protoc.* **16**, 1998, 105–117.

Johnston, M. & Davis, R.W., (1984). Sequences that regulate the divergent GAL1-GAL10 promoter in

Saccharomyces cerevisiae. *Mol. Cell. Biol.* **4**, 8, 1440–1448.

Jones, C.G., Keeling, C.I., Ghisalberti, E.L., Barbour, E.L., Plummer, J. a & Bohlmann, J., (2008). Isolation of cDNAs and functional characterisation of two multi-product terpene synthase enzymes from sandalwood, Santalum album L. *Arch. Biochem. Biophys.* **477**, 1, 121–30.

Kampranis, S.C. & Makris, A.M., (2012). Developing a Yeast Cell Factory for the Production of Terpenoids *Comput. Struct. Biotechnol. J.* **3**, 4, 1–7.

Keim, V., Manzano, D., Fernández, F.J., Closa, M., Andrade, P., Caudepón, D., Bortolotti, C., Vega, M.C., Arró, M. & Ferrer, A., (2012). Characterization of Arabidopsis FPS Isozymes and FPS Gene Expression Analysis Provide Insight into the Biosynthesis of Isoprenoid Precursors in Seeds *PLoS One* **7**, 11, e49109.

Kirby, J., Nishimoto, M., Chow, R.W.N., Pasumarthi, V.N., Chan, R., Chan, L.J.G., Petzold, C.J. & Keasling, J.D., (2014). Use of nonionic surfactants for improvement of terpene production in Saccharomyces cerevisiae *Appl. Environ. Microbiol.* **80**, 21, 6685–6693.

Kollner, G.T., Schnee, C., Gershenzon, J. & Degenhardt, J.J., (2004). The variability of sesquiterpenes emitted from two Zea mays cultivars is controlled by allelic variation of two terpene synthase genes encoding stereoselective multiple product enzymes *Plant Cell* **16**, 5, 1115–1131.

Kulkarni, R., Pandit, S., Chidley, H., Nagel, R., Schmidt, A., Gershenzon, J., Pujari, K., Giri, A. & Gupta, V., (2013). Characterization of three novel isoprenyl diphosphate synthases from the terpenoid rich mango fruit. Vol. 71. Elsevier Ltd.

Lashbrooke, J.G., Young, P.R., Dockrall, S.J., Vasanth, K. & Vivier, M.A., (2013). Functional characterisation of three members of the Vitis vinifera L. carotenoid cleavage dioxygenase gene family *BMC Plant Biol.* **13**, 1, 156.

Li, Y. & Pfeifer, B.A., (2014). Heterologous production of plant-derived isoprenoid products in microbes and the application of metabolic engineering and synthetic biology *Curr. Opin. Plant Biol.* **19**, 8–13.

Liu, J., Zhang, W., Du, G., Chen, J. & Zhou, J., (2013). Overproduction of geraniol by enhanced precursor supply in Saccharomyces cerevisiae *J. Biotechnol.* **168**, 4, 446–451.

Liu, L., Redden, H. & Alper, H.S., (2013). Frontiers of yeast metabolic engineering: diversifying beyond ethanol and Saccharomyces. *Curr. Opin. Biotechnol.* **24**, 6, 1–8.

Lücker, J., El Tamer, M.K., Schwab, W., Verstappen, F.W.A., van der Plas, L.H.W., Bouwmeester, H.J. & Verhoeven, H.A., (2002). Monoterpene biosynthesis in lemon (Citrus limon) *Eur. J. Biochem.* **269**, 13, 3160–3171.

Mahmoud, S.S. & Croteau, R.B., (2002). Strategies for transgenic manipulation of monoterpene biosynthesis in plants *Trends Plant Sci.* **7**, 8, 366–373.

Marienhagen, J. & Bott, M., (2013). Metabolic engineering of microorganisms for the synthesis of plant natural products. *J. Biotechnol.* **163**, 2, 166–78.

Martin, D.M. & Bohlmann, J., (2004). Identification of Vitis vinifera (-)-alpha-terpineol synthase by in silico screening of full-length cDNA ESTs and functional characterization of recombinant terpene synthase. *Phytochemistry* **65**, 9, 1223–9.

Martin, D.M., Aubourg, S., Schouwey, M.B., Daviet, L., Schalk, M., Toub, O., Lund, S.T. & Bohlmann, J., (2010). Functional annotation, genome organization and phylogeny of the grapevine (Vitis vinifera) terpene synthase gene family based on genome assembly, FLcDNA cloning, and enzyme assays. *BMC Plant Biol.* **10**, 1, 226.

Martin, V.J.J., Pitera, D.J., Withers, S.T., Newman, J.D. & Keasling, J.D., (2003). Engineering a mevalonate pathway in Escherichia coli for production of terpenoids. *Nat. Biotechnol.* **21**, 7, 796–802.

Moses, S.B.G., Otero, R.R.C. & Pretorius, I.S., (2005). Domain engineering of Saccharomyces cerevisiae exoglucanases. *Biotechnol. Lett.* **27**, 5, 355–62.

Moyo, M., (2017). The interaction between Vitis vinifera and fungal pathogens : A molecular approach using characterized grapevine mutants.

Mumberg, D., Muller, R. & Funk, M., (1994). Regulatable promoters of Saccharomyces cerevisiae: comparison of transcriptional activity and their use for heterologous expression. *Nucleic Acids Res.* **22**, 25, 5767–5768.

Muntendam, R., Melillo, E., Ryden, A. & Kayser, O., (2009). Perspectives and limits of engineering the isoprenoid metabolism in heterologous hosts. *Appl. Microbiol. Biotechnol.* **84**, 6, 1003–19.

Murashige, T. & Skoog, F., (1962). A revised medium for rapid growth and bioassays with tobacco tissue culture *Physiol. Plant.* **15**, 473–497.

Mutwil, M., (2020). Computational approaches to unravel the pathways and evolution of specialized metabolism *Curr. Opin. Plant Biol.* **55**, 38–46.

Nguyen, T.-D., MacNevin, G. & Ro, D.-K., (2012). De Novo Synthesis of High-Value Plant Sesquiterpenoids

in Yeast In: Methods Enzymol. (1st ed.). Vol. 517. Elsevier Inc. 261–278.

Ooms, G., Hooykaas, P.J.J., Moolenaar, G. & Schilperoort, R.A., (1981). Crown gall plant tumors of abnormal morphology, induced by Agrobacterium tumefaciens carrying mutated octopine Ti plasmids; analysis of T-DNA functions *Gene* **14**, 1–2, 33–50.

Oswald, M., Fischer, M., Dirninger, N. & Karst, F., (2007). Monoterpenoid biosynthesis in Saccharomyces cerevisiae. *FEMS Yeast Res.* **7**, 3, 413–21.

Pan, Z., Herickhoff, L. & Backhaus, R.A., (1996). Cloning, characterization, and heterologous expression of cDNAs for farnesyl diphosphate synthase from the guayule rubber plant reveals that this prenyltransferase occurs in rubber particles *Arch. Biochem. Biophys.* **332**, 1, 196–204.

Pardo, E., Rico, J., Gil, J.V. & Orejas, M., (2015). De novo production of six key grape aroma monoterpenes by a geraniol synthase-engineered S. cerevisiae wine strain *Microb. Cell Fact.* **14**, 1, 136.

Polakowski, T., Stahl, U. & Lang, C., (1998). Overexpression of a cytosolic hydroxymethylglutaryl-CoA reductase leads to squalene accumulation in yeast. *Appl. Microbiol. Biotechnol.* **49**, 1, 66–71.

Reed, J. & Osbourn, A., (2018). Engineering terpenoid production through transient expression in Nicotiana benthamiana *Plant Cell Rep.* **37**, 10, 1431–1441.

Reid, K.E., Olsson, N., Schlosser, J., Peng, F. & Lund, S.T., (2006). An optimized grapevine RNA isolation procedure and statistical determination of reference genes for real-time RT-PCR during berry development. *BMC Plant Biol.* **6**, 27.

Rico, J., Pardo, E. & Orejas, M., (2010). Enhanced production of a plant monoterpene by overexpression of the 3-hydroxy-3-methylglutaryl coenzyme A reductase catalytic domain in Saccharomyces cerevisiae. *Appl. Environ. Microbiol.* **76**, 19, 6449–54.

Roach, C.R., Hall, D.E., Zerbe, P. & Bohlmann, J.J., (2014). Plasticity and Evolution of (+)-3-Carene Synthase and (-)-Sabinene Synthase Functions of a Sitka Spruce Monoterpene Synthase Gene Family associated with Weevil Resistance. *J. Biol. Chem.* **289**, 34, 23859–23869.

Robinson, A.L., Boss, P.K., Heymann, H., Solomon, P.S. & Trengove, R.D., (2011). Development of a sensitive non-targeted method for characterizing the wine volatile profile using headspace solid-phase microextraction comprehensive two-dimensional gas chromatography time-of-flight mass spectrometry. *J. Chromatogr. A* **1218**, 3, 504–17.

Rodriguez, S., Kirby, J., Denby, C.M. & Keasling, J.D., (2014). Production and quantification of sesquiterpenes in Saccharomyces cerevisiae, including extraction, detection and quantification of terpene products and key related metabolites *Nat. Protoc.* **9**, 8, 1980–1996.

Rusdi, N., Goh, H.-H., Sabri, S., Ramzi, A., Mohd Noor, N. & Baharum, S., (2018). Functional Characterisation of New Sesquiterpene Synthase from the Malaysian Herbal Plant, Polygonum Minus *Molecules* **23**, 6, 1370.

Salvagnin, U., Malnoy, M., Thöming, G., Tasin, M., Carlin, S., Martens, S., Vrhovsek, U., Angeli, S. & Anfora, G., (2018). Adjusting the scent ratio: using genetically modified Vitis vinifera plants to manipulate European grapevine moth behaviour *Plant Biotechnol. J.* **16**, 1, 264–271.

Scalcinati, G., Knuf, C., Partow, S., Chen, Y., Maury, J., Schalk, M., Daviet, L., Nielsen, J. & Siewers, V., (2012). Dynamic control of gene expression in Saccharomyces cerevisiae engineered for the production of plant sesquitepene α-santalene in a fed-batch mode. *Metab. Eng.* **14**, 2, 91–103.

van Schie, C.C.N., Haring, M.A. & Schuurink, R.C., (2012). Prenyldiphosphate Synthases and Gibberellin Biosynthesis In: Isoprenoid Synth. Plants Microorg. Springer New York, New York, NY 213–232.

Schilmiller, A.L., Schauvinhold, I., Larson, M., Xu, R., Charbonneau, A.L., Schmidt, A., Wilkerson, C., Last, R.L. & Pichersky, E., (2009). Monoterpenes in the glandular trichomes of tomato are synthesized from a neryl diphosphate precursor rather than geranyl diphosphate. *Proc. Natl. Acad. Sci. U. S. A.* **106**, 26, 10865–70.

Schmidt, A. & Gershenzon, J., (2008). Cloning and characterization of two different types of geranyl diphosphate synthases from Norway spruce (Picea abies). *Phytochemistry* **69**, 1, 49–57.

Schmidt, A., Wachtler, B., Temp, U., Krekling, T., Seguin, A. & Gershenzon, J., (2010). A Bifunctional Geranyl and Geranylgeranyl Diphosphate Synthase Is Involved in Terpene Oleoresin Formation in Picea abies *Plant Physiol.* **152**, 2, 639–655.

Shelton, D., Zabaras, D., Chohan, S., Wyllie, S.G., Baverstock, P., Leach, D. & Henry, R., (2004). Isolation and partial characterisation of a putative monoterpene synthase from Melaleuca alternifolia *Plant Physiol. Biochem.* **42**, 11, 875–882.

Shen, J., Zeng, Y., Zhuang, X., Sun, L., Yao, X., Pimpl, P. & Jiang, L., (2013). Organelle pH in the arabidopsis endomembrane system *Mol. Plant* **6**, 5, 1419–1437.

Shi, P., Fu, X., Liu, M., Shen, Q., Jiang, W., Li, L., Sun, X. & Tang, K., (2017). Promotion of artemisinin content in Artemisia annua by overexpression of multiple artemisinin biosynthetic pathway genes *Plant Cell,*

Tissue Organ Cult. **0**, 0, 0.

Silhavy, D., Molnár, A., Lucioli, A., Szittya, G., Hornyik, C., Tavazza, M. & Burgyán, J., (2002). A viral protein suppresses RNA silencing and binds silencing-generated, 21- to 25-nucleotide double-stranded RNAs *EMBO J.* **21**, 12, 3070–3080.

Simkin, A.J., Miettinen, K., Claudel, P., Burlat, V., Guirimand, G., Courdavault, V., Papon, N., Meyer, S., Godet, S., St-pierre, B., Giglioli-guivarc, N., Fischer, M.J.C., Memelink, J., Clastre, M., Giglioli-Guivarc'H, N., Fischer, M.J.C., Memelink, J. & Clastre, M., (2013). Characterization of the plastidial geraniol synthase from Madagascar periwinkle which initiates the monoterpenoid branch of the alkaloid pathway in internal phloem associated parenchyma. *Phytochemistry* **85**, January, 36–43.

Slaghenaufi, D. & Ugliano, M., (2018). Norisoprenoids, Sesquiterpenes and Terpenoids Content of Valpolicella Wines During Aging: Investigating Aroma Potential in Relationship to Evolution of Tobacco and Balsamic Aroma in Aged Wine *Front. Chem.* **6**, March, 1–13.

Szkopińska, A. & Płochocka, D., (2005). Farnesyl diphosphate synthase; regulation of product specificity. *Acta Biochim. Pol.* **52**, 1, 45–55.

Takahashi, S., Yeo, Y., Greenhagen, B.T., McMullin, T., Song, L., Maurina-Brunker, J., Rosson, R., Noel, J.P. & Chappell, J., (2007). Metabolic engineering of sesquiterpene metabolism in yeast *Biotechnol. Bioeng.* **97**, 1, 170–181.

Del Terra, L., Lonzarich, V., Asquini, E., Navarini, L., Graziosi, G., Suggi Liverani, F. & Pallavicini, A., (2013). Functional characterization of three Coffea arabica L. monoterpene synthases: insights into the enzymatic machinery of coffee aroma. *Phytochemistry* **89**, May, 6–14.

Thabet, I., Guirimand, G., Guihur, A., Lanoue, A., Courdavault, V., Papon, N., Bouzid, S., Giglioli-Guivarc'h, N., Simkin, A.J. & Clastre, M., (2012). Characterization and subcellular localization of geranylgeranyl diphosphate synthase from Catharanthus roseus *Mol. Biol. Rep.* **39**, 3, 3235–3243.

Thomas, B.J. & Rothstein, R., (1989). Elevated recombination rates in transcriptionally active DNA. *Cell* **56**, 4, 619–30.

Turek, C. & Stintzing, F.C., (2013). Stability of essential oils: A review *Compr. Rev. Food Sci. Food Saf.* **12**, 1, 40–53.

Vandermoten, S., Haubruge, É. & Cusson, M., (2009). New insights into short-chain prenyltransferases: structural features, evolutionary history and potential for selective inhibition *Cell. Mol. Life Sci.* **66**, 23, 3685–3695.

Varming, C., Andersen, M.L. & Poll, L., (2006). Volatile monoterpenes in black currant (Ribes nigrum L.) juice: effects of heating and enzymatic treatment by beta-glucosidase. *J. Agric. Food Chem.* **54**, 6, 2298–302.

Verwaal, R., Wang, J., Meijnen, J.-P., Visser, H., Sandmann, G., van den Berg, J. a & van Ooyen, A.J.J., (2007). High-level production of beta-carotene in Saccharomyces cerevisiae by successive transformation with carotenogenic genes from Xanthophyllomyces dendrorhous. *Appl. Environ. Microbiol.* **73**, 13, 4342–50.

Vidal, J.R., Gomez, C., Cutanda, M.C., Shrestha, B.R., Bouquet, A., Thomas, M.R. & Torregrosa, L., (2010). Use of gene transfer technology for functional studies in grapevine *Aust. J. Grape Wine Res.* **16**, SUPPL. 1, 138–151.

Wang, G. & Dixon, R. a, (2009). Heterodimeric geranyl(geranyl)diphosphate synthase from hop (Humulus lupulus) and the evolution of monoterpene biosynthesis. *Proc. Natl. Acad. Sci. U. S. A.* **106**, 24, 9914–9.

Wang, K., (2006). Agrobacterium Protocols. (2nd ed.). Vol. 343. Humana Press, New Jersey.

Wang, K. & Ohnuma, S., (1999). Chain-length determination mechanism of isoprenyl diphosphate synthases and implications for molecular evolution. *Trends Biochem. Sci.* **24**, 11, 445–51.

Williams, D.C., McGarvey, D.J., Katahira, E.J. & Croteau, R., (1998). Truncation of limonene synthase preprotein provides a fully active "pseudomature" form of this monoterpene cyclase and reveals the function of the amino-terminal arginine pair. *Biochemistry* **37**, 35, 12213–20.

Wriessnegger, T. & Pichler, H., (2013). Yeast metabolic engineering – targeting sterol metabolism and terpenoid formation *Prog. Lipid Res.* **52**, 3, 277–293.

Wrolstad, R. & Jennings, W., (1963). Chromatostrip isomerization of terpenes *J. Chromatogr.* **18**, 318–324.

Xiao, H. & Zhong, J.-J., (2016). Production of Useful Terpenoids by Higher-Fungus Cell Factory and Synthetic Biology Approaches *Trends Biotechnol.* **xx**, 1–14.

Xiao, M., Zhang, Y., Chen, X., Lee, E.-J., Barber, C.J.S., Chakrabarty, R., Desgagné-Penix, I., Haslam, T.M., Kim, Y.-B., Liu, E., MacNevin, G., Masada-Atsumi, S., Reed, D.W., Stout, J.M., Zerbe, P., Zhang, Y., Bohlmann, J., Covello, P.S., De Luca, V., Page, J.E., Ro, D.-K., Martin, V.J.J., Facchini, P.J. & Sensen, C.W., (2013). Transcriptome analysis based on next-generation sequencing of non-model plants producing specialized metabolites of biotechnological interest *J. Biotechnol.* **166**, 3, 122–134.

Xie, X., Kirby, J. & Keasling, J.D., (2012). Functional characterization of four sesquiterpene synthases from

Ricinus communis (Castor bean) *Phytochemistry* **78**, 20–28.

Yin, J.L., Wong, W.S., Jang, I.C. & Chua, N.H., (2017). Co-expression of peppermint geranyl diphosphate synthase small subunit enhances monoterpene production in transgenic tobacco plants *New Phytol.* **213**, 3, 1133–1144.

Young, P.R., (2004). Molecular analyses of candidate carotenoid biosynthetic genes in <i>Vitis vinifera<i/> L. Stellenbosch University.

Zhang, X., Niu, M., Teixeira da Silva, J.A., Zhang, Y., Yuan, Y., Jia, Y., Xiao, Y., Li, Y., Fang, L., Zeng, S. & Ma, G., (2019). Identification and functional characterization of three new terpene synthase genes involved in chemical defense and abiotic stresses in Santalum album *BMC Plant Biol.* **19**, 1, 115.

Zhao, J., Bao, X., Li, C., Shen, Y. & Hou, J., (2016). Improving monoterpene geraniol production through geranyl diphosphate synthesis regulation in Saccharomyces cerevisiae *Appl. Microbiol. Biotechnol.* **100**, 10, 4561–4571.

Zhao, Y.J., Chen, X., Zhang, M., Su, P., Liu, Y.J., Tong, Y.R., Wang, X.J., Huang, L.Q. & Gao, W., (2015). Molecular cloning and characterisation of farnesyl pyrophosphate synthase from Tripterygium wilfordii *PLoS One* **10**, 5, 1–13.

Zhu, F., Suzuki, K., Okada, K., Tanaka, K., Nakagawa, T., Kawamukai, M. & Matsuda, H., (1997). Cloning and Functional Expression of a Novel Geranylgeranyl Pyrophosphate Synthase Gene from Arabidopsis thaliana in Escherichia coli *Plant Cell Physiol.* **38**, 3, 357–361.

Zhuang, X. & Chappell, J., (2015). Building terpene production platforms in yeast *Biotechnol. Bioeng.* **112**, 9, 1854–1864.

Appendix A   To Chapter 2

Table A-i Primers used in this study. Underlined sequences indicate restriction endonuclease recognition site addition.

Name	Sequence (5' to 3')	Amplicon size (kb)	Description
VvTPS39-5'	<u>GTCGAC</u>ATGGCTCTTTCCATGCTTTCTTCAA	1773	Amplifies the full-length CDS of the *Vitis vinifera TPS39*. *SalI* RE site
VvTPS39-3'	TTATTCAGAACTCAAACTGGGAATG		
VvTPS39trunc-5'	<u>GTCGAC</u>ATGGCTTCTCGTCCAGGAAACCAAT	1698	Amplifies a truncated version of *VvTPS39* without N-terminal plastid-targeting sequence. *SalI* RE site and start codon
VvTPS39-3'	TTATTCAGAACTCAAACTGGGAATG		
M13pUCF	CCCAGTCACGACGTTGTAAAACG	Varies	Universal primers to PCR any cassette from pGEM-T Easy
M13pUCR	AGCGGATAACAATTTCACACAGG		
attB1 adapter	GGGGACAAGTTTGTACAAAAAAGCAGGCT	Varies	Universal *att*B adapter primers used for Gateway® cloning
attB2 adapter	GGGGACCACTTTGTACAAGAAAGCTGGGT		
VviTPS39_B1	aaaaagcaggctATGGCTCTTTCCATGCTTTC	1797	Template specific primers containing 12 nucleotides of the *att*B sites (lowercase)
VviTPS39_trunc_B1	aaaaagcaggctatgGCTTCTCGTCCAGGAAACC	1722	
VviTPS39_B2	agaaagctgggtTTATTCAGAACTCAAACTGGGAATG		
VviGPStrunc-5'	<u>GTCGAC</u>ATGGTTTTGGGCTGTAGAGAAACTTATTC	1148	Amplifies the truncated CDS of the *Vitis vinifera GPS*. *SalI* RE site and start codon
VviGPS-3'	ACTCTTCTGGTTCTTCATTTAGTTCTTG		
VviGPS-5'	<u>GTCGAC</u>ATGTTATTCTCCAGGGGATTTTCTC	1283	Amplifies full-length CDS of the *Vitis vinifera GPS*. *SalI* RE site
VviGPS-3'	ACTCTTCTGGTTCTTCATTTAGTTCTTG		
nptII-5'	TCTGATGCCGCCGTGTTC	402	Screening for gene integration. Amplifies kanamycin resistant gene on pART27 construct
nptII_3'	GAGCCCCTGATGCTCTTCGT		
VviActin-5'	GATACTGAAGATATCCAGCCCCTCG	521 bp for cDNA and 713 bp for gDNA	Intron spanning primers designed to amplify region of actin encoding gene (VIT_204s0044g00580)
VviActin-3'	GCATGGGGAAGTGCATAACCTT		

Name	Sequence (5' to 3')	Amplicon size (kb)	Description
CaMVp	GACGTAAGGGATGACGCACAAT	1865	3' gene specific primer in combination with 5' primer specific to CaMV promoter to screen for transgene integration
VviTPS39	TTATTCAGAACTCAAACTGGGAATG		
SctHMG1-5'	ATGGCAGCAGACCAATTGGTGAAAACTG	1590	Amplifies truncated *HMG* from *Saccharomyces cerevisiae*. *SalI* RE site
SctHMG1-3'	GTCGACTTAGGATTTAATGCAGGTGACGG		
ScIDI1-5'	CTCGAGTTATAGCATTCTATGAATTTGCC	867	Amplifies *IDI1* isomerase from *S. cerevisiae*. *SalI* RE site
ScIDI1-3'	TCGAGATGACTGCCGACAACAATAG		
PGK1p-5'	AATATTCGATTAATTTTTTTTTCTTTCCTCTTTT	717	Amplify the *PGK1* promoter from the yeast expression vector pCEL15. *XbaI* RE site
PGK1p-3'	TCTAGAATTTGTTGTAAAAGTAGATAATTACTTCCTTG		
PGK1p-5'	AATATTCGATTAATTTTTTTTTCTTTCCTCTTTT	Varies	Amplify the expression cassette from PGK1p-IDI1-CYCt
CYC1t-3'	ATACCCGGGATCCTCTTCGCTATTACGCCAG		
pBS-5'	GGTACCCCTGATTCTGTGGATAAC	1196	Used for amplifying cassette from generic pBS vector. *SalI* RE sites
pBS-3'	GGTACCGGCCGCAAATTA		
ScURA3-5'	AATATTGCTGTCAAACATGAGAATTG	1146	Isolate the *URA3* gene from YEplac195 vector. *SspI* and *SalI* RE site
ScURA3-3'	GGTACCCCTTTCGTCTTCAAGAATTA		
ScADE2-5'	ACTGCACAGAACAAAAACCTGCAGGAAACGAAGATAAATCCTTCATGCTCGAAAAAGAT	2518	Isolate the *ADE2* gene from *S. cerevisiae*
ScADE2-3'	CACTCAAAGGCGGTAATACGGTTATCCACAGAATCAGGGGCGGTACAGTCACTGGAATCG		
ScTRP1-5'	GAGGGAGGGCATTGGTGAC	798	Isolate the *TRP1* gene from *S. cerevisiae*
ScTRP1-3'	GCCTGCAGGCAAGTGCAC		

Table A-ii Constructs used and generated in this study. NA = not applicable.

Plasmid	Description	Expression cassette	Source or reference
pCEL15	*PGK1p* region PCR-amplified from this vector	NA	Moses *et al.* (2005)
p424MET25	*CYC1t* region PCR-amplified from this vector	NA	Mumberg *et al.* (1994)
pGEM-T-Easy	*E. coli* general cloning vector	NA	Promega
pBlueScript SK II+	Cloning vector used as backbone to construct yeast expression vector	NA	Stratagene cloning systems
YIplac128	*LEU2* gene PCR-amplified from this vector	NA	Gietz & Akio (1988)
YIplac204	*TRP1* gene PCR-amplified from this vector	NA	Gietz & Akio (1988)
YEplac195	*URA3* gene PCR-amplified from this vector	NA	Gietz & Akio (1988)
pART7	Primary cloning vector	CaMV35Sp::OCSt::nptII	Gleave (1992)
pART27	Binary vector	NA	Gleave (1992)
pBS-URA3	pBlueScript SK II+ [*URA3* - P$_{PGK1}$]	PGK1p::CYC1t::URA3	This study
pGEM-TPS39	Cloning vector containing *VviTPS39, Spe*I and *Sal*I RE sites	NA	This study
pBS-PGK1p-TPS39	pBlueScript SK II+ [*URA3* - P$_{PGK1}$ - *VviSBTPS39*], linearise with *Apa*I	PGK1p::VviSBTPS39::CYCt::URA3 Amp^R	This study
pBS-PGK1p-TPS39trunc	pBlueScript SK II+ [*URA3* - P$_{PGK1}$ - *VviSBTPS39trunc*], linearise with *Apa*I	PGK1p::VviSBTPS39trunc::CYCt::URA3 Amp^R	This study
YIplac128-tHMG1	YIplac128 [*LEU2* - P$_{PGK1}$ - *tHMG1*], linearise with *Eco*Rv	PGK1p::tHMG1::CYCt LEU2 Amp^R	This study
pGEM-T-Easy-IDI1	pGEM-T-Easy [*ADE2* - P$_{PGK1}$ - *IDI1*], linearise with *Hpa*I	PGK1p::IDI1::CYCt::ADE2	This study
pBS-TRP1	pBlueScript SK II+ [*TRP1* - P$_{PGK1}$]	PGK1p::CYCt::TRP1	This study
pBS-PGK1p-GPStrunc	pBlueScript SK II+ [*TRP1* - P$_{PGK1}$ – *VviGPS*], linearise with *Eco*81I	PGK1p::VviGPS::CYCt::TRP1 Amp^R	This study

83

Plasmid	Description	Expression cassette	Source or reference
pAG426GAL	Episomal *S. cerevisiae* Gateway® cloning vector	GAL1p::CYC1t::URA3	Alberti *et al.* (2007)
pAG426GAL-TPS39	426GAL-ccdB + *VviSBTPS39*	GAL1p::VviSBTPS39::CYC1t::URA3	This study
pAG426GAL-TPS39trunc	426GAL-ccdB + *VviSBTPS39trunc*	GAL1p::VviSBTPS39trunc::CYC1t::URA3	This study
pART7-GPS	Full-length *GPS* isolated from *Vitis vinifera* and cloned into pART7 expression cassette	CaMV35Sp::VviGPS::OCSt::nptII	This study
pART27-GPS	pART7 expression cassette containing *VviGPS* cloned into pART27	CaMV35Sp::VviGPS::OCSt::nptII	This study
pART7-TPS39	Full-length *TPS39* isolated from *Vitis vinifera* and cloned into pART7 expression cassette	CaMV35Sp::VviTPS39::OCSt::nptII	This study
pART27-TPS39	pART7 expression cassette containing *VviTPS39* cloned into pART27	CaMV35Sp::VviTPS39::OCSt::nptII	This study
P19	anti-posttranscriptional gene silencing protein		
pCB355-GFP	pCB301 parental vector. 35S from pGREEN and mGFP5ER		M. Campa (unpublished)

84

Table A-iii Yeast strains used and generated in this study.

Strain	Description	Source or reference
W303-1A	MAT a ade2-1 can1-100 ura3-1 leu2-3,112 his3-11,15 trp1-1	Thomas & Rothstein (1989)
GT01	MAT a ade2-1 can1-100 ura3-1::URA3 - P_{PGK1} leu2-3,112 his3-11,15 trp1-1	This study
GT02	MAT a ade2-1 can1-100 ura3-1::URA3 - P_{PGK1} – VviTPS39 leu2-3,112 his3-11,15 trp1-1	This study
GT03	MAT a ade2-1, can1-100 ura3-1::URA3 - P_{PGK1} – VviTPS39 leu2-3::LEU2 - P_{PGK1} – tHMG1, his3-11,15, trp1-1	This study
GT04	MAT a ade2-1::ADE2 - P_{PGK1} – IDI1 can1-100 ura3-1::URA3 - P_{PGK1} leu2-3,112 his3-11,15 trp1-1	This study
GT05	MAT a ade2-1::ADE2 - P_{PGK1} – IDI1 can1-100 ura3-1::URA3 - P_{PGK1} – VviTPS39 leu2-3,112 his3-11,15 trp1-1	This study
GT06	MAT a ade2-1 can1-100 ura3-1::URA3 - P_{PGK1} – VviTPS39 leu2-3 his3-11,15 trp1-1::TRP1 - P_{PGK1} – VviGPS	This study
GT07	MAT a ade2-1::ADE2 - P_{PGK1} – IDI1 can1-100 ura3-1::URA3 - P_{PGK1} – VviTPS39 leu2-3::LEU2 - P_{PGK1} – tHMG1 his3-11,15 trp1-1	This study
GT08	MAT a ade2-1 can1-100 ura3-1::URA3 - P_{PGK1} – VviTPS39 leu2-3::LEU2 - P_{PGK1} – tHMG1 his3-11,15 trp1-1::TRP1 - P_{PGK1} – VviGPS	This study
GT09	MAT a ade2-1::ADE2 - P_{PGK1} – IDI1 can1-100 ura3-1::URA3 - P_{PGK1} – VviTPS39 leu2-3 his3-11,15 trp1-1::TRP1 - P_{PGK1} – VviGPS	This study
GT11	MAT a ade2-1::ADE2 – P_{PGK1} – IDI1 can1-100 ura3-1::URA3 - P_{PGK1} – VviTPS39 leu2-3::LEU2 - P_{PGK1} – tHMG1 his3-11,15 trp1-1	This study
GT14	MAT a ade2-1::ADE2 - P_{PGK1} – IDI1 can1-100 ura3-1::URA3 - P_{GAL1} – VviTPS39full-length leu2-3::LEU2 - P_{PGK1} – tHMG1 his3-11,15 trp1-1	This study
GT15	MAT a ade2-1::ADE2 - P_{PGK1} – IDI1 can1-100 ura3-1::URA3 - P_{GAL1} – VviTPS39trunc leu2-3::LEU2 - P_{PGK1} – tHMG1 his3-11,15 trp1-1	This study

Appendix B   To Chapter 2

Table B-i Volatile analysis of yeast cultures expressing *VviSBTPS39.* Average of peak area normalised to IS (3-octanol) and cell count (OD$_{600}$) with ± standard deviation between four repeats. Values significantly different (student's *t*-test with p < 0.05) from the control yeast are indicated in red (higher) and blue (lower). Compounds confirmed with the authentic standard are indicated with asterisks (*). ND = not detected.

Compounds	Control	VviSBTPS39
α-thujene	ND	0.0019 ± 0.0007
β-myrcene*	0.002 ± 0.0001	0.0099 ± 0.0011
α-phellandrene	ND	0.0037 ± 0.0004
α-terpinene	ND	0.0118 ± 0.0018
Limonene*	0.0005 ± 0.0001	0.0047 ± 0.0009
Eucalyptol*	ND	0.0021 ± 0.00002
γ-terpinene	ND	0.0229 ± 0.0046
Terpinolene	ND	0.0028 ± 0.0007
Linalool*	0.0038 ± 0.0002	0.0064 ± 0.0005
(-)-terpinen-4-ol*	ND	0.0242 ± 0.0005
trans-β-farnesene	0.0068 ± 0.0008	0.0078 ± 0.0006
α-terpineol*	0.0004 ± 0.00002	0.0022 ± 0.0001
α-bergamotene	0.0009 ± 0.0001	0.0009 ± 0.0001
Methionol	0.0019 ± 0.0004	0.0032 ± 0.0002
β-bisabolene	0.0004 ± 0.0001	0.0006 ± 0.0001
Farnesene	0.0018 ± 0.0002	0.002 ± 0.0002
β-citronellol*	0.0031 ± 0.0001	0.0068 ± 0.0002
Geraniol	0.0012 ± 0.0001	0.0034 ± 0.0001
Nerolidol	0.0059 ± 0.0006	0.0069 ± 0.0003

Appendix C   To Chapter 2

Table C-i Effect of temperature before and during SPME on the volatile profile observed in yeast expressing *VviSBTPS39*. Terpenes expressed as average percentage of the total monoterpene or sesquiterpene peak area with ± standard deviation between three or more repeats. Compounds listed in order of retention time; Asterisks (*) indicate peak identity confirmed with an authentic standard. No heat treatment – vials were kept at room temperature before analysis; heat treatment – vials were placed in a 100°C oven for 1 h and allowed to cool to room temperature before analysis; 30°C extraction – SPME at 30°C; 60°C extraction – SPME at 60°C. The compounds produced through rearrangement of sabinene according to the study by Wrolstad and Jennings (1963) are presented in red. The monoterpene compounds were divided into four clusters based on the effect of the various temperature treatments on the relative peaks. ND = not detected.

| Class	Compounds#	Retention time (min)	No heat treatment		Heat treatment		Cluster
			30°C extraction (%)	60°C extraction (%)	30°C extraction (%)	60°C extraction (%)	
Monoterpenes	α-thujene	11.9	17.8 ± 1.5	8.5 ± 0.5	10.5 ± 0.7	3.1 ± 0.4	A
	β-pinene	14.2	0.6 ± 0.1	0.3 ± 0.005	0.8 ± 0.1	0.2 ± 0.03	A
	Sabinene	14.6	34.7 ± 4.2	11.1 ± 0.8	16.5 ± 3.2	3.8 ± 0.8	A
	β-myrcene	15.7	5.3 ± 0.4	6.6 ± 2.8	8 ± 0.7	5.4 ± 1.9	B
	α-phellandrene	16.0	1.4 ± 0.1	0.6 ± 0.3	1.4 ± 0.1	0.8 ± 0.3	A
	α-terpinene*	16.5	7.6 ± 0.7	7.4 ± 3	14.2 ± 0.8	6.1 ± 2.8	B
	Limonene*	17.1	3.7 ± 0.3	6.7 ± 0.2	5.2 ± 0.4	2.9 ± 1.8	B
	Eucalyptol	17.3	ND	0.4 ± 0.02	0.1 ± 0.02	0.5 ± 0.04	C
	β-phellandrene	17.4	2.5 ± 0.2	2.9 ± 0.3	2.5 ± 0.2	3.2 ± 0.4	B
	γ-terpinene	18.5	15.3 ± 1.5	23.7 ± 1.1	26.1 ± 1.2	27.2 ± 2.3	D
	ρ-cymene	19.3	8.8 ± 1.2	11.2 ± 1.3	11 ± 0.8	11.9 ± 0.5	B
	Terpinolene	19.6	2 ± 0.2	2.8 ± 0.2	3 ± 0.1	3.5 ± 0.4	D
	Linalool*	26.4	ND	0.4 ± 0.04	ND	1.1 ± 0.2	C
	(-)-terpinen-4-ol*	28.5	0.4 ± 0.1	10.8 ± 3.1	0.7 ± 0.1	21.2 ± 2.5	C
	α-terpineol*	30.6	ND	0.6 ± 0.1	ND	0.8 ± 0.02	C
	β-citronellol*	31.8	ND	2.2 ± 0.3	ND	2.8 ± 0.5	C
	Geraniol*	33.8	ND	3.8 ± 0.7	ND	5.4 ± 0.6	C
Sesquiterpenes	Nerolidol*	37.7	ND	30 ± 1.3	ND	51.7 ± 8.3	-
	Farnesol*	43.9	ND	70 ± 1.3	ND	48.3 ± 8.3	-

Appendix D   To Chapter 2

Table D-i Average of the selected ion peak area normalised to the IS and cell count (OD_{600}) of the various yeast strains heterologously expressing *VviSBTPS39* with various combinations of the MVA pathway genes. Values significantly different (student's *t*-test with $p < 0.05$) from the yeast expressing only *VviSBTPS39* are indicated in red (higher) and blue (lower) with N=3.

Strain	VviSBTPS39	+ tHMG1	+ IDI1	+ VviGPS	+tHMG1 & IDI1	+tHMG1 & VviGPS	+IDI1 & VviGPS
α-thujene	0.0228	0.0121	0.0418	0.0152	0.0277	0.0144	0.0715
β-pinene	0.0019	0.0011	0.00368	0.0014	0.0027	0.0014	0.0064
Sabinene	0.1859	0.0853	0.3400	0.1225	0.1921	0.0941	0.5096
β-myrcene	0.0155	0.0094	0.0343	0.0120	0.0270	0.0122	0.0606
α-phellandrene	0.0016	0.0009	0.0029	0.0010	0.0024	0.0012	0.0062
α-terpinene	0.0121	0.0095	0.0252	0.0103	0.0290	0.0129	0.0580
Limonene	0.0105	0.0061	0.0222	0.0081	0.0173	0.0077	0.0380
β-phellandrene	0.0054	0.0030	0.0105	0.0038	0.0081	0.0039	0.0195
Eucalyptol	0.0003	0.0002	0.0005	0.0002	0.0004	0.0001	0.0003
γ-terpinene	0.0252	0.0197	0.0536	0.0222	0.0602	0.0265	0.1157
ρ-cymene	0.0089	0.0055	0.0139	0.0067	0.0126	0.0075	0.0243
α-terpinolene	0.0036	0.0024	0.0071	0.0028	0.0076	0.0034	0.0150
(-)-terpinen-4-ol	0.0007	0.0007	0.0019	0.0008	0.0024	0.0009	0.0037
Total monoterpene	0.294	0.156	0.557	0.207	0.390	0.186	0.929
Fold change in total monoterpenes	**1**	**0.53**	**1.89**	**0.70**	**1.32**	**0.63**	**3.16**

Table D-ii Average of the selected ion peak area normalised to IS and cell count (OD_{600}). The student's *t*-test ($p < 0.05$) was used to determine significant differences (indicated by red values) in normalised compound peak areas between the yeast strain heterologously expressing a full-length version of *VviSBTPS39* compared to the truncated versions of the *VviTPS* wherein the predicted plastid-targeting sequence has been removed with n=3.

Construct	VviSBTPS39full	VviSBTPS39trunc
α-thujene	0.0135	0.0228
α-pinene	0.0010	0.0013
Camphene	0.00001	0.00003
Sabinene	0.0091	0.0155
β-pinene	0.0009	0.0012
Myrcene	0.0019	0.0033
α-phellandrene	0.0007	0.0012
α-terpinene	0.0050	0.0088
ρ-cymene	0.0072	0.0111
Limonene	0.0014	0.0023
Eucalyptol	0.0003	0.0004
γ-terpinene	0.0093	0.0162
α-terpinolene	0.0016	0.0029
Menthol	0.0001	0.0001
(-)-terpinen-4-ol	0.0009	0.0014
α-terpineol	0.0001	0.0001
Fenchone	0.0001	0.0001
Citronellol	0.0005	0.0006
Total monoterpenes	0.0536	0.0893
Fold change in total monoterpenes	**1**	**1.67**

Appendix E   To Chapter 2
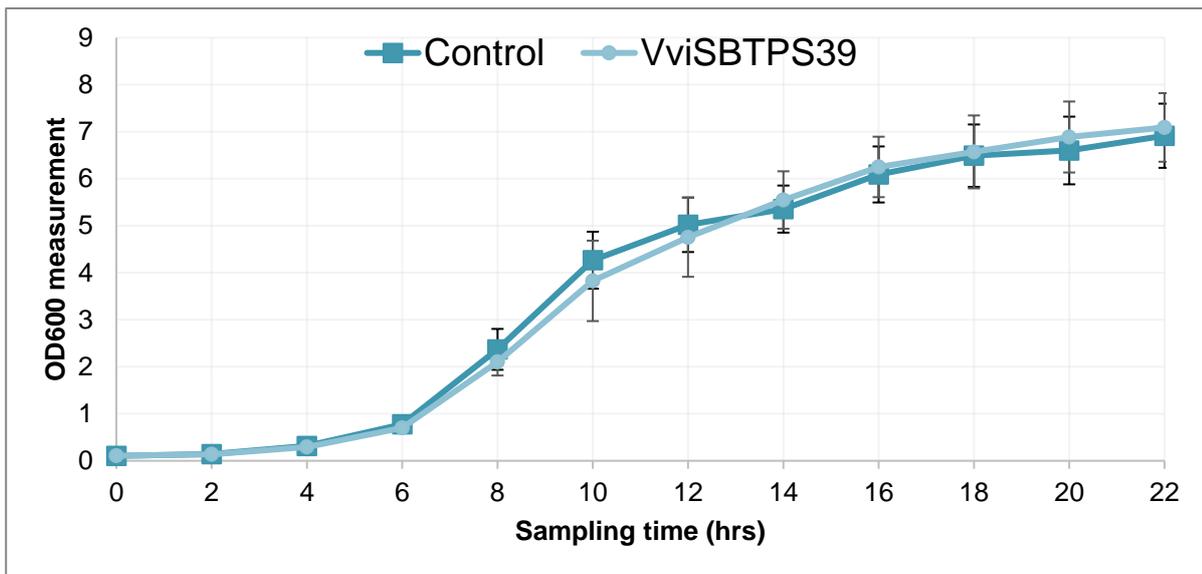
Figure 2.9 Growth curve with yeast strains. Each point represents OD_{600} average of three cultures with error bars denoting the standard deviation.

90

Appendix F   To Chapter 2

Table F-i Average peak area normalised to IS (3-octanol) and fresh weight of grapevine tissue with ± standard deviation. Asterisks (*) indicate compound identity confirmed with an authentic standard. Peak areas of the transformed plants that were significantly different (student's *t*-test with p < 0.05) from the control plants are indicated in red (higher than control) or blue (lower than control).

Compounds	Control	VviSBTPS39
β-myrcene	0.15 ± 0.03	0.14 ± 0.03
Limonene*	0.22 ± 0.03	0.18 ± 0.03
Eucalyptol*	0.02 ± 0.003	0.02 ± 0.004
δ-3-carene	0.15 ± 0.01	0.15 ± 0.03
ρ-cymene	0.05 ± 0.05	0.09 ± 0.01
α-terpinolene	0.12 ± 0.02	0.11 ± 0.03
Cis-linalool oxide*	0.2 ± 0.02	0.29 ± 0.1
Adamantane	0.08 ± 0.14	0 ± 0
trans-linalool oxide*	0.05 ± 0.04	0.07 ± 0.07
Menthone	0.32 ± 0.23	0.04 ± 0.08
Menthone_2	0.12 ± 0.09	0.02 ± 0.03
Linalool*	0.72 ± 0.08	0.53 ± 0.1
Bicyclo[4.1.0]heptane, 7-(methylethylidene)-	0.02 ± 0.01	0.03 ± 0.02
Vitispirane	0.26 ± 0.07	0.42 ± 0.22
α-terpineol-like	0.05 ± 0.02	0.09 ± 0.02
Hotrienol	0.14 ± 0.01	0.13 ± 0.09
β-fenchyl alcohol	0.05 ± 0.09	0.21 ± 0.05
Menthol	0.75 ± 0.53	0.1 ± 0.2
β-cyclocitral	0.1 ± 0.03	0.16 ± 0.04
Ocimenol	0.18 ± 0.06	0.3 ± 0.06
α-terpineol*	1.45 ± 0.05	1.2 ± 0.19
Citral	0.02 ± 0.003	0.06 ± 0.04
Geraniol*	0.08 ± 0.01	0.07 ± 0.02
β-damascenone*	0.5 ± 0.15	0.65 ± 0.38
Geranyl acetone*	0.18 ± 0.05	0.27 ± 0.14
α-ionone*	0.1 ± 0.05	0.13 ± 0.02

Appendix G   To Chapter 2

Table G-i Volatile terpene analysis of whole *N. benthamiana* leaves agroinfiltrated with the empty expression construct (Control_empty), or expression construct containing *VvSBTPS39.* Average of non-normalised peak area from at least 11 biological repeats (with leaves 1 and 2 sampled per plant) ± standard deviation. Compounds which were significantly different ($p < 0.05$) from the control are presented in red. ND = not detected.

Compounds	Control_empty	VviSBTPS39
α-thujene	ND	519373.8 ± 313020.8
δ-3-carene	ND	21266.8 ± 10020.9
Sabinene	ND	289214.7 ± 183054.1
β-pinene	ND	18919.6 ± 9038.9
Myrcene	348.3 ± 1206.4	ND
α-phellandrene	ND	28199.7 ± 23951.9
α-terpinene	ND	182288.8 ± 146379.1
p-cymene	ND	286966 ± 178606.1
β-phellandrene	ND	38501.5 ± 29583.1
Eucalyptol	ND	8342.9 ± 4960.7
β-terpinene	ND	346429.8 ± 253468.9
Terpinolene	ND	64868.4 ± 52868.5
Linalool	564.7 ± 1413.3	ND
(-)-terpinen-4-ol	ND	5063.7 ± 4008.9
β-cyclocitral	44.5 ± 154.2	ND
(*E*)-β-caryophyllene	348.3 ± 539.6	182 ± 603.6
Sesquiterpene_1	ND	ND
Sesquiterpene_2	ND	ND
α-muurolene	6265.7 ± 6722.2	ND
Sesquiterpene_3	47.8 ± 165.7	ND

Table G-ii Average peak area normalised to IS (Anisole-d$_8$) and fresh weight of *N. benthamiana* tissue with ± standard deviation. Peak areas of the transformed plants that were significantly different (student's *t*-test with $p < 0.05$) from the respective control plants are indicated in red (higher than control). ND = not detected.

Compounds	VviSBTPS39-control	VviSBTPS39-VviGPS
α-thujene	0.05 ± 0.07	0.03 ± 0.05
Sabinene	0.03 ± 0.06	ND
α-phellandrene	0.09 ± 0.12	0.02 ± 0.04
α-terpinene	0.7 ± 0.61	0.27 ± 0.09
p-cymene	0.99 ± 0.72	0.48 ± 0.19
β-phellandrene	ND	ND
λ-terpinene	1.19 ± 0.99	0.49 ± 0.15
Terpinolene	0.16 ± 0.13	0.06 ± 0.03
Linalool	0.1 ± 0.06	0.1 ± 0.07
Menthol	ND	ND
(-)-terpinen-4-ol	1.22 ± 1.02	0.42 ± 0.14
α-terpineol	0.01 ± 0.02	ND
β-cyclocitral	0.03 ± 0.01	0.06 ± 0.02
Total monoterpenes	**4.57 ± 3.74**	**1.93 ± 0.76**
(*E*)-β-caryophyllene	ND	ND
Sesquiterpene_1	ND	ND
Sesquiterpene_2	ND	ND
α-muurolene	0.01 ± 0.01	0.01 ± 0.01
Sesquiterpene_3	ND	ND
Total sesquiterpenes	**0.01 ± 0.01**	**0.01 ± 0.01**

Compounds	VviSBTPS39-control	VviSBTPS39-VviGPS

Chapter 3 Characterisation of a eucalyptol and α-thujene synthase from *Vitis vinifera*

3.1 Introduction

With the increasing number of plant genomes being sequenced, the functional annotation of genes continues to be a major impediment to the better understanding of plant metabolism. This is especially true for genes involved in specialised metabolism which has undergone extensive expansion and specialisation, often in a very species-specific manner. Terpenes form a significant portion of the specialised metabolome of plants. The substrates for terpenes are produced through the activity of isoprenyl diphosphate synthases (IDSs) via consecutive condensation reactions of isopentenyl diphosphate (IPP) to its isomer dimethylallyl diphosphate (DMAPP). In *Arabidopsis thaliana,* a single-copy gene and gene pair encode geranyl diphosphate synthase (GPS) and farnesyl diphosphate synthase (FPS), respectively (Cunillera *et al.*, 1996; Bouvier *et al.*, 2000; Closa *et al.*, 2010; Vranová *et al.*, 2013). In *Vitis vinifera* (grapevine), these enzymes are predicted to be encoded by single-copy genes (PLAZA, https://bioinformatics.psb.ugent.be/plaza/versions/plaza_v3_dicots/).

Unlike the IDS genes, terpene synthases (TPSs) that are responsible for channelling IDS substrates into various terpene backbones are encoded by extended gene families. The variation in the specific enzyme activity of TPSs is one of the main reasons for the large diversity of terpenes found in nature (Fridman & Pichersky, 2005; Tholl, 2006; Degenhardt *et al.*, 2009; Martin *et al.*, 2010; Karunanithi & Zerbe, 2019). With 152 *VviTPS*-like gene models identified (69 predicted to be functional), the *V. vinifera TPS* gene family is one of the largest compared to other plant species such as *Arabidopsis thaliana*, *Oryza sativa*, *Populus trichocarpa* and *Jatropha curcas* L. (Aubourg *et al.*, 2002; Tuskan *et al.*, 2006; Jaillon *et al.*, 2007; Martin *et al.*, 2010; Chen *et al.*, 2011; Xiong *et al.*, 2016). To date, only *Eucalyptus spp.* has been shown to contain more *TPSs* than grapevine, with more than a hundred *TPSs* predicted to be functional in *Eucalyptus grandis* and *Eucalyptus globulus* (Külheim *et al.*, 2015; Butler *et al.*, 2018).

Terpene synthases are often difficult to characterise because sequence similarity does not always indicate similar functions or acceptance of the same substrate. Conversely, enzymes that are very dissimilar in sequence can sometimes catalyse the same reaction (Fridman & Pichersky, 2005; Pazouki & Niinemets, 2016). Approximately half of the previously characterised monoterpene and sesquiterpene synthases have been shown to produce multiple products (Degenhardt *et al.* 2009). However, sequence analysis of the active site has not yielded conserved features in TPS that conclusively point toward the ability of certain enzymes to form several products. One motif that might play a role in enhancing multiple product formation is the NSE/DTE motif (Fridman & Pichersky, 2005; Degenhardt *et al.*, 2009).

94

The identification and quantification of the terpene compounds produced through a specific TPS, typically via heterologous expression studies, are necessary in order to functionally characterise *TPS* genes (Martin & Bohlmann 2004). In total, 58 grapevine terpene synthases, associated with 35 gene models, have been functionally characterised to date (Lücker, Bowen, *et al.*, 2004; Martin & Bohlmann, 2004; Martin *et al.*, 2009, 2010; Zhu *et al.*, 2014; Drew *et al.*, 2016; Dueholm *et al.*, 2019; Smit *et al.*, 2019). Various approaches can be followed to determine the product profiles of the isolated TPSs – each approach with its own advantages and disadvantages, as discussed in Chapter 2 of this thesis (Fischer *et al.*, 2013; Li & Pfeifer, 2014). The functional characterisation of the grapevine *TPS* genes was carried out through heterologous expression in bacteria (Lücker, Bowen, *et al.*, 2004; Martin & Bohlmann, 2004; Martin *et al.*, 2009, 2010; Zhu *et al.*, 2014); yeast (Smit *et al.*, 2019), and plants (Drew *et al.*, 2016; Dueholm *et al.*, 2019; Smit *et al.*, 2019).

Here, the aim was to characterise four *VviTPS* and two *VviIDS* utilising the expression systems and analytical methods that were developed and described in Chapter 2. The VviTPS genes included one putative sesquiterpene synthase and three monoterpene synthase genes. The monoterpene synthase indicator gene used in the previous chapter for method development was also included in this chapter for further characterisation. The sesquiterpene synthase and two of the monoterpene synthases corresponded to previously characterised genes. The two *VviIDSs* included the *VviGPS* used in the previous chapter to evaluate the system, as well as an *VviFPS* isolated in a previous study (Young, 2004) but which could not be functionally characterised. The characterisation involved sequence analysis, prediction of the expression profile in grapevine, and functional characterisation using the expression systems and analytical methods developed and evaluated in Chapter 2.

3.2   Materials and methods

3.2.1   Isolating genes, updating gene annotations, and determining predicted gene expression profiles

Protocols for DNA isolation, manipulation, and cloning were based on those described by Sambrook *et al.* (1989). The isolation of the coding sequences of the grapevine terpenoid pathway genes, bacterial strains, transformation methods, and growth conditions were performed according to the methods outlined in Chapter 2. Primers and plasmids used in this study are listed in **To Chapter** 3

Table A-i and **Table A-ii**, respectively.

The isolated grapevine cDNA sequences were subjected to a BLAST analysis against the VCost.v3 annotation (https://urgi.versailles.inra.fr/blast/) of the 12X.2 assembly of the *V. vinifera* cv. PN40024 sequenced genome (Canaguier *et al.*, 2017) using default settings. Deduced amino acid sequences were generated with the toolbox available on the CLC Main Workbench (Version 7, CLC Bio-Qiagen, Denmark) with the subcellular localisations predicted using ProtComp Version 9.0

(http://www.softberry.com/berry.phtml) and TargetP 1.1 (http://www.cbs.dtu.dk/services/TargetP/) (Nielsen *et al.*, 1997; Emanuelsson *et al.*, 2000).

Gene and protein sequences from the 12X.v2 and genome assembly and VCost.v3 annotation were downloaded from https://urgi.versailles.inra.fr/Species/Vitis/Annotations (Canaguier *et al.*, 2017). Available sequences of functionally characterised TPSs and IDSs from other plant species were downloaded from GenBank (https://www.ncbi.nlm.nih.gov/genbank/). *VviIDS* orthologs in *A. thaliana* were identified using the default settings of the BLASTp tool in PLAZA 3.0 Dicots (https://bioinformatics.psb.ugent.be/plaza/versions/plaza_v3_dicots/) (Altschul *et al.*, 1997).

Multiple sequence alignments (MSA) and the construction of phylogenetic trees were done using CLC Main Workbench (Version 7, CLC Bio-Qiagen, Denmark). MSA with deduced full-length protein sequences were generated using default settings with the characteristic motifs set as fixed alignment points. The phylogenetic trees were created using maximum-likelihood phylogeny with the neighbor-joining construction method, with the Dayhoff (PAM) substitution model set at four substitution-rate categories. The gamma distribution parameter was estimated when performing 1000 bootstrap replicas.

The grapevine gene atlas [GEO Accession GSE36128 (Fasoli *et al.*, 2012)] was used to determine the expression patterns of the putative terpenoid genes. Probe ambiguity for the putative *VviTPSs* and *VviIDSs* was determined according to the following method: The 60 bp probe sequences were downloaded from the GEO database (Edgar *et al.*, 2002) for the NimbleGen 090918 *V. vinifera* exp HX12 platform (https://www.ncbi.nlm.nih.gov/geo/query/acc.cgi?acc=GPL13936). By using the BLAST function in CLC Main Workbench, the gene model sequences of the putative terpenoid pathway genes were aligned against the probe sequences with allowance of two nucleotides mismatch. The identified probe sequences were then compared against the CDS sequences of the 12X.v2 chromosome assembly (https://urgi.versailles.inra.fr/Species/Vitis/Annotations) using BLAST, to determine ambiguity of the probes. RMA-normalised expression data for each probe was downloaded from https://www.ncbi.nlm.nih.gov/geo/query/acc.cgi?acc=GSE36128. The expression data for each of the identified probes was used to calculate the average of the three sample replicates. Probes mapping to a gene but not correlating with the other gene-specific probes were not included in the calculation of the average gene expression values. The correlation of the expression values was determined with heatmap construction using the ClustVis web interface (https://biit.cs.ut. ee/clustvis/), unit variance was used for scaling, whereas Pearson correlation was selected for clustering-distance calculation and the average distances of all possible pairs selected as the linkage method (Metsalu & Vilo, 2015).

3.1.1 Construction of yeast expression vectors, transformation, genetic characterisation, and terpene analysis

The *VviTPS* sequences were excised from pGEM-TPS subclones with the restriction enzymes listed in **Table A-ii** and cloned into the corresponding sites of pBS-PGK1p-URA3 to yield pBS-PGK1p-VvTPSx. A full-length and truncated version of *VviPNTPS41* was also cloned into the Gateway®-compatible yeast expression vector pAG426GAL (Alberti *et al.*, 2007), as described for *VviSBTPS39* in Chapter 2.

Yeast transformation and subsequent genetic characterisation were conducted according to the methods discussed in Chapter 2. The strains that were used in this study are listed in **Table A-iii**. Analysis of the total potential terpene and determination of the terpene profile for the purpose of characterisation was also performed as described in Chapter 2.

3.1.2 Grapevine transformation, growth conditions, genetic characterisation, and terpene analysis

The uncharacterised putative transgenic *V. vinifera* cv. Merlot population transformed with *VviPTPS27* was obtained from the grapevine transformation and regeneration platform of the Institute for Wine Biotechnology (IWBT) at Stellenbosch University. The construction of the *VviPTPS27* plant expression vector, grapevine transformation, and regeneration of transgenic callus were performed according to the method described in Chapter 2 for *VviSBTPS39.* The regenerated population was maintained on Murashige & Skoog (MS) media (Murashige & Skoog, 1962) without selection with 11 transgenic lines available. The hardening-off method for transgenic grapevine plants, growth conditions for grapevine, genetic characterisation of these lines, as well as total potential analyses of volatile terpenes were done according to the methods described in Chapter 2.

3.1.3 Tobacco agroinfiltration for transient expression

In addition to the transient expression study conducted with *VviSBTPS39* and *VviGPS* in Chapter 2, the *A. tumefaciens*-mediated infiltration of *VviPTPS27* and *VviFPS* into *N. benthamiana* is also described in this chapter. The cloning method that was used for the plant expression construct containing *VviPTPS27* is described in Section 3.1.2. The isolation and subsequent cloning of *VviFPS* into pART27 were performed according to methods described by Young (2004). The methods that were used for transient expression via agroinfiltration of *N. benthamiana* leaves and for the analysis of volatile terpenes from whole leaves and ground tissue are described in Chapter 2.

3.1.4 Data analysis

Data were analysed using SIMCA® (Version 16, Sartorius Stedim Biotech, Göttingen, Germany), Microsoft Office Excel 2016 (Microsoft Corporation, Redmond, WA, USA), and STATISTICA version 13.2 (http://software.dell.com/products/statistica/).

97

3.3   Results

3.3.1   Updating the gene annotations of selected grapevine terpenoid pathway genes, and construction of phylogenetic trees

The sequences of the putative *VviIDSs* and the four predicted *VviTPSs* were analysed and results are summarised in **Table 3.1** and **Table 3.2**, respectively. The *VviIDS* and *VviTPS* sequences were mapped to the closest gene model and named according to the standard grapevine nomenclature and VCost.v3 annotation (Grimplet *et al.*, 2014; Canaguier *et al.*, 2017).

The constructed phylogenetic tree showed clear grouping of the *A. thaliana* IDS protein sequences based on the chain lengths of the products formed by these enzymes (**Figure B-i**). The predicted VviGPS and VviFPS grouped with the respective IDSs from *A. thaliana.* Utilisation of the *A. thaliana* coding sequences for *AtGPS1* (At2g34630), *AtFPS1* (At4g17190), and *VviFPS2* (At5g47770) as query sequences in a BLAST search of the VCost.v3 annotation (https://urgi.versailles.inra.fr/blast/) of the PN40042 genome did not yield any additional sequences that putatively encode either a GPS or a FPS.

The two highly conserved aspartate-rich regions, which are common to isoprenyl diphosphate synthases and crucial for enzymatic activity (Koyama *et al.*, 1993; Ohnuma *et al.*, 1996; Vandermoten *et al.*, 2009), were identified in the isolated sequences. The two regions are composed of a $DDx_{2\text{-}4}D$ sequence with the designations of the first (FARM) and second aspartate-rich motifs (SARM). The FARM sequence forms part of the chain-length determination (CLD) region (Wang & Ohnuma, 1999), whereas the SARM sequence is located further downstream in the C-terminal (Koyama *et al.*, 1993; Vandermoten *et al.*, 2009). Both motifs were identified in the isolated sequences (**Figure B-ii** and **Figure B-iii**). The CLD sequences of the *VviGPS* genes were consistent with those described by Vandermoten *et al.* (2009) for plant homodimer GPSs (ASxxHDDxxD), whereas the CLD sequence of the VviFPS was the same as the one identified in the AtFPS sequences. The predicted subcellular localisation of the VviGPS was uncertain with the most likely localisation being the mitochondria, although subcellular targeting to the plastid was also predicted. As expected, the VviFPS was predicted to localise in the cytosol.

Table 3.1 Analysis of the isolated gene sequences putatively encoding *VviIDSs.*

Gene ID	Isolated	V2 ID*	VCost_v3 ID**	Splicing variant	mTP^	cTP^	Protein length	Characteristic motifs present	Arabidopsis thaliana orthologs		
									Gene annotation	Gene ID	Reference
VviGPS	This study	VIT_215s0024g00850.1	Vitvi15g00079	Yes	Yes#	?#	321	Yes	GPS1 (PPPS)	At2g34630	Bouvier *et al.* (2000) Hsieh *et al.* (2011)
VviFPS	Young (2004)	VIT_219s0015g01010	Vitvi19g00729	No	No	No	341	Yes	FPS2	At4g17190	Delourme *et al.* (1994) Cunillera *et al.* (1996) Cunillera *et al.* 1997) Cunillera *et al.* 2000) Keim *et al.* (2012)
									FPS1	At5g47770	

All three sequences were isolated from cDNA synthesised from total RNA extracted from *Vitis vinifera* L. cv. Pinotage leaves (Young, 2004). *Closest gene model accession based on BLAST on http://genomes.cribi.unipd.it/grape/ website. **Annotation and ID as found on the https://urgi.versailles.inra.fr/Species/Vitis website. ^ Predicted subcellular localisation based on sequence analysis described in section 3.2. mTP – mitochondrial transit peptide; cTP – chloroplastic transit peptide. # The putative localisation of the VviGPS was determined for both splicing variants, subcellular localisation was predicted to be to the mitochondria, but the proteins could also be localised to the chloroplast.

The RRX$_8$W motif found in the N-terminal and the DDXXD and NSE/DTE motifs in the metal-binding (C-terminal) domain was identified in all the isolated VviTPS sequences (**Table 3.2**; Bohlmann *et al.*, 1998; Aubourg *et al.*, 2002; Christianson, 2006). One of the putative terpene synthases, *VviPTPS27*, was predicted to localise to the cytosol and grouped into the *TPS-a* subfamily based on sequence analysis. This subfamily usually comprises sesquiterpene synthases. The VviTPS-a subfamily phylogenetic tree (**Figure B-iv**), containing the VviPTPS27 protein sequence, showed the closest grouping with characterised isolates that also mapped to the *VviPTPS27* gene model. The coding sequences for these characterised TPSs were isolated from Gewürztraminer, Muscat of Alexandria, and Shiraz, and encoded three (*E*)-β-caryophyllene synthases (Martin *et al.*, 2010; Smit *et al.*, 2019) and an isocaryophyllene synthase (Dueholm *et al.*, 2019). MSA of these isolates (
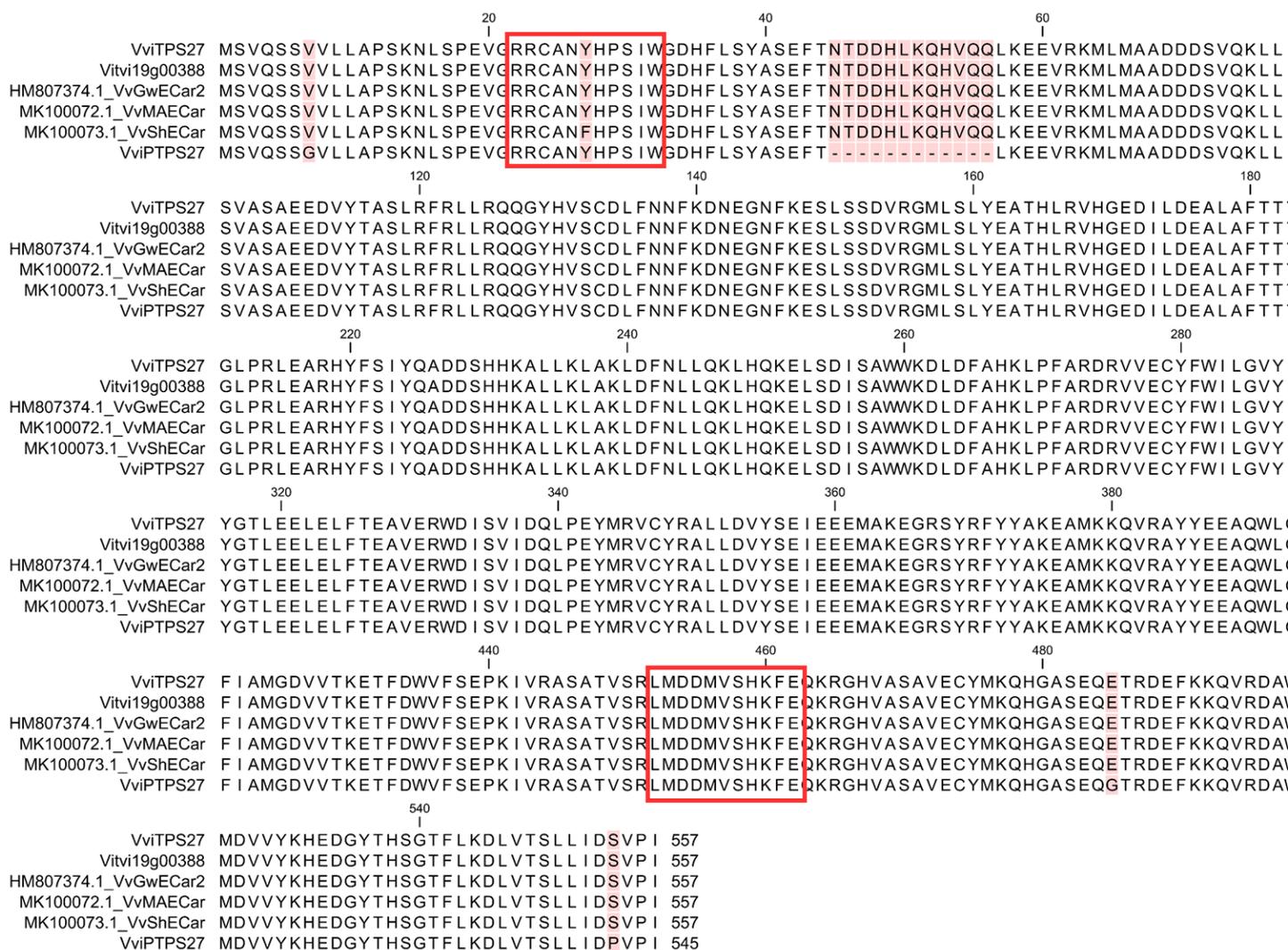
Figure B-v) showed high sequence similarity except for a gap in the N-terminal of VviPTPS27 isolated in this study.

The other three putative terpene synthases were predicted to have a targeting sequence for sublocalisation to the plastid and are classified as belonging to the *TPS-b* subfamily of terpenoid synthases. Monoterpene synthases from angiosperms typically fall in this subfamily of TPSs (Bohlmann *et al.*, 1998; Martin *et al.*, 2010). The VviTPS-b subfamily phylogenetic tree containing

the VviSBTPS39, VviPNTPS41, and VviPNTPS44 protein sequences is shown in **Figure B-vi**. VviSBTPS39 subdivides with two α-terpineol synthases isolated from Gewürztraminer (Martin & Bohlmann, 2004) and an (E)-β-ocimene/myrcene synthase isolated from Cabernet Sauvignon (Martin *et al.*, 2010). The two α-terpineol synthases and the *VviSBTPS39* isolated in this study mapped to the *VviTPS39* gene model while the (E)-β-ocimene/myrcene synthase was shown to map to the *VviTPS38* gene model (Martin *et al.*, 2010). The MSA of VviSBTPS39 with the other isolates mapping to the same gene model are shown in **Figure B-vii**. Phylogenetic analysis did not indicate close grouping of the VviPNTPS41 protein sequence to any of the previously characterised isolates used in the construction of the phylogenetic tree (**Figure B-vi**), and MSA that was conducted with gene models showed characteristic motifs and high sequence similarity (**Figure B-ix**). The VviPNTPS44 protein sequence grouped closest to two (+)-α-pinene synthases, isolated from Pinot noir, mapping to the same gene model (Martin *et al.*, 2010). The alignment with these sequences is shown in **Figure B-viii**.

101

Table 3.2 Analysis of isolated gene sequences putatively encoding for VviTPSs.

Gene ID	Vitis vinifera cv.	V2 ID*	VCost_v3 ID**	VCost_v3 annotation**	Splicing variant	TPS subfamily	cTP^	Protein length	Motifs	Previous characterised isolates in *V. vinifera*		
										Annotation	Cultivar	Reference
VviPTPS27	Pinotage	VIT_219s0014g04900.1	Vitvi19g00388	VviTPS27	Yes	TPS-a	No	545	Yes	(*E*)-β-caryophyllene synthase	Gewürztraminer	Martin *et al.* (2010)
											Muscat of Alexandria Shiraz	Smit *et al.* (2019)
										Isocaryophyllene synthase	Shiraz	Dueholm *et al.* (2019)
VviSBTPS39	Sauvignon blanc	VIT_213s0067g00370	Vitvi13g01307	VviTPS39	No	TPS-b	Yes	590	Yes	(-)-α-terpineol synthase	Gewürztraminer	Martin & Bohlmann (2004)
VviPNTPS41	Pinot noir	VIT_213s0067g03700	Vitvi13g01439	VviTPS41	No	TPS-b	Yes	590	Yes	-	-	-
VviPNTPS44	Pinot noir	VIT_213s0067g03790	Vitvi13g01877	VviTPS44	No	TPS-b	Yes	593	Yes	(+)-α-pinene synthase	Pinot noir	Martin *et al.* (2010)

*Closest gene model accession based on BLAST on the http://genomes.cribi.unipd.it/grape/ website. **Annotation and ID as found on the https://urgi.versailles.inra.fr/Species/Vitis website. ^ Predicted subcellular localisation based on sequence analysis described in section 3.2. cTP – chloroplastic transit peptide. The cultivars from which the *VviTPSs* were isolated are indicated with an abbreviation before the TPS (Pinot noir – PN, Sauvignon blanc – SB).

3.3.2 Gene expression profiling of putative terpenoid pathway genes from *Vitis vinifera* from gene atlas data

The predicted expression profiles of the genes that were investigated in this study was determined by using the publicly available gene atlas data from *V. vinifera* cv. Corvina (Fasoli *et al.*, 2012). Due to the high level of gene duplication observed in the *VviTPS* family (Martin *et al.*, 2010), the specificity of probe sequences were determined for the coding sequences. Results of the mapping of the NimbleGen probes to the gene sequences are summarised in **Table C-i**. Probe ambiguity for the *VviTPS* sequences was high, with only the *VviTPS39* sequence having four probes that uniquely bind to it. No ambiguity was observed for the *VviIDSs,* with four unique probes binding to the sequences. The expression of the *VviIDS* and *VviTPS* genes that were analysed in this study are summarised in a correlation heatmap (**Figure 3.1**) and illustrated in more detail in Appendix C with gene expression visualised according to the sampled organs.

Figure 3.1 Correlation heatmap generated with average gene expression values. Rows are centred with unit variance scaling applied to the rows. Both rows and columns are clustered using Pearson correlation distance and average linkage.

Expression of the two *VviIDS* genes*,* the *VviGPS* and *VviFPS* remained relatively constant throughout different organs and developmental stages. The lowest expression for *VviGPS* was

observed in pollen (**Figure C-ix**), whereas increased levels of expression was seen in the seeds during mid-ripening (**Figure C-ii**). *VviFPS* expression was decreased in the winter bud at E-L stage 1 (**Figure C-iv**). The highest gene expression was observed in the flower (**Figure C-viii**) at stage E-L 20 and E-L 23, as well as in the pooled carpel and stamen samples (**Figure C-ix**). The expression of the predicted sesquiterpene synthase (*VviTPS27*) was also the highest in the flower tissue, although not in the stamen, at the E-L 20 and E-L 23 stages (**Figure C-viii**). Expression levels for *VviTPS27* was otherwise relatively low in the other developmental stages and tissues. The correlation heatmap (**Figure 3.1**) shows grouping of *VviFPS1* and *VviTPS27* with highest expression in the flower tissue.

The expression of *VviTPS39* was relatively low in berry bunch tissue with higher expression seen in the vegetative tissue – specifically the young tendril (**Figure C-v**). *VviTPS41* expression was relatively low in all tissue types, except in the stamen (**Figure C-ix**) and green stem (**Figure C-vii**). A spike in *VviTPS44* expression levels was observed in the pollen, as illustrated in **Figure C-ix**. The gene was also highly expressed in the tissue culture plants, especially when compared to the other *VviTPS* genes that were analysed (**Figure C-x**).

3.3.3 Yeast expression system

3.3.3.1 *Volatile analysis of VviTPS genes in Saccharomyces cerevisiae*

In addition to the *VviSBTPS39* cloning that was described in the previous chapter, the full-length cDNA sequences of *VviPTPS27, VviPNTPS41,* and *VviPNTPS44* were cloned into a yeast expression vector (**Table A-ii**) with an expression cassette containing the *VviTPSs* integrated into the genome of an *S. cerevisiae* W303-1A strain (**Table A-iii**). The headspace (HS) solid phase microextraction (SPME) coupled with gas chromatography (GC) – mass spectrometry (MS) method described in Chapter 2 to determine TPS gene functionality was also used for these genes and the volatile analysis data is shown in **Table D-i**. Visual comparison of the detected terpenes shows that the two yeast cultures expressing *VviPTPS27* and *VviPNTPS41* (**Figure 2.2**a & b) did not produce any unique terpenes, except for the small peak identified as eucalyptol that was detected in the *VviPNTPS41*-expressing yeast culture. Instead, the control strain culture contained higher levels of the detected compounds – specifically the peaks putatively identified as sesquiterpenes. The yeast culture expressing *VviPNTPS44* had a terpene profile that was almost indistinguishable from the control yeast strain in terms of identified peaks and areas (**Figure 3.2**c).
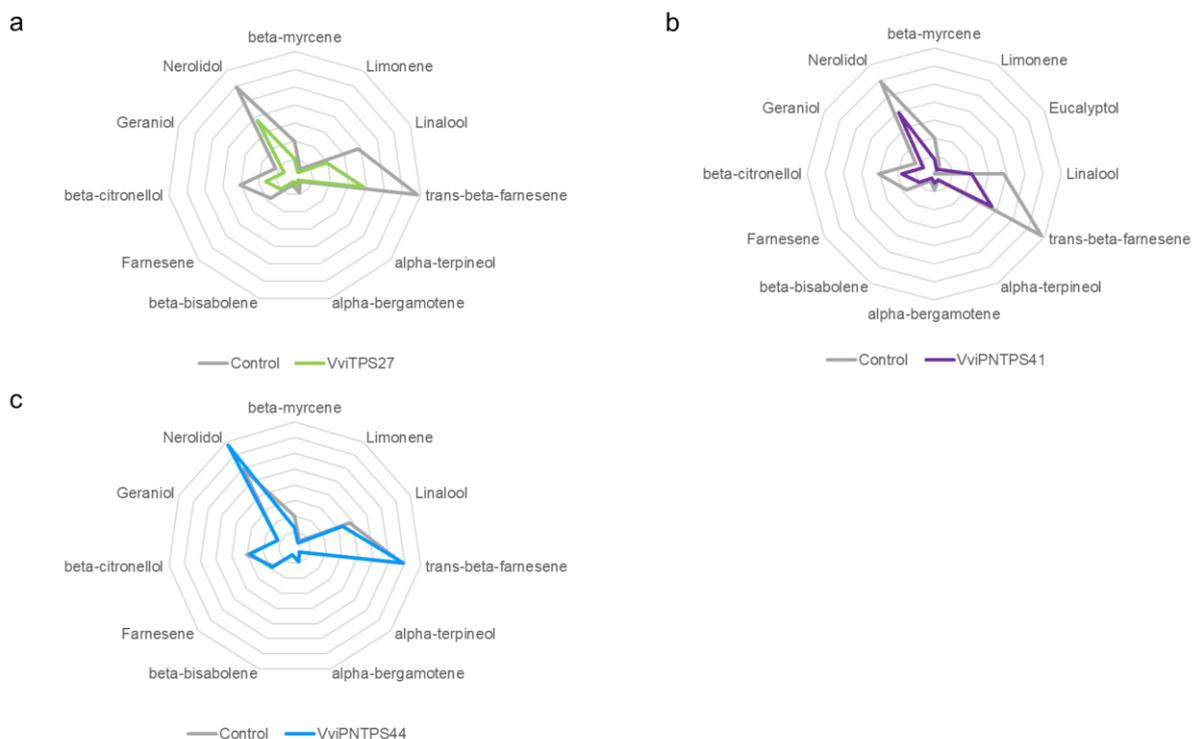
Figure 3.2 Terpene analysis results of the yeast cultures heterologously expressing the various *VviTPS* genes in comparison to the control yeast (grey line in all the figures). a – Control strain versus *VviPTPS27*-expressing strain (green line), b – Control strain versus *VviTPS41*-expressing strain (purple line), and c – Control strain versus *VviTPS44*-expressing strain (blue line), The average peak areas (selected ion count), normalised to the internal standard (3-octanol) and cell counts (OD_{600} reading) are shown.

3.3.4   Plant expression systems

3.3.4.1   Ectopic expression of VviTPS genes in grapevine

Two grapevine populations transformed with *VviTPS* genes under the control of a constitutive promoter were investigated in this study. The population that was transformed with *VviSBTPS39* was characterised in Chapter 2, whereas the *VviPTPS27*-expressing grapevine population was characterised according to the same methods and is discussed in this chapter.

3.3.4.1.1 Genetic characterisation of grapevine population

The results for the genetic characterisation of the population that was transformed with *VviPTPS27* are summarised in **Table 3.3**. The primers that were used for PCR screening are listed in **To Chapter** 3

Table A-i, with results showing that all the lines were successfully transformed with the *VviPTPS27* expression cassette, except for line 3. Gene expression analysis with the actin gene (VIT_204s0044g00580) serving as a positive control (**To Chapter** 3

Table A-i) indicated that the grapevine population ectopically expressed the *VviPTPS27* gene – except for line 3, previously shown to be an untransformed line.

106

Table 3.3 Summary of the genetic characterisation of the *V. vinifera* cv. Merlot population transformed with *VviPTPS27.*

Transgenic lines	Gene integration		Gene expression			
	nptII PCR with gDNA	CaMVp & VviTPS27 PCR with gDNA	Northern blot with actin probe (control)	Actin PCR with cDNA (control)	Northern blot with VviTPS27 probe	VviTPS27 PCR with cDNA
Merlot_#WT	-	-	+	+	-	-
Merlot_#3	-	-	+	+	-	-
Merlot_#8	+	+	+	+	+	+
Merlot_#9	+	+	+	+	+	+
Merlot_#17	+	+	+	+	+	+
Merlot_#18	+	+	+	+	+	+
Merlot_#19	+	+	+	+	+	+
Merlot_#24	+	+	+	+	+	+
Merlot_#25	+	+	+	+	-	-
Merlot_#35	+	+	+	+	+	+
Merlot_#36	+	+	+	+	+	+
Merlot_#37	+	+	+	+	+	+

3.3.4.1.2 Volatile analysis of tissue culture plants from transgenic grapevine population

Volatile analysis of tissue cultured plants using the method that was evaluated in Chapter 2 did not detect any sesquiterpenes. The *VviPTPS27*-expressing lines did not show a clear separation between the transformed population and the control plants when orthogonal projections to latent structures discriminant analysis (OPLS-DA) was applied (**Figure 2.5Figure 2.5**). However, there were some compounds that were present in significantly lower amounts ($p<0.05$) in the *VviPTPS27*-transformed plants, compared to the control (**Table E-i**).

107
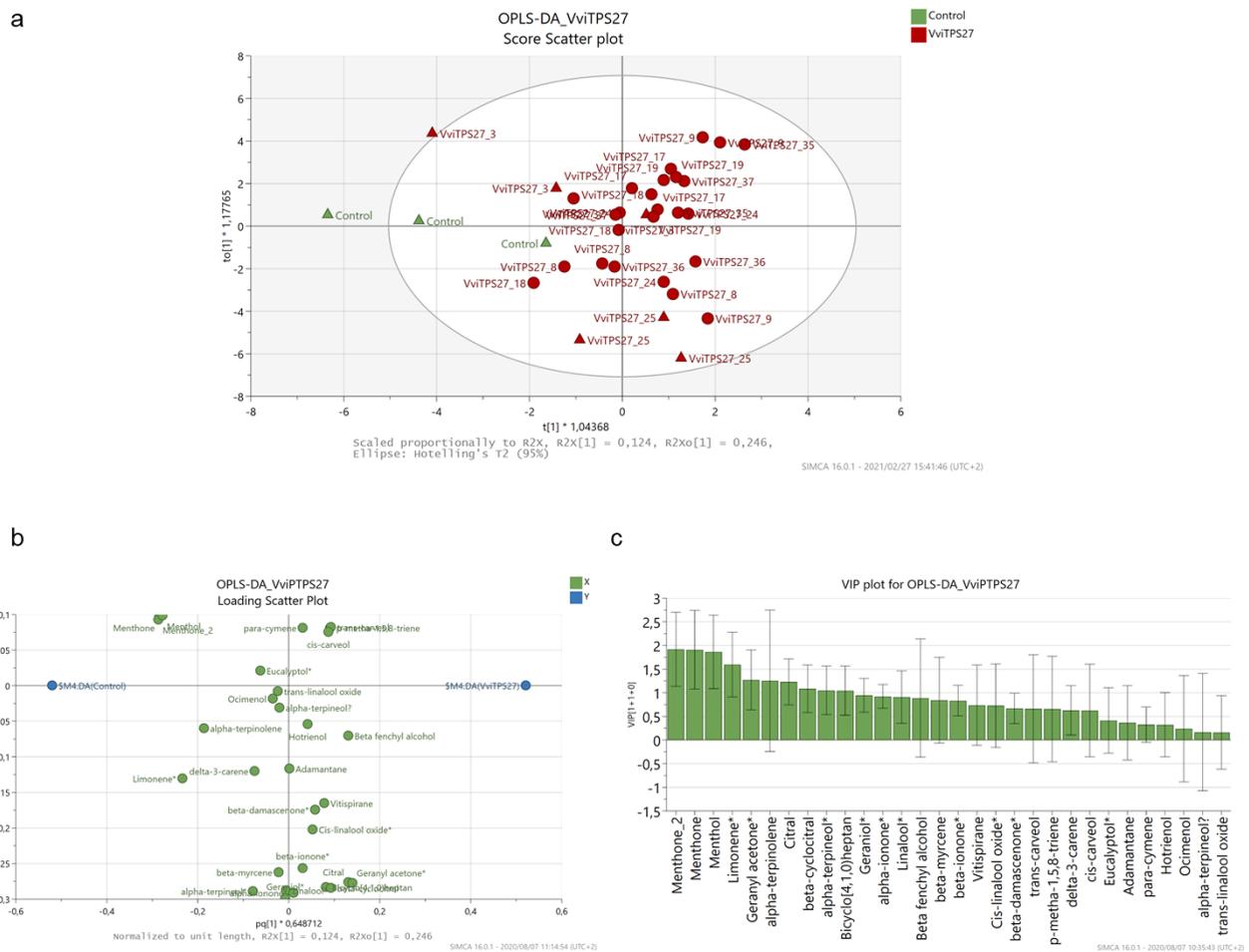
Figure 3.3 OPLS-DA analysis of volatile compounds detected in tissue culture plants of *Vitis vinifera* L. cv. Merlot transformed with *VviPTPS27* in comparison to untransformed plants. The loading score plot (a) illustrates the separation of the samples with the lines not expressing *VviPTPS27* indicated with triangles. The loading score plot (b) indicates the variables that drove the separation (if any) between the samples in (a).

3.3.4.2 *Terpene production utilising a heterologous plant expression platform: transient expression in <u>N. benthamiana</u>*

Agroinfiltration of *VviPTPS27* into *N. benthamiana* for transient expression was performed as described in Chapter 2. OPLS-DA of the non-normalised peak areas of the detected volatile compounds utilising the whole-leaf analysis method indicated that the variables that drove the separation between the control and agroinfiltrated plants were predominantly those of peaks that were putatively identified as sesquiterpenes (**Figure 2.7**). The results are summarised in **Table F-i** with the peak areas that are significantly different from the control plants highlighted in red.
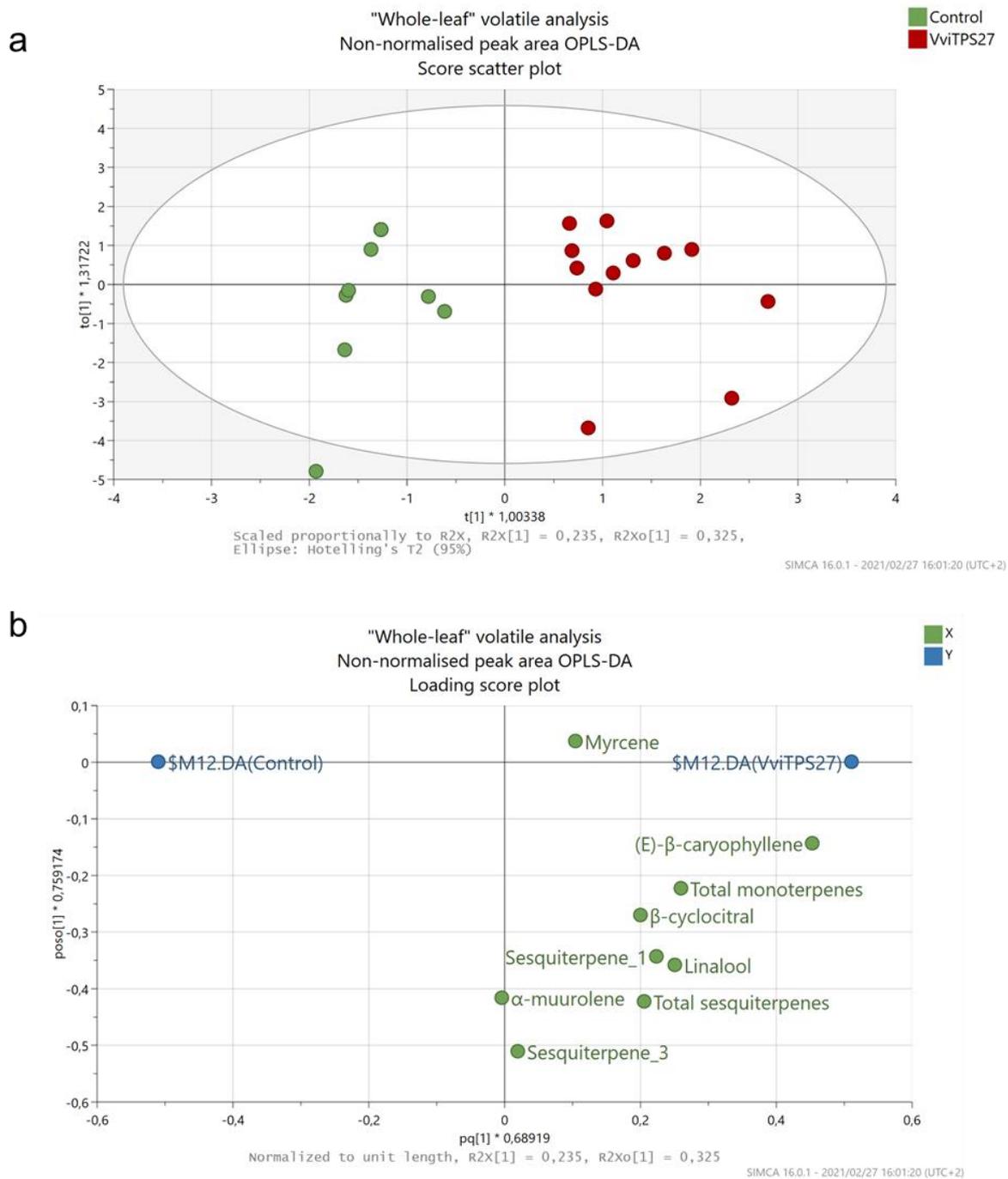
Figure 3.4 OPLS-DA of head-space volatiles produced by *N. benthamiana* plants agroinfiltrated either with an empty expression vector (control) or *VviPTPS27* with the score scatter plot (a) showing separation between control and *VviPTPS27* samples. The loading scatter plots (b) indicate the variables that drove the separation.

The *N. benthamiana* plants were also agroinfiltrated with pART27-VviPTPS27 in combination with either pART27-empty (control), pART27-VviGPS, or pART27-VviFPS. The peak areas were normalised to the internal standard peak area (Anisole-d_8) and the fresh weight (g) of each sample. There were no significant ($p<0.05$) differences in the normalised peak areas of terpene compounds

109

measured in plants that were infiltrated with *VviPTPS27* in combination with either *VviGPS* or *VviFPS* in comparison to the mono-infiltrated plants (**Table F-ii**).

3.3.5   Terpene profiles of monoterpene synthases

The monoterpene profiles produced by the yeast expression system, using the Gateway® expression vector by VviSBTPS39 and VviPNTPS41, as well as the monoterpenes produced by VviSBTPS39 in the *N. benthamiana* plant expression system are listed in **Table 2.2**. Both of these monoterpene synthases formed multiple products. Nevertheless, the profile remained consistent between repeats. The main compound that was produced by VviSBTPS39 in both the yeast and the plant systems was α-thujene, whereas eucalyptol was the main compound produced by VviPNTPS41 in terms of the relative peak area under the conditions used for analysis.

Table 3.4 Monoterpene profiles for the two monoterpene synthases. [a]Components listed in the order of elution on an HP 5MS capillary column and named according to identification methods listed in ID. [b]CAS number of compounds listed. [c]Retention time (in minutes) of the compounds detected. [d]Compound identification method: MS – comparison of mass spectra with MS libraries (Wiley and NIST), RI – comparison of calculated retention index with those reported in literature, Std – identification based on comparison with authentic standard. [e]Compounds detected in the yeast expression system over-expressing *VviSBTPS39*. [f]Compounds detected in plant (*N. benthamiana*) expression system transiently expressing *VviSBTPS39*. [g]Compounds detected in yeast expression system over-expressing *VviPNTPS41*. [e-g]Terpenes were analysed in the headspace at ambient temperature, expressed as % ratio of the total monoterpene peak area with ± standard deviation. The main compound in terms of relative peak area is highlighted in red for each expression system. ND = not detected.

Compound[a]	CAS[b]	RT[c]	ID[d]	Terpene peak ratio (%)		
				VviSBTPS39[e]	VviSBTPS39[f]	VviPNTPS41[g]
α-thujene	2867-05-2	7.278	MS, RI	24.3 ± 1.4	30.4 ± 2.4	11.4 ± 1.7
α-pinene	80-56-8	7.402	MS, RI	1.3 ± 0.4	1.2 ± 0.2	7.1 ± 1.5
Camphene	79-98-5	7.722	MS, RI	0.03 ± 0.005	ND	0.2 ± 0.03
Sabinene	3387-41-5	8.262	MS, RI	18.1 ± 1.1	20.2 ± 4.7	7.3 ± 1.4
β-pinene	127-91-3	8.328	MS, RI	1.4 ± 0.3	1.1 ± 0.2	3.4 ± 0.6
Myrcene	123-35-3	8.602	MS, RI, Std	4.4 ± 0.9	0.6 ± 0.9	2 ± 0.2
α-phellandrene	99-83-2	8.885	MS, RI	1.8 ± 0.5	1.3 ± 0.4	0.8 ± 0.1
α-terpinene	99-86-5	9.149	MS, RI, Std	10.5 ± 1.1	8.7 ± 1.7	5.1 ± 0.6
p-cymene	99-87-6	9.313	MS, RI	10.2 ± 3.2	13.9 ± 3.4	8.1 ± 1.2
β-phellandrene	555-10-2	9.389	MS, RI	ND	2 ± 0.4	ND
Limonene	138-86-3	9.404	MS, RI, Std	2.8 ± 0.2	ND	1.5 ± 0.1
Eucalyptol	470-82-6	9.458	MS, RI, Std	0.5 ± 0.1	0.4 ± 0.2	35.7 ± 5.6
γ-terpinene	99-85-4	10.025	MS, RI, Std	17.8 ± 0.5	16.7 ± 2.3	8.8 ± 1
Terpinolene	586-62-9	10.604	MS, RI	3.6 ± 0.6	3.1 ± 0.6	1.6 ± 0.2
Linalool	78-70-6	10.79	MS, RI, Std	0.2 ± 0.02	0.1 ± 0.2	0.7 ± 0.4
Menthol	89-78-1	12.224	MS, RI	0.1 ± 0.1	ND	0.2 ± 0.1
(-)-terpinen-4-ol	562-74-3	12.335	MS, RI, Std	2.1 ± 0.6	0.4 ± 0.4	1.3 ± 0.2
α-terpineol	10482-56-1	12.57	MS, RI, Std	0.3 ± 0.1	0.03 ± 0.05	5 ± 1
α-fenchene	471-84-1	12.808	MS	ND	0.3 ± 0	ND
Fenchone	2774-84-7	12.873	MS	0.1 ± 0.1	ND	ND
β-cyclocitral	432-25-7	13.122	MS	ND	0.03 ± 0.03	ND
β-citronellol	106-22-9	13.193	MS, Std	0.7 ± 0.5	ND	0.4 ± 0.2
Geraniol	106-24-1	13.668	MS, RI, Std	ND	0.2 ± 0.2	ND

3.4   Discussion

3.4.1   Functionality of isoprenyl diphosphate synthases

Two putative isoprenyl diphosphate synthase genes isolated from grapevine were included in the yeast and/or plant systems used for TPS characterisation in this study. Sequence analyses indicated that these isolates had the characteristic motifs for GPS and FPS. Phylogeny with *A. thaliana* isoprenyl diphosphate synthases further supported the identification of these two sequences. The expression profiles of the two *VviIDSs,* based on the results of the gene atlas generated by Fasoli *et al.* (2012), showed relatively consistent gene expression across the various plant organs, tissues, and developmental stages that were analysed. In some instances, such as during bud and flower development, the expression of *VviFPS* correlated with the expression of *VviPTPS27* (predicted to be a sesquiterpene synthase).

The heterologous expression of the two genes did not yield conclusive results in terms of functionality with the systems that were used. *VviGPS* expressed in yeast increased monoterpene levels only when expressed in combination with *ScIDI1*, whereas co-infiltration of the full-length *VviGPS* with *VviSBTPS39* in *N. benthamiana* did not result in a significant difference in the measured monoterpenes. These results indicate that *VviGPS* is likely to be functional, but other enzymes can affect the activity of heterologously-expressed *VviGPS*. The putative *VviFPS* was used only in co-infiltration into *N. benthamiana* and could not be shown to affect either mono- or sesquiterpene levels.

3.4.2   Cultivar differences influence terpene synthase functionality

Functionality of the putative sesquiterpene synthase gene (*VviPTPS27*) could not be conclusively shown in either the yeast or grapevine expression systems, even though sequence analyses predicted the gene to encode a functional enzyme. Agroinfiltration into *N. benthamiana* for transient expression was used as an additional test for functionality. Headspace analysis from the whole leaves identified various compounds that had mass spectra characteristic of sesquiterpenes, with the additional detection of some monoterpenes in both the control and the plants transiently expressing *VviPTPS27*. The results indicate that *VviPTPS27* most likely is a (*E*)-β-caryophyllene synthase, but the levels of sesquiterpene that were produced was very low, which is most likely why characterisation in the yeast and grapevine expression systems could not be achieved. This is in accordance with previously characterised isolates mapping to the same gene model (Martin *et al.*, 2010; Smit *et al.*, 2019). Previous studies have shown that cultivar differences in *VviTPS* isolate sequences can influence gene function (Martin *et al.*, 2010; Drew *et al.*, 2016; Smit *et al.*, 2019). MSA of these characterised isolates (Figure B-v) indicated a 12-amino acid gap in the N-terminal domain adjacent to the RRX$_8$W motif in *VviPTPS27* and this sequence difference could possibly

influence the activity of the enzyme. It would be interesting to evaluate whether this deletion influences the folding of the protein and hence the active site.

As discussed by Smit *et al.* (2019), the relative expression based on the gene atlas data (Fasoli *et al.*, 2012) of *VviTPS27* is especially high during the later stages of flower development. Due to the potential role the products of the enzyme encoded by *VviTPS27* could have on plant–environment interactions, it has received more attention than most of the other *VviTPSs* investigated in this study (Martin *et al.*, 2010; Matarese *et al.*, 2014; Salvagnin *et al.*, 2016; Smit *et al.*, 2019). However, based on the lower activity of the VviPTPS27 (Pinotage) that was characterised in this study compared to VviMATPS27 (Muscat of Alexandria) and VviSHTPS27 (Shiraz) that were characterised by Smit *et al.* (2019), it is likely that the enzyme does not extensively contribute to flower bouquet in Pinotage.

Advances in the assembly of genome sequences troubled with high heterozygosity is allowing for higher quality genome sequencing of grapevine (Chin *et al.*, 2013; Doi *et al.*, 2014; Chin *et al.*, 2016; Gordon *et al.*, 2016; Pryszcz & Gabaldón, 2016; Ricker *et al.*, 2016; Seo *et al.*, 2016; Vij *et al.*, 2016; Huddleston *et al.*, 2017; Minio *et al.*, 2019). Genomes from various grapevine cultivars such as Cabernet Sauvignon, Chardonnay, Carménère, and Zinfandel have been or are being sequenced and annotated, which presents the opportunity to delve deeper into the cultivar differences found in specialised metabolism genes (Minio *et al.*, 2019; Vondras *et al.*, 2019; Zhou *et al.*, 2019). As an alternative to the relatively expensive exercise of genome sequencing, other methods such as studying expressed gene isoforms (Iso-Seq) using single-molecule real-time sequencing (SMRT) technology have also been developed (Minio, Massonnet, Figueroa-Balderas, Vondras, *et al.*, 2019). This technology enables the identification of cultivar-specific genes through the sequencing of full-length transcripts that can then be used as a reference for transcriptomic/expression studies.

3.4.3   The effect of functional characterisation systems on observed gene functionality

According to the functional characterisation by Martin *et al.* (2010), *VviTPS44* isolated from Pinot noir encodes a (+)-α-pinene synthase. In addition, the volatile analysis conducted by Matarese *et al.* (2014) showed increased levels of α-pinene in the flower, correlating to increased expression in the pollen. These results are supported by gene atlas data from this study. The highest relative *VviTPS44* gene expression was observed in the pollen, followed by tissue culture plants (root and pooled seedling samples) and senescing leaves.

However, heterologous expression of *VviPNTPS44* in yeast followed by volatile analysis, did not indicate any differences in the terpene profile, compared to the control strain, under the conditions used. Sequence comparison with previously characterised isolates mapping to the same gene model indicated high sequence similarity with only two amino acids differing. It is possible that the enzyme activity of VviTPS44 was very low and due to the methods used in this study detectable levels of terpenes could not be produced. Although it fell outside the scope of this study, future studies could

113

therefore include optimisation of the system such as removing the predicted targeting sequence and/or increasing substrate availability to the yeast. Alternatively, transient expression in *N. benthamiana* could also be considered.

3.4.4 Novel gene annotations: *VviTPS39* encodes an α-thujene synthase and *VviTPS41* a eucalyptol (1,8-cineole) synthase

Previous full-length cDNA isolates mapping to the *VviTPS39* gene model were functionally characterised as (-)-α-terpineol synthases, based on the main compound that was produced with the *in vitro* method that was utilised (Martin & Bohlmann, 2004). However, the main terpene produced by the full-length as well as the truncated cDNA isolates mapping to *VviTPS39* in this study, was α-thujene (Table 3.4). Based on these findings, it is proposed that the protein translated from the cDNA isolated from *V. vinifera* cv. Sauvignon blanc mapping to the *VviTPS39* gene model should be renamed to an α-thujene synthase (VviSBThu).

The full-length cDNA isolated from *V. vinifera* cv. Pinot noir which mapped to the previously uncharacterised *VviTPS41* gene model, produced eucalyptol (1,8-cineole) as the main compound when heterologously expressed in yeast (Table 3.4). The functional annotation of the enzyme was therefore established as a eucalyptol synthase (VviPNEuc). This is the first grapevine monoterpene synthase reported to produce eucalyptol as the main product. At a high concentration, eucalyptol contribution to the aroma of wine is seen as a negative aspect, with the wine described as having a "*Eucalyptus*" character. However, at moderate levels it denotes a fresh, camphoraceous odour that is considered as a desired characteristic in certain Cabernet Sauvignon wines (Saliba *et al.*, 2009). A study by Capone *et al.* (2012) attributed high levels of eucalyptol in the berry to the proximity of some vineyards to *Eucalyptus* trees. However, eucalyptol was detected in the grape berry by Kalua and Boss (2009) irrespective of the grapevine's proximity to the *Eucalyptus* trees, which indicates *de novo* synthesis in the grapevine. It was proposed that limonene and α-terpineol could be converted to eucalyptol (Fariña *et al.*, 2005). However, the functional characterisation of *VviPNTPS41* showed that a grapevine terpene synthase exists that may contribute to eucalyptol production in grapevine.

Tentative gene expression profiles were determined for *VviTPS39* and *VviTPS41* by utilising the gene atlas from *V. vinifera* cv. Corvina (Fasoli *et al.*, 2012). According to these expression data, these two terpene synthases are not highly expressed during berry development. However, it is well known that the expression profiles and levels, as well as the functionality of terpene synthases can differ among cultivars as discussed in Section 3.4.2. It would, therefore, be beneficial to further investigate the expression profiles of these characterised terpene synthases in other cultivars, especially those cultivars known to have higher eucalyptol levels in the berry.

Nevertheless, most of the monoterpenes produced by VviSBThu and VviPNEuc were shown to be present in grapevine in a study by Chalal *et al.* (2015) where the VOCs of whole grapevine plants were analysed. Sabinene has also been detected in wine samples from the Nero d'Avola grapevine cultivar (Verzera *et al.*, 2015) and has been identified in ripening Sauvignon blanc berries (Joubert *et al.*, 2016). Other studies have identified (-)-terpenin-4-ol in the grapevine berries of various cultivars (Erp *et al.*, 1976; Jesús Ibarz *et al.*, 2006; Loscos *et al.*, 2007; Noguerol-Pato *et al.*, 2013). Alternatively, the activity of these terpene synthases in the vegetative tissue, or materials other than grapes (MOG), could impact the wine quality when berries are harvested in a manner that includes these tissues during pressing or fermentation (Capone *et al.*, 2012).

In addition, terpene products often undergo modifications through the action of other enzymes (Martin *et al.*, 2010). A prominent example being the oxidation of α-guaiene to (-)-rotundone through the activity of a cytochrome P450 (CYP) (Takase *et al.*, 2016). The aroma detection threshold of (-)-rotundone in wine is very low (16 ng/L) and imparts a "black pepper" aroma to some Shiraz wines (Wood *et al.*, 2008). Further modification of terpene products *in planta* can therefore alter the product profile observed with *in vivo* enzyme assays and should be considered during the functional characterisation of terpene synthases (Croteau & Cane, 1985; Donaldson & Luster, 1991; Chang *et al.,* 2007; Gavira *et al.*, 2013). The terpene profile can also be affected by various other conditions: Cornwell *et al.* (1999) showed that during leaf aging in *Melaleuca* species, (+)-sabinene, *cis*-, and *trans*-sabinene hydrate are converted to (-)-terpenin-4-ol. It is thus possible that the terpenes produced via the enzymatic activity of various terpene synthases, including the α-thujene and eucalyptol (1,8-cineole) synthases characterised in this study, are converted through various chemical and/or enzymatic reactions in the plant into different terpene compounds.

3.5   Conclusion

Although the data generated from genomic and transcriptomic analyses provide invaluable information, functional characterisation of genes remains essential. This is especially true for genes involved in specialised metabolism. This study aimed to functionally characterise genes from the grapevine terpenoid pathway. In pursuit of this aim, various characterisation methods were evaluated including the expression system and the method with which the products were analysed. For the first time, the previously uncharacterised *VviPNTPS41* was shown to encode a eucalyptol synthase – indicating the inherent ability of grapevine to produce the compound *de novo*. In addition, *VviPTPS27* was confirmed to encode a (*E*)-β-caryophyllene synthase, but with much lower enzyme activity than the other isolates mapping to the same gene model. In contrast to the previously characterised isolates mapping to the same gene model, *VviSBTPS39* was proposed to encode an α-thujene synthase and not (-)-α-terpineol synthase. These results support the observation that gene sequence variation between cultivars can contribute to differences in the observable phenotypes.

3.6   Acknowledgements

3.7   References

Alberti, S., Gitler, A.D. & Lindquist, S., (2007). A suite of Gateway cloning vectors for high-throughput genetic analysis in Saccharomyces cerevisiae *Yeast* **24**, 10, 913–919.

Altschul, S.F., Madden, T.L., Schäffer, a a, Zhang, J., Zhang, Z., Miller, W. & Lipman, D.J., (1997). Gapped BLAST and PSI-BLAST: a new generation of protein database search programs. *Nucleic Acids Res.* **25**, 17, 3389–402.

Aubourg, S., Lecharny, a & Bohlmann, J., (2002). Genomic analysis of the terpenoid synthase (AtTPS) gene family of Arabidopsis thaliana. *Mol. Genet. Genomics* **267**, 6, 730–45.

Baranauskiene, R., Venskutonis, P.R., Viškelis, P. & Dambrauskiene, E., (2003). Influence of Nitrogen Fertilizers on the Yield and Composition of Thyme (Thymus vulgaris) *J. Agric. Food Chem.* **51**, 26, 7751–7758.

Bohlmann, J., Meyer-Gauen, G. & Croteau, R., (1998). Plant terpenoid synthases: molecular biology and phylogenetic analysis. *Proc. Natl. Acad. Sci. U. S. A.* **95**, 8, 4126–33.

Bouvier, F., Suire, C., D'Harlingue, A., Backhaus, R.A. & Camara, B., (2000). Molecular cloning of geranyl diphosphate synthase and compartmentation of monoterpene synthesis in plant cells *Plant J.* **24**, 2, 241–252.

Butler, J.B., Freeman, J.S., Potts, B.M., Vaillancourt, R.E., Grattapaglia, D., Silva-Junior, O.B., Simmons, B.A., Healey, A.L., Schmutz, J., Barry, K.W., Lee, D.J., Henry, R.J., King, G.J., Baten, A. & Shepherd, M., (2018). Annotation of the Corymbia terpene synthase gene family shows broad conservation but dynamic evolution of physical clusters relative to Eucalyptus *Heredity (Edinb).* **121**, 1, 87–104.

Canaguier, A., Grimplet, J., Gaspero, G. Di, Scalabrin, S., Duchêne, E. & Choisne, N., (2017). A new version of the grapevine reference genome assembly (12X.v2) and of its annotation (VCost.v3) *Genomics Data* **14**, July, 56–62.

Capone, D.L., Jeffery, D.W. & Sefton, M. a, (2012). Vineyard and fermentation studies to elucidate the origin of 1,8-cineole in Australian red wine. *J. Agric. Food Chem.* **60**, 9, 2281–7.

Chalal, M., Winkler, J.B., Gourrat, K., Trouvelot, S., Adrian, M., Schnitzler, J.-P., Jamois, F. & Daire, X., (2015). Sesquiterpene volatile organic compounds (VOCs) are markers of elicitation by sulfated laminarine in grapevine *Front. Plant Sci.* **6**, May, 1–9.

Chen, F., Tholl, D., Bohlmann, J. & Pichersky, E., (2011). The family of terpene synthases in plants: a mid-size family of genes for specialized metabolism that is highly diversified throughout the kingdom. *Plant J.* **66**, 1, 212–29.

Chin, C.S., Alexander, D.H., Marks, P., Klammer, A.A., Drake, J., Heiner, C., Clum, A., Copeland, A., Huddleston, J., Eichler, E.E., Turner, S.W. & Korlach, J., (2013). Nonhybrid, finished microbial genome assemblies from long-read SMRT sequencing data *Nat. Methods* **10**, 6, 563–569.

Chin, C.S., Peluso, P., Sedlazeck, F.J., Nattestad, M., Concepcion, G.T., Clum, A., Dunn, C., O'Malley, R., Figueroa-Balderas, R., Morales-Cruz, A., Cramer, G.R., Delledonne, M., Luo, C., Ecker, J.R., Cantu, D., Rank, D.R. & Schatz, M.C., (2016). Phased diploid genome assembly with single-molecule real-time sequencing *Nat. Methods* **13**, 12, 1050–1054.

Christianson, D.W., (2006). Structural biology and chemistry of the terpenoid cyclases. Vol. 106.

Closa, M., Vranová, E., Bortolotti, C., Bigler, L., Arró, M., Ferrer, A. & Gruissem, W., (2010). The Arabidopsis thaliana FPP synthase isozymes have overlapping and specific functions in isoprenoid biosynthesis, and complete loss of FPP synthase activity causes early developmental arrest *Plant J.* **63**, 3, 512–525.

Cornwell, C.P., Leach, D.N. & Wyllie, S.G., (1999). The Origin of Terpinen-4-ol in the Steam Distillates of Melaleuca argentea, M. dissitiflora and M. linariifolia *J. Essent. Oil Res.* **11**, 1, 49–53.

Croteau, R. & Cane, D.E., (1985). Monoterpene and sesquiterpene cyclases *Methods Enzymol.* **110**, 383–405.

Cunillera, N., Arró, M., Delourme, D., Karst, F., Boronat, A. & Ferrer, A., (1996). Arabidopsis thaliana Contains Two Differentially Expressed Farnesyl-Diphosphate Synthase Genes *J. Biol. Chem.* **271**, 13, 7774–7780.

Cunillera, N., Boronat, A. & Ferrer, A., (1997). The Arabidopsis thaliana FPS1 gene generates a novel mRNA that encodes a mitochondrial farnesyl-diphosphate synthase isoform *J. Biol. Chem.* **272**, 24, 15381–15388.

Cunillera, N., Boronat, A. & Ferrer, A., (2000). Spatial and temporal patterns of GUS expression directed by 5′ regions of the Arabidopsis thaliana farnesyl diphosphate synthase genes FPS1 and FPS2 *Plant Mol. Biol.* **44**, 6, 747–758.

Degenhardt, J., Köllner, T.G. & Gershenzon, J., (2009). Monoterpene and sesquiterpene synthases and the origin of terpene skeletal diversity in plants. *Phytochemistry* **70**, 15–16, 1621–37.

Delourme, D., Lacroute, F. & Karst, F., (1994). Cloning of an Arabidopsis thaliana cDNA coding for farnesyl diphosphate synthase by functional complementation in yeast *Plant Mol. Biol.* **26**, 6, 1867–1873.

Demetzos, C., Angelopoulou, D. & Perdetzoglou, D., (2002). A comparative study of the essential oils of Cistus salviifolius in several populations of Crete (Greece) *Biochem. Syst. Ecol.* **30**, 7, 651–665.

Doi, K., Monjo, T., Hoang, P.H., Yoshimura, J., Yurino, H., Mitsui, J., Ishiura, H., Takahashi, Y., Ichikawa, Y., Goto, J., Tsuji, S. & Morishita, S., (2014). Rapid detection of expanded short tandem repeats in personal genomics using hybrid sequencing *Bioinformatics* **30**, 6, 815–822.

Drew, D.P., Andersen, T.B., Sweetman, C., Møller, B.L., Ford, C. & Simonsen, H.T., (2016). Two key polymorphisms in a newly discovered allele of the Vitis vinifera TPS24 gene are responsible for the production of the rotundone precursor α-guaiene *J. Exp. Bot.* **67**, 3, 799–808.

Dueholm, B., Drew, D.P., Sweetman, C. & Simonsen, H.T., (2019). In planta and in silico characterization of five sesquiterpene synthases from Vitis vinifera (cv. Shiraz) berries *Planta* **249**, 1, 59–70.

Edgar, R., Domrachev, M. & Lash, A.E., (2002). Gene Expression Omnibus: NCBI gene expression and hybridization array data repository. *Nucleic Acids Res.* **30**, 1, 207–10.

Emanuelsson, O., Nielsen, H., Brunak, S. & von Heijne, G., (2000). Predicting subcellular localization of proteins based on their N-terminal amino acid sequence *J.Mol.Biol.* **300**, 4, 1005–1016.

Erp, A., Bull, S., Schreier, P., Drawert, F., Junker, A., Weihenstephan, D.-F.- & Germany, W., (1976). Identification of volatile constituents from grapes *J. Agric. Food Chem.* **24**, 2, 331–336.

Fariña, L., Boido, E., Carrau, F., Versini, G. & Dellacassa, E., (2005). Terpene compounds as possible precursors of 1,8-cineole in red grapes and wines *J. Agric. Food Chem.* **53**, 5, 1633–1636.

Fasoli, M., Dal Santo, S., Zenoni, S., Tornielli, G.B., Farina, L., Zamboni, A., Porceddu, A., Venturini, L., Bicego, M., Murino, V., Ferrarini, A., Delledonne, M. & Pezzotti, M., (2012). The Grapevine Expression Atlas Reveals a Deep Transcriptome Shift Driving the Entire Plant into a Maturation Program *Plant Cell* **24**, 9, 3489–3505.

Fischer, M.J.C., Meyer, S., Claudel, P., Perrin, M., Ginglinger, J.F., Gertz, C., Masson, J.E., Werck-Reinhardt, D., Hugueney, P. & Karst, F., (2013). Specificity of Ocimum basilicum geraniol synthase modified by its expression in different heterologous systems. *J. Biotechnol.* **163**, 1, 24–9.

Fridman, E. & Pichersky, E., (2005). Metabolomics, genomics, proteomics, and the identification of enzymes and their substrates and products. *Curr. Opin. Plant Biol.* **8**, 3, 242–8.

Gleave, A.P., (1992). A versatile binary vector system with a T-DNA organisational structure conducive to efficient integration of cloned DNA into the plant genome *Plant Mol. Biol.* **20**, 6, 1203–1207.

Gordon, D., Huddleston, J., Chaisson, M.J.P., Hill, C.M., Kronenberg, Z.N., Munson, K.M., Malig, M., Raja, A., Fiddes, I., Hillier, L.W., Dunn, C., Baker, C., Armstrong, J., Diekhans, M., Paten, B., Shendure, J., Wilson, R.K., Haussler, D., Chin, C.-S., Eichler, E.E. & Performed, A.R., (2016). Long-read sequence assembly of the gorilla genome deposited SMRT sequencing data into SRA HHS Public Access **352**, 6281, 1–21.

Grimplet, J., Adam-Blondon, A.-F., Bert, P.-F., Bitz, O., Cantu, D., Davies, C., Delrot, S., Pezzotti, M., Rombauts, S. & Cramer, G.R., (2014). The grapevine gene nomenclature system. *BMC Genomics* **15**, 1, 1077.

Hazzit, M., Baaliouamer, A., Faleiro, M.L. & Miguel, M.G., (2006). Composition of the essential oils of Thymus and Origanum species from Algeria and their antioxidant and antimicrobial activities *J. Agric. Food Chem.* **54**, 17, 6314–6321.

Hsieh, F.L., Chang, T.H., Ko, T.P. & Wang, A.H.J., (2011). Structure and mechanism of an arabidopsis medium/long-chain-length prenyl pyrophosphate synthase *Plant Physiol.* **155**, 3, 1079–1090.

Huddleston, J., Chaisson, M.J.P., Steinberg, K.M., Warren, W., Hoekzema, K., Gordon, D., Graves-Lindsay, T.A., Munson, K.M., Kronenberg, Z.N., Vives, L., Peluso, P., Boitano, M., Chin, C.S., Korlach, J., Wilson, R.K. & Eichler, E.E., (2017). Discovery and genotyping of structural variation from long-read haploid genome sequence data *Genome Res.* **27**, 5, 677–685.

Jaillon, O., Aury, J.-M., Noel, B., Policriti, A., Clepet, C., Casagrande, A., Choisne, N., Aubourg, S., Vitulo, N., Jubin, C., Vezzi, A., Legeai, F., Hugueney, P., Dasilva, C., Horner, D., Mica, E., Jublot, D., Poulain, J., Bruyère, C., Billault, A., Segurens, B., Gouyvenoux, M., Ugarte, E., Cattonaro, F., Anthouard, V., Vico, V., Del Fabbro, C., Alaux, M., Di Gaspero, G., Dumas, V., Felice, N., Paillard, S., Juman, I., Moroldo, M., Scalabrin, S., Canaguier, A., Le Clainche, I., Malacrida, G., Durand, E., Pesole, G., Laucou, V., Chatelet, P., Merdinoglu, D., Delledonne, M., Pezzotti, M., Lecharny, A., Scarpelli, C., Artiguenave, F., Pè, M.E., Valle, G., Morgante, M., Caboche, M., Adam-Blondon, A.-F., Weissenbach, J., Quétier, F. & Wincker, P., (2007). The grapevine genome sequence suggests ancestral hexaploidization in major angiosperm

phyla. *Nature* **449**, 7161, 463–7.

Jesús Ibarz, M., Ferreira, V., Hernández-Orte, P., Loscos, N. & Cacho, J., (2006). Optimization and evaluation of a procedure for the gas chromatographic–mass spectrometric analysis of the aromas generated by fast acid hydrolysis of flavor precursors extracted from grapes *J. Chromatogr. A* **1116**, 1–2, 217–229.

Joubert, C., Young, P.R., Eyeghe-Bickong, H.A. & Vivier, M.A., (2016). Field-grown grapevine berries use carotenoids and the associated xanthophyll cycles to acclimate to UV exposure differentially in high and low light (shade) conditions *Front. Plant Sci.* **7**, June, 786.

Kalua, C.M. & Boss, P.K., (2009). Evolution of Volatile Compounds during the Development of Cabernet Sauvignon Grapes (Vitis vinifera L.) *J. Agric. Food Chem.* **57**, 9, 3818–3830.

Karunanithi, P.S. & Zerbe, P., (2019). Terpene Synthases as Metabolic Gatekeepers in the Evolution of Plant Terpenoid Chemical Diversity *Front. Plant Sci.* **10**, October, 1–23.

Keim, V., Manzano, D., Fernández, F.J., Closa, M., Andrade, P., Caudepón, D., Bortolotti, C., Vega, M.C., Arró, M. & Ferrer, A., (2012). Characterization of Arabidopsis FPS Isozymes and FPS Gene Expression Analysis Provide Insight into the Biosynthesis of Isoprenoid Precursors in Seeds *PLoS One* **7**, 11, e49109.

Khan, M., Al-Saleem, M.S.M. & Alkhathlan, H.Z., (2016). A detailed study on chemical characterization of essential oil components of two Plectranthus species grown in Saudi Arabia *J. Saudi Chem. Soc.* **20**, 6, 711–721.

Koyama, T., Obata, S., Osabe, M., Takeshita, A., Yokoyama, K., Uchida, M., Ishino, T. & Ogura, T., (1993). Thermostable farnesyl diphosphate synthase of bacillus stearothermophilus: Molecular cloning, sequence determination, overproduction, and purification *J. Biochem.* **113**, 3, 355–263.

Külheim, C., Padovan, A., Hefer, C., Krause, S.T., Köllner, T.G., Myburg, A.A., Degenhardt, J. & Foley, W.J., (2015). The Eucalyptus terpene synthase gene family. *BMC Genomics* **16**, 1, 450.

Li, Y. & Pfeifer, B.A., (2014). Heterologous production of plant-derived isoprenoid products in microbes and the application of metabolic engineering and synthetic biology *Curr. Opin. Plant Biol.* **19**, 8–13.

Loscos, N., Hernandez-Orte, P., Cacho, J. & Ferreira, V., (2007). Release and formation of varietal aroma compounds during alcoholic fermentation from nonfloral grape odorless flavor precursors fractions *J. Agric. Food Chem.* **55**, 16, 6674–6684.

Lücker, J., Bowen, P. & Bohlmann, J., (2004). Vitis vinifera terpenoid cyclases: functional identification of two sesquiterpene synthase cDNAs encoding (+)-valencene synthase and (−)-germacrene D synthase and expression of mono- and sesquiterpene synthases in grapevine flowers and berries *Phytochemistry* **65**, 19, 2649–2659.

Martin, D.M. & Bohlmann, J., (2004). Identification of Vitis vinifera (-)-alpha-terpineol synthase by in silico screening of full-length cDNA ESTs and functional characterization of recombinant terpene synthase. *Phytochemistry* **65**, 9, 1223–9.

Martin, D.M., Toub, O., Chiang, A., Lo, B.C., Ohse, S., Lund, S.T. & Bohlmann, J., (2009). The bouquet of grapevine (Vitis vinifera L. cv. Cabernet Sauvignon) flowers arises from the biosynthesis of sesquiterpene volatiles in pollen grains. *Proc. Natl. Acad. Sci. U. S. A.* **106**, 17, 7245–50.

Martin, D.M., Aubourg, S., Schouwey, M.B., Daviet, L., Schalk, M., Toub, O., Lund, S.T. & Bohlmann, J., (2010). Functional annotation, genome organization and phylogeny of the grapevine (Vitis vinifera) terpene synthase gene family based on genome assembly, FLcDNA cloning, and enzyme assays. *BMC Plant Biol.* **10**, 1, 226.

Matarese, F., Cuzzola, A., Scalabrelli, G. & D'Onofrio, C., (2014). Expression of terpene synthase genes associated with the formation of volatiles in different organs of Vitis vinifera *Phytochemistry* **105**, 12–24.

Metsalu, T. & Vilo, J., (2015). ClustVis: A web tool for visualizing clustering of multivariate data using Principal Component Analysis and heatmap *Nucleic Acids Res.* **43**, W1, W566–W570.

Minio, A., Massonnet, M., Figueroa-Balderas, R., Vondras, A.M., Blanco-Ulate, B. & Cantu, D., (2019). Iso-Seq Allows Genome-Independent Transcriptome Profiling of Grape Berry Development *G3 Genes|Genomes|Genetics* **9**, 3, 755–767.

Minio, A., Massonnet, M., Figueroa-Balderas, R., Castro, A. & Cantu, D., (2019). Diploid Genome Assembly of the Wine Grape Carménère *G3 Genes|Genomes|Genetics* **9**, 5, 1331–1337.

Murashige, T. & Skoog, F., (1962). A revised medium for rapid growth and bioassays with tobacco tissue culture *Physiol. Plant.* **15**, 473–497.

Nielsen, H., Engelbrecht, J., Brunak, S. & Von Heijne, G., (1997). Identification of prokaryotic and eukaryotic signal peptides and prediction of their cleavage sites *Protein Eng.* **10**, 1, 1–6.

Noguerol-Pato, R., González-Álvarez, M., González-Barreiro, C., Cancho-Grande, B. & Simal-Gándara, J., (2013). Evolution of the aromatic profile in Garnacha Tintorera grapes during raisining and comparison with that of the naturally sweet wine obtained *Food Chem.* **139**, 1–4, 1052–1061.

Ohnuma, S., Nakazawa, T., Hemmi, H., Hallberg, a M., Koyama, T., Ogura, K. & Nishino, T., (1996). Conversion from farnesyl diphosphate synthase to geranylgeranyl diphosphate synthase by random

chemical mutagenesis. *J. Biol. Chem.* **271**, 17, 10087–95.

Pazouki, L. & Niinemets, Ü., (2016). Multi-Substrate Terpene Synthases: Their Occurrence and Physiological Significance *Front. Plant Sci.* **7**, July, 1–16.

Pryszcz, L.P. & Gabaldón, T., (2016). Redundans: An assembly pipeline for highly heterozygous genomes *Nucleic Acids Res.* **44**, 12, e113.

Ricker, N., Shen, S.Y., Goordial, J., Jin, S. & Fulthorpe, R.R., (2016). PacBio SMRT assembly of a complex multi-replicon genome reveals chlorocatechol degradative operon in a region of genome plasticity *Gene* **586**, 2, 239–247.

Saliba, A.J., Bullock, J. & Hardie, W.J., (2009). Consumer rejection threshold for 1,8-cineole (eucalyptol) in Australian red wine *Food Qual. Prefer.* **20**, 7, 500–504.

Salido, S., Altarejos, J., Nogueras, M., Sánchez, A., Pannecouque, C., Witvrouw, M. & De Clercq, E., (2002). Chemical studies of essential oils of Juniperus oxycedrus ssp. badia *J. Ethnopharmacol.* **81**, 1, 129–134.

Salvagnin, U., Carlin, S., Angeli, S., Vrhovsek, U., Anfora, G., Malnoy, M. & Martens, S., (2016). Homologous and heterologous expression of grapevine E-(β)-caryophyllene synthase (VvGwECar2) *Phytochemistry* **131**, 76–83.

Seo, J.S., Rhie, A., Kim, J., Lee, S., Sohn, M.H., Kim, C.U., Hastie, A., Cao, H., Yun, J.Y., Kim, J., Kuk, J., Park, G.H., Kim, J., Ryu, H., Kim, J., Roh, M., Baek, J., Hunkapiller, M.W., Korlach, J., Shin, J.Y. & Kim, C., (2016). De novo assembly and phasing of a Korean human genome *Nature* **538**, 7624, 243–247.

Smit, S.J., Vivier, M.A. & Young, P.R., (2019). Linking Terpene Synthases to Sesquiterpene Metabolism in Grapevine Flowers *Front. Plant Sci.* **10**, February, 1–18.

Takase, H., Sasaki, K., Shinmori, H., Shinohara, A., Mochizuki, C., Kobayashi, H., Ikoma, G., Saito, H., Matsuo, H., Suzuki, S. & Takata, R., (2016). Cytochrome P450 CYP71BE5 in grapevine (Vitis vinifera) catalyzes the formation of the spicy aroma compound (-)-rotundone *J. Exp. Bot.* **67**, 3, 787–798.

Tholl, D., (2006). Terpene synthases and the regulation, diversity and biological roles of terpene metabolism. *Curr. Opin. Plant Biol.* **9**, 3, 297–304.

Thomas, B.J. & Rothstein, R., (1989). Elevated recombination rates in transcriptionally active DNA. *Cell* **56**, 4, 619–30.

Tuskan, G.A., DiFazio, S., Jansson, S., Bohlmann, J., Grigoriev, I., Hellsten, U., Putnam, M., Ralph, S., Rombauts, S., Salamov, A., Schein, J., Sterck, L., Aerts, A., Bhalerao, R.R., Bhalerao, R.P., Blaudez, D., Boerjan, W., Brun, A., Brunner, A., Busov, V., Campbell, M., Carlson, J., Chalot, M., Chapman, J., Chen, G.L., Cooper, D., Coutinho, P.M., Couturier, J., Covert, S., Cronk, Q., Cunningham, R., Davis, J., Degroeve, S., Dřjardin, A., DePamphilis, C., Detter, J., Dirks, B., Dubchak, I., Duplessis, S., Ehlting, J., Ellis, B., Gendler, K., Goodstein, D., Gribskov, M., Grimwood, J., Groover, A., Gunter, L., Hamberger, B., Heinze, B., Helariutta, Y., Henrissat, B., Holligan, D., Holt, R., Huang, W., Islam-Faridi, N., Jones, S., Jones-Rhoades, M., Jorgensen, R., Joshi, C., Kangasjärvi, J., Karlsson, J., Kelleher, C., Kirkpatrick, R., Kirst, M., Kohler, A., Kalluri, U., Larimer, F., Leebens-Mack, J., Leplé, J.C., Locascio, P., Lou, Y., Lucas, S., Martin, F., Montanini, B., Napoli, C., Nelson, D.R., Nelson, C., Nieminen, K., Nilsson, O., Pereda, V., Peter, G., Philippe, R., Pilate, G., Poliakov, A., Razumovskaya, J., Richardson, P., Rinaldi, C., Ritland, K., Rouzé, P., Ryaboy, D., Schmutz, J., Schrader, J., Segerman, B., Shin, H., Siddiqui, A., Sterky, F., Terry, A., Tsai, C.J., Uberbacher, E., Unneberg, P., Vahala, J., Wall, K., Wessler, S., Yang, G., Yin, T., Douglas, C., Marra, M., Sandberg, G., Van De Peer, Y. & Rokhsar, D., (2006). The genome of black cottonwood, Populus trichocarpa (Torr. & Gray) *Science (80-.).* **313**, 5793, 1596–1604.

Vandermoten, S., Haubruge, É. & Cusson, M., (2009). New insights into short-chain prenyltransferases: structural features, evolutionary history and potential for selective inhibition *Cell. Mol. Life Sci.* **66**, 23, 3685–3695.

Venditti, A., Bianco, A., Frezza, C., Serafini, M., Giacomello, G., Giuliani, C., Bramucci, M., Quassinti, L., Lupidi, G., Lucarini, D., Papa, F. & Maggi, F., (2016). Secondary Metabolites, Glandular Trichomes and Biological Activity of Sideritis montana L. subsp. montana from Central Italy *Chem. Biodivers.* **13**, 10, 1380–1390.

Verzera, A., Tripodi, G., Dima, G., Condurso, C., Scacco, A., Cincotta, F., Giglio, D.M.L., Santangelo, T. & Sparacio, A., (2015). Leaf removal and wine composition of Vitis vinifera L. cv. Nero d'Avola: the volatile aroma constituents *J. Sci. Food Agric.*

Vij, S., Kuhl, H., Kuznetsova, I.S., Komissarov, A., Yurchenko, A.A., Van Heusden, P., Singh, S., Thevasagayam, N.M., Prakki, S.R.S., Purushothaman, K., Saju, J.M., Jiang, J., Mbandi, S.K., Jonas, M., Hin Yan Tong, A., Mwangi, S., Lau, D., Ngoh, S.Y., Liew, W.C., Shen, X., Hon, L.S., Drake, J.P., Boitano, M., Hall, R., Chin, C.S., Lachumanan, R., Korlach, J., Trifonov, V., Kabilov, M., Tupikin, A., Green, D., Moxon, S., Garvin, T., Sedlazeck, F.J., Vurture, G.W., Gopalapillai, G., Kumar Katneni, V., Noble, T.H., Scaria, V., Sivasubbu, S., Jerry, D.R., O'Brien, S.J., Schatz, M.C., Dalmay, T., Turner, S.W., Lok, S., Christoffels, A. & Orbán, L., (2016). Chromosomal-Level Assembly of the Asian Seabass Genome Using Long Sequence Reads and Multi-layered Scaffolding *PLoS Genet.* **12**, 4, 1–35.

Vondras, A.M., Minio, A., Blanco-Ulate, B., Figueroa-Balderas, R., Penn, M.A., Zhou, Y., Seymour, D., Ye, Z., Liang, D., Espinoza, L.K., Anderson, M.M., Walker, M.A., Gaut, B. & Cantu, D., (2019). The genomic diversification of grapevine clones *BMC Genomics* **20**, 1, 972.

Vranová, E., Coman, D., Gruissem, W., Vranov, E., Coman, D., Gruissem, W., Vranová, E., Coman, D. & Gruissem, W., (2013). Network Analysis of the MVA and MEP Pathways for Isoprenoid Synthesis *Annu. Rev. Plant Biol.* **64**, 1, 665–700.

Wang, K. & Ohnuma, S., (1999). Chain-length determination mechanism of isoprenyl diphosphate synthases and implications for molecular evolution. *Trends Biochem. Sci.* **24**, 11, 445–51.

Wood, C., Seibert, T., Parker, M., Capone, D.L., Elsey, G.M., Pollnitz, A.P., Eggers, M., Meier, M., Vossing, T., Widder, S., Krammer, G., Sefton, M. a & Herderich, M., (2008). Spice up your life - The rotundone story. In: Expr. Multidiscip. Flavour Sci. 483–486.

Xiong, W., Wu, P., Jia, Y., Wei, X., Xu, L., Yang, Y., Qiu, D., Chen, Y., Li, M., Jiang, H. & Wu, G., (2016). Genome-wide analysis of the terpene synthase gene family in physic nut (Jatropha curcas L.) and functional identification of six terpene synthases *Tree Genet. Genomes* **12**, 5, 97.

Young, P.R., (2004). Molecular analyses of candidate carotenoid biosynthetic genes in <i>Vitis vinifera<i/> L. Stellenbosch University.

Zhou, Y., Minio, A., Massonnet, M., Solares, E., Lv, Y., Beridze, T., Cantu, D. & Gaut, B.S., (2019). The population genetics of structural variants in grapevine domestication *Nat. Plants* **5**, 9, 965–979.

Zhu, B.-Q., Cai, J., Wang, Z.-Q., Xu, X.-Q., Duan, C.-Q. & Pan, Q.-H., (2014). Identification of a Plastid-Localized Bifunctional Nerolidol/Linalool Synthase in Relation to Linalool Biosynthesis in Young Grape Berries *Int. J. Mol. Sci.* **15**, 12, 21992–22010.

Appendix A   To Chapter 3

Table A-i Primers used in study. Underlined sequences indicate restriction endonuclease recognition site additions.

| Name	Sequence (5' to 3')	Amplicon size (bp)	Description
VviTPS27-5' VviTPS27-3'	<u>GTCGAC</u>ATGTCTGTTCAGTCTTCAGGGGTAC TCATATTGGCACAGGATCAATTAGC	1674	Amplifies the full-length CDS of the *Vitis vinifera TPS27* gene. *SalI* RE site
VviTPS44-5' VviTPS44-3'	<u>TCTAGA</u>ATGGCTCTTCTGACGCTTTCTT <u>GTCGAC</u>CTATACAGGGGAAATAGGCTCA	1773	Amplifies the full-length CDS of the *Vitis vinifera TPS44* gene. *XbaI* RE site on 5' primer and *SalI* RE site on 3' pirmer.
VvTPS41-5' VvTPS41-3'	<u>TCTAGA</u>ATGGCTCTTTTCATGCTTTCTTC <u>GTCGAC</u>CTAGACCAGGGGAATGG	1782	Amplifies the full-length CDS of the *Vitis vinifera TPS41* gene. *XbaI* RE site on 5' primer and *SalI* RE site on 3' pirmer.
M13pUCF M13pUCR	CCCAGTCACGACGTTGTAAAACG AGCGGATAACAATTTCACACAGG	Varies	Universal primers to PCR any cassette from pGEM-T Easy
attB1 adapter attB2 adapter	GGGGACAAGTTTGTACAAAAAAGCAGGCT GGGGACCACTTTGTACAAGAAAGCTGGGT	Varies	Universal *att*B adapter primers used for Gateway® cloning
VviTPS41_B1 VviTPS41_trunc_B1 VviTPS41_B2	aaaaagcaggctATGGCTCTTTTCATGCTTTC aaaaagcaggct<u>ATG</u>TGCGTGGTTGTCAATAGAC agaaagctgggtCTAGACCAGGGGAATGGG	1797 1674	Template-specific primers containing 12 nucleotides of the attB sites (lowercase)
nptII-5' nptII_3'	TCTGATGCCGCCGTGTTC GAGCCCCTGATGCTCTTCGT	402	Screening for gene integration. Amplifies kanamycin-resistant gene on pART27 construct
VviActin-5' VviActin-3'	GATACTGAAGATATCCAGCCCCTCG GCATGGGGAAGTGCATAACCTT	521 bp for cDNA and 713bp for gDNA	Intron-spanning primers designed to amplify region of actin-encoding gene (VIT_204s0044g00580)
CaMVp VviTPS27	GACGTAAGGGATGACGCACAAT TCATATTGGCACAGGATCAATTAGC	1730	3' gene-specific primer in combination with 5' primer specific to CaMVp to screen for transgene integration

Table A-ii Constructs generated and used in study. NA = not applicable.

Plasmid	Description	Expression cassette	Source or reference
pGEM-T-Easy	*E. coli* general cloning vector	NA	Promega
pART7	Primary cloning vector	CaMV35Sp::OCSt::nptII	Gleave (1992)
pART27	Binary vector	NA	Gleave (1992)
pBS-URA3	pBlueScript SK II+ [*URA3* - P*PGK1*]	PGK1p::CYC1t::URA3	This study
pGEM-TPS27	Cloning vector containing *VviTPS27, Spe*I and *Sal*I RE sites	NA	This study
pGEM-TPS41	Cloning vector containing *VviTPS41, Xba*I and *Sal*I sites RE sites	NA	This study
pGEM-TPS44	Cloning vector containing *VviTPS44, Xba*I and *Sal*I sites RE sites	NA	This study
pBS-PGK1p-TPS27	pBlueScript SK II+ [*URA3* - P*PGK1* – *VviSBTPS27*], linearise with *Apa*I	PGK1p::VviSBTPS27::CYCt::URA3 Amp^R	This study
pBS-PGK1p-TPS39	pBlueScript SK II+ [*URA3* - P*PGK1* - *VviSBTPS39*], linearise with *Apa*I	PGK1p::VviSBTPS39::CYCt::URA3 Amp^R	This study
pBS-PGK1p-TPS41	pBlueScript SK II+ [*URA3* - P*PGK1* – *VviPNTPS41*], linearise with *Apa*I	PGK1p::VviPNTPS41::CYCt::URA3 Amp^R	This study
pBS-PGK1p-TPS44	pBlueScript SK II+ [*URA3* - P*PGK1* – *VviPNTPS44*], linearise with *Apa*I	PGK1p::VviPNTPS44::CYCt::URA3 Amp^R	This study
pBS-PGK1p-GPStrunc	pBlueScript SK II+ [*TRP1* - P*PGK1* – *VviGPS*], linearise with *Eco*81I	PGK1p::VviGPS::CYCt::TRP1 Amp^R	This study
pAG426GAL	Episomal *S. cerevisiae* Gateway® cloning vector	GAL1p::CYC1t::URA3	Alberti *et al.* (2007)
pAG426GAL-TPS39	426GAL-ccdB + *VviSBTPS39*	GAL1p::VviSBTPS39::CYC1t::URA3	This study
pAG426GAL-TPS39trunc	426GAL-ccdB + VviSBTPS39trunc	GAL1p::VviSBTPS39trunc::CYC1t::URA3	This study
pAG426GAL-TPS41	426GAL-ccdB + *VviPNTPS41*	GAL1p::VviPNTPS41::CYC1t::URA3	This study
pAG426GAL-TPS41trunc	426GAL-ccdB + VviPNTPS41trunc	GAL1p::VviPNTPS41trunc::CYC1t::URA3	This study
pART27-FPS	Full-length *FPS* isolated from *Vitis vinifera* and cloned pART7 expression cassette. The expression cassette containing *FPS* was then cloned into pART27 plant expression vector	CaMV35Sp::VviFPS::OCSt::nptII	Young (2004)

122

Plasmid	Description	Expression cassette	Source or reference
pART27-GPS	pART7 expression cassette containing *VviGPS* cloned into pART27	CaMV35Sp::VviGPS::OCSt::nptII	This study
pART27-TPS39	pART7 expression cassette containing *VviTPS39* cloned into pART27	CaMV35Sp::VviTPS39::OCSt::nptII	This study
pART7-TPS27	Full-length *TPS27* isolated from *Vitis vinifera* and cloned into pART7 expression cassette	CaMV35Sp::VviTPS27::OCSt::nptII	This study
pART27-TPS27	pART7 expression cassette containing *VviTPS27* cloned into pART27	CaMV35Sp::VviTPS27::OCSt::nptII	This study
P19	anti-posttranscriptional gene silencing protein		

123

Table A-iii Yeast strains used and generated in study.

Strain	Description	Source or reference
W303-1A	MAT a ade2-1 can1-100 ura3-1 leu2-3,112 his3-11,15 trp1-1	Thomas & Rothstein (1989)
GT07	MAT a ade2-1::ADE2 - P_{PGK1} – IDI1 can1-100 ura3-1::URA3 - P_{PGK1} – VviTPS39 leu2-3::LEU2 - P_{PGK1} – tHMG1 his3-11,15 trp1-1	This study
GT10	MAT a ade2-1::ADE2 – P_{PGK1} – IDI1 can1-100 ura3-1::URA3 - P_{PGK1} – VviTPS27 leu2-3::LEU2 - P_{PGK1} – tHMG1 his3-11,15 trp1-1	This study
GT11	MAT a ade2-1::ADE2 - P_{PGK1} – IDI1 can1-100 ura3-1::URA3 - P_{PGK1} – VviTPS41 leu2-3::LEU2 - P_{PGK1} – tHMG1 his3-11,15 trp1-1	This study
GT12	MAT a ade2-1::ADE2 - P_{PGK1} – IDI1 can1-100 ura3-1::URA3 – P_{GAL1} – VviTPS44 leu2-3::LEU2 - P_{PGK1} – tHMG1 his3-11,15 trp1-1	This study
GT13	MAT a ade2-1::ADE2 - P_{PGK1} – IDI1 can1-100 ura3-1::URA3 - P_{GAL1} – VviTPS39full-length leu2-3::LEU2 - P_{PGK1} – tHMG1 his3-11,15 trp1-1	This study
GT14	MAT a ade2-1::ADE2 - P_{PGK1} – IDI1 can1-100 ura3-1::URA3 - P_{GAL1} – VviTPS39trunc leu2-3::LEU2 - P_{PGK1} – tHMG1 his3-11,15 trp1-1	This study
GT15	MAT a ade2-1::ADE2 - P_{PGK1} – IDI1 can1-100 ura3-1::URA3 - P_{GAL1} – VviTPS41full-length leu2-3::LEU2 - P_{PGK1} – tHMG1 his3-11,15 trp1-1	This study
GT16	MAT a ade2-1::ADE2 - P_{PGK1} – IDI1 can1-100 ura3-1::URA3 - P_{GAL1} – VviTPS41trunc leu2-3::LEU2 - P_{PGK1} – tHMG1 his3-11,15 trp1-1	This study

Appendix B   To Chapter 3
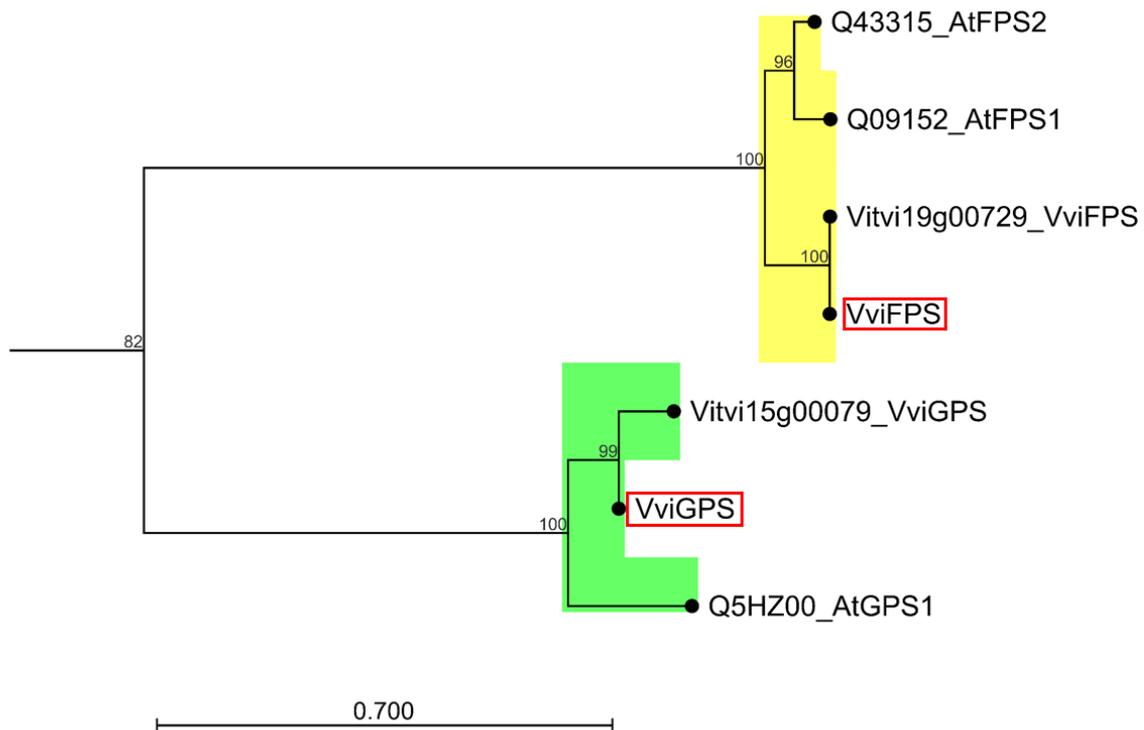
Figure B-i Phylogenetic tree construction of *Vitis vinifera* (Vvi) and *Arabidopsis thaliana* (At) short-chain isoprenyl diphosphate synthase (IDS) sequences with the two IDSs studied in this chapter (highlighted with red boxes). Multiple sequence alignment (MSA) with amino acid sequences using the characteristic sequences as fixed alignment points followed by maximum-likelihood phylogeny with the neighbor-joining construction method, with the Dayhoff (PAM) substitution model set at four substitution-rate categories. Subtree colouring to indicate the various groupings: yellow – farnesyl diphosphate synthase (FPS) and green – geranyl diphosphate synthase (GPS).
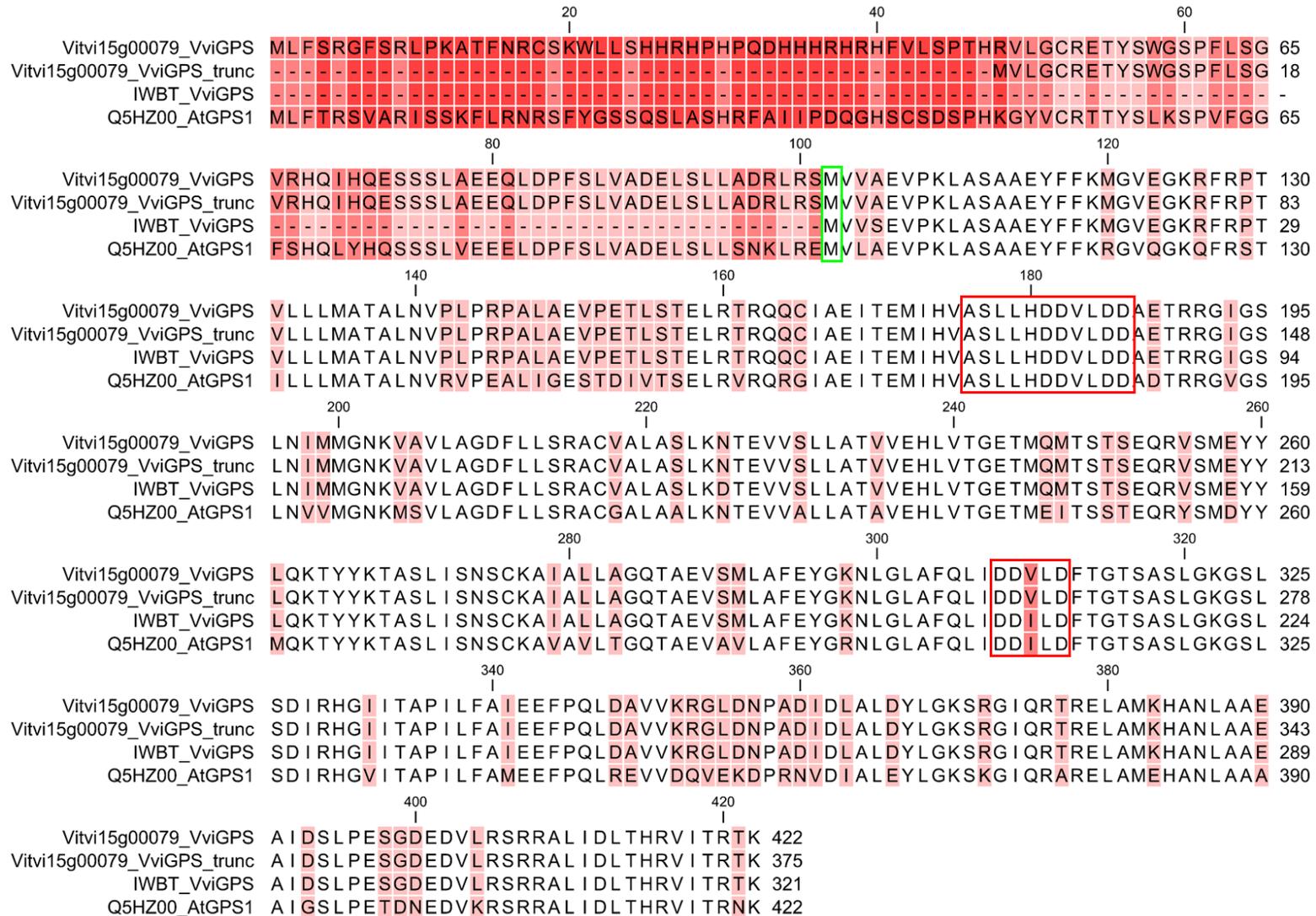
Figure B-ii Multiple sequence alignment of VviGPS with predicted geranyl diphosphate synthase sequences from *Arabidopsis thaliana.* Dissimilarity in sequence shown in light red with the two characteristic motifs highlighted with red boxes: Chain-length determination (CLD) region, which includes the first aspartate rich motif (FARM), with the second aspartate rich motif (SARM) located further downstream.
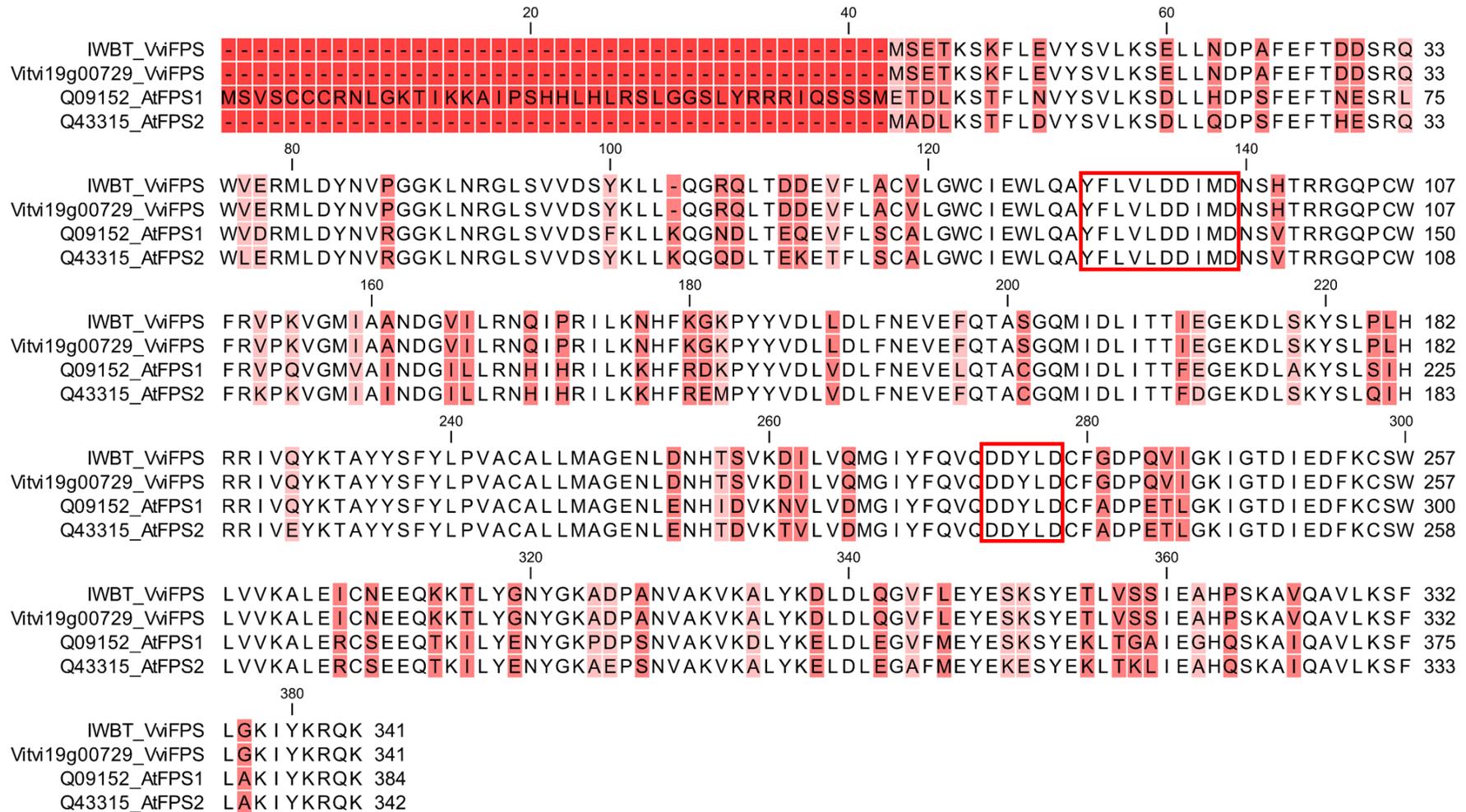
Figure B-iii Multiple sequence alignment of VviFPS (the isolated sequence and gene model to which it maps) with predicted farnesyl diphosphate synthase sequences from *Arabidopsis thaliana*. Dissimilarity in sequence shown in different shades of red with the two characteristic motifs highlighted with red boxes: Chain-length determination (CLD) region (including the first aspartate rich motif (FARM)) and the second aspartate rich motif (SARM).

127
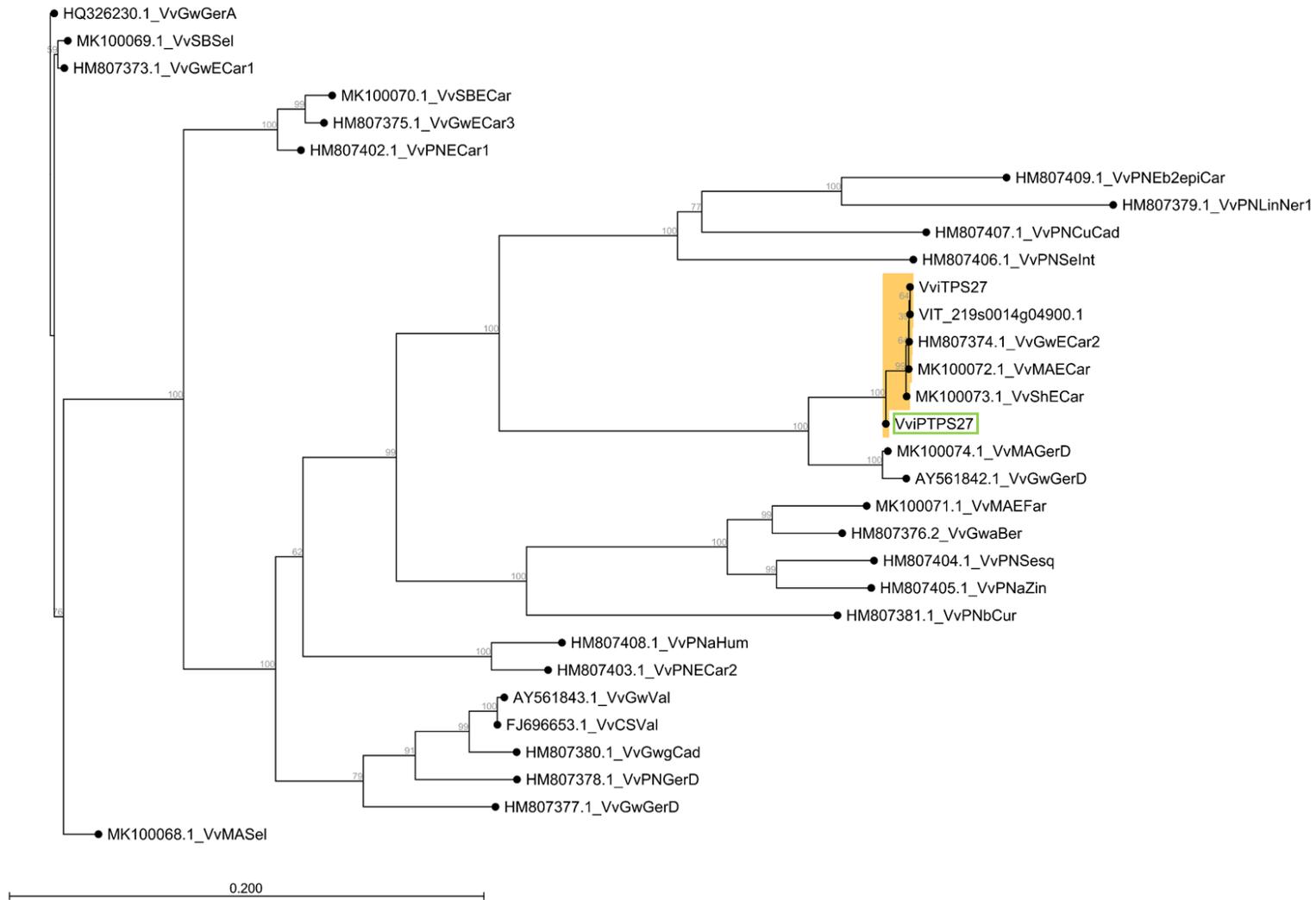
Figure B-iv Phylogenetic tree of previously characterised VviTPS-a subfamily isolates and the isolated sequence from this study (green box). The gene model and previously characterised isolates to which it maps closest to is highlighted with yellow colouring of the subtree. Bootstrap % values shown at each branchpoint.

128
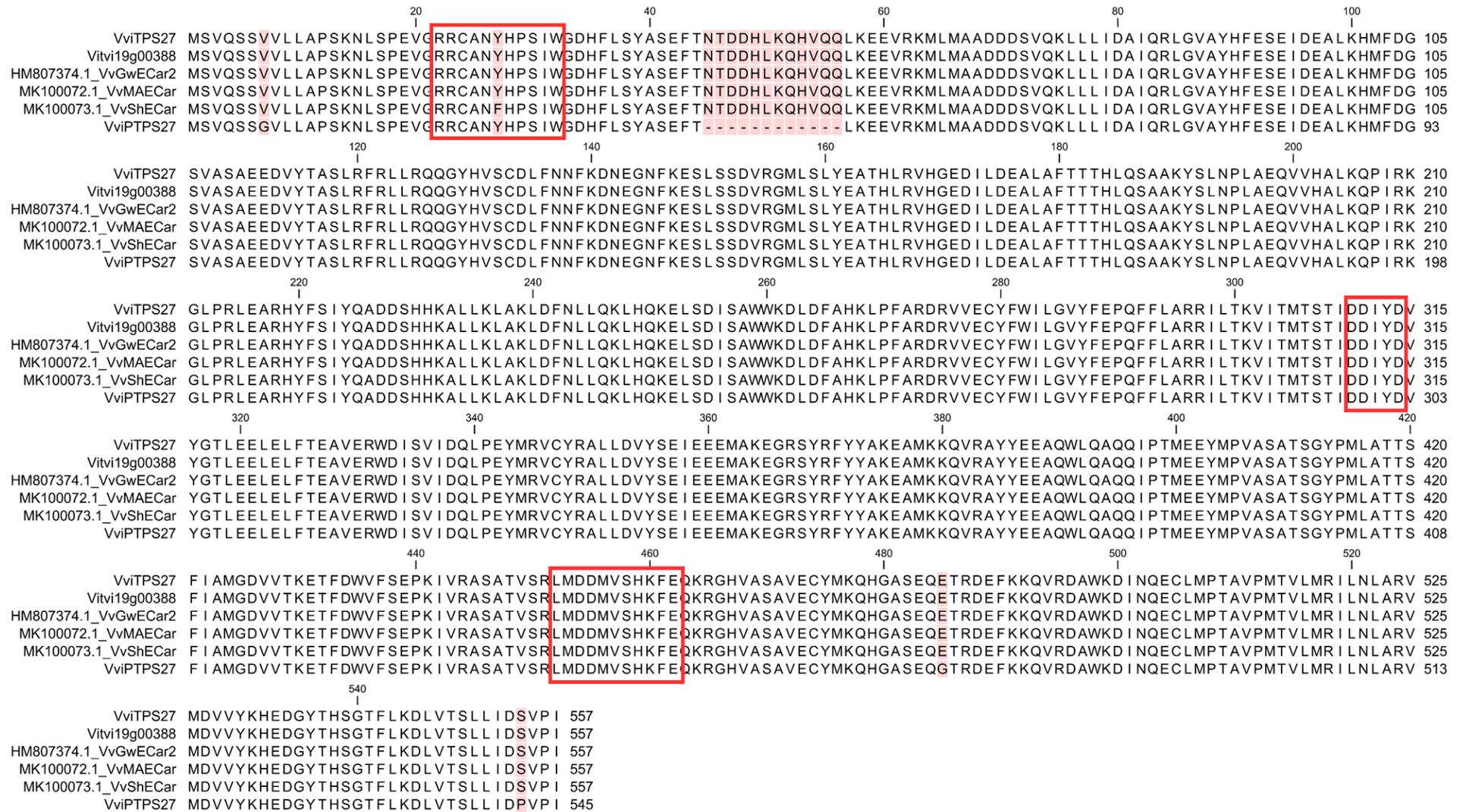
Figure B-v Multiple sequence alignment of *VviTPS27* with three previously characterised (*E*)-β-caryophyllene synthases mapping to the same gene model and grouping closest to *VviTPS27* in the phylogenetic tree. Dissimilarity in sequences are shown in light red with the three characteristic motifs highlighted with red boxes. RR(x)8W, DDXXD, and NSE/DTE motifs highlighted with red boxes.

129
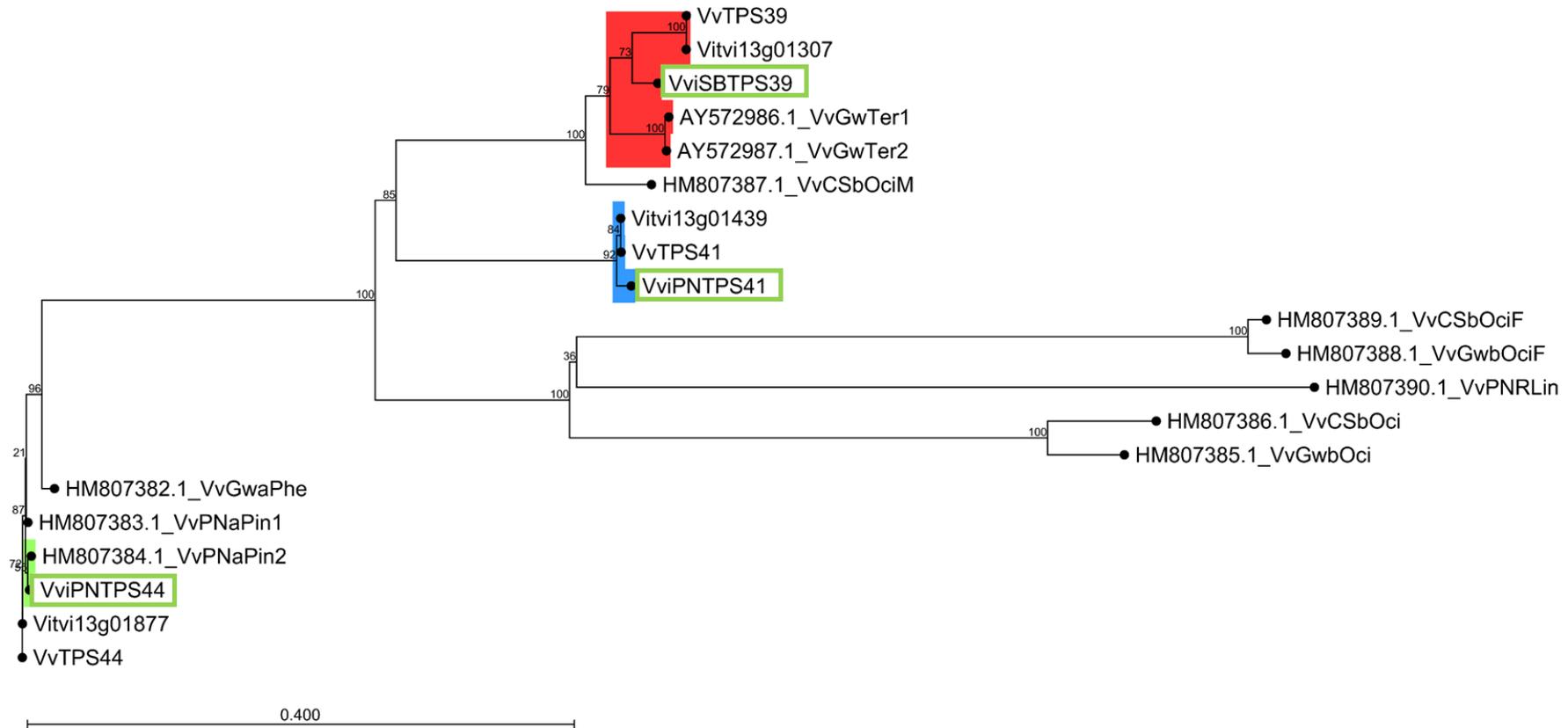
Figure B-vi Phylogenetic tree of previously characterised VviTPS-b subfamily isolates and the isolated sequenced from this study (green box) and the gene models to which it maps to - VviTPS39 (red), VviTPS41 (blue) and VviTPS44 (green). Bootstrap % values are shown at each branchpoint.

130
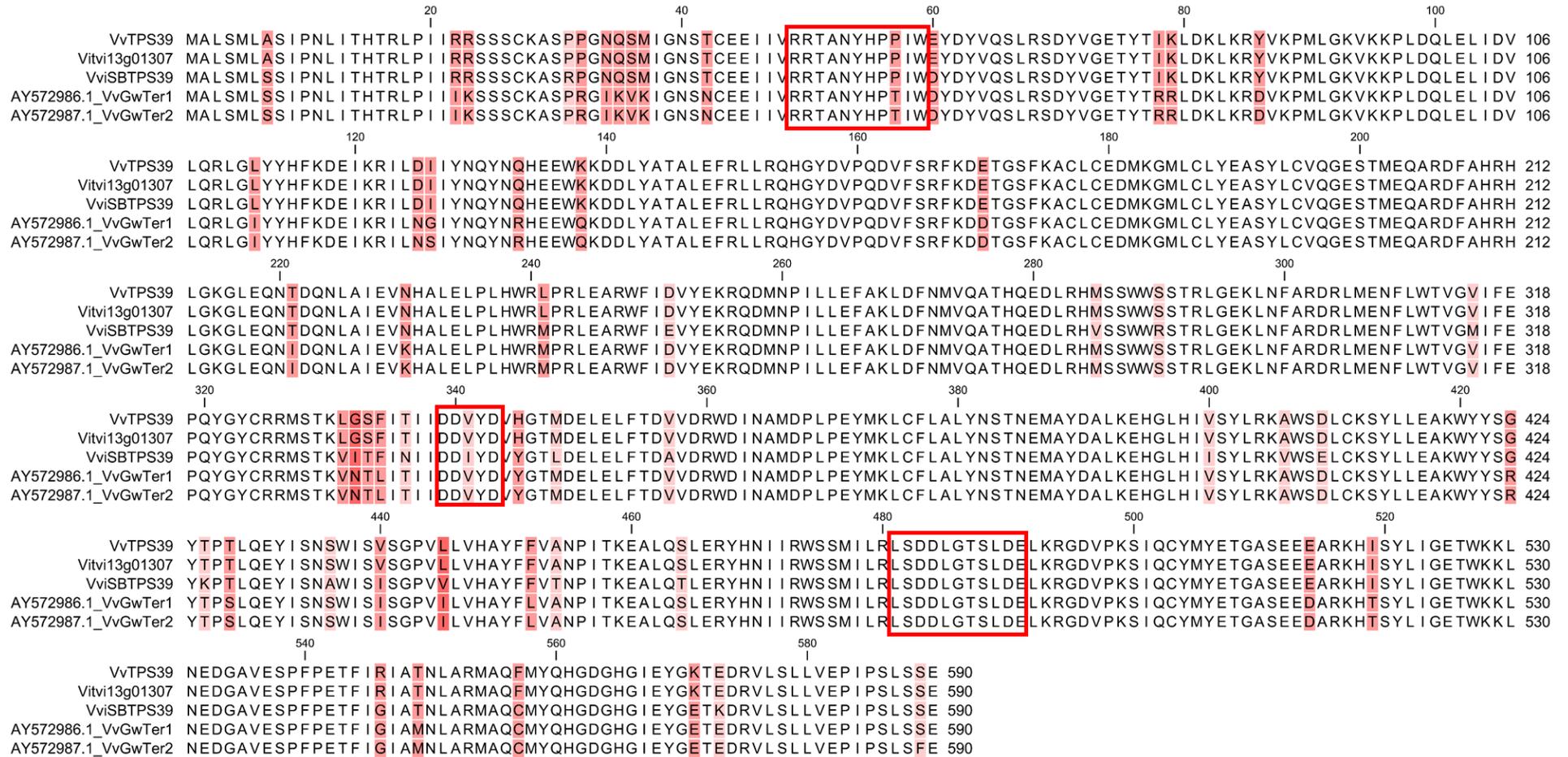
Figure B-vii Multiple sequence alignment of *VviSB39* with three previously isolated characterised as two α-terpineol synthases and a (E)-β-ocimene/myrcene synthases grouping closest to *VviSBTPS39* in the phylogenetic tree. The two α-terpineol synthases map to the same gene model. Dissimilarity in sequence shown in light red with the three characteristic motifs highlighted with red boxes. Characteristic motifs (RRX8W, DDXXD, and NSE/DTE) are highlighted in red.
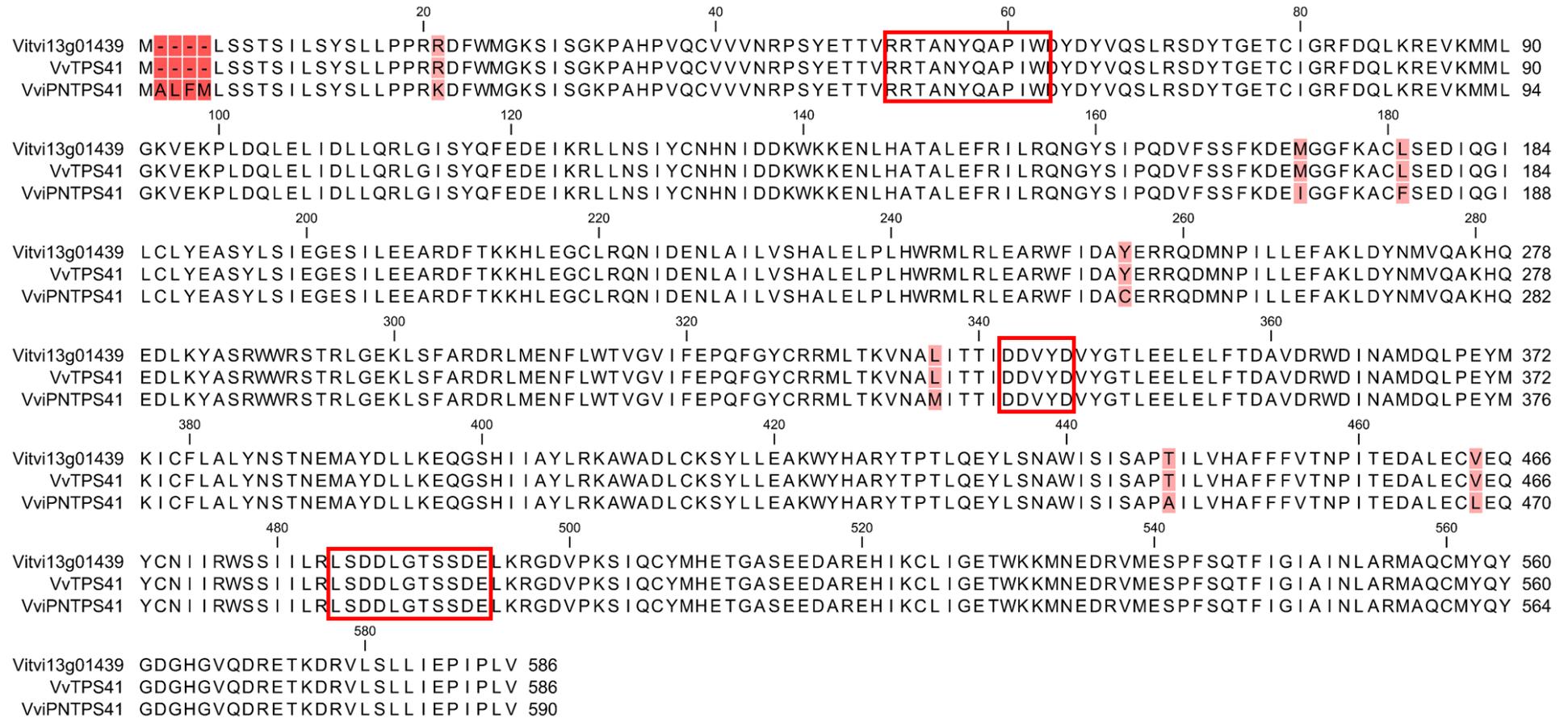
Figure B-viii Multiple sequence alignment of the *VviTPS* gene model mapping closely to the *VviPNTPS41* isolated in this study. Characteristic motifs (RRX8W, DDXXD, and NSE/DTE) are highlighted in red.

Figure B-ix Multiple sequence alignment of functionally characterised *VviTPS*s mapping closely to *VviPNTPS44* isolated in this study. Characteristic motifs (RRX8W, DDXXD, and NSE/DTE) are highlighted in red.

Appendix C   To Chapter 3

Table C-i Non-ambiguous probes for the putative *VviIDS* and *VviTPS* genes*. *CRIBI_V2.1 and **VCost_v3 accession as found on the https://urgi.versailles.inra.fr/Species/Vitis website. ***Unique NimbleGen probes as determined in this study.

Gene ID	V2 ID*	VCost_v3 ID**	Unique probes***	NimbleGen	Comment
VviGPS	VIT_215s0024g00850	Vitvi15g00079	VitusP00074268 VitusP00074267 VitusP00074261 VitusP00074263		No probe ambiguity per V1 annotated gene
VviFPS1	VIT_219s0015g01010	Vitvi19g00729	VitusP00136068 VitusP00136072 VitusP00136073 VitusP00136074		No probe ambiguity per V1 annotated gene
VviTPS27	VIT_219s0014g04900	Vitvi19g00388	VitusP00133021 VitusP00133022		
VviTPS39	VIT_213s0067g00370	Vitvi13g01307	VitusP00051229 VitusP00051231 VitusP00051238 VitusP00051235		
VviTPS41	VIT_213s0067g03700	Vitvi13g01439	VitusP00051425 VitusP00051421		
VviTPS44	VIT_213s0067g03790	Vitvi13g01877	VitusP00051468		Re-annotation show binding of probe to VviTPS112 (Vitvi13g01869) and VviTPS114 (Vitvi13g01448)
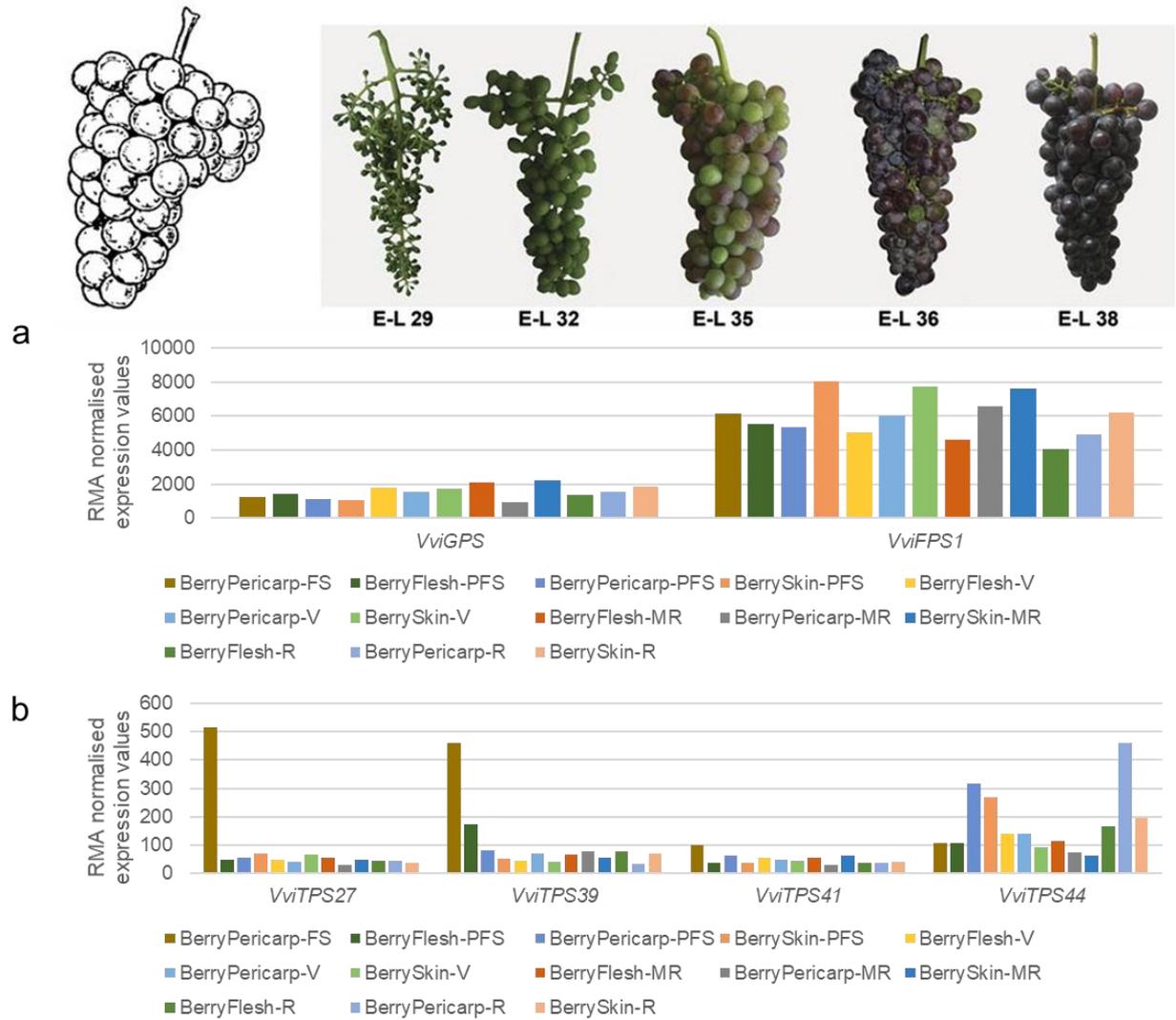
Figure C-i Average gene expression from selected probes in the berry tissues sampled during the various stages of berry development, these being: fruit set (FS, E-L 29), post-fruit set (PFS, E-L 32), véraison (V, E-L 35), mid-ripening (MR, E-L 36), and ripe stage (R, E-L 38).
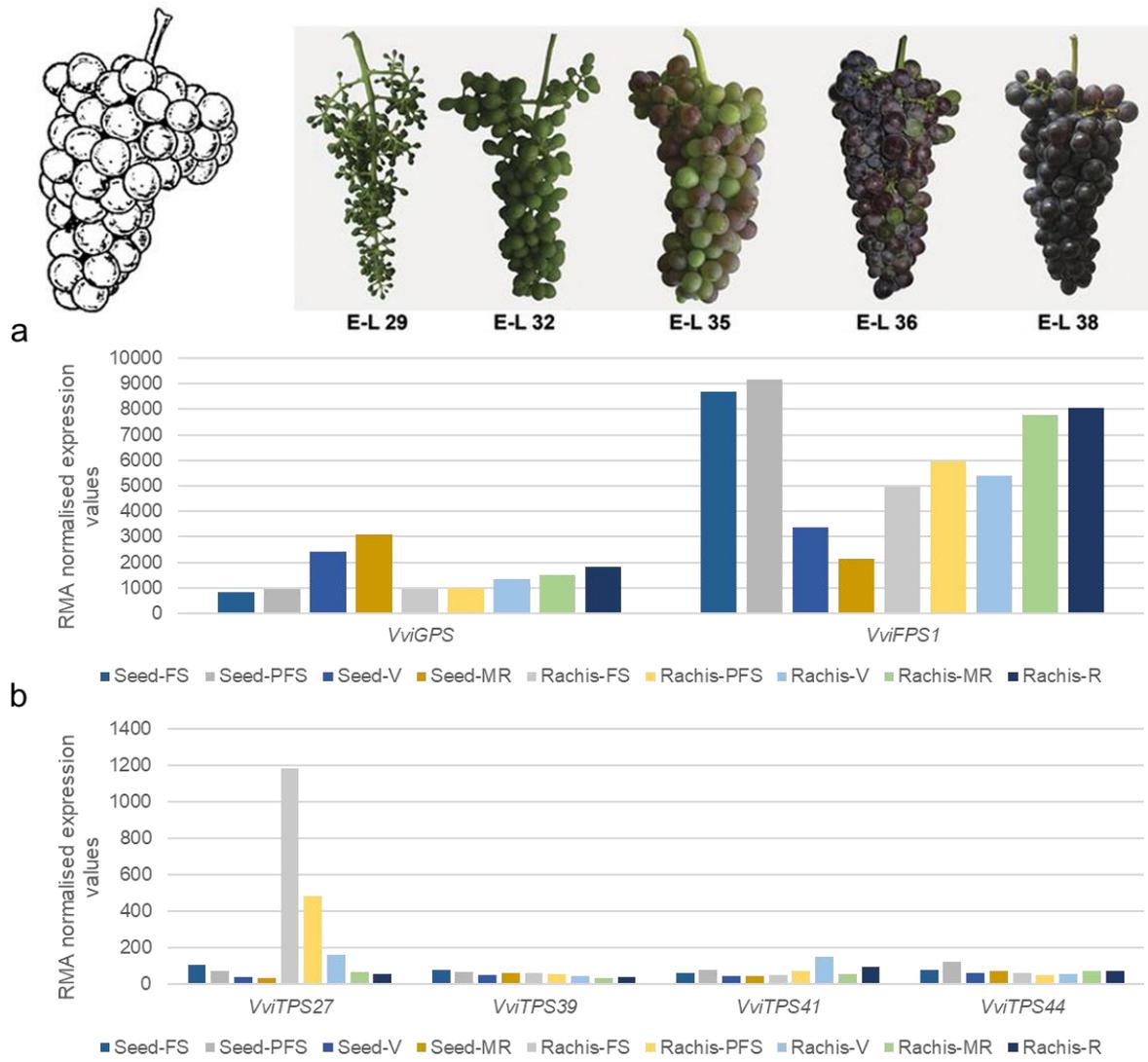
Figure C-ii Average gene expression from selected probes in the seeds and rachis sampled during the various stages of berry development, these being: fruit set (FS, E-L 29), post-fruit set (PFS, E-L 32), véraison (V, E-L 35), mid-ripening (MR, E-L 36), and ripe stage (R, E-L 38).

136

PHW

a

b

Figure C-iii Average gene expression from selected probes in berries sampled during the three post-harvest withering stages (1 to 3 months).

137
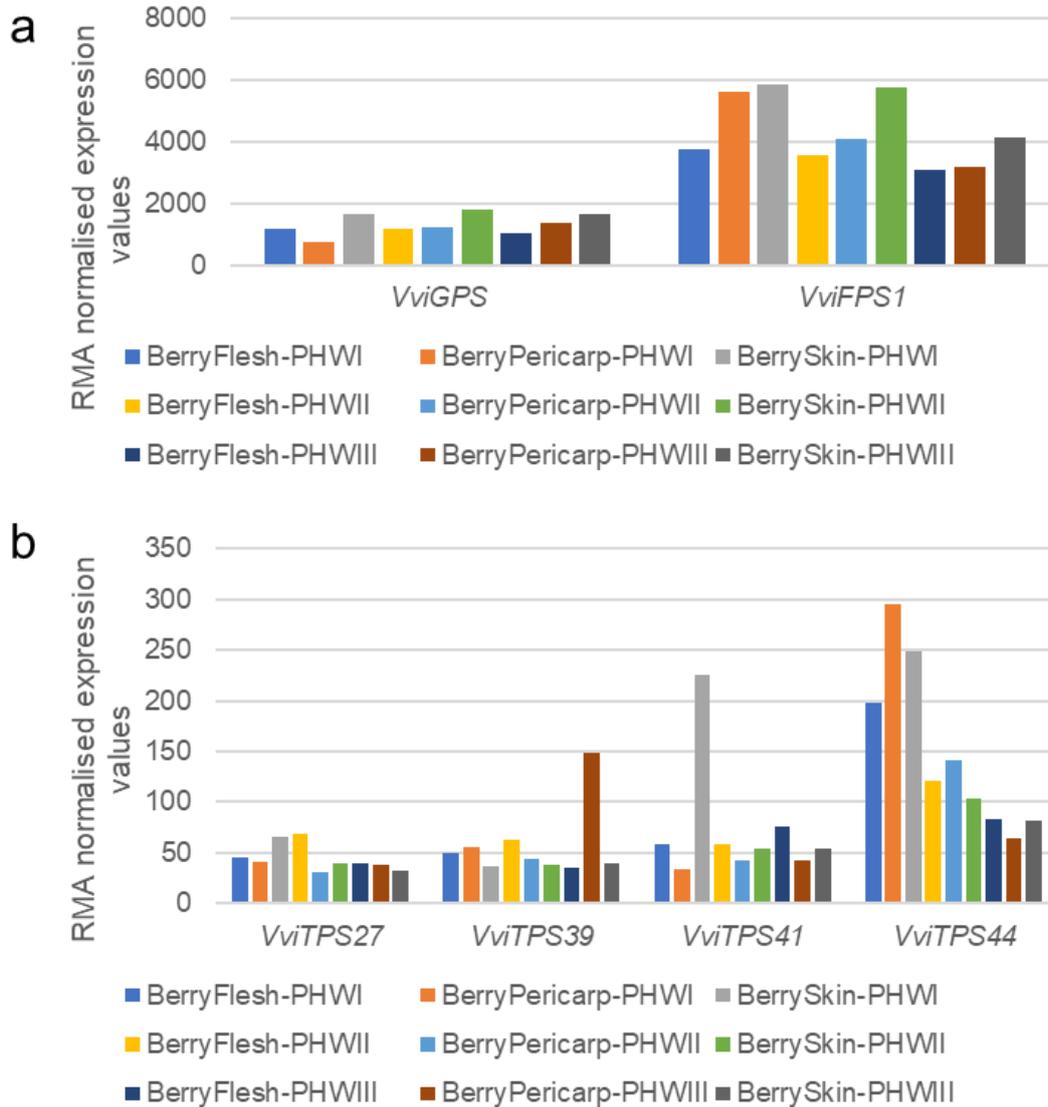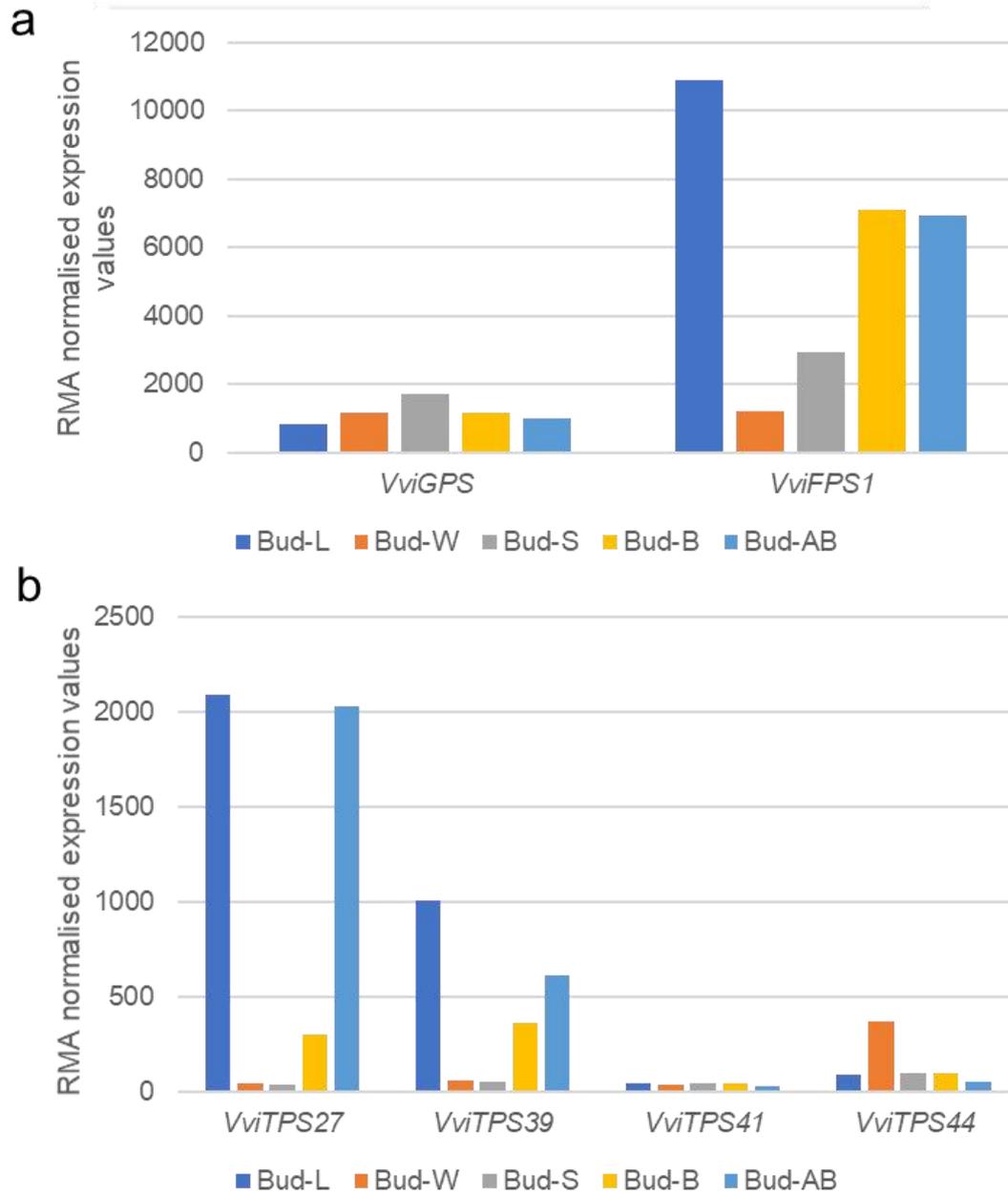
Figure C-iv Average gene expression from selected probes in bud tissue sampled in the latent bud (L, E-L 23), winter bud (W, E-L 1), during bud swell (S, E-L 2), bud burst (B, E-L 4), and after bud burst (AB, E-L 5).
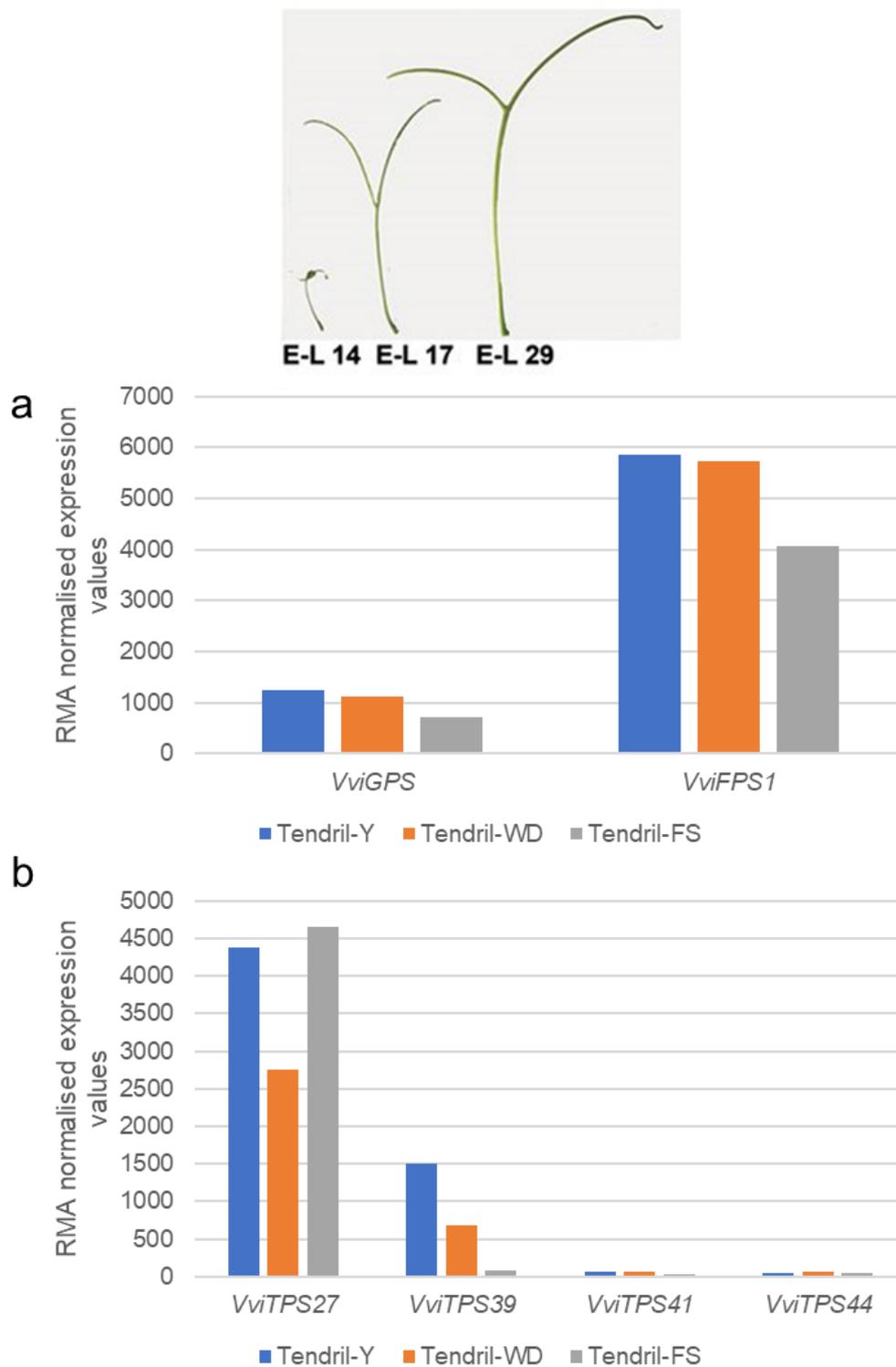
Figure C-v Average gene expression from selected probes in the young tendril (Y, E-L 14), well-developed tendril (WD, E-L 17), and mature tendril at fruit set (FS, E-L 29).
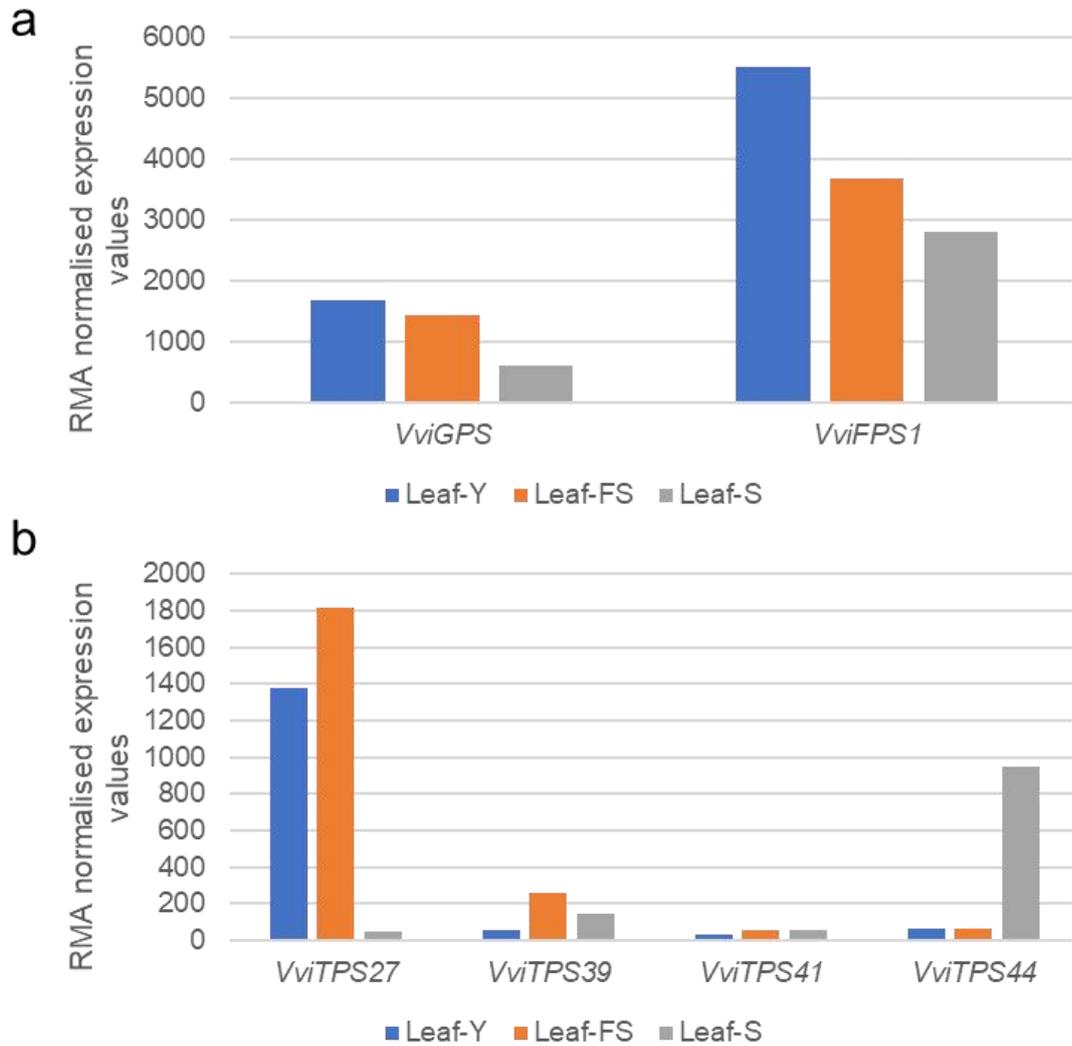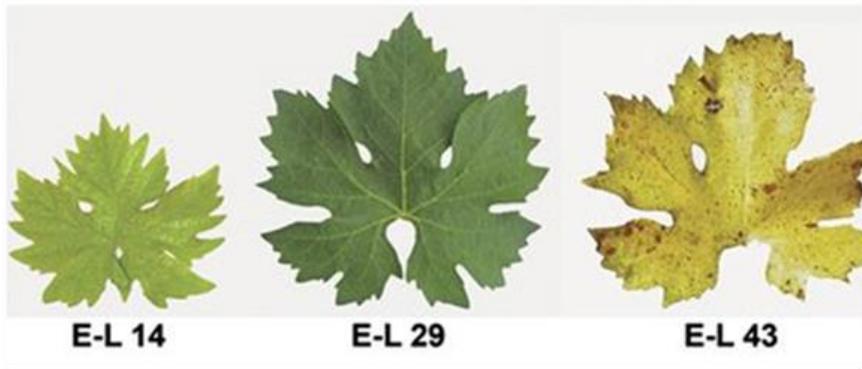
Figure C-vi Average gene expression from selected probes in the young leaf (Y, E-L 14), mature leaf at fruit set (FS, E-L 29), and the senescing leaf (S, E-L 43).
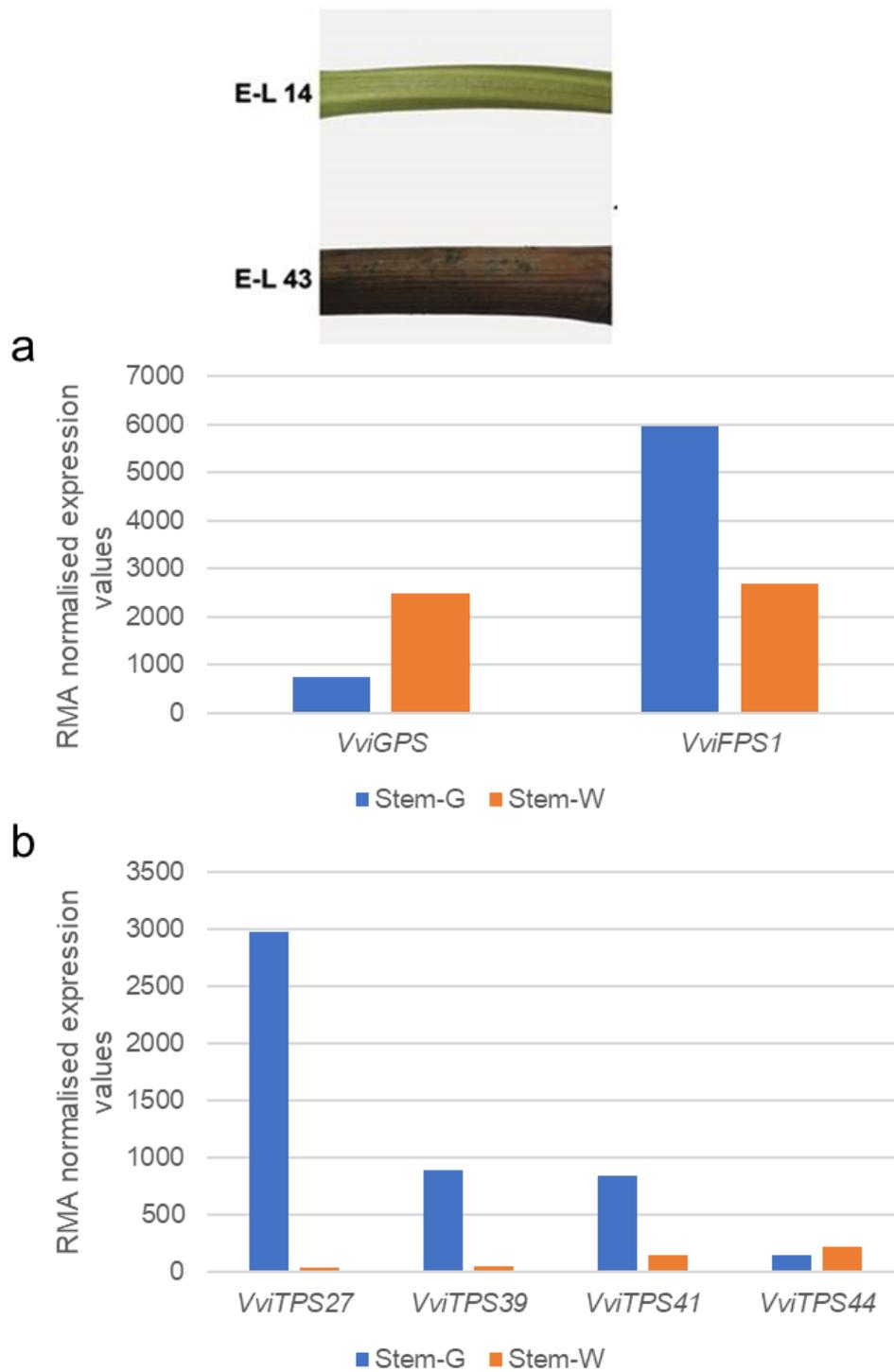
Figure C-vii Average gene expression from selected probes in the green stem (G, E-L 14) and the woody stem (W, E-L 43).

141
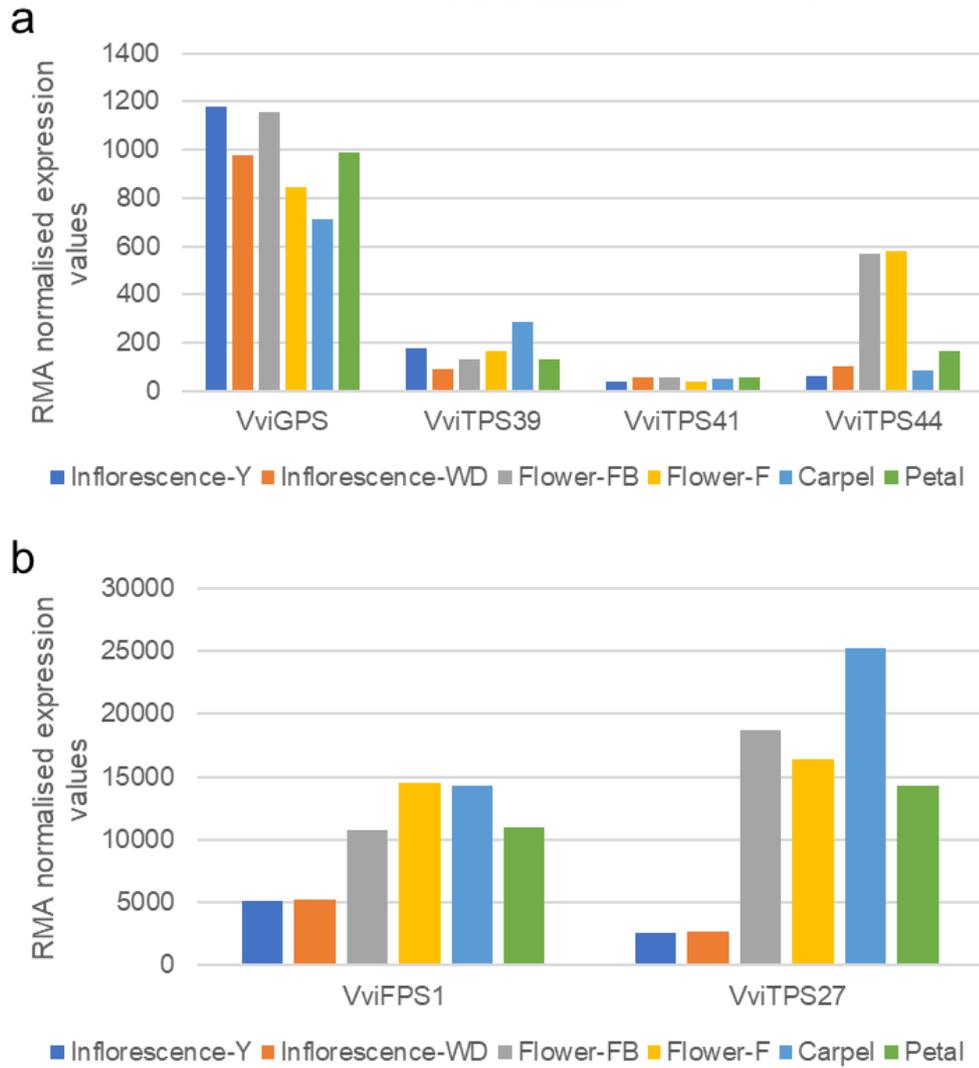
Figure C-viii Average gene expression from selected probes in young inflorescence (Y, E-L 14), well-developed inflorescence (WD, E-L 17), in flowers at the 10% caps off (FB, E-L 20) and 50% caps off (F, E-L 23), as well as the pooled carpel and petal tissue of flowers at the E-L 20 and E-L 23 stages of development.

142

E-L 20 / E-L 23 **E-L 25**

a

b
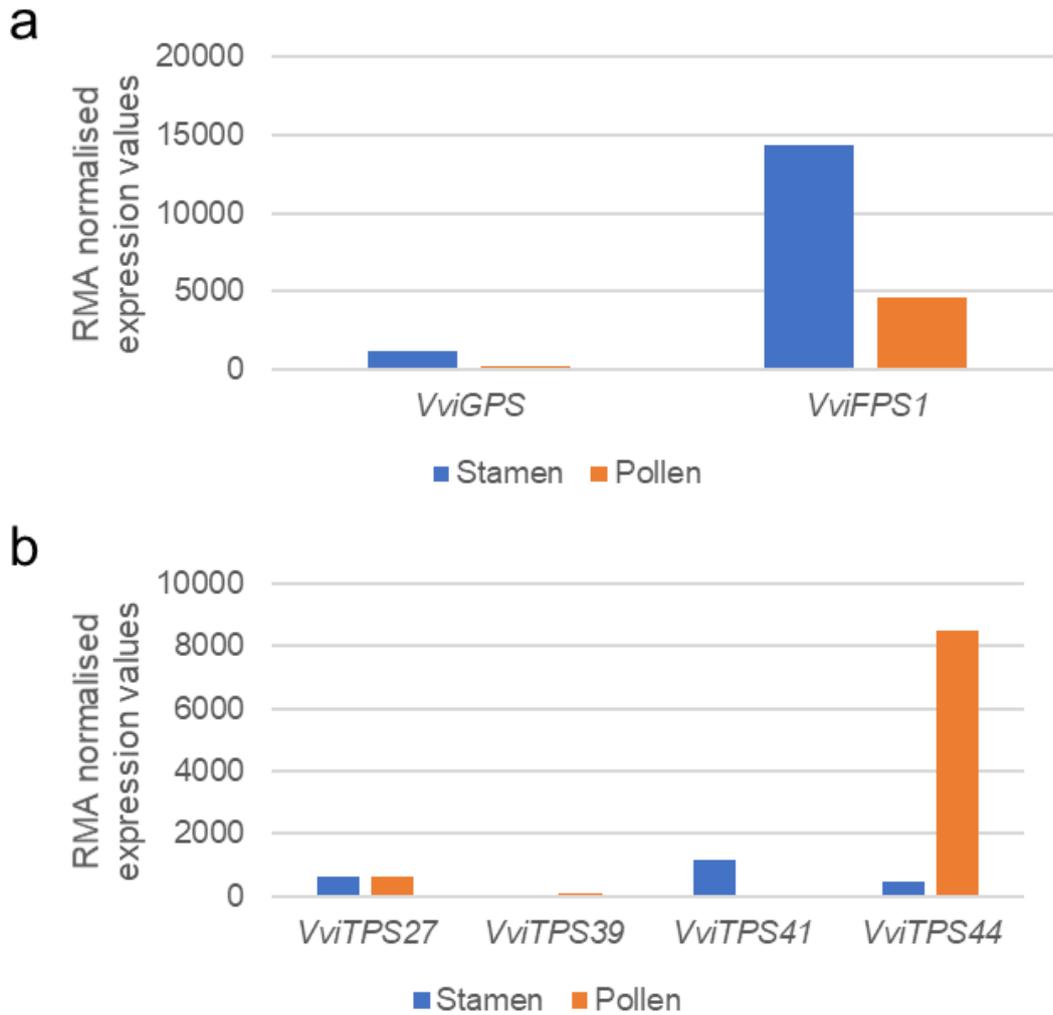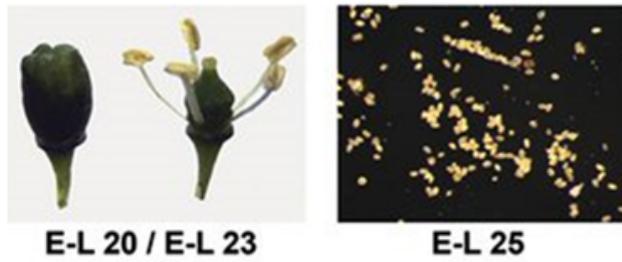
Figure C-ix Average gene expression from selected probes in the pooled stamen tissue of flowers at the E-L 20 and E-L 23 stages of development, as well as pollen from flowers with more 50% caps off (E-L 25).

143
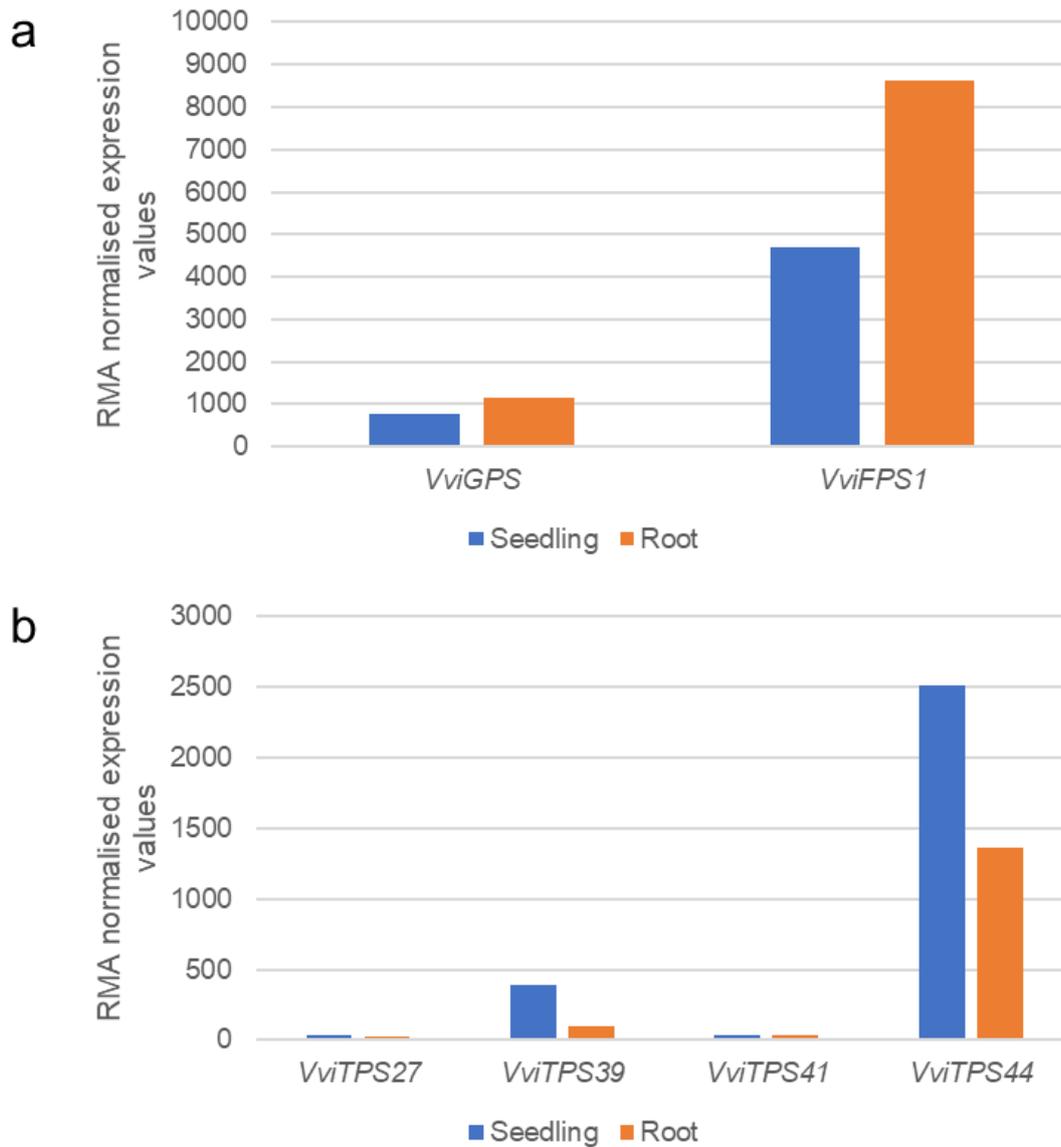
Figure C-x Average gene expression from selected probes in the pooled seedling tissue at three stages of development and root samples from *in vitro* cultured plantlets.

Appendix D   To Chapter 3

Table D-i Volatile analysis of yeast cultures expressing the four *VviTPSs.* Average of peak area normalised to IS (3-octanol) and cell count (OD_{600}) with ± standard deviation between four repeats. Values significantly different (student's *t*-test with $p < 0.05$) from the control yeast are indicated in red (higher) and blue (lower). #Peak ID confirmed with authentic standard are indicated with asterisks (*). ND = not detected.

Compounds#	Control	VviTPS27	VviPNTPS41	VviPNTPS44
β-myrcene*	0.002 ± 0.0001	0.001 ± 0.0001	0.0008 ± 0.0005	0.0013 ± 0.0009
Limonene*	0.0005 ± 0.0001	0.0003 ± 0.00003	0.0002 ± 0.0002	0.0004 ± 0.0002
Eucalyptol*	ND	ND	0.0004 ± 0.0003	ND
Linalool*	0.0038 ± 0.0002	0.0019 ± 0.0001	0.002 ± 0.0001	0.0033 ± 0.0001
trans-β-farnesene	0.0068 ± 0.0008	0.0038 ± 0.0005	0.0036 ± 0.0004	0.0069 ± 0.0009
α-terpineol*	0.0004 ± 0.00002	0.0002 ± 0.00002	0.0004 ± 0.00003	0.0004 ± 0
α-bergamotene	0.0009 ± 0.0001	0.0005 ± 0.0001	0.0005 ± 0.0001	0.0009 ± 0.0001
Methionol	0.0019 ± 0.0004	0.0019 ± 0.0001	0.0019 ± 0.0001	0.0027 ± 0.0005
β-bisabolene	0.0004 ± 0.0001	0.0002 ± 0.00003	0.0003 ± 0.00004	0.0005 ± 0.0001
Farnesene	0.0018 ± 0.0002	0.001 ± 0.0002	0.001 ± 0.0001	0.0019 ± 0.0002
β-citronellol*	0.0031 ± 0.0001	0.0016 ± 0.0001	0.0018 ± 0.0002	0.0029 ± 0.0003
Geraniol	0.0012 ± 0.0001	0.0006 ± 0.00004	0.0007 ± 0.0002	0.0012 ± 0.0004
Nerolidol	0.0059 ± 0.0006	0.0038 ± 0.0003	0.0039 ± 0.0008	0.0078 ± 0.0015

Appendix E   To Chapter 3

Table E-i Average peak area normalised to internal standard (3-octanol) and fresh weight of grapevine tissue with ± standard deviation. Asterisks (*) indicate compound identity confirmed with authentic standard. Peak areas of the transformed plants which were significantly different (student's *t*-test with p<0.05) from the control plants are indicated in blue (lower than control).

Compounds	Control	VviTPS27
β-myrcene	0.15 ± 0.03	0.16 ± 0.05
Limonene*	0.22 ± 0.03	0.17 ± 0.03
Eucalyptol*	0.02 ± 0.003	0.02 ± 0.008
δ-3-carene	0.15 ± 0.01	0.14 ± 0.03
ρ-cymene	0.05 ± 0.05	0.07 ± 0.07
α-terpinolene	0.12 ± 0.02	0.1 ± 0.02
Cis-linalool oxide*	0.2 ± 0.02	0.27 ± 0.11
Adamantane	0.08 ± 0.14	0.05 ± 0.12
trans-linalool oxide*	0.05 ± 0.04	0.06 ± 0.07
Menthone	0.32 ± 0.23	0.04 ± 0.13
Menthone_2	0.12 ± 0.09	0.01 ± 0.05
Linalool*	0.72 ± 0.08	0.77 ± 0.28
Bicyclo[4.1.0]heptane, 7-(methylethylidene)-	0.02 ± 0.01	0.04 ± 0.05
Vitispirane	0.26 ± 0.07	0.37 ± 0.16
α-terpineol-like	0.05 ± 0.02	0.05 ± 0.02
Hotrienol	0.14 ± 0.01	0.15 ± 0.09
B-fenchyl alcohol	0.05 ± 0.09	0.1 ± 0.06
Menthol	0.75 ± 0.53	0.11 ± 0.34
β-cyclocitral	0.1 ± 0.03	0.15 ± 0.06
Ocimenol	0.18 ± 0.06	0.17 ± 0.07
α-terpineol*	1.45 ± 0.05	1.35 ± 0.23
Citral	0.02 ± 0.003	0.05 ± 0.04
Geraniol*	0.08 ± 0.01	0.1 ± 0.05
β-damascenone*	0.5 ± 0.15	0.76 ± 0.37
Geranyl acetone*	0.18 ± 0.05	0.3 ± 0.16
α-ionone*	0.1 ± 0.05	0.12 ± 0.05

Appendix F   To Chapter 3

Table F-i Volatile terpene analysis of whole *Nicotiana benthamiana* leaves agroinfiltrated with the empty expression construct (Control_empty), or expression constructs containing *VviPTPS27*. Average of non-normalised peak areas from at least 11 biological repeats (with Leaf 1 & 2 sampled per plant) ± standard deviation. Compounds that are significantly different (student's *t*-test with $p < 0.05$) from the control are presented in red. ND = not detected.

Compounds	Control_empty	VviPTPS27
α-thujene	ND	ND
δ-3-carene	ND	ND
Sabinene	ND	ND
β-pinene	ND	ND
Myrcene	348.3 ± 1206.4	1461.4 ± 2825.9
α-phellandrene	ND	ND
α-terpinene	ND	ND
p-cymene	ND	ND
β-phellandrene	ND	ND
Eucalyptol	ND	ND
λ-terpinene	ND	ND
Terpinolene	ND	ND
Linalool	564.7 ± 1413.3	2189.9 ± 1703.4
(-)-terpinen-4-ol	ND	ND
β-cyclocitral	44.5 ± 154.2	273.8 ± 412
(E)-β-caryophyllene	348.3 ± 539.6	5233.3 ± 1723.9
Sesquiterpene_1	ND	104.9 ± 199.3
Sesquiterpene_2	ND	75 ± 259.8
α-muurolene	6265.7 ± 6722.2	6377.7 ± 3077.2
Sesquiterpene_3	47.8 ± 165.7	71.8 ± 168

Table F-ii Average peak area normalised to internal standard (Anisole-d$_8$) and fresh weight of *Nicotiana benthamiana* tissue with ± standard deviation. No significant difference (student's *t*-test with $p < 0.05$) in peak areas of the transformed plants in comparison to the respective control plants could be shown. ND = not detected.

Compounds	VviPTPS27-control	VviPTPS27-VviGPS	VviPTPS27-VviFPS
α-thujene	ND	ND	ND
Sabinene	ND	ND	ND
α-phellandrene	ND	ND	ND
α-terpinene	ND	ND	ND
p-cymene	ND	ND	ND
β-phellandrene	ND	ND	ND
λ-terpinene	ND	ND	ND
Terpinolene	ND	ND	ND
Linalool	0.06 ± 0.03	0.07 ± 0.05	0.06 ± 0.02
Menthol	0.004 ± 0.01	0.009 ± 0.01	0.01 ± 0.01
(-)-terpinen-4-ol	0.01 ± 0.01	0.02 ± 0.02	0.01 ± 0.02
α-terpineol	ND	ND	ND
βcyclocitral	0.05 ± 0.01	0.05 ± 0.03	0.04 ± 0.01
Total monoterpenes	0.12 ± 0.05	0.15 ± 0.09	0.13 ± 0.05
(E)-β-caryophyllene	0.02 ± 0.003	0.01 ± 0.008	0.01 ± 0.001
Sesquiterpene_1	ND	ND	0.003 ± 0.004
Sesquiterpene_2	0.001 ± 0.001	0.001 ± 0.002	ND
α-muurolene	0.02 ± 0.02	0.02 ± 0.005	0.02 ± 0.004
Sesquiterpene_3	0.002 ± 0.004	ND	ND
Total sesquiterpenes	0.04 ± 0.02	0.03 ± 0.01	0.03 ± 0.002

Appendix G   To Chapter 3

Table G-i Identified compounds information table. Compounds[a] listed in the order of elution on HP 5MS capillary column and named according to identification methods listed in ID column. [b]CAS number of compounds listed. [c]Retention time (in minutes) of the compounds detected. [d]Retention index (RI) calculated using the retention time of the compounds as well as the retention times of the saturated alkane mix (C7 – C40). RI Lit.– based on comparison of calculated RI with those reported by [e]Hazzit *et al.* (2006), [f] Venditti *et al.* (2016), [g]Khan *et al.* (2016), [h]Baranauskiene *et al.* (2003), [i]Salido *et al.* (2002), and [j]Demetzos *et al.* (2002). [k]Methods used to identify compounds listed, MS – comparison of mass spectra with MS libraries (Wiley and NIST), RI – comparison of calculated retention index with those reported in literature, Std – identification based on comparison with authentic standard. [L]Mass ion used to quantify identified peak, followed by qualifier ions used. [m]Odour characteristics of compounds as listed on www.pherobase.com.

Compounds[a]	CAS[b]	RT[c]	RI[d]	RI Lit.[e]	RI Lit.[f]	RI lit.[g]	RI lit.[h]	RI lit.[i]	RI lit.[j]	ID[k]	Quant. ion[L]	Qual. ion1	Qual. ion2	Qual. ion3	Qual. ion4	Odour characteristics[m]
Anisole-d$_8$	54887-54-6	6.98	913							Std	116	84	70	81	98	
α-thujene	2867-05-2	7.278	927	925	924	928	934	928		MS, RI	93	91	77	79	136	Woody, Herbal, Green
δ-3-carene	13466-78-9	7.407	933				1007	1010		MS, RI	93	91	77	136	121	Citrus fruit, Orange peel
α-pinene	80-56-8	7.402	933	939			942	936		MS, RI	93	77	121	136		Terpeny, Fruity, Sweet, Green, Woody, Pine, Citrus, Lime, Camphor
Camphene	79-92-5	7.722	948	951			949	951		MS, RI	93	121	79	107		Sweet, Fruity, Camphor, Pine, Oily, Herbal
Sabinene	3387-41-5	8.262	973	973	932	975	970	974		MS, RI	93	91	77	136	94	Fresh, Citrus, Spicy, Sweet, Woody
β-pinene	127-91-3	8.328	976	978	974	978	974	978		MS, RI	93	91	69	136	121	Musty, Green, Sweet, Pine, Resin, Turpentine, Woody
Myrcene	123-35-3	8.602	989	992	988		987	990		Std, MS, RI	93	69	79	53	136	Metallic, Musty, Geranium, Sweet, Fruity, Ethereal, Soapy, Lemon, Spicy, Woody
α-phellandrene	99-83-2	8.885	1002	1007	1002	1006	1000	1005		MS, RI	93	91	77	136	119	Fruity, Minty, Herbal, Citrus, Lime, Pepper, Juniper

Compounds[a]	CAS[b]	RT[c]	RI[d]	RI Lit.[e]	RI Lit.[f]	RI lit.[g]	RI lit.[h]	RI lit.[i]	RI lit.[j]	ID[k]	Quant. ion[L]	Qual. ion1	Qual. ion2	Qual. ion3	Qual. ion4	Odour characteristics[m]
α-terpinene	99-86-5	9.149	1015	1017		1018	1014	1016		Std, MS, RI	121	93	136	77	119	Gasoline-like, Ethereal, Fruity, Lemon
p-cymene	99-87-6	9.313	1024	1026		1027	1024	1025		MS, RI	119	134	91	117	77	Lemon, Fruity, Fuel-like, Sweet, Herbal, Spicy
β-phellandrene	555-10-2	9.389	1027	1045						MS, RI	93	91	136	68	121	Terpeny, Fruity, Minty, Herbal
Limonene	138-86-3	9.404	1028	1044	1024	1031		1030		Std, MS, RI	68	79	136	121		Licorice, Green, Citrus, Ethereal, Fruity
Eucalyptol	470-82-6	9.458	1031	1046		1036	1031			Std, MS, RI	81	108	111	154	139	Camphor, Minty, Sweet, Liquorices, Mentholic, Pine
γ-terpinene	99-85-4	10.025	1059	1060		1061	1061	1059		Std, MS, RI	93	91	136	121	77	Citrus, Terpeny, Herbal, Fruity, Sweet
Terpinolene	586-62-9	10.604	1087	1093		1090	1087			MS, RI	93	121	136	91	79	Woody, Fruity, Sweet, Piney, Anise
Linalool	78-70-6	10.79	1096	1104		1101	1097		1098	Std, MS, RI	71	93	55	136		Muscat, Sweet, Green, Floral, Lemon, Parsley, Lavender, Fruity
Menthol	89-78-1	12.224	1171						1173	MS, RI	71	81	95	123		Fresh, Green, Cool, Herbal
(-)-terpinen-4-ol	562-74-3	12.335	1177	1177	1174	1180	1174	1178	1177	Std, MS, RI	71	111	93	69	154	Terpeny, Woody, Sweet, Herbal, Pine, Musty, Fruity, Licorices, Moldy
α-terpineol	10482-56-1	12.57	1190	1190		1194	1190	1191	1183	Std, MS, RI	59	93	121	136	139	Peach, Anise, Oily, Fruity, Floral, Minty, Toothpaste
α-fenchene	471-84-1	12.808	1202				950			MS	93	121	81	67	136	Fruity, Fresh, Camphor
Fenchone	1195-79-5	12.873	1206							MS	81	69	53	91		
β-cyclocitral	432-25-7	13.122	1220							MS						Sweet, Mild, Green, Grassy, Floral, Hay

150

Compounds[a]	CAS[b]	RT[c]	RI[d]	RI Lit.[e]	RI Lit.[f]	RI lit.[g]	RI lit.[h]	RI lit.[i]	RI lit.[j]	ID[k]	Quant. ion[L]	Qual. ion1	Qual. ion2	Qual. ion3	Qual. ion4	Odour characteristics[m]
β-Citronellol	106-22-9	13.193	1224							Std, MS, RI	69	123	68	138		Rose, Sour, Green, Clove, Sweet, Citrus, Floral, Fresh
Nerol	106-25-2	13.197	1224			1229				MS, RI	69	93	121	79	136	Floral, Rose, Citrus, Marine
Isogeraniol	5944-20-7	13.308	1231							MS	109	81	154	139		Floral
Geraniol	106-24-1	13.668	1251			1256	1254			Std, MS, RI	69	93	123	84	111	Rose, Geranium, Floral, Sweet, Fruity, Citrus
α-citral	141-27-5	13.948	1267							MS	69	84	94	136	152	Citrus, Lemon, Peely, Green
Isoterpinolene	586-63-0	15.527	1360							MS	93	136	79	105		
4-Terpinenyl acetate	(4821-04-09)	15.527	1360							MS	121	93	136	105		
(E)-β-caryophyllene	87-44-5	16.623	1428	1417	1417	1428		1420	1418	MS, RI	93	133	69	161	204	Musty, Green, Spicy, Woody, Terpeny, Fruity, Sweet
Sesquiterpene_1	NA	17.056	1456							MS	79	105	161	204	91	
Sesquiterpene_2	NA	17.125	1460							MS	105	93	119	147	163	
α-muurolene	31983-22-9	17.599	1490	1497		1506		1499	1495	MS, RI	105	161	93	204	147	Woody
Sesquiterpene_3	NA	17.783	1502							MS	161	107	133	119	79	
Nerolidol	7212-44-4	18.715	1565	1551				1565		MS, RI	69	93	107	161		
cis-nerolidol	142-50-7					1542										Waxy, Rose, Apple, Green, Citrus
trans-nerolidol	40716-66-3															Waxy, Floral

151

Chapter 4 Annotation and evaluation of a tobacco population overexpressing the *VviGGPS1*

4.1 Introduction

Functional gene annotation not only requires the determination of the products synthesised by the enzyme encoded by the gene, but also an investigation into the possible role that the gene and the expression thereof may play within an organism. Studies of the geranylgeranyl diphosphate synthase (GGPS) gene family in *Arabidopsis thaliana* has shown that knowledge of the product (GGPP) formed does not equate to an understanding of the functional role within the plant (Beck *et al.*, 2013; Ruiz-Sola, Barja, *et al.*, 2016; Ruiz-Sola, Coman, *et al.*, 2016).

In plants, GGPS can catalyse the successive addition of isopentenyl diphosphate (IPP) to either dimethylallyl diphosphate (DMAPP), geranyl diphosphate (GPP) or farnesyl diphosphate (FPP) to produce the C20 prenyl diphosphate GGPP (Vandermoten *et al.*, 2009). Unlike the sublocalisation of geranyl diphosphate synthase (GPS) and farnesyl diphosphate synthase (FPS) to the plastid and cytosol, respectively, various isoforms of GGPS are targeted to the different subcellular organelles with GGPP biosynthesis occurring in the cytosol, mitochondria, and plastids of plants. Production of GGPP at the various sites within the cell allows for its utilisation in various reactions to synthesise primary and specialised (secondary) metabolites (Beck *et al.*, 2013; Vranová *et al.*, 2013).

In general, GGPSs function as homodimers, but studies have shown binding of GGPS to a small-subunit GGPS to form a heterodimer, altering the product length (Orlova *et al.*, 2009; Gutensohn *et al.*, 2013) or enzyme activity (Zhou *et al.*, 2017; Wang, Huang, *et al.*, 2018). The heterodimeric GPS found in *Humulus lupulus* consists of a large (LSU) and small subunit (SSU), with the SSU being inactive on its own. However, the LSU is capable of producing GPP, FPP and GGPP from IPP and DMAPP in an *in vitro* environment (Wang & Dixon, 2009). The GPS.LSU isolated from *Malus domestica* (apple) can also produce GGPP when not in a heterodimeric form (Tholl *et al.*, 2004). The majority of GGPSs are capable of only synthesising GGPP, but there are some short-chain isoprenyl diphosphate synthases (IDSs) with bifunctional capabilities. A study by Cervantes-Cervantes *et al.* (2006) showed an FPS isolated from maize capable of producing GGPP, depending on the length of the N-terminus. An IDS from *Picea abies* capable of producing substantial amounts of GPP and GGPP, but not FPP, *in vivo* has also been reported (Schmidt *et al.*, 2010).

Analysis of annotated plant genomes predict GGPS gene families ranging from one (in algae *Micromonas commoda* and *Chlamydomonas reinhardtii)* to 22 putative *GGPS* orthologs identified in *P. abies* (https://bioinformatics.psb.ugent.be/plaza/versions/plaza_v4_dicots/). The *GGPS* gene family in *Arabidopsis thaliana* is the most well-studied with 12 paralogs identified, 10 of which are functional (Zhu, Suzuki, Okada, Tanaka, Nakagawa, Kawamukai, Matsuda, *et al.*, 1997; Zhu, Suzuki,

Saito, *et al.*, 1997; Okada *et al.*, 2000; Wang & Dixon, 2009; Beck *et al.*, 2013). Analysis of the grapevine genome by Leng *et al.* (2017) identified four *VviGGPSs*. *VviGGPS1* and *VviGGPS2* most likely originated from a segregation duplication event, while the other two genes are predicted to encode for the LSU and SSU of a putative heterodimeric GGPS (Leng *et al.*, 2017). Coman *et al.*, (2014) identified an additional two grapevine proteins as putative homologs to the small subunit of the heterodimeric GPS (SSUII) and polyprenyl diphosphate synthase (PPPS).

Heterologous expression and determination of enzyme functionality either via functional complementation or *in vitro* methods are generally used for IDS functional characterisation (Oh *et al.*, 2000). However, assigning gene function(s) to specific GGPSs is hampered by the difficulty associated with studying paralogous gene families (Coman *et al.*, 2014). Additionally, determining gene functionality in an *in vivo* (microbial) or *in vitro* system does not provide extensive information on the endogenous role of an enzyme in a multicellular plant (Camagna *et al.*, 2019). The *in planta* environment can also not be easily imitated or understood in an *in vitro* assay because of various factors such as enzyme activity, assay conditions (pH, IPP/DMAPP ratio and buffer composition), enzyme truncation and interference of purification tags (van Schie *et al.*, 2012). Altering gene expression in either the native host or in another plant species enables a more comprehensive characterisation of the gene function, as the effect of the altered gene can be studied at various developmental stages as well as under different environmental conditions.

Tobacco has been used as a model plant for the study of plant somatic cell genetics including transformation technology and genetic engineering since the twentieth century (Gebhardt, 2016) and more recently, *Nicotiana attenuata* has become a useful model for studying insect herbivore – plant interactions (Schuman & Baldwin, 2016). The ease with which *Nicotiana benthamiana* can be infiltrated with *Agrobacterium tumefaciens* (agroinfiltration) has made this species an attractive option for functional screening (Gebhardt, 2016). Draft genome sequences are available for three *Nicotiana tabacum* varieties (Sierro *et al.*, 2014) as well as for *N. benthamiana* (Bombarely *et al.*, 2012)*,* which further supports the use of tobacco as model organism for various genetic applications.

In this study, the annotation of the *VviGGPS* gene family was updated with the putative expression profile of these genes determined based on available expression data. Furthermore, an existing transgenic *N. tabacum* L. Havana Petit SR1 population expressing the *VviGGPS1* gene under the control of a constitutive promoter was targeted for further evaluation. The *VviGGPS1* gene was previously shown to be functional via complementation in *Escherichia coli* (Young, 2004). The available transgenic tobacco population was already genetically characterised to confirm transgene presence and expression in the T1 population (unpublished data), but no phenotyping or chemotyping of the population was available. Here the re-establishment of the transgenic population from seed-stocks is described, as well as the first description of the unique morphological features of the lines, carotenoid, and chlorophyll pigment analysis from leaves, as well as basic physiological

153

analysis under different growth conditions to confirm stable and unique *VviGGPS1* related phenotypes.

4.2 Material and methods

4.2.1 Updating the *VviGGPS* gene family annotation, determining the expression profiles, multiple sequence alignment and phylogenetic tree construction

The predicted *VviGGPS* sequences described by Coman *et al.* (2014) were downloaded from Uniprot (https://www.uniprot.org/) with the protein sequences mapped to the VCost.v3 gene annotations using the tBLASTn function (https://urgi.versailles.inra.fr/blast/). The predicted *VviGGPS* sequences (V1 accessions) from the Leng *et al.*, (2017) study were downloaded from (https://plants.ensembl.org/index.html) and the corresponding VCost.v3 annotations determined and predicted coding sequence downloaded (https://urgi.versailles.inra.fr/Species/Vitis/Annotations).

The subcellular localisations of the deduced protein sequences were predicted using ProtComp Version 9.0 (http://www.softberry.com/berry.phtml) and TargetP 1.1 (http://www.cbs.dtu.dk/services/TargetP-1.1/index.php) algorithms (Nielsen *et al.*, 1997; Emanuelsson *et al.*, 2000).

Characterised GGPS sequences from *A. thaliana* were downloaded from UniProt (https://www.uniprot.org/) and named according to the nomenclature laid out in Beck *et al.* (2013). The characteristic motifs were identified and highlighted (Wang & Ohnuma, 1999; Vandermoten *et al.*, 2009; Coman *et al.*, 2014). Multiple sequence alignments (MSA) and generation of phylogenetic trees of the GGPS sequences, including the predicted GGPS sequence from grapevine was done using CLC Main Workbench (Version 7, CLC Bio-Qiagen, Denmark). MSA with deduced protein sequences were done using default settings with the characteristic motifs used as fixed alignment points and the gap cost set at cheap. The phylogenetic trees were generated using maximum-likelihood phylogeny with the neighbour-joining construction method, with the Dayhoff (PAM) substitution model set at four substitution-rate categories. The gamma distribution parameter was estimated when performing 1000 bootstrap replicas. Using a keyword search of "geranylgeranyl diphosphate synthase" and "geranylgeranyl pyrophosphate synthase" on the https://www.ncbi.nlm.nih.gov/nucleotide/ website, 167 complete coding sequences predicted or shown to encode for GGPS in plants were downloaded from Genbank (https://www.ncbi.nlm.nih.gov/genbank/). Translation into protein sequences was performed using CLC Main Workbench with MSA with the predicted grapevine sequences and phylogenetic tree construction done as described above.

The *in silico* expression profile based on the data generated by Fasoli *et al.* (2012) for the putative grapevine *GGPS* gene family identified by Leng *et al.* (2017), as well the additional genes annotated by Coman *et al.* (2014), was determined using the method described in Chapter 3 of this thesis.

4.2.2   Plant growth conditions

The seed stocks of a previously established transgene tobacco population overexpressing *VviGGPS1* was obtained from the seed bank of the South African Grape and Wine Research Institute (SAGWRI), Stellenbosch University. Since the population was already genetically characterised, this data is provided in Appendix A to Chapter 4, alongside the relevant information of the transformation itself.

The genetically characterised transgenic as well as the control (untransformed) *N. tabacum* L. Havana Petit SR1 seeds were surface sterilised for 30 min using a chlorine vapour-phase method (Clough & Bent, 1998) and germinated on half-strength Murashige and Skoog (MS) media (Murashige & Skoog, 1962) supplemented with 0.75% (w/v) sucrose and adjusted with KOH to pH 5.7 prior to autoclaving. Selection of transformants was achieved with the addition of kanamycin (100 µg/mL) to media after autoclaving. The germinating seeds were maintained in a climaroom under irradiance from F36W/GRO fluorescent tubes (Feilo Sylvania Europe Ltd., Newhaven, UK) on a long day (LD) cycle (16 h light, 8 h dark) with temperature maintained at 25°C and relative humidity kept ≥ 50% with a humidifier. Kanamycin-resistant seedlings of a similar size were transferred to coco-peat plugs (Jiffy International AS, Kristiansand, Norway) hydrated with 0.1% (v/v) Sporekill® (Hygrotech, Stellenbosch, South Africa) and allowed to acclimatise to lower humidity conditions over a one-week period. The coco-peat plugs containing the hardened-off plantlets were transferred to 0.5 L pots with a Hygromix (Hygrotech) and vermiculite mixture (1:1) which had been hydrated overnight with 0.1% (v/v) Sporekill® (Hygrotech) solution). Plants were watered as needed with equal measurements of water given to all plants. Nutrients were given weekly with the addition of 0.5 g/L Hygrofert (Hygrotech) to the water. The plants were placed in a randomised manner and routinely moved around across the growth areas used for tobacco to ensure that individual plants within a line did not group together. Seedlings were moved to the greenhouse during the hardening-off period unless stated otherwise. Irradiance in the greenhouse was natural light with the temperature maintained below 26°C and relative humidity maintained ≥ 50% during the day.

Climatic conditions were monitored with dual channel internal temperature and relative humidity loggers (TinyTag® TGP-4500, Gemini dataloggers, UK) in both the climaroom as well as the greenhouse. Photosynthetically active radiation (PAR) in µmol photons m^{-2} s^{-1} within the 400 to 700 nm range was also monitored at 5 min intervals in the greenhouse with the use of Millivolt input data logger (TinyTag® TGPR-1001, Gemini dataloggers, UK) attached to a quantum sensor (LI-COR Environmental, model LI190, Lincoln, NE, USA). A sensor was placed at each of the growth areas

to measure PAR at the region of plant growth. PAR measurements were used in the following equation to obtain the daily light integral (DLI) in mol photons m^{-2} d^{-1} where x is the hours of light (Runkle, 2006a).

$$PAR\ (\mu mol\ m^{-2}\ s^{-1}) \times (3600\ \times x\ hrs\ of\ light\ per\ day)\ \times\ 10^{-6}$$

The value is used to define the amount of PAR that is supplied to the plants per day and has been shown to influence various aspects of plant growth and is often utilised to describe greenhouse lighting conditions (Kaczperski *et al.*, 1991; Catley & Brooking, 1996; Oh *et al.*, 2009).

When seeds were required, the flowering heads were isolated with plastic bags containing small aeration holes to prevent cross-pollination but still allow gas exchange. Some of the lines displayed an extreme flower phenotype and natural self-pollination was not possible, in these cases artificial self-pollination was performed by removing the stamen and dusting the anther onto the stigma. Seed pods were harvested when browning was seen on the pedicel with seeds stored at room temperature in cryotubes.

4.2.2.1 Environmental conditions used for the phenotypic characterisations

The location and measured environmental parameters were used to divide the growth conditions into three categories, with the PAR measurements taken over the growth period converted to DLI values and described in **Table 4.1**.

Table 4.1 Summary of the environmental conditions under which plants were kept for phenotypic characterisations.

Facility	Season	Abbreviation	DLI (mol m^{-2} d^{-1})	Temperature (°C)	Relative humidity (%)
Climaroom (CR)	NA	CR_LL	Set at: 3.5 Measured: 4.4	Set at: 25 Measured: 23.7 ± 1.7	Set at: > 50 Measured: 54.8 ± 12.1
Greenhouse (GH)	Autumn	GH_HL	Set at: Natural light Measured at position 1: 8.69 Measured at position 2: 10.18	Set at: < 25 Measured: 21.9 ± 5.1	Set at: > 50 Measured: 66.2 ± 17.4
Greenhouse (GH)	Winter	GH_LL	Set at: Natural light Measured at position 1: 3.01 Measured at position 2: 4.3	Set at: < 25 Measured: 21.9 ± 5.1	Set at: > 50 Measured: 66.2 ± 17.4

As can be expected, higher fluctuations in the temperature and relative humidity were observed in the greenhouse compared to the climaroom. The DLI values in the greenhouse fluctuated across

the various days but the average during the Autumn season was much higher than what was seen during the winter growth period. The DLI in the climaroom under artificial light was comparable to the greenhouse DLI in the winter season while the increased day length during the autumn season resulted in a higher calculated DLI. These values are expected since the DLI values are affected by the season, cloud cover and day length with the DLI values found inside greenhouses compared to values measured outside often reduced by 35-50 % due to glazing materials and structure of the greenhouse with seasonal variation of DLI observed when no additional light is supplied in the greenhouse (Korczynski *et al.*, 2002). DLI values generally vary between 1 to 25 mol m^{-2} d^{-1} within the greenhouse (Faust *et al.*, 2005) which corresponds to the calculated values in this study.

Plants moved to the greenhouse (GH) were subdivided into three groups based on the stage at which the plants were moved to the greenhouse: Late – Plants maintained in the climaroom under low light (CR_LL) for most of the development and moved to GH at late stage (1 week before analysis); Mid – Plants maintained at CR_LL and moved to GH at the three- to four-leaf stage; Early – Plants moved to GH during the hardening-off stage.

4.2.3 PCR screening of transgenic plant population

The T1 generation had been previously genetically characterised by Dr PR Young with the methods and results summarised in Appendix A, whereas a T2 generation was generated from the T1 plants in this study. The gDNA was extracted from ground leaf tissue obtained from the T1 generation plants based on the method described by (Reid *et al.*, (2006). PCR screening using GoTaq® DNA polymerase (Promega, Madison, Wisconsin, USA) with primers (**Table 4.2**) specific to the kanamycin-resistant (*nptII*) gene and *VviGGPS1* were done to ensure the presence of the transgene before allowing subsequent self-pollination and seed formation from the T1 generation to produce the T2 generation.

Table 4.2 Primers used in study. Underlined sequences indicate restriction endonuclease recognition site addition.

| Name	Sequence (5' to 3')	Amplicon size (bp)	Description
nptII-5' nptII-3'	TCTGATGCCGCCGTGTTC GAGCCCCTGATGCTCTTCGT	402	Screening for gene integration. Amplifies kanamycin resistant gene on pART27 construct
VviGGPS-5' VviGGPS-3'	<u>CTCGAG</u>ATGAATACTGTGAATCTGGGC <u>CAACTGG</u>TCAGACCATTGAGACAAC	1128	Primers initially used to isolate the *VviGGPS1* gene and later used to screen for the transgene in tobacco
PlScreen-5' PlScreen-3'	GATACTAGCCCCTGGGGCAC CCTTCGCAAGACCCTTCCTC	1749	Flanking primers to screen for gene integration and for PCR-labelling with DIG

4.2.4   Phenotyping

Various approaches, summarised in **Table 4.3**, were used to do initial characterisation of the plant population.

Table 4.3 Summary of analysis done on vegetative and reproductive organs. LMA – leaf mass (fresh weight) per area.

Transgenic lines	Seed germination	Morphology		Physiological measurements	Metabolite analysis	
		Initial	Growth conditions		Photosynthetic & LMA	Leaf surface
Control_SR1	Yes	Yes	Yes	Yes	Yes	Yes
VviGGPS_1.3	Yes	Yes	Yes	Yes	Yes	Yes
VviGGPS_2.4	Yes	Yes	No	No	Yes	No
VviGGPS_3.4	Yes	Yes	Yes	No	Yes	No
VviGGPS_4.1	Yes	Yes	No	No	Yes	No
VviGGPS_6.4	Yes	Yes	Yes	No	Yes	Yes
VviGGPS_9.1	Yes	Yes	Yes	No	Yes	Yes
VviGGPS_10.4	Yes	Yes	Yes	Yes	Yes	Yes
VviGGPS_12.3	Yes	Yes	No	No	Yes	No

A simplified workflow of the analysis is shown in **Figure 4.1** to outline the experimental design. The available *VviGGPS1* transgenic population consisted of eight lines with seed germination assays done for all the lines available. The initial phenotyping, performed for all the lines, evaluated the similarity or dissimilarity with the untransformed control plants. The various transgenic phenotypes were categorised based on organ affected and the trait which was presented. The preliminary screening indicated that the transgenic phenotype differed between lines and was affected by the growth conditions. This initiated the selection of six lines along with the untransformed control plants, for further morphological phenotyping under the different conditions described in the previous Section (4.2.2). Four of these five selected lines were also included in the analysis of the leaf surface metabolites. Analysis of the photosynthetic compounds in conjunction with leaf mass (fresh weight) per area (LMA) determination was performed for all the available lines and the untransformed control plants at one growth condition. Based on the results from phenotyping at different growth conditions and the photosynthetic metabolite analysis, two lines were selected for physiological measurements which consisted of photosynthetic measurement using the infrared gas analyser (IRGA) system and thermal imaging of leaves.
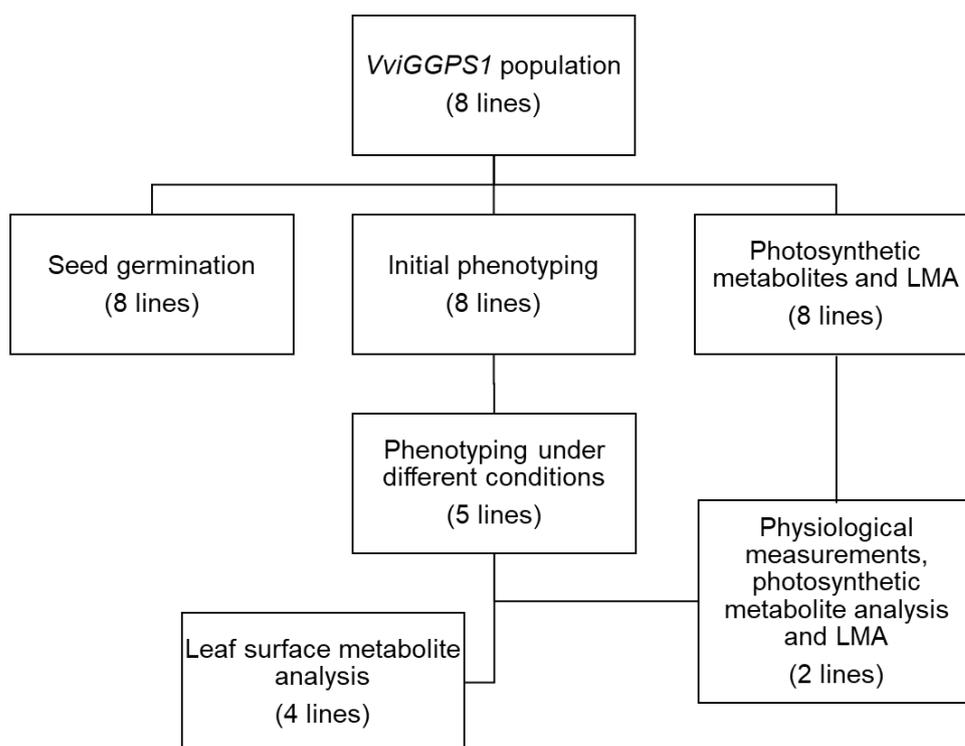
Figure 4.1 Simplified diagram outlining the workflow for the characterisation of the *VviGGPS1* tobacco population. All lines were included in seed germination, initial phenotyping, and photosynthetic metabolite with leaf mass per area (LMA) analysis. Based on the results from the analysis of all the lines, five lines were selected for phenotyping of plants grown under different conditions. The results from phenotyping under different growth conditions as well as the photosynthetic metabolite with LMA analysis led to the selection of two lines for physiological measurement in combination with photosynthetic metabolite and LMA analysis. In addition, four lines were selected based on the phenotyping results for leaf surface metabolite analysis.

4.2.4.1   Seed germination assay

The seed germination assay used was based on the method described by Lee *et al.* (2010). The T2 transgenic tobacco (*N. tabacum*) seeds were germinated on half-strength MS medium (Murashige & Skoog, 1962) with 0.75 % (w/v) sucrose and 0.6% (w/v) phytagel to solidify the medium. Seeds were spaced 1 cm apart on the plate. Micropore™ tape (3M South Africa) was used to seal the plates which were kept at 25°C under lights at a short-day (SD) cycle (8 h light, 16 h dark). Each assay consisted of one plate for every transformed plant line, with a total of eight transgenic lines available, as well as the control (wild type) line. At least 50 seeds per plate were analysed, with the assay repeated six times.

Germination rate was determined by counting seeds at 24-hour intervals for duration of 14 days. Seeds were scored as germinated when the radicle/primary root had clearly protruded through the seed coat (Avery, 1933), with the germination percentage plotted on a line graph. The germination rate was further investigated with the coefficient of velocity of germination calculated according to the method described by Kotowski (1962) and discussed by Ranal and Santana (2006).

4.2.4.2 Vegetative and reproductive morphology

When referring to leaf number, the leaves were counted from the youngest mature leaf (≥ 10 cm) down to the oldest leaf as shown in Figure 4.2 (Basson, 2017). Some of the transgenic plants displayed a phenotype where the apical dominance was reduced with internodes between leaves shortened or not discernible, in these instances where the leaf number could not be easily determined the leaves were numbered according to leaf size.
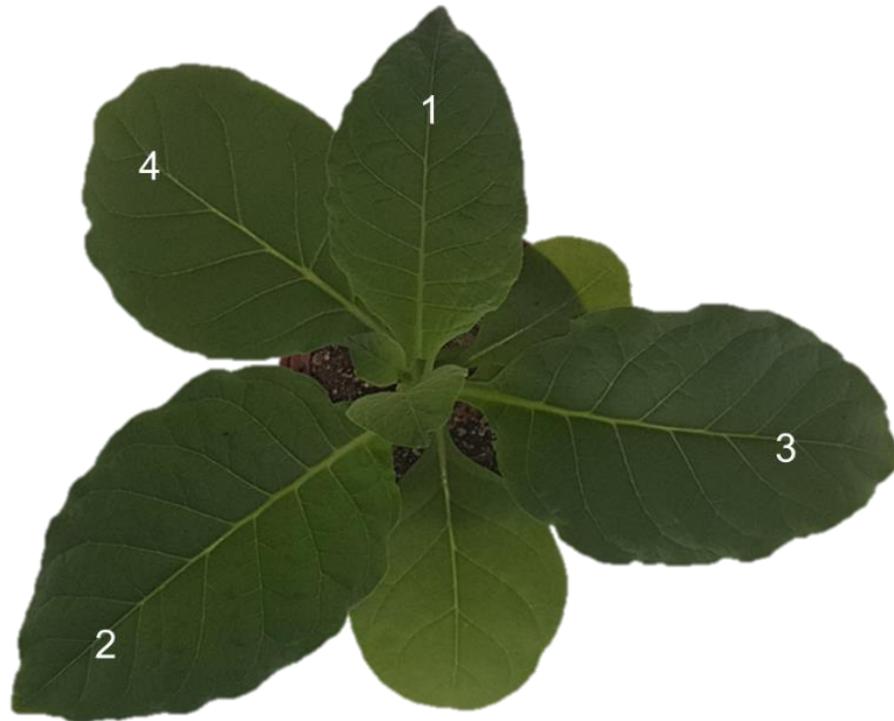
Figure 4.2 Leaf numbering of the tobacco plants. Leaves were numbered from youngest, fully expanded leaf (Leaf 1) to oldest leaf (Leaf 4).

During the initial phenotypic observations, all the available transgenic lines were screened. Distinct phenotypes in the transgenic population were recorded and the nomenclature of the visual observations of the vegetative and reproductive phenotypes were based on a study done by Wang *et al.* (2017) wherein the various phenotypes were divided into categories and subcategories. Within a category, the plant was scored based on the number of subcategories that displayed an abnormal phenotype, i.e., if there are three subcategories and two of these were abnormal in the plant then a score of two was given. Flowers were photographed on graph paper [A4 with 2/10/20 mm ruling

160

(RBE Stationery Manufacturers (Pty) Ltd, Milnerton, South Africa)] to determine the length of corolla and style.

Following the initial screening and annotation of transgenic phenotypes observed, five lines were selected for further study. These transgenic lines, in combination with the control plants were grown under the various conditions as outlined in the previous section (4.2.2). At least 12 individual plants per line were studied under each growth condition except during the GH_HL_Late growth condition when only 5 plants per line were used.

4.2.4.2.1 Computed tomography scanning of leaf surfaces

A transgenic leaf with a visible leaf surface phenotype and a control leaf of the same age were analysed using the micro-computed tomography (CT) scanner system (General Electric Sensing and Inspection Technologies/Phoenix X-ray, Wunstorff, Germany) at the CT Scanning unit of the Central Analytical Facility (CAF) at Stellenbosch University (du Plessis *et al.*, 2016). Generated data were viewed, and images generated with the myVGL 3.1 software (Volume Graphics, Heidelberg, Germany).

4.2.4.3 Measurement of physiological parameters

4.2.4.3.1 Photosynthesis

The control plants as well as two transgenic lines were selected for measurements of photosynthetic parameters using the IRGA method. Two plant populations, with at least eight individual plants per line, were used for the measurements. The plants were grown in the greenhouse from an early stage of development (moved to GH during hardening-off stage) during the autumn and winter season. Photosynthetic measurements were done at the four- to five-leaf stage of plant growth with leaf 1 and 2 used for photosynthetic measurements.

A LI-6400XT portable photosynthesis system (LI-COR Biosciences, Lincoln, NE, USA) was used to measure the rate of CO_2 uptake in single leaves. Conditions in the leaf chamber were set at a saturating irradiance (PPFD) of 1000 µmol photons $m^{-2}s^{-1}$, CO_2 concentration of 400 µmol mol^{-1} and a flow rate of 300 µmol min^{-1} with relative humidity kept above 45% and the block temperature maintained at 23°C with the stomatal ratio set at 0.5. Measurements were conducted between 10 am and 2 pm, individual plants were moved to a room without natural light for measurements and thermal imaging with the maximum time out of the GH kept below 10 min. Readings were logged after photosynthesis readings had stabilised, at least 2 min after clamping the chamber onto the leaf. Matching of IRGAs was done after every four readings, or more often if deemed necessary.

4.2.4.3.2 Thermal imaging

In addition to the photosynthesis measurements, infrared thermal imaging was done to determine to Crop Water Stress Index (CWSI). The FLIR A-series (Model A615) (FLIR Systems, Portland USA)

161

camera was used with a resolution of 640 x 480 pixels. The camera measures temperature in the range of -20 °C to +2000 °C. The thermal sensitivity of the camera is <0.05 °C @ +30 °C /50 mK with a spatial resolution of 0.68 milliradians at 25°C. Each pixel was considered as an effective temperature reading in degree Celsius (°C). Thermal images were taken of each individual plant before photosynthesis measurements. The thermal imager was mounted on a tripod with plants placed directly underneath at approximately 30 cm distance from the lens. Temperature and relative humidity readings were taken every minute with a dual-channel internal temperature and relative humidity logger (TinyTag® TGP-4500, Gemini dataloggers, UK) in the room used for thermal imaging. Temperature at time of imaging was used during processing of images using a customized code written in MATLAB® (MathWorks Inc., Natick, MA, USA) by Dr Carlos Poblete-Echeverría (Department of Viticulture and Oenology, Stellenbosch University) to extract the relevant data (Sepúlveda-Reyes *et al.*, 2016). Emissivity was set at 0.95 with reflection temperature determined using an aluminium foil set at the position the plants was placed. Extracted data were used to the CWSI according to the method developed by (Idso *et al.*, 1981) and adapted by Jones, (1999) with the following equation:

$$CWSI = \frac{Tc - Twet}{Tdry - Twet}$$

Wherein T_c is the temperature (°C) measured with logger at the time of image taken. T_{wet} is the temperature (°C) of the leaf at the coolest end of the leaf temperature spectrum with T_{dry} the temperature (°C) at warmest end leaf temperature spectrum. The CWSI value ranges from 0 to 1, with lower values indicating increased transpiration (i.e., the higher transpiration results in a cooler leaf temperature).

4.2.5   Analysis of photosynthetic and leaf surface metabolites.

4.2.5.1   Carotenoid and chlorophyll profiling in leaves with reverse-phase ultra-performance liquid chromatography

Extraction of carotenoids and chlorophylls from 25 mg of frozen, ground leaf tissue was done according to the method described by Lashbrooke *et al.* (2010) for grape berry tissue with the method only altered by decreasing the extraction buffer volume to 1.6 mL. Three extraction repeats per biological repeat were done. The analysis method of extracted compounds utilising reverse-phase ultra-performance liquid chromatography (RP-UPLC) and quantification of pigments as described by Young *et al.*, (2016). The de-epoxidation ratio was determined as described by Thayer and Björkman (1990).

Initial carotenoid and chlorophyll analysis was done on leaf three of all eight available transgenic lines as well as the control plants, with six biological repeats per line. These plants were grown under low-light conditions in the climaroom and leaves were harvested at the four- to five-leaf stage of plant growth. Additionally, leaf mass (fresh weight) per area (LMA) was determined for each leaf before carotenoid and pigment analysis according to the method described by Cornelissen *et al.* (2003) and shown in the formula below.

$$\frac{Fw\ (g)\ of\ leaf\ x\ 1000}{weight\ of\ leaf\ area\ on\ paper\ (g)\ x\ \frac{area\ cm^2}{weight\ (g)\ of\ paper}}$$

4.2.5.2   Hexane extraction and analysis of compound on the tobacco leaf surface

GGPP is a substrate for various metabolites including diterpenes, analysis of these non-volatile terpenoids was done based on a protocol outlined in Bach *et al.* (2014). Five lines were selected for analysis with the wild-type included as a control. Two populations were analysed, with one population grown in CR_LL and the other population grown in the greenhouse under high light (GH_HL), with three individual plants per line harvested. Three leaf discs (1.5 cm in diameter) were punched out from leaf 1 of each plant. The leaf discs were placed in a Pyrex® glass vial with 2 mL hexane and 2 mg/L tetracosane (IS) followed by extraction at 25°C for 2 h with rotation. Leaf discs were removed from the vial and samples were stored at -20°C until the samples could be concentrated with nitrogen evaporation and resuspended in 250 μL hexane.

One microlitre of extract was injected with separation and detection of compounds done on an Agilent 7890N gas chromatograph (Agilent, Palo Alto, CA, USA) system coupled to a CTC CombiPal Analytics auto-sampler and an Agilent 5977B inert XL EI/CI MSD mass spectrometer (MS) detector through a transfer line. Separation was done using the HP-5MS (Agilent) capillary column (30 m × 250 μm × 0.25μm). (Agilent Technologies, Little Falls, Wilmington, USA). Helium was used as carrier gas with a constant flow rate of 1 mL/min with the purge flow set at 15 mL/min for 1 min. The oven parameters were as follows: initial temperature was set at 60°C and maintained for 2 min, followed by a linear increase to a temperature of 200°C at a rate of 20°C/min, temperature was held at 200°C for 1 min. The temperature was then increased to 310°C at a rate of 7°C/min and kept at this final temperature for 5 min. The total run time was 30.714 min.

Detection was performed in electron impact mode (70 eV) and operated in scan mode. The scan parameters were set at *m/z* ranging from 50 to 450.

For unknown compounds, the initial identification was done by comparing the mass spectra to the NIST and Wiley275.L mass spectral libraries.

163

4.2.6   Data analysis

Generated data was analysed using SIMCA® (Version 16, Sartorius Stedim Biotech, Göttingen, Germany). Microsoft Office Excel 2016 (Microsoft Corporation, Redmond, WA, USA) and Statistica™ (version 13.2, Dell, Round Rock, USA) were used to visualise data in graphs and for statistical analysis.

4.3   Results

4.3.1   Updating sequence analysis, determining the expression profile of *VviGGPS* gene family, and phylogenetic tree construction with characterised plant GGPSs

The sequences of the predicted *VviGGPS* gene family (Coman *et al.*, 2014; Leng *et al.*, 2017) were re-analysed and mapped to the VCost.v3 gene annotations with the characteristic motifs identified and the subcellular localisation predicted, the results are summarised in **Table 4.4**.

The coding sequence isolated by Young (2004) mapping to the *VviGGPS1* gene sequence annotated by Leng *et al.* (2017) was therefore renamed to *VviGGPS1.*

Table 4.4 Predicted *VviGGPS* gene family with corresponding V2* and VCost.v3** gene annotation as listed on https://urgi.versailles.inra.fr/Species/Vitis website with the presence of a splicing variant for each gene model noted based on VCost_v3 annotation. ^ predicted subcellular localisation based on Vcost.v3 sequence analysis described in methods section, cTP – chloroplastic transit peptide, ? - subcellular localisation was uncertain. The sequences were analysed for the characteristic motifs of GGPSs which included the two CxxxC motifs (1st and 2nd), the first aspartate rich motif (FARM) and the second aspartate rich motif (SARM). Five amino acids upstream and including FARM is the chain length determination (CLD) region. In VviPPPS the FARM and 2nd CxxxC motif had undergone evolutionary changes with both motifs consisting of the DDxxD sequence. The SARM sequence in VviSSUII had undergone changes with the motif consisting of DDxxK sequence (Camon *et al.*, 2014).

Gene ID	V2 ID*	Vcost.v3 ID**	Splicing variant	Targeting sequence^	Protein length	Characteristic motifs present	Arabidopsis thaliana orthologs		
							Gene annotation	Gene ID	Reference
VviGGPS1	VIT_204s0023g01210	Vitvi04g01230	No	cTP	368	1st CxxxC FARM SARM	AtGGPS11	AT4G36810	Okada *et al.* (2000) Ruiz-Sola, Coman, *et al.* (2016)
VviGGPS2	VIT_218s0001g12000	Vitvi18g00922	No	?	371	1st CxxxC FARM SARM			
VviGGPS-SS	VIT_219s0090g00530	Vitvi19g00506	No	?	298	1st CxxxC FARM 2nd CxxxC	AtGGPS12	AT4G38460	Wang & Dixon (2009)
VviGGPS-LS	VIT_205s0020g01240	Vitvi05g00289	No	?	290	1st CxxxC FARM SARM	AtGGPS11	AT4G36810	Okada *et al.* (2000) Ruiz-Sola, Coman, *et al.* (2016)
VviPPPS	VIT_219s0014g00070	Vitvi19g00005	Yes	?	421	FARM 2nd CxxxC	AtPPPS	At2g34630	Hsieh et al. (2011)
VviSSUII	VIT_203s0038g03050	Vitvi03g01420	No	?	637	-			
		Vitvi03g01421	No	cTP	341	1st CxxxC FARM 2nd CxxxC SARM	AtGGPS12	AT4G38460	Wang & Dixon (2009)
		Vitvi03g01422	Yes	?	640	-			
		Vitvi03g01423	No	Yes	261	1st CxxxC SARM	AtGGPS12	AT4G38460	Wang & Dixon (2009)

The GGPS sequences identified and downloaded from public databases were analysed in terms of the characteristic motifs; these being the chain-length determination (CLD) region which includes the first aspartate rich motif (FARM), the second aspartate rich motif (SARM) and the two CxxxC (where x is any hydrophobic amino acid) motifs.

Protein sequences of the extensively characterised GGPS family from *A. thaliana* were used to produce a phylogenetic tree containing the predicted grapevine GGPS sequences (**Figure 4.3**). The subtrees were coloured according to the characteristic motifs, with motifs shown, and function of characterised IDSs. Based on this phylogenetic tree, the IDSs group according to the chain-length of the products produced. The small subunit (SSU) of GGPSs cluster together while the predicted large subunit (LS) GGPS from grapevine groups with the GGPSs from *A. thaliana* and grapevine. Based on the branch lengths, the VviGGPSs and VviGGPS-LS map closest to AtGGPS11 while VviGGPS-SS and VviSSUII map closest to AtGGPS12. The two VviSSUII gene loci, Vitvi03g01420 and Vitvi03g01422, did not contain any of the characteristic motifs in their sequence and did not map closely to any of the characterised AtGGPSs.

In addition to the phylogenetic tree construction with the *A. thaliana* GGPS sequences, the VviGGPSs were also incorporated into a phylogenetic tree with published sequences which are reported to encode plant GGPSs. Some of the downloaded sequences did not contain the CLD region or had premature stop codons and were therefore not included in the multiple sequence alignment and phylogenetic tree construction, reducing the number of sequences used to 157 from the original 167. The resulting phylogenetic tree is shown in **Figure B-i** with different branches highlighted based on the characteristic motifs. Sequences mapping closely to VviGGPSs are shown while some of the subtrees were collapsed with the membership number per subtree indicated. VviGGPS1, VviGGPS2 and VviGGPS-LS all have the motifs characteristic of GGPSs while VviGGPS-SS and VviSSUII (Vitvi03g01421) have motifs indicative of SSUII activity (Coman *et al.*, 2014). Although the protein sequence encoded by Vitvi03g01423 (predicted to be VviSSUII) grouped with the other SSUII sequences, it did not contain the FARM and second CxxxC motifs.
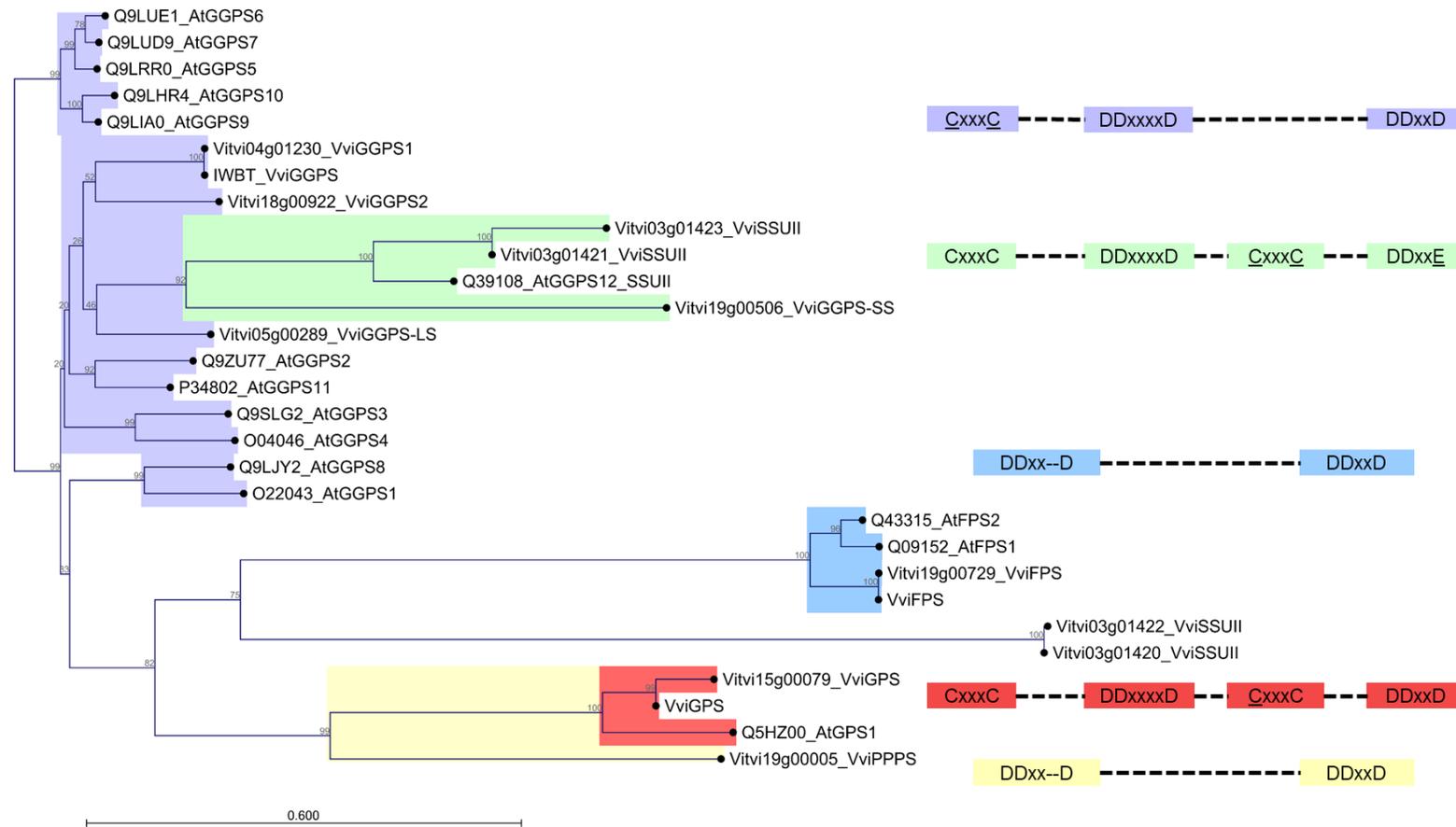
Figure 4.3 Unrooted phylogenetic tree of predicted and characterised isoprenyl diphosphate synthase from *Vitis vinifera* (Vvi) and *Arabidopsis thaliana* (At). Multiple sequence alignment (MSA) using the amino acid sequences was done using the characteristic motifs as fixed points with the end gap cost set at cheap. A Neighbour-Joining tree was constructed with the MSA using the Dayhoff (PAM) substitution model with default settings and 1000 pseudoreplicates to obtain a bootstrap value. The subtrees of the phylogenetic tree are highlighted according to the motifs that determine enzyme function.

167

The Gene Atlas expression data (Fasoli *et al.*, 2012) was used to determine the expression profile for the predicted *VviGGPSs.* Probe ambiguity, when mapped to the VCost.v3 annotation was low, with most of the predicted genes having either four or three unique probes, the only exception being the putative *VviSSUII* where re-annotation split the predicted gene into four with one predicted to have a splicing variant (**Table 4.4**). The correlation heatmap (**Figure 4.4**) summarises the expression profile of the putative *VviGGPSs* utilising the gene atlas data while Appendix C compares the expression values between predicted *VviGGPSs* in more detail with values grouped according to tissue analysed.

The expression of the various *VviGGPSs* is relatively ubiquitous in the different grapevine tissues and developmental stages, although expression of *VviGGPS1* was higher in the vegetative tissues with lowest expression levels observed in the berry. *VviGGPS2* generally had the highest expression levels apart from equivalent or higher expression of *VviSSUII* during post-harvest withering in the berry and higher expression of *VviGGPS1* in the seedling and *VviPPPS* in the leaf and young bud. The expression of small and large subunits of *VviGGPSs* correlated, but with lower expression compared to the other predicted *VviGGPSs*.
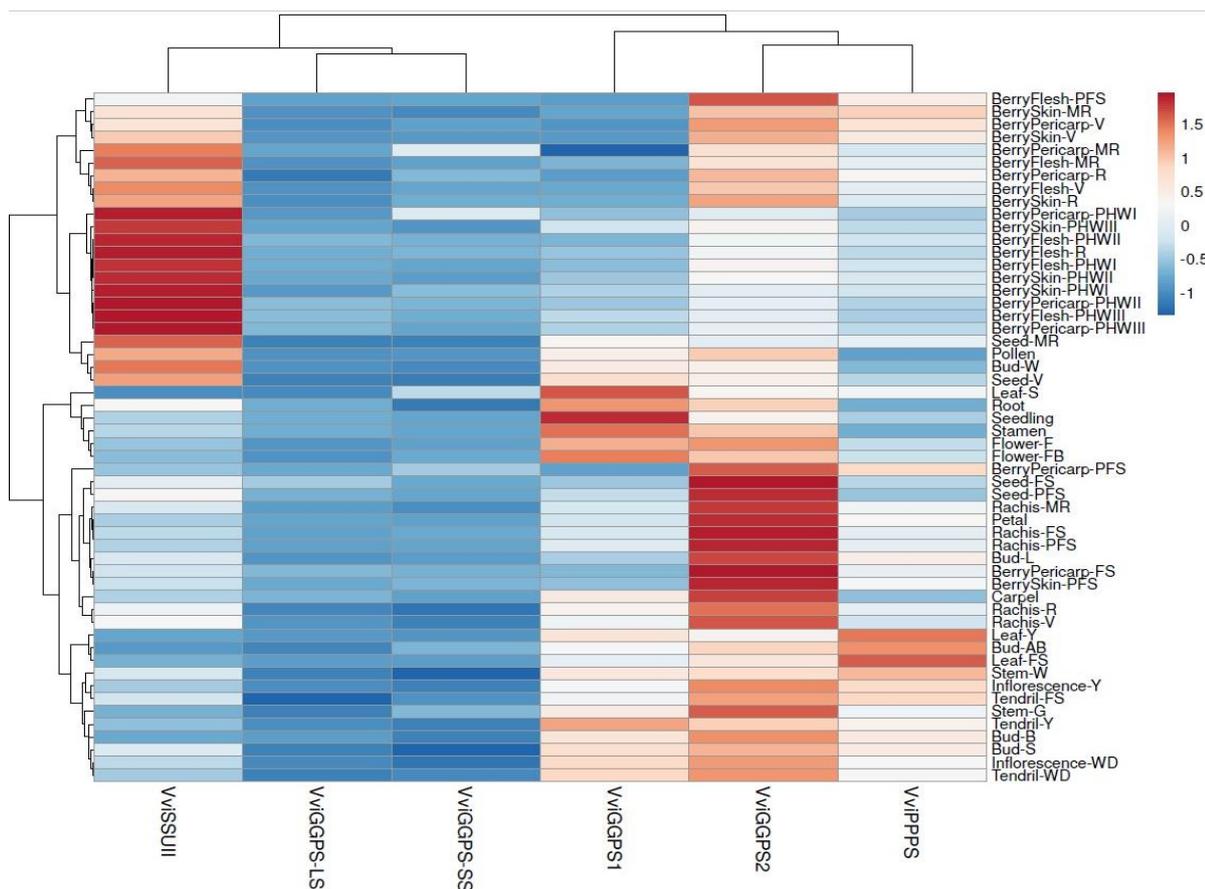
Figure 4.4 Correlation heatmap generated with average gene expression values. Rows are centred with unit variance scaling is applied to rows, both rows and columns are clustered using Pearson correlation distance and average linkage.

4.3.2 Genetic characterisation of *Nicotiana tabacum* population transformed with *VviGGPS1*

The *VviGGPS1* gene isolated and cloned into the plant expression pART27 vector under the control of the CaMV 35S promoter and nopaline synthase (nos) terminator by Young (2004) was shown to be functional via complementation in *E. coli* (A4.1).

Based on sequence analysis results of the previous section, the gene was mapped to *VviGGPS1* (4.3.1). The expression vector containing *VviGGPS1* was transformed into tobacco and genetic characterisation of the T1 generation was repeated to confirm transgene expression and number of integration events. Seeds produced with self-fertilisation of the T1 population were stored, constituting the T2 population. The T2 population plants were PCR screened before commencing further phenotyping of the population. Results show that the transgene was expressed in all the lines tested, with no expression detected in the control plants (**Figure A-ii**) with the results summarised in **Table 4.4**. All the lines were used for the initial phenotypic characterisation, with results obtained used as the basis for subsequent analysis.

Table 4.4 Summary of genetic characterisation of the T1 and T2 generation of the *Nicotiana tabacum* plant population transformed with *VviGGPS* under the control of a constitutive promoter.

Analysis	Control SR1	VviGGPS 1.3	VviGGPS 2.4	VviGGPS 3.4	VviGGPS 4.1	VviGGPS 6.4	VviGGPS 9.1	VviGGPS 10.4	VviGGPS 12.3
PCR	-	+	+	+	+	+	+	+	+
Northern Hybridisation	-	+	+	+	+	+	+	+	+
Southern Hybridisation*	0	2	2	2	1	2	3	1	2

*Number of independent integrations into the tobacco genome

4.3.3 Descriptive phenotyping of transgenic tobacco population

4.3.3.1 Seed germination

Error! Reference source not found.A comparison of the germination rate between the transgenic *VviGGPS1* seeds and the control seeds did not indicate any global differences (**Figure 4.5**). However, there were some slight differences when each line was compared individually to the control (**Figure D-i**). At time-points between day four and nine, some lines had a significantly higher (**Figure D-i**b, d, e and g) or significantly lower (**Figure D-i**c) seed germination percentage. Lines VviGGPS_1.3 (**Figure D-i**a) and VviGGPS_12.3 (**Figure D-i**h) showed a lower seed germination percentage at the end of the observation period but the germination rate was not significantly different from the control seeds. Calculation of the germination coefficient (**Figure D-ii**) show line

VviGGPS_10.4 having a significantly higher coefficient compared to the control line. In contrast, line VviGGPS_9.1 had a lower coefficient **Figure D-ii**.
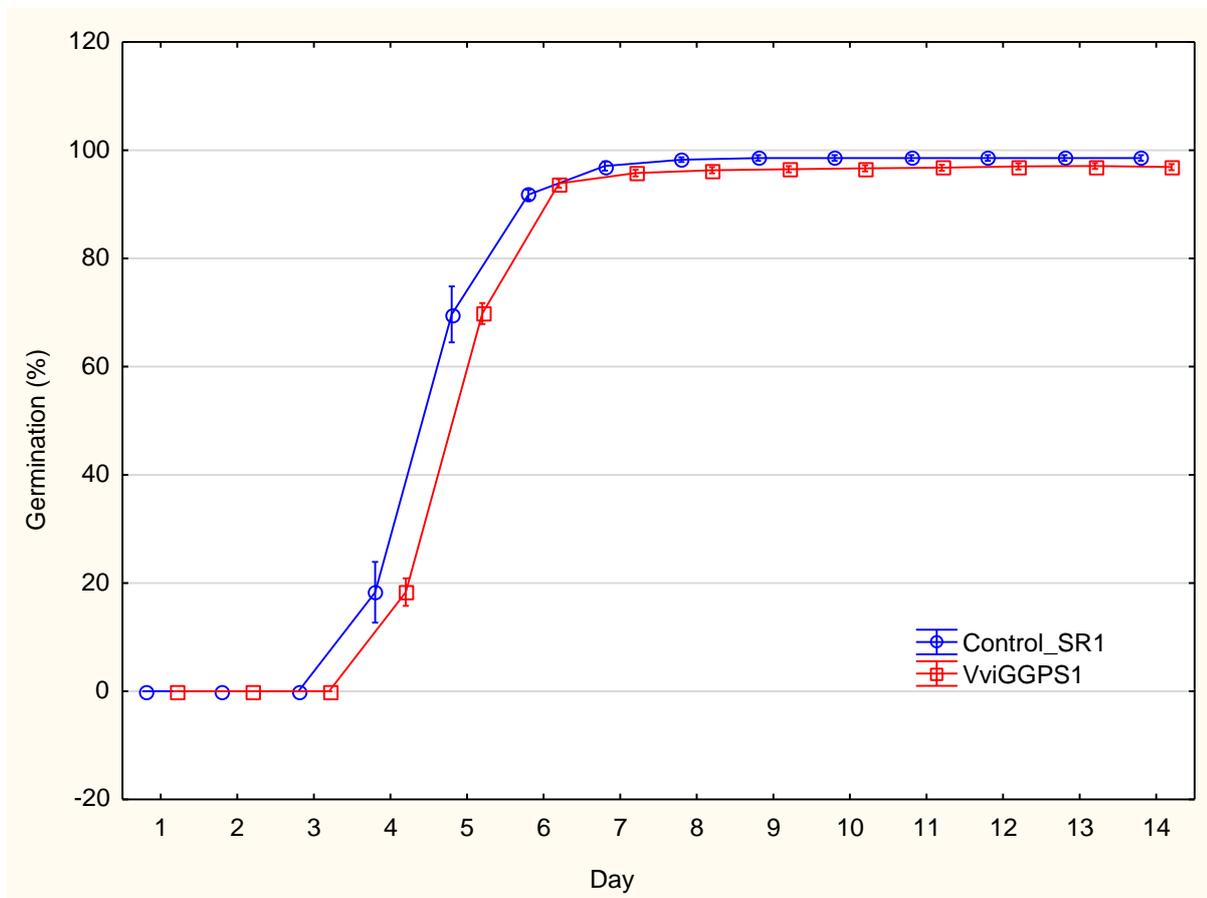
Figure 4.5 Germination of transgenic seeds in comparison to untransformed (control) seeds. The average of the eight *VviGGPS1* transgenic lines was used with each point an average of six repeats per line with error bars indicating the standard error between repeats. For the control seeds, each point indicates an average of six repeats of the experiment. No significant differences between the transgenic and control seeds could be determined with student's t-test ($p < 0.05$).

4.3.3.2   Vegetative and reproductive phenotypes observed in the transgenic population

The transgenic plants displayed various morphological characteristics in the vegetative and reproductive organs with some lines having a more severe abnormal phenotype compared to the wild-type control. There was no clear correlation between the number of gene integrations and phenotype observed. The various phenotypes observed in the transgenic lines when grown under different conditions are described in Table 4.5 and

170

Table 4.6 as well as which lines displayed these phenotypes.

Some leaves had a more lanceolate shape (Table 4.5 – 2a) and this phenotype was especially prominent in the T0 generation, decreasing with each generation. Leaf vein formation was occasionally affected with either disordered leaf vein development, which was associated with deformed leaf shape, or bifurcation of the main leaf vein (Table 4.5 – 5). A reduced or complete absence of apical dominance (Table 4.5 – 1b) were observed in some plants, specifically in line VviGGPS_1.3 and sometimes line VviGGPS_10.4, with the plants growing in a rosette shape with short or no internodes and leaf number was often difficult to determine. The severity of this phenotype would sometimes lessen as the plant aged and a flowering head could form. However, in some instances the plants were unable to switch to the reproductive phase, especially when plants were transferred to the greenhouse at an early stage of development. If flower formation was required, the plants were kept in the climaroom or only moved to the greenhouse at a later stage. Multiple shoot formation was often seen in plants that displayed the lack of apical dominance phenotype but could also occur in plants where apical dominance was present. Usually, one shoot appeared more dominant and was used for measurements and sampling.

In contrast to the vegetative phenotype, the reproductive phenotype (

Table 4.6) did not seem to be influenced by the environmental conditions except where reduced apical dominance delayed or prevented flowering. Some of the more apparent phenotypes were lighter coloration or sometimes a variegated pigmentation of the petals (

Table 4.6– 2) and less pronounced indentations of the petal lobes (

Table 4.6 – 1a). Elongated styles (

174

Table 4.6 – 1c) were associated with lighter petal colour except for line VviGGPS_3.4 where the flowers appeared normal except for the light pink colouration of the petals. This line also did not display any abnormal vegetative phenotype. Instances where the style was much longer than the stamen, conventional self-fertilisation could not occur. It was therefore necessary to artificially pollinate the flowers by removing the stamen and dusting the stigma with the mature anther. Necrotic flower buds were also a common transgenic phenotype with many buds undergoing premature abscission (

Table 4.6 – 1d) and only a few developing to mature flowers. Although not measured or counted, the flower buds in plants with the "necrotic flower bud" phenotype seemed smaller, and a larger number of buds were formed during the flowering phase compared to the control plants.

Table 4.5 Description of various vegetative phenotypes observed within the *VviGGPS*-expressing tobacco population.

Major category	Subcategory	Description	Lines displaying phenotype	Visual representation
1. Shoot apex	a. Multiple shoots	More than one primary shoot forms when seedling is transferred to soil. Usually associated with a lack of apical dominance	VviGPPS_1.3 VviGPPS_2.4 VviGPPS_4.1 VviGPPS_6.4 VviGPPS_9.1 VviGPPS_10.4	
	b. Lack of apical dominance	The plants display lack of apical dominance, it can range in severity and is usually associated with multiple shoots formation. Difficult to assign leaf number with these plants and in severe cases these plants fail to form a flowering head	VviGPPS_1.3 VviGPPS_2.4 VviGPPS_4.1 VviGPPS_6.4 VviGPPS_10.4	

177

Major category	Subcategory	Description	Lines displaying phenotype	Visual representation
2. Leaf shape	a. Twisted leaf apex	The leaf apex has some twist to it with the leaf apex having an acuminate shape rather than the acute shape associated with tobacco leaves. Associated with abnormal leaf surface and shape	VviGPPS_1.3 VviGPPS_2.4 VviGPPS_4.1 VviGPPS_6.4 VviGPPS_9.1 VviGPPS_10.4	
	b. Lanceolate	Leaves have an elongated shape compared to the wild-type plants. This phenotype was especially visible in the T0 population.	VviGPPS_1.3 VviGPPS_2.4 VviGPPS_4.1 VviGPPS_6.4 VviGPPS_9.1 VviGPPS_10.4	
	c. Involute leaf margins	Upward curling of the leaves but also frilly lead edges	VviGPPS_1.3 VviGPPS_2.4 VviGPPS_4.1 VviGPPS_6.4 VviGPPS_9.1 VviGPPS_10.4	
	d. Deformed	Irregular-shaped leaves, distinctly different from wild-type. Associated with leaf surface that is also different than the wild-type plants	VviGPPS_1.3 VviGPPS_10.4	

178

Major category	Subcategory	Description	Lines displaying phenotype	Visual representation
	e. Disordered vein	Abnormal vein development. Associated with abnormal/deformed leaf shape. Bifurcation of the main vein, have only been observed in line 1.3 in plants lacking apical dominance where it looks as if two leaves fused together.	VviGPPS_1.3 VviGPPS_2.4 VviGPPS_4.1 VviGPPS_6.4 VviGPPS_10.4	
3. Leaf surface and texture	a. Pockmarked	Not as visually prominent as the "rough and rugose" surface, the leaves look as if it has small pockmarks that covers it	VviGPPS_1.3 VviGPPS_2.4 VviGPPS_4.1 VviGPPS_6.4 VviGPPS_9.1 VviGPPS_10.4	
	b. Rough & rugose and crunchy	The leaf surface has a "bubbly" surface which looks rougher than the wild-type leaves. In extreme cases the leaf seems to be thicker than the wild-type and the texture of the leaf is much more brittle (folding breaks the leaf) unlike the wild-type leaves.	VviGPPS_1.3 VviGPPS_2.4 VviGPPS_4.1 VviGPPS_6.4 VviGPPS_10.4	

179

Table 4.6 Description of various reproductive phenotypes observed within the *VviGGPS*-expressing tobacco population.

Major category	Subcategory	Description	Lines displaying phenotype	Visual representation
1. Flower organs and sterility	a. Underdeveloped lobes	General category for any abnormalities in corolla. The most common being the smaller lobes with less pronounced indentations	VviGPPS_1.3 VviGPPS_2.4 VviGPPS_4.1 VviGPPS_6.4 VviGPPS_9.1 VviGPPS_10.4 VviGPPS_12.3	
	b. Elongated filament	The filament protrudes over the corolla. Usually, the style is also longer which means that self-fertilisation is possible. It seems that the floral tube is shorter than the wild-type flowers rather than the style and filament being longer.	VviGPPS_6.4 VviGPPS_9.1 VviGPPS_10.4 VviGPPS_12.3	
	c. Elongated style	The style protrudes over the corolla, it is also much longer than the filament which means that natural self-fertilisation is not possible. The elongated style is usually visible from early flower development	VviGPPS_1.3 VviGPPS_2.4 VviGPPS_6.4 VviGPPS_9.1 VviGPPS_10.4	

180

Major category	Subcategory	Description	Lines displaying phenotype	Visual representation
	d. Necrotic flower buds	Flower buds become necrotic and fall of during early flower development. These flower buds are also smaller than the wild-type flower buds with more flower buds present on the flowering head	VviGPPS_1.3 VviGPPS_2.4 VviGPPS_6.4 VviGPPS_9.1 VviGPPS_10.4 VviGPPS_12.3	
	e. Incomplete dehiscence	Not all the anthers go through dehiscence or dehiscence is delayed in some anthers.	VviGPPS_4.1 VviGPPS_9.1	
	f. Browning stigma	The stigma part of the pistil starts browning and drying out before fertilisation has occurred. These flowers cannot be fertilised and eventually wither and fall off.	VviGPPS_10.4	

181

Major category	Subcategory	Description	Lines displaying phenotype	Visual representation
2. Flower colour	a. Pale pink	The flower has a much lighter pink coloration compared to the wild-type flower	VviGPPS_1.3 VviGPPS_2.4 VviGPPS_3.4 VviGPPS_6.4 VviGPPS_9.1 VviGPPS_10.4 VviGPPS_12.3	
	b. Variegated	The coloration of the petal is more variegated with some dark pink present in certain areas	VviGPPS_3.4 VviGPPS_6.4	

Although the severity of the phenotypes ranged across individual plants, only the presence or absence of a certain abnormal phenotype was noted. Individual plants with extreme phenotypes that hindered propagation inevitability did not survive past the T0 generation. The phenotypes observed in the T1 and later generations therefore included only those that did not prevent production of the next generation.

### 4.3.3.2.1 Transgenic phenotypes observed under various growth conditions

Initial observations found that the environmental conditions influenced some of the phenotypes observed, the vegetative organs (leaves and apical meristem) being especially affected.

Figure 4.**6** summarises the effect that growth conditions had on the vegetative phenotype observed in the selected lines grown under various conditions.
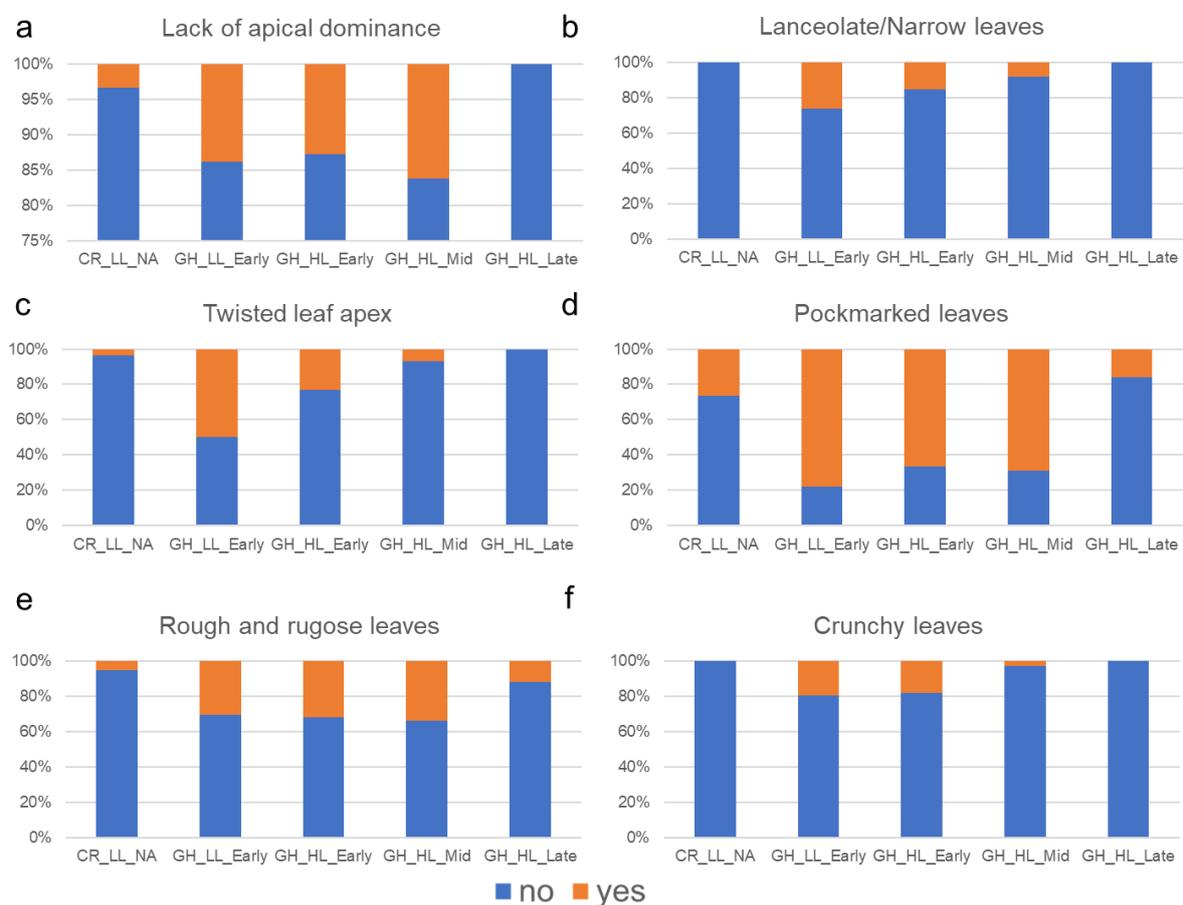
Figure 4.6 Phenotypic observations of transgenic plants grown under different conditions. Observations of five lines (VviGGPS_1.3, VviGGPS_3.4, VviGGPS_6.4, VviGGPS_9,1 and VviGGPS_10.4) with at least 12 plants per line except during the GH_HL_Late growth condition when only 5 plants per line were used. The percentage of plants displaying the abnormal phenotype are shown when grown in the climaroom (CR) at low-light (LL) compared to when grown in the greenhouse (GH) at low light (LL) and high light (HL) from an early or mid-growth stage. The growth conditions are described in **Error! Reference source not found.** while the

abnormal phenotypes are described in Table 4.5. Observations were binary, i.e., if the abnormal phenotype was observed then it was marked as "yes" while if it was not observed it was marked as "no".

The abnormal phenotypes occurred at a higher frequency in the transgenic population when the plants were moved to the greenhouse from an early or mid-growth stage of development. From these results the phenotypes displayed did not seem to be affected between plants moved to the greenhouse during the hardening-off period (early) or at around the three- to four-leaf stage (mid), except for the "crunchy" leaf phenotype, which was more often observed when the plants had been grown in the greenhouse from an early stage. Transgenic plants moved to the greenhouse at a late stage of development had a frequency of abnormal phenotype which was comparable to plants kept in the climaroom.

4.3.3.3 *Measurement of carotenoids and photosynthetic pigment in low-light climaroom*

The results for the carotenoid and chlorophyll analysis in the transgenic population as well as control plants when grown in the low-light conditions of the climaroom are summarised in **Table E-i**. Values significantly ($p < 0.05$) different from the control plants are shown in red with bar graphs shown in **Figure 4.7**.Lines VviGGPS_1.3, VviGGPS_6.4 and VviGGPS_9.1 had higher levels of Neoxanthin, Violaxanthin, lutein, chlorophyll a and b. Antheraxanthin, zeaxanthin and lutein epoxide levels were below the LOD and/or LOQ in many samples and was therefore not included in the results shown. The ratio of chlorophyll a to chlorophyll b was significantly ($p < 0. 05$) lower in lines VviGGPS_9.1 and VviGGPS_12.3.
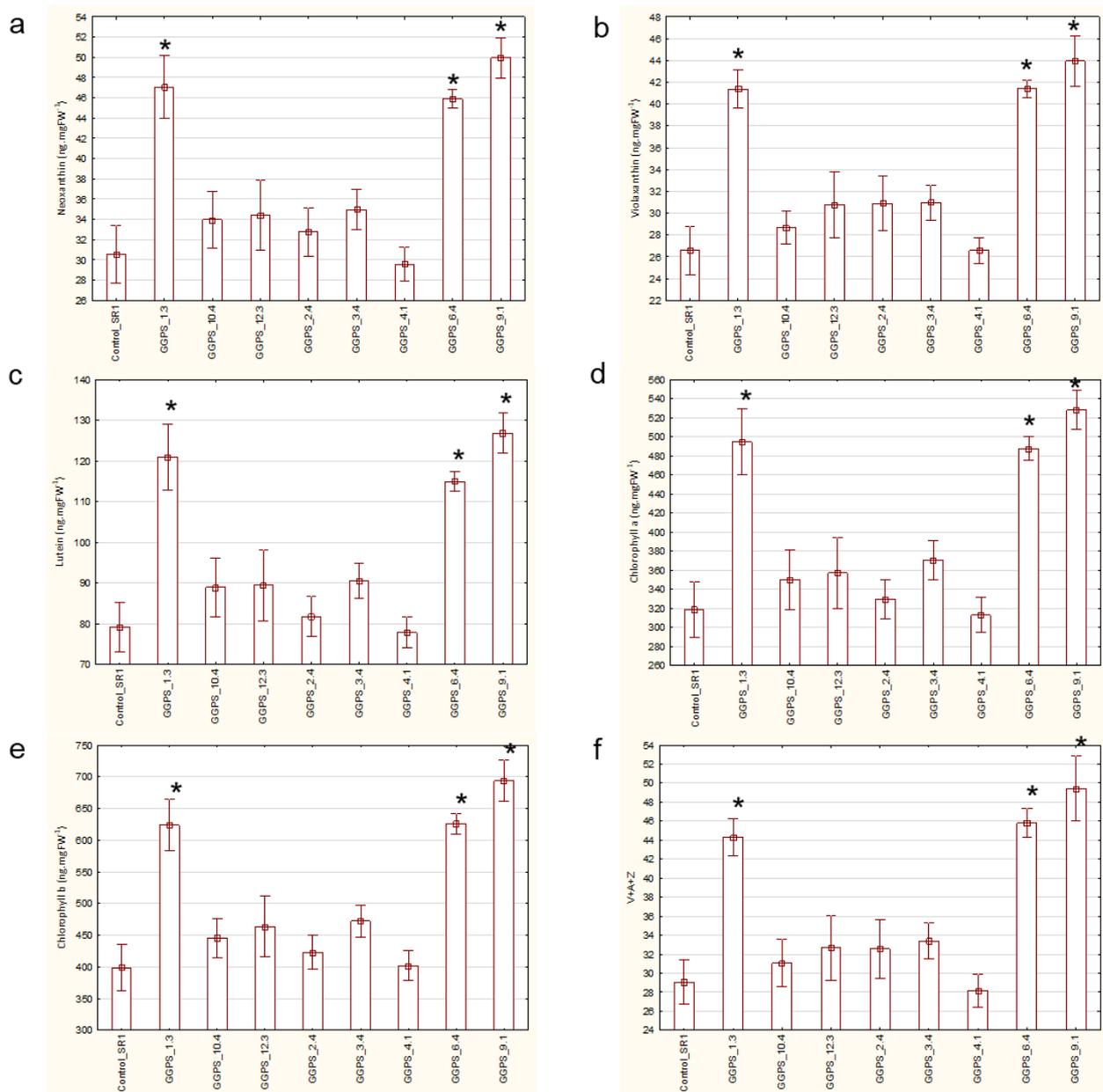
Figure 4.7 Carotenoid and pigment analysis of Leaf 3 sampled in plants grown in climaroom (low-light) with six plants per line sampled and analysed. Significant differences from the control population (Control_SR1) highlighted in red. Carotenoid and pigment concentrations shown as ng.mgFW^{-1}. Bar graph show average and error bars the standard error. Asterisks(*) indicate significant difference from Control_SR1 determined with the student's *t*-test (p < 0.05).

4.3.3.4 Physiological measurements taken in the autumn and winter season

For physiological measurements, two transgenic lines were analysed in comparison to the wild-type tobacco plants. The two lines chosen were VviGGPS_1.3 and VviGGPS_10.4, line VviGGPS_1.3 was shown to have two transgenic integration events with a severe morphological phenotype and increased levels of photosynthetic metabolites. Line VviGGPS_10.4 had one transgenic integration event and displayed some of the morphological phenotypes but did not show any significant

185

difference in photosynthetic metabolites measured. The plants were grown in the greenhouse from an early stage of development and since irradiance in the greenhouse was wholly dependent on the natural light the growth conditions were categorised as GH_HL (autumn) and GH_LL (winter) as described in section (4.2.2.1). During the two growth seasons the light conditions differed with the autumn (GH_HL) season having a DLI value that was more than double that of the winter (GH_LL) season.

The results of the IRGA photosynthetic measurements taken over the two growth periods are compared in **Figure 4.8**. During the GH_HL growth period, leaf 1 and 2 of the transgenic lines had significantly ($p < 0.05$) higher photosynthetic rates, conductance, and transpiration (**Figure 4.8**a, c & e) when compared to leaf 1 and 2 of the control plants. The vapour temperature deficit (Vpd) was significantly ($p < 0.05$) lower in transgenic plants compared to the control plants (**Figure 4.8**g). In contrast, photosynthetic measurements taken of the plant population grown in the GH_LL growth period showed significantly ($p < 0.05$) lower photosynthetic rates, conductance, and transpiration (**Figure 4.8**b, d & f) in line VviGGPS_1.3 (leaf 1 and 2) and in leaf 1 of line VviGGPS_10.4 when compared to the control population while the Vpd was significantly higher in the transgene leaves except for leaf 2 of VviGGPS_10.4 (**Figure 4.8**h).

In addition to the physiological measurements using the IRGA system, thermal imaging was also done with the same plants. An example of the thermal image is shown in **Figure F-i** with the calculated Crop water stress index (CWSI) in relation to the stomatal conductance determined with the IRGA shown in **Figure F-ii**. There was no significant difference in the CWSI between the control and transgenic plants grown in the GH_HL growth period, even though the stomatal conductance measurements were significantly higher in leaf 1 and 2 in both transgenic lines analysed. During the GH_LL growth period the CWSI was significantly higher in leaf 2 of line VviGGPS_1.3 and VviGGPS_10.4 in comparison to the control leaf 2. The stomatal conductance measured in leaf 2 of the transgenic lines was lower than the control, but only significant different in line VviGGPS_1.3.
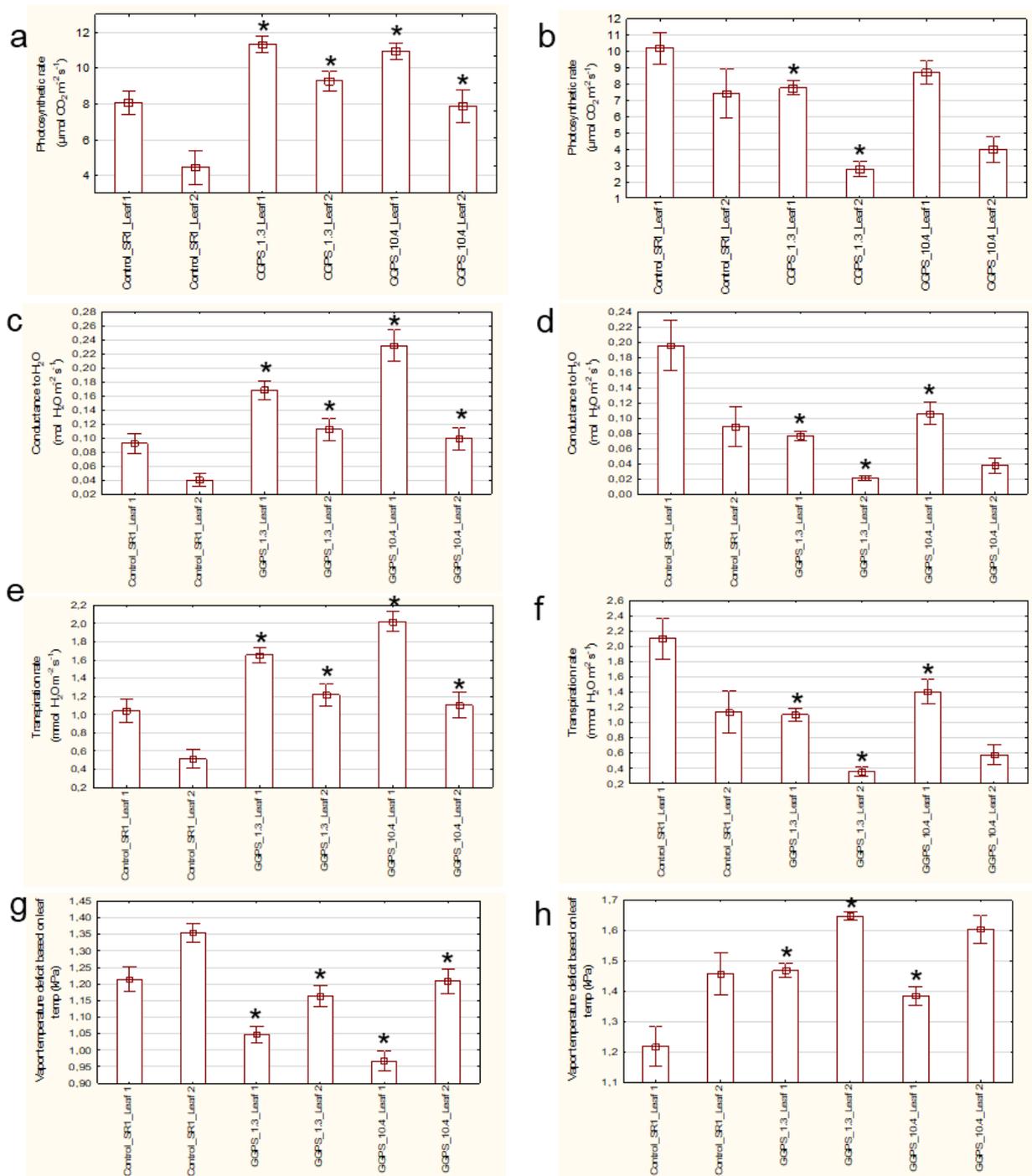
Figure 4.8 Photosynthetic parameters measured of leaf 1 & 2 taken of at least 8 plants per line (Control_SR1, GGPS_1.3 and GGPS_10.4 with T1 and T2 pooled) over two day period during the autumn (a, c, e, g) and winter (b, d, f, h) growth season. Bar graphs show average and error bars the standard error. *indicates significant difference from Control_SR1 for the respective leaves determined with the student's t-test ($p < 0.05$).

4.3.3.5 Leaf surface visualisation and metabolite analysis

One of the most visually arresting and frequently observed transgenic phenotypes was when the leaf surface was affected. The leaf surface phenotypes, as well as their frequency within the population, are described in more detail in Section 4.3.3.2. The abnormal leaf surface transgene phenotype

187

initiated further analysis using CT scanning of the leaves to get a better idea of the differences between the control and transgenic leaves. Unfortunately, CT scanning is not a high throughput method and is better suited for items with a rigid structure, since even small movements during the scanning process can affect the image generated. Nonetheless, leaves of the same age were analysed from the control plant and line VviGGPS_1.3, which displayed the "rough and rugose" leaf surface phenotype (**Figure 4.9**). From the imaging of the upper (adaxial) leaf side it seems that the trichomes are distributed more evenly across the leaf surface and are smaller on the control leaf (**Figure 4.9**a) compared to the transgenic leaf (**Figure 4.9**b). On the bottom (abaxial) side of the leaf, the number of trichomes appeared more sparsely distributed on the transgenic leaf (**Figure 4.9**d) than on the control leaf (**Figure 4.9**c).
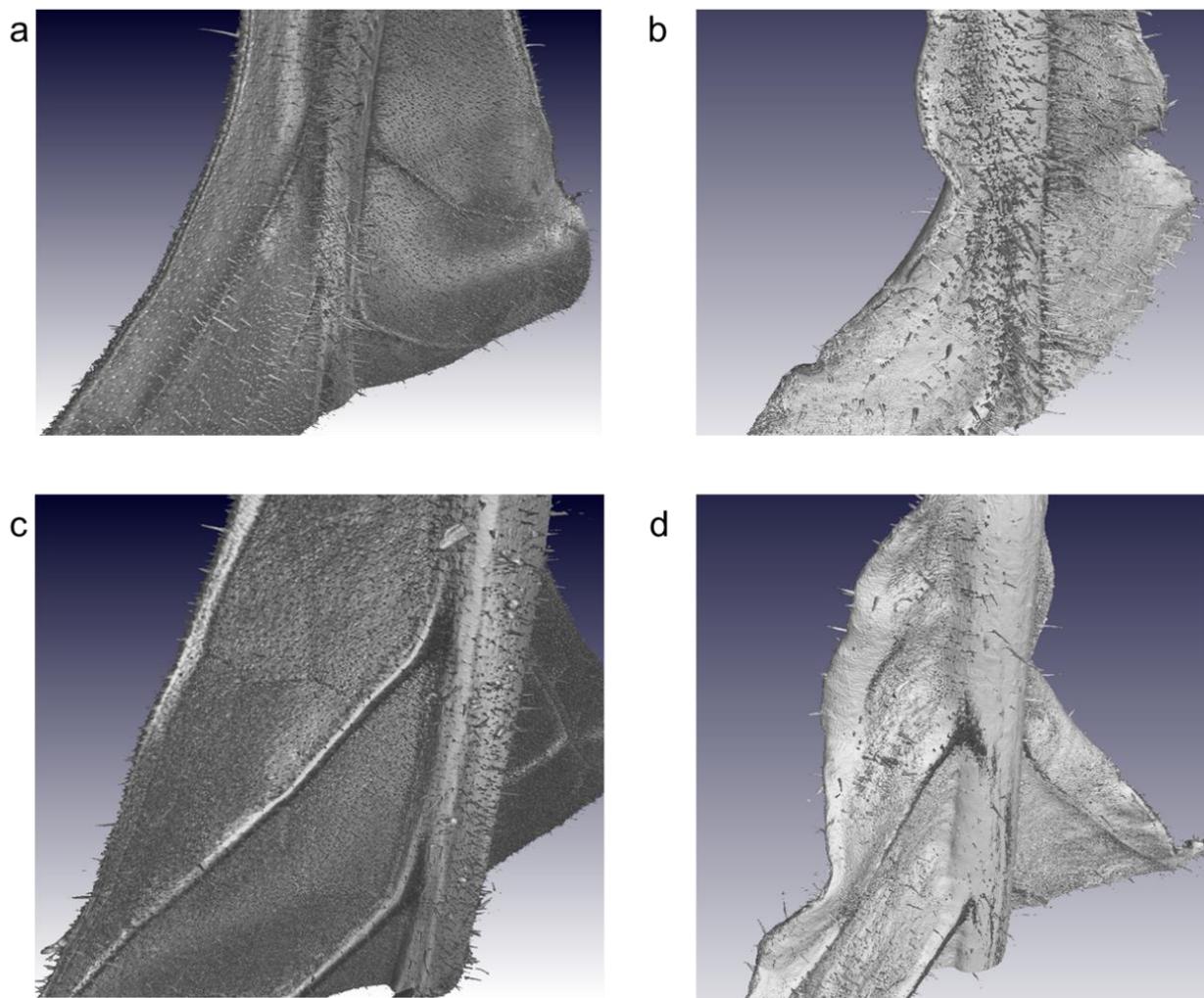
Figure 4.9 CT scanner results comparing leaf from control (a and c) to a transgenic (line VviGGPS_1.3) leaf showing the abnormal "pockmarked" leaf phenotype (b and d). View of the adaxial (a and b) and abaxial (c and d) of leaf.

188

Hexane extraction was used for the analysis of non-volatile (or low volatility) terpenoids such as diterpenes and triterpenes (Bach *et al.*, 2014). Leaves were sampled from plants grown in the climaroom (CR_LL) and in the greenhouse (GH_HL) which allowed a comparison between transgenic and control plants as well as between different growth conditions. Various peaks were identified with identification based on mass spectra done if possible, otherwise peaks were named according to retention time. Peak area was normalised to IS peak area and analysed via PCA to get an indication of the sample separation (**Figure 4.10**a). There was no clear separation between the control (circle) and transgenic plants (triangle) when grown in the climaroom or the greenhouse (**Figure 4.10**a). However, there was separation based on the growth conditions with plants grown in the climaroom (CR_LL) grouping together as indicated by red circle (**Figure 4.10**a). OPLS using growth conditions as the y-variable showed clear separation between the two groups (**Figure 4.10**b) and the variables driving the separation are displayed in **Figure 4.10**c.
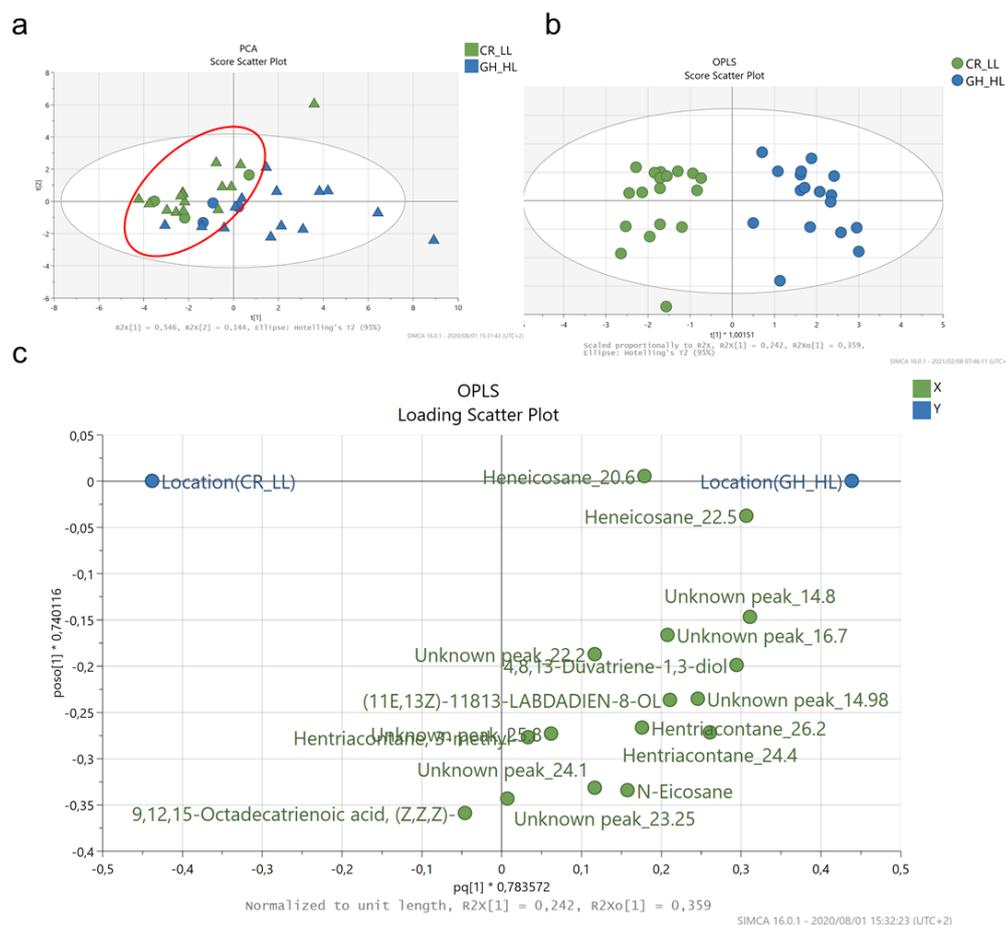
Figure 4.10 Analysis of hexane extract from leaf surface. PCA (a) was done to determine separation with transgenic plant samples indicated by triangle and control samples by circle while the location at which the plants were grown are indicated by green (climaroom at low light – CR_LL) and blue (greenhouse at high light – GH_HL). OPLS with location as y-variable (b) show clear separation based on growth conditions with the variable driving the separation shown in the loading scatter plot (c).

The normalised peak areas are summarised in **Table G-i** with the peaks significantly different (p<0.05) from the control samples under the same growth conditions highlighted in red. These results show that most of the transgene lines have higher levels of the putative diterpenes, (11E,13Z)-11813-Labdadien-8-ol and 4,8,13-Duvatriene-1,3-diol, but this was only significantly higher in line VviGGPS_9.1. Interestingly, line VviGGPS_1.3 did not follow the same trend with lower levels of these compounds measured compared to the control. As indicated by the separation shown in the PCA plot, the growth conditions had a palpable effect on the peak areas. Compounds that were significantly different (p<0.05) between different growth conditions within the same line are indicated with an asterisk in **Table G-i**. For the peaks that were significantly different, higher levels of the leaf surface compounds were observed in samples from plants grown in the greenhouse (GH_HL). However, only the transgenic plants showed any notable response to the growth conditions with no significant differences observed between control plants grown in the climaroom (CR_LL) versus control plants grown in the greenhouse (GH_HL).

4.4 Discussion

4.4.1 The grapevine *GGPS* gene family consists of several members with the predicted duplicated genes *VviGGPS1* and *VviGGPS2* displaying variable expression

The previously annotated *VviGGPS* gene family (Coman *et al.*, 2014; Leng *et al.*, 2017) was updated in this study. All the identified *VviGGPS* sequences were translated to their protein sequence with the characteristic motifs identified. Short-chain diphosphate synthases have two conserved aspartate-rich regions which are located on opposite sides of the active site when the enzyme is folded. These motifs have been shown to play an important role in the catalytic activity of the enzyme and are appropriately named FARM and SARM (Blanchard & Karst, 1993; Koyama *et al.*, 1993; Song & Poulter, 1994). FARM is in region II of the amino acid sequence, while SARM is located further downstream in region VI (Vandermoten *et al.*, 2009). FARM also forms part of the CLD region that is associated with the determination of product length (Wang & Ohnuma, 1999). In addition, the CxxxC motifs required for the interaction between different subunits in heterodimer were identified (Wang & Dixon, 2009; Beck *et al.*, 2013; Coman *et al.*, 2014).

According to Leng *et al.* (2017), *VviGGPS1* and *VviGGPS2* are the results of a segregation duplication event, with VviGGPS1 predicted to be localised to the chloroplast and VviGGPS2 to the mitochondria. Using the ProtComp Version 9.0 and TargetP 1.1 databases, the subcellular localisation of the predicted VviGGPSs based on the on Vcost.v3 genome annotation was updated in this study. Localisation of VviGGPS1 to the chloroplast was confirmed, but VviGGPS2 localisation was uncertain. These duplicated genes also displayed differential expression patterns according to the gene atlas data (Fasoli *et al.*, 2012), although Leng *et al.*, (2017) found that the expression profile

was comparable in the ripening grape berry but supported the gene atlas results in that *VviGGPS2* expression was significantly higher than *VviGGPS1.*

Coman *et al.*, (2014) identified a putative grapevine homolog to the polyprenyl pyrophosphate synthase (PPPS), also known as solanesyl diphosphate synthase (SPS), which had been previously characterised in *A. thaliana* (Hsieh *et al.*, 2011; Ducluzeau *et al.*, 2012). The PPPS is believed to be a neofunctionalisation of a GGPS and encodes for an enzyme capable of producing medium (C25) to long (C45) chain isoprenyl diphosphates (Hsieh *et al.*, 2011), which are utilised for the isoprenoid side chain in plastoquinone and ubiquinone biosynthesis (Hirooka *et al.*, 2003; Jun *et al.*, 2004; Ducluzeau *et al.*, 2012; Jones *et al.*, 2013; Liu *et al.*, 2019).

The large subunit GGPS sequence contains the first CxxxC, FARM and SARM motifs and can be active on its own (Tholl *et al.*, 2004) but that is not always the case (Burke *et al.*, 1999). Since the first CxxxC motif is crucial for the interaction between the large subunit and the small subunit, this motif cannot be modified (Wang & Dixon, 2009), as is seen with some of the other GGPSs (Coman *et al.*, 2014). The putative VviGGPS-LS contains all these motifs and groups more closely with the predicted small subunit VviGGPSs which support its initial annotation.

Based on the two studies by Coman *et al.* (2014) and Leng *et al.* (2017) there were two genes predicted to encode for the small subunit GGPS in grapevine (VviGGPS-SS and VviSSUII). This enzyme has been shown to be inactive on its own but can function in a heterodimer with the LS GGPS to produce either GPP or GGPP (Burke & Croteau, 2002b; Tholl *et al.*, 2004). The SSU protein sequence contains two CxxxC motifs and the FARM motif but lacks a conserved SARM motif, which results in a loss of GGPS activity (Burke *et al.*, 1999; Tholl *et al.*, 2004; Wang & Dixon, 2009). The aspartate-rich motifs are required for substrate binding as well as product length determination, but only one aspartate rich motif is necessary if the enzyme uses a diphosphate substrate with the additional aspartate motif required for the isopentenyl diphosphate which is incorporated into the growing allylic substrate (Song & Poulter, 1994; Tarshis *et al.*, 1996; Sacchettini & Poulter, 1997). One of the annotated grapevine genes predicted to encode for VviSSUII by Coman *et al.* (2014) was split into four genes based on the Vcost.v3 re-annotation, with only one gene (Vitvi03g01421) encoding for a protein containing two CxxxC motifs, in addition to the FARM and a modified version of the SARM motif. Based on the importance of the CxxxC motif in the interaction between the small and large subunit to form the heterodimer (Wang & Dixon, 2009), it can concluded that only the gene encoding for VviSSUII containing these motifs is functional. This protein was also predicted to localise to the plastid and gene atlas expression analysis of the *VviSSUII* gene showed relatively high expression in the grape berry, especially during the post-harvest withering phase. Tholl *et al.* (2004) hypothesised that GGPS-SSU plays a key regulating role in GGP production, and indirectly monoterpene biosynthesis, due to the correlating expression profile with monoterpene emission.

191

Further investigation into VviSSUII function and its role in monoterpene biosynthesis could yield some interesting results.

4.4.2   Over-expression of *VviGGPS1* results in pleiotropic phenotypes which are affected by the (light) environment

The established transgenic population, generated by PR Young and expressing *VviGGPS1,* consisted of eight independently transformed lines, with the number of integration events ranging from one to three. As a first point of characterisation of the transgene population and since GGPP is the branchpoint substrate for the biosynthesis of phytohormones which can play a role in seed germination (McCarty, 1995; Miransari & Smith, 2014), assays were done using the seeds produced from the T2 generation plants to investigate whether *VviGGPS1* transgene expression affected germination. Some lines displayed differences in the germination rate or germination percentage compared to the control but generally there was not a clear difference between the transgene and control lines. Line VviGGPS_9.1 had a significantly lower rate of germination compared to the control, which could be due to increased levels of abscisic acid (ABA) while the increased germination rate observed in line VviGGPS_10.4 could be due to higher gibberellin (GA) levels (Miransari & Smith, 2014). However, these phytohormones were not measured during the study and further investigation would be required to support this hypothesis. Also, the reason for these opposing germination rate phenotypes in two lines could be due to the position effect when utilising *Agrobacterium*-mediated plant transformation (Gelvin, 2003). GGPP is utilised in the biosynthesis of carotenoid and the isoprenoid phytol side-chain of chlorophyll (Von Wettstein *et al.*, 1995; Bollivar, 2006; Lichtenthaler, 2007; Ruiz-Sola & Rodríguez-Concepción, 2012; Kim *et al.*, 2013), with the carotenoids also being precursors for abscisic acid (ABA) and strigolactones (Nambara & Marion-Poll, 2005; Saeed *et al.*, 2017). Altered levels of these compounds could affect the transgene phenotype and were therefore analysed in the available lines (Umehara *et al.*, 2008; Ji *et al.*, 2009; Procházková *et al.*, 2009; Dall'Osto *et al.*, 2010; Moreno *et al.*, 2016; Yang *et al.*, 2017). The leaf samples were taken from plants grown in the climaroom under low light conditions which did not require the de-epoxidation of violaxanthin to zeaxanthin via antheraxanthin as a means of protection against photoinhibition and photooxidation. The latter two xanthophyll compounds were therefore below the levels of quantification and/or detection (Jeffrey *et al.*, 1974; Demmig-Adams *et al.*, 1989; Lichtenthaler, 2007). Three of the eight available lines showed increased levels of Chlorophyll a & b, lutein, neoxanthin and violaxanthin in comparison to the control plants. Biosynthesis of these compounds are under various regulatorily controls due to their importance in normal plant functioning (Cazzonelli & Pogson, 2010; Kim *et al.,* 2013; Llorente *et al.*, 2017), however, these results indicate that transgene *GGPS* expression can result in increased availability of GGPP which could be directed towards carotenoid and chlorophyll biosynthesis. A previous study wherein a *GGPS* isolated

from *Gentiana lutea* was overexpressed in tobacco resulted in significantly higher levels of β-carotene (Ji *et al.*, 2009).

An initial observation was that the vegetative phenotype was not always consistent and could be affected by the growth conditions. The available lines were therefore phenotypically characterised under various growth conditions to establish whether external factors influenced the phenotype displayed by the transgene plants as well as to assist in the selection of a few lines which could be studied more in-depth. Lines which displayed all (VviGGPS_1.3), most (VviGGPS_6.4 and VviGGPS_10.4), some (VviGGPS_9.1) or few (VviGGPS_3.4) of the abnormal phenotypes were grown at different conditions with the observed vegetative morphology used as a measurement of the impact the environment had on the plant phenotype. Since the greenhouse is solely reliant on natural light the daily light integral (DLI) was used to describe the light environment, since the value incorporates the light intensity as well as the day length. Even though the calculated DLI of the greenhouse at low light (winter season) was comparable to the climaroom, the plants grown in the greenhouse from an early stage displayed a higher frequency of the abnormal phenotype which was comparable to plants grown in the greenhouse at high light (autumn season). A review by Matsubara, (2018) highlighted the need to study plants grown under fluctuating conditions instead of the consistent environment strived for in growth chambers. To get a better idea of the phenotype a plant will have in a realistic situation, plants should ideally be grown in the field setup. However this is not always possible especially in cases where genetically modified plants are studied (https://www.loc.gov/law/help/restrictions-on-gmos/south-africa.php) (Slot *et al.*, 2018). A metabolite analysis study conducted by (Annunziata *et al.*, 2017) compared *A. thaliana* plants grown under artificial versus natural light. The results indicated that the use of artificial light was likely not representative of natural conditions. Greenhouses with natural light irradiance are a good alternative wherein the plants can be contained in a GMO approved area but with natural light fluctuation, although the DLI is much lower compared to the outside environment due to roofing material and structural obstructions (Runkle, 2006b). Results from this study supports these findings as it became clear that the phenotype in plants grown under the relatively consistent conditions of the climaroom were much less severe than what was seen in plants growing in the greenhouse.

Compared to the vegetative phenotype, the transgene flower phenotype was much more constant within lines and did not seem to be affected by the environmental conditions except when the plant could not switch to the reproductive phase due to the lack of apical dominance phenotype. The most commonly and easily observed transgene flower phenotypes were the light coloration of the corolla and the elongated style. These phenotypes were studied in more depth and discussed in the following Chapter. Some of the abnormal flower phenotypes such as elongated filaments, incomplete anther dehiscence and browning of the stigma were observed only a few times during the entire study and were therefore noted but not discussed. Line VviGGPS_4.1 seemed to have an extended

flowering time, with new flowers being formed when some of the seed pods have already matured. Since only the days to flowering were measured this observation could only be anecdotal in this study.

The altered leaf surface phenotype observed in some of the transgenic plants initiated a more in-depth analysis thereof. Based on the CT scanning results it looked as if the trichome distribution and/or quantity was affected in the transgenic plant. Diterpenes are produced and accumulate in the trichomes of tobacco (Sallaud *et al.*, 2012). In addition, GGPP is the substrate for diterpene biosynthesis. It was therefore decided to analyse the leaf surface metabolites, which includes metabolites stored in the trichomes as well as in the cuticular wax, of the tobacco leaves. The line (VviGGPS_1.3) displaying the most severe leaf surface phenotype did not show significantly different levels of any of the detected peaks. The results did indicate that some of the lines did have significantly higher levels of some of the compounds / peaks compared to the control and that the environmental conditions could impact some of the compounds. The influence of the environmental conditions on metabolite levels, especially secondary metabolites, is not surprising (Demkura & Ballaré, 2012; Llusia *et al.*, 2012; Liu, Cao, *et al.*, 2017; Kanagendran *et al.*, 2018) and any further analysis should take the growth conditions into consideration.

Based on the phenotyping results, two lines (VviGGPS_1.3 and VviGGPS_10.4) were selected for further study of the photosynthetic parameters in comparison to the control line. Both lines displayed a vegetative phenotype under low-light conditions which was intensified when plants were moved to high-light at an early or mid-growth stage of development. Carotenoid and pigment analysis of plants grown in the climaroom showed that the one line (VviGGPS_1.3) had significantly higher levels of neoxanthin, violaxanthin, lutein and chlorophyll a & b while the other line (VviGGPS_10.4) showed no significant differences to the control. These two lines were chosen since they were phenotypically different from the control plants, with one line also being metabolically different in terms of compounds involved in photosynthesis.

The photosynthetic rate of line VviGGPS_1.3 was significantly lower than the control plants during the winter growth season, while VviGGPS_10.4 showed no significant difference in the photosynthetic rate. In contrast, measurements during the Autumn growth season showed that both transgenic plants (line VviGGPS_1.3 and VviGGPS_10.4) were able to maintain a higher photosynthetic rate than the control plants. These results highlight the importance that growth conditions, specifically light, have on the phenotype observed in the *VviGGPS1* over-expressing plants.

Additionally, thermal imaging was included in the physiological measurements. The principle of this technique is the measurement of the leaf temperature which can related to the stomatal aperture and can therefore be used as an indirect measurement of the plants' photosynthetic capability

194

(Jones, 2018). The main advantage of using this method is that it is high throughput however, it does not provide the same amount of information as the IRGA system.

4.5   Conclusion

In this chapter the first aim was to update the *in silico* characterisation of the *VviGGPS* gene family. Genome annotation identified five genes encoding for GGPS, two of these were predicted to encode the SSUII while another gene putatively encoded the LSU. Two of the identified genes were predicted to encode the homomeric GGPS but only VviGGPS1 was predicted to localise to the plastids. From these results it can be concluded that *VviGGPS1* is responsible for GGPP biosynthesis in the plastid, which is the branchpoint substrate to produce various primary and secondary (specialised) metabolites.

The second aim was to conduct a preliminary characterisation of the already established tobacco transgene population over-expressing *VviGGPS1,* which can then serve as the basis for a more in-depth study. A difficulty associated with plant transformation is the variance associated with the transformation and plant regeneration method. Characterisation of the *VviGGPS1* over-expressing plant population highlighted this, as it was clear that the phenotype displayed across the lines differed. Bhat & Srinivasan (2008) recommend doing reciprocal backcross between the T_0 generation and the untransformed plants to create backcross progenies (BC_1F_1) which will contain a higher proportion of single copy transgenes. Limiting the population to individuals with only one transgene and increasing the number of independent transformants studied to at least 10 could eliminate or compensate for some of the problems associated with plant transformation methods wherein the transgene cannot be targeted to a specific locus (Birch, 1997; Bhat & Srinivasan, 2008). Backcrossing will also yield non-transgenic plants which could serve as a better control than the untransformed plants since these plants would have gone through regeneration or tissue culture which could have resulted in some variation in the population which is not attributed to the transgene (Bhat & Srinivasan, 2008). Future studies should take these consider these recommendations when establishing a transgenic population.

Multiple plant populations were grown under artificial light (climaroom) as well as under natural irradiance (greenhouse). It was found that growing the transgenic plants under natural light, which fluctuated throughout the day, resulted in an intensified transgenic phenotype that was also more consistent within a line. Plants have the capacity to respond to a changing environment through phenotypic plasticity with Bradshaw (1965) stating that the way in which an organism reacts to different environments is a characteristic that is just as important as the features observed in a homogeneous environment. Although the major hindrance for growing plants under a more natural irradiance and temperature is the resulting low reproducibility (high variance) making statistical analysis challenging, this should be weighed against the relevance of the results obtained. For

further analysis of the tobacco population over-expressing *VviGGPS1* it was decided to continue growing the plants under natural light in the greenhouse, increasing the individual plants per line whenever possible to compensate for the variation conferred with the fluctuating growth conditions.

4.6 Acknowledgements

4.7 References

Annunziata, M.G., Apelt, F., Carillo, P., Krause, U., Feil, R., Mengin, V., Lauxmann, M.A., Köhl, K., Nikoloski, Z., Stitt, M. & Lunn, J.E., (2017). Getting back to nature: A reality check for experiments in controlled environments *J. Exp. Bot.* **68**, 16, 4463–4477.

Avery, G.S.J., (1933). Structure and Germination of Tobacco Seed and the Developmental Anatomy of the Seedling Plant *Am. J. Bot.* **20**, 5, 309–327.

Bach, S.S., Bassard, J.-É., Andersen-Ranberg, J., Møldrup, M.E., Simonsen, H.T. & Hamberger, B., (2014). High-Throughput Testing of Terpenoid Biosynthesis Candidate Genes Using Transient Expression in Nicotiana benthamiana In: M. Rodríguez-concepción (ed). Plant Isoprenoids. 245–255.

Basson, C.E., (2017). Transcriptomic analysis of disease resistance responses using a tobacco-Botrytis cinerea pathosystem.

Beck, G., Coman, D., Herren, E., Ruiz-Sola, M.Á., Rodríguez-Concepción, M., Gruissem, W. & Vranová, E., (2013). Characterization of the GGPP synthase gene family in Arabidopsis thaliana *Plant Mol. Biol.* **82**, 4–5, 393–416.

Bhat, S.R. & Srinivasan, R., (2008). Molecular and genetic analyses of transgenic plants *Handb. New Technol. Genet. Improv. Legum.* **163**, 385–402.

Birch, R.G., (1997). Plant Transformation: Problems and Strategies for Practical Application *Annu. Rev. Plant Biol.* **48**, 297–326.

Blanchard, L. & Karst, F., (1993). Characterization of a lysine-to-glutamic acid mutation in a conservative sequence of farnesyl diphosphate synthase from Saccharomyces cerevisiae *Gene* **125**, 185–189.

Bollivar, D.W., (2006). Recent advances in chlorophyll biosynthesis *Photosynth. Res.* **89**, 3.

Bombarely, A., Rosli, H.G., Vrebalov, J., Moffett, P., Lukas, A., Martin, G.B., Mueller, L.A., Moffett, P., Mueller, L.A. & Martin, G.B., (2012). A Draft Genome Sequence of Nicotiana benthamiana to Enhance Molecular Plant-Microbe Biology Research *Mol. Plant-Microbe Interact.* **25**, 12, 1523–1530.

Bradshaw, A.D., (1965). Evolutionary Significance of Phenotypic Plasticity in Plants In: Adv. Genet. Vol. 13 115–155.

Burke, C. & Croteau, R., (2002). Interaction with the small subunit of geranyl diphosphate synthase modifies the chain length specificity of geranylgeranyl diphosphate synthase to produce geranyl diphosphate *J. Biol. Chem.* **277**, 5, 3141–3149.

Burke, C.C., Wildung, M.R. & Croteau, R., (1999). Geranyl diphosphate synthase: cloning, expression, and characterization of this prenyltransferase as a heterodimer. *Proc. Natl. Acad. Sci. U. S. A.* **96**, 23, 13062–7.

Camagna, M., Grundmann, A., Bar, C., Koschmieder, J., Beyer, P. & Welsch, R., (2019). Enzyme fusion removes competition for geranylgeranyl diphosphate in carotenogenesis *Plant Physiol.* **179**, 3, 1013–1027.

Catley, J.L. & Brooking, I.R., (1996). Temperature and light influence growth and flower production in Heliconia "Golden Torch" *HortScience* **31**, 2, 213–217.

Cazzonelli, C.I. & Pogson, B.J., (2010). Source to sink: regulation of carotenoid biosynthesis in plants *Trends*

Plant Sci. **15**, 5, 266–274.

Cervantes-Cervantes, M., Gallagher, C.E., Zhu, C. & Wurtzel, E.T., (2006). Maize cDNAs Expressed in Endosperm Encode Functional Farnesyl Diphosphate Synthase with Geranylgeranyl Diphosphate Synthase Activity *PLANT Physiol.* **141**, 1, 220–231.

Clough, S.J. & Bent, A.F., (1998). Floral dip: a simplified method for Agrobacterium-mediated transformation of Arabidopsis thaliana. *Plant J.* **16**, 6, 735–43.

Coman, D., Altenhoff, A., Zoller, S., Gruissem, W. & Vranová, E., (2014). Distinct evolutionary strategies in the GGPPS family from plants. *Front. Plant Sci.* **5**, May, 230.

Cornelissen, J.H.C., Lavorel, S., Garnier, E., Díaz, S., Buchmann, N., Gurvich, D.E., Reich, P.B., Steege, H. ter, Morgan, H.D., Heijden, M.G.A. van der, Pausas, J.G. & Poorter, H., (2003). A handbook of protocols for standardised and easy measurement of plant functional traits worldwide *Aust. J. Bot.* **51**, 4, 335.

Dall'Osto, L., Cazzaniga, S., Havaux, M. & Bassi, R., (2010). Enhanced photoprotection by protein-bound vs free xanthophyll pools: A comparative analysis of chlorophyll b and xanthophyll biosynthesis mutants *Mol. Plant* **3**, 3, 576–593.

Demkura, P. V. & Ballaré, C.L., (2012). UVR8 mediates UV-B-induced arabidopsis defense responses against botrytis cinerea by controlling sinapate accumulation *Mol. Plant* **5**, 3, 642–652.

Demmig-Adams, B., Winter, K., Krüger, A. & Czygan, F.C., (1989). Light response of CO2 assimilation, dissipation of excess excitation energy, and zeaxanthin content of sun and shade leaves *Plant Physiol.* **90**, 3, 881–886.

Ducluzeau, A., Wamboldt, Y., Elowsky, C.G., Mackenzie, S.A., Schuurink, R.C. & Basset, G.J.C., (2012). Gene network reconstruction identifies the authentic trans -prenyl diphosphate synthase that makes the solanesyl moiety of ubiquinone-9 in Arabidopsis *Plant J.* **69**, 2, 366–375.

Emanuelsson, O., Nielsen, H., Brunak, S. & von Heijne, G., (2000). Predicting subcellular localization of proteins based on their N-terminal amino acid sequence *J.Mol.Biol.* **300**, 4, 1005–1016.

Fasoli, M., Dal Santo, S., Zenoni, S., Tornielli, G.B., Farina, L., Zamboni, A., Porceddu, A., Venturini, L., Bicego, M., Murino, V., Ferrarini, A., Delledonne, M. & Pezzotti, M., (2012). The Grapevine Expression Atlas Reveals a Deep Transcriptome Shift Driving the Entire Plant into a Maturation Program *Plant Cell* **24**, 9, 3489–3505.

Faust, J.E., Holcombe, V., Rajapakse, N.C. & Layne, D.R., (2005). The effect of daily light integral on bedding plant growth and flowering *HortScience* **40**, 3, 645–649.

Gallois, P. & Marinho, P., (1995). Leaf Disk Transformation Using Agrobacterium tumefaciens-Expression of Heterologous Genes in Tobacco In: Plant Gene Transf. Expr. Protoc. Humana Press, New Jersey 39–48.

Gebhardt, C., (2016). The historical role of species from the Solanaceae plant family in genetic research *Theor. Appl. Genet.* **129**, 12, 2281–2294.

Gelvin, S.B., (2003). Agrobacterium-mediated plant transformation: the biology behind the "gene-jockeying" tool. *Microbiol. Mol. Biol. Rev.* **67**, 1, 16–37, table of contents.

Gutensohn, M., Orlova, I., Nguyen, T.T.H., Davidovich-Rikanati, R., Ferruzzi, M.G., Sitrit, Y., Lewinsohn, E., Pichersky, E. & Dudareva, N., (2013). Cytosolic monoterpene biosynthesis is supported by plastid-generated geranyl diphosphate substrate in transgenic tomato fruits. *Plant J.* (April, 22), 351–363.

Hirooka, K., Bamba, T., Fukusaki, E. & Kobayashi, A., (2003). Cloning and kinetic characterization of *Arabidopsis thaliana* solanesyl diphosphate synthase *Biochem. J.* **370**, 2, 679–686.

Hood, E.E., Gelvin, S.B., Melchers, L.S. & Hoekema, A., (1993). New Agrobacterium helper plasmids for gene transfer to plants *Transgenic Res.* **2**, 4, 208–218.

Hsieh, F.L., Chang, T.H., Ko, T.P. & Wang, A.H.J., (2011). Structure and mechanism of an arabidopsis medium/long-chain-length prenyl pyrophosphate synthase *Plant Physiol.* **155**, 3, 1079–1090.

Idso, S.B., Reginato, R.J., Jackson, R.D. & Pinter, P.J., (1981). Foliage and air temperatures: Evidence for a dynamic "equivalence point" *Agric. Meteorol.* **24**, 223–226.

Jeffrey, S.W., Douce, R. & Benson, A.A., (1974). Carotenoid Transformations in the Chloroplast Envelope *Proc. Natl. Acad. Sci.* **71**, 3, 807–810.

Ji, J., Wang, G., Wang, J. & Wang, P., (2009). Functional analysis of multiple carotenogenic genes from *Lycium barbarum* and *Gentiana lutea* L. for their effects on β-carotene production in transgenic tobacco *Biotechnol. Lett.* **31**, 2, 305–312.

Jones, H.G., (1999). Use of infrared thermometry for estimation of stomatal conductance as a possible aid to irrigation scheduling *Agric. For. Meteorol.* **95**, 3, 139–149.

Jones, H.G., (2018). Thermal imaging and infrared sensing in plant ecophysiology *Adv. Plant Ecophysiol. Tech.* 135–151.

Jones, M.O., Perez-Fons, L., Robertson, F.P., Bramley, P.M. & Fraser, P.D., (2013). Functional characterization of long-chain prenyl diphosphate synthases from tomato *Biochem. J.* **449**, 3, 729–740.

Jun, L., Saiki, R., Tatsumi, K., Nakagawa, T. & Kawamukai, M., (2004). Identification and subcellular

197

localization of two solanesyl diphosphate synthases from Arabidopsis thaliana *Plant Cell Physiol.* **45**, 12, 1882–1888.

Kaczperski, M.P., Carlson, W.H. & Karlsson, M.G., (1991). Growth and Development of Petunia × hybrids as a Function of Temperature and Irradiance *J. Am. Soc. Hortic. Sci.* **116**, 2, 232–237.

Kanagendran, A., Pazouki, L., Bichele, R., Külheim, C. & Niinemets, Ü., (2018). Temporal regulation of terpene synthase gene expression in Eucalyptus globulus leaves upon ozone and wounding stresses: relationships with stomatal ozone uptake and emission responses *Environ. Exp. Bot.* **155**, August, 552–565.

Kim, S., Schlicke, H., Van Ree, K., Karvonen, K., Subramaniam, A., Richter, A., Grimm, B. & Braam, J., (2013). Arabidopsis chlorophyll biosynthesis: An essential balance between the methylerythritol phosphate and tetrapyrrole pathways *Plant Cell* **25**, 12, 4984–4993.

Korczynski, P.C., Logan, J. & Faust, J.E., (2002). Mapping monthly distribution of daily light integrals across the contiguous United States *Horttechnology* **12**, 1, 12–16.

Kotowski, F., (1962). Temperature relations to germination of vegetable seed. *Proc. Am. Soc. Hortic. Sci.* **23**, 176–184.

Koyama, T., Obata, S., Osabe, M., Takeshita, A., Yokoyama, K., Uchida, M., Ishino, T. & Ogura, T., (1993). Thermostable farnesyl diphosphate synthase of bacillus stearothermophilus: Molecular cloning, sequence determination, overproduction, and purification *J. Biochem.* **113**, 3, 355–263.

Lashbrooke, J.G., Young, P.R., Strever, a. E., Stander, C. & Vivier, M. a., (2010). The development of a method for the extraction of carotenoids and chlorophylls from grapevine leaves and berries for HPLC profiling *Aust. J. Grape Wine Res.* **16**, 2, 349–360.

Lee, Y.P., Baek, K.-H., Lee, H.-S., Kwak, S.-S., Bang, J.-W. & Kwon, S.-Y., (2010). Tobacco seeds simultaneously over-expressing Cu/Zn-superoxide dismutase and ascorbate peroxidase display enhanced seed longevity and germination rates under stress conditions *J. Exp. Bot.* **61**, 9, 2499–2506.

Leng, X., Wang, P., Wang, C., Zhu, X., Li, X., Li, H., Mu, Q., Li, A., Liu, Z. & Fang, J., (2017). Genome-wide identification and characterization of genes involved in carotenoid metabolic in three stages of grapevine fruit development *Sci. Rep.* **7**, 1, 4216.

Lichtenthaler, H.K., (2007). Biosynthesis, accumulation and emission of carotenoids, α-tocopherol, plastoquinone, and isoprene in leaves under high photosynthetic irradiance *Photosynth. Res.* **92**, 2, 163–179.

Liu, H., Cao, X., Liu, X., Xin, R., Wang, J., Gao, J., Wu, B., Gao, L., Xu, C., Zhang, B., Grierson, D. & Chen, K., (2017). UV-B irradiation differentially regulates terpene synthases and terpene content of peach *Plant. Cell Environ.* **40**, 10, 2261–2275.

Liu, M., Ma, Y., Du, Q., Hou, X., Wang, M. & Lu, S., (2019). Functional analysis of polyprenyl diphosphate synthase genes involved in plastoquinone and ubiquinone biosynthesis in salvia miltiorrhiza *Front. Plant Sci.* **10**, July, 1–16.

Llorente, B., Martinez-Garcia, J.F., Stange, C. & Rodriguez-Concepcion, M., (2017). Illuminating colors: regulation of carotenoid biosynthesis and accumulation by light *Curr. Opin. Plant Biol.* **37**, 49–55.

Llusia, J., Llorens, L., Bernal, M., Verdaguer, D. & Peñuelas, J., (2012). Effects of UV radiation and water limitation on the volatile terpene emission rates, photosynthesis rates, and stomatal conductance in four Mediterranean species *Acta Physiol. Plant.* **34**, 2, 757–769.

Matsubara, S., (2018). Growing plants in fluctuating environments: why bother? *J. Exp. Bot.* **69**, 20, 4651–4654.

McCarty, D.R., (1995). Genetic Control and Integration of Maturation and Germination Pathways in Seed Development *Annu. Rev. Plant Physiol. Plant Mol. Biol.* **46**, 1, 71–93.

McGarvey, P. & Kaper, J.M., (1991). A simple and rapid method for screening transgenic plants using the PCR. *Biotechniques* **11**, 4, 428–32.

Miransari, M. & Smith, D.L., (2014). Plant hormones and seed germination *Environ. Exp. Bot.* **99**, 110–121.

Moreno, J.C., Cerda, A., Simpson, K., Lopez-Diaz, I., Carrera, E., Handford, M. & Stange, C., (2016). Increased *Nicotiana tabacum* fitness through positive regulation of carotenoid, gibberellin and chlorophyll pathways promoted by *Daucus carota* lycopene β-cyclase (*Dclcyb1*) expression *J. Exp. Bot.* **67**, 8, 2325–2338.

Murashige, T. & Skoog, F., (1962). A revised medium for rapid growth and bioassays with tobacco tissue culture *Physiol. Plant.* **15**, 473–497.

Nambara, E. & Marion-Poll, A., (2005). Abscisic Acid Biosynthesis and Catabolism *Annu. Rev. Plant Biol.* **56**, 1, 165–185.

Nielsen, H., Engelbrecht, J., Brunak, S. & Von Heijne, G., (1997). Identification of prokaryotic and eukaryotic signal peptides and prediction of their cleavage sites *Protein Eng.* **10**, 1, 1–6.

Oh, S.K., In Jeong Kim, Dong Ho Shin, Yang, J., Kang, H. & Han, K.H., (2000). Cloning, characterization, and heterologous expression of a functional geranylgeranyl pyrophosphate synthase from sunflower (Helianthus annuus L.) *J. Plant Physiol.* **157**, 5, 535–542.

198

Oh, W., Cheon, I.H., Kim, K.S. & Runkle, E.S., (2009). Photosynthetic daily light integral influences flowering time and crop characteristics of *Cyclamen persicum* *HortScience* **44**, 2, 341–344.

Okada, K., Saito, T., Nakagawa, T., Kawamukai, M. & Kamiya, Y., (2000). Five geranylgeranyl diphosphate synthases expressed in different organs are localized into three subcellular compartments in Arabidopsis. *Plant Physiol.* **122**, April, 1045–1056.

Orlova, I., Nagegowda, D.A., Kish, C.M., Gutensohn, M., Maeda, H., Varbanova, M., Fridman, E., Yamaguchi, S., Hanada, A., Kamiya, Y., Krichevsky, A., Citovsky, V., Pichersky, E. & Dudareva, N., (2009). The Small Subunit of Snapdragon Geranyl Diphosphate Synthase Modifies the Chain Length Specificity of Tobacco Geranylgeranyl Diphosphate Synthase in Planta *Plant Cell* **21**, 12, 4002–4017.

du Plessis, A., le Roux, S.G. & Guelpa, A., (2016). The CT Scanner Facility at Stellenbosch University: An open access X-ray computed tomography laboratory *Nucl. Instruments Methods Phys. Res. Sect. B Beam Interact. with Mater. Atoms* **384**, 42–49.

Procházková, D., Haisel, D. & Wilhelmová, N., (2009). Content of carotenoids during ageing and senescence of tobacco leaves with genetically modulated life-span *Photosynthetica* **47**, 3, 409–414.

Ranal, M. a. & Santana, D.G. De, (2006). How and why to measure the germination process? *Rev. Bras. Botânica* **29**, 1, 1–11.

Reid, K.E., Olsson, N., Schlosser, J., Peng, F. & Lund, S.T., (2006). An optimized grapevine RNA isolation procedure and statistical determination of reference genes for real-time RT-PCR during berry development. *BMC Plant Biol.* **6**, 27.

Ruiz-Sola, M.Á. & Rodríguez-Concepción, M., (2012). Carotenoid Biosynthesis in Arabidopsis: A Colorful Pathway *Arab. B.* **10**, e0158.

Ruiz-Sola, M.Á., Coman, D., Beck, G., Barja, M.V., Colinas, M., Graf, A., Welsch, R., Rütimann, P., Bühlmann, P., Bigler, L., Gruissem, W., Rodríguez-Concepción, M. & Vranová, E., (2016). Arabidopsis GERANYLGERANYL DIPHOSPHATE SYNTHASE 11 is a hub isozyme required for the production of most photosynthesis-related isoprenoids *New Phytol.* **209**, 1, 252–264.

Ruiz-Sola, M.Á., Barja, M.V., Manzano, D., Llorente, B., Schipper, B., Beekwilder, J. & Rodriguez-Concepcion, M., (2016). A Single Arabidopsis Gene Encodes Two Differentially Targeted Geranylgeranyl Diphosphate Synthase Isoforms *Plant Physiol.* **172**, 3, 1393–1402.

Runkle, E., (2006a). Do you know what your DLI is? *Greenh. Prod. News* **December**, 66.

Runkle, E., (2006b). Daily Light Integral Defined *Greenh. Prod. News* November, 70.

Sacchettini, J.C. & Poulter, C.D., (1997). Creating isoprenoid diversity. *Science* **277**, 5333, 1788–9.

Saeed, W., Naseem, S. & Ali, Z., (2017). Strigolactones biosynthesis and their role in abiotic stress resilience in plants: A critical review *Front. Plant Sci.* **8**, August, 1–13.

Sallaud, C., Giacalone, C., Töpfer, R., Goepfert, S., Bakaher, N., Rösti, S. & Tissier, A., (2012). Characterization of two genes for the biosynthesis of the labdane diterpene Z -abienol in tobacco (Nicotiana tabacum) glandular trichomes *Plant J.* **72**, 1, 1–17.

van Schie, C.C.N., Haring, M.A. & Schuurink, R.C., (2012). Prenyldiphosphate Synthases and Gibberellin Biosynthesis In: Isoprenoid Synth. Plants Microorg. Springer New York, New York, NY 213–232.

Schmidt, A., Wachtler, B., Temp, U., Krekling, T., Seguin, A. & Gershenzon, J., (2010). A Bifunctional Geranyl and Geranylgeranyl Diphosphate Synthase Is Involved in Terpene Oleoresin Formation in Picea abies *Plant Physiol.* **152**, 2, 639–655.

Schuman, M.C. & Baldwin, I.T., (2016). The Layers of Plant Responses to Insect Herbivores *Annu. Rev. Entomol.* **61**, 1, 373–394.

Sepúlveda-Reyes, D., Ingram, B., Bardeen, M., Zúñiga, M., Ortega-Farías, S. & Poblete-Echeverría, C., (2016). Selecting canopy zones and thresholding approaches to assess grapevine water status by using aerial and ground-based thermal imaging *Remote Sens.* **8**, 10, 1–16.

Sierro, N., Battey, J.N.D., Ouadi, S., Bakaher, N., Bovet, L., Willig, A., Goepfert, S., Peitsch, M.C. & Ivanov, N. V, (2014). The tobacco genome sequence and its comparison with those of tomato and potato *Nat. Commun.* **5**, May, 1–9.

Slot, M.M., van de Wiel, C.C.M., Kleter, G.A., Visser, R.G.F. & Kok, E.J., (2018). The assessment of field trials in GMO research around the world and their possible integration in field trials for variety registration *Transgenic Res.* **27**, 4, 321–329.

Song, L. & Poulter, C.D., (1994). Yeast farnesyl-diphosphate synthase: Site-directed mutagenesis of residues in highly conserved prenyltransferase domains I and II *Proc. Natl. Acad. Sci. U. S. A.* **91**, 8, 3044–3048.

Tarshis, L.C., Proteau, P.J., Kellogg, B.A., Sacchettini, J.C. & Poulter, C.D., (1996). Regulation of product chain length by isoprenyl diphosphate synthases. *Proc. Natl. Acad. Sci. U. S. A.* **93**, 26, 15018–23.

Thayer, S.S. & Björkman, O., (1990). Leaf Xanthophyll content and composition in sun and shade determined by HPLC *Photosynth. Res.* **23**, 3, 331–343.

Tholl, D., Kish, C.M., Orlova, I., Sherman, D., Gershenzon, J., Pichersky, E. & Dudareva, N., (2004). Formation of Monoterpenes in Antirrhinum majus and Clarkia breweri Flowers Involves Heterodimeric Geranyl

199

Diphosphate Synthases *Plant Cell* **16**, 4, 977–992.

Umehara, M., Hanada, A., Yoshida, S., Akiyama, K., Arite, T., Takeda-Kamiya, N., Magome, H., Kamiya, Y., Shirasu, K., Yoneyama, K., Kyozuka, J. & Yamaguchi, S., (2008). Inhibition of shoot branching by new terpenoid plant hormones *Nature* **455**, 7210, 195–200.

Vandermoten, S., Haubruge, É. & Cusson, M., (2009). New insights into short-chain prenyltransferases: structural features, evolutionary history and potential for selective inhibition *Cell. Mol. Life Sci.* **66**, 23, 3685–3695.

Vranová, E., Coman, D., Gruissem, W., Vranov, E., Coman, D., Gruissem, W., Vranová, E., Coman, D. & Gruissem, W., (2013). Network Analysis of the MVA and MEP Pathways for Isoprenoid Synthesis *Annu. Rev. Plant Biol.* **64**, 1, 665–700.

Wang, D., Wang, S., Chao, J., Wu, X., Sun, Y., Li, F., Lv, J., Gao, X., Liu, G. & Wang, Y., (2017). Morphological phenotyping and genetic analyses of a new chemical-mutagenized population of tobacco (Nicotiana tabacum L.) *Planta* 11.

Wang, G. & Dixon, R. a, (2009). Heterodimeric geranyl(geranyl)diphosphate synthase from hop (Humulus lupulus) and the evolution of monoterpene biosynthesis. *Proc. Natl. Acad. Sci. U. S. A.* **106**, 24, 9914–9.

Wang, K. & Ohnuma, S., (1999). Chain-length determination mechanism of isoprenyl diphosphate synthases and implications for molecular evolution. *Trends Biochem. Sci.* **24**, 11, 445–51.

Wang, Q., Huang, X.-Q., Cao, T.-J., Zhuang, Z., Wang, R. & Lu, S., (2018). Heteromeric Geranylgeranyl Diphosphate Synthase Contributes to Carotenoid Biosynthesis in Ripening Fruits of Red Pepper (Capsicum annuum var. conoides) *J. Agric. Food Chem.* **66**, 44, 11691–11700.

Von Wettstein, D., Gough, S. & Kannangara, C.G., (1995). Chlorophyll biosynthesis *Plant Cell* **7**, 7, 1039–1057.

Yang, X., Chen, L., He, J. & Yu, W., (2017). Knocking out of carotenoid catabolic genes in rice fails to boost carotenoid accumulation, but reveals a mutation in strigolactone biosynthesis *Plant Cell Rep.* **36**, 10, 1533–1545.

Young, P.R., (2004). Molecular analyses of candidate carotenoid biosynthetic genes in <i>Vitis vinifera<i/> L. Stellenbosch University.

Young, P.R., Eyeghe-Bickong, H.A., du Plessis, K., Alexandersson, E., Jacobson, D.A., Coetzee, Z., Deloire, A. & Vivier, M.A., (2016). Grapevine Plasticity in Response to an Altered Microclimate: Sauvignon Blanc Modulates Specific Metabolites in Response to Increased Berry Exposure. *Plant Physiol.* **170**, 3, 1235–1254.

Zhou, F., Wang, C.-Y., Gutensohn, M., Jiang, L., Zhang, P., Zhang, D., Dudareva, N. & Lu, S., (2017). A recruiting protein of geranylgeranyl diphosphate synthase controls metabolic flux toward chlorophyll biosynthesis in rice *Proc. Natl. Acad. Sci.* (June, 12), 201705689.

Zhu, F., Suzuki, K., Okada, K., Tanaka, K., Nakagawa, T., Kawamukai, M., Matsuda, H., Zhu, X.F., Suzuki, K., Okada, K., Tanaka, K., Nakagawa, T., Kawamukai, M. & Matsuda, K., (1997). Cloning and Functional Expression of a Novel Geranylgeranyl Pyrophosphate Synthase Gene from *Arabidopsis thaliana* in *Escherichia coli Plant Cell Physiol.* **38**, 3, 357–361.

Zhu, X., Suzuki, K., Saito, T., Okada, K., Tanaka, K., Nakagawa, T., Matsuda, H. & Kawamukai, M., (1997). Geranylgeranyl pyrophosphate synthase encoded by the newly isolated gene GGPS6 from Arabidopsis thaliana is localized in mitochondria *Plant Mol. Biol.* **35**, 3, 331–341.

Appendix A   To Chapter 4

A4.1   Functional complementation of isolated VviGGPS

The isolation and cloning of the *VviGGPS* gene into the pART27 plant expression construct is described in (Young, 2004) with functional complementation in *E. coli* and analysis via HPLC of carotenoids produced to confirm gene functionality done by Young (unpublished) with results shown in **Figure A-i** .
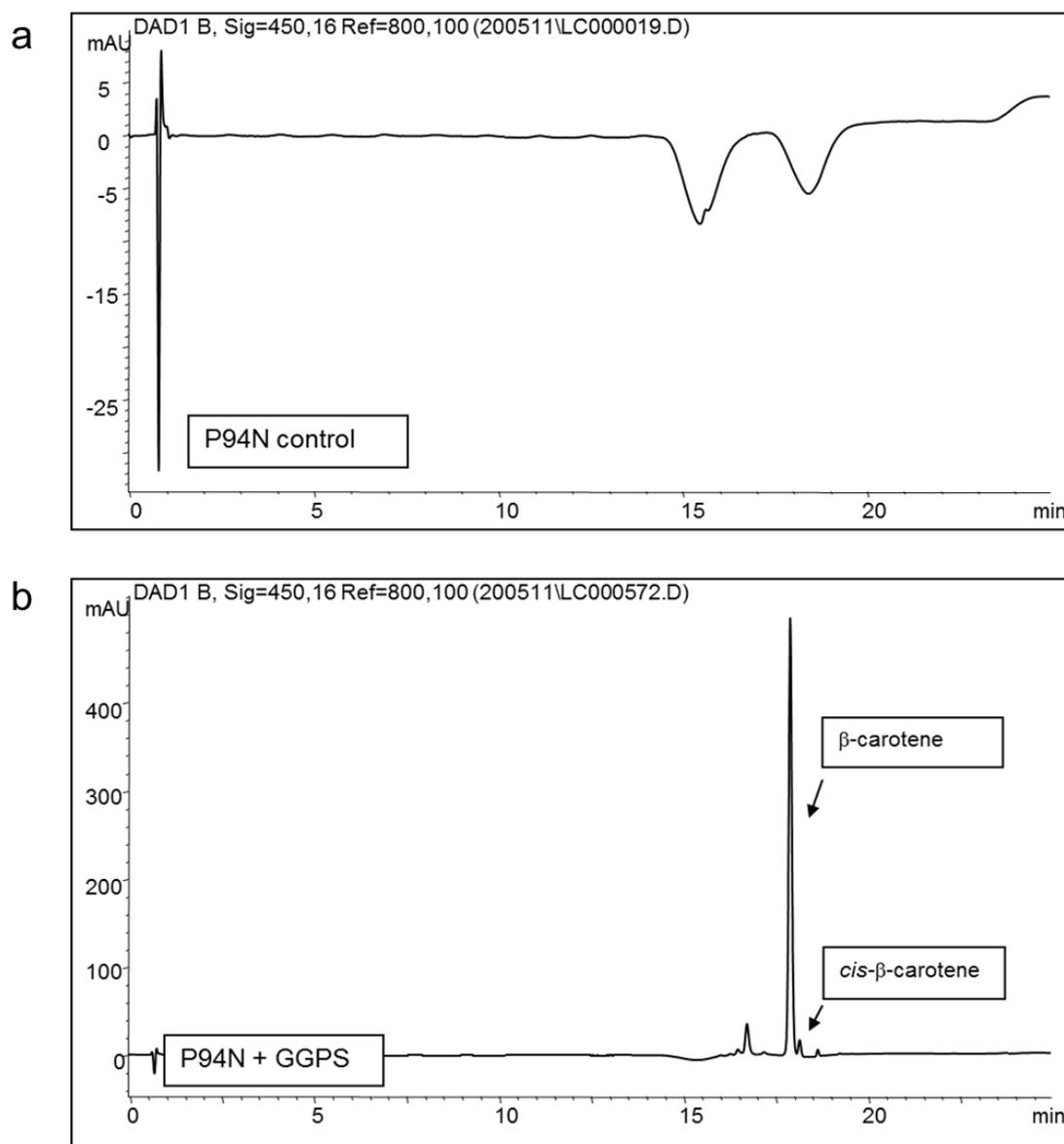
Figure A-i HPLC analysis of the *E. coli* cultures expressing the empty expression vector (a) and the vector containing the isolated *VviGGPS* (b).

A4.2   Plant transformation and genetic characterisation of transformants

Plant transformation and genetic characterisation was done by Young (unpublished) with the methods and materials utilised described below.

The construct was transformed into *Agrobacterium tumefaciens* strain EHA105 (Hood *et al.*, 1993) with electroporation. For plant transformation, tobacco plantlets (*Nicotiana tabacum* L. cv. Petit Havana SR1) were grown *in vitro* on MS medium (Murashige & Skoog, 1962) and incubated at 26°C with 16 h light 8 h dark (LD) photoperiod. The protocol established by Gallois & Marinho (1995) was used to transform tobacco leaf discs with pART27-*VviGGPS* construct. Transformed leaf discs were encouraged to form shoots on MS media supplemented with 0.5 µg/mL 6-benzyl-aminopurine (BAP). Induction of rooting was done by culturing plantlets on MS media supplemented with 0.1 µg/mL 1-Naphthaleneacetic acid (NAA). Selection for the transformed plant material was maintained with the addition of 100 µg/mL kanamycin to the media. Several putative primary transgenic lines (T0) were selected.

The T0 generation plants were hardened-off and allowed to develop to the flowering stage with the T1 generation produced through self-fertilisation of the T0 flowers. Nucleic acid was extracted from the T1 generation plants using the method described by McGarvey & Kaper (1991) for genomic DNA (gDNA) and total RNA extracted using TRIzol reagent (Invitrogen, Carlsbad, USA) according to the manufacturer's instructions.

The T1 generation was genetically characterised with gene copy number and clonal copies determined with Southern hybridisation and transgene expression established with northern hybridisation. Gel electrophoresis, nucleic acid transfer to membranes, hybridisation and detection of probes were done according to methods described in the DIG application manual 2008 (Roche Diagnostics GmbH, Mannheim, Germany). The probes were PCR-labelled according to the supplier' instructions (Roche Diagnostics GmbH, Mannheim, Germany). For Southern blot, the gDNA was RNAse-treated before overnight enzyme digestion with *Eco*RV. The northern and Southern hybridisation results are shown in **Figure A-ii** for the lines included in this chapter.
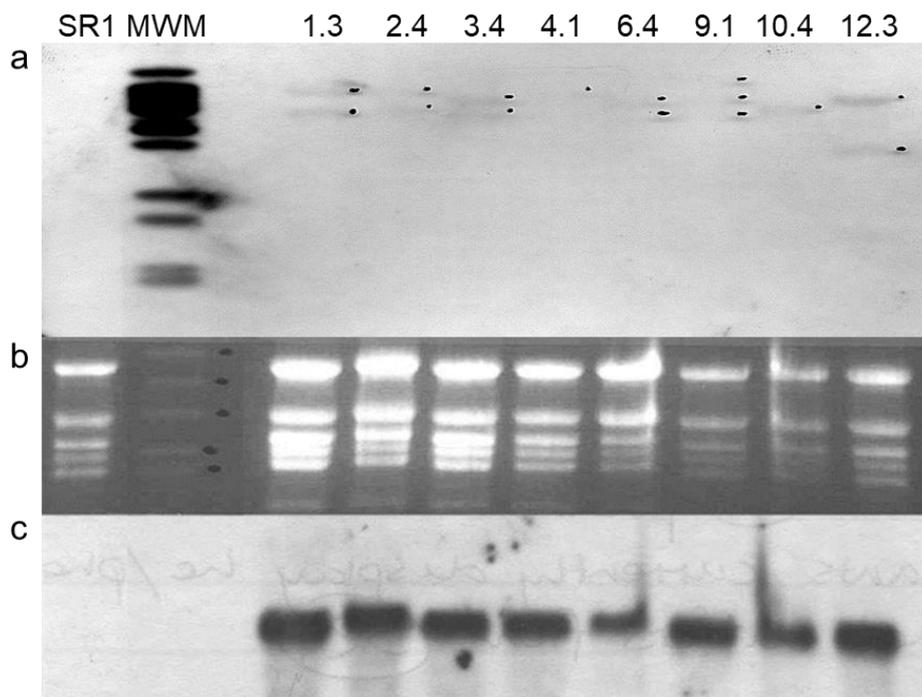
Figure A-ii Genetic characterisation of T1 tobacco population transformed with *VviGGPS* under the control of a constitutive promoter. Southern hybridisation to determine copy number (a), total RNA gel (b) and northern blot (c) to determine transgene expression. The molecular weight marker (MWM) for the Southern hybridisation was λDNA-*Bst*EII digest with total genomic DNA isolated from tobacco digested with *Eco*RV. MWM for the northern hybridisation was RiboRuler™ High Range RNA Ladder.

Appendix B   to Chapter 4
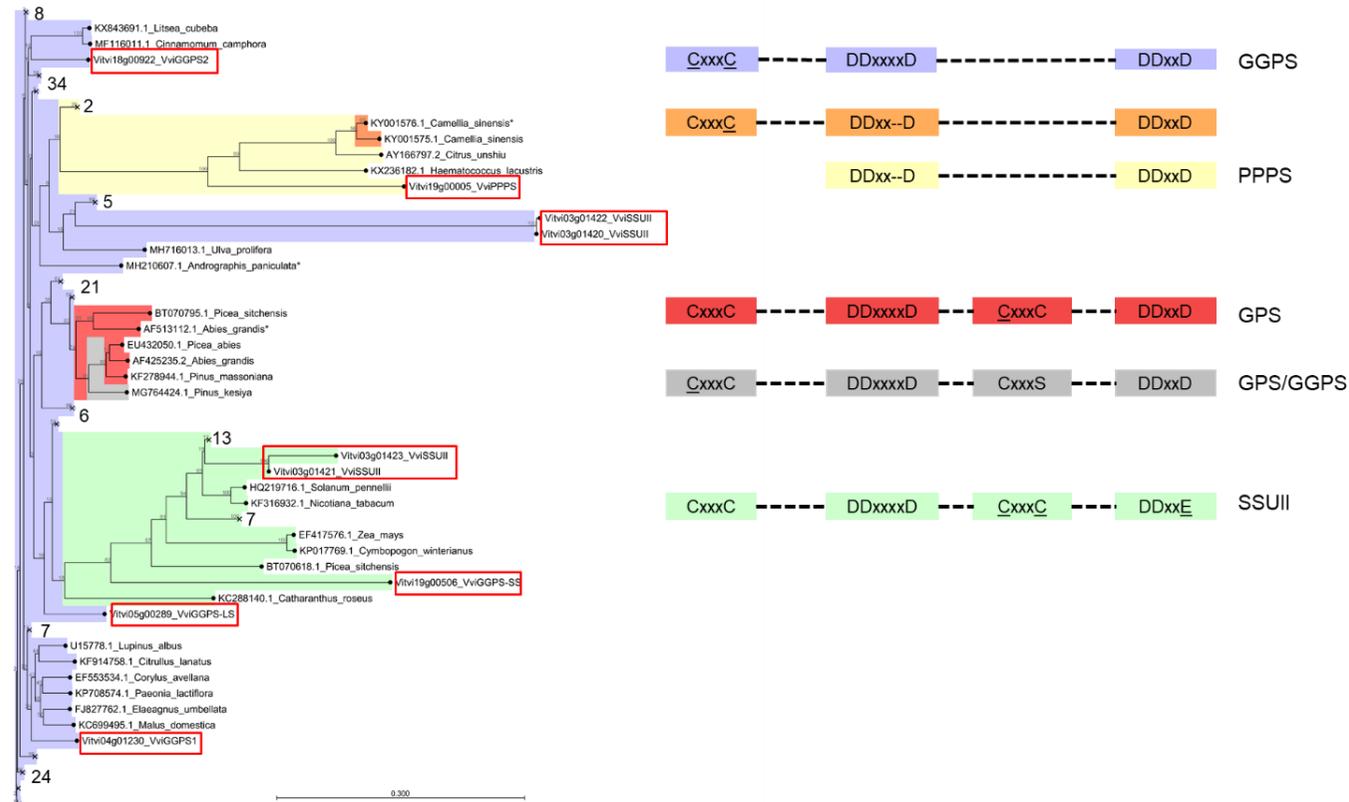
Figure B-i Unrooted phylogenetic tree of predicted and characterised geranylgeranyl diphosphate synthase (GGPSs) of plants. Sequences were retrieved from Genbank and converted to amino acid sequences. Multiple sequence alignment (MSA) using the amino acid sequences was done using the characteristic motifs as fixed points with the end gap cost set at cheap. A Neighbour-Joining tree was constructed with the MSA using the Dayhoff (PAM) substitution model with default settings and 1000 pseudoreplicates to obtain a bootstrap value. The subtrees of the phylogenetic tree are highlighted according to the motifs. The characteristic motifs detected in the sequences are summarised on the right with underlined letters indicating variable amino acid residues. Putative homologs based on the characteristic motifs described by Coman et al. (2014) are shown. GGPS – geranyl geranyl diphosphate synthase; PPPS – polyprenyl diphosphate synthase; GPS – geranyl diphosphate synthase; GPS/GGPS – bifunctional GPS/GGPS; SSUII – small subunit of heterodimeric GPS. Branches were collapsed with the number of members shown, sequences with high similarity isolated from the same species were collapsed to one representative and indicated with (*). The predicted grapevine sequences are highlighted with red boxes.

Appendix C   To Chapter 4

Table C-i Non-ambiguous probes for the putative VviIDSs and VviTPSs. *CRIBI_V2.1 and **VCost_v3 accession as found on the https://urgi.versailles.inra.fr/Species/Vitis website. ***Unique NimbleGen probes as determined in this study. Probes highlighted show low correlation with other probes mapping to the same gene and were therefore not used for the calculation of the average.

Gene ID	V2 ID*	VCost_v3 ID**	Unique NimbleGen probes***	Comment
VviGGPS1	VIT_204s0023g01210	Vitvi04g01230	VitusP00182585 VitusP00182586 VitusP00182588	
VviGGPS2	VIT_218s0001g12000	Vitvi18g00922	VitusP00118512 VitusP00118518 VitusP00118514 VitusP00118516	No probe ambiguity per V3 annotated gene
VviGGPS-LS	VIT_205s0020g01240	Vitvi05g00289	VitusP00197681 VitusP00197689 VitusP00197686	
VviGGPS-SS	VIT_219s0090g00530	Vitvi19g00506	VitusP00139585 VitusP00139592 VitusP00139589 VitusP00139587	No probe ambiguity per V3 annotated gene
VviSSUII	VIT_203s0038g03050	Vitvi03g01420	VitusP00171005	Probe binding to Vitvi03g01422
		Vitvi03g01421	No Probe	
		Vitvi03g01422	VitusP00171005	Probe binding to Vitvi03g01420
		Vitvi03g01423	No Probe	
VviPPPS	VIT_219s0014g00070	Vitvi19g00005	VitusP00133691 VitusP00133694 VitusP00133697 VitusP00133696	No probe ambiguity per V3 annotated gene

205
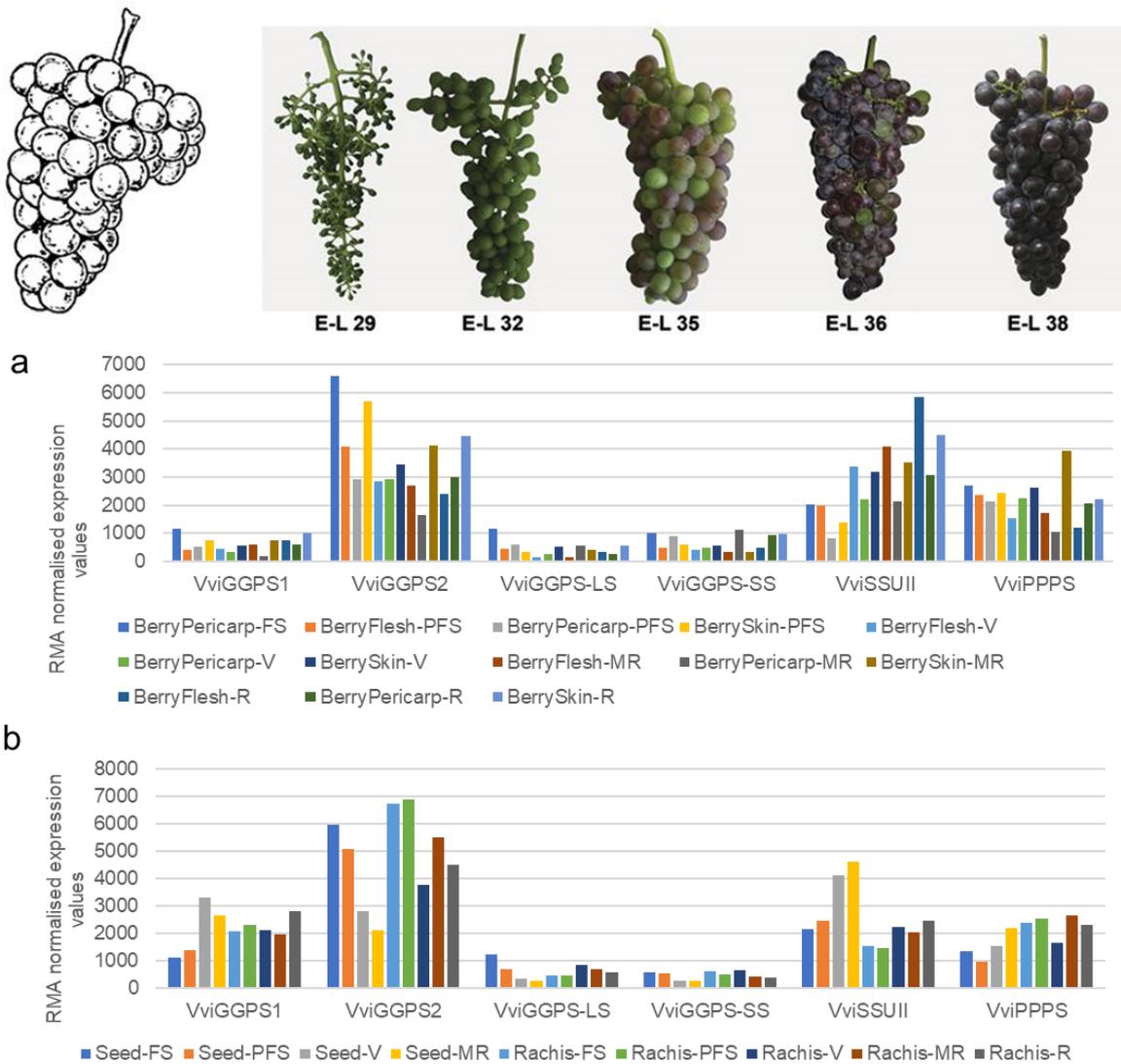
Figure C-i Average gene expression from selected probes in the berry bunch sampled during the various stages of berry development, these being fruit set (FS, E-L 29), post fruit set (PFS, E-L 32), véraison (V, E-L 35), mid-ripening (MR, E-L 36) up until ripe stage (R, E-L 38). Expression shown in various tissue of berry bunch with the berry skin, pericarp and flesh in top graph (a) and the seeds and rachis in the bottom graph (b).
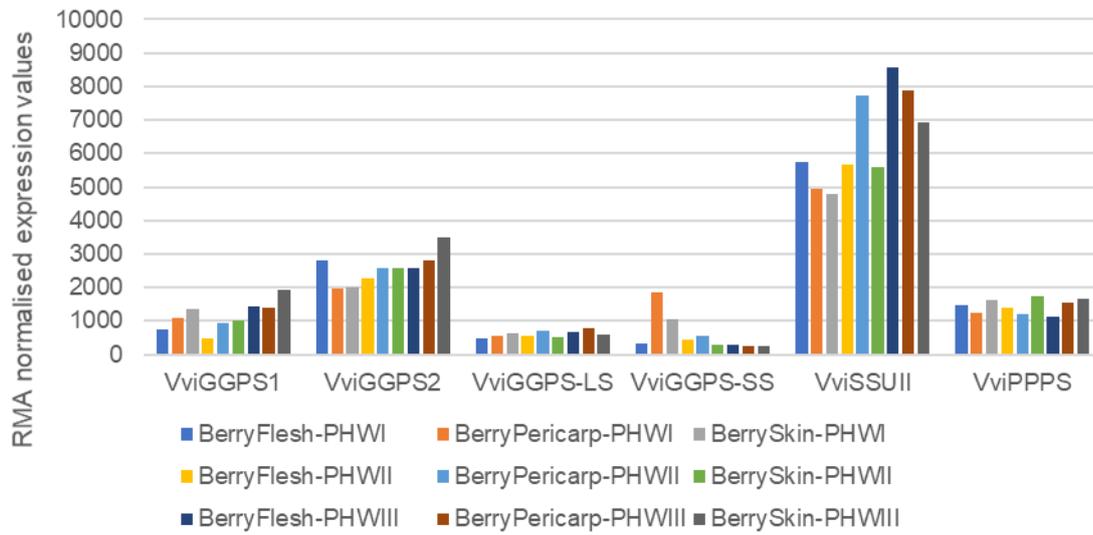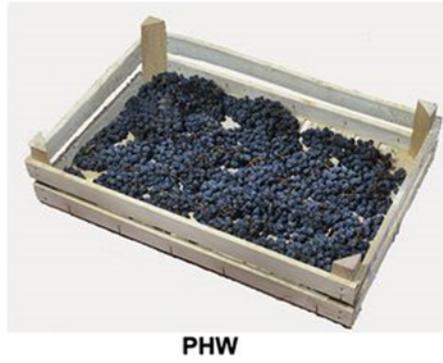
206

PHW

Figure C-ii Average gene expression from selected probes in berries sampled during the three post-harvest withering stages (1 to 3 months).
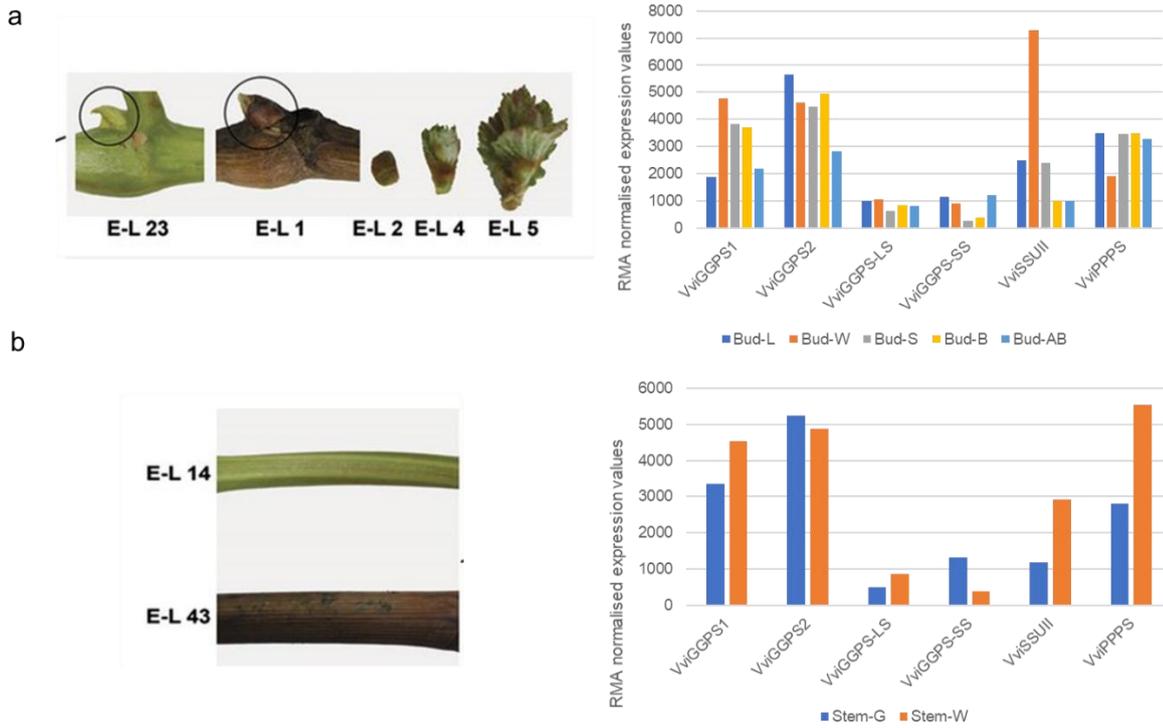
Figure C-iii Average gene expression from selected probes in bud tissue (a) sampled in the latent bud (L, E-L 23), winter bud (W, E-L 1), during bud swell (S, E-L 2), bud burst (B, E-L 4) and after bud burst (AB, E-L 5) and the stem (b) sampled in the green stem (G, E-L 14) and the woody stem (W, E-L 43).

208
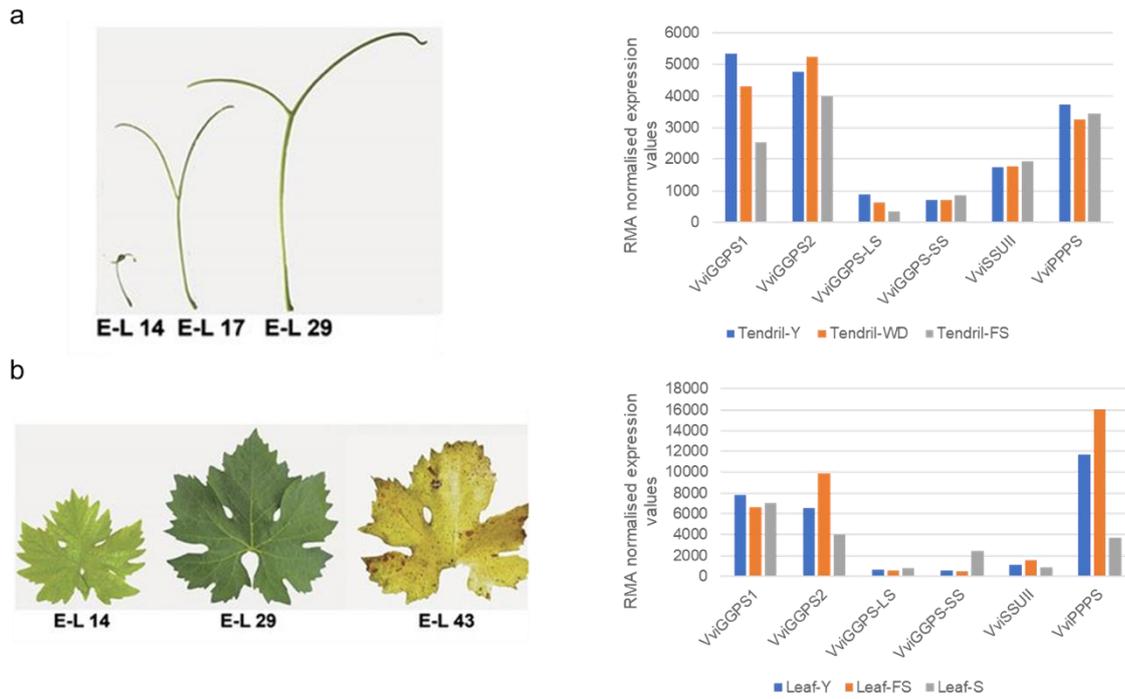
Figure C-iv Average gene expression from selected probes in the Tendril (a) at the young (Y, E-L 14), well – developed (WD, E-L 17) and mature (FS, E-L 29) stages of development and in the leaf (b) at the young (Y, E-L 14), mature (FS, E-L 29) and senescing (S, E-L 43) stages of leaf development.

209

a

b
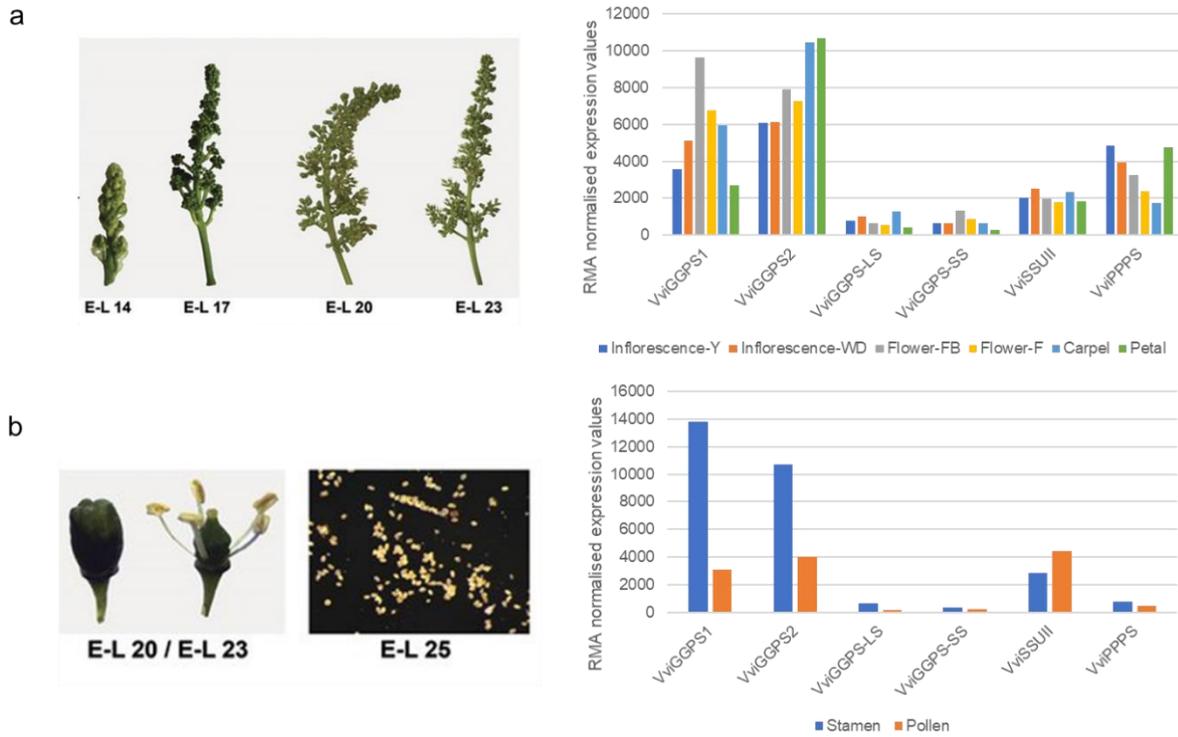
Figure C-v Average gene expression from selected probes in the flower (a) at young inflorescence (Y, E-L 14), well-developed inflorescence (WD, E-L 17), in flowers at the 10% caps off (FB, E-L 20) and 50% caps off (F, E-L 23) as well as the pooled carpel and petal tissue of flowers at E-L 20 and E-L 23 stages of development. Expression in the pooled stamen tissue of flowers at E-L 20 and E-L 23 stages of development as well as the pollen from flowers with more 50% caps off (E-L 25) is shown in figure b.
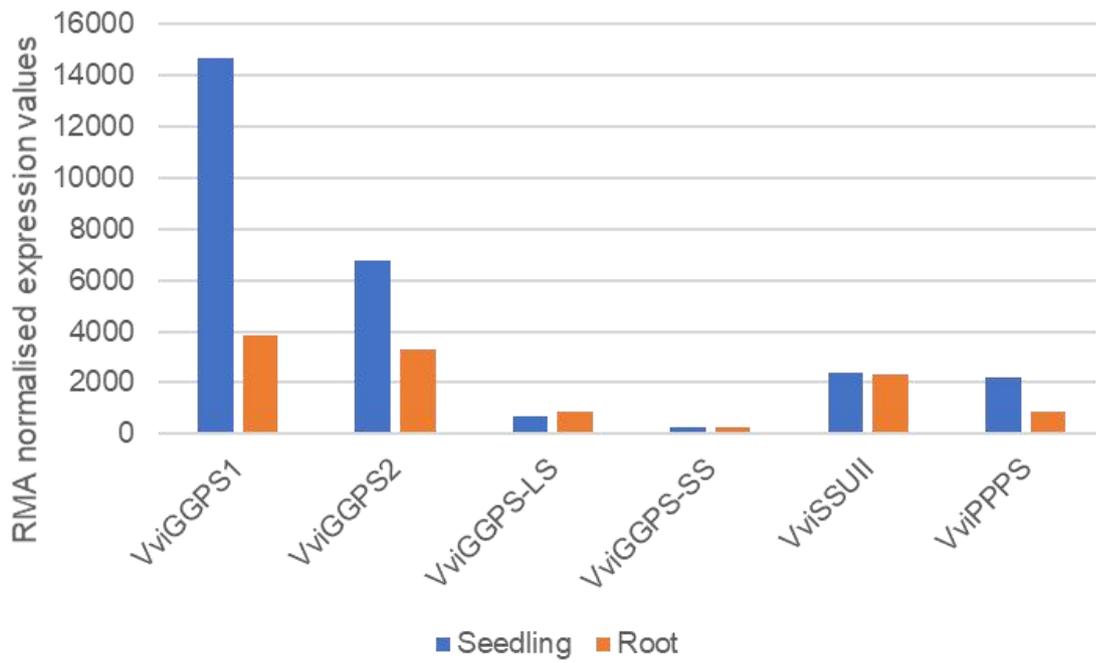
210

Figure C-vi Average gene expression from selected probes in the pooled seedling tissue at three stages of development and root samples from in vitro cultured plantlets.

Appendix D   To Chapter 4
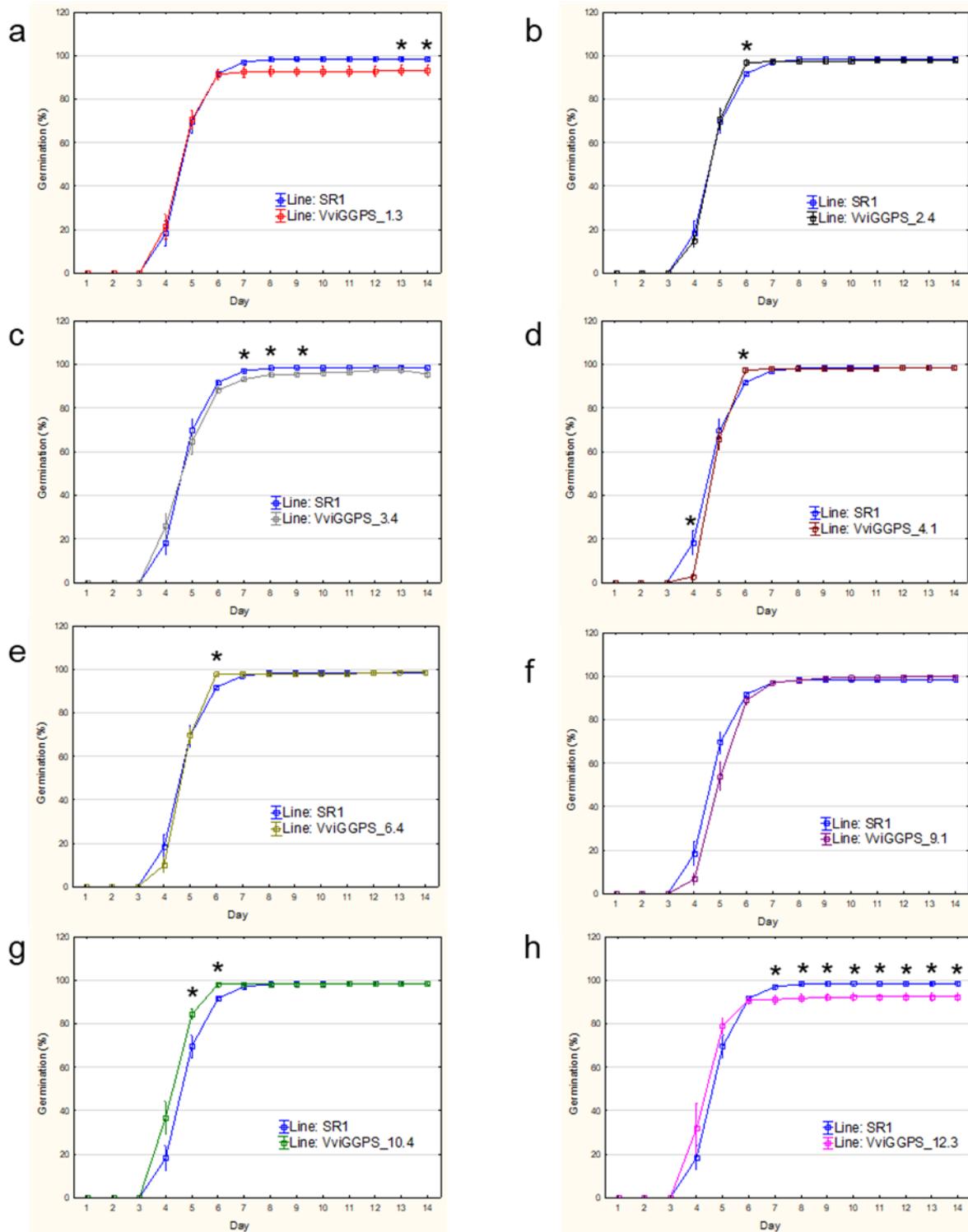
Figure D-i Germination of transgenic seeds in comparison to untransformed (control) seeds. Each point is an average of six repeats with error bars indicating the standard error between repeats. *indicates significant difference of transgenic seed from control seeds as determined with student's *t*-test (p < 0.05).
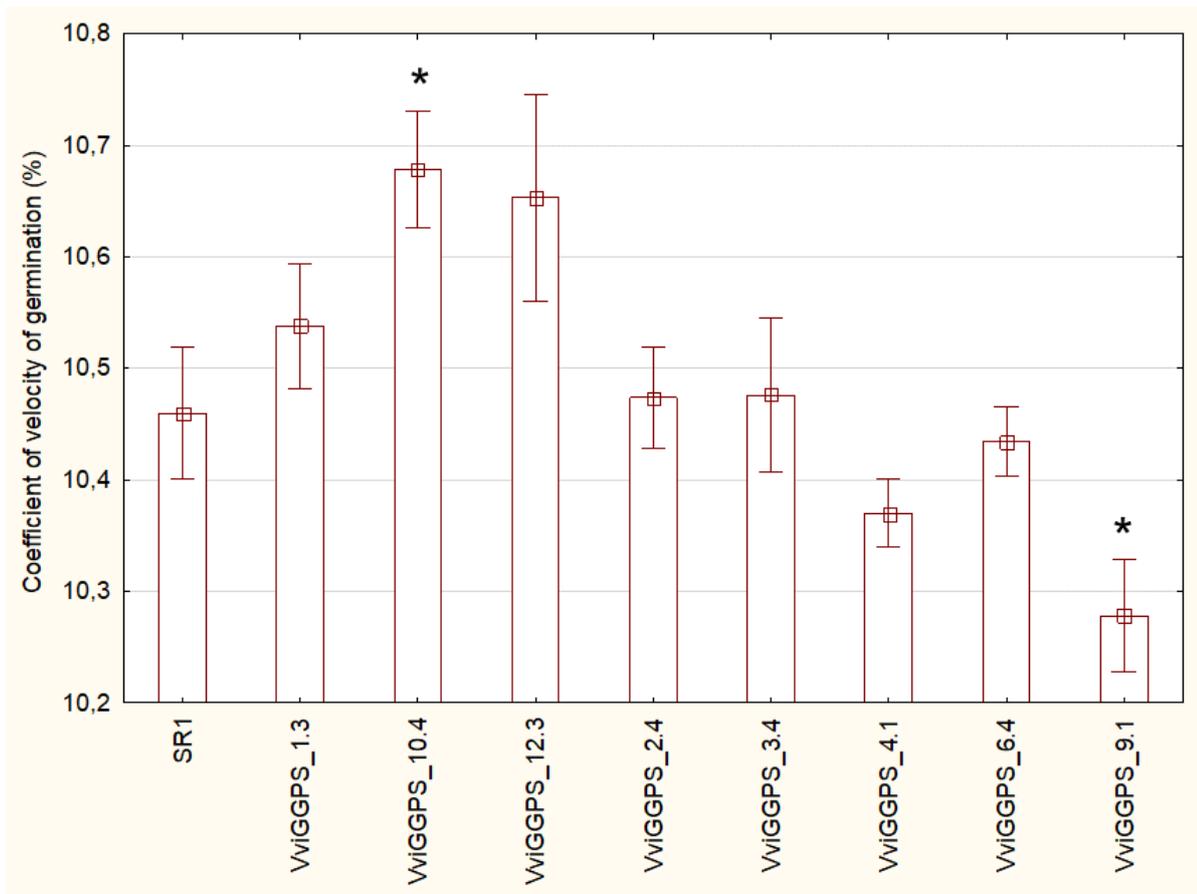
Figure D-ii Germination rate determined based on method described by (Kotowski, 1962). Bar graph show average of six repeats and error bars the standard error. *indicates significant difference of transgenic seed from control seeds as determined with student's *t*-test ($p < 0.05$).

213

Appendix E   To Chapter 4

Table E-i Leaf 3 sampled in plants grown in climaroom (low-light) with six plants per line sampled and analysed. Significant differences from the control population (Control_SR1) highlighted in red. Carotenoid and pigment concentrations shown as ng.mgFW^{-1}. Levels/peak area for Lutein epoxide, Antheraxanthin and Zeaxanthin was below the LOD and/or LOQ for many samples with the results not included in the Table (The DEPS ratio was therefore not calculated).

|	Control_SR1	VviGGPS_1.3	VviGGPS_2.4	VviGGPS_3.4	VviGGPS_4.1	VviGGPS_6.4	VviGGPS_9.1	VviGGPS_10.4	VviGGPS_12.3
LMA (mg/cm^2)	28.3 ± 1.5	34.5 ± 16.8	28.7 ± 3.6	29.3 ± 1.5	27.8 ± 2.6	28.6 ± 2.5	26.9 ± 2.6	28.1 ± 11	27.8 ± 1.2
length/width	1.6 ± 0.1	1.7 ± 0.1	1.8 ± 0.1	1.7 ± 0.2	1.7 ± 0.1	1.7 ± 0.1	1.7 ± 0.2	1.8 ± 0.1	1.8 ± 0.2
Neoxanthin	30.6 ± 7	47.1 ± 7.6	32.8 ± 5.8	35 ± 4.8	29.6 ± 4.2	45.9 ± 2.2	50 ± 4.8	34 ± 6.9	34.4 ± 8.5
Violaxanthin	26.6 ± 5.5	41.4 ± 4.3	30.9 ± 6	31 ± 4	26.6 ± 2.9	41.4 ± 2	43.9 ± 5.8	28.7 ± 3.6	30.8 ± 7.3
Lutein	79.2 ± 14.7	120.9 ± 20.1	81.9 ± 12	90.5 ± 10.5	77.9 ± 9.4	115 ± 6.1	126.8 ± 11.8	88.9 ± 17.8	89.5 ± 21.4
ß-carotene	815.2 ± 22.1	809.3 ± 13.8	818.9 ± 30.2	825.9 ± 28.8	824.3 ± 18.3	811.8 ± 24.9	828.9 ± 35	816.3 ± 36.4	811.3 ± 16.9
Chlorophyll a	318.6 ± 71.3	494.6 ± 84.6	329.6 ± 49.7	370.6 ± 50.5	312.8 ± 44.9	487.7 ± 29.9	528.2 ± 49.4	350.3 ± 77	357.2 ± 91
Chlorophyll b	398.9 ± 90.8	624 ± 99.5	422.8 ± 65.6	472.3 ± 60.9	402.1 ± 58.6	625.9 ± 39.8	694 ± 80.2	445.6 ± 76	463.5 ± 117.6
Chl a/b ratio	0.8 ± 0.03	0.79 ± 0.03	0.78 ± 0.03	0.79 ± 0.02	0.78 ± 0.01	0.78 ± 0.02	0.76 ± 0.03	0.78 ± 0.04	0.77 ± 0.01
V+A+Z	29.1 ± 5.7	44.3 ± 4.7	32.6 ± 7.6	33.4 ± 4.7	28.1 ± 4.3	45.8 ± 3.8	49.4 ± 8.4	31.1 ± 6.1	32.7 ± 8.4

Appendix F   To Chapter 4
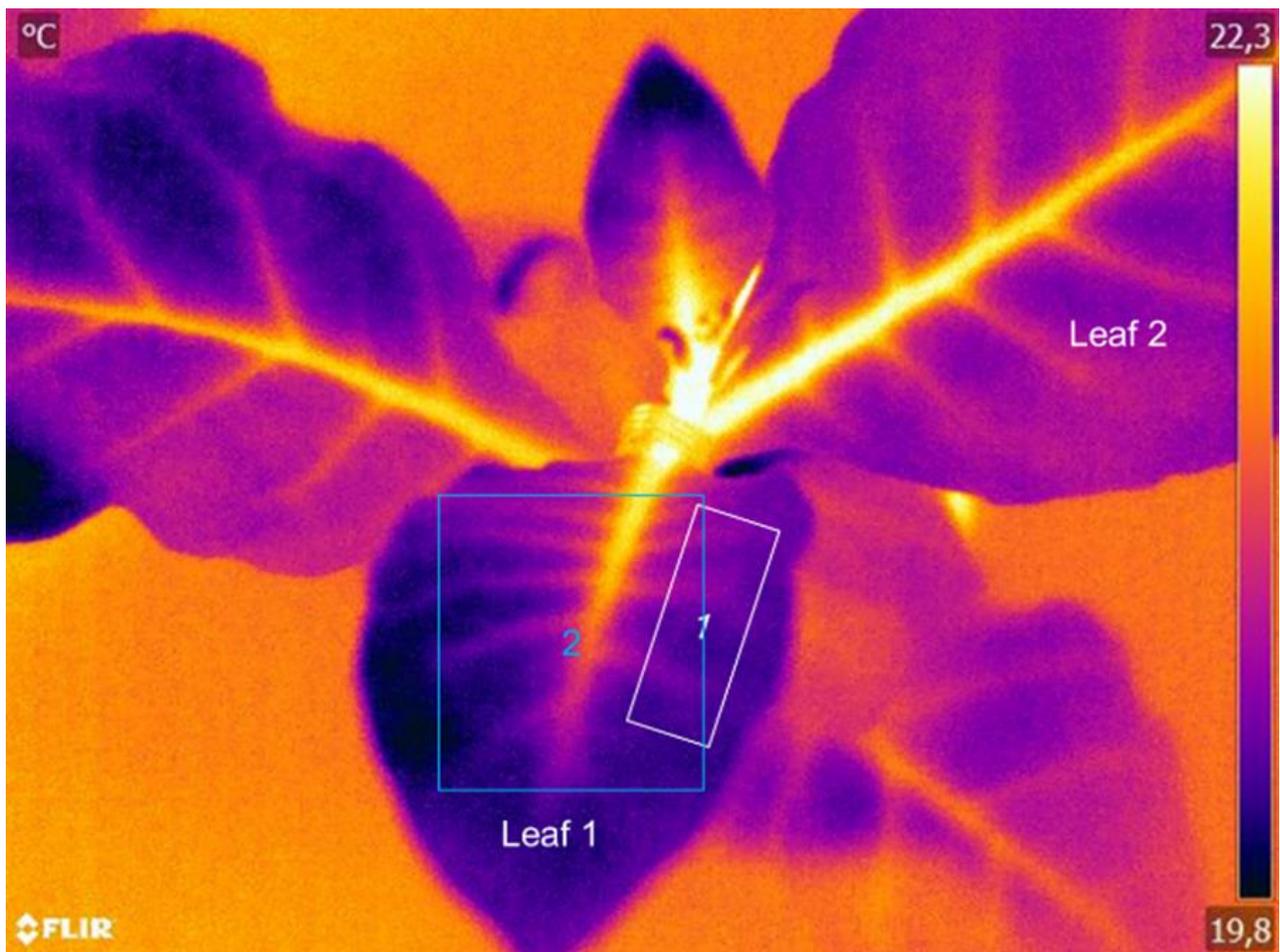
Figure F-i Example of thermal images taken of tobacco plants. Leaves 1 and 2 are marked. Two methods for selection of area processed were used when processing the images, either a small are that did not include the main leaf vein were selected (white square with number one) or the maximum leaf area with main leaf vein included were selected (blue square with number two). The temperature range in the image is shown on the right side.
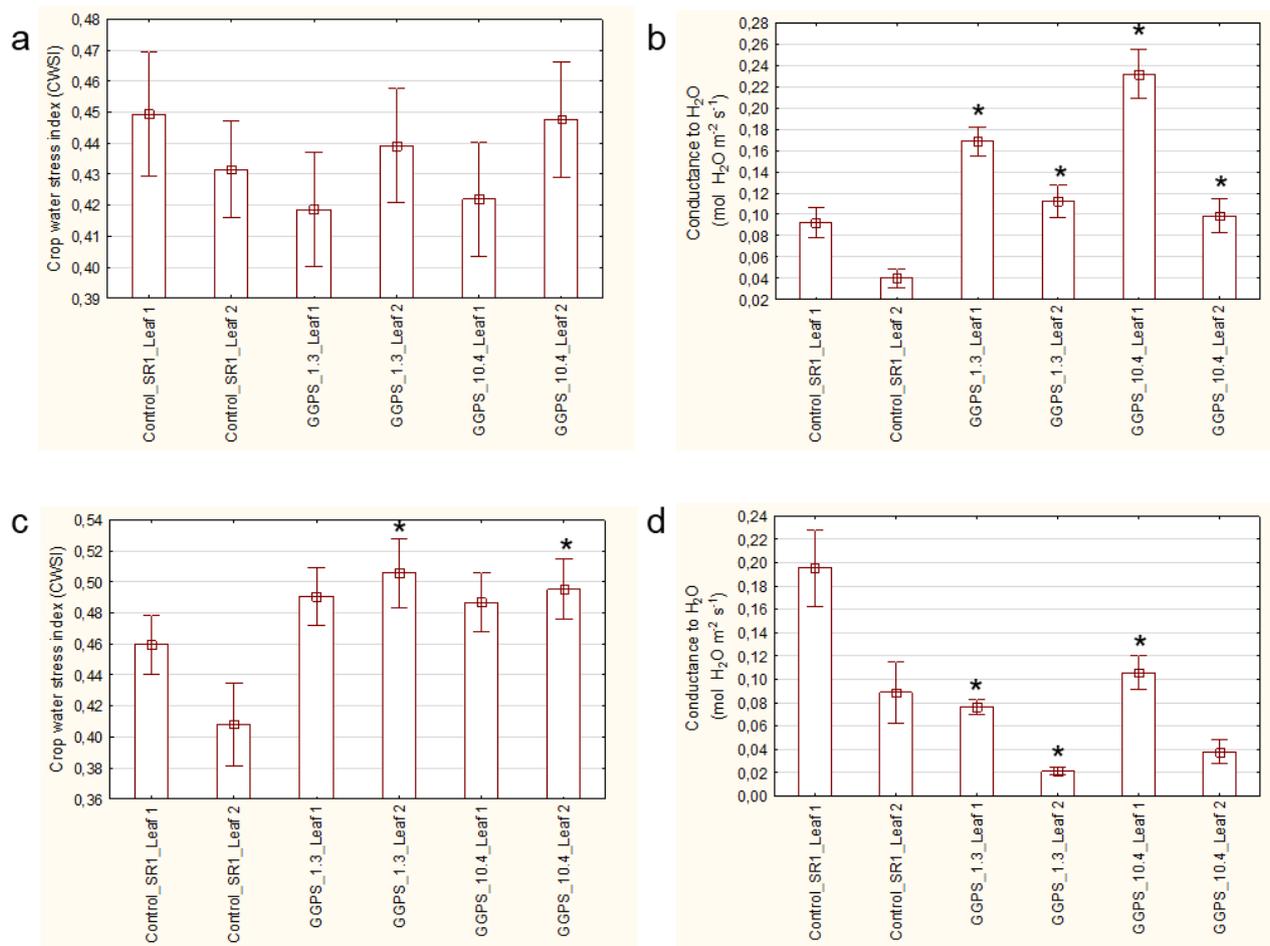
Figure F-ii Crop water stress index (CWSI) calculated based on the thermal imaging (a & c) of leaf 1 & 2 in comparison to the stomatal conductance (b & d) measured of the same leaf. 8 plants per line (Control_SR1, GGPS_1.3 and GGPS_10.4 with T1 and T2 pooled) during the autumn (a & b) and winter (c & d) growth season used for measurements. Bar graph show average and error bars the standard error. * indicates significant difference from Control_SR1 determined with student's *t*-test (p < 0.05).

216

Appendix G   To Chapter 4

Table G-i Summary of the peaks detected in hexane extract of the leaf surface. ^Some peaks could be putatively annotated via mass spectra comparison, peaks with same annotation was differentiated with addition of retention time to the name. Peaks that could not be annotated were named according to retention time. Two plant populations were grown consisting of the various lines with three repeats of each line in each population. The two populations were grown in the climaroom under low light (CR_LL) and in the greenhouse under high light (GH_HL). Values highlighted in red were significantly different (t-test, p<0.05) from control under same growth conditions while values highlighted with an asterisk (in GH_HL column) were significantly different (t-test, p<0.05) between growth conditions but within the same line. # peak not detected in one or more biological repeat.

| Compounds	Retention time (min)	Control_SR1		VviGGPS_1.3		VviGGPS_3.4		VviGGPS_6.4		VviGGPS_9.1		VviGGPS_10.4	
		CR_LL	GH_HL	CR_LL	GH_HL	CR_LL	GH_HL	CR_LL	GH_HL	CR_LL	GH_HL	CR_LL	GH_HL
(11E,13Z)-11813-Labdadien-8-ol	14.6	5.43	5.79	2.89	4.23	4.98	8.98	6.12	14.27	4.07	11.98*	5.35	7.21
9,12,15-Octadecatrienoic acid, (Z,Z,Z)-	14.78	17.80	11.21	10.82	7.96	14.18	12.83	16.38	14.75	13.94	17.95	16.28	17.09
Unknown peak_14.8	14.8	1.36	2.43	0.79	1.14	1.67	2.80*	1.76	3.38*	1.02	4.28*	1.31	2.02
Unknown peak_14.98	14.98	3.30	3.29	1.51	2.39	2.83	5.25*	3.21	6.18	2.37	6.45*	3.14	3.69
4,8,13-Duvatriene-1,3-diol	15.95	5.33	6.38	2.90	5.41	5.12	10.96*	5.74	13.17	3.91	13.35*	5.46	9.76
Unknown peak_16.7#	16.7	0.49	0.55	0.18	0.37	0.40	0.67	0.53	0.92	0.37	1.09*	0.54	0.45
Heneicosane_20.6#	20.6	0.71	0.92	0.92	0.85	0.94	1.08	0.45	1.59*	0.66	0.94	0.95	0.72
Unknown peak_22.2#	22.2	ND	0.31	0.27	0.11	0.42	0.45	0.41	0.34	0.23	0.72	0.54	0.75
Heneicosane_22.5#	22.5	0.71	0.85	0.66	0.84	0.68	1.26*	0.49	1.14*	0.50	1.08*	0.48	1.03*
N-Eicosane#	23.24	0.59	0.72	0.65	0.66	1.02	1.33	0.92	1.84	0.38	1.09	2.31	1.47
Unknown peak_23.25#	23.25	0.20	0.19	0.28	0.22	ND	0.45	0.31	0.30	0.32	0.41	0.44	0.41
Unknown peak_24.1#	24.1	1.43	0.92	0.97	0.57	1.65	2.60	1.67	1.79	0.96	2.39	1.94	2.60
Hentriacontane_24.4	24.4	1.40	2.50	1.81	1.59	1.81	3.95*	1.58	3.66	1.19	3.82*	2.50	3.77
Hentriacontane, 3-methyl-#	25.07	0.97	1.07	0.63	0.80	1.21	1.39	1.00	1.38	0.53	1.05	1.91	1.15
Eicosane#	25.28	ND	0.19	ND	ND	ND	0.89	0.92	ND	0.67	0.22	ND	ND
Unknown peak_25.8#	25.8	0.55	0.65	0.61	0.15	0.57	1.00	0.62	0.68	0.42	1.09	0.93	0.57
Hentriacontane_26.2#	26.2	1.04	2.42	1.12	1.55	1.73	2.44	1.78	2.51	1.73	3.46*	2.83	2.00

Chapter 5   Overexpression of the grapevine geranylgeranyl diphosphate synthase (*VviGGPS1)* gene in tobacco alters plant morphology and chemotypes indicative of changes in gibberellin metabolism

5.1   Introduction

Geranylgeranyl diphosphate (GGPP) is a branchpoint substrate that is utilised in the biosynthesis of various compounds required during plant growth. These metabolites include phytohormones (gibberellin, abscisic acid and strigolactones), compounds essential for the photosynthetic and electron transport systems (carotenoids, tocopherols and quinones) and diterpenes involved in plant-environment interactions (Lange & Ghassemian, 2003; de Boer & Leeuwen, 2012; Zerbe *et al.*, 2013; Jassbi *et al.*, 2017). The central role that GGPP plays in plant metabolism is highlighted in **Figure 5.1** with the various compounds derived from GGPP shown.

Although the *GGPS* gene family is not as expansive as other gene families, such as the *TPSs*, it has been found that multiple GGPS isoforms function in plants (Beck *et al.*, 2013; Wang, Lin, *et al.*, 2018; Barja *et al.*, 2020; Kamran *et al.*, 2020). Characterisation of GGPSs generally involves isolation of the enzyme or the putative gene, followed by heterologous expression and/or enzyme assays in order to determine functionality (Laferriere & Beyer, 1991; Aitken *et al.*, 1995), sometimes involving endogenous expression and compartmentation studies (Kuntz *et al.*, 1992; Scolnik & Bartley, 1994; Badillo *et al.*, 1995; Zhu, Suzuki, Saito, *et al.*, 1997; Okada *et al.*, 2000; Thabet *et al.*, 2012; Beck *et al.*, 2013).

Even though numerous *GGPS* genes have been functionally characterised, the ectopic expression of *GGPS* genes in a plant system followed by characterisation of the transgenic plant population has only been done by a few studies (Tata *et al.*, 2016). Previous studies in which GGPS levels were altered in tobacco, either via silencing of endogenous gene expression or heterologous expression of *GGPS* genes isolated from other plant species, had various effects on the chemical composition (chemotype) and/or morphological phenotype. Silencing of the *Nicotiana attenuata GGPS* (EF382626) *in planta* lowered levels of the defensive 17-hydroxygeranyllinalool diterpene glycosides but did not significantly alter the phenotype of the plant (Jassbi *et al.*, 2008; Heiling *et al.*, 2010). Ji *et al.*, (2009) transformed tobacco with *GGPS* isolated from *Gentiana lutea* L. The transgenic population had a slight increase in β-carotene but were phenotypically similar to the control population. Over-expressing *GGPS* isolated from sunflower (*Helianthus annuus*) in *N. tabacum* cv. Xanthi resulted in enhanced growth in the transgenic population, which was attributed to the measured increase in bioactive gibberellin (Tata *et al.*, 2016).

218
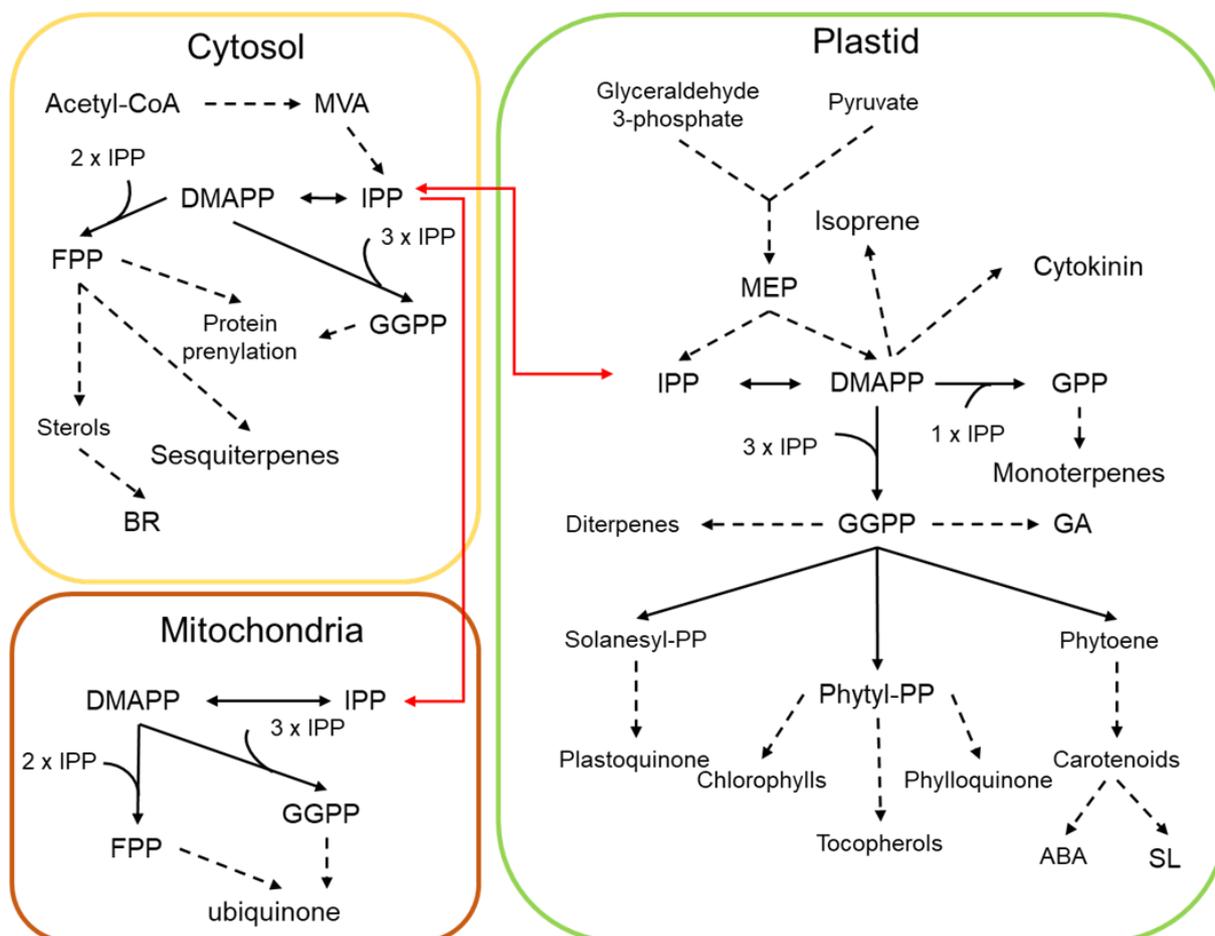
Figure 5.1 Terpenoid pathway representation in plants illustrating the central role of GGPP in the biosynthesis of various metabolites involved in primary and secondary metabolism. The universal C5 isoprenoid precursors isopentenyl diphosphate (IPP) and dimethylallyl diphosphate (DMAPP) can be synthesized by the MVA pathway in the cytosol or the methylerythritol 4-phosphate (MEP) pathway in plastids, and then transported among cell compartments. Addition of IPP molecules to DMAPP produces prenyl diphosphates of increasing chain length, such as geranyl diphosphate (GPP, C10), farnesyl diphosphate (FPP, C15) and geranylgeranyl diphosphate (GGPP, C20). These are the starting points to produce various terpenoids, including the plant hormones brassinosteroids (BR), cytokinins (CK), gibberellins (GA), abscisic acid (ABA) and strigolactones (SL). GGPP is synthesized in different compartments by GGPP synthase (GGPS) enzymes. Some of the enzymes that channel GGPP to specific isoprenoid pathways are indicated. Dashed arrows indicate multiple steps. Red arrows represent transport of isoprenoid precursors between cell compartments.

The different phenotypes observed in these studies can be explained by the presence of multiple GGPSs in plants, with the in-depth analysis of the *AtGGPSs* gene family showing that it can include multiple members with GGPSs localised to various cellular compartments performing different functions (functional diversification) or with overlapping functionality (sub-functionalisation) (Zhu, Suzuki, Okada, Tanaka, Nakagawa, Kawamukai, Matsuda, *et al.*, 1997; Zhu, Suzuki, Saito, *et al.*, 1997; Okada *et al.*, 2000; Wang & Dixon, 2009; Beck *et al.*, 2013; Coman *et al.*, 2014). The effect of ectopic expression or gene silencing of a *GGPS* in a plant system will therefore be influenced by the type of GGPS (of which the expression has been altered) as well as the native GGPSs.

Based on the results of an initial phenotyping analysis of a transgenic tobacco population overexpressing the *VviGGPS1* gene from grapevine, (described in Chapter 4 of this thesis), the tobacco plant population overexpressing *VviGGPS1* was grown under the environmental conditions that lead to the most discernible vegetative phenotypes (plants moved to a high light greenhouse environment from an early developmental stage). A more detailed analysis of the abnormal phenotype was undertaken in this Chapter which was broadly divided into phenotyping of morphology and physiology and chemotyping (metabolite analysis). Analyses falling under the first category included measurement of growth, photosynthesis, in-depth study of the leaf surface, and quantitative analyses of the vegetative and reproductive morphology. Chemotyping involved analysis of carotenoids and photosynthetic pigments, flavonoid compounds and cuticular wax. The results from these analyses expanded on the current knowledge and were used to formulate a hypothesis regarding the biological role *VviGGPS1* plays in the grapevine.

5.2   Material and methods

5.2.1   Phenotyping of morphology and physiology

5.2.1.1   *Leaf mass per area (LMA) and morpho-colorimetric analysis*

In order to quantify phenotypic observations, an image analysis method used by Fuentes *et al.*, (2018) on grapevine leaves was adapted to analyse tobacco leaves with the same parameters generated. The leaves of a plant population grown under greenhouse conditions were scanned at the highest resolution to TIF file format using bizhub 223 (Konica Minolta, South Africa) scanner. Sampling was done at the time when flower bud formation became visible. The transgenic plants that displayed the "lack of apical dominance" phenotype which was associated with the inability to form a flowering head were sampled on the last sampling day, irrespective of whether a flower bud could be observed. Leaves 1 to 4 were harvested from each plant and scanned with at least six biological repeats (individuals) per line sampled. The images were analysed using a modified code written in MATLAB® version R2017b (MathWorks Inc., Natick, MA. USA). Calibration of the scanner was done by analysing scanned images of a black square of paper with known dimensions (Fuentes *et al.*, 2018).

After scanning, the fresh weight of the leaves was determined. The leaves were placed in a 70°C oven for ~ 48 hours until no further weight loss was detected, after which the dry weight of each leaf was measured and leaf mass (dry weight) per area (LMA) was determined using the area calculated during the image analysis described above.

5.2.1.2   *Scanning electron microscope (SEM) imaging*

Samples for scanning electron microscopy (SEM) were obtained by punching out leaf discs (1.5 cm in diameter) near the leaf apex with either the main leaf vein in the middle of the disc (if trichome

images were required) or the disc was punched out on either side of the main leaf vein (stomatal images). The discs were placed on 1% (w/v) water agar plates to prevent excessive water loss before analysis, the fresh leaf discs were mounted on aluminium stubs with carbon tape and analysed with no coating. Electron microscopy was performed on a LEO® 1450VP SEM at the Electron microscopy (EM) unit of the Central Analytical Facility (CAF) at Stellenbosch University (Stellenbosch, South Africa). SEM settings were as following: Spot size = 300, ETH target = 7 kV, Fil target = 2.655 A, Z = 18 – 20 mm, brightness at ± 49, Contrast at ± 65, working distance at ± 6 mm (4-7 mm). Between 7 and 10 images at 150x magnification were taken from a single leaf disc, the time used for each leaf disc was restricted to < 30 min to avoid excessive drying of the sample. Stomatal area and count per image were done using a code written in MATLAB® version R2017b (MathWorks Inc., Natick, MA. USA).

5.2.2   Chemotyping

5.2.2.1   Carotenoid and chlorophyll profiling in leaves with RP-UPLC

Extraction and analysis of carotenoids and chlorophylls from leaf 1 of plants grown in the greenhouse in the autumn season (GH_HL) were done as described in Section 4.2.5.1 of Chapter 4 of this thesis. Physiological measurements of the same plants were done a day before sampling.

5.2.2.2   Total anthocyanin determination and flavonoid profiling of flower corolla

Flowers were harvested at four different developmental stages (**Figure 5.2**), the corolla was cut just above the sepal with the stamen and pistil removed and immediately frozen in liquid nitrogen. At least three independent biological replicates (individual plants) were sampled per line. The samples were finely ground with liquid nitrogen and ~ 25 mg were measured off in triplicate for extraction.

Total anthocyanin concentration was determined in the corolla from the stage 4 flowers based on spectrophotometric methods described in Honda *et al.* (2002), Huang *et al.* (2012) and Tuan *et al.* (2015). The extraction buffer consisted of 500 µL methanol with 1% (v/v) HCl, extraction was done at 8 °C for 24 h in the dark with continuous shaking. The extracts were centrifuged at 16500 RCF for 5 min, the supernatant was carefully pipette into a microtiter plate for measurements. Absorbance was measured at 530 nm, 620 nm and 650 nm with the equation used to normalise the anthocyanin absorbance at OD530 being [(OD530-OD650) – 0.2 x (OD650-OD620)], as described by Tuan *et al.*, (2015). The adapted absorbance measurement was normalised to the specific weight of the sample. Cyanidin-3-glucoside (Sigma-Aldrich, Steinheim, Germany) was used as a standard with dilutions made in the same buffer used for extractions at 5 µg/mL, 10 µg/mL, 15 µg/mL, 30 µg/mL, and 50 µg/mL.
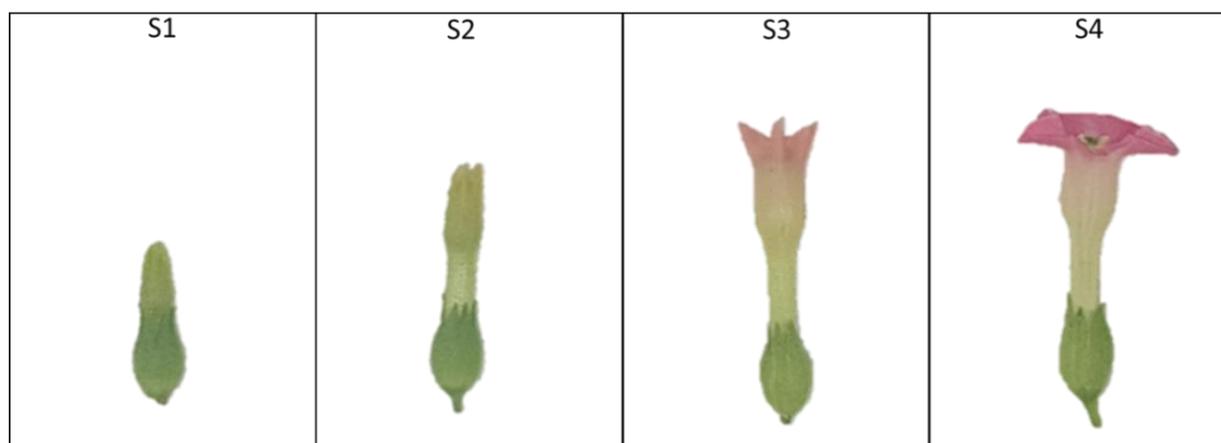
Figure 5.2 Different flower stages sampled for phenolic extraction. Stage 1 – 3 before anthesis with Stage 4 being a fully developed flower.

Non-acidic extraction and analysis of flavonoids from the corolla tissue was done with the flowers harvested at all four developmental stages. 750 µL chloroform:methanol:H_2O (1:3:1) with 25 mg/L p-coumaric acid (IS) was added to each vial and mixed with a ball mill (Retsch® mill MM 400, Haan, Germany) for 2 min at 30 Hz at room temperature. Samples were centrifuged at 16 500 RCF for 10 min and 200 µL supernatant was carefully transferred into amber vials for analysis. Flavonoid compounds were analysed with a Waters ACQUITY UPLC system (Waters, Stainleys) equipped with a diode array detector (DAD). The compounds were separated on a Waters UPLC BEH C18 column (2.1 mm x 100 mm, 1.7 µm) and the column temperature was set to 35°C with the flow rate at 0.3 mL/min. The mobile phases were composed of (A) 2% (v/v) formic acid in dH_2O and (B) 2% (v/v) formic acid in acetonitrile. The following gradient program with a linear increase in mobile phase was applied: from 0 to 24 min; 0% to 24% B; from 24 to 25 min, 24% to 65% B; from 25 to 26 min, 65% B; from 26 to 26.1 min, 65% to 100% B, maintained at 100% B until 27 min then decreased to 1% B from 27 to 27.1 min and maintained at 1% B until 28 min. The control of the instrument, the acquisition and processing of the generated data were done using Empower 2 software from Waters® and the injection volume was 5 µL. The quantification of the compounds was conducted at 280 nm for flavon-3-ols, 320 nm for phenolic acids, 360 nm for flavanols and 520 nm for anthocyanins. The peak area of detected compounds was normalised to the IS peak area and the sample fresh weight.

Peak identification with authentic standards were done if available. Some samples were also run on a UPLC-MS using the same separation method to facilitate peak identification of unknown peaks (CAF, Stellenbosch, South Africa), with peaks putatively annotated based on the MS spectra. Otherwise, the peaks were labelled according to the wavelength at which the peak was most visible and the numbered according to the retention time. Multiple peaks were identified as phenolic acids but could not be accurately named and were therefore numbered.

222

5.2.2.3 Extraction, derivatisation, and analysis of cuticular wax components

For the analysis of the cuticular wax, a plant population moved to a greenhouse (high light conditions) at an early stage of development was used. Five leaf discs (1.5 cm in diameter) were punched out along the main vein of leaf 2 with two extractions done per leaf. The method of extraction was based on the protocol developed by Kurdyukov *et al.*, (2006). Glassware was used for sample preparation to avoid high background noise. For extraction, 5 mL chloroform with tetracosane (4 µg/mL) as internal standard was added to the leaf discs and shaken for 1 min. The extract was poured into Pyrex® glass tubes and evaporated under nitrogen until ~ 1 mL volume. The concentrated extract was transferred to 1 mL micro-reaction vessels (Supelco) with glass Pasteur pipettes and further evaporated to ~200 µL. Derivatisation was done with the addition of 40 µL bis-(N,N-trimethylsilyl)-trifluoroacetamide (BSTFA) (Supelco) and 40 µL anhydrous, 99.8%, pyridine (Sigma-Aldrich, Steinheim, Germany), followed by incubation for 40 min at 70°C. The samples were transferred to GC vials with inserts, capped and analysed via GC-MS. To determine the retention index, 10 µL of a 1000 µg/mL C_7-C_{40} saturated alkane mix (Supelco) was added to 90 µL chloroform and analysed using the same GC-MS method.

The extraction (1 µL) was injected with separation and detection of compounds done using an Agilent 6890N gas chromatograph (Agilent, Palo Alto, CA, USA) system coupled to a CTC CombiPal Analytics auto-sampler and an Agilent 5977B inert XL EI/CI MSD mass spectrometer detector through a transfer line. Separation was done using the ZB-SemiVolatiles w/GUARDIAN™ (Zebron™ Phenomenex) capillary column (30 m × 250 µm × 0.25µm) (Promolab Pty Ltd T/A Separations, Randburg, South Africa). Helium was used as carrier gas with a constant flow rate of 1 mL/min with the purge flow set at 30 mL/min for 2 min. The oven parameters were as follows: initial temperature was set at 100℃ and maintained for 2 min, followed by an increase to a temperature of 180℃ at a rate of 15℃/min. The temperature was increased to 250°C at 5°C/min and held for 3 min, this was followed by 20°C/min increase to the final temperature of 320°C where it was held for 12 min. The total run time was 39.83 min.

Detection was performed in electron impact mode (70 eV) and operated in scan mode. The scan parameters were set at m/z ranging from 40 to 650.For unknown compounds, the initial identification was done by comparing the mass spectra to the NIST and Wiley275.L mass spectral libraries.

5.2.3 Data analysis

Generated data was analysed using SIMCA® (Version 16, Sartorius Stedim Biotech, Göttingen, Germany). Microsoft Office Excel 2016 (Microsoft Corporation, Redmond, WA, USA) and STATISTICA version 13.2 (http://software.dell.com/products/statistica/) were used to visualise data in graphs and for statistical analysis.

223

5.3   Results

Based on the general phenotypic observations described in Chapter 4, specific lines were selected for more in-depth characterisation under the growth conditions found to be most conducive to the abnormal phenotype. **Table 5.1** summarises the lines included in the various analyses of vegetative and reproductive organs.

Table 5.1 Summary of analysis done on vegetative and reproductive organs.

	Morphology		Growth parameters	Morpho-colorimetric	Days before flowering	LMA	Photosynthesis (IRGA)	Leaf surface (SEM)	Metabolite Analysis		
									Carotenoid and pigment	Cuticular wax	Flower Phenolic
	Vegetative	Flower									
Control_SR1	Yes	Yes	Yes	Yes	Yes	Yes	Yes	Yes	Yes	Yes	Yes
VviGGPS_1.3	Yes	Yes	Yes	Yes	Yes	Yes	Yes	Yes	Yes	Yes	Yes
VviGGPS_3.4	Yes	Yes	Yes	Yes	Yes	Yes	Yes	No	No	No	No
VviGGPS_6.4	Yes	Yes	Yes	Yes	Yes	Yes	Yes	No	No	No	Yes
VviGGPS_9.1	Yes	Yes	Yes	Yes	Yes	Yes	Yes	No	No	No	Yes
VviGGPS_10.4	Yes	Yes	Yes	Yes	Yes	Yes	Yes	Yes	Yes	Yes	Yes

5.3.1 Vegetative and reproductive phenotypes observed in transgenic population

Although some individual lines displayed a phenotype that was particularly noticeable, there were vegetative and reproductive transgenic phenotypes which could be observed across various lines. The percentage of the most observed phenotypes within a population grown at the conditions shown to increase the frequency and/or intensity of the phenotype are presented with a photographic example in **Figure 5.3**.

The most common vegetative phenotype observed was the pockmarked leaf surface with just under 70% of the transgenic population displaying this phenotype. In more extreme cases the leaf surface looked rough with large indentations that could be described as a "bubbled" leaf surface with the incidence rate within a population of around 30%. The texture of some of these leaves differed from the control leaves with a more crunchy or brittle appearance where a slight folding of the leaves would result in it breaking with just under 20% of the population displaying this phenotype. The leaf shape was also altered in some individuals with curling of the leaf margin, twisted leaf apex and more lanceolate shape seen at a population incidence rate between 15 - 23%.

In comparison the abnormal phenotype observed in the flowers were much more prevalent. The pale pink coloration was seen in almost 90% of the transgene population with lines also sometimes having a more variegated coloration of the corolla. Generally, in lines where the flower colour was affected, the lobes also showed less indentation, and the style was elongated (or is longer that the flower tube and filament). Another prominent transgene phenotype was the premature abscission of flower buds, with around 70% of the population displaying this phenotype.
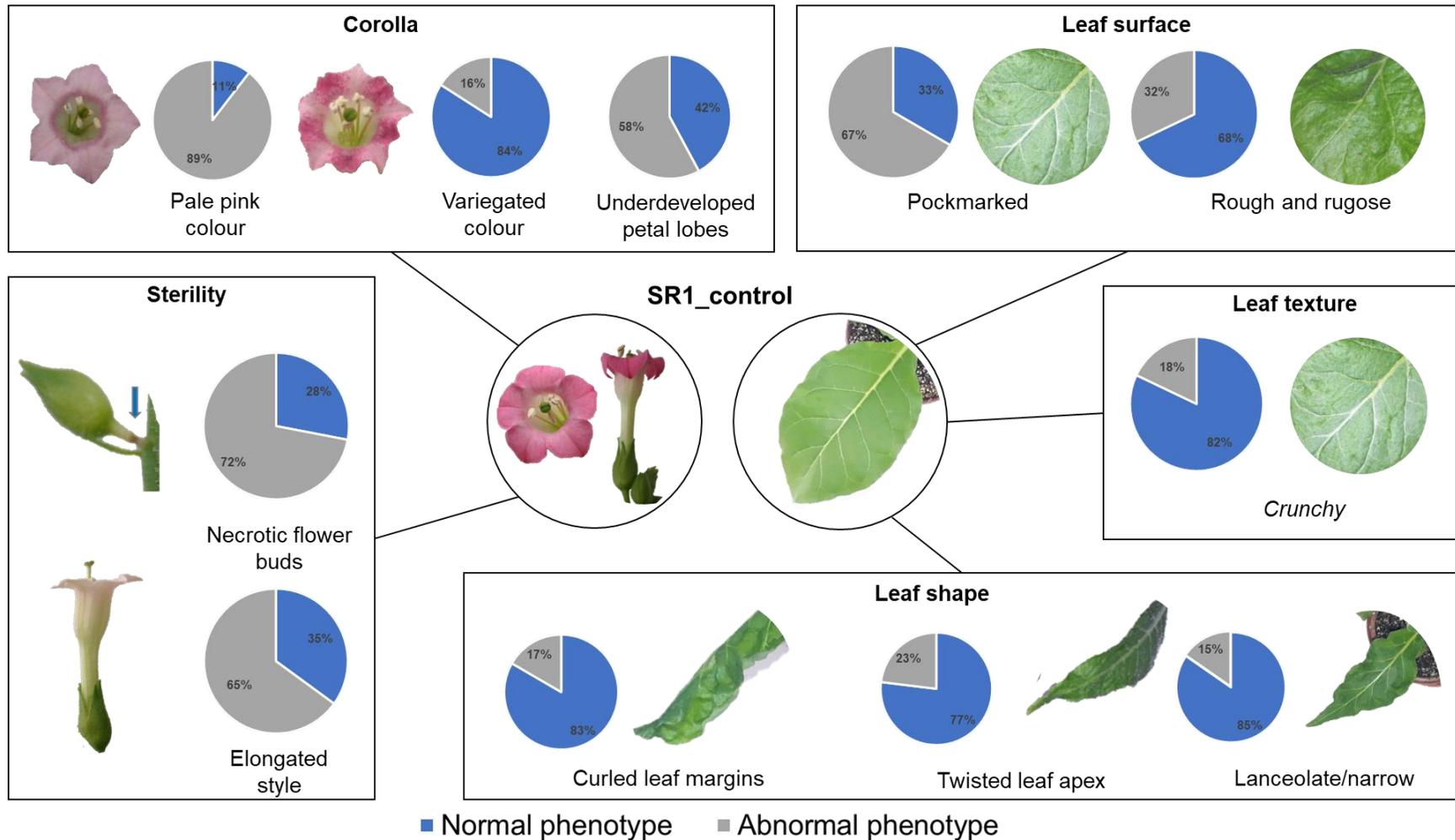
Figure 5.3 Visual summary of some of the prevalent transgenic phenotypes observed. Control (SR1) plant flower and leaf are shown in circles with examples of some of the transgenic phenotypes observed shown in squares together with the pie graph representing the percentage of plants displaying the abnormal phenotype in a population of selected lines (1.3, 3.4, 6.4, 9.1 and 10.4). For flower phenotyping the T1 generation was studied with 5 biological repeats per line while the T1 and T2 generation (8 biological repeats per line) were studied for vegetative phenotyping. Supplementary Table 5.1 describes the various phenotypes observed in more detail as well as the other phenotypes that were less prevalent within a population.

227

### 5.3.2   Leaf morphology and coloration

Visual observation of the leaves indicated morphological differences between the control and transgenic population. In order to quantify these differences, the leaves were scanned and the resulting images were used to extract morphometric parameters of each leaf (Fuentes *et al.*, 2012, 2018). PCA analysis indicated a separation spectrum according to leaf age (**Figure 5.4**a) and between the control and transgenic plants (**Figure 5.4**) which prompted an OPLS analysis with the genotype used as the y-variable (**Figure 5.5**). Most control samples grouped separately from the transgenic samples (**Figure 5.5**a) with the Loading Scatter Plot (**Figure 5.5**b) indicating which measurements drive the separation. Comparison of the measured parameters in **Figure A-i** gave more information on the morphological differences between the control and transgenic leaves.

The leaf area (**Figure A-i**a) of the transgenic plants was generally smaller in the older leaves except for line VviGGPS_1.3 which had a reduced area in all four leaves. The eccentricity value is the length to width ratio, with rounder shapes having values closer to 1. The eccentricity value shows a downward trend as the leaf age increases (**Figure A-i** b), apart from line VviGGPS_1.3 where the values remained high even with increasing leaf age. The maximum length (**Figure A-i** c) and perimeter (**Figure A-i** e) was significantly shorter in the transgenic leaves when compared to the control leaves for all leaf ages. The minimum leaf length (**Error! Reference source not found.**d) of line VviGGPS_1.3 was significantly shorter in leaf 3 and 4 compared to the control leaves. The fractal dimension (**Figure A-i** f) calculations showed that the transgenic leaves had significantly higher values than what was seen in the control leaves except for the leaves 2 and 3 of line 1.3.
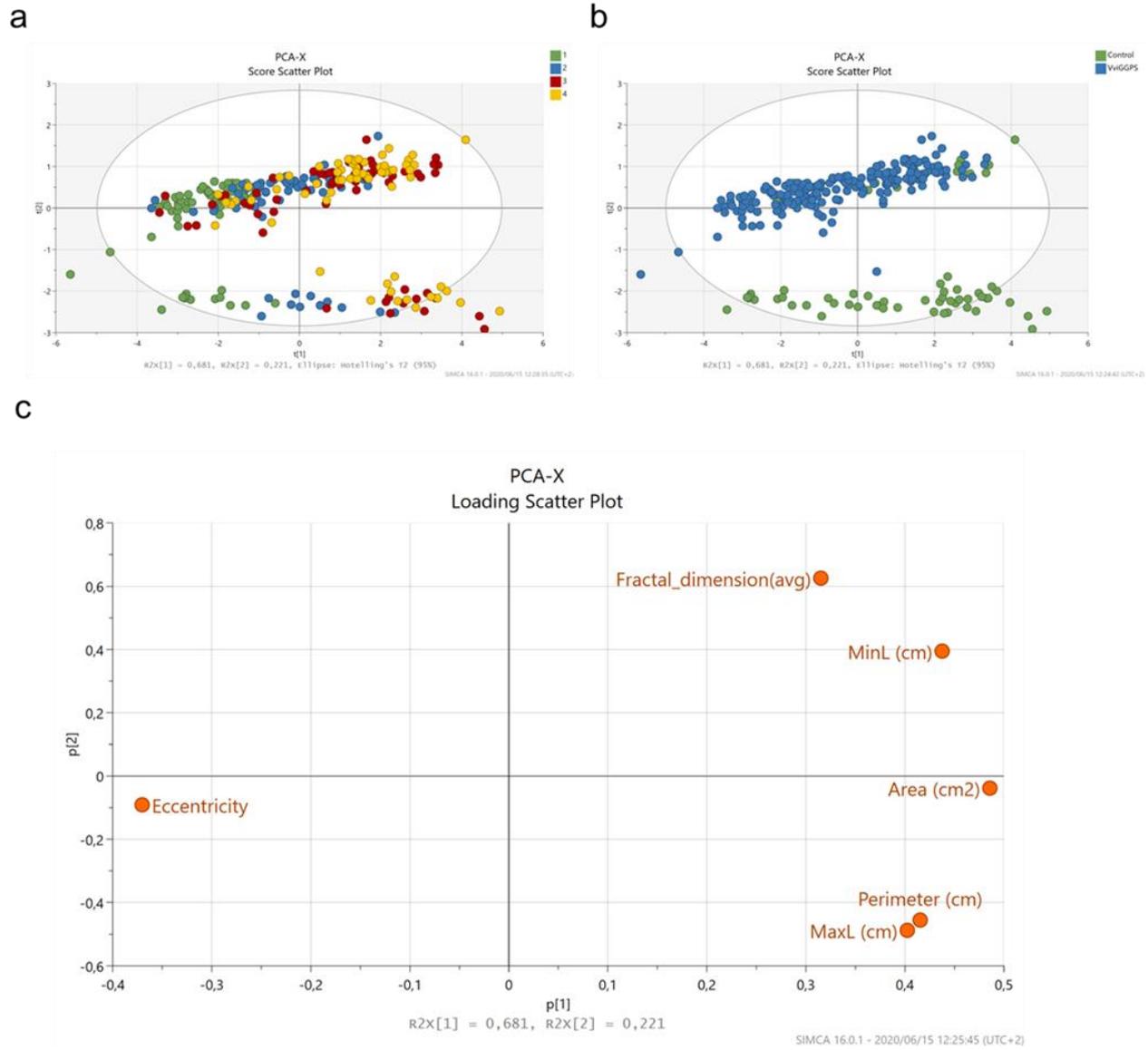
Figure 5.4 PCA plot with morphometric parameters as x-variables. All lines and leaves measured included in analysis. Separation of samples coloured according to leaf number shown in the Score Scatter Plot (a) with the separation between transgene and control samples shown in Score scatter Plot (b) and the x-variables driving the separation shown in the Loading Scatter plot (b).

229
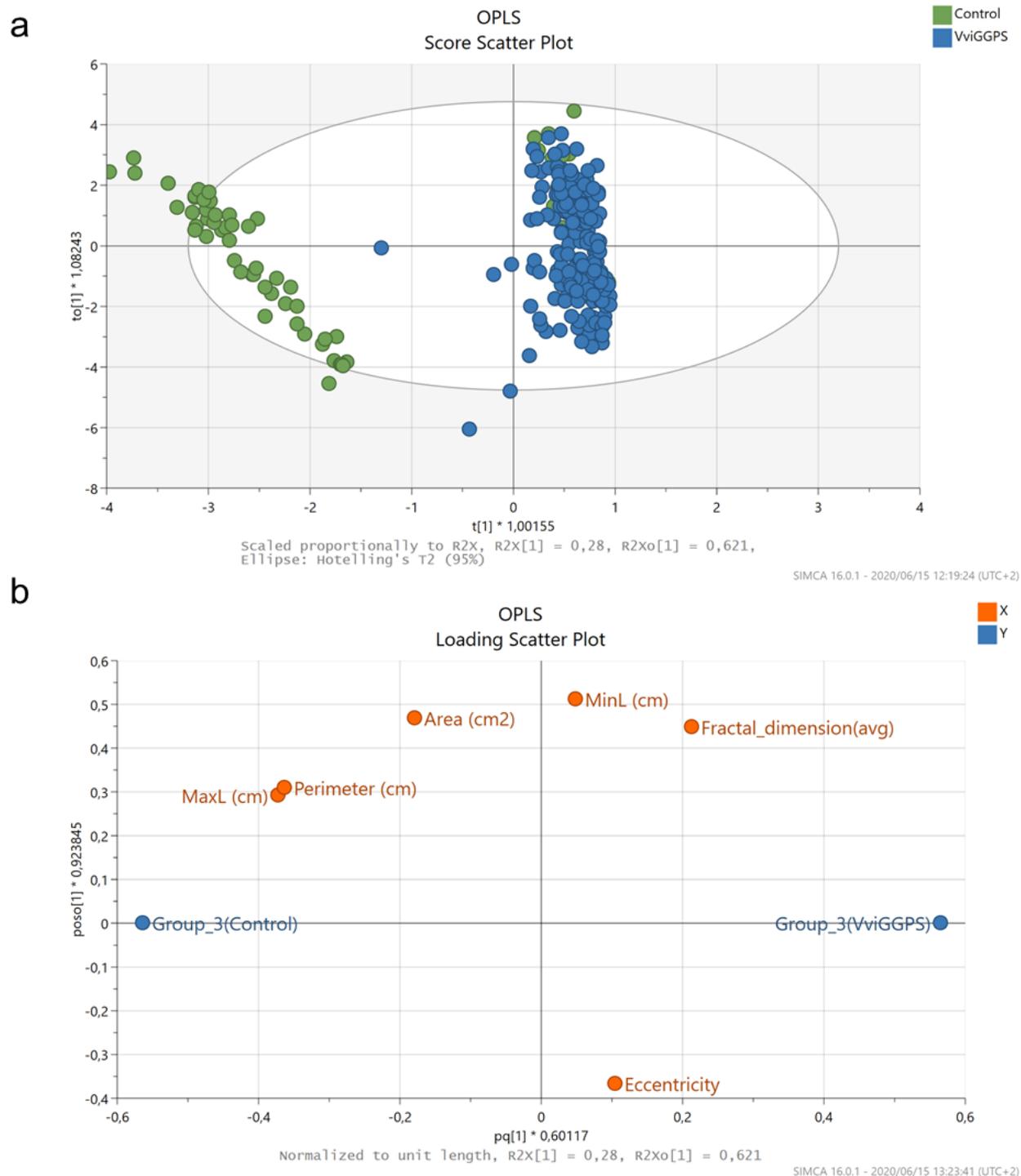
Figure 5.5 OPLS plot with morphometric parameters as x-variables and the transgenic lines as the y-variable, all lines and leaves measured were included in analysis. Separation of samples shown in the Score Scatter Plot (a) and x-variables driving the separation shown in the Loading Scatter plot (b).

The other dataset generated from the scanned leaves using the method developed by Fuentes *et al.*, (2012) was the RGB and CieLab colour scale variables. PCA with these values did not yield a clear grouping of the control and transgenic leaves (not shown) although OPLS indicated two variables driving the limited separation that can be seen (Figure A-ii). These two variables were the

230

red and green colours (part of the RGB colour scale) with comparison between control and the various transgenic lines showing that the red colour was significantly ($p < 0.05$) higher in the transgenic plants compared to the control plants (**Figure 5.6**a) in all the leaves analysed, while the green colour was only significantly higher in some of the leaves (**Figure 5.6**b).
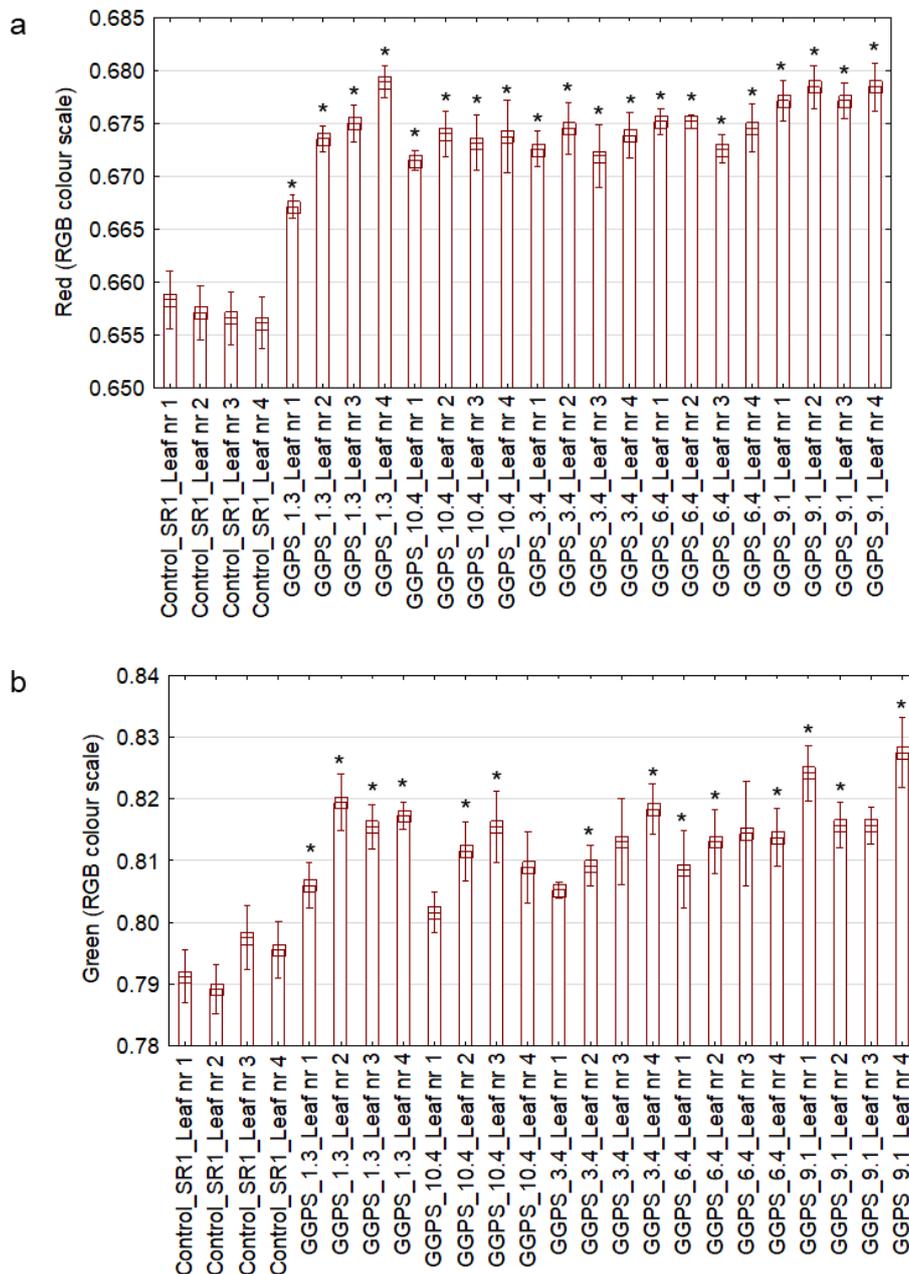
Figure 5.6 Colorimetric analysis of scanned leaves showing the RGB colour scale as described by (Fuentes *et al.*, 2018). Leaves were harvested when buds were visible in the control plants. Four leaves per plant with 16 plants measured for Control_SR1, GGPS_1.3 and GGPS_10.4 (T1 and T2 pooled), 6 plants studied for GGPS_3.4, GGPS6.4 and GGPS9.1 (T2 generation). Bar graph show average and error bars the standard error of the repeats. * indicates significant difference from respective leaves of control plants determined with t-test ($p < 0.05$).

231

5.3.3 Growth and biomass accumulation

Plant growth and biomass was measured in selected lines and results summarised in **Figure 5.7**. The days to flowering for most transgenic lines were similar to the control plants except for line VviGGPS_1.3, which showed a marked increase in the time for plants to start flowering (**Figure 5.7**a). Although not as prominent as line VviGGPS_1.3, line VviGGPS_10.4 also showed a significant increase in the number of days before the plants entered the reproductive stage. Height and internode length (**Figure 5.7**b & c) showed no significant differences between transgenic and control plants except for line VviGGPS_1.3. However, stem diameter was significantly lower in all the transgenic plants compared to the control plants (**Figure 5.7**d). Significantly higher dry weights (g) per area (cm^2) of the leaves were observed in lines VviGGPS_1.3, VviGGPS_9.1 and VviGGPS_10.4 (**Figure 5.7**e).
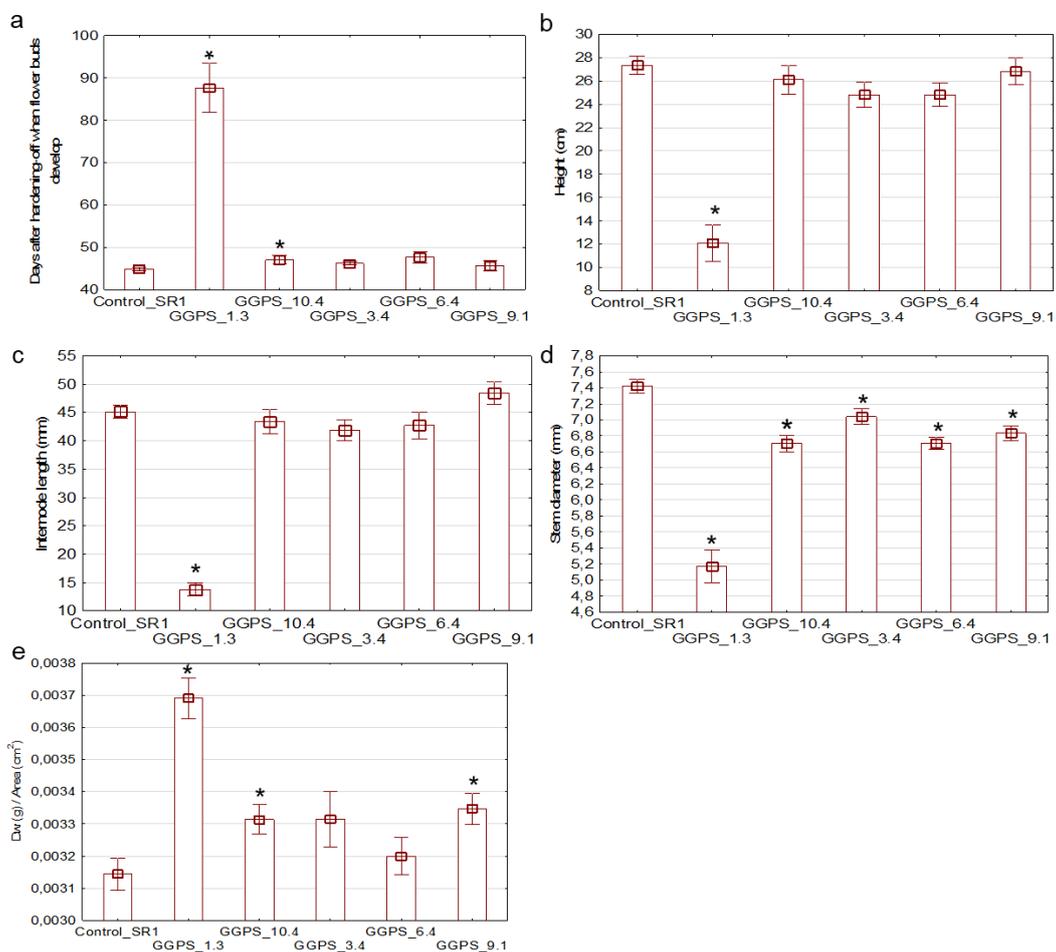
Figure 5.7 Days before flowering (a) measured in T1 and T2 generation plants studied (results pooled) with 16 plants per line studied. Height (b), internode length (c), stem diameter (d) and LMA (e) measured when buds were visible in the control plants. 16 plants measured for Control_SR1, GGPS_1.3 and GGPS_10.4 (T1 and T2 pooled), 6 plants studied for GGPS_3.4, GGPS6.4 and GGPS9.1 (T2 generation). Three internode (leaf 1 & 2, leaf 2 & 3 and leaf 3 & 4) and two stem diameter (leaf 2 and leaf 3) measurements made per plant with readings pooled (bar graph show average and error bars the standard error). *indicates significant difference from control plants determined with t-test (p < 0.05).

232

5.3.4 Photosynthesis measurements coupled with carotenoid and pigment determination in leaves

During the autumn growth period, leaves 1 and 2 of the transgenic lines had significantly ($p < 0.05$) higher photosynthetic rates, conductance, and transpiration (**Figure 5.8** a – c) when compared to leaves 1 and 2 of the control plants. The vapor temperature deficit (Vpd) was significantly ($p < 0.05$) lower in transgenic plants compared to the control plants (**Figure 5.8**d).
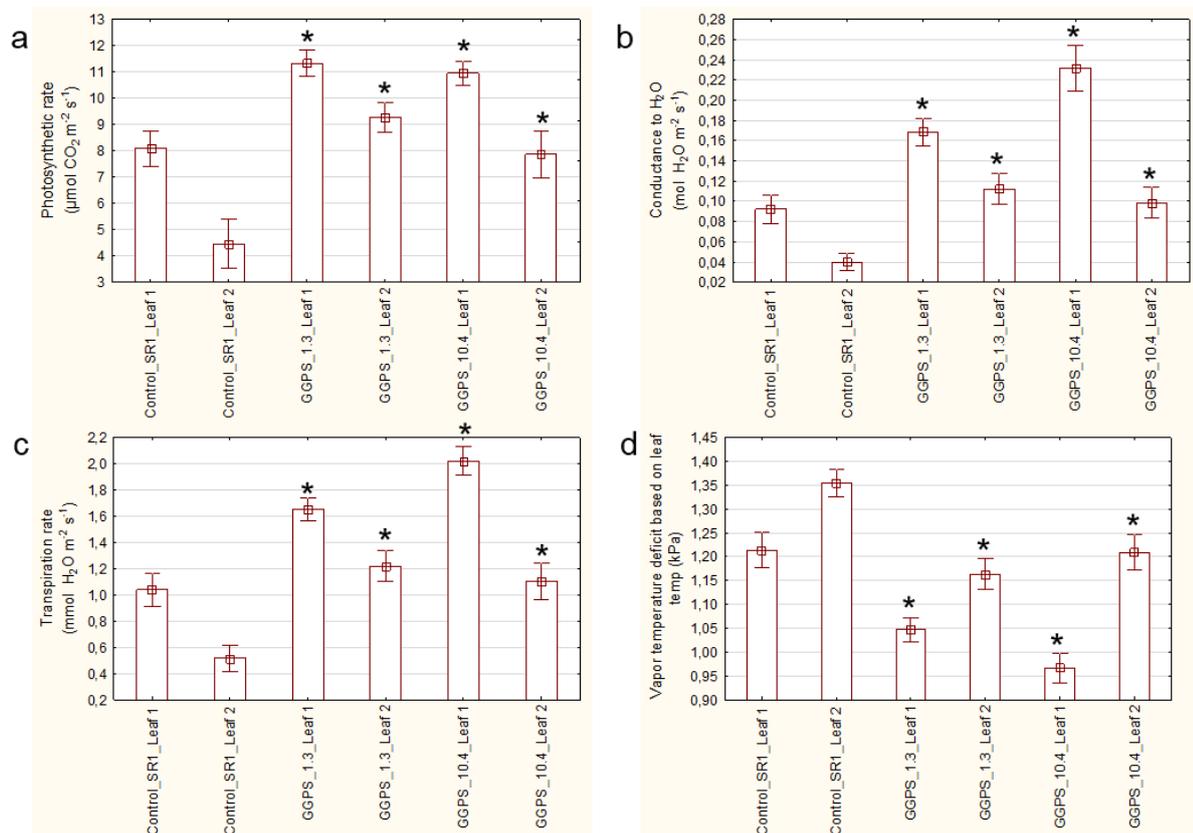
Figure 5.8 Photosynthetic parameters measured of leaves 1 & 2 taken of 12 plants per line (Control_SR1, GGPS_1.3 and GGPS_10.4 with T1 and T2 pooled) over two day period during the autumn growth season. Bar graphs show average and error bars the standard error. * indicates significant difference from Control_SR1 determined with student t-test ($p < 0.05$) for each leaf.

Leaf 1 of the plants used for the photosynthesis measurements described above were sampled for carotenoid and pigment analysis. The leaves were sampled the day after the photosynthetic measurements were taken during the same period in the day. The results are summarised in **Table B-iError! Reference source not found.**, with **Figure 5.9** showing the compounds which were significantly ($p < 0.05$) different. The only other significant difference was seen with the chlorophyll a to b ratio in line VviGGPS_10.4 which was significantly higher (**Table B-i**)

233
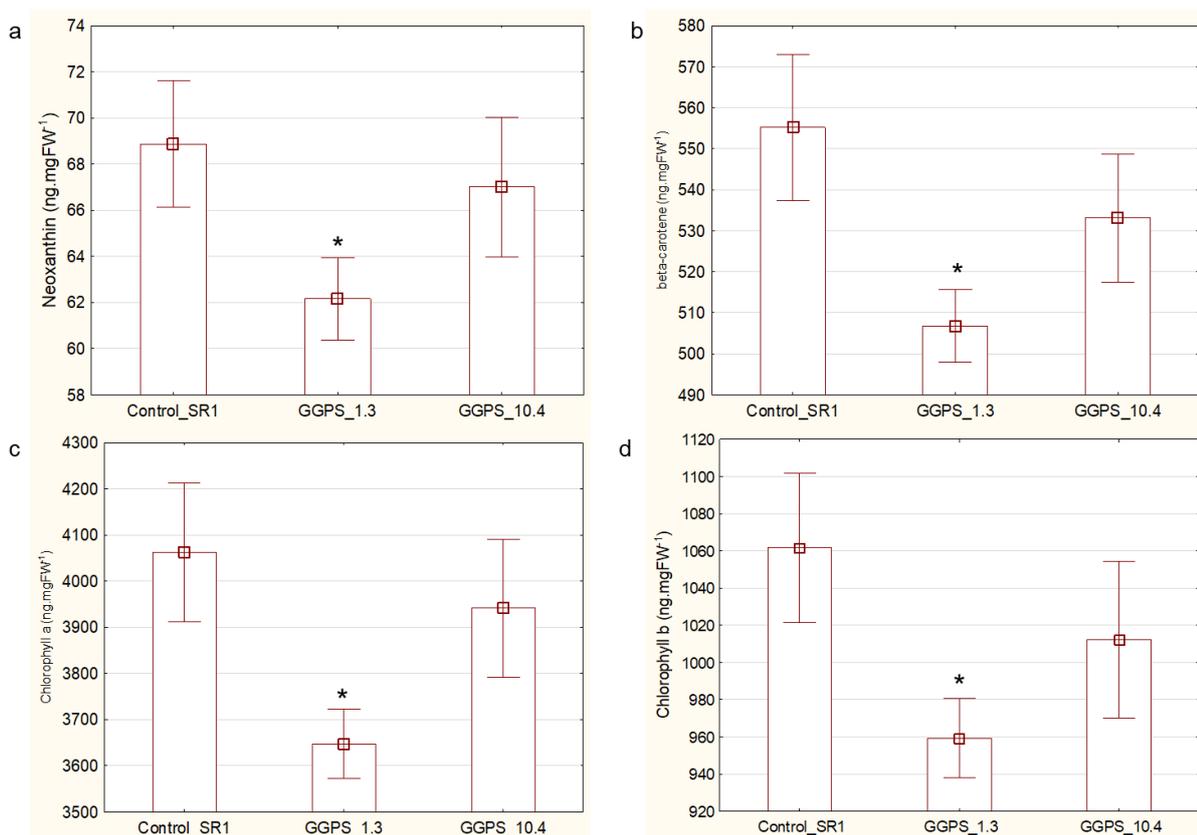
Figure 5.9 Carotenoid and pigment analysis of leaf 1 taken of 8 plants per line (Control_SR1, GGPS_1.3 and GGPS_10.4 with T1 and T2 pooled) during the autumn growth season. Bar graphs show average and error bars the standard error. * indicates significant difference from Control_SR1 determined with student t-test ($p < 0.05$).

### 5.3.5   Stomatal count and size determination

Leaf discs taken from control and line VviGGPS_1.3 plants were analysed via microscopy (SEM), with multiple images taken per disc on the adaxial and abaxial side. Measurement of the stomata as well as the number of stomata per image was determined with the average shown in **Figure 5.10**. The VviGGPS_1.3 leaf discs had significantly fewer stomata than the control on the abaxial as well as the adaxial leaf side (**Figure 5.10**a). Statistical analysis of stomatal size measurements indicated that there were significant differences in the area (**Figure 5.10**b), length (**Figure 5.10**c) and width (**Figure 5.10**d).

234
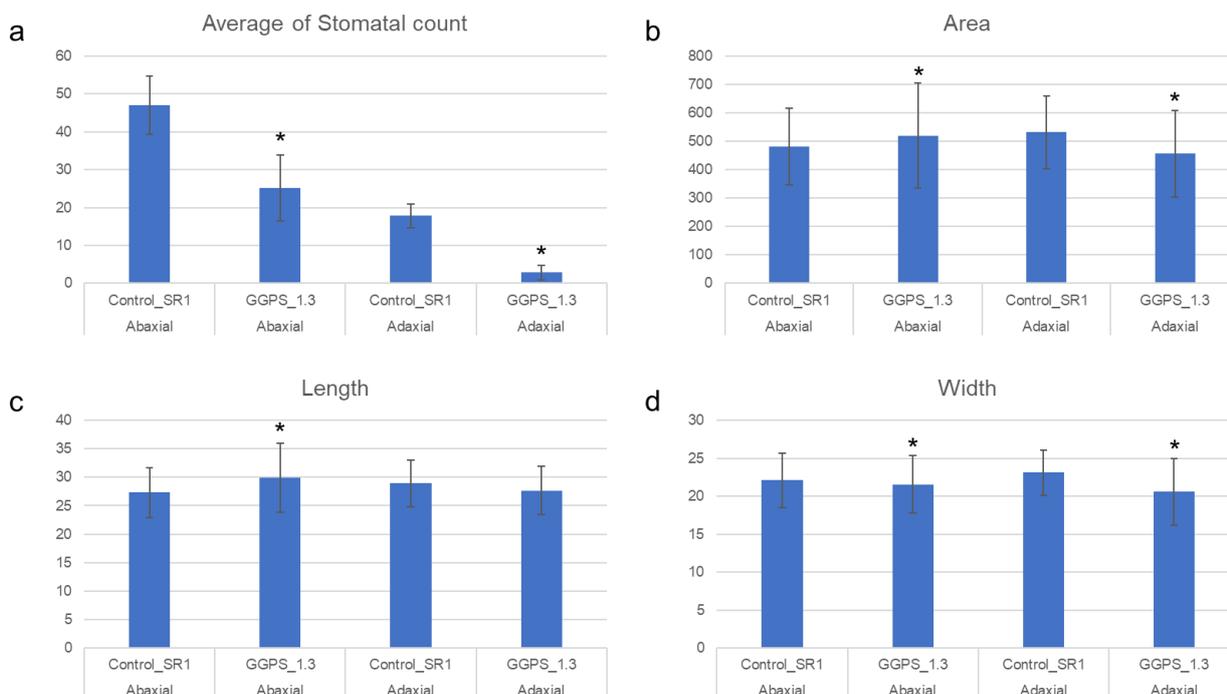
Figure 5.10 Bar graphs showing the average stomata per leaf disc (a), area of stomata (b), length of stomata (c) and width of stomata (d) with the standard deviation indicated by the error bars. Two plants per line were sampled with between 7 and 10 images taken per leaf disc and the significant difference (p < 0.01) determined with student t-test when control and transgene were compared indicated with an asterisk.

5.3.6 Leaf surface metabolites characterisation

Further analyses of the plant surface metabolites were done on selected lines (VviGGPS_1.3 and VviGGPS_10.4) with plants grown in the greenhouse from the hardening-off stage. The extracellular lipids soluble in organic solvents was extracted and identified via GC-MS with various fatty acid, alkane and other compounds identified. The peaks were integrated and normalised to the internal standard (tetracosane) peak area. The average normalised area of the putatively annotated peaks is shown in **Table C-i**. Variation between extraction (technical) repeats was very high for some peaks, as indicated by an asterisk in **Error! Reference source not found.**. PCA was done for all the samples using the peak areas as variables (excluding the peaks with high variability between technical repeats) to determine whether there was separation between the transgenic and control plants based on the compounds extracted from the leaf surface (**Figure C-i**a). The VviGGPS_1.3 line separated from the Control_SR1 samples as indicated by the red circle (Figure C-ia) which led to an OPLS with samples from just the control plants and the VviGGPS_1.3 lines (**Figure 5.11**a). The blue and yellow circles in the loading scatter plot (**Figure 5.11**b) indicate which peaks were driving the separation between the control and transgenic samples.
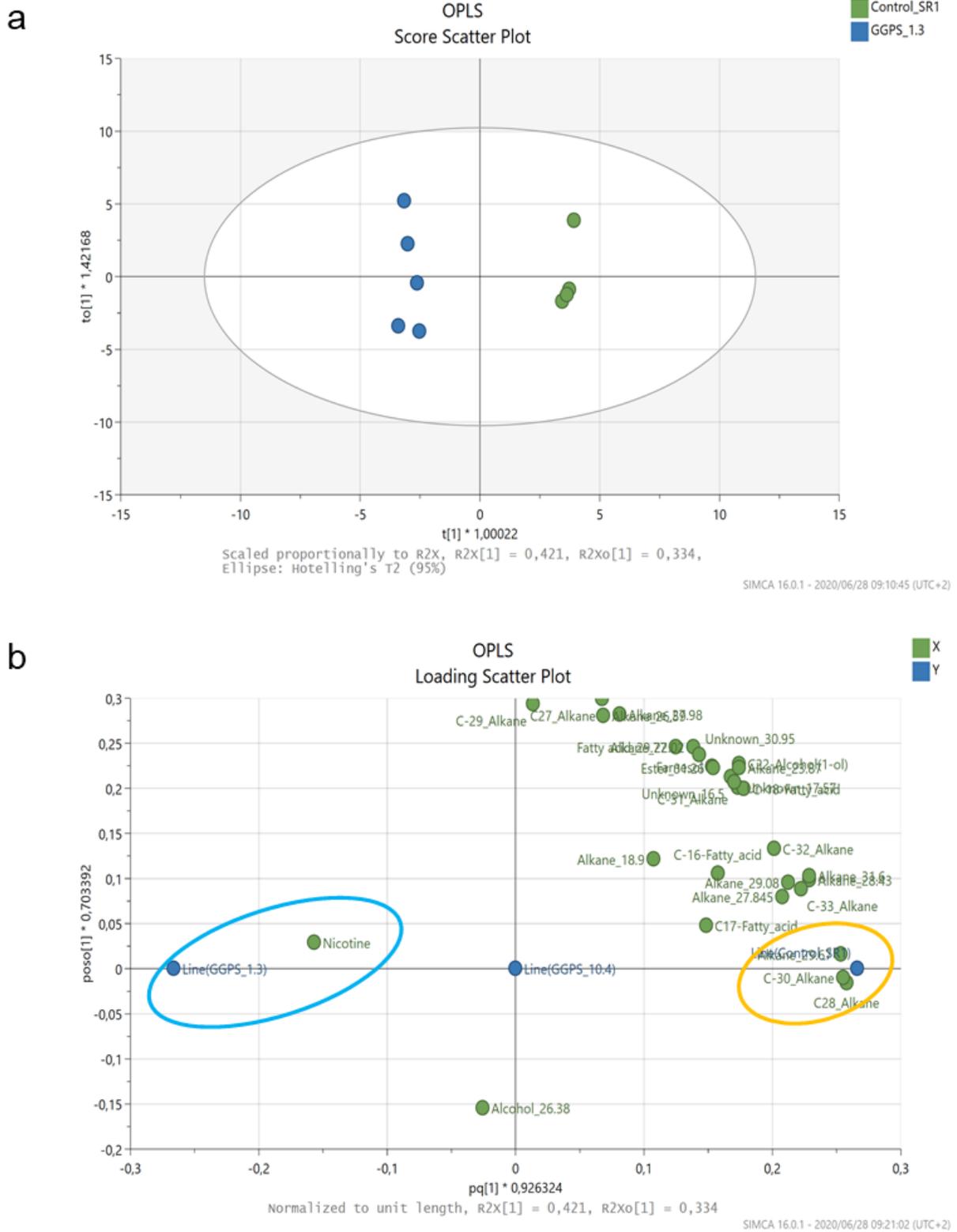
Figure 5.11 Based on the separation of GGPS_1.3 from Control_SR1 samples in the PCA score scatter plot, an OPLS was performed with these two lines (a) with the loading scatter plot (b) indicating the peak driving the separation.

Comparison of the peak areas identified as variables driving the separation between the transgenic and control plants are shown in Figure 5.12. Except for the putatively identified nicotine (**Figure 5.12**a), the VviGGPS_1.3 line had significantly ($p < 0.05$) lower levels of the three alkane compounds (**Figure 5.12**c - d).
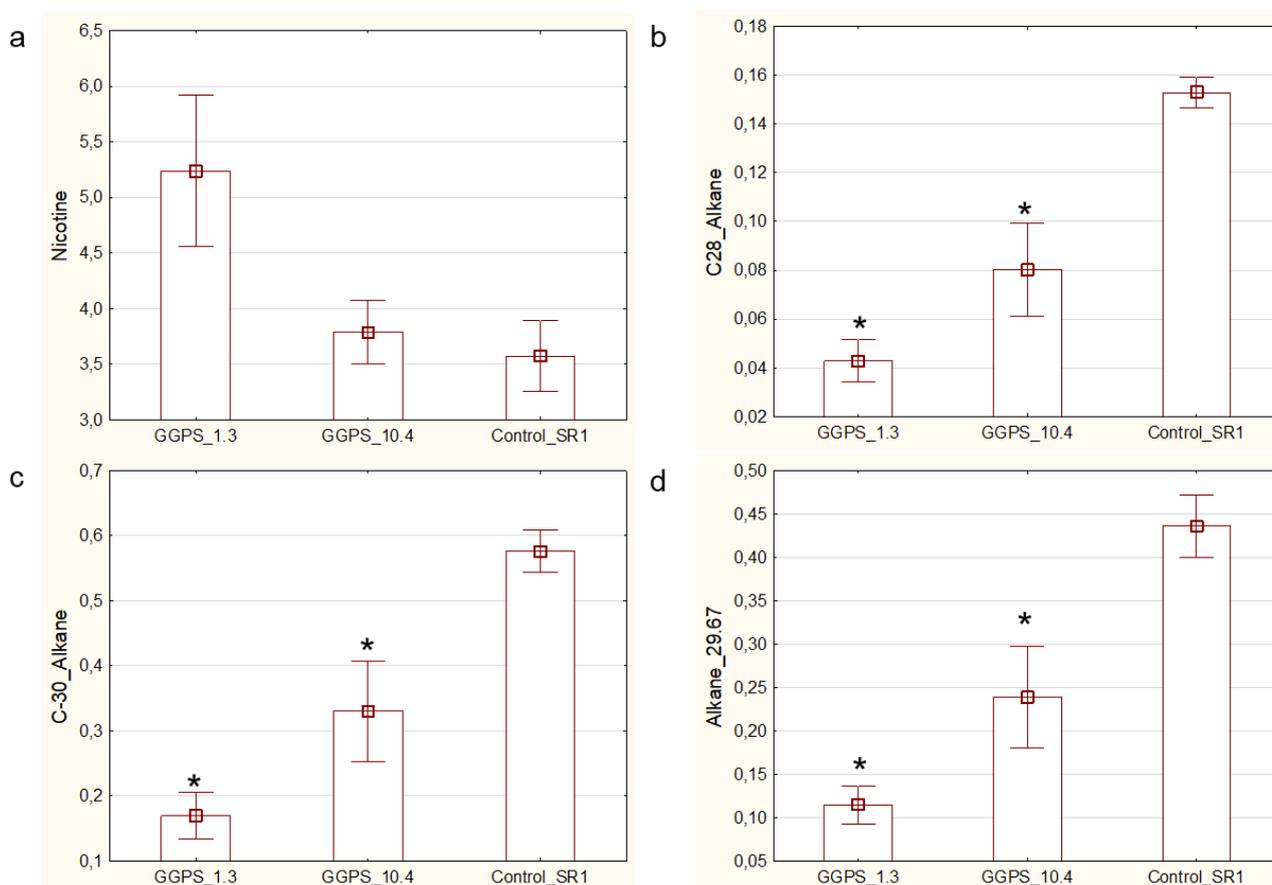
Figure 5.12 Comparison of the average peak area of compounds identified in the OPLS to drive the separation between transgenic and control samples. Bar graphs show average and error bars the standard error. * indicates significant difference from Control_SR1 determined with t-test ($p < 0.05$).

5.3.7 Flower phenotyping and flavonoid composition of corolla

A prominent phenotype observed in the flowers of some of the transgenic lines was the elongated style that protruded above the corolla. A representative sample of the control versus the transgenic flowers at different developmental stages are shown in Figure 5.13a, with measured length of the flower corolla tube and the pistil at the time of anthesis shown in the graph (Figure 5.13b). The severity of this phenotype ranged from only slightly extending above the corolla at the time of anthesis to the sigma and the upper part of the style being clearly visible even at early flower development (Figure 5.13a). Natural self-fertilisation was not possible in the transgenic flowers with the elongated style phenotype due the position of the stigma above the anther. Length

237

measurements (Figure 5.13b) show that for the transgenic flowers the corolla tube was significantly ($p < 0.05$) shorter than that of the control flowers, while the style length remained the same.
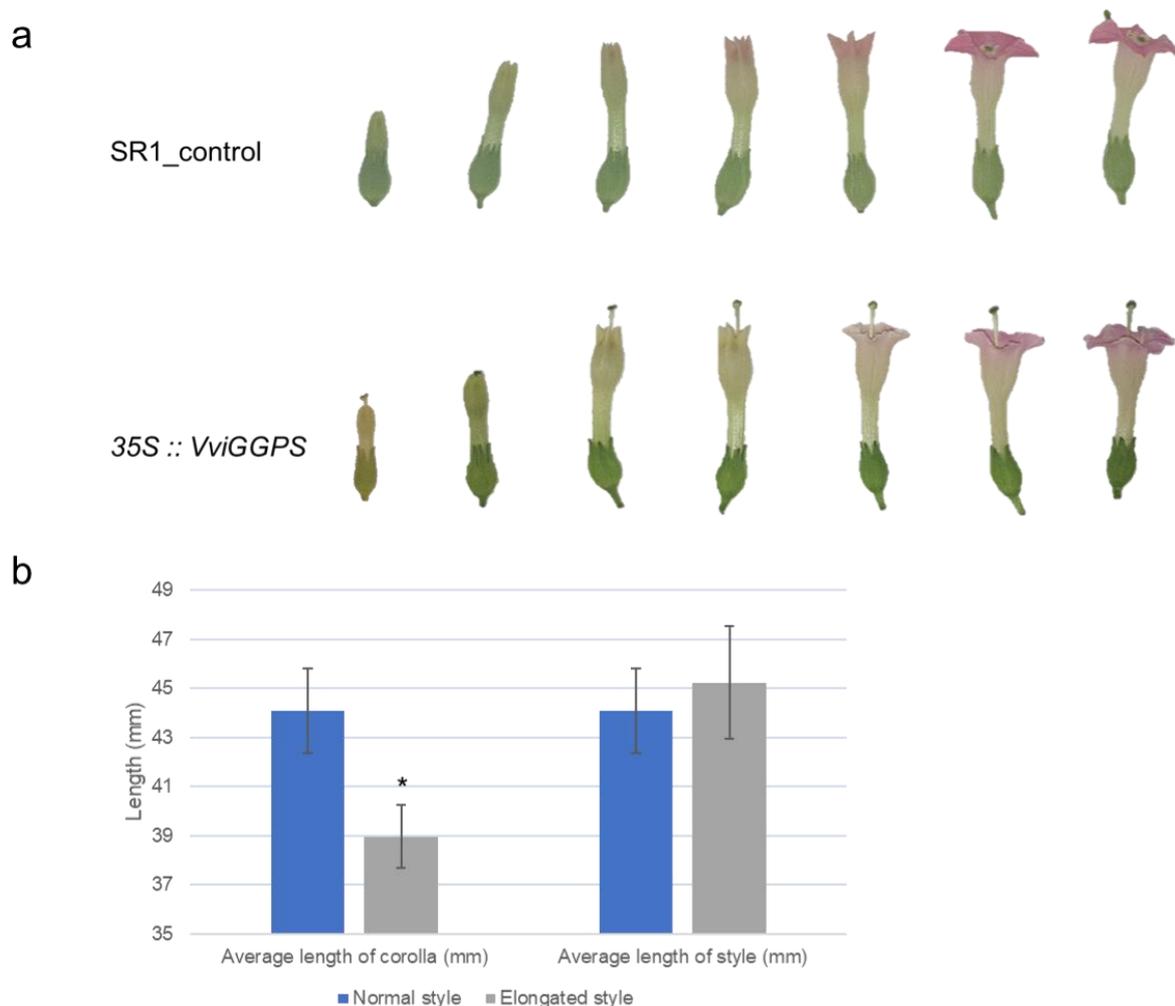
Figure 5.13 Representative sample of flowers at various stages of development from SR1_control compared to tobacco over-expression *VviGGPS* with the length (mm) of flowers is indicated with ruler on right (a). The measured length of the corolla tube and the style of flowers with a normal or elongated style are compared in the graph (b) with significant difference ($p < 0.01$) indicated with an asterisk. The style and corolla tube length for the normal flowers are the same but the style in the abnormal flowers extend above the petals of the corolla.

Total anthocyanin analysis using an acidified extraction buffer and spectrophotometric measurement showed that the transgenic flowers at stages 4 (fully developed flower) had significantly less anthocyanin compared to the control flowers (Figure D-i). The reduced anthocyanin levels were also phenotypically visible in the light pink coloration of the corolla.

Profiling of the flavonoid composition of the corolla from flowers harvested at four different developmental stages (Figure 5.14a) was done to further investigate the variation of the transgenic flower from the control flower. Various peaks were detected at the four wavelengths with peak

238

identification done when possible, only standards for epicatechin and catechin were available while the other peaks were putatively annotated based on mass spectra or otherwise labelled according to wavelength and peak number. PCA with the normalised peak area as variables show separation of the samples based on genotype as well as the developmental stage (**Figure 5.14**b). Samples from Stage 3 and 4 (circled in blue) were used for OPLS-DA (**Figure 5.14**c) with the variables driving the separation shown in **Figure 5.14**d.
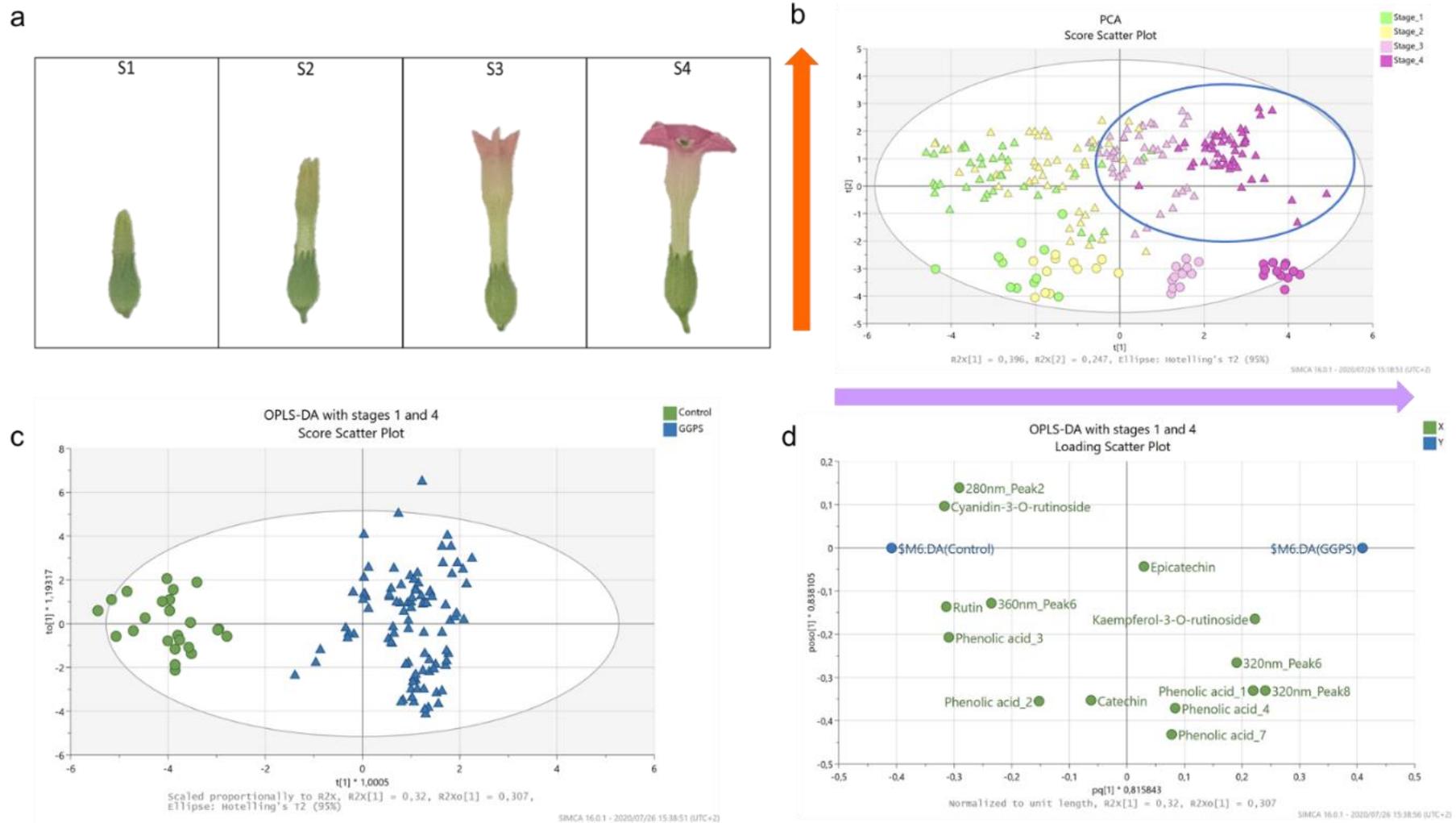
Figure 5.14 Flowers were sampled at four different stages during development (a) for flavonoid profiling. Samples in PCA score scatter plot was coloured according to developmental stages (b) with the direction of separation indicated with a purple while the transgenic plant samples were indicated by triangles and the control plant samples with circles, direction of separation according to genotype indicated by orange arrow. Stages 3 and 4 was used for OPLS-DA with genotype set as the y-variable (c) with the loading scatter plot showing the variables driving the separation between these groups (d).

240

The variables driving the separation between the transgene and control flowers in the OPLS-DA (**Figure 5.14**c & d) were selected for analysis of variance (ANOVA). Peak areas of rutin and a peak putatively identified only as a phenolic acid (phenolic acid_3) (**Figure 5.15**a & b) were significantly higher in the control samples when compared to the transgenic samples at each developmental stage and remained relatively constant during flower development only declining in the fully developed flower (Stage 4). ANOVA of Cyanidin-3-O-glucoside (**Figure 5.15**e) and the unidentified peak at 280nm (**Figure 5.15**c) showed a significant increase in the peak area as the flower developed in the control plant. cyanidin-3-O-glucoside (**Figure 5.15**e) remained low in the transgenic flower during development and this was supported by the results from total anthocyanin determination (**Figure D-i**). Two peaks identified at the 320 nm wavelength, Phenolic acid_1 and peak 8 (**Figure 5.15**h & i), had significantly lower peak areas in the control flowers compared to the transgenic flowers during stages 1 to 3. The peak areas steadily decreased during flower development until there was no significant difference between control and transgenic flower samples in the fully developed flower (Stage 4). The normalised areas of the unidentified peak 6 (**Figure 5.15**d) at the 360nm wavelength and the phenolic acid peak 2 (**Figure 5.15**f) decreased during flower development and there was only a significant difference at the Stage 1 with higher peak areas observed in the control flowers. The peak putatively identified as kaempferol-3-O-rutinoside (**Figure 5.15**g) was significantly higher in line VviGGPS_6.4 and VviGGPS_10.4 compared to the other lines and control samples, with levels increasing between Stage 1 to Stage 2 but then stabilising.
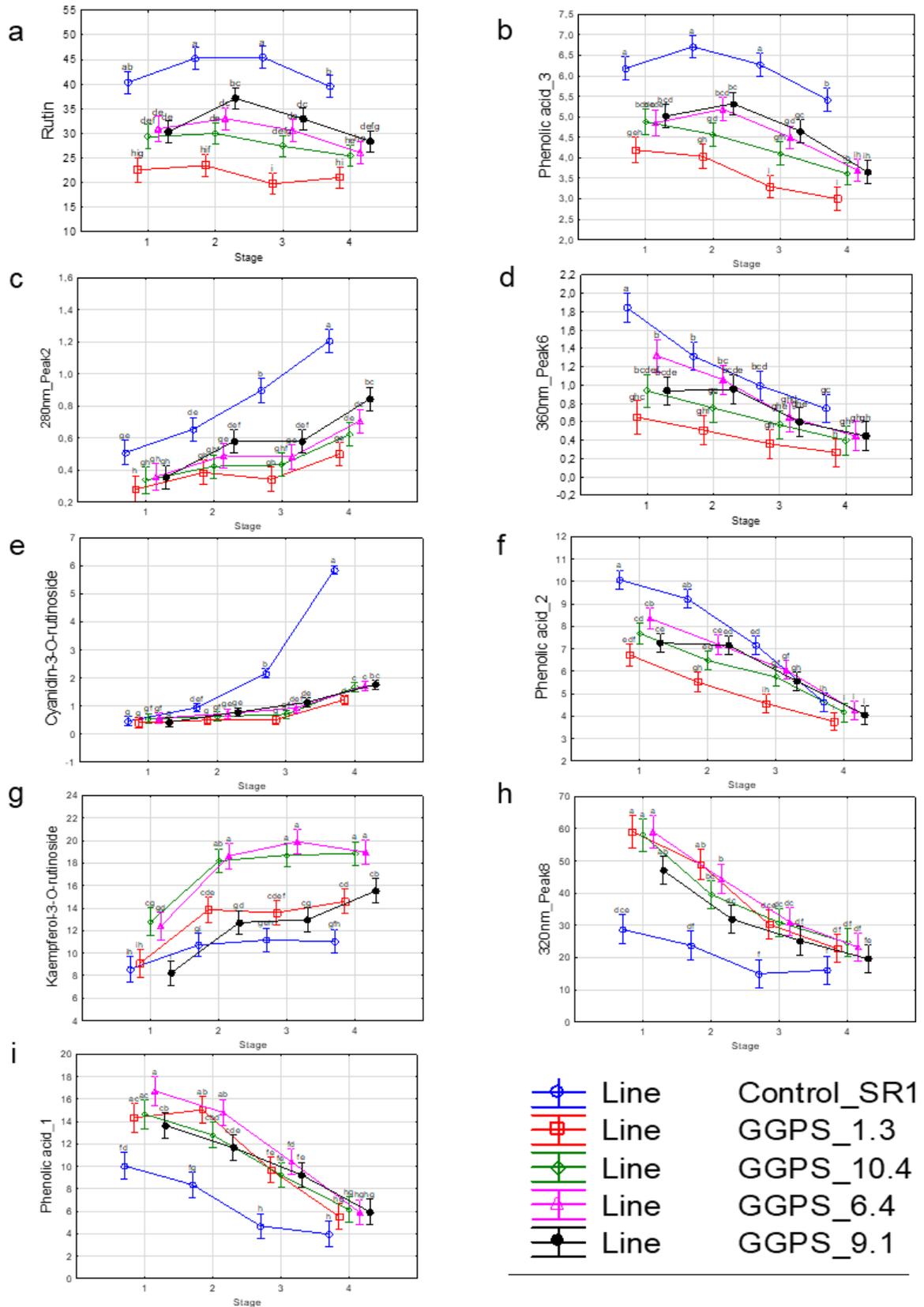
Figure 5.15 ANOVA of peaks driving the separation with Tukey HSD post-hoc test (α = 0.05) to determine significant differences and indicated by letters.

5.4   Discussion

5.4.1   Biomass and plant growth

Based on the results from the previous chapter it was decided to continue with further analysis on plants that had been moved to greenhouse conditions at an early stage of growth. Analysis of the growth profile of the transgenic population in comparison to the control plants did not point to an overall population difference except for decreased stem diameter in all lines studied. However, line VviGGPS_1.3 had a significantly different growth profile compared to the control plants. Flowering time was delayed, the plants had a reduced height with shorter internodes and thinner stems, while the biomass (weight per area) was higher. Line VviGGPS_10.4 also showed a delay in flowering time, and lines VviGGPS_9.1 and VviGGPS_10.4 an increase in biomass.

The abnormal phenotype, specifically of line VviGGPS_1.3, could be due to altered levels of gibberellin. In a study by Gallego-Giraldo *et al.*, (2008) the increase in the level of active gibberellin in the tobacco apical shoots inhibits transition to flowering with the final stem length increased due to higher number of vegetative internodes. In the case of line VviGGPS_1.3 the stem length was not increased (quite the opposite) but the transition to flowering was delayed in line VviGGPS_1.3 and VviGGPS_10.4. Dwarfism was observed in tomato plants over-expressing a phytoene synthase gene (*PSY)* with the phenotype attributed to a decrease in gibberellin through the diversion of the GGPP substrate away from phytohormone production (Fray *et al.*, 1995). Gibberellin has been shown to affect LEAFY (LFY) transcription in *Arabidopsis* (Blázquez *et al.*, 1998) with over-expression of LFY as well as ectopic expression of *N. tabacum* LEAFY – like gene in tobacco resulting in altered phyllotaxy of both flowers and leaves with the primordia developing incorrectly (Ahearn *et al.*, 2001). Another locus activated by gibberellin is the FLOWERING LOCUS T (FT) as seen in *Arabidopsis* (Mutasa-Göttgens & Hedden, 2009). Heterologous expression of *FLOWERING LOCUS T (FT)* from *Gossypium hirsutum* in tobacco having a pleiotropic effect on the transgenic plants which included formation of lateral shoots (multiple shoot formation), increased axillary bud set and altered leaf development (Li *et al.*, 2015).

5.4.2   Leaf morphology and coloration

General observations of the transgenic plant populations indicated that some of the leaves were smaller and had a leaf shape that was different from the control plants of the same population. All phenotypes could be observed in one leaf but were not necessarily linked. Quantitative analysis of the transgenic leaves in comparison to the control plants confirmed that the transgenic leaves were smaller. Calculation of the fractal dimension based on the box-

243

counting method also showed significant differences between most transgenic leaves compared to the control plants. The fractal dimension is used to describe the leaf shape complexity (Cope *et al.*, 2012) with a higher value indicating a more complex shape (Fuentes *et al.*, 2018). The transgenic leaves generally had higher value compared to the control leaves with the curled leaf margin phenotype being the likely cause for the higher FD value. Some of the leaves also seemed to have a darker green colour than the control plants with the RGB results indicating that there might basis to these anecdotal observations.

Ectopic expression of *psy* genes in *N. tabacum* Petit Havana SR1 resulted in various phenotypic aberrations including curled (involute and revolute) leaf margin and altered leaf texture that closely resembled the transgenic leaf phenotype observed in this study (Busch *et al.*, 2002). Although the study did not include phytohormone analysis, another study involving ectopic over-expression of *psy* genes in tomato plants showed that gibberellin levels were lower, most likely due to diversion of GGPP to the carotenoid biosynthesis branch (Fray *et al.*, 1995). *Nicotiana sylvestris* and *N. tabacum* cv. Hicks *MM* plants over-expressing *NtFPF1* (*FLOWERING PROMOTING FACTOR* from Tobacco) displayed a wrinkled leaf appearance especially in the later formed leaves which resembles the "bubbly" phenotype observed in this study (Smykal *et al.*, 2004). The *NtFPF1* over-expressing plants showed an enhanced responsiveness to GA$_3$ treatment indicating a connection between the phytohormone and the gene. Based on these studies the transgenic leaf phenotype could be due to altered gibberellin levels, specifically a lower level of the phytohormone.

5.4.3   Photosynthesis and photosynthetic compounds

In Chapter 4, the effect of the growth conditions on the abnormal transgenic population was investigated with photosynthetic measurements of selected lines grown in the autumn and winter growth season showing a differential response depending on the environmental conditions. Measurements during the Autumn growth season showed that the transgenic plants (line VviGGPS_1.3 and VviGGPS_10.4) were able to maintain a higher photosynthetic rate than the control plants and the biomass (dry weight per area) of these leaves were also higher than the control plants (5.3.3).

The DLI has a significant effect on plant growth and flowering, although the specific impact can be species-dependent the general trend is higher biomass and flower number with increasing DLI (Korczynski *et al.*, 2002; Faust *et al.*, 2005). The reason for the effect of light on the plant phenotype could be connected to phytochrome-interacting factors (PIFs) which has been shown to regulate carotenoid biosynthesis (Toledo-Ortiz *et al.*, 2010), with the overproduction of GGPP possibly allowing for higher levels of carotenoids as well as

chlorophyll being produced. However, photosynthetic pigment analysis of the leaves showed a 10% decrease in chlorophyll a & b in line VviGGPS_1.3 compared to the control plants when grown in the greenhouse, which is contrast to the almost 60% increase of chlorophyll a & b compared to the control plants when grown in the climaroom (Chapter 4). No significant difference in the photosynthetic pigments were measured in line VviGGPS_10.4, which is consistent with the results obtained from the climaroom grown plants, however, the Chl a/b ratio was higher in the greenhouse grown plants. Neoxanthin and β-carotene was also found to be significantly lower in the greenhouse grown VviGGPS_1.3 line in comparison to the control. The high light conditions resulted in quantifiable levels of antheraxanthin and zeaxanthin, however, none of the compounds involved in the violaxanthin cycle were significantly different from the control plants. The other xanthophyll cycle present in higher plants, although taxonomically restricted, involves lutein epoxidation to lutein epoxide and has not been shown to exist in tobacco (Procházková *et al.*, 2009; Goss & Latowski, 2020). However, a peak corresponding to the retention time and wavelength of lutein epoxide was detected in the tobacco leaf samples, which indicates that this light sensitive pathway could be present in tobacco.

Carotenoid and pigment analysis of the greenhouse grown plants could not provide a viable reason for the increased photosynthetic rate in the transgene plants. The sessile nature of plants necessitates a sophisticated method of monitoring the environment and the ability to react appropriately to stimuli. Due to the importance of light in photosynthesis various processes within the plant are affected by this stimulus (Lymperopoulos *et al.*, 2018) with phytohormones playing an essential role in signalling (Ljung *et al.*, 2015). The interaction of sucrose, produced through photosynthesis, with various phytohormones including gibberellin could explain the phenotypes observed in the transgenic population (Ljung *et al.*, 2015). The increased photosynthetic rate could therefore be ascribed to higher levels of gibberellin since the phytohormone has been shown to activate *AtFT1* expression (Mutasa-Göttgens & Hedden, 2009) with over-expression of *GhFT1* in tobacco affecting photosynthesis. Although the authors of the study reasoned that the higher chlorophyll content was the reason for the increased photosynthetic rate, it is possible that *FT1* has a pleiotropic effect with chlorophyll levels correlating to photosynthesis but not necessary directly affecting it (Li *et al.*, 2015).

Using SEM, the stomata of the control and transgene (VViGGPS_1.3) leaves were investigated in more detail to determine whether stomatal density could be influencing the higher rate of stomatal conductance measured. Interestingly, the results showed that the transgenic line had fewer stomata than the control, which is contradictory to the higher stomatal rate measured. Several phytohormones, including gibberellin, have been shown to

regulate stomatal development, with GA treatment of *A. thaliana* resulting in an increase in hypocotyl stomatal density (Saibo *et al.*, 2003; Qi & Torii, 2018). However, it should be noted that the plants used for SEM analysis were greenhouse-grown in the winter with the reduced light possibly affecting stomatal development. In addition, the small sample size is not ideal for statistical analysis. Based on these shortcomings it is recommended that future studies should use plants grown in autumn (higher light) and with the number of plants and lines sampled increased.

5.4.4 Coloration of corolla

A prominent transgenic phenotype observed was the light pink coloration of the flower petals. Analysis of the phenolic composition showed that the light colour was due to decreased levels of anthocyanins. Previous studies wherein expression of genes in the carotenoid pathway were altered in *N. tabacum* also resulted in decreased coloration of the flowers. The phenolic compounds were not measured in these studies and therefore decreased anthocyanin levels cannot be credited as the cause of the lighter petal colour as was shown in this study (Busch *et al.*, 2002; Ji *et al.*, 2009). Although GGPP does not lead directly to anthocyanin biosynthesis (**Figure 5.1**), gibberellin has been shown to antagonise anthocyanin biosynthesis through the degradation of DELLA proteins (Li *et al.*, 2014) and a study by Loreti *et al.*, (2008) showed repression of anthocyanin pathway genes through the addition of Gibberellic acid (GA). Increased levels of GA in this study's transgenic plants, specifically during flower development, could be the cause of the lower levels of anthocyanin in the corolla, although it will require measurement of the phytohormone to support this hypothesis. An alternative hypothesis could be that increased flow through one pathway, due to ectopic expression of *VviGGPS1,* could affect the flux through another seemingly unrelated pathway.

5.4.5 Elongated style and filament

Length measurement of the flower style and corolla showed that the elongated style phenotype observed in many of the lines was due to the corolla or flower tube being shorter in the mature transgenic flowers compared to the control plants. Constitutive over-expression of *AGL20,* which is regulated by the GA pathway, in *Arabidopsis* and its homologue (*MADSA*) in *N. tabacum* Maryland Mammoth altered the flower phenotype including an elongated pistil/style which prevented self-pollination (Borner *et al.*, 2000). The study did not include measurements of the corolla to quantitatively compare the transgenic flower with control flowers. Some of the transgenic flowers also displayed elongated filaments with stamen development modulated by phytohormones, specifically gibberellins and jasmonates

(Marciniak & Przedniczek, 2019). It therefore seems as if gibberellin also plays a role in the elongated style and filament phenotype.

5.4.6 Premature bud abscission

A phenotype that was often observed in transgenic plants and linked to light colour of the petal and elongated style (or smaller corolla) was the premature abscission of flower buds. The formation of multiple buds but with the inability to mature to flowers phenotype was also observed during a study wherein *psy* genes were ectopically expressed in tobacco (Busch *et al.*, 2002) and when *GhFT1* was heterologously expressed in tobacco (Li *et al.*, 2015). As mentioned previously, this phenotype (in addition to other characteristics) was connected to lower levels of gibberellin. Studies of the *tap3 (APETALA3) A. thaliana* mutants showed that the parthenocarpic phenotype characteristic of this mutation was affected by the growth conditions. This can be linked to this study where the greenhouse-grown plants displayed lower levels of fruit set. This study found that increased GA biosynthesis, activated in the ovaries and associated with abnormal stamen, triggered parthenocarpy in the mutant plants (Okabe *et al.*, 2019). From general observations of the transgenic population in this study it did not seem as though parthenocarpy occurred, once the bud could develop into a flower and fertilisation was possible there was fruit set. However, the study did show that environmental conditions influenced the phenotype observed which could be due to GA activity.

5.5 Conclusion

Five *GGPSs* were identified in grapevine based on sequence analysis of the genome (Coman *et al.*, 2014; Leng *et al.*, 2017). Although not as extensive as the *Arabidopsis GGPS* gene family, the presence of multiple *VviGGPS* members indicate that some sub-functionalisation is likely. Two of these *GGPSs* were predicted to be the products of gene duplication and contained all the characteristic motifs of GGPSs functioning as homodimers and producing GGPP. One of these genes was predicted to encode for enzyme which localises to plastids and was over-expressed in tobacco.

Previous studies in which *GGPSs* were ectopically expressed in plants indicated that the effect on the phenotype would not be predicable. A study in which a bifunctional IDS was over-expressed in spruce did not result in altered levels of the primary terpenoids or the resin mono- and diterpenes even though the substrates, GPP and GGPP, of these metabolites were shown to be higher. Instead, increased levels of geranylgeranyl fatty acid esters were produced which were shown to play a role in plant defence (Nagel *et al.*, 2014). Silencing of *GGPS* in *N. attenuata* resulted in decreased diterpenes but not phytoene or phytol (Jassbi *et al.*, 2008) while over-expression of *GGPS* from *G. lutea* in tobacco increased β-carotene levels only

247

slightly with the phenotype otherwise appearing normal. In contrast, the overexpression of *HaGGPS* in tobacco had a positive effect on the growth of the transgene plants with increased biomass and seed yield reported with elevated levels of gibberellin cited as the cause of the phenotype (Tata *et al.*, 2016). It is understandable that the biosynthesis of primary (central) metabolites are tightly regulated and since GGPP is a branchpoint substrate utilised in various pathways it is expected that increased levels would not necessarily translate to an increase in all the metabolites derived from GGPP. A recent study by Camagna *et al.*, (2019) highlighted the importance of the downstream enzymes in shuttling GGPP to the various pathways. Ectopic expression of *AtGGPS11* in *A. thaliana* did not result in a significant increase of carotenoids but over-expression of *AtPSY* on its own or in combination with *AtGGPPS11* did result in a significant increase in these compounds. In addition, over-expression of genes encoding for enzymes involved in carotenoid biosynthesis reactions downstream of GGPS resulted in higher levels of β-carotene in comparison to what was achieved with *GlGGPS* over-expression (Ji *et al.*, 2009). In rice, the flux towards chlorophyll biosynthesis is orchestrated through the "recruitment" of OsGGPS1 to a metabolon in the thylakoid which represents just one of the mechanisms used in allocating GGPP to the many terpenoid biosynthetic branches (Zhou *et al.*, 2017).

Characterisation of the tobacco population ectopically expressing *VviGGPS1* showed that the phenotype, comprising of the morphology, metabolome, and physiology, was affected with the environment playing a role in the severity and frequency of the phenotype observed. Metabolite levels, such as carotenoids and diterpenes which utilise GGPP as a substrate, were affected in some lines and under some conditions but it was not consistently altered. It should be noted that in all the studies mentioned above, wherein *GGPSs* were studied *in planta,* there was no mention that the transgenic plants were grown under various conditions to determine whether the environment influenced the phenotype. It is therefore possible that growing the plants under different conditions could affect the phenotype as seen in this study. Interestingly, ectopic expression of *PSY* in *N. tabacum* plants displaying a phenotype closely resembling the phenotype observed in this study (Busch *et al.*, 2002). The severity of the phenotype ranged across lines but some of the observed phenotypes included curling of the leaf edge, altered leaf surface, excessive bud formation with failure to form flowers and pale to white flowers. The authors referred to another study where *psy* was over-expressed in plants and a decrease in gibberellin, due to diversion of GGPP to carotenoids instead of GA biosynthesis, was given as the cause of the phenotype (Fray *et al.*, 1995). However, this only addressed the dwarf phenotype observed in some of the high transgene expressors and not the altered leaf, bud, and flower phenotype. Another study showed that co-suppression of phytoene synthase in tomato plants resulted in pale flowers (Fray & Grierson, 1993) but

248

tomato flower coloration is due to xanthophyll accumulation (Galpaz *et al.*, 2006) and not anthocyanins so it cannot be the cause for the light coloration seen in the transgene tobacco flowers.

The pleiotropic phenotype in the transgenic tobacco population over-expressing *VviGGPS1* indicates the possibility of a phytohormone playing a role. GGPP is the substrate (indirectly or directly) to various phytohormones, one of these being gibberellin (**Figure 5.1**). Although phytohormones were not measured in this study, the phenotype observed in the transgenic population indicated that the gibberellin levels were affected with the various abnormal phenotypes discussed above and placed into context with previous studies to support this hypothesis. However, the transgenic phenotype presents a contradictory picture with some phenotypes observed in the *VviGGPS1* transgene population seemingly attributed to decreased levels of gibberellin while other phenotypes are due to higher levels of the phytohormone. Based on the biosynthesis pathway for gibberellin (**Figure 5.1**) and the predicted plastid localisation of VviGGPS1 it makes sense that over-expression of *VviGGPS1* would result in an increased production of gibberellin but biosynthesis and response to this phytohormone is under various regulatory mechanisms. A possible explanation might be that increased levels of gibberellin in different tissue and/or different developmental stages as well as the ratio of gibberellin to other phytohormones results in different characteristics observed.

It is generally thought that GGPP is synthesised by the consecutive addition of three IPPs to DMAPP (**Figure 5.1**). However, Van Schie *et al.*, (2007; 2012) presented the hypothesis that GGPP destined for gibberellin biosynthesis requires GPP and IPP as the starting substrates. Through this substrate specificity the various GGPSs can produce different GGPP pools for gibberellin and terpenoid biosynthesis. Taking this into consideration it is a possibility that *VviGGPS1* encodes for a GGPS that has a substrate specificity for GPP and IPP, producing GGPP used for gibberellin production, which can explain why the various phenotypes observed in the transgenic population are linked to altered levels of the hormone and why other GGPP derived metabolites was not always affected (based on phenotype and metabolite analysis).

5.6   Acknowledgements

5.7   References

Ahearn, K.P., Johnson, H. a, Weigel, D. & Wagner, D.R., (2001). NFL1, a Nicotiana tabacum LEAFY-like gene, controls meristem initiation and floral structure. *Plant Cell Physiol.* **42**, 10, 1130–1139.

Aitken, S.M., Attucci, S., Ibrahim, R.K. & Gulick, P.J., (1995). A cDNA Encoding Geranylgeranyl Pyrophosphate Synthase from White Lupin *Plant Physiol.* **108**, 2, 837–838.

Badillo, A., Steppuhn, J., Deruère, J., Camara, B. & Kuntz, M., (1995). Structure of a functional geranylgeranyl pyrophosphate synthase gene from Capsicum annuum *Plant Mol. Biol.* **27**, 2, 425–428.

Barja, M.V., Ezquerro, M., Diretto, G., Florez-Sarasa, I., Feixes, E., Fiore, A., Karlova, R., Fernie, A., Beekwilder, J. & Rodriguez-Concepcion, M., (2020). Several geranylgeranyl diphosphate synthase isoforms supply metabolic substrates for carotenoid biosynthesis in tomato.

Beck, G., Coman, D., Herren, E., Ruiz-Sola, M.Á., Rodríguez-Concepción, M., Gruissem, W. & Vranová, E., (2013). Characterization of the GGPP synthase gene family in Arabidopsis thaliana *Plant Mol. Biol.* **82**, 4–5, 393–416.

Blázquez, M.A., Green, R., Nilsson, O., Sussman, M.R. & Weigel, D., (1998). Gibberellins promote flowering of Arabidopsis by activating the LEAFY promoter *Plant Cell* **10**, 5, 791–800.

de Boer, A.H. & Leeuwen, I.J.D.V., (2012). Fusicoccanes: diterpenes with surprising biological functions *Trends Plant Sci.* **17**, 6, 360–368.

Borner, R., Kampmann, G., Chandler, J., Gleißner, R., Wisman, E., Apel, K. & Melzer, S., (2000). A MADS domain gene involved in the transition to flowering in Arabidopsis *Plant J.* **24**, 5, 591–599.

Busch, M., Seuter, A. & Hain, R., (2002). Functional Analysis of the Early Steps of Carotenoid Biosynthesis in Tobacco *Plant Physiol.* **128**, 2, 439–453.

Camagna, M., Grundmann, A., Bar, C., Koschmieder, J., Beyer, P. & Welsch, R., (2019). Enzyme fusion removes competition for geranylgeranyl diphosphate in carotenogenesis *Plant Physiol.* **179**, 3, 1013–1027.

Coman, D., Altenhoff, A., Zoller, S., Gruissem, W. & Vranová, E., (2014). Distinct evolutionary strategies in the GGPPS family from plants. *Front. Plant Sci.* **5**, May, 230.

Cope, J.S., Corney, D., Clark, J.Y., Remagnino, P. & Wilkin, P., (2012). Plant species identification using digital morphometrics: A review *Expert Syst. Appl.* **39**, 8, 7562–7573.

Faust, J.E., Holcombe, V., Rajapakse, N.C. & Layne, D.R., (2005). The effect of daily light integral on bedding plant growth and flowering *HortScience* **40**, 3, 645–649.

Fray, R.G. & Grierson, D., (1993). Identification and genetic analysis of normal and mutant phytoene synthase genes of tomato by sequencing, complementation and co-suppression *Plant Mol. Biol.* **22**, 4, 589–602.

Fray, R.G., Wallace, A., Fraser, P.D., Valero, D., Hedden, P., Bramley, P.M. & Grierson, D., (1995).

Fuentes, S., De Bei, R. & Tyerman, S.D., (2012). Image analysis techniques applied to canopies, berries, plant tissues and leaves. In: Int. Conf. Agric. Eng.

Fuentes, S., Hernández-Montes, E., Escalona, J.M., Bota, J., Gonzalez Viejo, C., Poblete-Echeverría, C., Tongson, E. & Medrano, H., (2018). Automated grapevine cultivar classification based on machine learning using leaf morpho-colorimetry, fractal dimension and near-infrared spectroscopy parameters *Comput. Electron. Agric.* **151**, February, 311–318.

Gallego-Giraldo, L., Ubeda-Tomás, S., Gisbert, C., García-Martínez, J.L., Moritz, T. & López-Díaz, I., (2008). Gibberellin homeostasis in tobacco is regulated by gibberellin metabolism genes with different gibberellin sensitivity *Plant Cell Physiol.* **49**, 5, 679–690.

Galpaz, N., Ronen, G., Khalfa, Z., Zamir, D. & Hirschberg, J., (2006). A Chromoplast-specific carotenoid Biosynthesis pathway is revealed by cloning of the tomato white-flower locus *Plant Cell* **18**, 8, 1947–60.

Goss, R. & Latowski, D., (2020). Lipid Dependence of Xanthophyll Cycling in Higher Plants and Algae *Front. Plant Sci.* **11**, April, 1–22.

Heiling, S., Schuman, M.C., Schoettner, M., Mukerjee, P., Berger, B., Schneider, B., Jassbi, A.R. & Baldwin, I.T., (2010). Jasmonate and ppHsystemin regulate key Malonylation steps in the biosynthesis of 17-Hydroxygeranyllinalool Diterpene Glycosides, an abundant and effective direct defense against herbivores in Nicotiana attenuata. *Plant Cell* **22**, 1, 273–292.

Honda, C., Kotoda, N., Wada, M., Kondo, S., Kobayashi, S., Soejima, J., Zhang, Z., Tsuda, T. & Moriguchi, T., (2002). Anthocyanin biosynthetic genes are coordinately expressed during red

coloration in apple skin *Plant Physiol. Biochem.* **40**, 11, 955–962.

Huang, W., Sun, W. & Wang, Y., (2012). Isolation and molecular characterisation of flavonoid 3'-hydroxylase and flavonoid 3', 5'-hydroxylase genes from a traditional Chinese medicinal plant, Epimedium sagittatum *Gene* **497**, 1, 125–130.

Jassbi, A.R., Gase, K., Hettenhausen, C., Schmidt, A. & Baldwin, I.T., (2008). Silencing geranylgeranyl diphosphate synthase in Nicotiana attenuata dramatically impairs resistance to tobacco hornworm *Plant Physiol.* **146**, 3, 974–986.

Jassbi, A.R., Zare, S., Asadollahi, M. & Schuman, M.C., (2017). Ecological Roles and Biological Activities of Specialized Metabolites from the Genus *Nicotiana*.

Ji, J., Wang, G., Wang, J. & Wang, P., (2009). Functional analysis of multiple carotenogenic genes from *Lycium barbarum* and *Gentiana lutea* L. for their effects on β-carotene production in transgenic tobacco *Biotechnol. Lett.* **31**, 2, 305–312.

Kamran, H.M., Hussain, S.B., Junzhong, S., Xiang, L. & Chen, L.-Q., (2020). Identification and Molecular Characterization of Geranyl Diphosphate Synthase (GPPS) Genes in Wintersweet Flower *Plants* **9**, 5, 666.

Korczynski, P.C., Logan, J. & Faust, J.E., (2002). Mapping monthly distribution of daily light integrals across the contiguous United States *Horttechnology* **12**, 1, 12–16.

Kuntz, M., Römer, S., Suire, C., Hugueney, P., Weil, J.H., Schantz, R. & Camara, B., (1992). Identification of a cDNA for the plastid-located geranylgeranyl pyrophosphate synthase from Capsicum annuum: correlative increase in enzyme activity and transcript level during fruit ripening *Plant J.* **2**, 1, 25–34.

Kurdyukov, S., Faust, A., Nawrath, C., Bär, S., Voisin, D., Efremova, N., Franke, R., Schreiber, L., Saedler, H., Métraux, J.-P. & Yephremov, A., (2006). The epidermis-specific extracellular BODYGUARD controls cuticle development and morphogenesis in Arabidopsis. *Plant Cell* **18**, 2, 321–39.

Laferriere, A. & Beyer, P., (1991). Purification of Geranylgeranyl Diphosphate Synthase From Sinapis-Alba Etioplasts *Biochim. Biophys. Acta* **1077**, 2, 167–172.

Lange, B.M. & Ghassemian, M., (2003). Genome organization in Arabidopsis thaliana: a survey for genes involved in isoprenoid and chlorophyll metabolism. *Plant Mol. Biol.* **51**, 6, 925–48.

Leng, X., Wang, P., Wang, C., Zhu, X., Li, X., Li, H., Mu, Q., Li, A., Liu, Z. & Fang, J., (2017). Genome-wide identification and characterization of genes involved in carotenoid metabolic in three stages of grapevine fruit development *Sci. Rep.* **7**, 1, 4216.

Li, C., Zhang, Y., Zhang, K., Guo, D., Cui, B., Wang, X. & Huang, X., (2015). Promoting Flowering, Lateral Shoot Outgrowth, Leaf Development, and Flower Abscission in Tobacco Plants Overexpressing Cotton FLOWERING LOCUS T (FT)-Like Gene GhFT1 *Front. Plant Sci.* **6**, June, 1–14.

Li, Y., Van Den Ende, W. & Rolland, F., (2014). Sucrose induction of anthocyanin biosynthesis is mediated by della *Mol. Plant* **7**, 3, 570–572.

Ljung, K., Nemhauser, J.L. & Perata, P., (2015). New mechanistic links between sugar and hormone signalling networks *Curr. Opin. Plant Biol.* **25**, 130–137.

Loreti, E., Povero, G., Novi, G., Solfanelli, C., Alpi, A. & Perata, P., (2008). Gibberellins, jasmonate and abscisic acid modulate the sucrose-induced expression of anthocyanin biosynthetic genes in Arabidopsis *New Phytol.* **179**, 4, 1004–1016.

Lymperopoulos, P., Msanne, J. & Rabara, R., (2018). Phytochrome and Phytohormones: Working in Tandem for Plant Growth and Development *Front. Plant Sci.* **9**, July, 1–14.

Marciniak, K. & Przedniczek, K., (2019). Comprehensive insight into gibberellin- and jasmonate-mediated stamen development *Genes (Basel).* **10**, 10.

Mutasa-Göttgens, E. & Hedden, P., (2009). Gibberellin as a factor in floral regulatory networks *J. Exp. Bot.* **60**, 7, 1979–1989.

Nagel, R., Berasategui, A., Paetz, C., Gershenzon, J. & Schmidt, A., (2014). Overexpression of an Isoprenyl Diphosphate Synthase in Spruce Leads to Unexpected Terpene Diversion Products That Function in Plant Defense *Plant Physiol.* **164**, 2, 555–569.

Okabe, Y., Yamaoka, T., Ariizumi, T., Ushijima, K., Kojima, M., Takebayashi, Y., Sakakibara, H., Kusano, M., Shinozaki, Y., Pulungan, S.I., Kubo, Y., Nakano, R. & Ezura, H., (2019). Aberrant Stamen Development is Associated with Parthenocarpic Fruit Set Through Up-Regulation of Gibberellin Biosynthesis in Tomato *Plant Cell Physiol.* **60**, 1, 38–51.

Okada, K., Saito, T., Nakagawa, T., Kawamukai, M. & Kamiya, Y., (2000). Five geranylgeranyl diphosphate synthases expressed in different organs are localized into three subcellular compartments in Arabidopsis. *Plant Physiol.* **122**, April, 1045–1056.

251

Procházková, D., Haisel, D. & Wilhelmová, N., (2009). Content of carotenoids during ageing and senescence of tobacco leaves with genetically modulated life-span *Photosynthetica* **47**, 3, 409–414.

Qi, X. & Torii, K.U., (2018). Hormonal and environmental signals guiding stomatal development *BMC Biol.* **16**, 1, 1–11.

Saibo, N.J.M., Vriezen, W.H., Beemster, G.T.S. & Van Der Straeten, D., (2003). Growth and stomata development of Arabidopsis hypocotyls are controlled by gibberellins and modulated by ethylene and auxins *Plant J.* **33**, 6, 989–1000.

van Schie, C.C.N., Haring, M.A. & Schuurink, R.C., (2012). Prenyldiphosphate Synthases and Gibberellin Biosynthesis In: Isoprenoid Synth. Plants Microorg. Springer New York, New York, NY 213–232.

Van Schie, C.C.N., Ament, K., Schmidt, A., Lange, T., Haring, M.A. & Schuurink, R.C., (2007). Geranyl diphosphate synthase is required for biosynthesis of gibberellins *Plant J.* **52**, 4, 752–762.

Scolnik, P. a & Bartley, G.E., (1994). Nucleotide Sequence of an Arabidopsis cDNA for Geranylgeranyl Pyrophosphate Synthase *Plant Physiol.* **104**, 4, 1469–1470.

Smykal, P., Gleissner, R., Corbesier, L., Apel, K. & Melzer, S., (2004). Modulation of flowering responses in different Nicotiana varieties *Plant Mol. Biol.* **55**, 2, 253–262.

Tata, S.K., Jung, J., Kim, Y.H., Choi, J.Y., Jung, J.Y., Lee, I.J., Shin, J.S. & Ryu, S.B., (2016). Heterologous expression of chloroplast-localized geranylgeranyl pyrophosphate synthase confers fast plant growth, early flowering and increased seed yield *Plant Biotechnol. J.* **14**, 1, 29–39.

Thabet, I., Guirimand, G., Guihur, A., Lanoue, A., Courdavault, V., Papon, N., Bouzid, S., Giglioli-Guivarc'h, N., Simkin, A.J. & Clastre, M., (2012). Characterization and subcellular localization of geranylgeranyl diphosphate synthase from Catharanthus roseus *Mol. Biol. Rep.* **39**, 3, 3235–3243.

Toledo-Ortiz, G., Huq, E. & Rodríguez-Concepción, M., (2010). Direct regulation of phytoene synthase gene expression and carotenoid biosynthesis by phytochrome-interacting factors. *Proc. Natl. Acad. Sci. U. S. A.* **107**, 25, 11626–31.

Tuan, P.A., Bai, S., Yaegaki, H., Tamura, T., Hihara, S., Moriguchi, T. & Oda, K., (2015). The crucial role of PpMYB10.1 in anthocyanin accumulation in peach and relationships between its allelic type and skin color phenotype *BMC Plant Biol.* **15**, 1, 280.

Wang, G. & Dixon, R. a, (2009). Heterodimeric geranyl(geranyl)diphosphate synthase from hop (Humulus lupulus) and the evolution of monoterpene biosynthesis. *Proc. Natl. Acad. Sci. U. S. A.* **106**, 24, 9914–9.

Wang, J., Lin, H.-X., Su, P., Chen, T., Guo, J., Gao, W. & Huang, L.-Q., (2018). Molecular cloning and functional characterization of multiple geranylgeranyl pyrophosphate synthases (ApGGPPS) from Andrographis paniculata *Plant Cell Rep.* **0**, 0, 0.

Zerbe, P., Hamberger, B., Yuen, M.M.S., Chiang, A., Sandhu, H.K., Madilao, L.L., Nguyen, A., Hamberger, B., Bach, S.S. & Bohlmann, J., (2013). Gene Discovery of Modular Diterpene Metabolism in Nonmodel Systems *Plant Physiol.* **162**, 2, 1073–1091.

Zhou, F., Wang, C.-Y., Gutensohn, M., Jiang, L., Zhang, P., Zhang, D., Dudareva, N. & Lu, S., (2017). A recruiting protein of geranylgeranyl diphosphate synthase controls metabolic flux toward chlorophyll biosynthesis in rice *Proc. Natl. Acad. Sci.* (June, 12), 201705689.

Zhu, F., Suzuki, K., Okada, K., Tanaka, K., Nakagawa, T., Kawamukai, M., Matsuda, H., Zhu, X.F., Suzuki, K., Okada, K., Tanaka, K., Nakagawa, T., Kawamukai, M. & Matsuda, K., (1997). Cloning and Functional Expression of a Novel Geranylgeranyl Pyrophosphate Synthase Gene from *Arabidopsis thaliana* in *Escherichia coli Plant Cell Physiol.* **38**, 3, 357–361.

Zhu, X., Suzuki, K., Saito, T., Okada, K., Tanaka, K., Nakagawa, T., Matsuda, H. & Kawamukai, M., (1997). Geranylgeranyl pyrophosphate synthase encoded by the newly isolated gene GGPS6 from Arabidopsis thaliana is localized in mitochondria *Plant Mol. Biol.* **35**, 3, 331–341.

Appendix A   To Chapter 5

Figure A-i Morphometric analysis of scanned leaves with various measurements shown as well as the Fractal dimension (f) calculated according to box-counting method (Fuentes *et al.*, 2018). Leaves harvested) when buds were visible in the control plants. Four leaves per plant with 16 plants measured for Control_SR1, GGPS_1.3 and GGPS_10.4 (T1 and T2 pooled), 6 plants studied for GGPS_3.4, GGPS6.4 and GGPS9.1 (T2 generation). Bar graph show average and error bars the standard error between repeats. *indicates significant difference from respective leaves of control plants determined with t-test (p < 0.05).
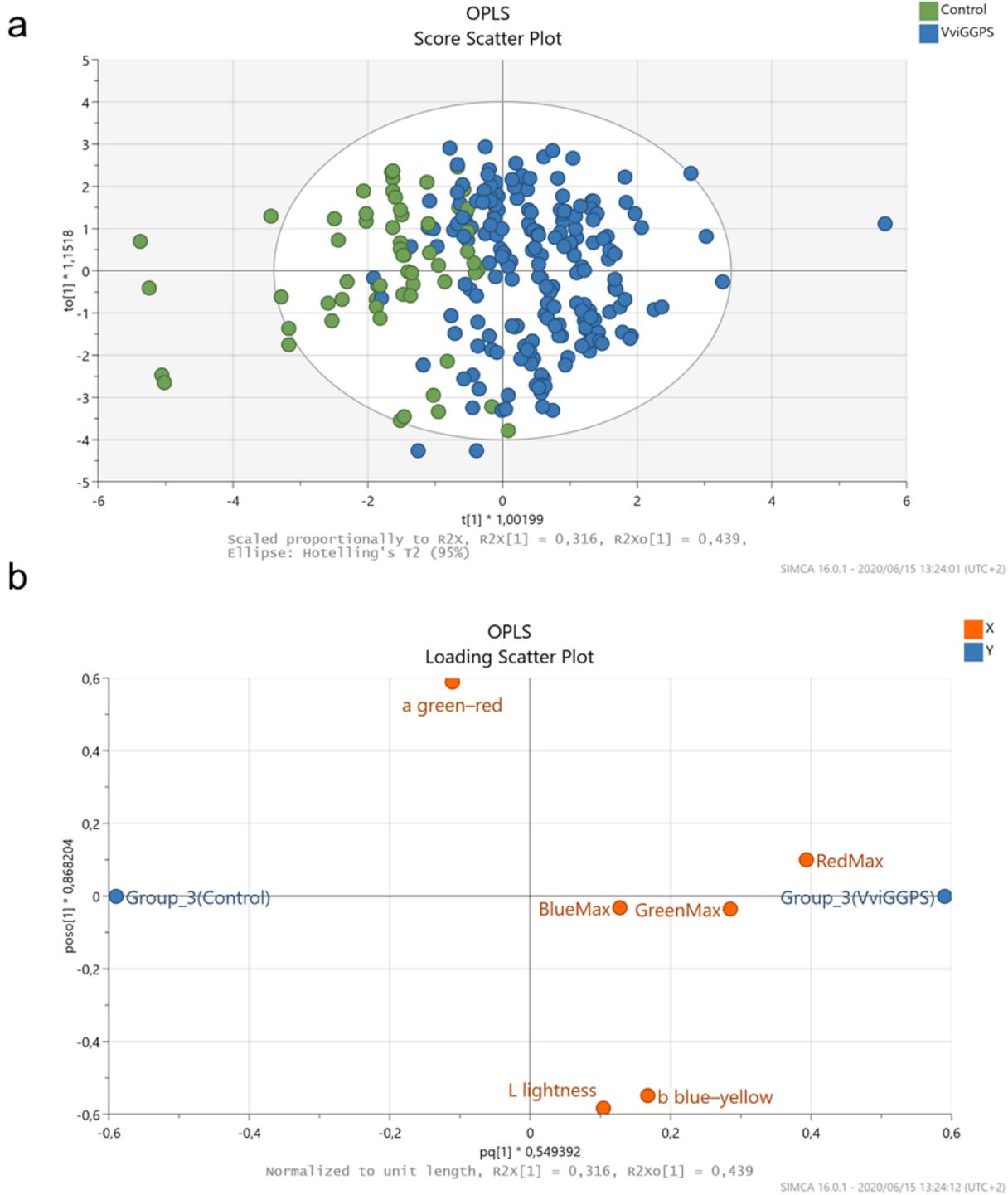
Figure A-ii OPLS plot with colorimetric parameters as x-variables and the presence of transgene as the y-variable. All lines and leaves measured included in analysis. Separation of samples shown in the Score Scatter Plot (a) and x-variables driving the separation shown in the Loading Scatter plot (b).

254

Appendix B   To Chapter 5

Table B-i Leaf 1 sampled in plants grown in Greenhouse during the Autumn growth period with six plants per line sampled and analysed. Significant differences from the control population (Control_SR1) highlighted in red. Carotenoid and pigment concentrations shown as ng.mgFW^{-1}.

| Compounds	Control_SR1	VviGGPS_1.3	VviGGPS_10.4
Neoxanthin	68.9 ± 7.7	62.2 ± 5.6	67 ± 9.5
Zeaxanthin	50.2 ± 39	42 ± 20.2	35.4 ± 35.6
β-carotene	555.2 ± 50.2	506.8 ± 28.1	533.1 ± 49.4
Antheraxanthin	12.5 ± 5.4	14.1 ± 5.9	10.6 ± 6.1
Lutein	115.7 ± 14.3	107 ± 9	115.1 ± 15.7
Lutein-epoxide	3.9 ± 1.4	3.5 ± 0.6	4.7 ± 1.2
Violaxanthin	55.6 ± 21.6	50.9 ± 11.5	69.8 ± 19.7
Chlorophyll a	4062.1 ± 423.7	3647.2 ± 237.3	3941.7 ± 473.2
Pheophytin a	45.1 ± 3.6	42 ± 3.1	43.8 ± 4.2
Chlorophyll b	1061.7 ± 114.1	959.3 ± 67.1	1012.2 ± 133.8
Pheophytin b	61.8 ± 5.8	58 ± 8.6	62.9 ± 6.8
DEPS ratio	0.4 ± 0.2	0.4 ± 0.1	0.3 ± 0.2
Chl a/b ratio	3.8 ± 0.1	3.8 ± 0.1	3.9 ± 0.1
V+A+Z	118.3 ± 24.3	107.1 ± 19.4	115.5 ± 24.8

Appendix C   To Chapter 5

Table C-i Summary of the cuticular wax analysis. Average of the normalised (to internal standard) peak areas detected with at least four biological per line with two technical (extraction) repeats per sample. *high standard deviation between extraction repeats detected in these peaks.

Compounds	Control_SR1	GGPS_1.3	GGPS_10.4
Nicotine	3.6 ± 0.6	5.2 ± 1.5	3.8 ± 0.6
Fatty acid_11.2*	0.02 ± 0.006	0.02 ± 0.01	0.02 ± 0.008
Neophytadiene*	0.01 ± 0.001	0.01 ± 0.008	0.01 ± 0.007
Fatty acid_11.95*	0.01 ± 0.002	0.01 ± 0.002	0.01 ± 0.002
C-16-Fatty_acid	0.03 ± 0.008	0.03 ± 0.004	0.03 ± 0.005
Thunbergol*	0.001 ± 0.001	0.0004 ± 0.0002	0.0005 ± 0.0003
Unknown_16.5	1 ± 0.3	0.4 ± 0.4	0.6 ± 0.3
Unknown_17.57	2.1 ± 0.4	1.1 ± 0.8	1.5 ± 0.6
Farnesol	0.2 ± 0.1	0.1 ± 0.1	0.1 ± 0.1
C17-Fatty_acid	0.03 ± 0.01	0.02 ± 0.005	0.02 ± 0.01
C-18-Fatty_acid	1.2 ± 0.3	0.6 ± 0.4	0.8 ± 0.4
Alkane_18.9	0.005 ± 0.0004	0.004 ± 0.0003	0.005 ± 0.0003
Alkane_22.02	0.03 ± 0.01	0.02 ± 0.01	0.03 ± 0.01
C22-Alcohol(1-ol)	0.05 ± 0.02	0.02 ± 0.01	0.03 ± 0.02
Alkane_23.87	0.02 ± 0.003	0.02 ± 0.002	0.02 ± 0.003
C27_Alkane	0.2 ± 0.03	0.2 ± 0.1	0.2 ± 0.03
Alcohol_26.38	0.01 ± 0.003	0.01 ± 0.003	0.01 ± 0.002
Alkane_26.59	0.03 ± 0.005	0.03 ± 0.007	0.03 ± 0.005
C28_Alkane	0.2 ± 0.01	0.04 ± 0.02	0.1 ± 0.04
C-29_Alkane	0.3 ± 0.04	0.3 ± 0.1	0.3 ± 0.04
Alkane_27.845	0.6 ± 0.1	0.3 ± 0.1	0.5 ± 0.2
Alkane_27.98	0.1 ± 0.01	0.1 ± 0.01	0.1 ± 0.01
C-30_Alkane	0.6 ± 0.1	0.2 ± 0.1	0.3 ± 0.2
Alkane_28.43	0.1 ± 0.02	0.02 ± 0.01	0.04 ± 0.02
C-31_Alkane	1.1 ± 0.1	0.9 ± 0.2	1 ± 0.1
Alkane_29.08	0.7 ± 0.1	0.4 ± 0.2	0.6 ± 0.2
C-32_Alkane	0.1 ± 0.03	0.1 ± 0.02	0.1 ± 0.04
Alkane_29.67	0.4 ± 0.1	0.1 ± 0.05	0.2 ± 0.1
Fatty acid_29.77	0.1 ± 0.02	0.04 ± 0.04	0.05 ± 0.02
C-33_Alkane	1 ± 0.1	0.5 ± 0.2	0.7 ± 0.2
C-37_ester*	0.02 ± 0.01	0.01 ± 0.01	0.01 ± 0.01
Unknown_30.95	0.4 ± 0.2	0.2 ± 0.2	0.3 ± 0.1
Ester_31.26	0.1 ± 0.02	0.02 ± 0.02	0.03 ± 0.02
Alkane_31.6	0.04 ± 0.01	0.02 ± 0.01	0.03 ± 0.01
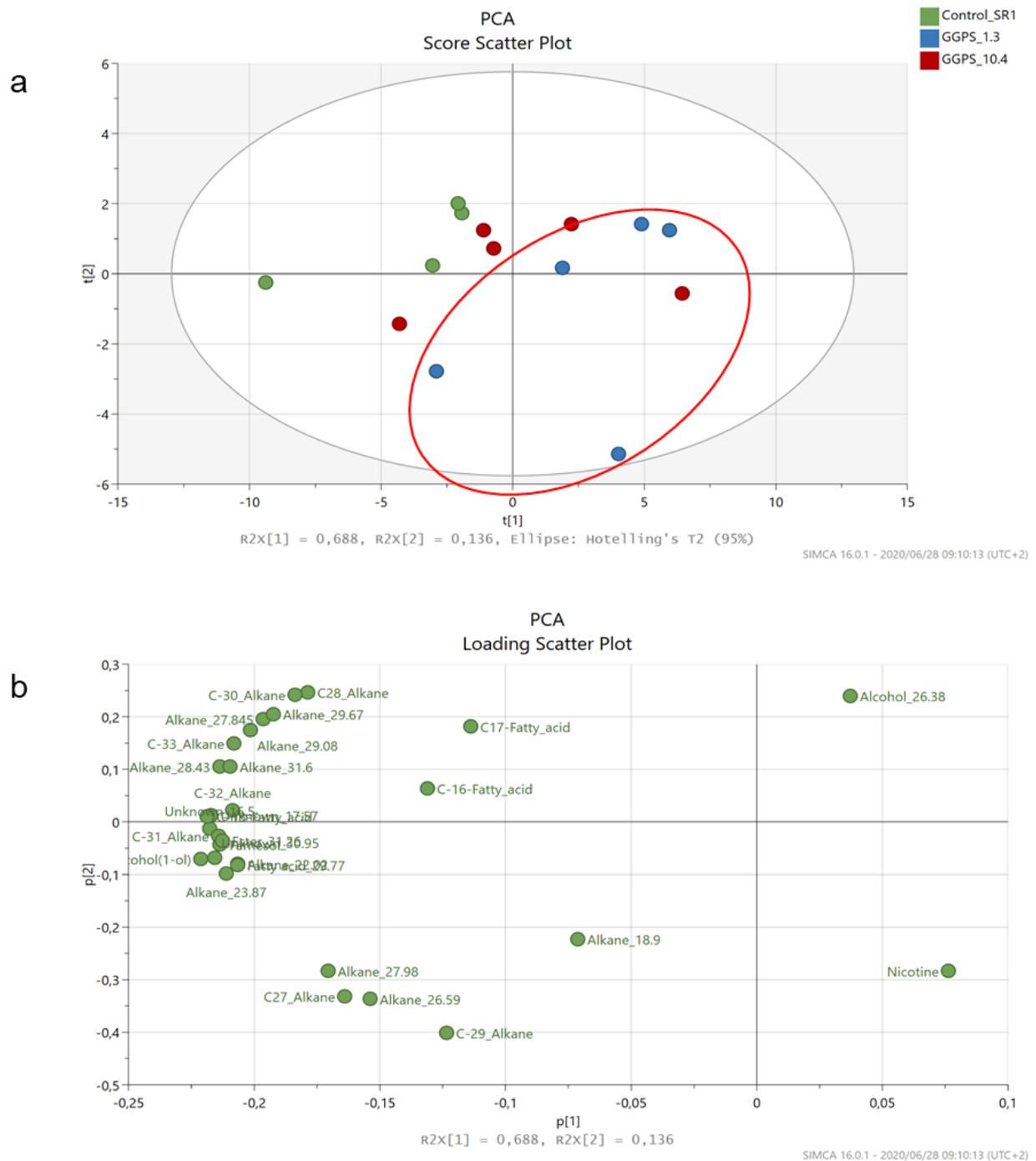
Figure C-i PCA (a) with all samples and identified peaks (excluding those with high variability between extraction repeats). Based on the separation of GGPS_1.3 from Control_SR1 samples as highlighted by red circle in the PCA score scatter plot (a), an OPLS was performed with these two lines (c) with the loading scatter plot (d) indicating the peak driving the separation.

257

Appendix D   To Chapter 5
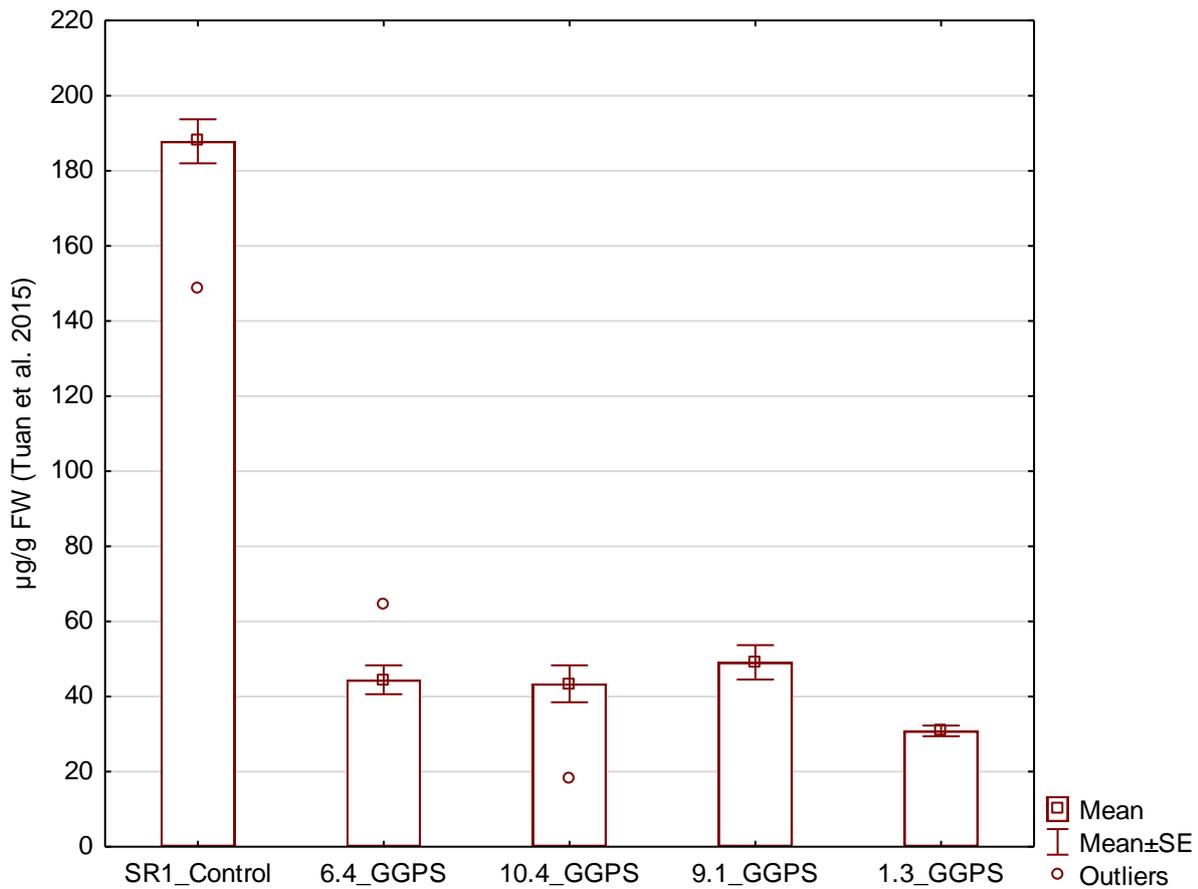
Figure D-i Total anthocyanin determination of corolla from stage 4 flowers. The spectrophotometric measurements were normalised to interference from chlorophyll based on method described by (Tuan *et al.*, 2015) and quantity determined with cyanidin-3-gluoside as a standard and expressed as µg per gram fresh weight of sample used.

Chapter 6   General discussion and conclusion

6.1   The scope of the study

Plants employ an extensive range of metabolites for their normal functioning, as well as to interact with their environment. Due to the everchanging environment and the inability to escape from it, plants need to be adaptable and therefore expanded on their repertoire of specialised metabolites utilised for plant-environment interactions (Pare & Tumlinson, 1999; Wink, 2003; Arimura *et al.*, 2008; Attaran *et al.*, 2008; Dudareva & Pichersky, 2008; Vickers, Gershenzon, *et al.*, 2009; Lee *et al.*, 2015; Abbas *et al.*, 2017; Korankye *et al.*, 2017; Tamiru *et al.*, 2017). This expansion can often be seen to have occurred in a species-specific manner (Hamberger & Bak, 2013; Karunanithi & Zerbe, 2019).

An important and highly represented group of plant metabolites is the terpenoids. Terpenoids include metabolites required for normal plant functioning, but most are specialised metabolites (Chen *et al.*, 2011; Pichersky & Lewinsohn, 2011). It is thought that plants were able to acquire the ability to produce specialised terpenoid metabolites through gene duplication and the subsequent neo-functionalisation of genes involved in primary terpenoid metabolism (Coman *et al.*, 2014; Liu *et al.*, 2016; Ilc *et al.*, 2018; Jiang *et al.*, 2019).

An important group of specialised terpenoids is the C5 - C20 terpenes, which have been shown to play various roles in plant defence against biotic and abiotic stress, attraction of pollinators and seed disseminators as well as in plant-plant communication (Pare & Tumlinson, 1999; Wink, 2003; Arimura *et al.*, 2008; Attaran *et al.*, 2008; Dudareva & Pichersky, 2008; Abbas *et al.*, 2017; Tamiru *et al.*, 2017). Two groups of enzymes play an important role in terpene biosynthesis, the short-chain isoprenyl diphosphate synthases (IDSs) and terpene synthases (TPSs). The IDS produce the substrates required by TPS to produce terpenes except for C5 terpenes which can be synthesised directly from the universal terpenoid precursor.

The increase in sequencing data from various plant genomes have shown that genes involved in terpenoid biosynthesis have undergone expansion, this is especially true for the TPS family (Coman *et al.*, 2014; Liu *et al.*, 2016; Ilc *et al.*, 2018; Jiang *et al.*, 2019). The extended *TPS* gene family is also seen in *Vitis vinifera* with cultivar-specific differences in the *TPS* sequences also observed (Kollner *et al.*, 2004; Jaillon *et al.*, 2007; Martin *et al.*, 2010). Sequence information, however, does not necessarily relate to activity of the encoded enzymes and does not provide information regarding product profile and/or the possibly functional role within the plant. Functional characterisation of the genes, which generally requires heterologous expression and product analysis, therefore remains an important (and time-consuming) step in annotating and ultimately understanding gene function (Camagna *et al.*, 2019).

259

The first aim of this study was to determine the product profile of *V. vinifera* genes involved in terpene biosynthesis using heterologous expression systems. This included the evaluation of different heterologous expression systems and analytical methods with the objective of obtaining a product profile which is an accurate representation of what is produced in the native plants system.

However, determining the product profile does not encompass the function of the gene within the plant. The second aim was therefore to evaluate and characterise an established transgenic population expressing a previously isolated and characterised *IDS* from *V. vinifera.*

6.2   Characterisation of the plant resources available to this study

Two established populations of *V. vinifera* cv. Merlot transformed with *TPS* gene mapping to *VviTPS27* and *VviTPS39,* respectively, were available to this study. The *VviTPS27* transgenic population consisted of 11 independent lines while the *VviTPS39* transgenic population consisted of six lines. The initial genotypical screening using PCR to determine integration of gene into genome were positive for most of the lines. However, ectopic expression could only be shown for the *VviTPS27* transgenic population.

Another plant resource available was *Nicotiana tabacum* L. Havana Petit SR1 population expressing *VviGGPS1.* This transgenic population was established with the T1 generation characterised in terms of gene integration as well as expression. The population consisted of eight lines with gene integration number varying from one to three and transgenic expression shown for all lines.

6.3   Major findings from the functional characterisation studies (general discussion)

6.4   The gene determines the method used

An expression system involving *Saccharomyces cerevisiae* as the heterologous host and *in vivo* production of terpene was assessed as an alternative for the functional characterisation of IDS and TPS genes. Two plant systems were also used and compared with the *S. cerevisiae* system. The plant systems consisted of *V. vinifera* (the native environment) and *Nicotiana benthamiana,* either through stable expression (*V. vinifera)* or transient expression (*N. benthamiana*).

These systems were compared with each other as well as the traditional method of heterologous expression in *Escherichia coli* which involves the *in vitro* analysis of terpenes. Based on the results it can be concluded that *S. cerevisiae* is a good alternative to the *E. coli* system since it has the benefits of being a microbiological system without the negative aspects of expressing a eukaryotic gene in a prokaryotic organism. Expression in *V. vinifera* has the benefit of the gene being ectopically expressed in its native environment but unfortunately transgenic expression could not be shown and although the volatile profile indicated differences between the control and transgenic plants it was not conclusive. In addition, the endogenous terpene production in *V. vinifera* resulted in relatively

high background noise. Establishing a stable transgenic *V. vinifera* population is also a time-consuming process which does not lend itself to being a high-throughput system. Transient expression in *N. benthamiana* proved to be a good alternative for a plant system since it is a relatively quick process, although not as quick as a microbiological system. It led to relatively high production of terpenes in transformed plants with low background noise observed. Also, the analysis system required minimal sample preparation, which increased convenience and decreased the risk of the terpene profile being altered due to the sample preparation methods used.

However, none of the systems evaluated proved to be adequate for the characterisation of the two *IDS* genes included in this study and it could not decisively be shown that these genes encode a VviGPS and VviFPS. Functional characterisation of these two genes would therefore require the conventional method using enzymes, produced through heterologous expression of the *IDS* genes, followed by incubation with the substrate(s) in enzyme assays (Pan *et al.*, 1996; Burke *et al.*, 1999).

6.4.1   Cultivar differences in genes involved in specialised metabolism

Although previously shown, this study confirmed that cultivar differences exist within the *TPS* gene family of *V. vinifera* (Drew *et al.*, 2016; Smit *et al.*, 2019). This can be seen in the sesquiterpene synthase mapping to the *VviTPS27* gene model. Although the isolate from the *V. vinifera* cv. Pinotage produced the same main product as found in previous studies for isolates mapping to the same gene model (Martin *et al.*, 2010; Smit *et al.*, 2019), the enzyme activity was very low. This is not a problem for assigning function to a gene if the levels produced are high enough, but it does indicate that cultivar difference can impact enzyme activity.

Characterisation of the monoterpene synthase isolated from *V. vinifera* cv. Sauvignon blanc and mapping to the *VviTPS39* gene model showed that the multi-product enzyme produced α-thujene as its main product. This contrasts with a previous study where isolates from *V. vinifera* cv. Gewürztraminer mapping to the same gene model produces α-terpineol as its main product. Although other aspects such the heterologous system and terpene analysis method used could have affected the product profile, sequence analysis did show species-specific differences which could affect enzyme functionality.

6.4.2   Novel characterisation of eucalyptol synthase supports the necessity for functional characterisation

Even though a vast majority of *TPS* genes from *V. vinifera* have been characterised, there remain genes which have not been annotated in terms of their product profile (Lücker, Bowen, *et al.*, 2004; Martin & Bohlmann, 2004; Martin *et al.*, 2009, 2010; Zhu *et al.*, 2014; Drew *et al.*, 2016; Dueholm *et al.*, 2019; Smit *et al.*, 2019). The heterologous expression of a *TPS* gene, isolated from *V. vinifera* cv. Pinot noir and which mapped to the previously uncharacterised *VviTPS41* gene model, showed

that this gene encodes a multi-product monoterpene synthase with eucalyptol as its main product. This is especially relevant since previous studies have attributed eucalyptol content in the grapevine to vineyard proximity to *Eucalyptus* trees (Capone *et al.*, 2012).

6.4.3 Ectopic expression of *VviGGPS1* gene in tobacco has a pleiotropic effect which suggest a phytohormone as a role player

Characterisation of a transgenic plant population constitutively expressing a target gene could enable a more holistic understanding of the functional role of the encoded product within the plant. An established and characterised *N. tabacum* L. Havana Petit SR1 population over-expressing *VviGGPS1* was used to obtain a better understanding of the function of this gene within the grapevine. The *VviGGPS* gene family annotation was updated to include all sequences previously identified (Coman *et al.*, 2014; Leng *et al.*, 2017) and the subcellular localisation, as well as the expression profiles predicted within grapevine tissues and organs. These results indicated that *VviGGPS1* is the only gene that encodes a monomeric GGPS which localises to the plastids with relatively high expression in vegetative tissue.

Characterisation of the *VviGGPS1*-expressing population included various methods such as classical visual phenotyping, physiological measurements as well as metabolite analysis. Classification of the morphological phenotype indicated that transgenic plants were affected in more than one aspect, including the growth habit, leaf shape and surface, as well as the buds and flowers. An initial screening of all the lines available lead to the selection of a few lines for further analysis. The first step in this analysis was to investigate the impact the environmental conditions have on the phenotype observed. Results showed that plants moved to the greenhouse where natural light provided the only irradiance at an early stage of growth displayed a much more severe transgenic phenotype. The physiological response in terms of photosynthesis and stomatal conductance was also affected in the transgenic plants depending on the growth conditions. At a higher daily light integral (DLI) the transgenic plants analysed were able to maintain an increased photosynthetic rate compared to the control plants. In contrast, the transgenic plants had a lower photosynthetic rate than the control plants at a lower DLI.

The preliminary characterisation of the transgenic population enabled the selection of lines for further analysis and determined the growth conditions most conducive to producing an intensified transgenic phenotype. Some of the visually observed phenotypes were studied in more depth to obtain quantitative measurements or to determine the metabolite affected. From this analysis it was shown that the anthocyanin levels were much lower in the transgenic flowers, which displayed a pale pink colour.

The pleiotropic nature of the transgenic phenotype indicates that a phytohormone is affected by the over-expression of *VviGGPS1* in *N. tabacum.* Taken together, the various phenotypes observed

262

could be indicative of gibberellin changes. However, it was not possible to determine whether the transgenic phenotypes observed were due to an increase or decrease in gibberellin levels. It was hypothesised that constitutive over-expression of *VviGGPS1* affected the various organs differently with developmental stage and environmental conditions playing an important with the interactive role of other phytohormones most likely affecting the plant phenotype.

6.5   Conclusions

The functional characterisation of genes requires an individualised approach and cannot be viewed in isolation. It therefore necessitates various methods of characterisation. The aims of this study consisted of the annotation of grapevine genes involved in terpenoid biosynthesis, this included the evaluation of various expression systems. This study satisfied the first aim through the novel annotation of a eucalyptol synthase and a re-annotation of a previously characterised gene to an α-thujene synthase. The various heterologous expression systems and methods for analysis were also evaluated which provides a basis for accelerating future functional characterisation studies of terpenoid related genes.

The second aim consisted of the characterisation of an established transgenic population to investigate the role of a branchpoint enzyme within the plant. Due to the myriad of paths that can be followed with GGPP as the substrate, the effect on the plant can be varied. The population was characterised in terms of its phenotype and a hypothesis was formulated regarding the metabolite affected through the expression of *VviGGPS1.* However, future studies will be required to support or disprove this hypothesis.

6.6   References

Abbas, F., Ke, Y., Yu, R., Yue, Y., Amanullah, S., Jahangir, M.M. & Fan, Y., (2017). Volatile terpenoids: multiple functions, biosynthesis, modulation and manipulation by genetic engineering *Planta* **246**, 5, 803–816.

Arimura, G.I., Garms, S., Maffei, M., Bossi, S., Schulze, B., Leitner, M., Mithöfer, A. & Boland, W., (2008). Herbivore-induced terpenoid emission in Medicago truncatula: Concerted action of jasmonate, ethylene and calcium signaling *Planta* **227**, 2, 453–464.

Attaran, E., Rostás, M. & Zeier, J., (2008). *Pseudomonas syringae* Elicits Emission of the Terpenoid (E,E)-4,8,12-Trimethyl-1,3,7,11-Tridecatetraene in *Arabidopsis* Leaves Via Jasmonate Signaling and Expression of the Terpene Synthase TPS4 *Mol. Plant-Microbe Interact.* **21**, 11, 1482–1497.

Burke, C.C., Wildung, M.R. & Croteau, R., (1999). Geranyl diphosphate synthase: cloning, expression, and characterization of this prenyltransferase as a heterodimer. *Proc. Natl. Acad. Sci. U. S. A.* **96**, 23, 13062–7.

Camagna, M., Grundmann, A., Bar, C., Koschmieder, J., Beyer, P. & Welsch, R., (2019). Enzyme fusion removes competition for geranylgeranyl diphosphate in carotenogenesis *Plant Physiol.* **179**, 3, 1013–1027.

Capone, D.L., Jeffery, D.W. & Sefton, M. a, (2012). Vineyard and fermentation studies to elucidate the origin of 1,8-cineole in Australian red wine. *J. Agric. Food Chem.* **60**, 9, 2281–7.

Chen, F., Tholl, D., Bohlmann, J. & Pichersky, E., (2011). The family of terpene synthases in plants: a mid-size family of genes for specialized metabolism that is highly diversified throughout the kingdom. *Plant J.* **66**, 1, 212–29.

Coman, D., Altenhoff, A., Zoller, S., Gruissem, W. & Vranová, E., (2014). Distinct evolutionary strategies in the GGPPS family from plants. *Front. Plant Sci.* **5**, May, 230.

Drew, D.P., Andersen, T.B., Sweetman, C., Møller, B.L., Ford, C. & Simonsen, H.T., (2016). Two key

polymorphisms in a newly discovered allele of the Vitis vinifera TPS24 gene are responsible for the production of the rotundone precursor α-guaiene *J. Exp. Bot.* **67**, 3, 799–808.

Dudareva, N. & Pichersky, E., (2008). Metabolic engineering of plant volatiles *Curr. Opin. Biotechnol.* **19**, 2, 181–189.

Dueholm, B., Drew, D.P., Sweetman, C. & Simonsen, H.T., (2019). In planta and in silico characterization of five sesquiterpene synthases from Vitis vinifera (cv. Shiraz) berries *Planta* **249**, 1, 59–70.

Hamberger, B. & Bak, S., (2013). Plant P450s as versatile drivers for evolution of species-specific chemical diversity *Philos. Trans. R. Soc. B Biol. Sci.* **368**, 1612, 20120426.

Ilc, T., Arista, G., Tavares, R., Navrot, N., Duchêne, E., Velt, A., Choulet, F., Paux, E., Fischer, M., Nelson, D.R., Hugueney, P., Werck-Reichhart, D. & Rustenholz, C., (2018). Annotation, classification, genomic organization and expression of the Vitis vinifera CYPome *PLoS One* **13**, 6, 1–22.

Jaillon, O., Aury, J.-M., Noel, B., Policriti, A., Clepet, C., Casagrande, A., Choisne, N., Aubourg, S., Vitulo, N., Jubin, C., Vezzi, A., Legeai, F., Hugueney, P., Dasilva, C., Horner, D., Mica, E., Jublot, D., Poulain, J., Bruyère, C., Billault, A., Segurens, B., Gouyvenoux, M., Ugarte, E., Cattonaro, F., Anthouard, V., Vico, V., Del Fabbro, C., Alaux, M., Di Gaspero, G., Dumas, V., Felice, N., Paillard, S., Juman, I., Moroldo, M., Scalabrin, S., Canaguier, A., Le Clainche, I., Malacrida, G., Durand, E., Pesole, G., Laucou, V., Chatelet, P., Merdinoglu, D., Delledonne, M., Pezzotti, M., Lecharny, A., Scarpelli, C., Artiguenave, F., Pè, M.E., Valle, G., Morgante, M., Caboche, M., Adam-Blondon, A.-F., Weissenbach, J., Quétier, F. & Wincker, P., (2007). The grapevine genome sequence suggests ancestral hexaploidization in major angiosperm phyla. *Nature* **449**, 7161, 463–7.

Jiang, S.Y., Jin, J., Sarojam, R. & Ramachandran, S., (2019). A Comprehensive Survey on the Terpene Synthase Gene Family Provides New Insight into Its Evolutionary Patterns *Genome Biol. Evol.* **11**, 8, 2078–2098.

Karunanithi, P.S. & Zerbe, P., (2019). Terpene Synthases as Metabolic Gatekeepers in the Evolution of Plant Terpenoid Chemical Diversity *Front. Plant Sci.* **10**, October, 1–23.

Kollner, G.T., Schnee, C., Gershenzon, J. & Degenhardt, J.J., (2004). The variability of sesquiterpenes emitted from two Zea mays cultivars is controlled by allelic variation of two terpene synthase genes encoding stereoselective multiple product enzymes *Plant Cell* **16**, 5, 1115–1131.

Korankye, E.A., Lada, R., Asiedu, S. & Caldwell, C., (2017). Plant Senescence: The Role of Volatile Terpene Compounds (VTCs) *Am. J. Plant Sci.* **08**, 12, 3120–3139.

Lee, G.W., Lee, S., Chung, M.-S., Jeong, Y.S. & Chung, B.Y., (2015). Rice terpene synthase 20 (OsTPS20) plays an important role in producing terpene volatiles in response to abiotic stresses *Protoplasma* **252**, 4, 997–1007.

Leng, X., Wang, P., Wang, C., Zhu, X., Li, X., Li, H., Mu, Q., Li, A., Liu, Z. & Fang, J., (2017). Genome-wide identification and characterization of genes involved in carotenoid metabolic in three stages of grapevine fruit development *Sci. Rep.* **7**, 1, 4216.

Liu, Y., Luo, S., Schmidt, A., Wang, G., Sun, G.-L., Grant, M., Kuang, C., Yang, M.-J., Jing, S.-X., Li, C.-H., Schneider, B., Gershenzon, J. & Li, S.-H., (2016). A Geranylfarnesyl Diphosphate Synthase Provides the Precursor for Sesterterpenoid (C 25) Formation in the Glandular Trichomes of the Mint Species Leucosceptrum canum *Plant Cell* **28**, 3, 804–822.

Lücker, J., Bowen, P. & Bohlmann, J., (2004). Vitis vinifera terpenoid cyclases: functional identification of two sesquiterpene synthase cDNAs encoding (+)-valencene synthase and (−)-germacrene D synthase and expression of mono- and sesquiterpene synthases in grapevine flowers and berries *Phytochemistry* **65**, 19, 2649–2659.

Martin, D.M. & Bohlmann, J., (2004). Identification of Vitis vinifera (-)-alpha-terpineol synthase by in silico screening of full-length cDNA ESTs and functional characterization of recombinant terpene synthase. *Phytochemistry* **65**, 9, 1223–9.

Martin, D.M., Toub, O., Chiang, A., Lo, B.C., Ohse, S., Lund, S.T. & Bohlmann, J., (2009). The bouquet of grapevine (Vitis vinifera L. cv. Cabernet Sauvignon) flowers arises from the biosynthesis of sesquiterpene volatiles in pollen grains. *Proc. Natl. Acad. Sci. U. S. A.* **106**, 17, 7245–50.

Martin, D.M., Aubourg, S., Schouwey, M.B., Daviet, L., Schalk, M., Toub, O., Lund, S.T. & Bohlmann, J., (2010). Functional annotation, genome organization and phylogeny of the grapevine (Vitis vinifera) terpene synthase gene family based on genome assembly, FLcDNA cloning, and enzyme assays. *BMC Plant Biol.* **10**, 1, 226.

Pan, Z., Herickhoff, L. & Backhaus, R.A., (1996). Cloning, characterization, and heterologous expression of cDNAs for farnesyl diphosphate synthase from the guayule rubber plant reveals that this prenyltransferase occurs in rubber particles *Arch. Biochem. Biophys.* **332**, 1, 196–204.

Pare, P.W. & Tumlinson, J.H., (1999). Plant Volatiles as a Defense against Insect Herbivores *Plant Physiol.* **121**, 2, 325–331.

Pichersky, E. & Lewinsohn, E., (2011). Convergent Evolution in Plant Specialized Metabolism *Annu. Rev. Plant*

Biol. **62**, 1, 549–566.

Smit, S.J., Vivier, M.A. & Young, P.R., (2019). Linking Terpene Synthases to Sesquiterpene Metabolism in Grapevine Flowers *Front. Plant Sci.* **10**, February, 1–18.

Tamiru, A., Bruce, T.J.A., Richter, A., Woodcock, C.M., Midega, C.A.O., Degenhardt, J., Kelemu, S., Pickett, J.A. & Khan, Z.R., (2017). A maize landrace that emits defense volatiles in response to herbivore eggs possesses a strongly inducible terpene synthase gene *Ecol. Evol.* **7**, 8, 2835–2845.

Vickers, C.E., Gershenzon, J., Lerdau, M.T. & Loreto, F., (2009). A unified mechanism of action for volatile isoprenoids in plant abiotic stress. *Nat. Chem. Biol.* **5**, 5, 283–91.

Wink, M., (2003). Evolution of secondary metabolites from an ecological and molecular phylogenetic perspective *Phytochemistry* **64**, 1, 3–19.

Zhu, B.-Q., Cai, J., Wang, Z.-Q., Xu, X.-Q., Duan, C.-Q. & Pan, Q.-H., (2014). Identification of a Plastid-Localized Bifunctional Nerolidol/Linalool Synthase in Relation to Linalool Biosynthesis in Young Grape Berries *Int. J. Mol. Sci.* **15**, 12, 21992–22010.